# Aromatic phosphorus heterocycles: from triazaphospholes to phosphorus derivatives of mesoionic carbenes

Inaugural-Dissertation

to obtain the academic degree

Doctor rerum naturalium (Dr. rer. nat.)

submitted to the Department of Biology, Chemistry, Pharmacy

of Freie Universität Berlin

by

LEA DETTLING

Berlin, 2024

This doctoral thesis was carried out between March 2020 and March 2024 at the Department Institute of Chemistry and Biochemistry, Inorganic Chemistry at Freie Universität Berlin under the supervision of Prof. Dr. Christian Müller.

1st reviewer: Prof. Dr. Christian Müller

2nd reviewer: Prof. Dr. Biprajit Sarkar

Date of defense:   05.09.2024

**Declaration of Independence**

Herewith I certify that I have prepared and written my thesis independently and that I have not used any sources and aids other than those indicated by me.

Berlin, 28.06.2024

_____

Lea Dettling

## Acknowledgments

**List of publications**

M. Papke, L. Dettling, J. A. W. Sklorz, D. Szieberth, L. Nyulászi, C.Müller, *Angew. Chem. Int. Ed.* **2017**, *56*, 16484-16489.

E. Yue†, L. Dettling†, J. A. W. Sklorz, S. Kaiser, M. Weber, C. Müller*, Chem. Commun*. **2022**, *58*, 310-313.

E. Yue, A. Petrov, D. S. Frost, L. Dettling, L. Conrad, F. Wossidlo, N. T.Coles, M. Weber, C. Müller, *Chem. Commun*. **2022**, *58*, 6184 - 6187.

L. Dettling†, M. Papke†, J. A. W. Sklorz, D. Buzsáki, Z. Kelemen, M. Weber, L. Nyulászi, C. Müller, *Chem. Commun*. **2022**, *58*, 7745-7748.

J. Lin, N. T. Coles, L. Dettling, L. Steiner, J. F. Witte, B. Paulus, C. Müller, *Chem. Eur. J.* **2022**, *28*, e20220340.

N. T. Coles, L. J. Groth, L. Dettling, D. S. Frost, M. Rigo, S. E. Neale, C. Müller, *Chem. Commun*. **2022**, *58*, 13580-13583.

L. Dettling, N. Limberg, R. Küppers, D. Frost, M. Weber, N. T. Coles, D. M. Andrada, C. Müller, *Chem. Commun.* **2023,** *59*, 10243–10246.

L. Dettling, M. Papke, M. Ernst, M. Weber, C. Müller, *Chem. Eur. J.* **2024**, e202400592.

†: These authors have contributed equally.

iv

**Summary (German)**

In dieser Arbeit werden detaillierte Untersuchungen an aromatischen 5-gliedrigen Heterocyclen vorgestellt, die ein niederkoordiniertes Phosphoratom enthalten, wie Triazaphosphole und die verwandten Triazaphospholeniumsalze.

Zunächst lag der Schwerpunkt auf den 1,2,3,4-Triazaphospholen. Neuartige Triazaphosphole mit elektronenziehenden Arylsulfonylsubstituenten am N(3)-Atom wurden synthetisiert. Erstmals konnte gezeigt werden, dass diese elektronenziehenden Tosyl- und Mesitylsulfonylgruppen einen großen Einfluss auf die Reaktivität des Heterocyclus haben. Nach der Koordination an ein Gold(I)-Zentrum wurde eine $N_2$-Freisetzung und die anschließende Bildung eines $N_2P_2$-Heterocyclus beobachtet. Dies zeigt eine bisher unbekannte Reaktivität dieser neuen Triazaphosphole und eröffnet einen neuen Zugang zu $N_2P_2$-Heterocyclen mit der Möglichkeit, bisher unzugängliche Substitutionsmuster zu erhalten.

Darüber hinaus wurde gezeigt, dass Triazaphosphole als Diene in [4+2]-Cycloadditionen mit dem elektronenarmen Hexafluor-2-butin reagieren und die entsprechenden $CF_3$-substituierten 2*H*-1,2,3-Diazaphosphol Derivate in einer konzertierten Cycloaddition-Cyclorevisions-Reaktion unter Pivaloylnitril-Eliminierung bilden. Sowohl die Koordinationschemie der Triazaphosphole als auch der Diazaphosphole wurde untersucht. Eine kristallographische Charakterisierung der gebildeten Koordinationsverbindungen bestätigte eindeutig, dass die Heterocyclen über das Phosphoratom an ein $W(CO)_5$-Fragment koordinieren. Der beobachtete Wolfram(0)-Pentacarbonylkomplex des Triazaphosphols ist das erste Beispiel für einen Wolframkomplex eines Triazaphosphols und eines der wenigen Beispiele für eine Koordinationsverbindung eines Triazaphosphols mit einer Koordination über das Phosphoratom.

Außerdem wurden Triazaphospholeniumsalze näher untersucht, da diese Verbindungsklasse erst kürzlich beschrieben wurde. Triazaphospholeniumsalze konnten durch die Alkylierung von Triazaphospholen mit Meerwein-Reagenzien synthetisiert werden. Zum ersten Mal wurden Triazaphospholeniumsalze mit einer TMS-Gruppe in der 5-Position beschrieben. Diese ermöglichten den Zugang zu neuartigen protodesilylierten Produkten. Außerdem bilden die $[BF_4]^-$ Salze der TMS-substituierten Triazaphospholenium-Kationen neuartige, bisher unbekannte $BF_3$-Addukte durch Eliminierung von TMS-F. Diese $BF_3$-Addukte konnten isoliert und vollständig charakterisiert werden, und es gelang ebenfalls Zugang zu den verwandten $BEt_3$-Addukten zu erhalten. Die $BR_3$-Addukte stellen eine neue und interessante Verbindungsklasse dar, da sie als Phosphoranaloga von Tetrazol-5-yliden mit einem abnormalen Substitutionsmuster betrachtet werden können. Die protodesilylierten Produkte sind ebenfalls

von Interesse, da die protodesilylierende Reaktion in klassischen Triazaphospholen selten beobachtet wird und diese das erste Beispiel für ein protodesilyliertes Triazaphospholeniumsalz darstellen.

Abschließend wurde die Reaktivität von Pyridylmethyl-funktionalisierten Triazaphospholen in Quaternisierungsreaktionen mit Meerwein-Reagenzien untersucht. Aufgrund der unterschiedlichen nukleophile der verschiedenen Stickstoffatome konnten Triazaphosphole chemoselektiv und schrittweise alkyliert werden. Die Wahl und Stöchiometrie des Alkylierungsreagenzes spielte dabei eine entscheidende Rolle und ermöglichte den gezielten Zugang zu einer großen Anzahl von mono- und di-kationischen Spezies. Diese neuartigen Triazaphosphole und Triazaphospholeniumsalze zeigen mit Cu(I)-Halogeniden eine vielseitige Koordinationschemie, die sich je nach Ladung des Liganden sowie der Art des Cu(I)-Halogenids in unterschiedlichen Koordinationsmodi manifestiert. Es wird ausschließlich eine Koordination über das Phosphoratom beobachtet. Damit erweitern diese Verbindungen die doch sehr kleine Anzahl an Koordinationsverbindungen des Triazaphosphol- sowie des Triazaphospholenium-Heterocyclus mit einer Koordination über das Phosphoratom**.**

## Summary (English)

In this thesis, detailed investigations were carried out on aromatic 5-membered heterocycles containing a low-coordinated phosphorus atom, such as triazaphosphospoles and the related triazaphospholenium salts.

Initially, the focus was placed on 1,2,3,4-triazaphospholes. Novel triazaphospholes with electron-withdrawing arylsulfonyl substituents on the N(3) atom were synthesized. For the first time it could be shown that these electron-withdrawing tosyl and mesitylsulfonyl groups have a major influence on the reactivity of the heterocycle. Upon coordination to a gold(I) center, an unprecedented $N_2$ release and the subsequent formation of a $N_2P_2$ heterocycle were observed. This shows a previously unknown reactivity of these new triazaphospholes and presents a new route to the $P_2N_2$ heterocycles with the possibility of gaining access to previously inaccessible substitution patterns.

Furthermore, it was shown that triazaphospholes react as dienes in [4+2]-cycloaddition reactions with the electron-poor hexafluoro-2-butyne giving the corresponding $CF_3$-substituted 2*H*-1,2,3-diazaphospholes in a concerted cycloaddition-cyclorevision reaction under pivaloyl nitrile elimination. Both the coordination chemistry of the triazaphosphole and that of the diazaphosphole were investigated. The crystallographic characterization of the formed coordination compounds clearly confirms that the heterocycles coordinate to a $W(CO)_5$ fragment *via* the phosphorus atom. The observed tungsten(0)-pentacarbonyl complex of the triazaphosphole is the first example of a tungsten complex of a triazaphosphole and one of the few examples of a coordination compound of a triazaphosphole with a coordination *via* the phosphorus atom.

A closer look was also taken at triazaphospholenium salts as this compound class has only recently been described. Triazaphospholenium salts could be synthesized by alkylation of triazaphospholes with Meerwein reagents. For the first time, triazaphospholenium salts with a TMS group in the 5-position have been synthesized, which provided access to novel protodesilylated products. In addition, these $[BF_4]^-$ salts of the TMS-substituted triazaphospholenium cations form novel, previously unknown $BF_3$ adducts by elimination of TMS-F. These $BF_3$ adducts were isolated and fully characterized, and a targeted synthesis of the related $BEt_3$ adducts could also be shown. The $BR_3$ adducts represent a new and interesting class of compounds, as they can be regarded as phosphorus analogues of tetrazol-5-ylidenes with an abnormal substitution pattern. The protodesilylated products are also of interest as the

protodesilylating reaction is rarely observed in classical triazaphospholes and this is the first example of a protodesilylated triazaphospholenium salt.

Finally, the reactivity of pyridylmethyl-functionalised triazaphospholes was investigated in quaternization reactions with Meerwein reagents. Due to the different nucleophilicity of the nitrogen atoms, both a chemoselective and a stepwise alkylation of the triazaphosphole derivative can be observed. The choice and stoichiometry of the alkylation reagent plays a crucial role, and allowed access to a large number of mono- and di-cationic species. The coordination chemistry of these charged triazaphospholes and the triazaphospholenium salts with Cu(I) halides shows a versatile coordination chemistry, which manifests itself in different coordination modes depending on the charge of the ligand and the type of Cu(I) halide. Only coordination *via* the phosphorus atom is observed. These compounds are some of the few examples in which coordination of the triazaphosphol and triazaphospholenium heterocycles occurs *via* the phosphorus atom.

## Table of abbreviations

| | |
|---|---|
| Å | Ångström |
| dcpm | 1,2-Bis(dicyclohexylphosphino)ethane |
| dppe | 1,2-bis(diphenylphosphino)ethane |
| DME | 1,2-dimethoxyethane |
| IDipp | 1,3-bis-(2,6-*diiso*propylphenyl)-imidazol-2-ylidene |
| DABCO | 1,8-diazabicyclo[2.2.2]octane |
| DBU | 1,8-diazabicyclo[5.4.0]undec-7-en |
| Ad | adamantyl group |
| Ar | aryl group |
| Bz | benzyl group |
| nBu | butyl group |
| δ | chemical shift |
| CuAAC | copper-catalyzed azide-alkyne cycloaddition |
| Cy | cyclohexyl group |
| d | days |
| DFT | density functional theory |
| Dipp | diisopropylpheny group |
| DMAD | dimethylacetylenedicarboxylate |
| diox | dioxan |
| ESPS | electrostatic potential surface |
| E | energy |
| eq | equivalent |
| G | Gibbs energy |
| $t_{1/2}$ | half-life time |
| HOMO | highest occupied molecular orbital |
| IR | infrared spectroscopy |
| *i*Pr | *iso*-propyl group |
| Λ | lamda |
| LUMO | lowest unoccupied molecular orbital |
| Mes | mesityl group |
| MIC | mesoionic carbene |
| Me | methyl group |
| NBO | natural bonding orbitals |
| NPA | natural population analysis |
| NHC | N-heterocyclic carbene |
| NHP | N-heterocyclic phosphenium |
| NICS | nuclear independent chemical shift |
| NMR | nuclear magnetic resonance |
| Ph | phenyl group |
| Py | pyridine group |
| RuAAC | ruthenium-catalyzed azide-alkyne cycloaddition |
| *s*Bu | secondary butyl group |
| σ | sigma |
| *Mes | supermesityl group |
| *T* | temperature |
| *t*Bu | *tert*-butyl group |

| | |
|---|---|
| THF | tetrahydrofuran |
| *t* | time |
| TS | transition state |
| TAP | triazaphosphole |
| Tripp | triisopropylphenyl group |
| TMS | trimethylsilyl group |
| TAS | tris(dimethylamino)sulfonium cation |
| UV | ultraviolet light |

**Table of content:**

## 1. Introduction

### 1.1 Low-coordinated phosphorus compounds

Phosphorus compounds can be described using the $\sigma, \lambda$ -nomenclature.[1] Within the group of phosphorus-containing compounds, those with a lower number of bonding partners ($\sigma$) than the valency ($\lambda$) of the heteroatom are called low-coordinated phosphorus compounds. Generally, these species contain P–C multiple bonds. Although originally considered as rather unstable due to the 'double bond rule', the possibility of kinetic or thermodynamic stabilization by space-filling substituents or aromatic systems makes this assumption outdated.[2] Nowadays, a large variety of very different low-coordinated phosphorus compounds are known and find applications in homogeneous catalysis, luminescent devices and functional materials.[3][4] The chemical properties of low-coordinated phosphorus compounds differ significantly from those of classical P(III) and P(V) compounds and are more closely related to those of unsaturated carbon compounds. Following the isolobal concept, the exchange of a $C(sp^2)$–H or $C(sp)$–H fragment with a trivalent phosphorus atom gives low-coordinated phosphorus compounds, which can be considered as the phosphorus analogues of prominent organic molecules (Figure 1).[5] $\sigma^1\lambda^3$ phosphaalkynes can be considered as the phosphorus equivalent of classical alkynes. Similarly, $\sigma^2\lambda^3$ phosphinines can be regarded as the phosphorus homologues of benzene, and $\sigma^2\lambda^3$ triazaphospholes can be considered as the phosphorus homologues of the well-known triazaphospholes.
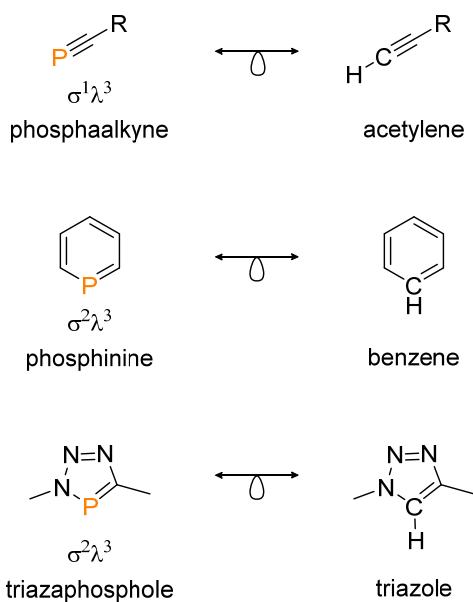


*Figure 1: Isolobal relationship between a trivalent phosphorus atom and a CH fragment, different low-coordinated phosphorus compounds with bonding partners ($\sigma$) of the phosphorus atom and its valency ($\lambda$).*

GIER published the first low-coordinated phosphorus compound in 1961, the phosphaacetylene (H–C≡P, Figure 2). It was synthesized by passing pure phosphine gas ($PH_3$) through a rotating electric arc between graphite electrodes and collecting the volatile products *in vacuo* at low temperatures. This compound is highly unstable and decomposes at temperatures above $T = -124$ °C.[6] The first air-, moisture and temperature stable low-coordinated phosphorus compound, 2,4,6-triphenylphosphabenzene was synthesized by MÄRKL in 1966 (Figure 2).[7] Shortly after, ASHE III successfully synthesized the unsubstituted Phosphinine (Figure 2) by treating 1,1-dibutyl-1,4-dihydrostannine with phosphorus tribromide, giving this route the name 'tin route'.[8] The first phosphaalkene was synthesized by BECKER in 1976 *via* a temperature-induced rearrangement leading to the formation of a P=C double bond (Figure 2).[9] It took 20 years from the first observation to finally find synthetic excess to a thermodynamically stable phosphaalkyne. BECKER and UHL found that additional stabilization could be achieved by using the space-filling *tert*-butyl-substituent (*t*Bu-substituent), sterically shielding the vulnerable P≡C bond (Figure 2).[10][11] Access to phosphaalkenes and phosphaalkynes finally made it possible for CARRIÉ and REGITZ to independently synthesize the first 1,2,3,4-triazaphospholes (Figure 2).[12][13] From the early 80s on low-coordinated phosphorus compounds became a vibrant area in the field of inorganic chemistry, just in 2021 GOICOECHEA and MÜLLER independently published two atom economic methods to access the cyaphide ion ([C≡P]⁻). The lack of effective synthesis methods for cyaphide salts led to this compound class being largely unexplored until recently.[14][15] These two compounds described by GOICOECHEA and MÜLLER are the first examples allowing the transfer of a cyaphide ion. The compound classes of phosphaalkynes and triazaphospholes will be discussed in more detail in the following chapters (Figure 2).
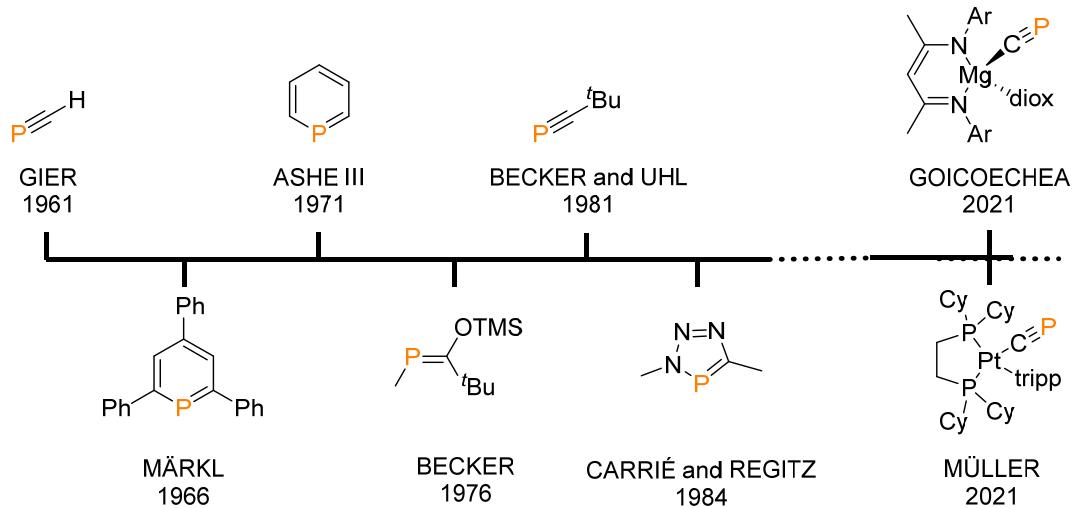


*Figure 2: Historical developments in low-coordinated phosphorus chemistry.*

## 1.2    Phosphaalkynes

Phosphaalkynes are an important class of low-coordinated phosphorus compounds. They display a versatile reactivity and furthermore, serve as valuable building blocks for the introduction of low-coordinated phosphorus moieties, for example in the synthesis of phosphinines and triazaphospholes, respectively.[16][13][17][18] The chemistry of these $\sigma^1\lambda^3$ C≡P triple bond containing compounds started in 1961 with the synthesis of the highly unstable phosphaacetylene by GIER.[6] The first kinetically stable phosphaalkyne, $^t$Bu–C≡P was synthesized around 20 years later (Figure 3, **3A**).[10][11] Due to its early availability, $^t$Bu–C≡P remains one of the most extensively investigated phosphaalkynes with regard to the reactivity of P≡C triple bonds in its compoundclass. Nowadays a variety of different kinetically stabilized phosphaalkynes are known (Figure 3, **3A-3I**). Ionic compounds like the well known Na(O–C≡P)[19][20][21] belong to the class of $\sigma^1\lambda^3$ phosphorus compounds as well (Figure 3, **3I**). The cyaphide anion ([C≡P]⁻), the higher homologue of the widely applied cyanide ion ([C≡N]⁻), has so far only been stabilized in complexes as $L_n$M–C≡P (Figure 3, **3J-3L**). The synthesis and crystallographic characterization of a transition metal complex with a terminal cyaphide ligand was first achieved by GRÜTZMMACHER and coworkers in 2006 (Figure 3, **3J**).[22] It was not until 2021 that GOICOECHEA and coworkers reported on the first cyaphide transfer reagent (Figure 3, **3K**). This compound enabled for Grignard-like reactivity and thus allows salt metathesis reactions to synthesize new cyaphido complexes.[14] Also in 2021, MÜLLER and coworkers were able to synthesize a terminal Pt(II) cyaphido complex (Figure 3, **3K**) that exhibits interesting reactivity at the C≡P ligand. It was shown that the corresponding [3+2]-cycloaddition product, a metallo-triazaphosphole, is formed selectively in the presence of an organic azide.[15]

A selection of phosphaalkynes and related compounds is shown in Figure 3 with NMR spectroscopic data and C≡P bond lengths in Å in the single crystal (if available). While different substituents have a noticeable effect on the variation of resonances in $^{31}$P NMR spectra, the bond length of the C≡P triple bond was typically found to be between 1.516 Å and 1.548 Å for neutral compounds and is as expected slightly elongated in the ionic compounds (1.555 - 1.634 Å) as well as in compounds of the type $L_n$M–C≡P (1.553 - 1.573 Å)
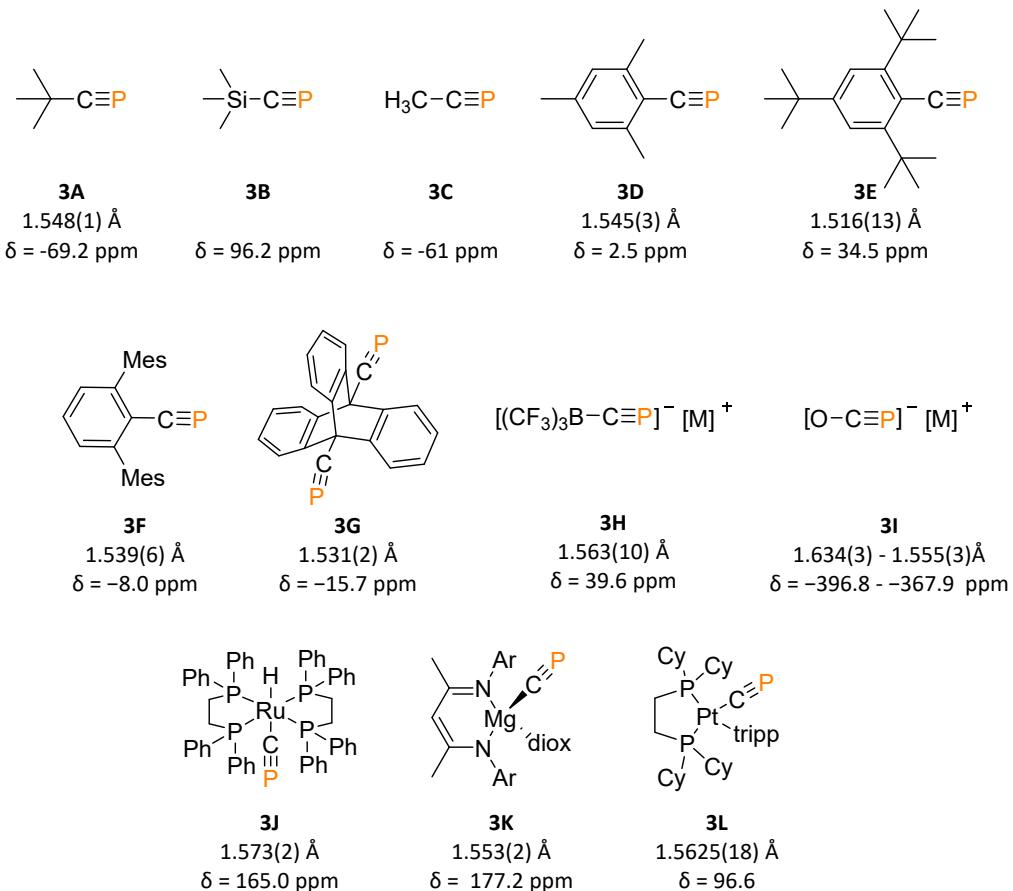
Figure 3: ^{31}P NMR spectroscopic data and bond lengths in Å of the C≡P moiety in tert-butyl-phosphaalkyne (*3A*),[23] trimethylsilyl-phosphaalkyne (*3B*),[24] methylphosphaalkyne (*3C*), mesitylphosphaalkyne (*3D*),[15] supermesitylphosphaalkyne (*3E*),[25] terphenylphosphaalkyne (*3F*),[26] diphosphaalkyne (*3G*),[27] phosphaethynyl complexes (*3H*),[28] sodium 2-phosphaethynolate anions (*3I*)[21]and the cyphido complexes [RuH(η[1]–C≡P)(dppe)₂] (*3J*),[22] [Mg(*[Dipp]NacNac*)(η[1]–C≡P)(Dioxan)] (*3K*)[14] and [(dcpm)Pt(η[1]–C≡P)–(Tripp)] (*3L*).[15]

### 1.2.1 Properties of phosphaalkynes

Already in 1983 Nixon, Suffolk and coworkers showed by photoelectron spectroscopic studies on *[t]*Bu-phosphaalkynes (*[t]*Bu–C≡P) and phenylphosphaalkynes (Ph–C≡P) that the π orbital of the C≡P bond (C≡P-π) represents the HOMO. As a consequence phosphaalkynes, like alkynes, tend to coordinate to a transition metal center *via* the π system (side-on coordination).[29] Similar results were observed by Jayasuriya and coworkers in 1992 in a molecular electrostatic potential (MEP) analysis also showing a preferred side-one reactivity.[30] In 1995 Nixon, Struchkov and coworkers showed by means of electron density distribution (EDD) studies on the *[t]*Bu phosphaalkyne (*[t]*Bu–C≡P) that a considerable excess of electron density is present at the C(sp) atom, resulting in a partial negative charge at the carbon atom and a partial positive charge at the phosphorus atom. In addition, the phosphorus lone pair was discussed to be significantly closer to the phosphorus atom than in related phosphaalkenes, which was attributed to the different hybridization of the phosphorus atom in both systems.[23] Mo, Yáñez and coworkers performed a combined theoretical (CCSD(T)/6-311+G(3df,2p)//QCISD/6-311+G(df,p)) and experimental study on the gas phase acidity of CH₃–C≡P and similar compounds. They showed that the

gas-phase acidity ($\Delta G°_{acidity}$) of H–C≡P is weaker than that of CH$_3$–C≡P. Furthermore the calculated values were in good agreement with the experimentally determined values (especially for CH$_3$–C≡P).[31] The different electronegativities of the phosphorus and the carbon atom (2.55 for C and 2.19 for P, Pauling scale) lead to a polarized C≡P bond. SICILIA, RUSSO and coworkers investigated the polarity of the C≡P bond of different R–C≡P moieties in 2008. The calculation of the natural charge using NBO analysis ((B3LYP/6-311+G(2d,2p)) resulted, for example, for the $^t$Bu–C≡P in a partial negative charge on the carbon atom of -0. 52 e and a partial positive charge on the phosphorus atom of +0.52 e.[32] More recently calculated natural charges (M06-2X/def2-TZVPP), published in 2023 by FERNÁNDEZ, GOICOECHEA and coworkers, gave similar results (for $^t$Bu–C≡P a partial negative charge at the carbon atom of −0.54 $e$ and a partial positive charge at the phosphorus atom of +0.50 $e$).[33] The partial charge of the phosphorus atom generally decreases with coordination to a metal center.[32][33] When examining the bonding situation between the R-fragment and the CP-fragment in $^t$Bu–C≡P the situation is best described by an electron sharing model. In transition metal cyaphido complexes bonding situation between the M-fragment and the CP-fragment [M]$^+$–[C≡P]$^-$ are better characterized by a dative bond (Figure 3, **3J** - **3L**).[33]

### 1.2.2    Synthesis of phosphaalkynes

Over the years, a variety of different methods for the synthesis of phosphaalkynes have been developed. Methodologically, $\beta$-elimination is the predominant synthetic route. Early synthesis methods of mostly short-lived phosphaalkynes required harsh reaction conditions to eliminate hydrogen halide from primary $\alpha$-halophosphanes or dihalophosphanes (Scheme 1, **1a**). However, the formed hydrogen halide can be involved in undesirable retro-reactions and has to be removed either by freezing out or by neutralization with a base.[34][35][36][37] A simplified route to kinetically unstable phosphaalkynes was published by DENIS and coworkers in 2001. Chemoselective reduction of dichlorophosphonates with dichloro(hydrido)aluminium (AlHCl$_2$) yielded 1,1-dichlorophosphines which were then converted into the corresponding phosphaalkynes in a bis-dehydrohalogenation reaction with 1,8-diazabicyclo[5.4.0]undec-7-en (DBU). This strong Lewis base was required, since weak Lewis bases only gave a complex product mixture, presumably due to partial release of HCl (Scheme 1, **1b**). Carrying out these reactions in dilute solutions makes handling of the reactive compound easier.[38] GRÜTZMACHER and RUSSEL further improved this method by using DABCO (1,8-diazabicyclo[2.2.2]octane) to initiate the dehydrohalogenation reaction and obtain the corresponding phosphaalkyne (Scheme 1, **1c**). While DABCO alone causes the conversion, rapid decomposition of this new phosphaalkyne is observed, presumably due to formed DABCO·HCl acting as a chloride anion source. This problem can be easily resolved by adding AgOTf (silver trifluoromethanesulfonate) to the reaction mixture. The method was used to prepare the silyl-substituted phosphaalkynes Ph$_3$Si–C≡P and

Me$_3$Si–C≡P on a multi-gram scale. However, the isolation of the silyl-substituted phosphaalkynes has so far been unsuccessful. In toluene or THF solution these phosphaalkynes only have a half-life time of: t$_{1/2}$ ≈ 1 day at $T$ = 23 °C, but can be stored for considerably longer at $T$ = −78 °C.[22][39] MÜLLER and coworkers were able to demonstrate that this route also allows access to aryl-substituted phosphaalkynes (R–C≡P, R = Mes, Tripp), in which case isolation is possible.[15]

In 1981 APPEL and coworkers showed that the related phenylphosphaalkyne (Ph–C≡P) can be synthesized by eliminating trimethylsilyl chloride from chloro(phenyl(trimethylsilyl)methylene)phosphane *via* flash vacuum pyrolysis at $T$ = 750 °C (Scheme 1, **1d**). The product was collected in a cooling trap at $T$ = −196 °C. Phenylphosphaalkyne (Ph–C≡P) is stable at low temperature, however, slow decomposition is observed above $T$ = −50 °C. $^{31}$P NMR spectroscopic studies revealed a half-life time of: t$_{1/2}$ ≈ 7 min at $T$ = 0 °C.[40] Similarly, trimethylsilylphosphaalkyne (Me$_3$Si–C≡P) was synthesized,[24] however, the method by GRÜTZMACHER and RUSSEL is nowadays more established due to the milder reaction conditions.
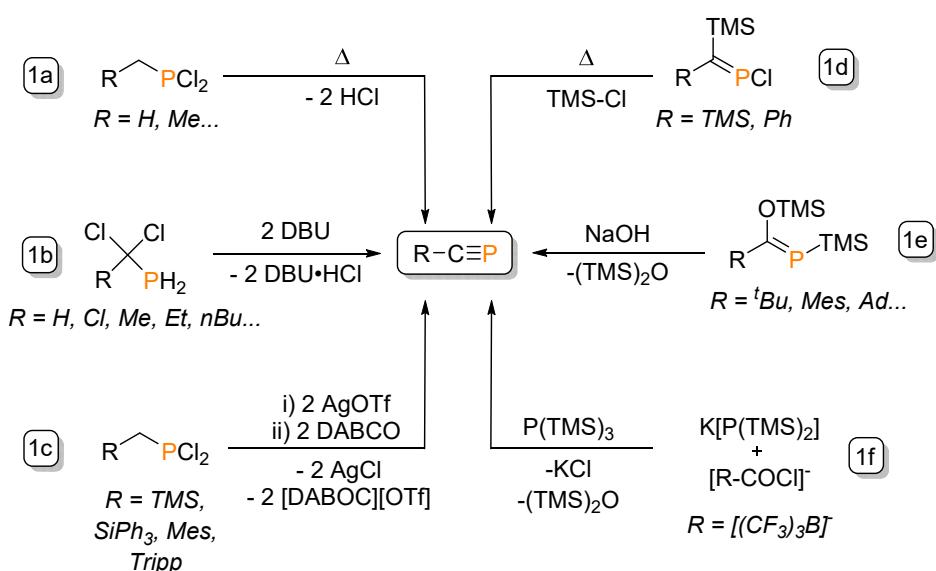


Scheme 1: Classical synthetic routes to phosphaalkynes.

In the same year (1981) BECKER and UHL synthesized $^t$Bu–C≡P *via* base-catalyzed hexamethyldisiloxane (TMS$_2$O) elimination from a suitable phosphaalkene (Scheme 1, **1e**).[11] These phosphaalkenes are normally prepared by treating a carboxylic acid chloride with tris(trimethylsilyl)phosphane, (P(TMS)$_3$), leading to the formal addition of a P(TMS)$_2$ fragment, followed by a subsequent 1,3 sigma tropic rearrangement of the trimethylsilyl group to the carbonyl oxygen atom, yielding the corresponding phosphaalkene. While the hexamethyldisilane elimination originally took place in a solution of sodium hydroxide (NaOH) in diglyme at $T$ = 20 °C, it was later found beneficial to perform the elimination reaction solvent free with sodium hydroxide (NaOH) at $T$ = 120-160 °C.[16][41][42][43][44] In the case of $^t$Bu–C≡P, purification of the product is achieved by a trap to trap condensation. This improved method

provides access to a wide range of new phosphaalkynes, such as the adamantylphosphaalkyne (Ad–C≡P)[41] and the 2,4,6-trimethylphenylphosphaalkyne (mesitylphosphaalkyne, Mes–C≡P).[44] Apart from the method used by GRÜTZMACHER and RUSSEL,[22][39] it remains the most commonly used method to synthesize phosphaalkynes.

The anionic borates [(CF$_3$)$_3$B–C≡P]$^-$ are obtained in a comparable synthesis, from acyl halide borates such as [(CF$_3$)$_3$B–COCl] and a mixture of K[P(TMS)$_2$] and P(TMS)$_3$.[28] The phosphide K[P(TMS)$_2$] can be obtained in a reaction of potassium *tert*-butoxide (KO$^t$Bu) with P(TMS)$_3$ (Scheme 1, **1f**).[45][46]

Another important phosphaalkyne compound is the phosphaethynolate anion ([O–C≡P]$^-$). The corresponding lithium salt Li(DME)$_2$(O–C≡P) was first synthesized by reacting lithium phosphide (Li[P(TMS)$_2$]) with dimethyl carbonate and characterized as early as 1992 by BECKER and coworkers (Scheme 2, **2a**).[19] However, this compound was not investigated further due to its thermodynamic instability. It took about 20 years until an improved synthetic route by GRÜTZMACHER and coworkers in 2011 provided access to the heavier analogs, in particular the much more stable Na(O–C≡P), thus making investigations into the properties and applications of this new functional group possible.[20] In 2014 the same group published an improved synthetic route, starting from red phosphorus, sodium, naphthalene and *tert*-butanol in solution, forming sodium phosphide (NaPH$_2$) *in situ* which was further reacted with ethylene carbonate giving Na(O–C≡P) on a multi-gram scale (Scheme 2, **2b**). This ultimately enabled the broad application of sodium phosphaethynolate (Na(O–C≡P)) in chemical transformations, e.g. as a ligand, in decarbonylating and deoxygenating processes and as a building block for novel heterocycles.[47] Concluding, GRÜTZMACHER *et al.* described in 2017 a synthetic method for industrial scale, where solid reagents are avoided; phosphine gas (PH$_3$) is utilized to generate sodium phosphide (NaPH$_2$) in a deprotonation reaction with sodium *tert*-butoxide (NaO$^t$Bu), which then reacts with dimethyl carbonate to form the sodium phosphaethynolate anion(Na(O–C≡P)) (Scheme 2, **2c**).[48]
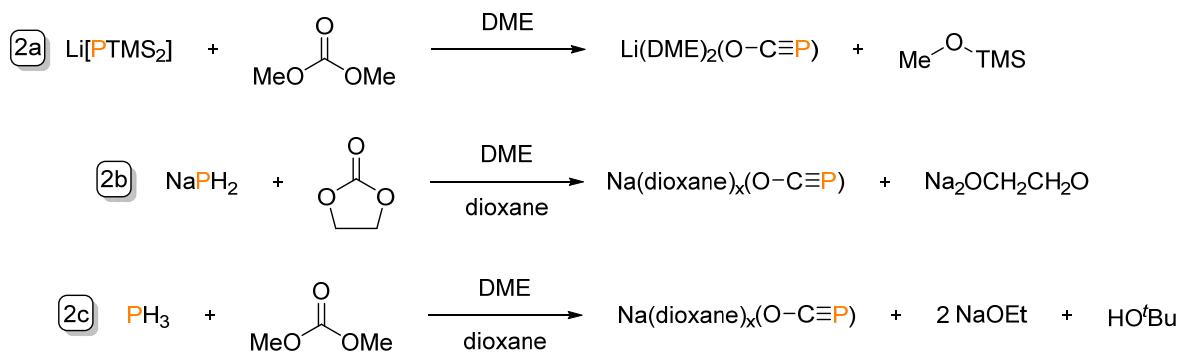


*Scheme 2: Selected synthesis routes to the 2-phosphaethinolate anion.*

Recently, CUMMINS and coworkers showed a method for the *in situ* preparation of the short-lived phosphaalkynes (R–C≡P, R = H, Me, Et, *i*Pr, *s*Bu). This procedure involves heating a dibenzo-7-

phosphanorbornadiene precursor (Ph$_3$PC(R)P(C$_{14}$H$_{10}$), R = H, Me, Et, $i$Pr, $s$Bu) to a temperature of $T$ = 20 °C – 80 °C, resulting in the thermolysis to anthracene (C$_{14}$H$_{10}$), triphenylphosphine (PPh$_3$) and the corresponding substituted phosphaalkynes (R–C≡P) (Scheme 3, **3a**). In reactions where anthracene and triphenylphosphine coproducts are tolerated, these phosphaalkyne precursors can be very useful.[49]
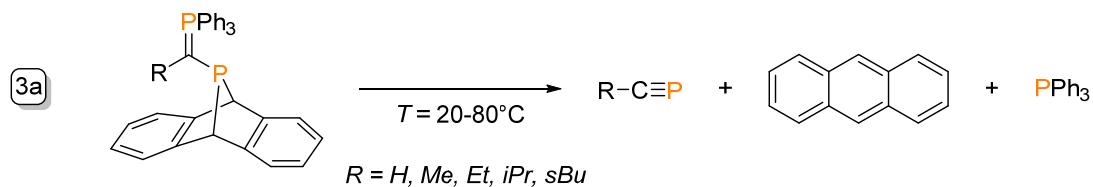


Scheme 3: Synthesis of short-lived phosphaalkynes from a dibenzo-7-phosphanorbornadiene.

For the cyaphide anion complexes L$_n$M–C≡P, different approaches were established to synthesize the before-mentioned terminal complexes (chapter 1.2, Figure 3, **3J** - **3L**). The approach of GRÜTZMMACHER *et al.* involves a ruthenium complex with a $\eta^1$-bonded silyl-phosphaalkyne (SiPh$_3$–C≡P). Cleavage of the Si–C bond with a slight excess of sodium phenoxide leads to the corresponding terminal cyaphido complex [RuH($\eta^1$–C≡P)(dppe)$_2$] (Figure 3, **3I,** Scheme 4, **4a**).[22] The approach of GOICOECHEA and coworkers published in 2023 starts from a sodium phosphaethynolate anion which is *in situ* silylated with *tris*(*iso*propyl)silyl trifluoromethanesulfonate (*i*Pr$_3$SiOTf) giving the corresponding phosphaalkyne (*i*Pr$_3$SiO–C≡P). Reductive C–O bond cleavage with Jones' magnesium(I) reagent ([Mg($^{Dipp}$NacNac)]$_2$) then yields the cyaphido-Grignard reagent [Mg($^{Dipp}$NacNac)($\eta^1$–C≡P)(Dioxan)] (Figure 3, **3J,** Scheme 4, **4b**).[14] In the same year MÜLLER and coworkers developed a photochemical approach. A platinum(0)complex with a side on ($\eta^2$) coordinated 1,3,5-*triiso*propylphenyl-substituted phosphaalkyne (Tripp–C≡P) can be irradiated with UV light ($\lambda_{max}$ = 405 nm, 4 × 15 W blacklight LED) which facilitates the C–C≡P bond activation and the formation of the desired terminal cyaphido complex at a platinum(II) center [(dcpm)Pt($\eta^1$–C≡P)–(Tripp)] (Figure 3, **3K,** Scheme 4, 4c).[15]
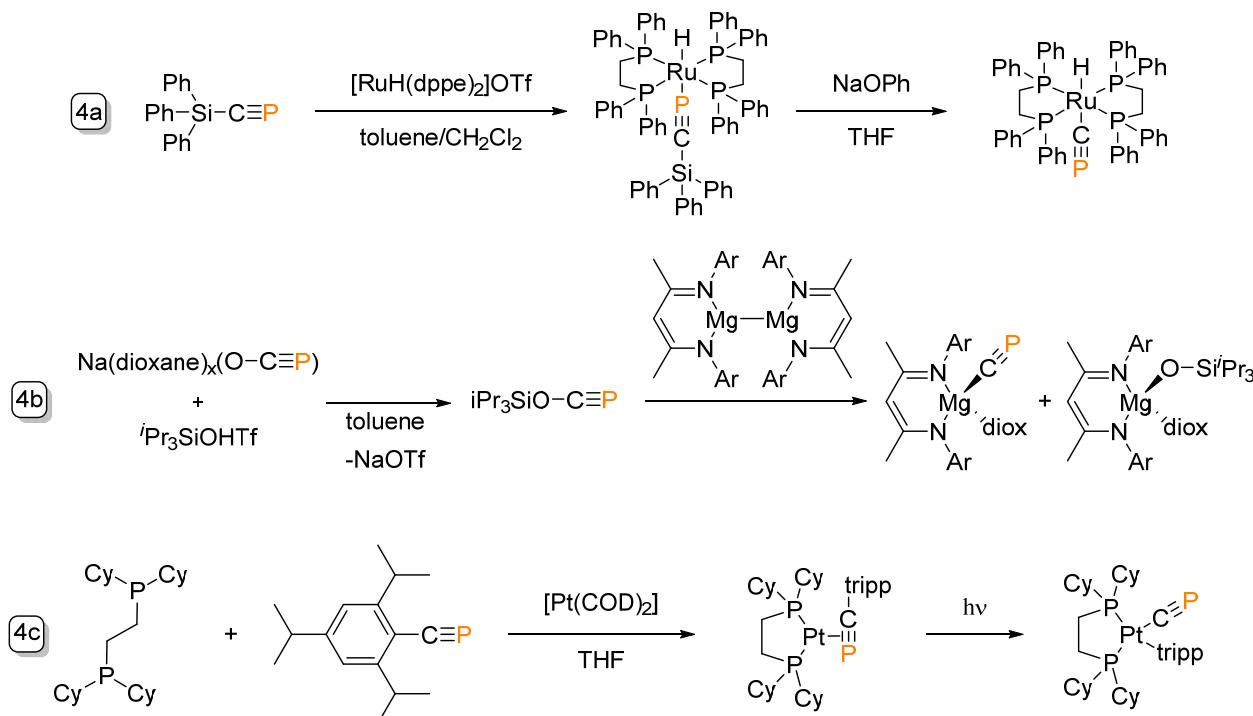
Scheme 4: Synthesis of different cyaphido complexes.

## 1.3    1,2,3,4-Triazaphospholes

This work will focus mainly on the substance class of the 1,2,3,4-triazaphospholes, their functionalization and coordination chemistry.[50][51][52][53] Initially synthesized by CARRIÉ and REGITZ in 1984,[12][13] these $\sigma^2\lambda^3$-phosphorus heterocycles can be considered the phosphorus analogues of the well-known triazoles (Figure 4).[54] In recent years they have gained more interest, as studies on their coordination chemistry and reactivity were carried out. The higher homologues of the 1,2,3,4-triazaphospholes the 1,2,3,4-triazaarsoles were first reported by MÜLLER and coworkers in 2016 (Figure 4).[55]
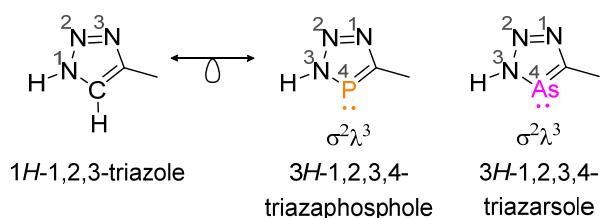


Figure 4: isolobal relationship between triazole, triazaphosphole and the higher arsenic homologue.

### 1.3.1 Structural and Electronic Properties of 3*H*-1,2,3,4-Triazaphospholes

1,2,3,4-triazaphospholes are low-coordinated, 5-membered planar heterocycles. Investigations by NYULÁSZI and coworkers on azaphospholes show a high degree of aromaticity for the 1,2,3,4-triazaphospholes, with the aromatic stability increasing with an increasing number of nitrogen atoms in the heterocycle.[56] In addition, HEINICKE and coworkers showed that these heterocycles have a high $\pi$-electron density at the phosphorus atom, due to the $\ddot{N}$–C=P $\leftrightarrow$ $N^+$=C–$P^-$ conjugation.[57][58] A comparison of the X-ray structural data analyses of selected literature-known triazaphospholes clearly shows the planarity of the five-membered aromatic {$PCN_3$} heterocycle. The average N–P–C bond angle is 85.35°-87.48°.[59][60][61][62][63] A direct comparison of the bond angles in a pyridyl-functionalized triazaphosphole (Figure 5, **5A**) with those of the structurally related triazole reveals a significantly smaller N–P–C angle (85.77°) than the N–C–C angle (105.01°). This effect is primarily attributed to the significantly longer P–C and P–N bonds and higher s-character of the phosphorus atom.[59] A similar phenomenon is also observed in the transition from pyridine to phosphinines.[64] The P=C double bond with an average length of 1.713 Å-1.723 Å is shorter than the bond length of a C–P single bond ($PPh_3$: 1.83 Å)[65] and longer than a localized C=P double bond ((diphenylmethylene)-(mesityl)phosphane, $Ph_2$C=PMes: 1.692 Å)[66].[59][60][61][62][63] While the bond angles and lengths are only slightly depending on the substitution pattern, the TMS group has a significant effect on the resonances observed in the $^{31}$P NMR spectra of these compounds. When comparing the chemical shift of compound **5C** (Figure 5: $\delta$ = 218.3 ppm) with its $^t$Bu-substituted derivative ($\delta$ = 174.0 ppm), a deviation of $\Delta\delta$ = 44.3 ppm is observed.[61] A similar observation can be made when comparing **5A** (Figure 5: $\delta$ = 167.5 ppm) with its TMS-substituted derivative ($\delta$ = 211.6 ppm), a difference of $\Delta\delta$ = 44.1 ppm is found.[59] However, replacing the $^t$Bu-group with a methyl group (Me) appears to have a minimal effect on the resonances in the $^{31}$P NMR spectra.[62][63] The $\pi$-electron-withdrawing character due to negative hyperconjugation of the TMS group directly bound to an aromatic system could explain this shielding and the associated downfield shift.[59][67]
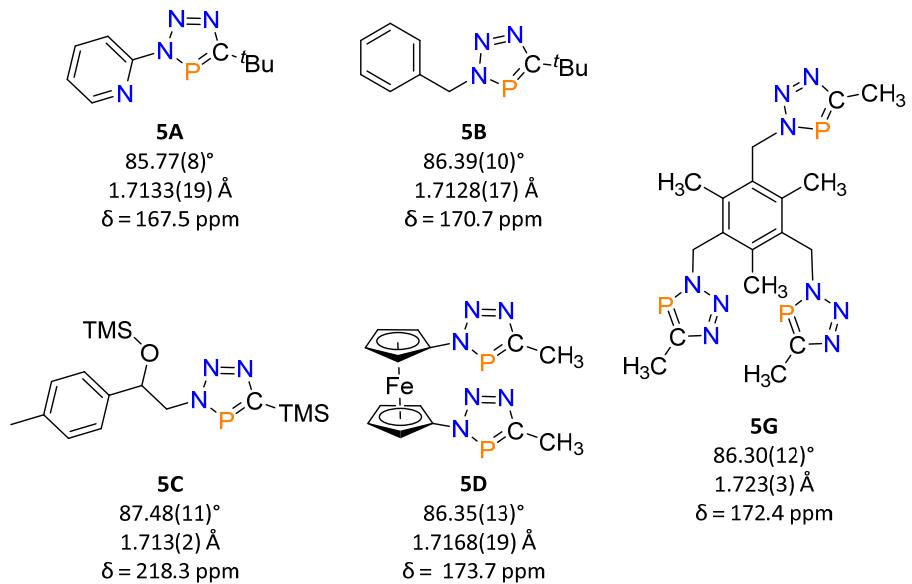
*Figure 5: $^{31}P$ NMR spectral data and P(1)-C(1) bond length in Å and N(3)-P(1)-C(1) bond angle in ° of 3-pyridine-5-tert-butyl-triazaphosphole (**5A**),[59] 3-benzyl-5-tert-butyl-triazaphosphole (**5B**),[60] 3-(2-ptolyl)-2-((trimethylsilyl)oxy)ethyl)-5-trimethylsilyl-triazaphosphole (**5C**),[61] 1,1'-bis(triazaphosphole)ferrocene (**5D**),[62] tris(triazaphosphole) (**5G**).[63]*

To gain insights into the electronic structure, MÜLLER and coworkers calculated the frontier molecular orbitals of the parent tetrazole and triazaphosphole (Figure 6).[55] The HOMO–LUMO gap in the triazaphosphole is found to be smaller than in the tetrazole. The LUMO exhibits a large coefficient with $\pi$-symmetry at the phosphorus atom, indicating $\pi$-accepting properties. In the corresponding tetrazole, this is much less pronounced. Upon examination of the donor capabilities of the low-coordinated system, the $\pi$-donor capabilities are indicated by a high degree of $\pi$-symmetry at the phosphorus atom in the HOMO. The σ-donor capabilities of the nitrogen atoms N(1) and N(2) are indicated by a $\sigma$-coefficient at these atoms in the HOMO−1. It is noteworthy that the order of the HOMO and HOMO−1 orbitals in the tetrazole is reversed in comparison to the triazaphosphole. A similar change in the order was also observed when comparing frontier orbitals of imines and phosphaalkenes.[68] The $\sigma$-donor properties of the phosphorus atom are evident through the $\sigma$-coefficient at phosphorus atom in the HOMO−2.
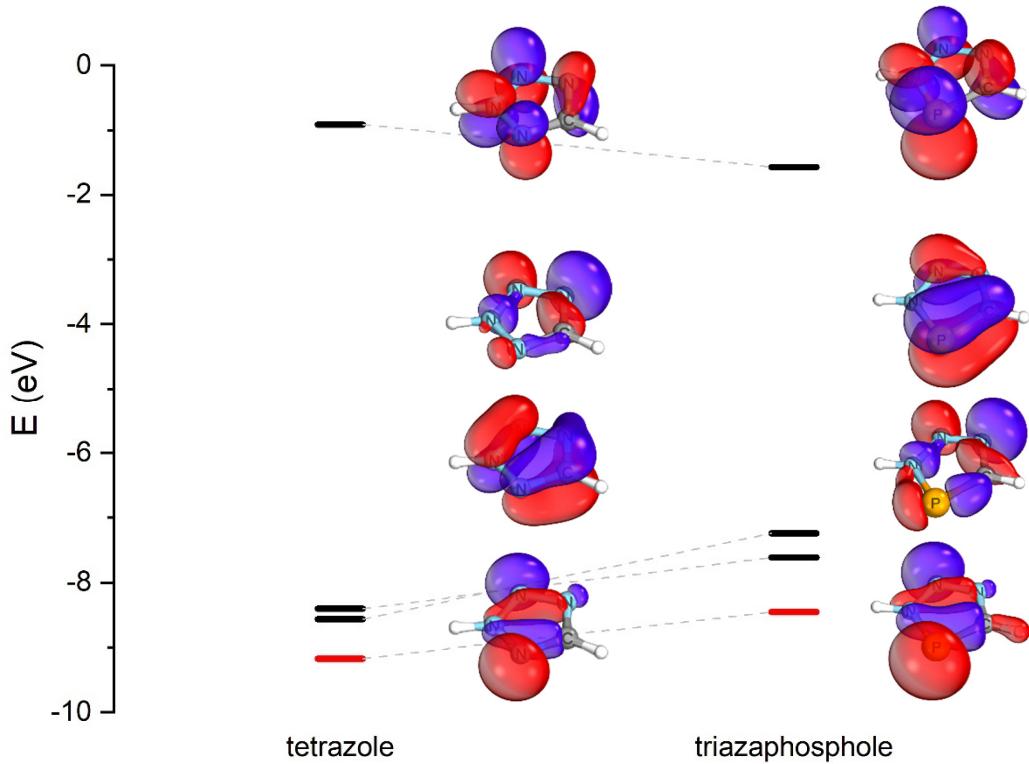
*Figure 6: Selected frontier molecular orbitals of the tetrazole(left) and triazaphosphole(right). Calculations at a DFT level (B3LYP, cc-pVTZ).[55]*

MÜLLER and FROST continued the investigations on the electronic structure of the triazaphosphole. Previous studies indicated that the phosphorus atom exhibited relatively weak σ-donor properties in comparison to the two N(1)- and N(2)-atoms as evidenced by the frontier orbitals (Figure 6: HOMO−1 vs. HOMO−2).[55] This was supported by NBO analyses (natural bonding orbitals, Figure 7) of the free electron pairs. The NBO analysis shows a relatively high s-character (70.5%) and a low p-character (29.4%) for the lone pair at the phosphorus atom. The higher s-character indicates the orbital being diffuse and potentially less suitable for coordination to transition metal centers than, for example, the N(1) or (N(1) atom with p-character: 62.8%, N(2)p-character: 56.3% respectively. In comparison, the lone pair at the phosphorus atom of the parent phosphinine (Figure 1, Chapter 1.1) is slightly less diffuse with only 61.7% s-character.[69]

s: 43.6%
p: 56.3%

s: 37.0%
p: 62.8%

s: 70.5%
p: 29.4%
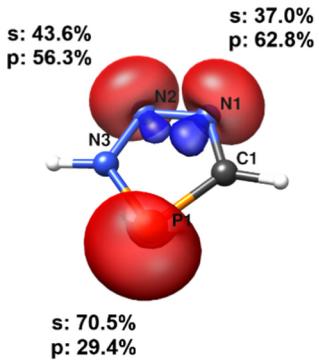
*Figure 7: The natural bonding orbitals representing free electron pairs with s- and p-character, as determined by the NBO analysis (isosurface value: 0.1 e/au3, B3LYP-D3/def2-TZVP).[69]*

The calculation of the natural population analysis (NPA) charges of the phosphinine and the triazaphosphole indicates a higher partial positive charge at the phosphorus atom of the triazaphosphole (NPA$_P$: 0.71$e$) than at the phosphorus atom of the phosphinine (NPA$_P$: 0.61$e$). These observations are in good agreement with the results of electrostatic potential surface plots (ESPS, Figure 8). The negative charge (red) in the triazaphosphole is concentrated around the N(1)- and N(2)-atoms, whereas the negative charge in the phosphinine is more evenly distributed over the ring system with a focus on the phosphorus atom. These calculations indicate that the phosphorus atom in the triazaphosphole will preferentially form coordination compounds with electron-rich and negatively charged metal centers.[69]
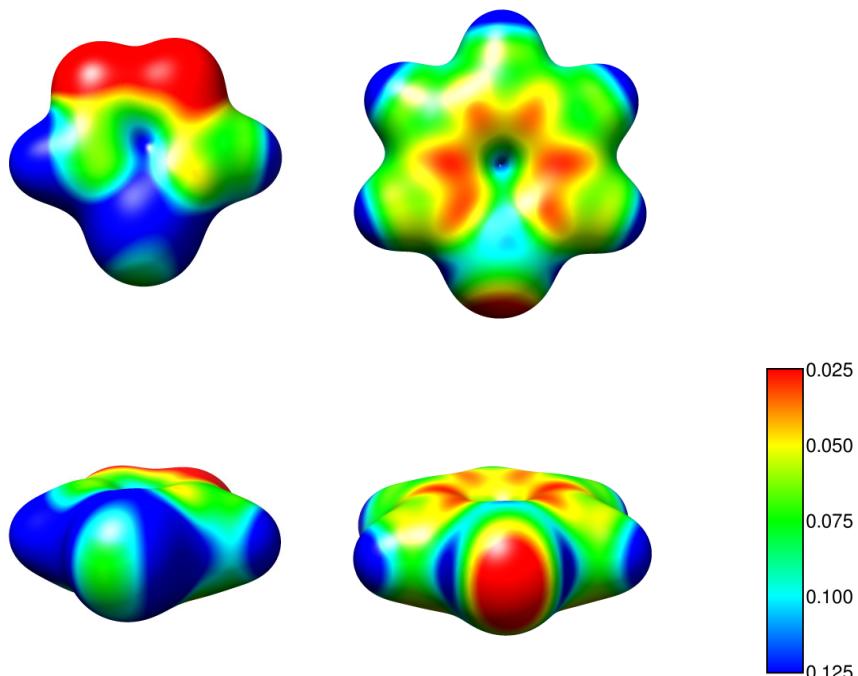


*Figure 8: Electrostatic potential surface (ESPS) plots of the unsubstituted triazaphosphole (left) and phosphinine (right). The electrostatic potentials (in a.u.) are mapped to the electron density isosurfaces of 0.02 e/au3, calculations were performed at the B3LYP-D3/def2-TZVP level. [69]*

## 1.3.2 Synthesis of 1,2,3,4-Triazaphospholes

The 3,5-disubstituted 1,2,3,4-triazaphospholes can be considered as the phosphorus analogues of the known 1,4-disubstituted 1,2,3-triazoles.[70][59] 1,2,3-Triazoles can be easily synthesized in a 1,3-dipolar cycloaddition reaction, typically involving the interaction between a $4\pi$ system (1,3-dipole) and a $2\pi$-dipolarophile.[33] This results in the formation of a five-membered heterocycle *via* a [3+2] cycloaddition. First described around 1960 by HUISGEN, the concerted [3+2] cycloaddition reaction between alkynes and organoazides leads to the formation of a mixture of isomers (1,4- and 1,5-regioisomers, Scheme 5, **5a**).[54][33]

Four decades later, SHARPLESS and MELDAL demonstrated independently that the 1,4-disubstituted regioisomer can be selectively obtained in the presence of suitable copper catalysts (Scheme 5, **5b**).[72][60] The use of the copper(I) catalyst leads not only to isomeric purity but also to an acceleration of the reaction by a factor of $10^7$ to $10^8$.[73] This process is also known as copper-catalyzed azide-alkyne cycloaddition (CuAAC). In 2005, FOKIN and coworkers described the counterpart, the ruthenium-catalyzed azide-alkyne cycloaddition (RuAAC), which allows access to the 1,5-disubstituted regioisomer (Scheme 5, **5c**).[74][75]
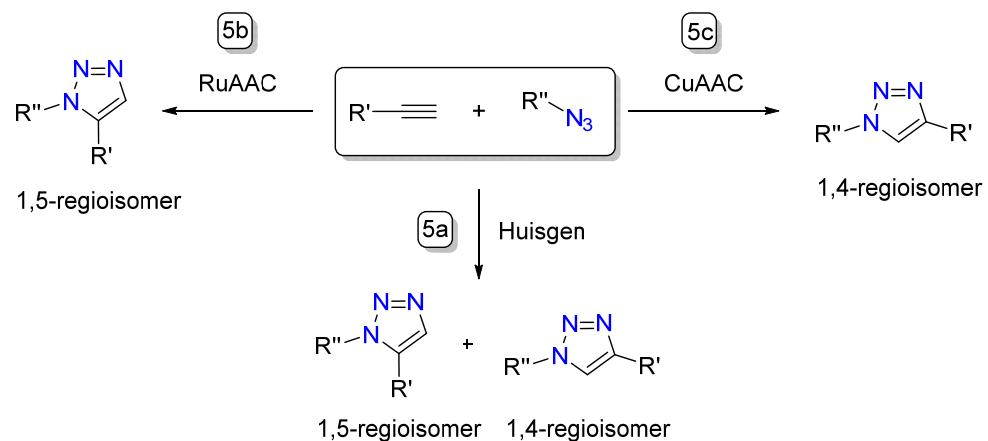


*Scheme 5: Huisgen cycloaddition (**5a**), ruthenium-catalysed azide-alkyne cycloaddition forming the 1,4-regioisomer (**5b**) selectively, and copper-catalysed azide-alkyne cycloaddition selectively forming the 1,5-regioisomer (**5c**).*

In 2001, SHARPLESS and coworkers introduced the term "click chemistry," defining it as a modular reaction with a wide scope that has high yields, is stereospecific, and merely yields by-products that can be easily separated without the use of chromatographic methods. In addition, the reaction should be insensitive to oxygen and water, contain only readily available starting materials, and take place in no solvent, benign or easy to removeable solvents. The isolation of the product should be possible without the use of chromatography, and the product should be stable under physiological conditions. Reactions that can be described as click reactions include, in addition to the 1,3-dipolar cycloaddition,

other cycloaddition reactions such as the Diels-Alder reaction, nucleophilic substitution reactions such as ring-opening reactions of epoxides and addition reactions involving C–C multiple bonds such as epoxidations.[76]

In 2022, SHARPLESS, MELDAL and BERTOZZI were awarded with the Nobel Prize in Chemistry for "the development of click chemistry and bioorthogonal chemistry". The copper-catalyzed azide-alkyne cycloaddition (CuAAC) in particular was named the "crown jewel" of click chemistry, due to its extensive range of potential applications, including the development of drugs, DNA mapping, and the production of materials with enhanced functionality.[77] BERTOZZI and coworkers has further developed click chemistry-based reactions, successfully applying them in bioorthogonal chemistry.[78]

The use of phosphaalkynes as dipolarophiles in a 1,3-dipolar cycloaddition leads to the formation of the 3,5-disubstituted 1,2,3,4-triazaphospholes, as first demonstrated by RÖSCH and REGITZ in 1984.[12] Due to the polarization of the phosphorus-carbon triple bond, no catalyst is required, and the 3,5-regioisomer is formed exclusively.[12][79] The steric demand of the starting materials has no influence on the stereoselectivity. Even the 1,3-dipolar cycloaddition of H–C≡P and Me–N$_3$ only results in the formation of the 3,5-regioisomer.[37] To this day, this remains the principal synthetic method for the preparation of 3,5-disubstituted triazaphospholes (Scheme 6).[80]



*R' = H, Me, TMS, $^t$Bu, Ad...*
*R" = Ph, Bz, Py, $^t$Bu, Ad, Dipp, 1,1'-diazidoferrocene, $C_6Me_3(CH_2N_3)_3$,...*
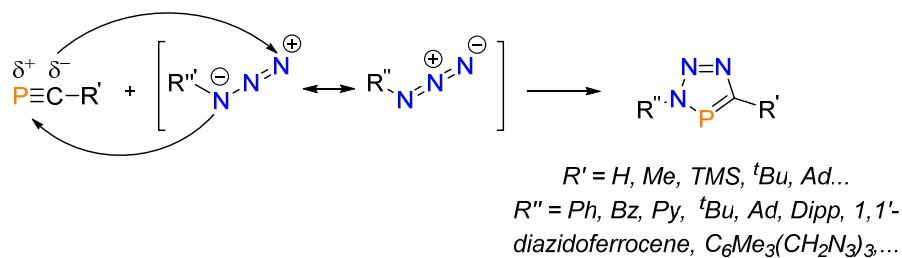
*Scheme 6: Reaction mechanism of the formation of different 1,2,3,4-triazaphospholes.*

A multitude of 1,2,3,4-triazaphosphole derivatives can be synthesized *via* this 1,3-dipolar cycloaddition reaction, including all of the aforementioned triazaphospholes (Figure 5: **5A-5E**). [59][60][61][62][63] This type of reaction is highly functional group tolerant, allowing a diverse range of derivatives.[79]

For example, it could be demonstrated that a 1,3-dipolar cycloaddition employing poly(allylazide) ({C$_3$H$_5$(N$_3$)}$_n$) as dipole, leads to the formation of a triazaphosphole-substituted polymer, as shown by JONES and coworkers (scheme 7, **7a**).[62] Furthermore, SO and coworkers showed that a triazaphosphole can be synthesized from a metal azide, specifically germanium(II)azide. The reaction with adamantylphosphaalkyne (Ad–C≡P) affords access to the corresponding 2,6-diiminophenylgermanium(II)triazaphosphole (Scheme 7, **7b**).[81]
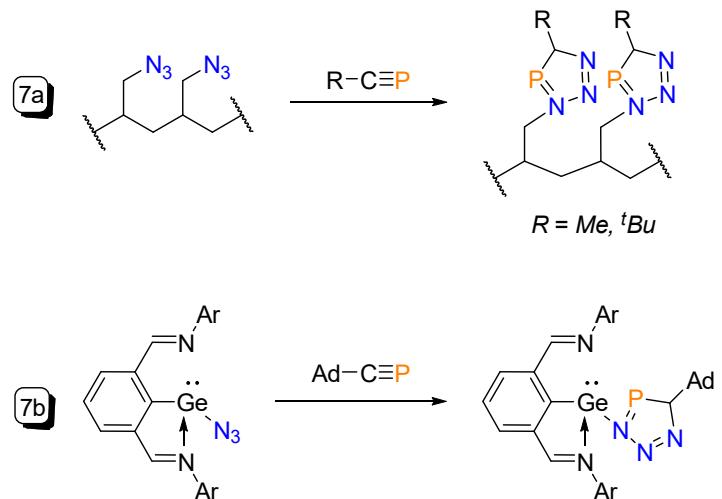
*Scheme 7: 1,3-dipolar cycloaddition reactions giving the corresponding poly triazaphosphole (**7a**) and 2,6-diiminophenylgermanium(II)triazaphosphole (**7b**) (Ad = adamantly; Ar = 2,6-$^i$Pr$_2$C$_6$H$_3$).*

FERNÁNDEZ, GOICOECHEA and coworkers conducted further computational studies on the factors influencing 1,3-dipolar cycloaddition reactions, such as regioselectivity, concertedness and aromaticity, with the reaction between $^t$Bu–N$_3$ and $^t$Bu–C≡P serving as an example. They showed that the [3+2]-cycloaddition reaction proceeds concertedly through the 5-membered transition state (TS), generating the corresponding triazaphosphole (TAP) in a strongly exergonic process (Figure 9). The calculated barriers are consistent with a reaction at room temperature, which is in line with the experimental data.[79][80]
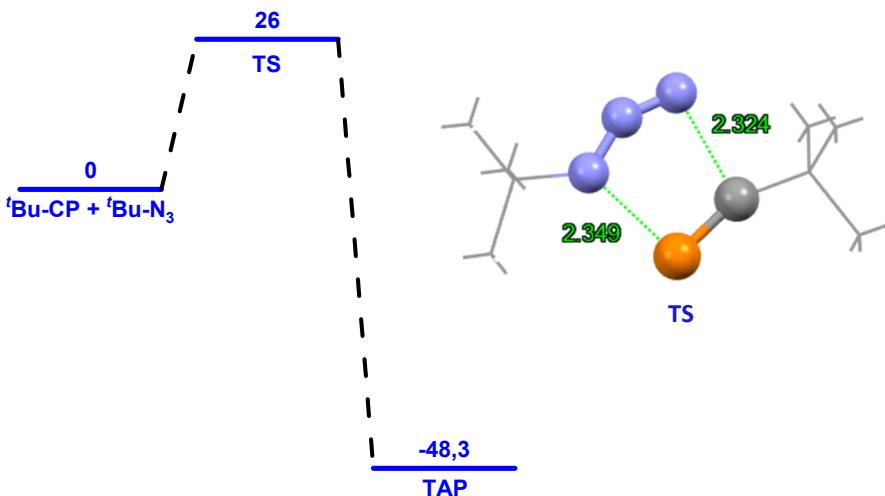


*Figure 9: computed reaction profile for the 1,3-dipolarcycloaddition (left), relative free energies (ΔG, at 298 K) are given in kcal/mol; C---N and P---N bond forming distances given in angstroms (middle). All data were computed at the PCM(toluene)-M06-2X/def2-TZVPP//PCM(toluene)-M06-2X/def2-SVP level.[79]*

As anticipated for [3+2] cycloadditions, the transition state (TS) can be regarded as aromatic, as evidenced by a strongly negative value of −21.9 ppm of the nuclear independent chemical shift (NICS) computed at the (3,+1) ring critical point of the five-membered transition state. With regard to the

regioselectivity of the cycloaddition reaction, only the 3,5-regioisomer, but not the 1,5-regioisomer, could be observed experimentally (Figure 10). Calculations of the free activation barriers ($\Delta G^{\neq}$) and reaction energies ($\Delta G_R$) indicate that product formation is mainly kinetically controlled. Additionally the 3,5-regioisomer is also thermodynamically favored. Furthermore, the polarized nature of the C≡P unit, which has already been reported in detail (Chapter 1.2.1) in connection with the charge accumulation on the substituted nitrogen atom of the azide dipole (Figure 10: −0.41 *e* compared to −0.09 *e* for the unsubstituted nitrogen), also leads to a strong preference for the formation of the 3,5-regioisomer.[79]
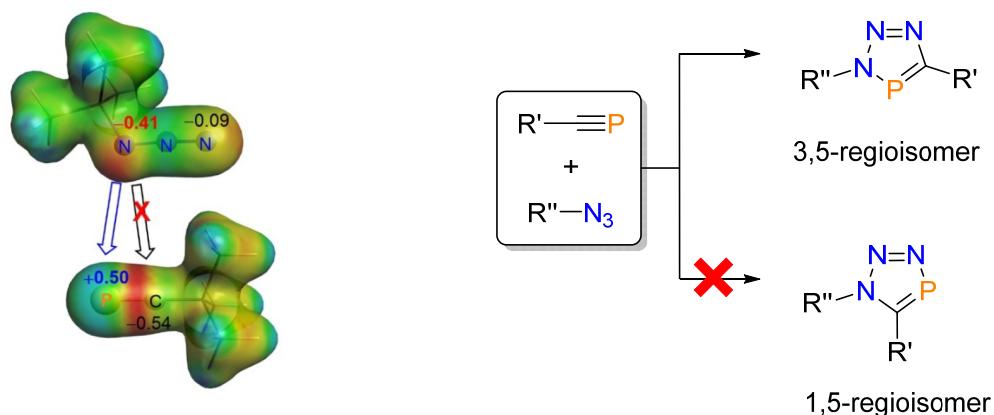


*Figure 10: Electrostatic potential maps and computed natural charges showing the preferred interaction between $^{t}$Bu-N₃ and $^{t}$Bu–C≡P.*

It has been shown that cyaphido complexes LnM–C≡P (Figure 3, **3J − 3L**) can also be used as dipolarophiles in 1,3-dipolar cycloaddition reactions. The first example was published in 2021 by MÜLLER and coworkers. The cyaphidoligand within the coordination sphere of a platinum center reacts with 2,6-*Diiso*propylphenyl-azide (Dipp–N₃), giving a 3,5-anionic triazaphospholato ligand in a regioselective manner (Figure 11, **11A**).[15]

GOICOECHEA and coworkers followed this approach and demonstrated that a broad range of metal cyaphido complexes can be readily reacted with azides, affording the corresponding metallo-triazaphospholes, which in turn can be converted into protonated triazaphospholes and iodo-triazaphospholes.[82][83]
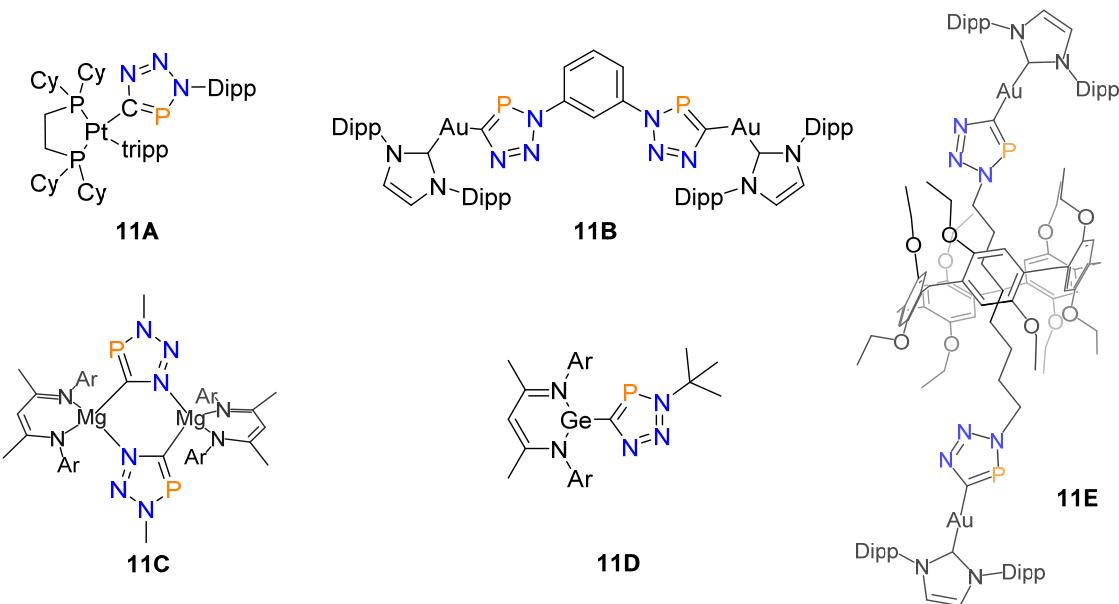
*Figure 11: A selection of triazaphospholes synthesized from cyaphido complexes.*

The addition of organic azides to Au(IDipp)(C≡P) results in the formation of gold(I) triazaphosphole complexes. The choice of different azides allows access to compounds with interesting properties. An example is that addition of a diazide gives rise to a bimetallic gold(I)1,3-bis(triazaphosphole) complex (Figure 11, **11B**).[82] Even access to inorganic rotaxanes is possible (Figure 11, **11E**).[83] Employing an electron-deficient bis-azide threaded with pillar[5]arene as 1,3-dipole and Au(IDipp)(C≡P) as the dipolarophil in a [3+2] cycloaddition, yields an inorganic rotaxane with gold(I) triazaphosphole stoppers (Figure 11, **11E**). The bulky and strongly bonded IDipp (1,3-bis-(2,6-*diiso*propylphenyl)-imidazol-2-ylidene) ligand prevented dethreading.[83] Cycloaddition with a magnesium cyaphido complex (Figure 3, **3K**), allows access to the corresponding dimeric magnesium(II) triazaphosphole with the two triazaphospholes bridging two magnesium centers *via* a carbon atom and the neighboring nitrogen atom (Figure 11, **11C**). The germanium(II) cyaphido complex, Ge(DippNacNac)(C≡P), yields the corresponding germanium(II) triazaphosphole complexes (Figure 11, **11D**) upon $^t$Bu-azide addition, thereby demonstrating that metal substitution at both the azide and phosphaalkene moiety is possible (see also: Scheme 7).[82] These experimental observations demonstrate that the P≡C triple bond of the cyaphide anion reacts in a similar manner as other phosphaalkynes in cyclisation reactions, a conclusion that was also confirmed computationally.[79]

The limiting factor of these [2+3] cycloaddition reactions is the availability of kinetically stable phosphaalkynes. Consequently, phosphaalkynes (R–C≡P) with R = Me, $^t$Bu, Mes*, TMS have been predominantly employed for the synthesis of triazaphospholes. One potential solution to this issue is the *in situ* preparation of the short-lived phosphaalkynes (R–C≡P, R = H, Me, Et, $^i$Pr, sBu) as described by CUMMINS and coworkers. The group demonstrated that H–C≡P is released (*T* = 80 °C in THF) from the corresponding precursor and reacts directly with tris(dimethylamino)sulfoniumazide (TASN₃) to

form the corresponding [TAS]$^+$ stabilized 1,2,3,4-phosphatriazolate anion ([HCPN$_3$]$^-$) anion (Scheme 8, **8a**).[84]
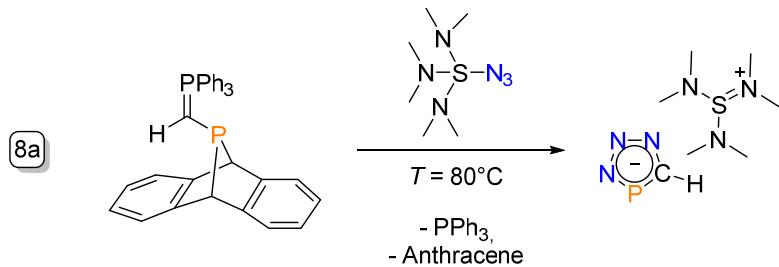


*Scheme 8: Synthesis of a 1,2,3,4-phosphatriazolate anion from a dibenzo-7-phosphanorbornadiene.*

Another approach is to start from phosphaalkenes. One of the very first triazaphospholes was synthesized by CARRIÉ and coworkers in 1984 *via* a 1,3-dipolar cycloaddition reaction from a chlorophosphaalkene (TMS$_2$C=P–Cl) with various organic azides (Scheme 9, **9a**). The primary formed cyclization adduct, dihydro-1,2,3,4 triazaphosphole, was found to aromatize spontaneously even at low temperatures under α-elimination of TMS-Cl resulting in the formation of the corresponding triazaphosphole.[13] Four years later MÄRKL and coworkers showed that 5-phenyl substituted triazaphospholes could be synthesized in the same way.[85] Similarly, SCHMIDPETER and coworkers employed the cationic 2-triphenylphosphonium-1-chlorophosphaalkene as a precursor for an otherwise inaccessible cationic phosphaalkyne. After the addition of an organic azide, the phaalkene afforded access to an unusual cationic 5-phosphonium-triazaphosphole salts *via* α-elimination of TMS–Cl. (Scheme 9, **9b**).[86]
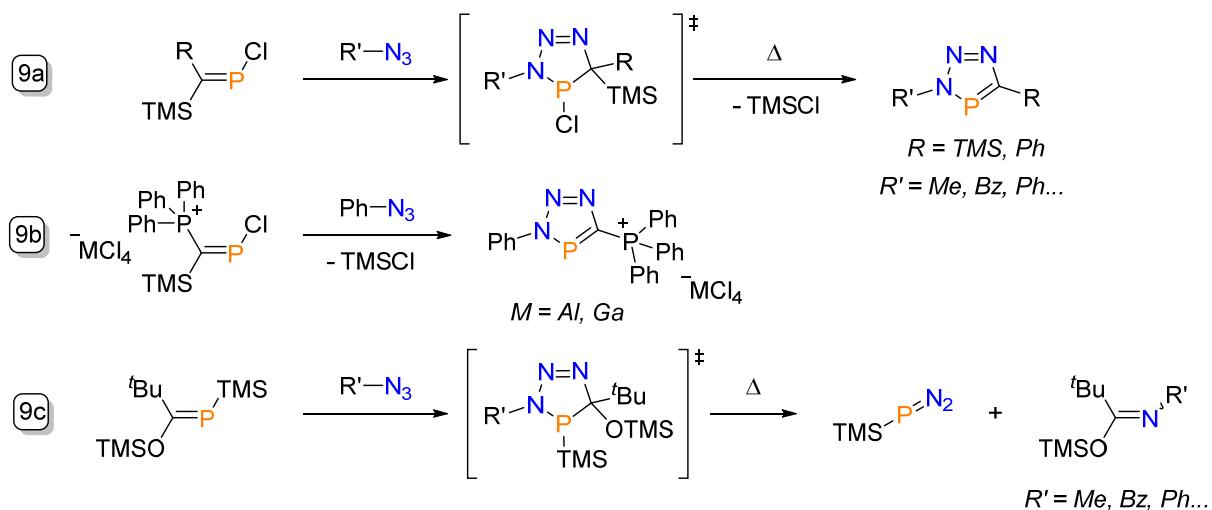


*Scheme 9: Triazaphosphole formation from phosphaalkenes.*

However, MÄRKL and coworkers found that even though phosphaalkynes could be synthesized by elimination of both trimethylsilylchloride and hexamethyldisilane, the reaction of an organic azide with (trimethylsilyl)(trimethylsilyloxy)phosphaalkyne did not lead to the formation of the desired

triazaphosphole under hexamethyldisilane elimination, but instead gave an intermediate with reversed regioselectivity, leading to a [3+2] cycloreversion and fragmentation (Scheme 9, **9c**).[85]

MÜLLER and FROST have recently shown that the triazaphosphole formation is also possible directly from the corresponding dihalophosphanes (R–CH$_2$–PCl$_2$). Under the influence of a base (most promisingly DABCO), a reactive species is generated *in situ* which undergoes a cycloaddition reaction with organic azides to give the corresponding triazaphosphole (Scheme 10, **10a**). This method eliminates the need for synthesis and isolation of a phosphaalkyne. It is of particular interest for the synthesis of triazaarsoles, as the number of synthetically accessible and kinetically stabilized arsaalkyne is very limited. [69]
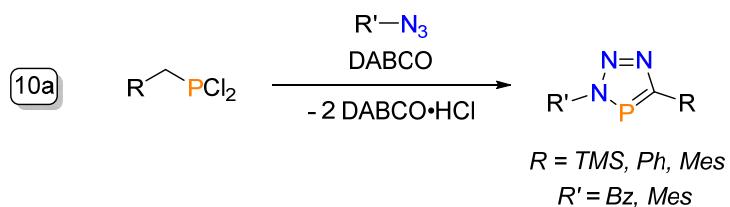


*Scheme 10: Triazaphosphole formation from the corresponding dihalophosphanes.*

MÜLLER and FROST were able to show that the synthesis of a 5-TMS-substituted triazaphosphole from the corresponding dihalophosphane precursor (TMS–CH$_2$–PCl$_2$) with DBU as a base produces not only the TMS-substituted triazaphosphole but also the protonated triazaphosphole (Scheme 11, **11a**). Addition of DBU to the TMS-substituted triazaphosphole however did not yield the corresponding protonated product, it is assumed that H–C≡P is released during the reaction is in fact responsible for the formation of the protonated triazaphosphole. Examples of DBU nucleophilically attacking α-chlorophosphanes to form ammonium-substituted phosphane salts are known in the literature.[87] The stabilization of the strong donor DBU could lead to the elimination of TMS–Cl and in continuation to the release of H–C≡P.[69]
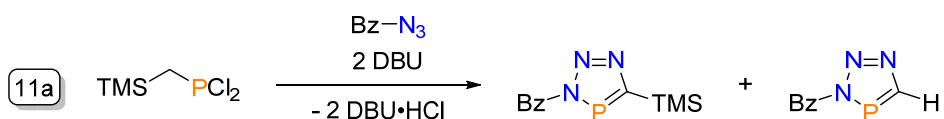


*Scheme 11: Synthesis of a 5-TMS-substituted triazaphosphole with DBU and protonated side product.*

As expected, the aromatically stabilized triazaphospholes are more stable than phosphaalkynes. Most of these thermally quite robust heterocycles can be handled in air for a short time.[80] Going as far as the ferrocene (Figure 5, **5D**) and polymer-based systems (Scheme 7, **7a**) being permanently stable in air,[62] while rotaxanes (Figure 11, **11E**) are even stable in air and moisture and can be purified by column chromatography without using Schlenk technique.[83]

### 1.3.3    Reactivity of 1,2,3,4-Triazaphospholes

Even though first synthesized in 1984, the reactivity of 1,2,3,4-triazaphosphole derivatives has only been explored to a very limited extent. Part of the motivation for this work was to gain a deeper understanding of the reactivity and coordination chemistry of these interesting compounds.

First observed by REGITZ and coworkers in 1984 and subsequently studied in greater depth by the same research group in 1987, it was demonstrated that in triazaphospholes, substituted in the 3-position with a proton (H) or a TMS group, these groups undergo a [1,5]-shift to the neighboring N(2) atom. This leads to the corresponding 2-H or 2-TMS triazaphospholes (Scheme 12, **12a-b**). The hydrolysis of the resulting 2-TMS triazaphosphole was performed by stirring a diethyl ether solution of the triazaphosphole with silica gel. (Scheme 12, **12b**).[12][88] REGITZ and coworkers showed that phenyl-substituted triazaphospholes undergo nitrogen cleavage during a flash vacuum pyrolysis at high temperatures ($T$ = 540 °C) yielding two isomeric 1,2- and 1,3-benzo-azaphospholes in a ratio of 4:1 (1,2 : 1,3)(Scheme 12, **12c**). However, high temperatures are needed as the same group also reported no reaction up until $T$ = 400 °C.[88]
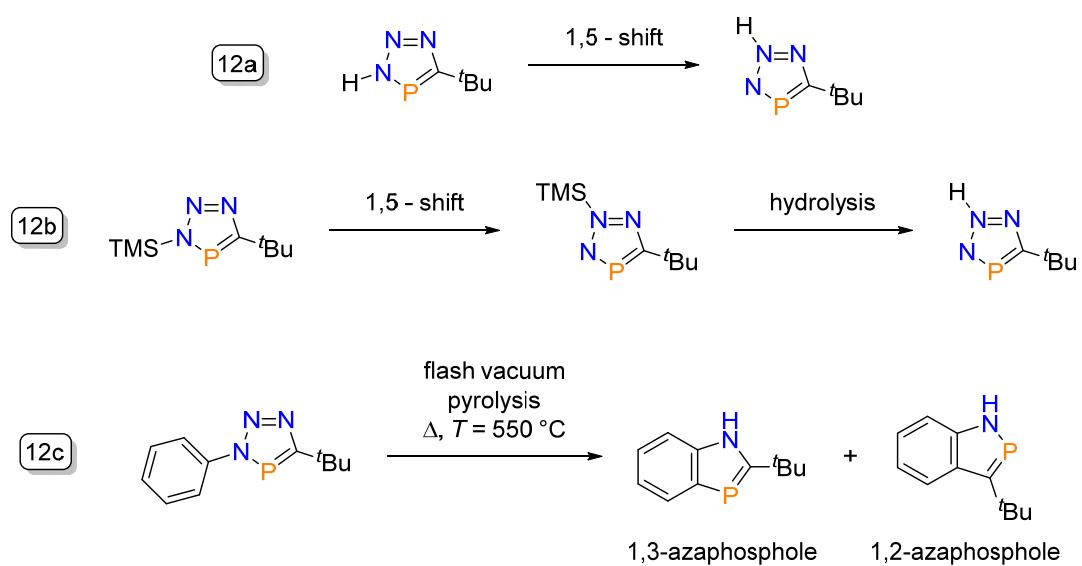


*Scheme 12: [1,5]-shift of the proton (H) yielding the corresponding 2-H triazaphosphole (**12a**), hydrolysis of the 2-TMS triazaphosphole (**12b**) and vacuum pyrolysis of a phenyl-substituted triazaphosphole (**12c**).[88]*

It took more than 20 years for the next study on the reactivity of triazaphospholes to be published. In 2000, KERTH and coworkers reported on the addition of an α-diazo-β-diketone to a triazaphosphole yielding the corresponding 1,3-diaza-2,4-diphosphetidine (Scheme 13, **13a**) under mild conditions ($T$ = r.t, $t$ =3d). This unexpected reactivity can be explained by the formation of a bicyclic intermediate in the dipolar 1,3-cycloaddition and a subsequent cleavage of $N_2$, resulting in a 4-imino-1,2,4($\lambda^5$)-diazaphosphole (Scheme 13, **13a,** intermediate). In a final step two 4-imino-1,2,4($\lambda^5$)-diazaphospholes dimerize to the corresponding 1,3-diaza-2,4-diphosphetidines.[89]
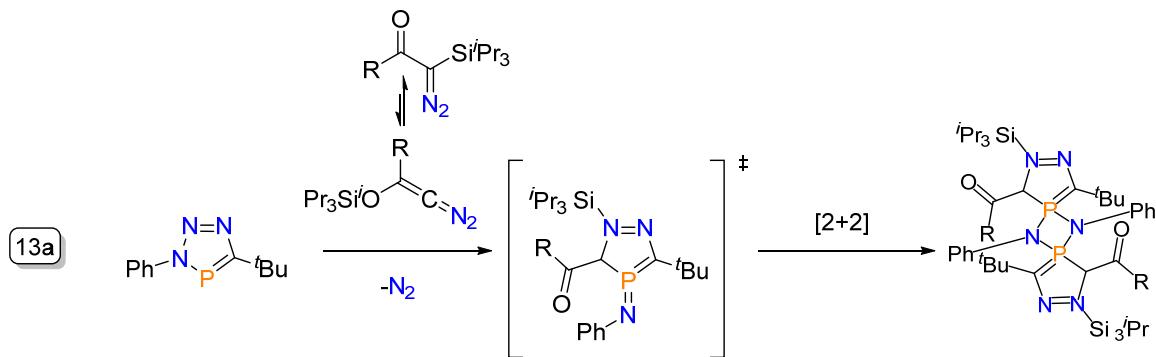
*Scheme 13: Dipolar 1,3-cycloadditio of an α-diazo-β-diketone (1,3-dipolemand a triazaphosphole (dipolarophile) giving a 1,3-diaza-2,4-diphosphetidines after dimerization.*

Recently a study GOICOECHEA and coworkers investigated the reactivity of metal triazaphosphole complexes. Starting from a dimeric magnesium(II) triazaphosphole (chapter 1.3.2, Figure 11, **11C**), cleavage of the polar M–C bond with an excess (4.0 eq) of pyridinium chloride yielded a protonated $^{t}$Bu-triazaphosphole (Scheme 14, **14a**). Another example of follow up chemistry of metal complexes is a halogenation of gold(I)-triazaphospholes (monomeric structure of Figure 11, **11B**) with iodine ($I_2$), resulting in a iodo-triazaphosphole, which is the first example of a halogenated triazaphosphole (Scheme 14, **14b**).[82]
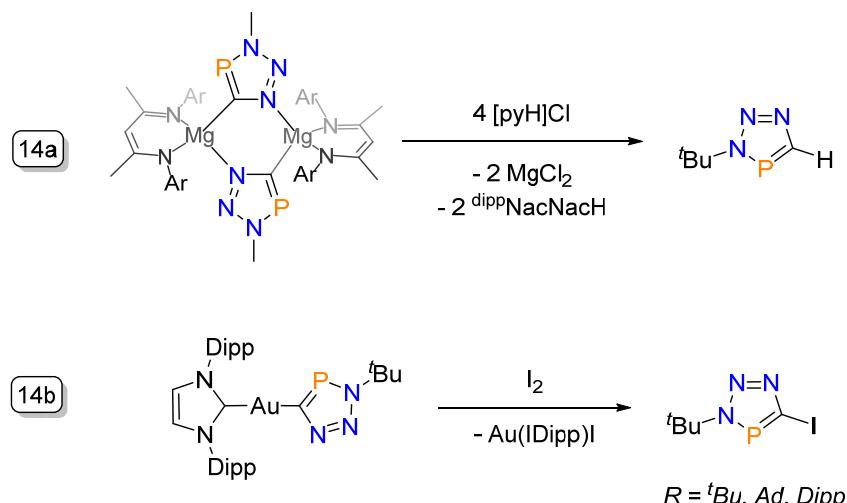


*Scheme 14: Synthesis of protonated-triazaphospholes (**14a**) and iodo-triazaphospholes (**14b**).*[82]

## 1.3.4　Coordination Chemistry of 1,2,3,4-Triazaphospholes
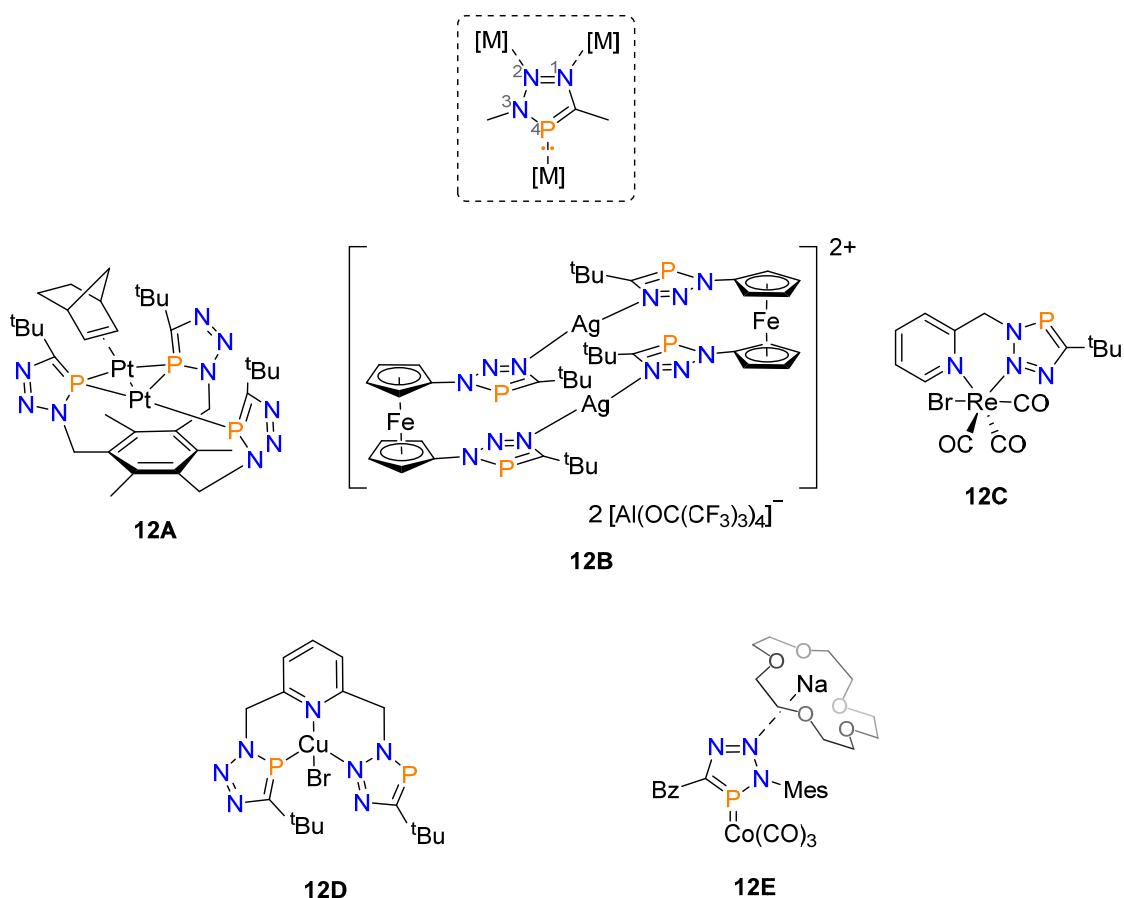


*Figure 12: Coordination chemistry of neutral 1,2,3,4-triazaphospholes.*

The examination of the frontier orbitals of triazaphospholes (Chapter 1.3.1, Figure 6) shows that triazaphospholes are ambidentate ligands. This means that they are able to coordinate to a metal centre *via* the low-coordinated phosphorus atom as well as *via* the nitrogen atoms N(1) and N(2)[80] The frontier orbitals also indicate that the low-coordinated phosphorus atom is a relatively weaker $\sigma$-donor and stronger $\pi$-acceptor This is also observed for other low-coordinated phosphorus compounds, such as phosphinines (Chapter 1.1, Figure1).[68][90] The lone pair at the nitrogen atom N(3) is integrated into the aromatic $\pi$-system and is therefore not available for coordination.[80] The first coordination compound containing a triazaphosphole ligand was synthesized 30 years after the first isolation of a triazaphosphole. In 2010 JONES and coworkers observed coordination of a tripodal triazaphosphole ligand (Chapter 1.3.1, Figure 5, **5E**) to an electron-rich Pt(0) center *via* the phosphorus atom (Figure 12, **12A**).[63] The addition of two equivalents of a [Pt(norbornene)₃] to the tripodal triazaphosphole resulted in the formation of an unusual bimetallic species, wherein one platinum center (Pt(1)) was coordinated by the three phosphorus centers of the ligand, while the other (Pt(2)) was coordinated by two bridging phosphorus atoms ($\mu_2$-P). The two $\mu_2$-P atoms have a distorted tetrahedral geometry, as opposed to the trigonal planar geometry of the $\eta^1$-phosphorus atom.[63] The

same group also reported on a dimeric cationic silver(I) complex three years later, which was obtained by addition of an equimolar amount of silver(I)polyfluoroalkoxyaluminates ([Au(Al(OC(CF$_3$)$_3$)$_4$)]) to a bis(triazaphosphole)ferrocene (Figure 5, **5D**). The silver(I) center coordinates, not to the phosphorus atom, but to the most electron rich nitrogen center of the heterocycle, the N(1) atom[91][60][92] (Figure 12, **12B**).[62] Coordination to the less electron rich N(2) atom is also possible and can be enforced by the chelating effect as shown by MÜLLER and coworkers in 2014. Functionalization at the 3-position of a triazaphosphole with a 2-pyridylmethyl-group opens up the possibility of accessing potential chelating ligands.[93] Equimolar addition of [Re(CO)$_5$Br] to the triazaphosphole yielded an octahedral [Re(CO)$_3$Br]-complex with the triazaphosphole acting as a chelating ligand coordinating to the rhenium(I) center *via* the N(2)-atom of the triazaphosphole moiety and the pyridine nitrogen donor (Figure 12, **12C**).[93] Furthermore, MÜLLER and PAPKE demonstrated that using a diazide, a di-triazaphosphole could be formed, which can act as a pincer ligand in the coordination to a copper(I) center. Interestingly, one triazaphosphole moiety exhibits a coordination mode similar to the one observed in the previously mentioned [Re(CO)$_3$Br]-complex,[93] whereas the second triazaphosphole moiety coordinates to the copper(I) center *via* the phosphorus atom (Figure 12, **12D**).[94] It is noteworthy that all examples previously mentioned are of the triazaphospholes acting as chelating ligands, with no documented example of a monodentate triazaphosphole ligand. Recently, MÜLLER and FROST investigated the reactivity of triazaphospholes towards metal precursors with a negatively charged central atom.[69] Equimolar addition of a triazaphosphole to sodium tetracarbonylcobaltate(−I) (Na[Co(CO)$_4$]) in toluene/DME yielded the first example of an anionic triazaphosphole complex. The negatively charged cobalt(−I) atom coordinates *via* the phosphorus atom to the triazaphosphole and, interestingly, the sodium atom is also coordinated to the heterocycle *via* the N(1) (Figure 12, **12E**). The P–Co bond distance is rather short, which indicates a considerable double bond character, derived from a superposition of the P → Co donation (σ-bond) and the Co → P back-donation (π-bond). A similar situation can be observed in the literature-known N-heterocyclic phosphenium cobaltate complexes making this a good example of the π-acceptor properties of triazaphospholes.[95]

### 1.4      1,2,3,4-Triazaphospholenium Salts

About 20 years before the synthesis of the first stable N-heterocyclic carbene (NHC, Figure 13, **13A**, R = R' = Adamantyl) by ARDUENGO III and coworkers in 1991,[96] FLEMING and coworkers synthesized the phosphorus analogues of these compounds, the 1,3,2-diazaphospholenium cations (Figure 13, **13B**, R=R'=Me).[97][98] These N-heterocyclic phosphenium (NHP) cations are valence isoelectronic to NHCs replacing the 'R–C–R' fragment with the valence isoelectronic 'R–P$^+$–R' fragment. NHCs are considered strong σ-donors leading to a wide range of applications as ligands in catalytic reactions.[99][100][101][102][103] A well-known example being the ruthenium-catalyzed olefin metathesis and the palladium-catalyzed

cross-coupling reactions.[104][105][106] In contrast, NHPs have a considerable $\pi$-acceptor capacity and a limited $\sigma$-donor capacity due to the formal positive charge at the phosphorus atom.[107][108]

Two coordination modes are observed primarily for the NHPs (Figure 13, Type 1 and Type 2). A planar P-coordination sphere and a relatively short P–M distance with a distinct double bond character. This double bond character is caused by the formation of an M → L $\pi$-bond from a filled metal d orbital to the empty p orbital of the phosphorus atom and a weaker dative L → M $\sigma$-bond from the lone pair of the phosphenium ligands to the metal center (Figure 13, **I**). [107][109][110][111][95] An analogy to a Fisher carbene can be drawn.[112][113][114] The second mode is reflected in a pyramidal geometry around the phosphorus atom upon metal coordination and elongated P–M bond distance. The pyramidal geometry is caused by the phosphorus lone pair remaining nonbonding. The NHP can be described as a cationic z-type[115] ligand, interacting with the metallocentre only through a dative M → P $\sigma$-bond (Figure 13, **II**).[112] Or it may be portrayed as a formally two-electron reduced phosphorus cation acting as an anionic x-type[115] phosphido ligand, coordinating to a formally two-electron oxidized metal center (Figure 13, **II**).[116][117][118]
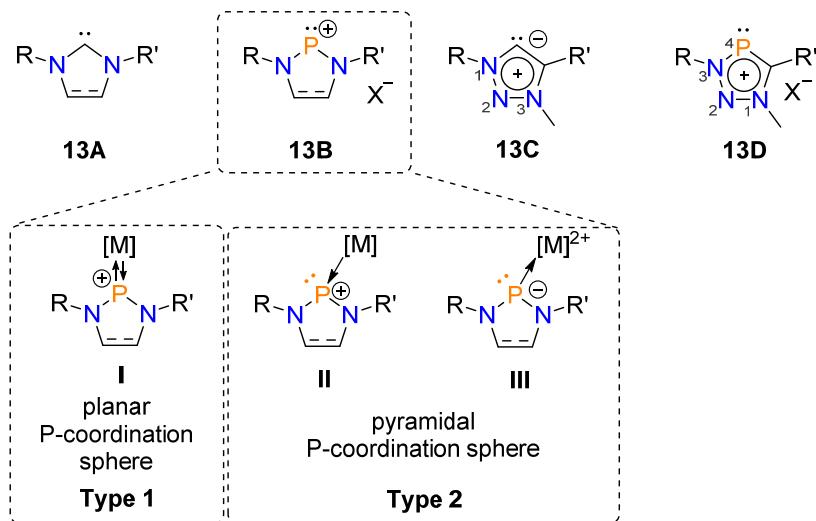


*Figure 13: The N-heterocyclic carbenes and their valence isoelectronic phosphorus analogues and different coordination modes of NHP (I and II).*

Since the synthesis of the first NHC 30 years ago, the NHC based ligand family has grown steadily. As mentioned, the Cu(I) catalyzed [3+2] cycloaddition of alkynes and organo-azides leads to the formation of 1,4-substituted 1,2,3-triazoles (see chapter 1.3.2).[72][119] The alkylation of the N(3) atom of these triazoles, for example with methyl iodine (MeI) results in the corresponding triazolium salts. [120][121][122] Direct metalation leads to the formation of the corresponding abnormal NHCs (aNHCs) or mesoionic carbene (MICs) complexes as first shown in 2008 by ALBRECHT and coworkers.[123] In 2010 BERTRAND and coworkers succeeded in synthesizing the free 1,2,3-triazol-5-ylide (Figure 13, **13C**).[124] The MICs show stronger $\sigma$-donor properties than the NHCs, which can be exploited in catalytic reactions and even lead to the MIC outperforming the classic NHC under certain conditions.[125] Considering the valence

isoelectronic relationship between the 'R–C–R' fragment and the 'R–P⁺–R' fragment, the 1,2,3,4-triazaspholenium salts (Figure 13, **13D**) are the phosphorus analogs of the 1,2,3-triazolylidenes. In 2017, MÜLLER and coworkers were able to report in detail for the first time on the synthesis and properties of these 1,2,3,4-triazaspholenium salts.[60]

Density function calculations to analyze the bonding situation were carried out exemplary on the 3-benzyl-5-*tert*-butyl triazaphosphole. The nucleus independent chemical shift (NICS) value of −11.6 ppm indicates a considerable degree of aromaticity. The charge of the natural bonding orbital (NBO) of +0.89 *e* is comparable to other phosphenium cations.[126][127]

*Table 1: CHELPEG charges of triazaphosphole and the triazaspholenium salt.[69]*
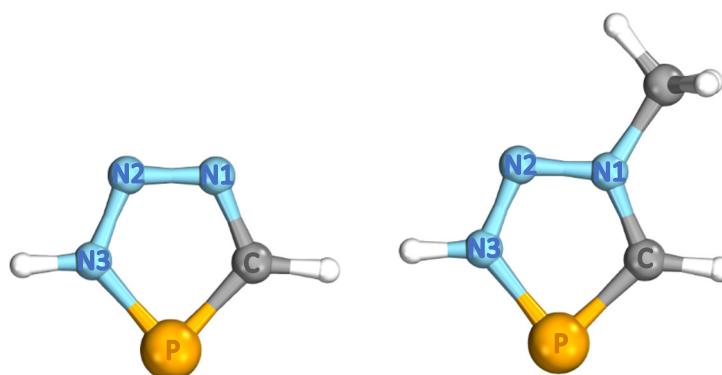


| ATOM | CHELPEG-Charges | |
|---|---|---|
| P | −0.10 | 0.24 |
| C | 0.26 | −0.15 |
| N(1) | −0.39 | 0.46 |
| N(2) | −0.29 | −0.32 |
| N(3) | 0.21 | 0.02 |
| TOTAL CHARGE | 0.00 | +1.00 |

FROST calculated the CHELPEG charges (Charges from Electrostatic Potentials using a grid-based method) comparing the triazaphosphole and the triazaspholenium salt, the largest charge change is observed at the N(1) atom, which is the most nucleophilic nitrogen atom in the triazaphosphole (−0.39 *e*) and the most positively charged after alkylation (+0.46 *e*). This strong charge change on the N1 atom also leads to a change in the charge distribution of the remaining ring atoms. After quaternization, the polarity of the P=C bond is reversed. In the triazaphosphole, the carbon atom is partially positively charged (0.26 *e*), while the phosphorus atom is weakly negatively charged (−0.10 *e*). In the 1,2,3,4-triazaspholenium cations, the phosphorus atom is positively charged (0.24 *e*), while the neighboring carbon atom is negatively charged (−0.15 *e*).[69] Comparison of the frontier orbitals of the triazaphosphole and the 1,2,3,4-triazaspholenium salts reveals the HOMO and

LUMO to be surprisingly similar in shape with both being delocalized across the five-membered ring, with large contributions from the bonding $\pi$ and antibonding $\pi^*$ orbitals of the P=C double bond .[60][69]

### 1.4.1 Synthesis of 1,2,3,4-Triazaphospholenium Salts

The first functionalization of a triazaphosphole at the N(1) nitrogen atom was published by JONES and coworkers in 2013.[1] The group initially intended to synthesize a silver coordination compound (see chapter 1.3.4 Figure 12, **12B**) with silver triflate (AgOTf). However, the protonation of a ferrocene-substituted triazaphosphole (see Chapter 1.3.1 Figure 5, **5D**) was observed instead (Scheme 15, **15a**). Subsequent investigations of the quaternization were conducted, but the attempt to selectively protonate the ferrocene-substituted triazaphosphole by adding triflic acid (HOTf) resulted in the formation of decomposition products.[62]
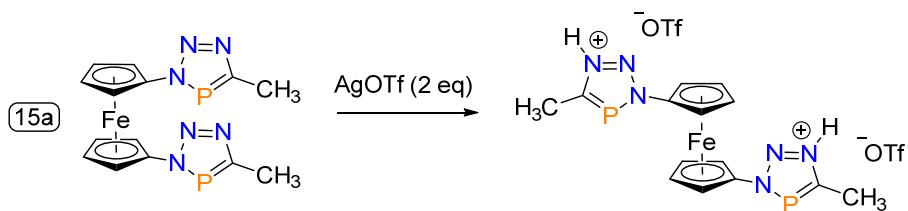


*Scheme 15: protonated ferrocene-substituted triazaphosphole.*

In 2017 MÜLLER and coworkers succeeded in the targeted synthesis of alkylated triazaphospholes.[60] Alkylation of the 3-benzyl-5-*tert*-butyl-1,2,3,4-triazaphosphole with an equimolar amount of trimethyloxonium tetrafluoroborate ([Me$_3$O][BF$_4$]) led to the formation of the desired 1,2,3,4-triazaphospholenium salt (Scheme 16, **16a**). Quaternization is possible with different Meerwein's salts (triethyloxonium tetrafluoroborate, triethyloxonium hexafluorophosphate), in contrast methyl iodide (MeI) shows no reactivity towards triazaphospholes.[60] This is surprising, since MeI is commonly used to form triazolium salts,[120][121][122] but can be explained by the fact that MeI is a much weaker methylation reagent compared to trimethyloxonium tetrafluoroborate.[128][129][130] In principle the methylation at the N(2) atom or the phosphorus atom is possible, but the N(1) nitrogen atom is expected to exhibit the highest electron density in accordance with theoretical calculations (chapter 1.4, table 1).[60][69] The quaternization of the N(1) nitrogen is also observed for the analogous triazoles.[91][92] Calculations furthermore revealed that the N(1)-alkylated product is the thermodynamicly favored product compared to the one where the N(2) atom (+5.6 kcal/mol) or the phosphorus atom (+26.3 kcal/mol) is alkylated.[60]
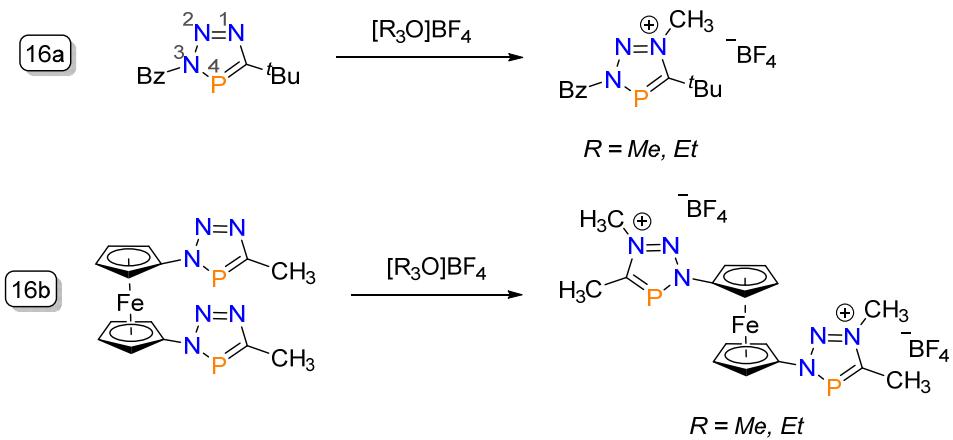
*Scheme 16: Synthesis of 1,2,3,4-triazaphospholenium salts by quarternisation of triazaphospholes with Meerwein's salts.[60][94]*

MÜLLER, PAPKE and FROST were able to show that the quaternization reaction works well regardless of the substitution pattern of the triazaphospholes. They synthesized a variety of novel triazaphospholenium salts, [69][94] including the alkylated ferrocene-substituted di-triazaphosphole (Scheme 16, **16b**), which was first protonated by Jones. Singel crystal X-ray diffraction studies of the compound shows that the two triazaphospholenium units are in *trans* orientation to each other, as previously observed for the product by JONES.[62][94]

Recently, the group of GOICOECHEA published a novel route towards trisubstituted triazaphospholes that can also be considered as the coordination compounds of triazaphospholenium salts.[82] They showed that the addition of the Lewis acidic $B(C_6F_5)_3$ to the N(1) atom of gold(I)-triazaphosphole (see chapter 1.3.2, Figure 11, **11B**), results in the formation of a Lewis Pair (scheme 17, **17a**).[82]
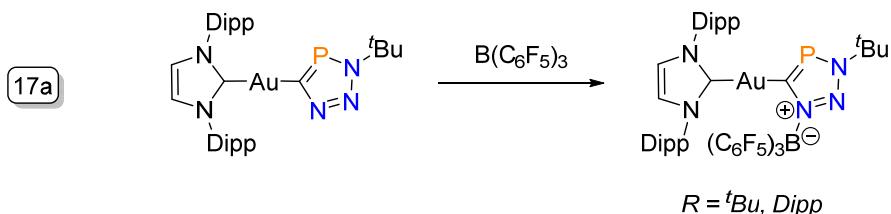


*Scheme 17: Coordination of a $B(C_6F_5)_3$ to a gold(I)1,3-bis(triazaphosphole) complex affording the corresponding Lewis adduct [82]*

## 1.4.2    Coordination Chemistry of 1,2,3,4-Triazaphospholenium Salts

The first coordination compound of triazaphospholenium salts was synthesized in 2017 by MÜLLER and coworkers. The addition of two equivalents of copper(I) bromide dimethyl sulfide (Cu(I)Br·SMe$_2$) yielded the corresponding dimeric neutral coordination compound (Scheme 18, **18a**). Two triazaphospholenium cations are bridged by a dianionic $[Cu_2Br_4]^{2-}$ unit. The copper-phosphorus bond is shorter than the sum of the van der Waals radii of both atoms,[131] but longer than an average dative

P(III) → Cu(I) bond[132][133][134][135] and the phosphorus atom adopts a pyramidal geometry with the [CuBr$_2$]$^-$ fragment pointing above the plane created by the heterocycle (Figure 14).[60]
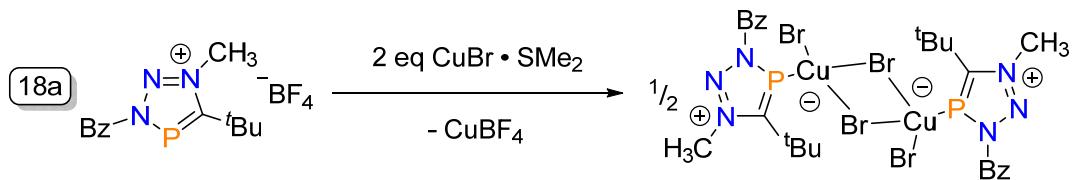


Scheme 18: Synthesis of dimeric neutral copper(I) coordination compound.
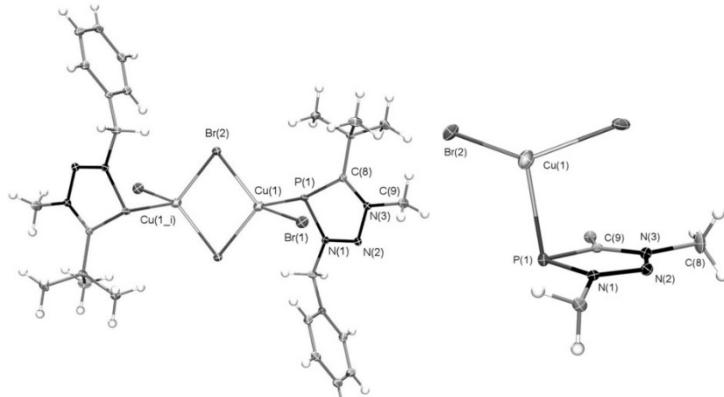


Figure 14: Molecular structure of the copper(I) complex in the crystal.[60]

Computational investigations of the copper-phosphorus bond using the atom-in-molecule (AIM) theory revealed a bond critical point between the phosphorus atom and copper(I) center with only a very low electron density. This indicates a bond with significant ionic character. Additionally, NBO calculations indicate that both the lone pair of the phosphorus atom and the $\pi$ orbital of the P=C double bond donate electron density into the vacant copper based d orbitals, and a weak Cu → P back bonding into the LUMO of the phosphorus atom is also observed.[60] Looking at the bonding situation of the trazaphospholenium copper(I) complex, parallels can be drawn to the type 2 coordination mode of NHP (chapter 1.4, Figure 13, II), in which an out-of-plane arrangement of the metal can also be observed (Figure 15).[112]
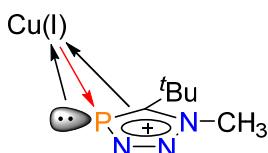


Figure 15: The metal -ligand interaction between a copper(I) center and the triazaphospholenium.[60][69]

MÜLLER and FROST lately also showed that the addition of a sodium tetracarbonylcobaltate(-I) (Na[Co(CO)$_4$]) leads to the unprecedented formation of coordination compound of a triazaphosphole ligating an [Co(CO)$_3$]$^-$ fragment trough the phosphorus atom (Scheme 19, **19a**).[69] The phosphorus coordination sphere is nearly planar, and the P–Co bond distance is surprisingly short with a bond length similar to the corresponding NHP complexes suggesting a double bond character (chapter 1.4,

Figure 13, I).[95] Both structural parameters and computational investigations of the orbital interactions indicate a coordination mode similar to type 1 of the NHP's. [69]
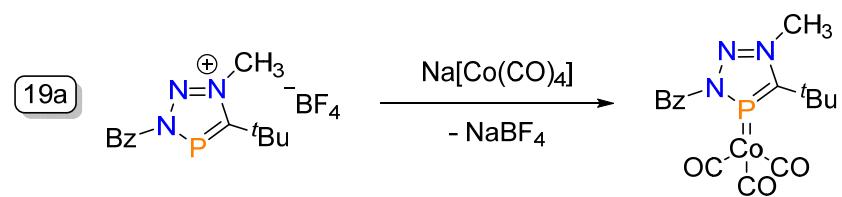


*Scheme 19: Synthesis of a neutral [Co(CO)₃]⁻ complex.*

## 2        Objective and Motivation

Low-coordinated phosphorus compounds are known to differ significantly from classical P(III) and P(V) compounds and can be more closely compared in their properties with unsaturated carbon compounds.[5] DFT studies indicate that the phosphorus atoms in these systems act as strong $\pi$-acceptor ligands and much weaker σ-donor ligands in the respective coordination compounds (see: chapter 1.3.1, Figure 6 (*frontier molecular orbitals*)). The reason is the relatively high s-character of the lone pair at the phosphorus atom (see: chapter 1.3.1, Figure 7 (*s- and p-character of lone pairs*)).[55][59] Following the isolobal concept, 1,2,3,4-triazaphospholes are considered the phosphorus analogues of the well known 1,2,3-triazoles. However, little has been published on these compounds and even less is known about their reactivity and coordination chemistry. When this work was started, there was only one crystallographically characterized example in the literature of a triazaphosphole coordinating to a metal center *via* the phosphorus atom.[63] The triazphospholenium salts were first introduced in 2017[60] by the group of Müller and are considered the phosphorus analogues of the again well known 1,2,3-triazolylidenes.[124] Computational analysis of the charge distribution on the ring atoms in the triazaphosphole and triazaphospholenium salts have shown clear differences between the two compound classes. Most prominently a reverse polarity along the P=C double bond, warranting a more intensive look into properties reactivity and coordination chemistry of the triazapholenium salts as well.

The first aim of this work was to broaden the triazaphosphole ligand library. Of special interest was the effect electron withdrawing substituents (arylsulfonyl group) would have on the reactivity of the heterocycle. Also, the behavior of triazaphospholes as dienes in [4+2] cycloaddition reactions was investigated, as it may provide access to new low-coordinated phosphorus-containing heterocycles.

The second aim was to further investigate triazphospholenium salts, as this compound class was only recently described. Little was known about their reactivity. At the beginning of this work only one example of a coordination compound with a cationic triazphospholenium ligand was documented. Of interest was the extent to which the replacement of the <sup>t</sup>Bu-group in the 5-position by a TMS-group influences the reactivity of the heterocycle. In addition, the degree to which the substitution in position 3 with a pyridine group has an influence on quaternisation reactions to form triazphospholenium salts was examined. In a second step, the coordination behavior of these newly synthesized charged triazaphospholes and the triazaphospholenium salts with copper(I) halides was investigated.

## 3     Au(I)-mediated N$_2$-elimination from triazaphospholes: a one-pot synthesis of novel N$_2$P$_2$-heterocycles

**Author contributions:**

The project concept originates from Julian A. W. Sklorz and Selina Kaiser and was continued by Erlin Yue. All synthesis procedures were reproduced by Lea Dettling, with some procedures significantly improved to address previously encountered synthesis and isolation issues. This was crucial for the successful publication of the project results. Additionally, Lea Dettling conducted experiments for mechanistic studies. Manuela Weber was responsible for the crystallographic characterization of several of the new compounds. Christian Müller supervised the project. Lea Dettling wrote the supporting information. The manuscript was written in collaboration with Erlin Yue, Lea Dettling and Christian Müller.

Check for updates

# Au(I)-mediated N$_2$-elimination from triazaphospholes: a one-pot synthesis of novel N$_2$P$_2$-heterocycles†

Erlin Yue, ‡$^{ab}$ Lea Dettling, ‡$^a$ Julian A. W. Sklorz,$^a$ Selina Kaiser,$^a$ Manuela Weber$^a$ and Christian Müller *$^a$

**Novel tosyl- and mesitylsulfonyl-substituted triazaphospholes were synthesized and structurally characterized. In an attempt to prepare the corresponding Au(I)-complexes with stoichiometric amounts of AuCl·S(CH$_3$)$_2$, cyclo-1,3-diphospha(III)-2,4-diazane-AuCl-complexes were obtained instead. Our here presented results offer a new strategy for preparing such coordination compounds selectively in a one-pot approach.**

According to the isolobal relationship between a trivalent P-atom and a C–H fragment, the 3,5-disubstituted 3H-1,2,3,4-triazaphosphole derivatives of type **B** are the phosphorus congeners of the well-studied 1,2,3-triazoles **A** (Chart 1).

These λ$^3$σ$^2$ phosphorus heterocycles can be prepared in a modular [3+2] cycloaddition reaction, starting from organic azides and phosphaalkynes, as first reported independently by Carrié and Regitz in 1984.[1] Generally, only one regioisomer is formed thermally and selectively, without the need of a copper-catalyst. 3H-1,2,3,4-triazaphosphole derivatives have a conjugated π-system with a high degree of aromaticity.[2] Typically, a whole variety of alkyl- and aryl-substituted as well as donor-functionalized azides (R-N$_3$) can be used for the preparation of triazaphospholes, but also TMS-N$_3$ or even H–N$_3$.[3] On the other hand, the substituent R' can only be varied to some extend due to the limited availability of the corresponding phosphaalkynes, although less sterically demanding phosphaalkynes can be generated *in situ* prior to the cycloaddition reaction.[4]

The first few reports on the coordination chemistry of triazaphospholes have only appeared in literature as recently as 2010.[5] As ambidentate ligands the coordination to a metal center can proceed either *via* the phosphorus atom or the nitrogen donors N(1) or N(2) (Chart 1, **C**).[6]

Despite the few reported examples on the coordination chemistry of 3H-1,2,3,4-triazaphosphole derivatives, very little is known about their reactivity.[7] N-Aryl/alkyl-substituted triazaphospholes are thermally robust and do not show any sign of reactivity upon irradiation with UV light (λ ≥ 280 nm).[7a] We therefore anticipated that the hitherto unknown introduction of an electron-withdrawing substituent at the N(3)-atom might change the coordination properties and reactivity of the corresponding heterocycle considerably. As a matter of fact, the phosphorus-lacking N-sulfonyl-1,2,3-triazoles show interesting chemical transformations in the presence of [Rh$_2$(OAc)$_4$].[8,9] Inspired by this fascinating reactivity, we started to transfer the chemistry of N-sulfonyl-1,2,3-triazoles to their phosphorus congeners and report here on our first results into this direction.

4-Methylbenzenesulfonylazide (**1a**) and mesitylsulfonylazide (**1b**) were prepared according to literature procedures.[10] As anticipated, the 1,3-dipolar cycloaddition reaction of **1a/b** with $^t$BuC≡P afforded the desired N-arylsulfonyl-substituted triazaphospholes **2a/b**, which were obtained as white solids in up to 85% yield after recrystallization from pentane (Scheme 1). Both compounds do not show any sign of decomposition when stored under inert conditions for several weeks.

$^a$ Freie Universität Berlin, Institute of Chemistry and Biochemistry, Fabeckstr. 34/36, Berlin 14195, Germany. E-mail: c.mueller@fu-berlin.de, yueerlin@yau.edu.cn

$^b$ Shaanxi Key Laboratory of Chemical Reaction Engineering, Key Laboratory of New Energy & New Functional Materials, College of Chemistry and Chemical Engineering, Yan'an University, Yan'an, Shaanxi 716000, People's Republic of China

† Electronic supplementary information (ESI) available. CCDC 1983603, 1983601 and 1983602. For ESI and crystallographic data in CIF or other electronic format see DOI: 10.1039/d1cc06205k

‡ These authors have contributed equally.
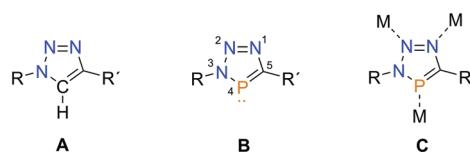


Chart 1 Triazaphosphole **A**, triazole **B** and possible coordination modes **C**.

**Scheme 1** Synthesis of triazaphospholes **2a/b**.

**Fig. 2** Resonance structures of **2b** and comparison of **2b** with **2c**.
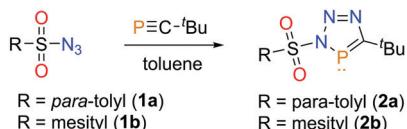
The hitherto unknown *N*-arylsulfonyl-triazaphospholes show single resonances in the $^{31}P\{^1H\}$ NMR at $\delta$(ppm) = 177.2 (**2a**) and $\delta$(ppm) = 175.2 (**2b**) in DCM-d$_2$. Although the *N*-arylsulfonyl group is supposed to be an electron withdrawing substituent, the resonances of **2a/b** in the $^{31}P\{^1H\}$ spectra are only slightly shifted more downfield compared to the literature known benzyl-substituted triazaphosphole **2c** ($\delta$(ppm) = 171.4, DCM-d$_2$, see Fig. 2).[1b,6b]

Single crystals of **2b** suitable for X-ray diffraction were obtained by slow diffusion of diethyl ether into a dichloromethane solution of the compound at low temperature. The molecular structure is shown in Fig. 1 along with selected bond lengths and angles. Compound **2b** crystallizes in the monoclinic space group $P2_1/c$. While the NMR spectroscopic data of **2a/b** are very similar to triazaphosphole **2c**, the crystallographic characterization of **2b** reveals a clear influence of the *N*-arylsulfonyl group on the bond distances within the P-heterocycle (Fig. 2 and Table 1). As a matter of fact, the N(1)–N(2) distance in **2b** is longer than in the known compound **2c**, while the N(2)–N(3) distance is shorter. Moreover, both the C(1)–N(3) and P(1)–N(1) bond lengths in **2b** are longer, while the C(1)–P(1) bond lengths is shorter compared to the situation in **2c**.[6b]

As also observed for *N*-sulfonamides, the N(1)–S(1) bond is with 1.7108(16) significantly shorter than the predicted value for pure S–N-single bonds, indicating the presence of a resonance structure with a partial S=N double bond (Fig. 2).[11]

Accordingly, the structural parameters are in line with a significant disruption of the aromaticity in **2b** along with more localized bonds (Fig. 2).

Apparently, the electronic structures of the hitherto unknown *N*-sulfonyl-substituted phosphorus heterocycles **2a/b** differ considerably from classical aryl- and alkyl-functionalized triazaphospholes. This should consequently also lead to a pronounced different chemical reactivity of **2a/b** in comparison
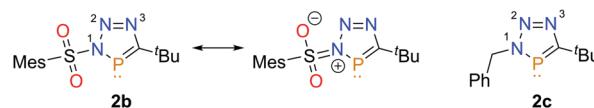
to **2c**. As we were primarily interested in the coordination chemistry of aromatic $\lambda^3\sigma^2$-phosphorus compounds, also with respect to applications, we first considered the reaction of **2a/b** with AuCl·S(CH$_3$)$_2$. It is well documented that phosphorus in low-coordination readily forms complexes with Au(I).[12]

Interestingly, a spontaneous and vigorous gas-evolution is observed when dichloromethane is added to a 1:1 mixture of either **2a** or **2b** and AuCl·S(CH$_3$)$_2$ at room temperature. The gas was identified as dinitrogen by means of GC-TCD. For triazaphosphole **2b** (R = mesityl), the $^{31}P\{^1H\}$ NMR spectrum of the slightly yellow reaction mixture shows only two resonances at $\delta$(ppm) = 133.9 and $\delta$(ppm) = 11.6 in a ratio of approximately 4:1. Stirring the reaction solution for 2 h at $T = 60\ ^\circ$C immediately after addition of the solvent leads, however, to a ratio of 20:1 (Fig. 3b). The isolation of the pure, air and moisture sensitive product **3b** in 36% yield was achieved by washing the reaction mixture with toluene. For **2a** (R = *p*-tolyl) the reaction seems to be less selective (see Fig. S10, ESI†).

Crystals of **3a** and **3b**, suitable for X-ray diffraction, could be obtained from both reaction mixtures. Dissolving the crystalline material of **3b** in dichloromethane gave indeed the identical resonance of the major product observed in the $^{31}P\{^1H\}$ NMR spectrum of the reaction mixture (Fig. 3c). Much to our surprise, the crystallographic characterization of **3a** and **3b** reveals the formation of a *cyclo*-1,3-diphospha(III)-2,4-diazane, rather than the presence of a simple triazaphosphole-Au(I) complex. Moreover, the *cyclo*-diphosphadiazane serves as a ligand, which binds to a total of two Au(I)Cl fragments *via* both phosphorus donors. The molecular structure of **3b** is depicted in Fig. 4, along with selected bond lengths and angles (for the
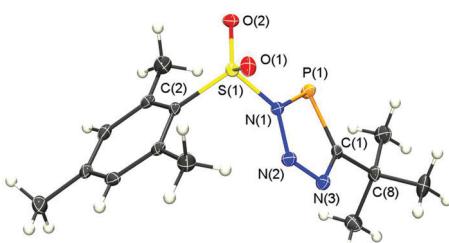
**Table 1** Comparison of selected bond lengths in **2b** and **2c**[6b]

|  | P(1)–C(1) | P(1)–N(1) | N(1)–N(2) | N(2)–N(3) | N(3)–C(1) |
|---|---|---|---|---|---|
| **2b** | 1.7047(16) | 1.7047(16) | 1.364(2) | 1.298(2) | 1.369(2) |
| **2c** | 1.7128(17) | 1.6834(19) | 1.340(2) | 1.314(2) | 1.351(3) |

**Fig. 1** Molecular structure of **2b** in the crystal. Displacement ellipsoids are shown at the 50% probability level. Selected bond lengths (Å) and angles (°): P(1)–N(1): 1.7047(16), N(1)–N(2): 1.364(2), N(2)–N(3): 1.298(2), N(3)–C(1): 1.369(2), C(1)–P(1): 1.715(2), N(1)–S(1): 1.7108(16), S(1)–O(1): 1.4232(14), S(1)–O(2): 1.4280(14). N(1)–P(1)–C(1): 85.35(9).
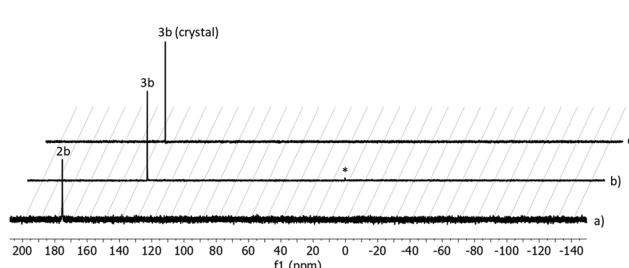
**Fig. 3** $^{31}P\{^1H\}$ NMR spectra of **2b** (a), the reaction mixture (b) and of the obtained crystals (c). (*): unidentified species.
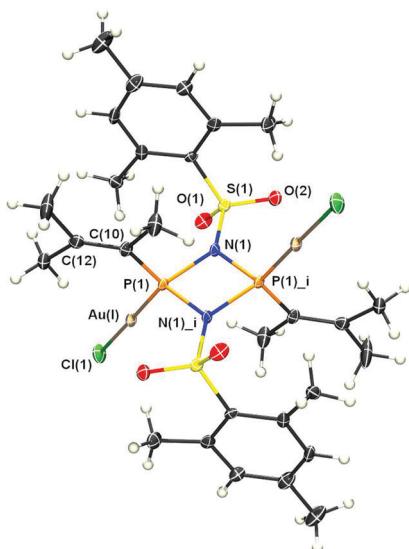
**Fig. 4** Molecular structure of **3b** in the crystal. Displacement ellipsoids are shown at the 50% probability level. Selected bond lengths (Å) and angels (°): P(1)–N(1): 1.730(3), N(1)–P(1)_i: 1.727(3), N(1)–S(1): 1.675(3), P(1)–Au(1): 2.2087(11), P(1)–C(10): 1.778(4), C(10)–C(12): 1.352(6). N(1)–P(1)–N(1)_i: 79.87(18), P(1)–N(1)–P(1)_i: 100.13(18).

single crystal X-ray structure of **3a** see Fig. S2, ESI†). Based on the structural characterization of **3a/b**, the novel and, in the case of **2b**, highly selective "one-pot" reaction with stoichiometric amounts of AuCl·S(CH₃)₂ under formation of a dinuclear *cyclo*-diphosphadiazane–Au(ɪ) complex is summarized in Scheme 2.

As a matter of fact, such N₂P₂ heterocylces are most commonly obtained as 1,3-dichloro-*cyclo*-1,3-diphospha(ɪɪɪ)-2,4-diazanes of the type [ClP(μ-NR)₂PCl] by reacting primary amines with PCl₃.[13] Subsequent reaction with appropriate nucleophiles leads to *cyclo*-diphosphadiazanes of the type [R′P(μ-NR)₂PR′] (R′ = alkyl, aryl; OR, NR″₂, NHR″), which can then be converted to the corresponding coordination compounds by reaction with an appropriate metal precursor.[14] Importantly, there are no reports on cyclodiphospha(ɪɪɪ)zanes featuring the exact susbstitution pattern of **3a/b**, potentially due to synthetic difficulties.[15] Therefore, our here described approach offers access to novel P₂N₂ heterocycles, which were so far not accessible.

**3b** crystallizes in the space group $P2_1/c$. In **3b** (as well as in **3a**, Fig. S2, ESI†) a perfectly planar P₂N₂-ring with both the R-groups and the Au(ɪ)Cl-fragments at the phosphorus atoms pointing in opposite directions (*trans* isomer) is present.
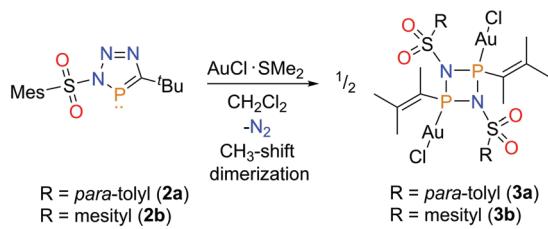
As observed for other *cyclo*-1,3-diphosphadiazanes, the nitrogen atoms are almost planar (sum of bond angles 359.3°), while the $\lambda^3,\sigma^3$-phosphorus atoms are pyramidally coordinated and bind each *via* the lone pair to the Au(ɪ) center.[14a] The P–N bond lengths of 1.730(3) Å and 1.727(3) Å are slightly shorter than observed in other *cyclo*-diphosphadizanes, which might be due to a reduced electrostatic repulsion between the P- and N-lone pairs, which are involved in an interaction with the metal center and the –SO₂R substituent, respectively.

The most striking feature of **3b** (and **3a**, Fig. S2, ESI†) is, however, that the ᵗBu-group of the original triazaphosphole was converted into an iso-pentenyl substituent. Obviously, a CH₃-shift took place during the conversion **2a/b → 3a/b**, which implies the formation of a carbene intermediate. This has also been observed by Fokin and co-worker during the Rh-catalyzed denitrogenative transformation of a ᵗBu-substituted 1-sulfonyl-1,2,3-triazole into a tetrasubstituted iminoalkene.[8]

The rather selective conversion **2a/b → 3a/b** requires the presence of stoichiometric amounts of AuCl·S(CH₃)₂. We could not observe the formation of any *cyclo*-diphosphadiazane upon heating **2a/b** in the absence of Au(ɪ). Moreover, the presence of the electron withdrawing *N*-sulfonyl-group at N(3) is crucial for the dinitrogenative generation of **3a/b**, as the PhCH₂-substituted triazaphosphole **2c** does not undergo the transformation to the corresponding N₂P₂-heterocycle.

Based on NMR-spectroscopic data, we propose the following mechanism for the conversion of the *N*-sulfonyl-triazaphosphole into the corresponding Au(ɪ)-complex: the Au(ɪ)Cl-fragment first coordinates to the donor-atoms of the phosphorus heterocycle in a dynamic exchange process (Scheme 3).[16] Due to the electron-withdrawing nature of the *N*-sulfonyl-group, the aromaticity of the triazaphosphole is strongly disrupted and ring-opening to [(**2a′/b′**)AuCl] is facilitated. Loss of dinitrogen gives the zwitterionic species [(**4a/b**)AuCl], for which a neutral resonance structure exist. According to the HSAB concept, we anticipate that the Au(ɪ)-fragment coordinates exclusively to the remaining soft phosphorus atom in [(**4a/b**)AuCl]. The neutral species is an



**Scheme 2** Synthesis of *cyclo*-1,3-diphospha-2,4-diazane-Au(ɪ)-complexes **3a/b**.
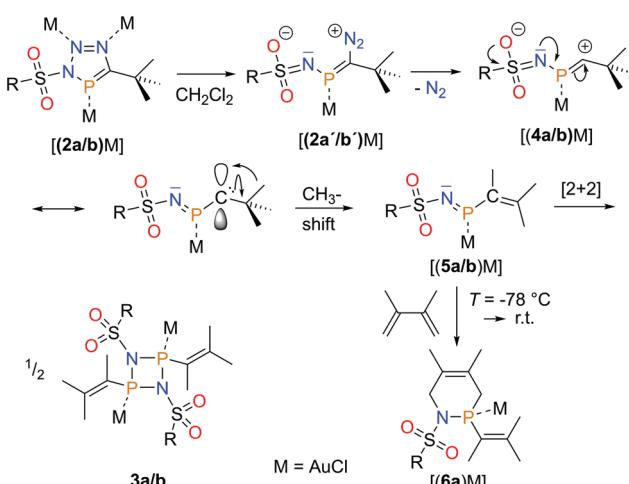


**Scheme 3** Proposed mechanism for the formation of **3a/b**.

iminophosphine-carbene, which undergoes a [1,2]-CH$_3$-shift to the more stable iminophosphine [(5a/b)AuCl]. Iminophosphinines are known to form dimers and even trimers from the parent monomer depending on the substituents on both the phosphorus and nitrogen atom. Dimerization of [(5a/b)AuCl], especially in presence of electron-withdrawing sulfonyl groups then leads to the observed main product 3a/b (Scheme 3).[17]

In order to identify the reactive iminophosphine [(5a/b)AuCl] as an intermediate in the proposed mechanism, N-tosyltriazaphosphole 2a and AuCl·SMe$_2$ were cooled to $T = -196$ °C and a solution of dimethylbutadiene as a trapping reagent in dichloromethane was condensed into the reaction vessel. The solution was first stored at $T = -78$ °C and then slowly warmed to room temperature over 6–8 hours. Subsequent $^{31}$P{$^1$H} NMR spectroscopy at room temperature showed only one major phosphorus resonance at $\delta$(ppm) = 104.0. Analysis of the product by means of ESI-MS indeed provided evidence for the expected trapping product [(6a)AuCl] (Scheme 3). Further confirmation for cyclodiphosphazane formation via dimerization of two iminophosphines is provided by a cross-reaction of a 1:1 mixture of 2a and 2b with AuCl·SMe$_2$ in DCM. In this case the $^{31}$P{$^1$H} NMR of the reaction mixture showed the formation of 3a and 3b as well as a third species at $\delta$(ppm) = 130.7, which we tentatively assigned to a mixed N-SO$_2$-Tol/N-SO$_2$-Mes substituted P$_2$N$_2$ ring. A similar cross reactivity in phosphazane chemistry has recently been described by Wright et al. as the authors also found evidence for the transient formation of monomeric phosphazane intermediates.[18]

We could demonstrate for the first time that 3H-1,2,3,4-triazaphosphole derivatives, containing electron-withdrawing N-sulfonyl-groups at the N$^3$ atom, are synthetically accessible. These phosphorus heterocycles show a remarkable different reactivity compared to their classical alkyl- or aryl-substituted counterparts. Interestingly, the hitherto unknown N-sulfonyl-1,2,3,4-triazaphospholes undergo a highly selective and unprecedented transformation to cyclo-1,3-diphospha(iii)-2,4-diazane-Au(i) complexes in the presence of stoichiometric amounts of AuCl·S(CH$_3$)$_2$ and loss of N$_2$. Single crystal X-ray diffraction studies show, that the trans-isomer of the substituted N$_2$P$_2$ heterocycle has been generated, while NMR-spectroscopic and mass-spectrometric investigations give insight into the mechanism of its formation. Our results pave the way to explore the chemistry of N-sulfonyl-substituted triazaphospholes in detail and provide a first step in transferring the fascinating chemistry, reported for the phosphorus-lacking N-sulfonyl-1,2,3-triazoles, to their isolobal phosphorus congeners.

## Conflicts of interest

There are no conflicts to declare.

## Notes and references

1 (a) Y. Y. C. Yeung Lam Ko and R. Carrié, J. Chem. Soc., Chem. Commun., 1984, 1640; (b) Y. Y. C. Yeung Lam, Ko, R. Carrié, A. Muench and G. Becker, J. Chem. Soc., Chem. Commun., 1984, 1634; (c) W. Rösch and M. Regitz, Angew. Chem., 1984, 96, 898; Angew. Chem. Int. Ed. Engl., 1984, 23, 900.
2 L. Nyulászi, Chem. Rev., 2001, 101, 1229.
3 See for example: (a) T. Allspach, M. Regitz, G. Becker and W. Becker, Synthesis, 1986, 31; (b) M. Regitz and P. Binger, Angew. Chem., Int. Ed. Engl., 1988, 27, 1484; (c) J. A. W. Sklorz and C. Müller, Eur. J. Inorg. Chem., 2016, 595.
4 J.-C. Guillemin, T. Janati and J.-M. Denis, J. Org. Chem., 2001, 66, 7864.
5 (a) S. L. Choong, C. Jones and A. Stasch, Dalton Trans., 2010, 39, 5774; (b) S. L. Choong, A. Nafady, A. Stasch, A. M. Bond and C. Jones, Dalton Trans., 2013, 42, 7775.
6 (a) J. A. W. Sklorz, S. Hoof, M. G. Sommer, F. Weißer, M. Weber, J. Wiecko, B. Sarkar and C. Müller, Organometallics, 2014, 33, 511; (b) J. A. W. Sklorz, S. Hoof, N. Rades, N. De Rycke, L. Könczöl, D. Szieberth, M. Weber, J. Wiecko, L. Nyulászi, M. Hissler and C. Müller, Chem. – Eur. J., 2015, 21, 11096.
7 (a) W. Rösch, T. Facklam and M. Regitz, Tetrahedron, 1987, 43, 3247; (b) J. Kerth, U. Werz and G. Maas, Tetrahedron, 2000, 56, 35; (c) M. Papke, L. Dettling, J. A. W. Sklorz, D. Szieberth, L. Nyulászi and C. Müller, Angew. Chem., 2017, 129, 16706; Angew. Chem. Int. Ed., 2017, 56, 16484.
8 N. Selander, B. T. Worrell and V. V. Fokin, Angew. Chem., 2012, 124, 13231; Angew. Chem. Int. Ed., 2012, 51, 13054.
9 For recent examples on rhodium(ii)-catalyzed reactions of N-sulfonyl-1,2,3-triazoles: (a) K. Pal, R. K. Shukla and C. M. R. Volla, Org. Lett., 2017, 19, 5764; (b) T. Miura, Q. Zhao and M. Murakami, Angew. Chem., Int. Ed., 2017, 56, 16645; (c) J. O. Strelnikova, N. V. Rostovskii, G. L. Starova, A. F. Khlebnikov and M. S. Novikov, J. Org. Chem., 2018, 83, 11232; (d) Y. Lv, A. A. Ogunlana, H. Li, D. Gao, C. Wang and X. Bao, Catal. Sci. Technol., 2018, 8, 3379; (e) C.-Z. Zhu, Y. Wei and M. Shi, Org. Chem. Front., 2019, 6, 2884; (f) J. Ge, X. Wu and X. Bao, Chem. Commun., 2019, 55, 6090; (g) N. Kahar, P. Jadhav, R. V. R. Reddy and S. Dawande, Chem. Commun., 2020, 56, 1207.
10 J. Wang, J. Mei, E. Zhao, Z. Song, A. Qin, J. Z. Sun and B. Z. Tang, Macromolecules, 2012, 45, 7692.
11 F. A. Cotton and P. F. Stokely, J. Am. Chem. Soc., 1970, 92, 294.
12 See for example: (a) N. Mézailles, L. Ricard, F. Mathey and P. Le Floch, Eur. J. Inorg. Chem., 1999, 2233; (b) M. Rigo, L. Hettmanczyk, F. J. L. Heutz, S. Hohloch, M. Lutz, B. Sarkar and C. Müller, Dalton Trans., 2017, 46, 86.
13 (a) A. Michaelis and G. Schroeter, Ber. Dtsch. Chem. Ges., 1894, 27, 490; (b) A. Schulz, A. Villinger and A. Westenkirchner, Inorg. Chem., 2013, 52, 11457; (c) J. Bresien, A. Hinz, A. Schulz, T. Suhrbier, M. Thomas and A. Villinger, Chem. – Eur. J., 2017, 23, 14738.
14 See for example: (a) M. M. Siddiqui, J. T. Mague and M. S. Balakrishna, Inorg. Chem., 2015, 54, 6063; (b) M. S. Balakrishna, V. Sreenivasa Reddy and S. S. Krishnamurthy, Coord. Chem. Rev., 1994, 129, 1; (c) G. G. Briand, T. Chivers and M. Krahn, Coord. Chem. Rev., 2002, 233–234, 237; (d) M. S. Balakrishna, in Copper(i) Chemistry of Phosphines, Functionalized Phosphines, and Phosphorus Heterocycles, ed. M. S. Balakrishna, Elsevier, 2019, ch. 11, pp. 345–373; (e) A. J. Plajer, J. Zhu, P. Pröhm, F. J. Rizzuto, U. F. Keyser and D. S. Wright, J. Am. Chem. Soc., 2020, 142, 1029.
15 For related species see: (a) A. Baceiredo, G. Bertrand, J.-P. Majoral and K. B. Dillon, J. Chem. Soc., Chem. Commun., 1985, 562; (b) F. L. Bowden, A. T. Dronsfield, R. N. Haszeldine and D. R. Taylor, J. Chem. Soc., Perkin Trans. 1, 1973, 516.
16 Low-temperature $^{31}$P{$^1$H} NMR measurements indicate a coordination of the Au(i)Cl fragment to the ambidentate triazaphosphole 2b. See ESI†.
17 See for example: (a) E. Niecke, W. Flick and S. Pohl, Angew. Chem., Int. Ed. Engl., 1976, 15, 309; (b) E. Niecke, R. Rüger and W. W. Schoeller, Angew. Chem., Int. Ed. Engl., 1981, 20, 10346; (c) N. Burford, T. S. Cameron, K. D. Conroy, B. Ellis, M. Lumsden, C. L. B. Macdonald, R. McDonald, A. D. Phillips, P. J. Ragogna, R. W. Schurko, D. Walsh and R. E. Wasylishen, J. Am. Chem. Soc., 2002, 124, 14012; (d) M. Lehmann, A. Schulz and A. Villinger, Struct. Chem., 2011, 22, 35; (e) M. Kuprat, M. Lehmann, A. Schulz and A. Villinger, Inorg. Chem., 2011, 50, 5784; (f) E. Niecke, M. Nieger and F. Reichert, Angew. Chem., 1988, 100, 1783.
18 A. J. Plajer, K. Bold, F. J. Rizzuto, R. García-Rodríguez, T. K. Ronson and D. S. Wright, Dalton Trans., 2017, 46, 12775.

## 4 A new access to diazaphospholes *via* cycloaddition–cycloreversion reactions on triazaphospholes

Lea Dettling, Martin Papke, Julian A. W. Sklorz, Dániel Buzsáki, Zsolt Kelemen, Manuela Weber, László Nyulászi and Christian Müller

**Author contributions:**

The project concept originates from Martin Papke and Julian A. W. Sklorz. Lea Dettling was responsible for the synthesis of coordination compounds as well as reproducing synthetic procedures for the purpose of complete analysis, necessary for the publication of the results. Quantum chemical calculations were performed by Dániel Buzsáki and Zsolt Kelemen. László Nyulászi supervised the quantum-chemical calculations and gave scientific advice. Manuela Weber and Martin Papke were responsible for the crystallographic characterization of several of the new compounds. Christian Müller supervised the project. Lea Dettling wrote the supporting information. The manuscript was written in collaboration between Lea Dettling, László Nyulászi and Christian Müller.
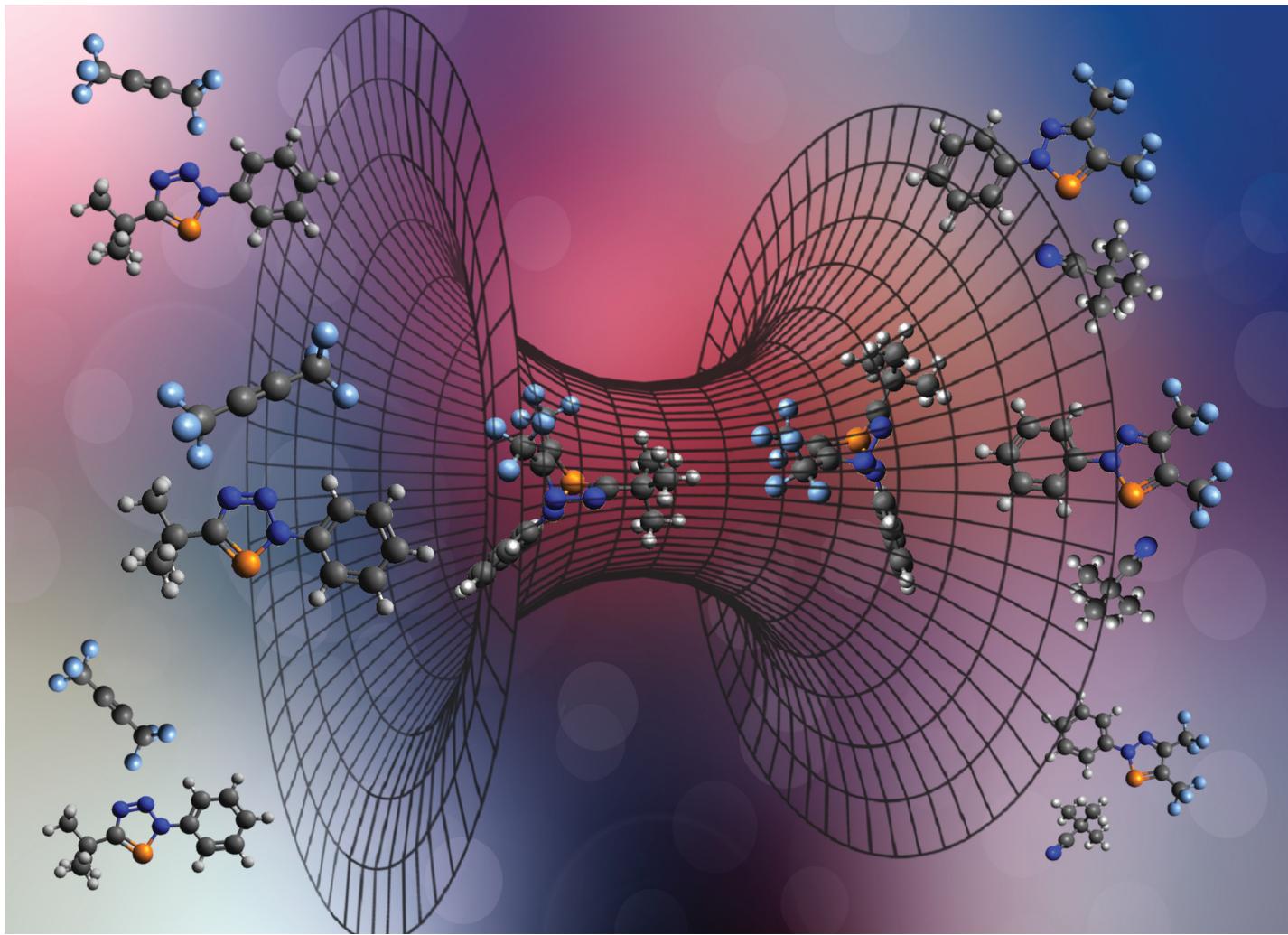
**Showcasing research from Professor Christian Müller's laboratory, Institute of Chemistry and Biochemistry, Freie Universität Berlin, Berlin, Germany**

A new access to diazaphospholes *via* cycloaddition–cycloreversion reactions on triazaphospholes

The image highlights the [4+2] cycloaddition reaction between an unsaturated 5-membered phosphorus heterocycle and hexafluoro-2-butyne, affording a $CF_3$-substituted diazaphosphole after cycloreversion and elimination of $^tBu$-C≡N.

ROYAL SOCIETY OF **CHEMISTRY**

rsc.li/chemcomm

# ChemComm

Check for updates

## A new access to diazaphospholes via cycloaddition–cycloreversion reactions on triazaphospholes†

Lea Dettling, [ID]‡[a] Martin Papke,‡[a] Julian A. W. Sklorz,[a] Dániel Buzsáki, [ID][b] Zsolt Kelemen,[b] Manuela Weber,[a] László Nyulászi [ID]*[b] and Christian Müller [ID]*[a]

A novel bis-CF₃-substituted diazaphosphole was synthesized selectively from hexafluoro-2-butyne and a 3H-1,2,3,4-triazaphosphole derivative. The [4+2] cycloaddition and subsequent cycloreversion reaction under elimination of pivaloyl nitrile affords the product in high yield. The heterocycle coordinates via the phosphorus atom to a W(CO)₅-fragment and shows stronger π-accepting properties than the triazaphosphole.

3,5-Disubstituted 3H-1,2,3,4-triazaphospholes (**B**) are the phosphorus congeners of the well-studied 1,2,3-triazoles (**A**), according to the isolobal relationship between a trivalent P-atom and a C–H fragment (Chart 1).

These $\lambda^3$, $\sigma^2$ phosphorus heterocycles have a conjugated π-system with a high degree of aromaticity.[1] They can easily be prepared regioselectively by a modular [3 + 2] cycloaddition reaction, starting from various aryl/alkyl-azides and phosphaalkynes.[2,3] Despite the fact that 3H-1,2,3,4-triazaphosphole derivatives have been synthesized independently by Carreé and Regitz already in 1984, the first reports on their coordination chemistry have not appeared in literature before 2010.[2,4] As ambidentate ligands the coordination of the heterocycle to a metal center might proceed either via the phosphorus atom or the nitrogen donors N¹ or N² (Chart 1, **C**). However, the η¹(P)-coordination mode has so far only been observed in a Pt(0)-complex.[4b]

Even less is known about the chemical reactivity of 3H-1,2,3,4-triazaphosphole derivatives. We could demonstrate that the cationic phosphorus analogues **D** of neutral mesoionic carbenes (1,2,3-triazolylidenes) can be obtained by quaternization of the N1 atom in **B** with Meerwein salts.[5] Moreover, we noticed that the introduction of electron-withdrawing N-sulfonyl groups at the N³-atom changes the reactivity of the corresponding triazaphosphole considerably. In the presence of stoichiometric amounts of AuCl·S(CH₃)₂, loss of N₂ and the formation of cyclo-1,3-diphospha(III)-2,4-diazane-Au(I) complexes of type **E** were observed.[6] Inspired by the fact that 6-membered azaphosphinines and 5-membered azaphospholes can undergo [4 + 2] cycloaddition reactions with various alkynes under subsequent nitrile elimination, we decided to investigate the reactivity of **B** towards alkynes in more detail with the aim to synthesize 2H-1,2,3-diazaphosphole derivatives (**G**) directly in one step (Chart 2).[7]

These heterocycles are otherwise only accessible by multistep synthetic procedures.[8] In fact, similar reactions with RC≡P elimination from oxadiphospholes and selenadiphospholes via a concerted mechanism have been reported.[9] Moreover, an imino-substituted diazaphosphole biradicaloid showed facile isonitrile cycloaddition, but no subsequent cycloreversion.[10]

The 3,5-disubstituted triazaphosphole **1** was prepared according to literature procedures from PhN₃ and ᵗBu-C≡P.[2a] Triazaphosphole **3** does not react with dimethyl

[a] *Freie Universität Berlin, Institute of Chemistry and Biochemistry, Fabeckstr. 34/36, 14195, Berlin, Germany. E-mail: c.mueller@fu-berlin.de*
[b] *Department of Inorganic and Analytical Chemistry, Budapest University of Technology and MTA-BME Computation Driven Chemistry Research Group, Műegyetem rkp. 3, H-1111, Budapest, Hungary.*
*E-mail: nyulaszi.laszlo@vbk.bme.hu*

† Electronic supplementary information (ESI) available. CCDC 2163856–2163858. For ESI and crystallographic data in CIF or other electronic format see DOI: **https://doi.org/10.1039/d2cc02269a**
‡ These authors have contributed equally.



**Chart 1** Triazole **A**, triazaphosphole **B** and possible coordination modes **C**. Selected examples (**D** and **E**) for the reactivity of **B**.
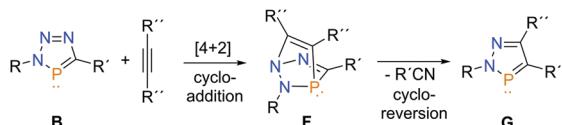
**Chart 2** Attempted synthesis of **G**, starting from **B** and an alkyne.



**Fig. 1** Molecular structure of **3** in the crystal. Displacement ellipsoids are shown at the 50% probability level. Selected bond lengths (Å) and angles (°): P(1)–N(2): 1.693(2), P(1)–C(8): 1.712(2), C(8)–C(7): 1.406(3), C(7)–N(1): 1.323(3), N(1)–N(2): 1.349(2), N(2)–C(1): 1.436(3). N(1)–N(2)–C(1)–C(2): 145.9(2).

acetylenedicarboxylate (DMAD) to diazaphosphole **2** (Scheme 1a). Using the stronger dienophile hexafluoro-2-butyne, however, elimination of $^t$Bu-C≡N and, according to $^{31}$P{$^1$H} NMR spectroscopy, quantitative formation of diazaphosphole **3** was observed (Scheme 1b). We could not detect the apparent intermediate **F** (Chart 2) during the course of the reaction. Interestingly, triazoles, such as **4**, did not react with CF$_3$C≡CCF$_3$ to the CF$_3$-substituted pyrazole **5**, although cycloaddition/cycloreversion reactions on 1,2,3-triazoles with DMAD have been reported in the literature (Scheme 1c).[11] This is particularly intriguing as 1-aryl-3,4-bis(trifluoromethyl)-substituted pyrazole motifs (**5**), are present in numerous pharmacologically relevant and bioactive nitrogen heterocycles and have to be prepared *via* a multistep synthesis.[12] Our novel diazaphosphole **3** thus represents a phosphorus derivative of this compound class.

Diazaphosphole **3** was obtained as an off-white solid in 87% isolated yield and shows a signal at $\delta$(ppm) = 234.4 (q, $^3J_{P-F}$ = 25.5 Hz) in the $^{31}$P{$^1$H} NMR spectrum (starting material **1**: $\delta$(ppm) = 174.3). For the CF$_3$-groups, resonances at $\delta$(ppm) = −53.3 (dq, $^3J_{F-P}$ = 25.5, $^5J_{F-F}$ = 7.4 Hz) and $\delta$(ppm) = −61.8 (qd, $^5J_{F-F}$ = 7.4 Hz, $^4J_{F-P}$ = 1.2 Hz) were observed in the $^{19}$F{$^1$H} NMR spectrum. Single crystals of **3** suitable for X-ray diffraction were obtained by slow evaporation of a dichloromethane solution and the molecular structure of **3** in the crystal is depicted in Fig. 1 along with selected bond lengths and distances.

Fig. 1 represents the first crystallographically characterized CF$_3$-substituted diazaphosphole. From the X-ray data it is evident that the heterocycle is fully planar and that the P(1)–C(8) and N(1)–N(2) bond distances in **3** are very similar to the ones observed in the starting material **1**,[13] with P–C and C–C bond lengths characteristic for aromatic compounds. The significantly negative NICS(1) values (see Table S1 in the ESI†)

are in accordance with aromaticity. Apparently, exchanging pivaloyl nitrile by a perfluorobutyne-moiety does not cause a significant structural change within the heterocycle. The same holds for the inter-ring N(2)–C(1) distance. Also, the N(2)–P(1)–C(8) and P(1)–N(2)–N(1) angles as well as the torsion angle N(1)–N(2)–C(1)–C(2) in **3** are very similar compared to the data found for triazaphosphole **1**.
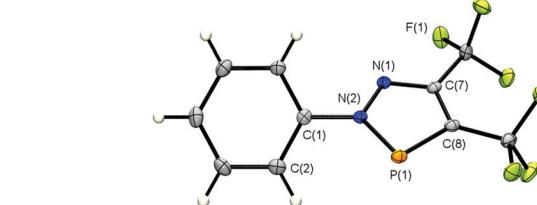
In order to understand the reaction mechanism, ωB97X-D/6-311 + G** DFT calculations (see ESI†) were performed after validating the optimized geometries with the X-ray data of **3** (see Table S2, ESI†). This level of theory was used successfully for cycloaddtion reactions before.[14]

The concerted cycloaddition–cycloreversion process (Fig. 2, Chart 2 and ESI†) is in full agreement with all experimental observations. The cycloaddition step **B→F** (Chart 2) is nearly thermoneutral, while the $^t$BuC≡N eliminating cycloreversion (forming **G**) is highly exergonic. Accordingly (see Hammond principle), the rate determining step of the overall reaction is **TS1**, that allows the formation of **3** (27.3 kcal mol$^{-1}$ activation Gibbs free energy) but not of **2** and **5** (barriers 31.9 kcal mol$^{-1}$,



**Fig. 2** ωB97X-D/6-311 + G**(PCM = toluene) Gibbs free energy ($T$ = 130 °C) profiles for the reactions in Scheme 1. Relative energies (in kcal mol$^{-1}$) are compared to the initial van der Waals complex of the reactants.
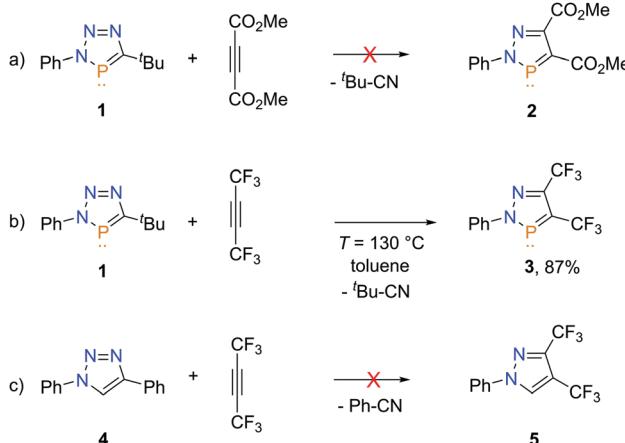


**Scheme 1** Reactivity of **1** and **4** towards electron-withdrawing alkynes.

36.9 kcal mol$^{-1}$, respectively). It is noteworthy that IRC calculations reveal, that the Ph substituent at the nitrogen atom should be in endo position with respect to the approaching/leaving group for any [4 + 2] cycloaddition step. The interconversion **F→F'** is needed prior to the retro cycloaddition step, by flattening the pyramidal nitrogen atom via a small barrier. The fact that no intermediate **F/F'** could be detected is in accordance with the very small barrier for the cycloreversion step.

A comparison of the Kohn–Sham orbitals of the parent CF$_3$-substituted diazaphosphole, the parent 2H-1,2,3-diazaphosphole and the parent 3H-1,2,3,4-triazaphosphole (Fig. S1, ESI†) shows, that in all three heterocycles, the π-type LUMO has a large coefficient at the phosphorus atom, indicating good π-acceptor properties when coordinated via the phosphorus atom to a metal center. While the orbital energies of the unsubstituted diazaphosphole are generally destabilized with respect to the triazaphosphole (Fig. S1, ESI†), in accordance with the observed ionization energies,[1] CF$_3$-substitution acts strongly stabilizing (Fig. S1, ESI†). Altogether, **3** should be a stronger π-acceptor than **1**. In all three compounds, the lone pair at the phosphorus atom (mixed with the nitrogen in-plane lone-pair) is represented by the HOMO−2 (CF$_3$-diazaphosphole: $E = -11.24$ eV; 3H-1,2,3,4-triazaphosphole: $E = -10.92$ eV; 2H-1,2,3-diazaphosphole: $E = -10.21$ eV). Consequently, triazaphospholes and diazaphospholes are expected to be rather weak σ-donors, as anticipated for low-coordinate phosphorus compounds. The π-donor properties of triazaphospholes and diazaphospholes are evident from the HOMOs, each having a large π-coefficient at the phosphorus atom, as it is known for other electron-rich phosphorus heterocycles.[15] Again, due to the energetically higher HOMO, triazaphosphole **1** should show stronger π-donor properties than the CF$_3$-substituted diazaphosphole **3**.

The interplay between the above described effects makes the coordination behavior of compound **3** highly interesting, also with respect to triazaphospholes. As a matter of fact, the coordination chemistry of 2H-1,2,3-diazaphospholes is largely unknown and only a few examples can be found in the literature. Chart 3 shows the possible coordination modes for this class of compounds. Analogous to triazaphospholes, diazaphospholes are ambidentate ligands and can coordinate to a metal center either via the phosphorus lone pair (**H**) or the nitrogen donor (**I**). This has been demonstrated in a few cases by van Koten, Schmidpeter and co-workers by using suitable Pt(II) and Pd(II) complexes as metal precursor.[16] The simultaneous coordination of a diazaphosphole to two metal fragments (**J**) has so far not been observed. Only recently, Erben and co-workers have investigated the synthesis and coordination chemistry of Si-bridged, chelating diazaphospholes.[17]
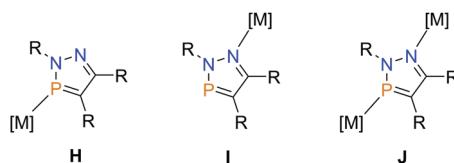
We decided to focus on the synthesis of a tungsten carbonyl complex of **3**, as it can provide valuable information on the electronic ligand properties via IR spectroscopy. Moreover, $^{31}$P NMR spectroscopy would immediately reveal, whether the coordination of the ligand to the W(CO)$_5$ fragment occurs via the phosphorus or the nitrogen donor. **3** was reacted with one equivalent of W(CO)$_6$ in THF at room temperature and under UV irradiation (Scheme 2). After only a short time, the formation of a single new resonance at $\delta$(ppm) = 217.3 was observed in the $^{31}$P{$^1$H} NMR spectrum, which corresponds to a coordination shift of $\Delta\delta$(ppm) = 17.1 compared to the starting material.[18] The selective reaction towards product **6** was complete within 68h. Interestingly, the signal of the product at $\delta$(ppm) = 217.3 shows tungsten satellites with a coupling constant of $^1J_{W-P} = 326.5$ Hz (Fig. S9, ESI†). This indicates that coordination of the ligand to the metal center occurs via the phosphorus atom, in agreement with the calculated 10.6 kcal mol$^{-1}$ preference of the coordination at phosphorus over nitrogen. For comparison reasons, we also reacted triazaphospholes **1** and **8** (Ar = 2,5-diisopropylphenyl, Dipp) with W(CO)$_6$ in THF at room temperature and under irradiation with UV light. The course of the reaction was again followed by means of NMR spectroscopy, which revealed a selective and quantitative formation of a new species within 5d. The new compounds (**7**, **9**) show a signal at $\delta$(ppm) = 136.1, respectively $\delta$(ppm) = 160.6 in the $^{31}$P{$^1$H} NMR spectrum ($\Delta\delta$(ppm) = 38.2, 39.7). Much to our surprise, these signals also show tungsten satellites ($^1J_{P-W} = 262.1$ Hz; 285.6 Hz), which verifies that also **1** and **8** coordinate via the phosphorus atom to the metal center. This is particularly interesting taking into account that a coordination via N$^1$ or N$^2$ (Chart 1) has so far been observed for the majority of triazaphosphole-based complexes.[4,19] The calculated 0.6 kcal mol$^{-1}$ energy difference between the two complexation modes of **1** indicates that subtle steric effects determine the complexation site in triazaphospholes.

A comparison of the IR spectra of **6**, **7** and **9** further shows, that the wavenumbers of the CO stretching frequencies are shifted to higher values in **6** compared to the ones found for **7** and **9** (Table 1). This is in line with the expected lower net-donor properties of **3** compared to **1** and **8**.

Thus, the CF$_3$-substituted diazaphosphole **3** is a stronger π-accepting ligand than triazaphospholes **1** and **8**, if coordination to the metal center proceeds via the phosphorus donor.



**Chart 3** Possible coordination modes (**H–J**) of diazaphospholes.
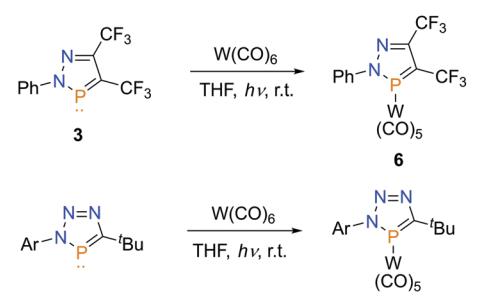


**Scheme 2** Synthesis of W(0)-complexes **6** and **7**.

| $\tilde{v}_{(CO)}$ [cm$^{-1}$] | | | |
|---|---|---|---|
| 6 | 2089 | 2017 | 2002 | 1934 |
| 7 | 2077 | 2023 | 1980 | 1885 |
| 9 | 2081 | 2000 | 1954 | 1934 |
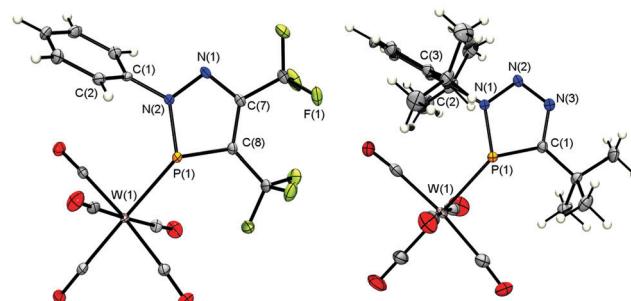


Fig. 3 Molecular structures of **6** (left) and **9** (right) in the crystal. Displacement ellipsoids are shown at the 50% probability level. Selected bond lengths (Å) and angles (°): **6**: P(1)–N(2): 1.677(2), P(1)–C(8): 1.707(2), C(8)–C(7): 1.413(3), C(7)–N(1), N(1)–N(2): 1.361(3), P(1)–W(1): 2.3890(6), N(2)–C(1): 1.441(3). N(1)–N(2)–C(2): 64.1(3). **7**: Only one independent molecule is shown. P(1)–N(2): 1.675(2), P(1)–C(1): 1.712(2), C(1)–N(3): 1.357(3), N(3)–N(2): 1.303(2), N(2)–N(1): 1.358(2), N(1)–C(2): 1.446(2), C(1)–C(14): 1.521(3), P(1)–W(1): 2.4512(5). N(1)–P(1)–C(1): 88.67(9), N(2)–N(1)–C(2)–C(3): 86.3(2).

Finally, single crystals of **6** and **9**, suitable for X-ray diffraction, could be obtained by slow evaporation of the solvent of a saturated solution of **6** and **9** in *n*-pentane. Fig. 3 shows the molecular structures of **6** and **9** in the crystal, along with selected bond lengths and angles. The W(0) complexes **6** and **9** show a slightly distorted octahedral coordination geometry and unequivocally confirm that the heterocycles coordinates *via* the phosphorus atom to the W(CO)$_5$ fragment. Compared to the solid state structure of the free ligand **3** (Fig. 1), the P(1)–C(8) and P(1)–N(2) bonds in **6** are slightly shortened upon coordination of the ligand to the metal center (1.707(2) Å and 1.677(2) Å in **6** *vs.* 1.712(2) Å and 1.693(2) Å in **3**). For steric reasons, the aryl rings in **6** and **9** are rotated out of the heterocyclic plane (see also Fig. 1).

We could demonstrate for the first time that a 3*H*-1,2,3,4-triazaphosphole derivative undergoes a selective [4 + 2] cycloaddition with hexafluoro-2-butyne with subsequent elimination of pivaloyl nitrile to afford a bis-CF$_3$-substituted diazaphosphole in high yield. According to the isolobal relationship between a trivalent phosphorus atom and a C–H fragment, this heterocycle represents a phosphorus congener of a bis-CF$_3$-substituted pyrazole, which finds applications as a bioactive nitrogen heterocycle. The novel diazaphosphole forms an (L)W(CO)$_5$-complex, in which the ligand coordinates *via* the phosphorus atom to the metal center. In combination with DFT-calculations, the experimental results show that the bis-CF$_3$-substituted diazaphosphole is a stronger π-acceptor than the corresponding triazaphosphole, which was used as a starting material. Our results demonstrate that bis-CF$_3$-substituted diazaphospholes are accessible in a facile manner. Their use as novel π-accepting ligands in coordination chemistry and homogeneous catalysis as well as the investigation of their potential bioactive properties is currently explored.

## Conflicts of interest

There are no conflicts to declare.

## Notes and references

1 L. Nyulászi, T. Veszprémi, J. Réffy, B. Burkhardt and M. Regitz, *J. Am. Chem. Soc.*, 1992, **114**, 9080.
2 (*a*) Y. Y. C. Yeung Lam, Ko, R. Carrié, A. Muench and G. Becker, *J. Chem. Soc., Chem. Commun.*, 1984, 1634; (*b*) W. Rösch and M. Regitz, *Angew. Chem., Int. Ed. Engl.*, 1984, **23**, 900.
3 L. Nyulászi, *Chem. Rev.*, 2001, **101**, 1229.
4 (*a*) S. L. Choong, A. Nafady, A. Stasch, A. M. Bond and C. Jones, *Dalton Trans.*, 2013, **42**, 7775; (*b*) S. L. Choong, C. Jones and A. Stasch, *Dalton Trans.*, 2010, **39**, 5774.
5 M. Papke, L. Dettling, J. A. W. Sklorz, D. Szieberth, L. Nyulászi and C. Müller, *Angew. Chem., Int. Ed.*, 2017, **56**, 16484.
6 E. Yue, L. Dettling, J. A. W. Sklorz, S. Kaiser, M. Weber and C. Müller, *Chem. Commun.*, 2022, **58**, 310.
7 (*a*) N. Avavari, P. Le Floch and F. Mathey, *J. Am. Chem. Soc.*, 1996, **118**, 11978; (*b*) A. Schmidpeter and H. Klehr, *Z. Naturforsch., B: Anorg. Chem., Org. Chem.*, 1983, **38**, 1484.
8 (*a*) G. Baccolini, R. Dalpozzo and E. Errani, *Tetrahedron*, 1987, **43**, 2755; (*b*) J. H. Weinmaier, G. Brunnhuber and A. Schmidpeter, *Chem. Ber.*, 1980, **113**, 2278; (*c*) F. Armbruster, U. Klingebiel and M. Noltemeyer, *Z. Naturforsch.*, 2006, **61b**, 225.
9 (*a*) A. Mack, U. Bergsträßer, G. J. Reiß and M. Regitz, *Eur. J. Org. Chem.*, 1999, 587; (*b*) S. Asmus, L. Nyulászi and M. Regitz, *J. Chem. Soc., Perkin Trans. 2*, 2001, 1968.
10 H. Beer, J. Bresien, D. Michalik, A.-K. Rölke, A. Schulz, A. Villinger and R. Wustrack, *J. Org. Chem.*, 2020, **85**, 14435.
11 Á. Díaz-Ortiz, A. de Cózar, P. Prieto, A. de la Hoz and A. Moreno, *Tetrahedron Lett.*, 2006, **47**, 8761.
12 (*a*) S. Eguchi. *Bioactive Heterocycles I*, Springer, Heidelberg, 2006; (*b*) Y. L. Yagupolskii, N. V. Pavlenko, I. I. Gerus, S. Peng and M. Nappa, *ChemistrySelect*, 2019, **4**, 4604.
13 J. A. W. Sklorz, S. Hoof, N. Rades, N. De Rycke, L. Könczöl, D. Szieberth, M. Weber, J. Wiecko, L. Nyulászi, M. Hissler and C. Müller, *Chem. – Eur. J.*, 2015, **21**, 11096.
14 S. Giese, D. Buzsáki, L. Nyulászi and C. Müller, *Chem. Commun.*, 2019, **55**, 13812.
15 C. Batich, E. Heilbronner, V. Hornung, A. J. Ashe III, D. T. Clark, U. T. Gobley, D. Kilcast and I. Scanlan, *J. Am. Chem. Soc.*, 1973, **95**, 929.
16 (*a*) J. G. Kraaijkamp, D. M. Grove, G. van Koten and A. Schmidpeter, *Inorg. Chem.*, 1988, **27**, 2612; (*b*) J. G. Kraaijkamp, G. van Koten, K. Vrieze, D. M. Grove, E. A. Klop, A. L. Spek and A. Schmidpeter, *J. Organomet. Chem.*, 1983, **256**, 375.
17 P. Kozáček, L. Dostál, A. Růžička, I. Císařová, Z. Černošek and M. Erben, *New J. Chem.*, 2019, **43**, 13388.
18 See also:(*a*) A. B. Grimm, S. Evariste, A. L. Rheingold, C. E. Moore and J. D. Protasiewicz, *J. Organomet. Chem.*, 2017, **851**, 9; (*b*) J. Heinicke, N. Gupta, S. Singh, A. Surana, O. Kühl, R. K. Bansal, K. Karaghiosoff and M. Vogt, *Z. Anorg. Allg. Chem.*, 2002, **628**, 2869.
19 J. A. W. Sklorz, S. Hoof, M. G. Sommer, F. Weißer, M. Weber, J. Wiecko, B. Sarkar and C. Müller, *Organometallics*, 2014, **33**, 511.

## 5 Phosphorus derivatives of mesoionic carbenes: synthesis and characterization of triazaphosphole-5-ylidene → BF₃ adducts

Lea Dettling, Niklas Limberg, Raphaela Küppers, Daniel Frost, Manuela Weber, Nathan T. Coles, Diego M. Andrada and Christian Müller

### Author contributions:

Lea Dettling designed the project and performed the majority of the experiments. Under Lea Detling's supervision, Niklas Limberg (during his internship) and Raphaela Küppers (during her B.Sc. thesis) contributed with experimental results. Daniel Frost gave scientific advice and helped synthesizing the protonated compound. Quantum chemical calculations were performed by Diego M. Andrada. Manuela Weber and Nathan T. Coles were responsible for the crystallographic characterization of several of the new compounds. Lea Dettling wrote the manuscript and the supporting information. Christian Müller supervised the project and revised the manuscript.

# ChemComm

Chemical Communications

rsc.li/chemcomm

**ROYAL SOCIETY OF CHEMISTRY**

**COMMUNICATION**
Christian Müller *et al.*
Phosphorus derivatives of mesoionic carbenes: synthesis and characterization of triazaphosphole-5-ylidene → BF$_3$ adducts

44

## COMMUNICATION

Check for updates

# Phosphorus derivatives of mesoionic carbenes: synthesis and characterization of triazaphosphole-5-ylidene → BF₃ adducts†‡

Lea Dettling, [iD] [a] Niklas Limberg,[a] Raphaela Küppers,[a] Daniel Frost, [iD] [a] Manuela Weber,[a] Nathan T. Coles, [iD] [b] Diego M. Andrada [iD] [c] and Christian Müller [iD] *[a]

**Trimethylsilyl-substituted triazaphospholes were synthesized by a [3+2] cycloaddition reaction between organic azides and (CH₃)₃Si–C≡P. In an attempt to isolate their *N*-alkylated products, the formation of BF₃ adducts of unprecedented triazaphosphol-5-ylidenes was found. The nature of the carbon_carbene–boron bond was investigated within the DFT framework, revealing a strong donation of electrons from the carbene carbon atom to the boron atom combined with weak back-bonding.**

According to the isolobal relationship between a trivalent phosphorus atom and a C–H fragment, 3*H*-1,2,3,4-triazaphosphole derivatives **A** are phosphorus analogues of the well-known 1,4-disubstituted 1,2,3-triazoles **B** (Fig. 1), which play a prominent role in the field of "click"-chemistry.[1] These heterocycles possess a high degree of aromaticity and can be obtained in a modular [3+2] cycloaddition reaction, starting from organic azides and phosphaalkynes.[2,3]

Although triazaphospholes were first synthesized as early as 1984, reports of their coordination chemistry were first published almost 30 years later.[3,4] Our group reported the coordination chemistry and photoluminescence properties of conjugated, pyridyl-functionalized triazaphospholes, bearing either ᵗBu or Si(CH₃)₃-substituents at the 5-position of the heterocycle.[5]

Little is known about the chemical reactivity of triazaphospholes. In addition to our observation that they undergo cycloaddition–cycloreversion reactions with CF₃C≡CCF₃ forming **C**, we found that triazapholenium salts **D** are accessible by
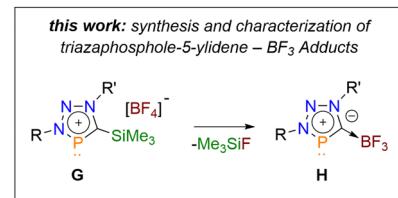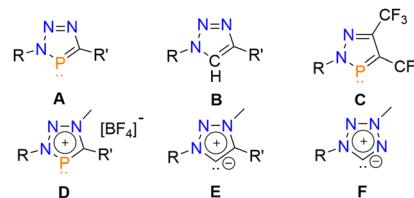


Fig. 1 Selected phosphorus and nitrogen based heterocycles and brief summary of this work (R/R′: alkyl-, aryl-group).

alkylation of triazaphospholes with Meerwein salts.[6,7] Because a negatively charged carbon atom is valence isoelectronic to a phosphorus atom, these cationic phosphorus heterocycles are formally phosphorus congeners of the well-known mesoionic 1,2,3-triazolylidenes **E** and show an interesting coordination chemistry.[7,8]

Inspired by our recent investigations on 6-membered, 2-Si(CH₃)₃-substituted aromatic phosphorus heterocycles (phosphinines), we became interested in reinvestigating Si(CH₃)₃-substituted triazaphospholes (**A**, R′ = Si(CH₃)₃), particularly with respect to the formation of the corresponding triazaspholenium salts (**D**, R′ = Si(CH₃)₃).[5,9] As Si(CH₃)₃-groups linked to an aromatic system generally provide interesting electronic effects to the aromatic ring, we anticipated that these compounds might also undergo chemical transformations, such as protodesilylations or C–Si bond cleavage reactions.[10]

Much to our surprise, we now found that BF₄⁻-salts of Si(CH₃)₃-substituted triazaspholenium cations (**G**) undergo elimination of FSi(CH₃)₃ to form selectively BF₃ adducts of unprecedented triazaphosphol-5-ylidenes (**H**). Interestingly,

[a] *Freie Universität Berlin, Institute of Chemistry and Biochemistry, Fabeckstr. 34/36, Berlin 14195, Germany. E-mail: c.mueller@fu-berlin.de*

[b] *School of Chemistry, University of Nottingham, University Park, Nottingham NG7 2RD, UK*

[c] *Universität des Saarlandes, Anorganische Chemie, Saarbrücken 66123, Germany*

**Scheme 1**  Synthesis of the triazaphospholenium salts **2a/2b**.



**Scheme 2**  Formation of **3a** and **4a** upon heating of **2a** in DME.
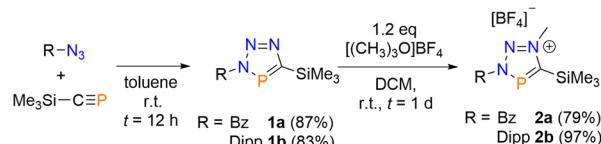
these heterocycles are the phosphorus congeners of tetrazol-5-ylidene carbenes (**F**) with an abnormal substitution pattern.[11]

The Si(CH₃)₃-substituted triazaphospholes **1a/b** were synthesized by [3+2] cycloaddition reactions from $Si(CH_3)_3-C\equiv P$ and benzyl azide (Bz-N₃) or diisopropylphenyl azide (Dipp-N₃), respectively in good yields (**1a**: 87%, **1b**: 83%, Scheme 1). As expected, both compounds show resonances in the downfield region of the $^{31}P\{^1H\}$ NMR spectrum, at $\delta$(ppm) = 214.8 (**1a**) and $\delta$(ppm) = 222.9 (**1b**).

Subsequently, we intended to convert **1a/b** into the corresponding Si(CH₃)₃-substituted triazaphospholenium salts of type **G** (Fig. 1). Using an analogous methodology to that of the $^tBu$-substituted derivatives, an equimolar mixture of compound **1a** and [Me₃O][BF₄] was vigorously stirred in dichloromethane at $T$ = 55 °C and the course of the reaction was followed by means of $^{31}P\{^1H\}$ NMR spectroscopy (Fig. S1, ESI†). After one hour, the formation of a new species was observed, which we attribute to the desired alkylated triazaphospholenium salt **2a**, due to its characteristic chemical shift at $\delta$(ppm) = 239.3.

However, considerable amounts of starting material were still present, while longer reaction times led to the formation of two more side-products. With the aim of preventing the formation of any side-products, [Me₃O][BF₄] was used in a slight excess and the reaction was kept at room temperature. After one day, **2a** was obtained as the sole product in an isolated yield of 79% (Scheme 1). Similarly, the triazaphospholenium salt **2b** was obtained in 97% isolated yield after washing the product with dry diethyl ether. **2b** shows a resonance at $\delta$(ppm) = 249.1 in the $^{31}P\{^1H\}$ NMR spectrum. In the $^1H$ NMR spectrum of the triazaphospholenium salts, the introduced CH₃-group can be detected as a characteristic singlet at $\delta$(ppm) = 4.52 (**2a**) and $\delta$(ppm) = 4.69 (**2b**), respectively.

Even though the Si(CH₃)₃-substituted triazaphospholenium salts **2a/b** were finally synthesized in high yields, we were still wondering about the formation of the observed side products (*vide supra*), particularly at higher reaction temperatures. Consequently, we investigated the thermal stability of **2a** by heating a solution of this compound in dimethoxyethane (DME) to $T$ = 60 °C. Interestingly, the complete conversion of **2a** to two new species (**3a**, **4a**) was observed by $^{31}P\{^1H\}$ spectroscopy after one day.

We were able to separate both compounds by means of either extraction (**3a**) or flash column chromatography (**4a**). Compound **3a** shows a resonance at $\delta$(ppm) = 206.7 in the $^{31}P\{^1H\}$ NMR spectrum, which corresponds to a chemical shift difference of $\Delta\delta$ = 32.6 ppm compared to the starting material **2a** ($\delta$(ppm) = 239.3). Interestingly, a new signal can be observed in the $^1H$ NMR spectrum at $\delta$(ppm) = 9.26. This resonance appears as a doublet with a coupling constant of
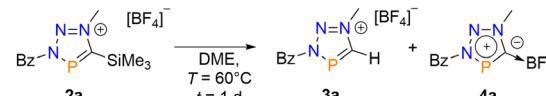
$^2J_{H-P}$ = 37.5 Hz, which is typical of protons in the α-position to a phosphorus atom. We therefore concluded that **3a** must have been formed by protodesilylation of **2a**, according to Scheme 2. The crystallographic characterization of **3a** indeed confirmed that protodesilylation of **2a** had occurred (Table S1, ESI†). Note, that the access to this compound would otherwise only be possible by cycloaddition reaction between an azide and hydrogen cyaphide (H–C≡P), or the cyaphido ligand (C≡P⁻), followed by a subsequent quaternization with Meerwein salt.[12]

Up to this point, the source of the proton still remains unknown. It should be noted, however, that protonated side-products have also been observed in the thermal degradation of free 1,2,3-triazol-5-ylidenes.[13]

Next, we turned our attention to the identification of the second species **4a**. Surprisingly, this compound shows a quartet in the $^{19}F\{^{31}P\}$ NMR spectrum at $\delta$(ppm) = −140.5 (q, $^1J_{F-B}$ = 37.7 Hz, Fig. S2, ESI†). Likewise, a quartet of doublets is observed in the corresponding $^{11}B$ NMR spectrum at $\delta$(ppm) = 0.6 (d, $^2J_{B-P}$ = 15.9 Hz, q, $^1J_{B-F}$ = 37.9 Hz). The chemical shifts and the coupling pattern is in line with the presence of a BF₃-carbene adduct. For instance, the classical Arduengo carbene adduct IMes → BF₃ (IMes = 1,3-dimesitylimidazol-2-ylidene) shows a resonance in the $^{19}F$ NMR spectrum at $\delta$(ppm) = −142.44 (q, $^1J_{F-B}$ = 34.6 Hz) and at $\delta$(ppm) = −1.36 (q, $^1J_{B-F}$ = 34.6 Hz) in the corresponding $^{11}B$ NMR spectrum.[15] A coupling to the phosphorus nucleus in **4a** would provide an additional splitting of the otherwise similar signals as can indeed be noticed in the $^{19}F$ NMR and the $^{11}B$ NMR spectra of **4a** ($^{19}F$ NMR: $\delta$(ppm) = −140.5 (d, $^2J_{F-P}$ = 14.6 Hz), $^{11}B$ NMR: $\delta$(ppm) = 0.6 ppm (d, $^1J_{B-P}$ = 15.9 Hz), Fig. S2, ESI†). Accordingly, the decoupled $^{11}B\{^{19}F\}$ NMR spectrum of **4a** shows only a doublet due to the $^1J_{B-P}$ coupling ($^{11}B\{^{19}F\}$ NMR: $\delta$(ppm) = 0.7 ($^1J_{B-P}$ = 15.8 Hz), Fig. S2, ESI†). Compound **4b** was synthesized in an analogous manner.

Single crystals of **4a**, suitable for X-ray diffraction, were obtained by layering a concentrated dichloromethane solution of **4a** with *n*-pentane and the molecular structure of **4a**, along with selected bond lengths and distances, is depicted in Fig. 2 (**4b**: Table S3, ESI†). The crystallographic characterization of **4a** indeed reveals the presence of an abnormal carbene → BF₃-adduct (Scheme 2). Compared to the protodesilylated triazaphospholenium salt **3a**, the P(1)–C(1) bond in **4a** is slightly elongated (**4a**: 1.711(2) Å; **3a**: 1.706(2) Å), while the N(1)–P(1)–C(1) bond angle is somewhat larger and closer to 90° (**4a**: 87.31(8)°; **3a**: 85.75(6)°). The C(1)–B(1) bond length of 1.640(3) Å) is very similar to the one found for the C–B-bond distance in the Lewis pairs of classical Arduengo carbenes (1.635(5) Å for IMes → BF₃ and 1.669(6) Å for 4,5-dichloro-IMes → BF₃).[14] Similar bond lengths and distances were observed also for **4b** (Table S3, ESI†). **4a** can be described as a BF₃ adduct of an unprecedented
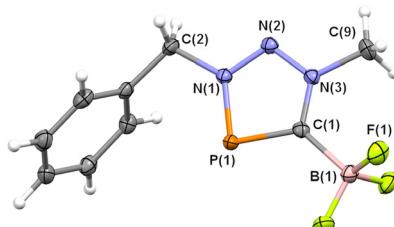
**Fig. 2** Molecular structure of **4a** in the crystal. Displacement ellipsoids are shown at the 50% probability level. Selected experimental and theoretical [B3LYP-D3(BJ)/def2-SVP] bond lengths (Å) and angles (°): P(1)–C(1): 1.711(2) [1.722], P(1)–N(1): 1.705(2) [1.755], N(1)–N(2): 1.309(2) [1.301], N(2)–N(3): 1.320(2) [1.316], N(3)–C(1): 1.354(2) [1.357], C(1)–B(1): 1.640(3) [1.667], N(1)–P(1)–C(1): 87.31(8) [86.2].



**Scheme 3** Synthesis of the triazaphospholenium salts **5a/5b** (a). Preparation of the BEt$_3$-adduct **7b** and the protodesilylated compound **6b** (b).

triazaphosphol-5-ylidene and thus as a phosphorus congener of the known tetrazol-5-ylidenes with an abnormal substitution pattern (**F**, Scheme 1).[11] Moreover, **4a/b** is again isoelectronic to the cationic part of the triazaphospholenium salt **D** (Fig. 1).

From a mechanistic point of view, **4a/b** is formed by elimination of FSiMe$_3$ from **2a/b**, which initially forms the carbene intermediate, that subsequently reacts with the remaining BF$_3$. This would be in line with observations reported by Borozov and co-workers for 1-ethyl-3-methyl-1*H*-imidazolium BF$_4^-$ (and respectively PF$_6^-$), which results in the formation of the corresponding NHC-based BF$_3$ and PF$_5$ Lewis pairs under rather harsh conditions.[15] In this respect, **4a/b** are also related to the GaCl$_3$ adducts of neutral tetrazaphospholes, reported by Schulz and co-workers.[16]

In case of the formation of **4a/b** the free carbene could not be observed spectroscopically, probably due to a rapid Lewis pair formation. However, the by-product FSiMe$_3$ was detected by means of $^1$H–, $^{19}$F– and $^{29}$Si–$^1$H–HMQC NMR spectroscopy and can easily be removed under vacuum. It is likely that the protonation of the carbene leads to the formation of **3a**. This would be in agreement with observation that 1,2,3-triazlylidenes can undergo migration of an alkyl group, that is bound to the most nucleophilic nitrogen atom, to the carbene carbon atom, while the formation of a protodesilylated side-product is also observed.[13]

Because **3a** and **4a** are apparently formed by competing reactions, the isolated yields were moderate. We therefore anticipated targeted syntheses of both compounds. While other electrophiles, such as CH$_3$I or CH$_3$OTf, are not suitable for quaternization reactions at triazaphospholes, we chose triethyloxonium hexafluorophosphate instead. This indeed yielded the corresponding triazaphospholenium salts **5a/b** in good isolated yields (**5a**: 80%, **5b**: 93%, Scheme 3a). Compounds **5a/b** provide again characteristic signals in the $^{31}$P{$^1$H} NMR spectra at δ(ppm) = 238.1 (**5a**) and δ(ppm) = 249.0 (**5b**), respectively. Additionally, the introduced ethyl group shows typical signals in the $^1$H NMR spectra (**5a**: δ(ppm) = 4.73 (q, *J* = 7.5 Hz), 1.74 (t, *J* = 7.3 Hz,); **5b**: δ(ppm) = 4.84 (q, *J* = 7.1 Hz), 1.69 (t, *J* = 7.1 Hz)).

We also anticipated that the addition of potassium fluoride (KF) in the presence of a Boron-based Lewis acid BR$_3$ should facilitate the formation of FSiMe$_3$ and the abnormal carbene → BR$_3$ adduct, while K[PF$_6$] might precipitate from the solution.
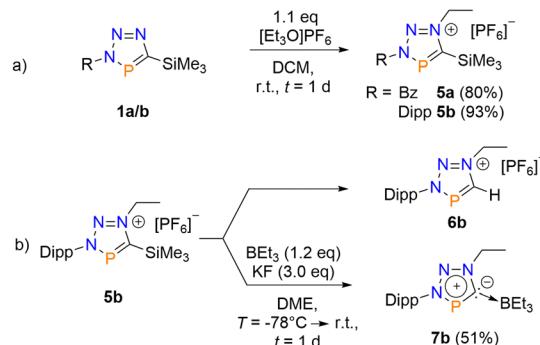
For this purpose, BH$_3$·SMe$_2$, BH$_3$·THF, BF$_3$·SMe$_2$, BF$_3$·OEt$_2$, and BEt$_3$, were used in combination with **5b**. Interestingly, except for BEt$_3$, the selective formation of the protodesilylated product **6b** was observed, most likely due to contaminations with H$_2$O/HF. On the other hand, in the presence of BEt$_3$, the BEt$_3$-adduct **7b** was selectively formed (Scheme 3b). This was confirmed by an X-ray structural analysis (Fig. 3). Compound **6b** was also independently synthesized and characterized crystallographically (see Table S4, ESI†).

Finally, we investigated the nature of the C$_{carb}$ → B bond by means of DFT calculations at the B3LYP-D3(BJ)/def2-SVP level of theory (see ESI† for details). We were particularly interested in the effect of the phosphorus atom on the donor–acceptor abilities of the abnormal carbene moiety.[17] The optimized structures are in good agreement with the experimentally measured ones (Fig. 2, 3 and Table S3 and Fig. S43, ESI†), with the C$_{carb}$–B bond lengths being slightly longer than those observed experimentally (**4a** 1.667 Å and **4b** 1.668 Å). The natural bond orbital analysis (Table S6 and Fig. S44, ESI†) indicates a strong donation of electrons as the BF$_3$ bears a negative partial charge of −0.47 (**4a**) and −0.46 (**4b**). The Wiberg bond orders indicate a single bond character with 0.71 au in **4a** and **4b**. The Bader topological analysis[18] reveals an electron accumulation between the carbene carbon atom and the boron atom with a bond critical point that possesses a
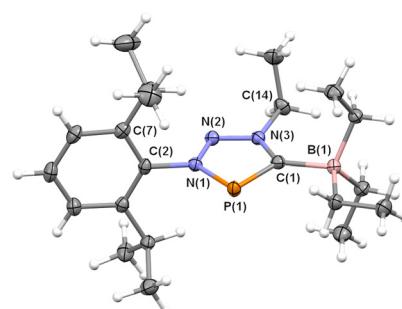


**Fig. 3** Molecular structure of **7b** in the crystal. Displacement ellipsoids are shown at the 50% probability level. Only one independent molecule in the asymmetric unit is shown. Selected bond lengths (Å) and angles (°): P(1)–C(1): 1.7306(10), P(1)–N(1): 1.7110(9), N(1)–N(2): 1.3146(12), N(2)–N(3): 1.3310(12), N(3)–C(1): 1.3629(13) C(1)–B(1): 1.6468(15); N(1)–P(1)–C(1): 88.26(4).
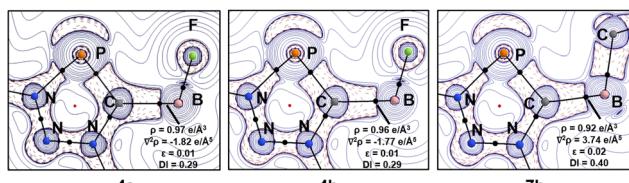
**Fig. 4** Laplacian distribution of the electron density of compounds **4a/b** and **7b** (B3LYP-D3(BJ)/def2-TZVP//B3LYP-D3(BJ)/def2-SVP). Contour line diagrams of the Laplacian distribution $\nabla^2\rho(r)$ in the PHC ring plane. Dashed red lines indicate areas of charge concentration ($\nabla^2\rho(r) < 0$) while solid blue lines show areas of charge depletion ($\nabla^2\rho(r) > 0$). The thick solid lines connecting the atomic nuclei are the bond paths and the small dots are the critical points. Bond Critical Points (in black), Ring Critical Points (in red).

relatively small electron density value ($\rho(r)$ 0.97 e Å$^{-3}$ **4a**, 0.96 e Å$^{-3}$ **4b**, and 0.92 e Å$^{-3}$ **7b**) with negative Laplacian values of $\nabla^2\rho(r) = -1.82$ e Å$^{-5}$ (**4a**) and $\nabla^2\rho(r) = -1.77$ e Å$^{-5}$ (**4b**), respectively a positive value of $\nabla^2\rho(r) = 3.74$ e Å$^{-5}$ for **7b** (Fig. 4). Additionally, we have performed energy decomposition analysis (EDA-NOCV)[19] to quantitatively assess the chemical bonding situation in these adducts, taking as fragments the neutral triazaphosphol-5-ylidenes (**4a/b**, **7b**) and BF$_3$ moieties (Table S7 and Fig. S45, ESI†). The bond dissociation energy is slightly weaker than in other borane adducts, with energies of 38.4 (**4a**), 37.5 (**4b**) and 40.0 (**7b**) kcal mol$^{-1}$.[20] However, the dissection into preparation energy and interaction energy suggests that the geometrical deformation of BF$_3$ or BEt$_3$ brings a significant energy penalty (31.0 and 26.0 kcal mol$^{-1}$).

The interaction energy is comparable to other known C$_{carbene}$ → B adducts, counting $-72.1$ (**4a**), $-70.7$ (**4b**) and $-68.4$ (**7b**) kcal mol$^{-1}$.[21] Further decomposition reveals an ionic nature of the bond with approximately 53% electrostatic interaction and 45% orbital interaction. Note that the electrostatic interaction refers to the electrostatic attraction between the charge distribution of the fragments, differentiating from the VB ionic bonds (for further details see ref. 20). The orbital term can be analysed with the Natural Orbitals for Chemical Valence (NOCV), where the σ-donation counts for ~80% of the orbital interaction, while the π-back donation is only ~5%. Fig. S46 (ESI†) shows a comparison of the frontier molecular orbital energies of the model systems 1,2,3-triazolylidene, tetra-zol-5-ylidene and triazaphosphole-5-ylidene.

The energy of the σ-lone pair on the carbene carbon atom is comparable to the triazole analogue and agrees with the strong donor properties towards BF$_3$ or BEt$_3$. On the other hand, the presence of a phosphorus atom provides less stabilization of the π* orbital, leading to relatively high π-acceptor properties.

In summary, we have found an access to BF$_3$ adducts of hitherto unknown triazaphosphol-5-ylidenes, which are the phosphorus analogs of tetrazol-5-ylidene carbenes with abnormal substitution pattern. Quantum chemical calculations reveal a strong σ-donor property and marginal π-accepting ligand properties. The access to transition metal complexes containing our novel triazaphosphole-5-ylidenes as ligands are currently performed in our laboratories.

## Conflicts of interest

There are no conflicts to declare.

## Notes and references

1 (a) *Phosphorus: The Carbon Copy: From Organophosphorus to Phospha-Organic Chemistry*, ed. K. B. Dillon, F. Mathey and J. F. Nixon, John Wiley & Sons, 1998; (b) J. A. W. Sklorz and C. Müller, *Eur. J. Inorg. Chem.*, 2016, 595.
2 L. Nyulászi, T. Veszprémi, J. Réffy, B. Burkhardt and M. Regitz, *J. Am. Chem. Soc.*, 1992, **114**, 9080.
3 (a) Y. Y. C. Yeung Lam, Ko, R. Carrié, A. Muench and G. Becker, *J. Chem. Soc., Chem. Commun.*, 1984, 1634; (b) W. Rösch and M. Regitz, *Angew. Chem., Int. Ed. Engl.*, 1984, **23**, 900.
4 (a) S. L. Choong, A. Nafady, A. Stasch, A. M. Bond and C. Jones, *Dalton Trans.*, 2013, **42**, 7775; (b) S. L. Choong, C. Jones and A. Stasch, *Dalton Trans.*, 2010, **39**, 5774.
5 J. A. W. Sklorz, S. Hoof, N. Rades, N. De Rycke, L. Könczöl, D. Szieberth, M. Weber, J. Wiecko, L. Nyulászi, M. Hissler and C. Müller, *Chem. – Eur. J.*, 2015, **21**, 11096.
6 L. Dettling, M. Papke, J. A. W. Sklorz, D. Buzsáki, Z. Kelemen, M. Weber, L. Nyulászi and C. Müller, *Chem. Commun.*, 2022, **58**, 7745.
7 M. Papke, L. Dettling, J. A. W. Sklorz, D. Szieberth, L. Nyulászi and C. Müller, *Angew. Chem., Int. Ed.*, 2017, **56**, 16484.
8 G. Guisado-Barrios, J. Bouffard, B. Donnadieu and G. Bertrand, *Angew. Chem., Int. Ed.*, 2010, **49**, 4759.
9 M. H. Habicht, F. Wossidlo, T. Bens, E. A. Pidko and C. Müller, *Chem. – Eur. J.*, 2018, **24**, 944.
10 M. Blug, O. Piechaczyk, M. Fustier, N. Mézailles and P. Le Floch, *J. Org. Chem.*, 2008, **73**, 3258; Y. Hatanaka and T. Hiyama, *J. Org. Chem.*, 1988, **53**, 918.
11 (a) W. P. Norris and R. A. Henry, *Tetrahedron Lett.*, 1965, **17**, 1213; (b) J. Müller, K. Öfele and G. Krebs, *J. Organometal. Chem.*, 1974, **82**, 383; (c) L. Schaper, X. Wei, P. J. Altmann, K. Öfele, A. Pöthig, M. Drees, J. Mink, E. Herdtweck, B. Bechlars, W. A. Herrmann and F. E. Kühn, *Inorg. Chem.*, 2013, **52**, 7031.
12 (a) W. J. Transue, A. Velian, M. Nava, M. A. Martin-Drumel, C. C. Womack, J. Jiang, G. L. Hou, X. Bin Wang, M. C. McCarthy, R. W. Field and C. C. Cummins, *J. Am. Chem. Soc.*, 2016, **138**, 6731; (b) T. E. Gier, *J. Am. Chem. Soc.*, 1961, **83**, 1769; (c) E. S. Yang, A. Mapp, A. Taylor, P. D. Beer and J. Goicoechea, *Chem. – Eur. J.*, 2023, e202301648; T. Görlich, D. Frost, N. Boback, N. T. Coles, B. Dittrich, P. Müller, W. D. Jones and C. Müller, *J. Am. Chem. Soc.*, 2021, **143**, 19365.
13 (a) G. Guisado-Barrios, J. Bouffard, B. Donnadieu and G. Bertrand, *Angew. Chem., Int. Ed.*, 2010, **49**, 4759; (b) J. Bouffard, B. K. Keitz, R. Tonner, G. Guisado-Barrios, G. Frenking, R. H. Grubbs and G. Bertrand, *Organometallics*, 2011, **30**, 2617.
14 A. J. Arduengo III, F. Davidson, R. Krafczyk, W. J. Marshall and R. Schmutzler, *Monatsh. Chem.*, 2000, **131**, 251.
15 C. Tian, W. Nie, M. V. Borzov and P. Su, *Organometallics*, 2012, **31**, 1751.
16 A. Villinger, P. Mayer and A. Schulz, *Chem. Commun.*, 2006, 1236.
17 D. Munz, *Organometallics*, 2018, **37**, 275.
18 R. F. W. Bader, *Atoms in Molecules: A Quantum Theory*, Clarendon, Oxford, 1990.
19 L. Zhao, M. von Hopffgarten, D. M. Andrada and G. Frenking, *WIREs Comput. Mol. Sci.*, 2018, **8**, e13450.
20 S. Dutta, S. M. De, S. Bose, E. Mahal and D. Koley, *Eur. J. Inorg. Chem.*, 2020, 638.
21 (a) A. Krapp, F. M. Bickelhaupt and G. Frenking, *Chem. – Eur. J.*, 2006, **12**, 9196; (b) I. Fernández, N. Holzmann and G. Frenking, *Chem. – Eur. J.*, 2020, **26**, 14194; (c) L. Zhao, S. Pan and G. Frenking, *J. Chem. Phys.*, 2022, **157**, 034105.

**6** **Chemoselective Post-Synthesis Modification of Pyridyl-Substituted, Aromatic Phosphorus Heterocycles: Cationic Ligands for Coordination Chemistry**

Lea Dettling, Martin Papke, Moritz Ernst, Manuela Weber, Christian Müller

**Author contributions:**

Lea Dettling and Martin Papke designed the project and performed the experiments. Lea Dettling reproduced all synthesis procedures to ensure full characterization. Martin Papke, Manuela Weber and Moritz Ernst were responsible for the crystallographic characterization of several of the new compounds. Lea Dettling wrote the manuscript and the supporting information. Christian Müller supervised the project and revised the manuscript.

# Chemoselective Post-Synthesis Modification of Pyridyl-Substituted, Aromatic Phosphorus Heterocycles: Cationic Ligands for Coordination Chemistry

Lea Dettling+,[a] Martin Papke+,[a] Moritz J. Ernst,[a] Manuela Weber,[a] and Christian Müller*[a]

Triazaphospholes are potential polydentate ligands due to the presence of both phosphorus and nitrogen donor atoms within the aromatic 5-membered heterocycle. The incorporation of an additional pyridyl-substituent opens up the possibility of a post-synthesis modification *via* chemoselective and also step-wise alkylation exclusively of the nitrogen atoms. This can be controlled by the choice and by the stoichiometry of the electrophile and allows the targeted synthesis of a variety of novel mono- and dicationic ligands. Reaction with Cu(I)-halides causes the formation of cuprates of the type $[CuX_n]^{(n-1)-}$, which enables coordination of the π-acidic phosphorus donor to the negatively charged metal core, which is favored over the coordination by a strongly σ-donating nitrogen atom. The use of cationic triazaphosphole derivatives can be used as a strategy to enforce the coordination of the ligand to an electron rich metal solely *via* the phosphorus atom. However, there is a subtle balance between the formation of either coordination polymers or dimeric structures, as the substitution pattern on the heterocycle and the nature of the halide have a large influence on the coordination motifs formed.

## Introduction

According to the isolobal relationship between a trivalent phosphorus atom and a C–H fragment, 3*H*-1,2,3,4-triazaphospholes (**A**, Figure 1) are the phosphorus analogues of the well-known 1,4-disubstituted 1,2,3-triazoles. These $\lambda^3\sigma^2$-phosphorus heterocycles are easily accessible *via* a [3 + 2] cycloaddition reaction of organic azides and phosphaalkynes, without the need of a catalyst.[1] First synthesized in 1984 by Carrié and Regitz independently,[2] triazaphospholes have recently gained more interest as continued studies, particularly on their coordination chemistry and reactivity, are currently carried out.[3] As ambidentate ligands, triazaphospholes can coordinate to a metal centre either *via* the low-coordinated phosphorus atom or *via* the nitrogen donors $N^1$ or $N^2$ (**B**, Figure 1). Since triazaphospholes, just as the aromatic phosphinines, have strong π-accepting properties, a coordination of the phosphorus atom to an electron-rich Pt(0) centre is enabled, as observed by Jones *et al.* (**C**, Figure 1).[4] In addition, the same group also reported on a Ag(I) complex (**D**, Figure 1),[5] in which
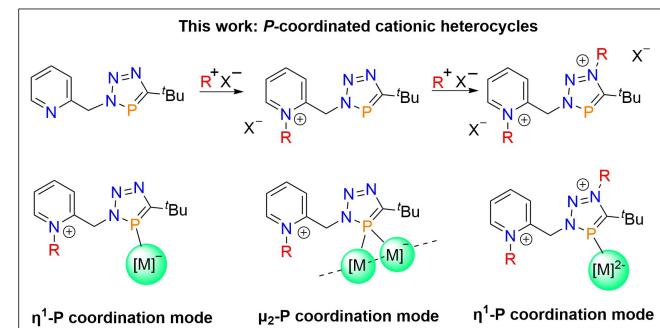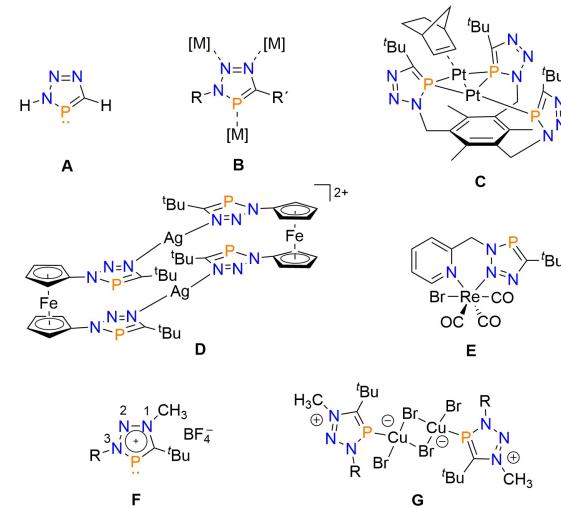


**Figure 1.** Triazaphosphole **A**, possible coordination modes **B**, triazaphospholenium salt (**F**) and coordination chemistry of triazaphospholes (**C**, **D**, **E**) and of triazaphospholenium salts (**G**).

[a]  M. Sc. L. Dettling,+ Dr. M. Papke,+ M. Sc. M. J. Ernst, M. Weber, Prof. Dr. C. Müller
Freie Universität Berlin
Institut für Chemie und Biochemie
Fabeckstr. 34/36, 14195 Berlin, Germany
E-mail: c.mueller@fu-berlin.de

[+]  These authors have contributed equally.

Supporting information for this article is available on the WWW under https://doi.org/10.1002/chem.202400592

the heterocycle binds *via* the $N^1$ atom to the metal centre. The functionalization of a triazaphosphole with a 2-pyridylmethyl-

**Chemistry–A European Journal**

Research Article
doi.org/10.1002/chem.202400592

**Chemistry
Europe**
European Chemical
Societies Publishing

group at the 3-position of the heterocycle opens up the possibility of accessing potential chelating ligands.

So far, however, only examples are known in which the triazaphosphole acts as an N,N-chelating ligand, as observed in the octahedral Re(CO)$_3$Br-complex **E** (Figure 1).[6] In this case the bidentate triazaphosphole coordinates *via* N$^2$ and the pyridine nitrogen donor.

Recently, we reported the successful synthesis of a triazaphospholenium salt by selectively alkylating the N$^1$-atom of the {PCN$_3$}-heterocycle with Meerwein's reagents (**F**, Figure 1, R = benzyl).[7] In accordance with the isolobal principle, the cationic heterocycles can be regarded as phosphorus congeners of the well-known 1,2,3-triazolylidenes, which are also referred to as mesoionic carbenes.[8] In the presence of Cu(I) salts, a neutral coordination compound of type **G** is formed (Figure 1), which is the first example of the coordination chemistry of this new ligand class.[7]

Based on our previous work, we decided to investigate the reactivity of pyridylmethyl-functionalized triazaphospholes with respect to alkylation reactions with electrophiles. We anticipated that the different electron densities at the nitrogen atoms may open up the possibility of a post-synthesis modification, for example a chemoselective and also a stepwise quaterniza-tion of the triazaphosphole derivative. This would allow the targeted synthesis of a variety of new cationic ligands, which might show an interesting coordination chemistry (Figure 1).

## Results and Discussion

Triazaphosphole **1** (Scheme 1) can be readily synthesized in high yield starting from *tert*-butylphosphaalkyne (ᵗBu–C≡P) and 2-(azidomethyl)-pyridine.[6] These [3 + 2] cycloaddition reactions between phosphaalkynes and azides are known to proceed regioselectively without a Cu(I) catalyst, as first demonstrated by Rösch and Regitz in 1984.[2] In light of our recently reported successful alkylation of the N$^1$-atom of benzyl-triazaphosphole **F** (Figure 1; R = benzyl) with Meerwein's salt,[7] compound **1** was reacted with one equivalent of trimethyloxonium tetrafluorobo-rate ([Me$_3$O][BF$_4$]) or triethyloxonium tetrafluoroborate ([Et$_3$O][BF$_4$]), respectively (Scheme 1).

The $^{31}$P{$^1$H} NMR spectrum of the reaction product **2a** reveals a single resonance at $\delta$(ppm) = 178.4 (**2b**: $\delta$(ppm) = 178.0). The rather small chemical shift difference compared to the starting material (**1**: $\delta$(ppm) = 172.4) is a first indication that the alkylation did not take place at one of the nitrogen atoms of the phosphorus heterocycle, but instead at the pyridine nitrogen atom. Moreover, the $^1$H NMR spectrum of **2a** show a
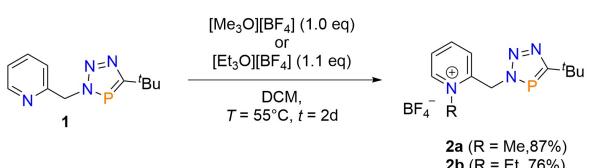
new singlet resonance in the aliphatic region at $\delta$(ppm) = 4.45 for one additional methyl group, while the $^1$H NMR spectrum of **2b** displays a quartet resonance at $\delta$(ppm) = 4.85 and a triplet resonance at $\delta$(ppm) = 1.63, as expected for the presence of an ethyl-substituent. Both results indicate a single, selective and quantitative alkylation. The $^1$H-$^{13}$C HMBC spectra (SI) of **2a/b** shows $^3J_{C\text{-}H}$ coupling between the carbon atoms of the pyridine ring and the protons of the methyl and ethyl groups, which is clear evidence for the alkylation of the nitrogen atom of the pyridine ring. Compounds **2a/b** were isolated as colourless solids and the molecular structure of **2b** was unambiguously confirmed by means of single crystal X-ray diffraction (Figure 2).

As expected, the alkylation of the nitrogen donor appears to have little effect on the bond lengths and angles within the molecule, which are comparable to those of the neutral pyridylmethyl-functionalized triazaphosphole derivatives.[6] The five-membered heterocycle is planar and the P(1)–C(1) bond length of 1.7205(12) Å is in-between the one of a P–C single bond (PPh$_3$: 1.83 Å)[9] and a P=C double bond ((diphenyl-methylene)-(mesityl)phosphane, MesP=CPh$_2$: 1.692 Å).[10] The N(1)–P(1)–C(1) angle of 86.33(5)° is close to 90°, which is also typical for neutral triazaphospholes.

The observation that the alkylation with Meerwein's salts takes place selectively at the pyridine nitrogen atom confirms the assumption that the electron density at the pyridine nitrogen atom is higher than that of all nitrogen atoms of the triazaphosphole.[7,8] In fact, a low basicity of the nitrogen atoms in the {PCN$_3$}-heterocycle has already been observed in the constitutional 1,2,4,3-isomers of triazaphospholes.[11]

Methyl iodide (MeI) is a frequently used reagent for the alkylation of 1,2,3-triazoles with the aim to access mesoionic carbenes.[12] Thus, reacting an excess of methyl iodide (4.0 eq) with compound **1** in acetonitrile at $T = 80\,°C$ leads to the formation of a light-yellow solid in very good yield (92%, Scheme 2). The $^{31}$P{$^1$H} NMR spectrum again shows a slightly shifted ($\Delta\delta = 5.0$ ppm) new signal at $\delta$(ppm) = 177.4, which is in the same region as observed for **2a** and **2b**. This indicates again, that the alkylation with MeI only takes place at the pyridine nitrogen atom. Further evidence is provided by the aliphatic region in the $^1$H NMR spectrum as well as by the
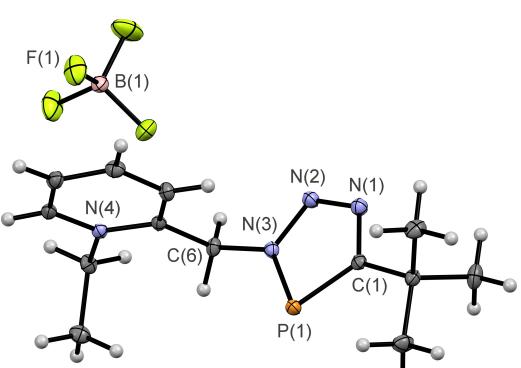


**Figure 2.** Molecular structure of **2b** in the crystal. Displacement ellipsoids are shown at the 50% probability level. Selected bond lengths (Å) and angles (°): P(1)–N(3): 1.6908(11), P(1)–C(1): 1.7205(12), N(4)–C(12): 1.4926(15); N(3)–P(1)–C(1): 86.33(5).



**Scheme 1.** Formation of the pyridinium-methyl-triazaphospholes **2a** and **2b**.

*Chem. Eur. J.* **2024**, e202400592 (2 of 10)

© 2024 The Authors. Chemistry - A European Journal published by Wiley-VCH GmbH

51
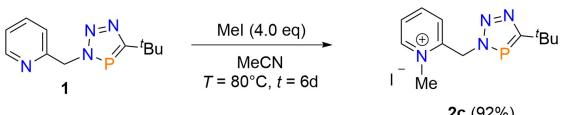
**Scheme 2.** Formation of the pyridinium-methyl-triazaphosphole **2c**.

corresponding ^{1}H-^{13}C HMBC spectrum (Figure S18). We therefore assume that compound **2c** has been formed selectively.

Interestingly, even when using a high excess of methyl iodide, no reaction at one of the nitrogen atoms of the heterocycle was observed. This clearly contrasts the observation that triazoles generally react with MeI. However, it is consistent with the fact that MeI is a much weaker methylating reagent compared to trimethyloxonium tetrafluoroborate and is particularly used for the alkylation of "soft" donor centers.[13]

We therefore anticipated that the alkylation of the nitrogen atom N[1] of the triazaphosphole, which is considered to show the highest electron density in accordance to the analogous triazoles, might be achieved by adding a second equivalent of Meerwein's salt.[7,14] Thus, 1.1 equivalents of trimethyloxonium tetrafluoroborate, respectively triethyloxonium tetrafluoroborate, were added to a solution of the triazaphosphole **2a** in dichloromethane (Scheme 3). After a reaction time of two days, the ^{31}P{^{1}H} NMR spectra of both reaction mixtures showed the formation of a new resonance with a chemical shift of $\delta$(ppm) = 212.2 (**3a'**) and 210.5 (**3a''**). This is indeed characteristic for alkylated triazaphospholes, the so called triazaphospholenium salts, which were recently reported by us for the first time.[7] Moreover, the aliphatic region in the ^{1}H NMR spectra shows only an additional resonance for the second methyl group (**3a'**: $\delta$(ppm) = 4.49), respectively two resonances for the ethyl group (**3a''**: $\delta$(ppm) = 4.83 (q), 1.63 (t)). A similar reactivity can be observed starting from the ethylpyridinium-triazaphosphole **2b** and trimethyloxonium tetrafluoroborate, yielding the triazaphospholenium salt **3b'**. Remarkably, the yields for the second reaction are as good as for the first alkylation (81% (**3a'**); 85% (**3a''**), 89% (**3b'**), Scheme 3a). A one-step synthesis of **3a'** and **3b''** directly from the **1** is also possible by adding two

equivalents of the corresponding Meerwein's salt and extending the reaction time to 4 days (Scheme 3b).

By diffusing dichloromethane into a concentrated solution of **3b''** in acetonitrile afforded single crystals of this compound, suitable for a crystallographic analysis (Figure 3). The solid-state structure of **3b''** clearly shows the presence of the anticipated dicationic heterocycle. Bond angles and lengths in the pyridine moiety are similar to the values found for **2b**. Likewise the bond lengths and angles of the triazaphospholenium ring are similar to the values observed for the benzyl-substituted triazaphospholenium salt (**3b''**: P(1)–C(1): 1.711(3), N(3)–P-(1)–C(1): 86.56(16); **F**: P–C: 1.723(2), N–P–C: 86.81(10), Figure 1).[7] The planarity of the heterocycle still suggests a high degree of aromaticity within the phosphorus heterocycle, while the P(1)–C(1) bond length is in-between the one of a single and a double bond.

From these results it can be concluded that the alkylation of the nitrogen atoms in triazaphospholes is chemoselective and can be controlled by the choice of alkylation reagent as well as by the stoichiometry of the alkylation reagent.

We were further interested in exploring the coordination chemistry of the novel monocationic compounds **2** and the dicationic heterocycles **3**. It is apparent that **2** and **3** cannot function as a chelating ligand anymore as observed for 2-pyridylmethyl-functionalized triazaphospholes (**E**, Figure 1).

Consequently, we anticipated that **2a–c** will either coordinate *via* the nitrogen atom N[1] and N[2] of the heterocycle or, alternatively, *via* the π-acidic phosphorus donor. In metal complexes containing the dicationic ligands **3**, a coordination should consequently exclusively occur *via* the phosphorus atom, as observed for the benzyl-substituted triazaphospholenium salt **F** (Figure 1).

In analogy to the formation of **G** from **F** (Figure 1), **2a** was reacted with 3.0 equivalents of CuBr·SMe$_2$ in THF (Scheme 4a). The ^{31}P{^{1}H} NMR spectra recorded from the reaction mixture showed a slightly shifted resonance at $\delta$(ppm) = 175.6 when compared to the staring material. Typically, only a marginal shift of the phosphorus resonance is observed upon coordination of a triazaphosphole to Cu(I) *via* the phosphorus atom.[7] After purification and removal of the byproduct CuBF$_4$, the new





**Figure 3.** Molecular structure of **3b''** in the crystal. Displacement ellipsoids are shown at the 50% probability level. Selected bond lengths (Å) and angles (°): P(1)–N(3): 1.698(4), P(1)–C(1): 1.711(3), N(1)–C(14): 1.492(4), N(4)–C(12): 1.507(5); N(3)–P(1)–C(1): 86.56(16).

**Scheme 3.** Formation of the pyridinium-methyl-triazaphospholium salts **3a'**, **3a''**, **3b'** and **3b''**.

*Chem. Eur. J.* **2024**, e202400592 (3 of 10)

52

**Chemistry–A European Journal**

Research Article
doi.org/10.1002/chem.202400592

**Chemistry**
**Europe**
European Chemical
Societies Publishing
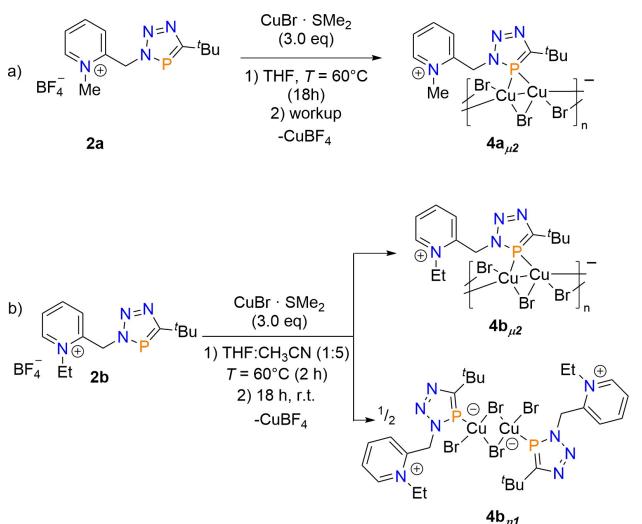
**Scheme 4.** Formation of Cu(I) coordination compounds of triazaphospholes **2a** and **2b**.

coordination compounds **4a**$_{\mu2}$ was obtained as yellow solid. Recrystallisation by cooling a saturated solution of **4a**$_{\mu2}$ in acetonitrile to $T = -21\,°C$ gave single crystals suitable for an X-ray crystal structure analysis. Recrystallisation from acetonitrile is, however, problematic as the products tend to decompose after some time under formation of [Cu(CH$_3$CN)$_4$]BF$_4$. Interestingly, the solid state structure of **4a**$_{\mu2}$ (Figure 4a) shows the formation of the neutral Cu(I) complex [LCu$_2$Br$_3$], consisting of the cationic ligand L$^+$ and the cuprate [Cu$_2$Br$_3$]$^-$. The phosphorus atom bridges two different Cu(I) centres (Cu(1), Cu(2)) in a $\mu_2$-P coordination mode. One bromido ligand acts as an additional bridging ligand for the two copper centres (Br(3)), while the two remaining bromido ligands (Br(1), (Br(2)) bridge

[LCu$_2$Br$_3$] units, forming a coordination polymer. Bond lengths of P(1)–Cu(1) = 2.2476(9) Å and P(1)–Cu(2) = 2.3065(9) Å are observed, while the Cu···Cu distance of 2.5499(6) Å is slightly shorter than the van der Waals distance $d$(Cu, Cu)$_{VDW}$ = 2.80 Å.[15] The five-membered heterocycle is still planar and shows comparable bond lengths and angles with compound **2a**.

It should be mentioned here that the bridging $\mu_2$-P coordination mode is common for low-coordinate phosphorus compounds. However, it has rarely been observed for triazaphospholes. To the best of our knowledge, only one example has been reported in literature, in which the heterocycle coordinates *via* the phosphorus atom in a bridging $\mu_2$-P coordination mode to a metal centre (**C**, Figure 1, electron rich Pt(0) centre).[4]

However, when the reaction mixture of **2b** and CuBr·SMe$_2$ was not worked up as described above for **2a** and **4a**$_{\mu2}$, two distinctive sets of crystals were directly formed from the solution at room temperature overnight. The X-ray crystallographic analysis of the yellow plates reveals a polymeric structure analogous to the one found for **4a**$_{\mu2}$, which is the coordination polymer **4b**$_{\mu2}$ (Scheme 4b, Table S4). On the other hand, the X-ray crystallographic analysis of the yellow blocks shows that a neutral Cu(I) dimer of the type [LCu$_2$Br$_4$] (**4b**$_{\eta1}$) has been formed additionally, which is not surprising for coordination compounds of copper halides (Scheme 4b, Figure 5).[17b] In comparison to **4b**$_{\mu2}$ the phosphorus atoms in **4b**$_{\eta1}$ (P(1)) only coordinate to one copper centre(Cu(1)) of the [Cu$_2$Br$_4$]$^{2-}$ core in an $\eta^1$ coordination mode (P(1)–Cu(1) = 2.2300(5) Å). Compared to the neutral Cu(I) dimer **G** (Figure 1), formed from the benzyl substituted triazapholenium salt and CuBr·SMe$_2$ (P(1)–Cu(1): 2.5251(5)), this bond is significantly shorter, suggesting a stronger P–Cu bond interaction in **4b**$_{\eta1}$.

Having synthesized the pyridinium-iodide **2c** (Scheme 2), we anticipated that this compound can directly be converted with CuI·SMe$_2$ to the corresponding coordination compound, without formation of CuBF$_4$ as byproduct (Scheme 5). When reacting **2c** with a slight excess of CuI·SMe$_2$, the $^{31}$P{$^1$H} NMR spectrum of the reaction mixture shows a single signal at
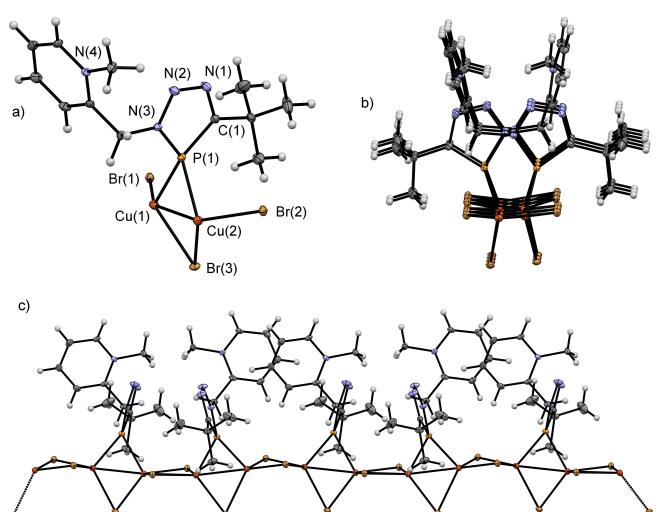


**Figure 4.** Molecular structure of **4a**$_{\mu2}$ in the crystal. Displacement ellipsoids are shown at the 50% probability level The solvent molecule (CH$_3$CN) is omitted for clarity. Selected bond lengths (Å) and angels (°): P(1)–N(3): 1.686(3), P(1)–C(1): 1.720(3), Cu(1)–P(1): 2.2476(9), Cu(2)–P(1): 2.3065(9), Cu(1)–Cu(2): 2.5499(6); N(3)–P(1)–C(1): 87.56(15), C(1)–P(1)–Cu(1): 135.26(12), Cu(1)–P(1)–Cu(2): 68.09(3).
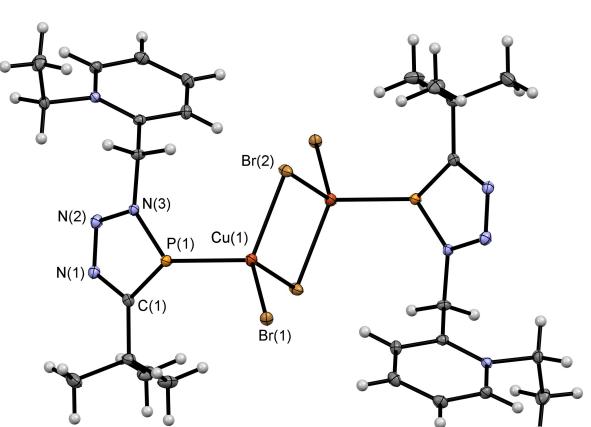


**Figure 5.** Molecular structure of **4b**$_{\eta1}$ in the crystal. Displacement ellipsoids are shown at the 50% probability level. Selected bond lengths (Å) and angels (°): **4b**$_{\eta1}$: P(1)–N(3): 1.6931(13), P(1)–C(1): 1.7258(15), Cu(1)–P(1): 2.2300(5); N(1)–P(1)–C(1): 86.61(7), Br(1)–Cu(1)–P(1): 108.350(16).

*Chem. Eur. J.* **2024**, e202400592 (4 of 10)

© 2024 The Authors. Chemistry - A European Journal published by Wiley-VCH GmbH

53

**Chemistry–A European Journal**

Research Article
doi.org/10.1002/chem.202400592

**Chemistry
Europe**
European Chemical
Societies Publishing
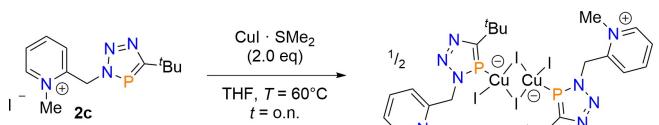
**Scheme 5.** Formation of copper(I) compound of triazaphsophole **2c**.

$\delta$(ppm) $= 170.8$, which is slightly shifted compared to the free ligand (**2c**: $\delta$(ppm) $= 177.4$).

The crystallographic characterization of **4c**$_{\eta 1}$ revealed, that indeed a dimer of the type $[L_2Cu_2I_4]$ had been formed, which is isostructural to **4b**$_{\eta 1}$ (Figure 6). Surprisingly, the use of CuI·SMe$_2$ instead of CuBr·SMe$_2$ has little effect on the structural parameter.

The phosphorus atom P(1) coordinates to the Cu(1) centre in an $\eta^1$ fashion, while the P(1)—Cu(1) bond length is only slightly shorter than in **4b**$_{\eta 1}$ (**4c**$_{\eta 1}$: 2.2382(6) Å; **4b**$_{\eta 1}$: 2.2300(5) Å). The trizaphsphole heterocycle is again planar and shows bond lengths and angles comparable to the ones observed in ligand **2c**.

Interestingly, in all coordination compounds described above, no coordination *via* one of the nitrogen atoms of the triazaphosphole ring is observed. This renders these compounds to one of the very few examples in which the coordination of the triazaphosphole heterocycle occurs *via* the $\pi$-acidic phosphorus atom. To the best of our knowledge, **4a–c** are the first Cu(I) complexes containing a triazaphosphole ligand with either a $\mu_2$-P or an $\eta^1$ coordination mode. Our results demonstrate, that the use of cationic triazaphospholes can thus be used as a strategy to enforce the coordination of the triazaphosphole to an electron rich metal *via* the phosphorus atom. As cuprates of the type $[CuX_n]^{(n-1)-}$ are formed, the coordination of the $\pi$-acidic phosphorus donor to the cuprate core is evidently favored over the coordination of a strongly $\sigma$-donating nitrogen atom.

Having explored the coordination chemistry of the monocationic heterocycles in the salts **2a–c** in detail, we turned our attention to the reaction of the dicationic systems **3a'–3b"** with CuBr·SMe$_2$. We chose for using 3 equivalents of the Cu(I) precursor to allow the formation of two equivalents of CuBF$_4$ as a byproduct and to enforce the generation of a mononuclear compound containing a $[CuBr_3]^{2-}$ core. Dissolving **3a'** in dichloromethane or THF turned out to be difficult, and the presumed product precipitated out of solution as an orange-coloured solid. The NMR spectroscopic characterization of this compound in CD$_3$CN showed only decomposition of the ligand. However, using **3a"** as a starting material proved to be more straightforward (Scheme 6). Even though the NMR spectroscopic characterization of the product **5** turned out to be difficult due to solubility reasons, we were able to obtain single crystals of **5**$_{\eta 1}$, suitable for crystallographic characterization, from a mixture of THF:CH$_3$CN (5:1). The molecular structure of **5**$_{\eta 1}$ in the crystal and the corresponding structural parameters are depicted in Figure 7.

As proposed from the stoichiometry of the reagents used, the solid state structure of **5**$_{\eta 1}$ reveals that a neutral mononuclear Cu(I) complex has indeed been formed, that shows that the phosphorus atom of the dicationic ligand coordinates in an $\eta^1$-fashion to a $[CuBr_3]^{2-}$ core.
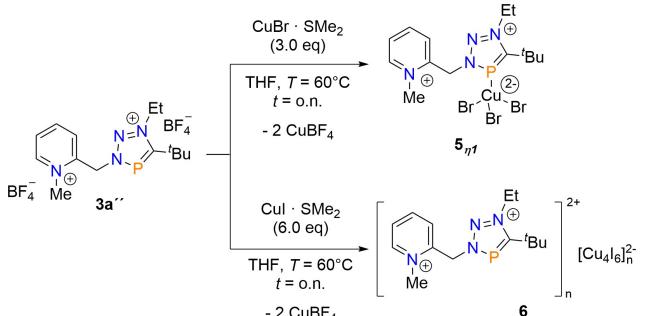


**Scheme 6.** Formation of Cu(I) compound of triazaphospholenium salts **3a"**.
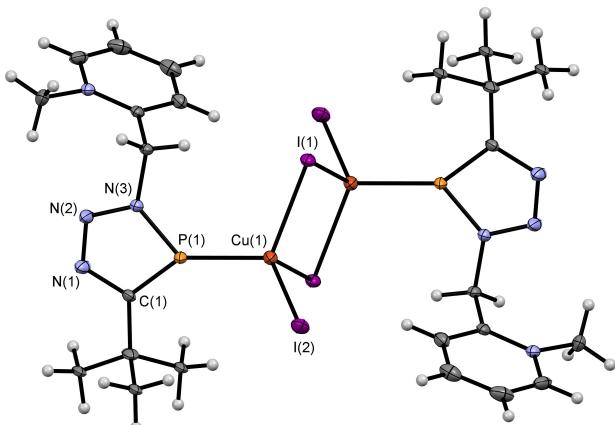


**Figure 6.** Molecular structure of **4c**$_{\eta 1}$ in the crystal. Displacement ellipsoids are shown at the 50% probability level. Selected bond lengths (Å) and angels (°): P(1)—N(3): 1.6816(19), P(1)—C(1): 1.725(2), Cu(1)—P(1): 2.2382(6); N(3)—P(1)—C(1): 87.11(10), I(2)—Cu(1)—P(1): 111.55(2).
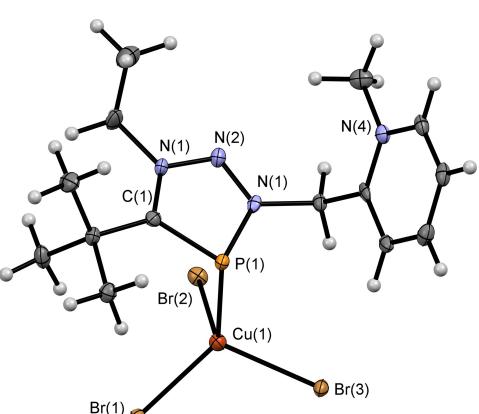


**Figure 7.** Molecular structure of **5**$_{\eta 1}$ in the crystal. Displacement ellipsoids are shown at the 50% probability level. Selected bond lengths (Å) and angels (°): P(1)—N(1): 1.703(4), P(1)—C(1): 1.730(5), Cu(1)—P(1): 2.4692(14); N(1)—P(1)—C(1): 86.4(2), N(1)—P(1)—Cu(1): 96.48(14).

**Chemistry–A European Journal**

Research Article
doi.org/10.1002/chem.202400592

**Chemistry Europe**
European Chemical
Societies Publishing

The triazaphospholenium heterocycle is planar, indicating that the aromaticity of the ligand is not disturbed. Nevertheless, the bonding situation in $5_{\eta1}$ deserves special attention, as the phosphorus atom adopts a pyramidal geometry and the Cu(I) is located below the plane of the heterocycle (N(1)–P(1)–Cu(1): 96.48(14)°). The P(1)–Cu(1) bond is with 2.4692(14) Å longer than observed in complexes $4a_{\mu2}$ (Cu(2)–P(1): 2.3065(9)) and $4b_{\eta1}$ (Cu(1)–P(1): 2.2300(5)) but shorter than the sum of the van der Waals radii of a phosphorus and a copper atom.[15] This arrangement is similar to the bonding situation observed in the previously reported Cu(I) complex of the benzyl substituted triazaphospholenium salt **G** (Figure 1). We therefore anticipate, that also in this case, the bonding situation in $5_{\eta1}$ can be described as an "inverse-dative" M→L donor-acceptor bond. Such a bonding situation has also been observed in Cu(I) coordination compounds of *N*-heterocyclic phosphenium cations.[15]

Furthermore, the reaction of CuI·SMe₂ with compound **3a''** afforded an orange solid (Scheme 6). The better solubility of the product compared to the $5_{\eta1}$ allowed for an NMR spectroscopic investigation. A new resonance in the $^{31}P\{^{1}H\}$ NMR spectrum of **6** was observed at $\delta(ppm) = 206.5$ (**3a''**: $\delta(ppm) = 210.5$). Single crystals suitable for a crystallographic characterization were obtained by cooling a saturated solution of **6** in acetonitrile to $T = -21\,°C$. Surprisingly, the structural analysis of **6** reveals the presence of an ion pair in the asymmetric unit between the dicationic ligand and a $[Cu_4I_6]^{2-}$ core with no direct coordination of the phosphorus atom P(1) to one of the Cu(I)-ions (Figure 8).

Moreover, the dicationic ligands are located between parallelly oriented polymeric ribbons of the anions. This structural motif is one of the very few examples known in literature.[16] Taking a closer look at the infinite $[Cu_4I_6]^{2-}_n$ polymer, it consists of edge-shared $[Cu_2I_2]$ rhombohedrons with the copper atoms of every second rhombohedron being bridged by an additional iodido ligand. The bridging iodide anion conveys the copper atoms in proximity, changing the distance between the copper atoms from Cu(1)–Cu(2)$_{nonbridged}$: 2.6985(10) to Cu(2)–Cu(3)$_{bridged}$: 2.5083(9). This is in accordance with literature reports on the formation of this type of $[Cu_4I_6]_n$ polymers.[17]

Lastly, CuBr·SMe₂ was added to **3b''** yielding $7_{\eta1}$ as an orange solid (Scheme 7).

The $^{31}P\{^{1}H\}$ NMR spectrum of $7_{\eta1}$ shows the formation of a new species with a resonance at $\delta(ppm) = 200.9$ (**3b''**: $\delta(ppm) = 210.1$). Single crystals of $7_{\eta1}$, suitable for a crystallographic characterization, were obtained from an acetonitrile solution. In the solid state, $7_{\eta1}$ shows a polymeric zigzag chain of $[CuBr_2]$ units, while the coordination sphere of each Cu(I) centre is completed by a dicationic ligand, which is $\eta^1$-coordinated *via* the π-acidic phosphorus atom P(1), and an additional bromido ligand. The remaining $[BF_4]^-$ anion completes the structure of $7_{\eta1}$ (Figure 9). The $^{19}F$ and $^{11}B$ NMR spectra also confirm the presence of the $[BF_4]^-$ counterion.
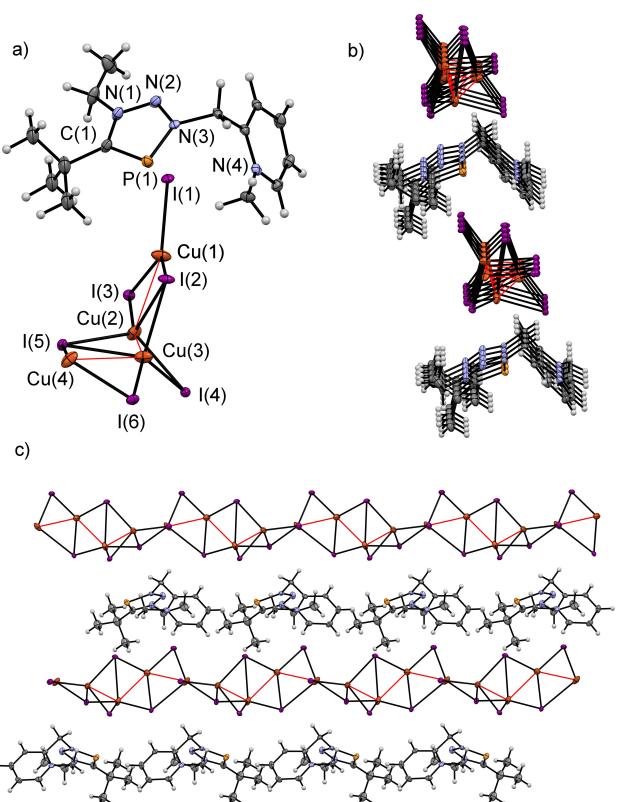


**Figure 8.** Molecular structure of **6** in the crystal. Displacement ellipsoids are shown at the 50% probability level. Selected bond lengths (Å) and angels (°): P(1)–N(3): 1.698(4), P(1)–C(1): 1.716(5), Cu(1)–Cu(2): 2.6985(10)Cu(2)–Cu(3): 2.5083(9) ; N(1)–P(1)–C(1): 87.1(2).
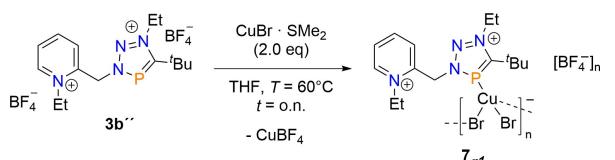


**Scheme 7.** Formation of copper(I) compound of triazaphospholenium salts **3b''**.

## Conclusions

We could demonstrate that pyridyl-functionalized triazaphospholes provide the possibility for a post-synthesis modification, affording a variety of mono- and dicationic species. This is achieved by a chemoselective and stepwise alkylation exclusively of the nitrogen atoms and can be controlled by the choice and by the stoichiometry of the used electrophile. This targeted synthesis opens up a fascinating coordination chemistry, as the reaction of the charged triazaphosphole derivatives with Cu(I)-halides causes the formation of cuprates of the type $[CuX_n]^{(n-1)-}$. Monocationic triazaphosphole derivatives from either coordination polymers containing $[Cu_2Br_3]^-$ cores, or dimeric structures with $[Cu_2Br_4]^{2-}$, respectively $[Cu_2I_4]^{2-}$ units. Dicationic triazaphospholenium salts, on the other hand, form mononuclear species containing a $[CuBr_3]^{2-}$ fragment, coordination polymers consisting of infinite *P*-coordinated

*Chem. Eur. J.* **2024**, e202400592 (6 of 10)

© 2024 The Authors. Chemistry - A European Journal published by Wiley-VCH GmbH

**Chemistry–A European Journal**

Research Article
doi.org/10.1002/chem.202400592

**Chemistry Europe**
European Chemical
Societies Publishing
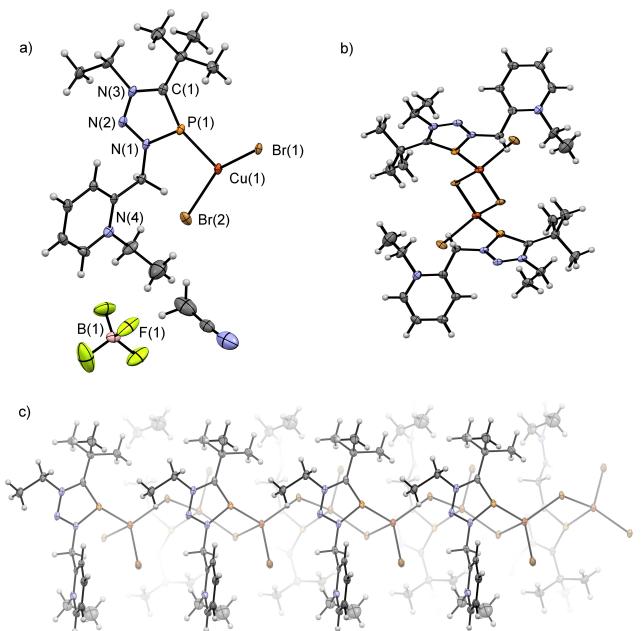
**Figure 9.** Molecular structure of **7$_{\eta1}$** in the crystal. Displacement ellipsoids are shown at the 50% probability level. The BF$_4$ anion and a CH$_3$CN molecule is omitted for clarity in b) and c). Selected bond lengths (Å) and angels (°): P(1)–N(1): 1.688(3), P(1)–C(1): 1.718(3), Cu(1)–P(1): 2.2088(9), N(1)–P(1)–C(1): 87.57(14).

[CuBr$_2$]$^-$ chains with integrated [BF$_4$]$^-$ ions, as well as cuprates with no direct coordination of the ligand to the polymeric [Cu$_4$I$_6$]$^{2-}$$_n$ chain. The substitution pattern on the heterocycle and the nature of the halide have a large influence on the coordination motifs formed and, consequently, there is a subtle balance between the formation of either coordination polymers or dimeric structures. In case of a direct Ligand-Cu interaction, the coordination of the ligand to the negatively charged metal core takes exclusively place *via* the π-acidic phosphorus donor, which is apparently favoured over the interaction *via* a strongly σ-donating nitrogen atom. Consequently, the use of cationic triazaphosphole derivatives can be used as a strategy to enforce the coordination of the ligand to an electron rich metal solely *via* the phosphorus atom, thus enabling the access to new coordination compounds of five-membered, aromatic phosphorus heterocycles.

## Experimental Section

### General Remarks

All reactions were preformed using an MBRAUN glovebox under an argon atmosphere or standard Schlenk techniques. All common solvents and chemicals were commercially available. 2-(Azidomethyl)pyridine,[18] (2,2-Dimethylpropylidyn)phosphan and (*tert*-butylphosphaalkyne)[19] were prepared by methods described in the literature. The temperatures reported are oil bath temperatures. Commercially available chemicals were used without further purification. DCM, MeCN and *n*-pentane were prepared using an MBRAUN Solvent Purification System MB-SPS 800. THF was dried

over K/benzophenone under argon and Et$_2$O was dried over Na under argon. ESIMS spectra were recorded on an Agilent 6210 ESI-TOF (4 kV) from Agilent Technologies. EI measurements were conducted with a modified device of a MAT 711 from Varian MAT. The intensities for the X-ray determinations were collected on a D8 Venture, Bruker Photon CMOS diffractometer with Mo/K$\alpha$ or Cu/K$\alpha$ radiation.[20] Semi-empirical or numerical absorption corrections were carried out by the SADABS or X-RED32 programs[21] Structure 535 solution and refinement were performed with the SHELX programs[22] included in OLEX2.[23] Hydrogen atoms were calculated for the idealized positions and treated with the 'riding model' option of SHELXL. Since some of the compounds crystallized together with disordered solvent molecules (partially close to special positions), the refinements of such structures were undertaken with the removal of the disordered solvent molecules using the solvent mask option of OLEX2. The representation of molecular structures was done using the Mercury 3.0 (2022).[24] Deposition Numbers https://www.ccdc.cam.ac.uk/services/structures?id=doi: 10.1002/chem.202400592 2331037 (for **2b**), 2331035 (for **3b′′**), 2331040 (for **4a$_{\mu2}$**), 2331042 (for **4b$_{\mu2}$**), 2331036 (for **4b$_{\eta1}$**), 2331038 (for **4c$_{\eta1}$**), 2331034 (for **5$_{\eta1}$**), 2331041 (for **6**), 2331039 (for **7$_{\eta1}$**) contain the supplementary crystallographic data for this paper. These data are provided free of charge by the joint Cambridge Crystallographic Data Centre and Fachinformationszentrum Karlsruhe http://www.ccdc.cam.ac.uk/structures. Details of the X-ray structure determinations and refinements are provided in Table S1–S9.

### 2-((5-(tert-Butyl)-3H-1,2,3,4-triazaphosphol-3-yl)methyl)pyridine (1)[6]

Triazaphosphole **1** was synthesized by condensing an excess of *tert*-butylphosphaalkyne into a solution of 2-(azidomethyl)pyridine (1.31 g, 9.75 mmol) in 60 mL THF. After stirring the reaction mixture for 12 hours at room temperature excess of the phosphaalkyne together with THF was condensed out of the reaction solution leaving an off white solid. Purification of the crude product was carried out by recrystallization from *n*-pentane. **1** was obtained as a colourless solid (1.97 g, 84%). $^1$H NMR (400 MHz, DCM-$d_2$): $\delta = 8.60$–8.53 (m, 1H, $H_{Ar}$), 7.69 (t, $J = 7.7$ Hz, 1H, $H_{Ar}$), 7.29–7.17 (m, 2H, $H_{Ar}$), 5.82 (d, $J = 6.8$ Hz, 2H, methylen), 1.44 (s, 9H, C(CH3)3) ppm. $^{31}$P{$^1$H} NMR (162 MHz, DCM-$d_2$): $\delta = 172.4$ ppm.

### 2-((5-(tert-butyl)-3H-1,2,3,4-triazaphosphol-3-yl)methyl)-1-methyl-pyridin-1-ium tetrafluoroborate (2a)

**1** (385 mg, 1.64 mmol) and trimethyloxonium tetrafluoroborate (243 mg, 1.64 mmol) were added in a Schlenk flask and dissolved in DCM (10 mL). The reaction mixture was stirred at $T = 55\,°C$ for two days. Removal of the solvent in vacuum gave an off white solid. Washing of the solid with diethyl ether (3×10 mL) and subsequent drying in vacuum yielded **2a** (483 mg, 87%) as a colorless solid. $^1$H NMR (400 MHz, DCM-$d_2$): $= 8.79$ (d, $J = 6.1$ Hz, 1H, $H$Ar), 8.37 (t, $J = 8.2$ Hz, 1H, $H$Ar), 7.92 (t, $J = 7.0$ Hz, 1H, $H$Ar), 7.34 (d, $J = 8.0$ Hz, 1H, $H$Ar), 6.20 (d, $J = 5.3$ Hz, 2H, methylen), 4.45 (s, 3H, N-C$H$3), 1.43 (s, 9H, C(C$H_3$)$_3$) ppm. $^{13}$C{$^1$H} NMR (101 MHz, DCM-$d_2$): $\delta = 200.4$ (d, $J = 57.6$ Hz, C$=$P), 153.5 (C$_{Ar}$), 147.8 (C$_{Ar}$), 146.7 (C$_{Ar}$), 128.0 (C$_{Ar}$), 128.0 (C$_{Ar}$), 51.5 (d, $J = 14.7$ Hz, methylen), 46.7 (N-C$H_3$), 35.8 (d, $J = 15.3$ Hz, $C$(CH3)3), 31.7 (d, $J = 7.7$ Hz, C(C$H_3$)$_3$) ppm. $^{31}$P{$^1$H} NMR (162 MHz, DCM-$d_2$): $\delta = 178.4$ ppm. $^{19}$F NMR (377 MHz, DCM-$d_2$): $\delta = -151.3$ ppm. $^{11}$B NMR (129 MHz, DCM-$d_2$): $\delta = -1.3$ ppm. **ESI-TOF** (m/z): 249.1295 g/mol (calculated: 249.1246 g/mol) [M]$^+$.

**Chemistry–A European Journal**

Research Article

doi.org/10.1002/chem.202400592

**Chemistry**
**Europe**
European Chemical
Societies Publishing

## 2-((5-(tert-Butyl)-3H-1,2,3,4-triazaphosphol-3-yl)methyl)-1-ethyl-pyridin-1-ium tetrafluoroborate (2 b)

**1** (171 mg, 0.73 mmol) and triethyloxonium tetrafluoroborate (153 mg, 0.80 mmol) were added in a Schlenk flask and dissolved in DCM (5 mL). The reaction mixture was stirred at $T = 55\,°C$ for two days. Removal of the solvent in vacuum gave an off white solid. Washing of the solid with diethyl ether (3×10 mL) and subsequent drying in vacuum yielded **2 b** (195 mg, 76%) as a colorless solid. ¹**H NMR** (400 MHz, DCM-$d_2$): $\delta = 8.86$ (dd, $J = 6.2$, 1.2 Hz, 1H, *H*Ar), 8.41 (td, $J = 7.9$, 1.4 Hz, 1H, *H*Ar), 8.02 (ddd, $J = 7.7$, 6.3, 1.5 Hz, 1H, *H*Ar), 7.53 (d, $J = 8.0$ Hz, 1H, *H*Ar), 6.23 (d, $J = 5.2$ Hz, 2H, methylen), 4.82 (q, $J = 7.3$ Hz, 2H, $CH_2CH_3$), 1.60 (t, $J = 7.3$ Hz, 3H, $CH_2CH_3$), 1.45 (d, $J = 1.4$ Hz, 9H, C(C*H*$_3$)3) ppm. ¹³**C{¹H} NMR** (101 MHz, DCM-$d_2$): $\delta = 200.4$ (d, $J = 57.6$ Hz, C=P), 152.7 (CAr), 146.7 (CAr), 146.4 (CAr), 129.4 (CAr), 128.7 (CAr), 54.9 ($CH_2CH_3$), 51.3 (d, $J = 14.9$ Hz, methylen), 36.0 (d, $J = 15.4$ Hz, $C(CH_3)_3$), 31.7 (d, $J = 7.6$ Hz, C(CH₃)₃), 16.1 ($CH_2CH_3$) ppm. ³¹**P{¹H} NMR** (162 MHz, DCM-$d_2$): $\delta = 178.0$ ppm. ¹⁹**F NMR** (377 MHz, DCM-$d_2$): $\delta = -152.1$ ppm. ¹¹**B NMR** (129 MHz, DCM-$d_2$): $\delta = -1.3$ ppm. ESI-TOF (m/z): 263.1432 g/mol (calculated: 263.1420 g/mol) [M]⁺.

## 2-((5-(tert-butyl)-3H-1,2,3,4-triazaphosphol-3-yl)methyl)-1-methyl-pyridin-1-ium iodide (2 c)

**1** (217 mg, 0.93 mmol) was dissolved in MeCN (15 mL) and methyl iodide (526 mg, 3.71 mmol) was added. The reaction mixture was stirred at $T = 80\,°C$ for six days, then cooled to room temperature and the solvent was removed *in vacuo*. Washing of the solid with diethyl ether (3 x 10 mL) and subsequent drying in vacuum yielded **2 c** (345 mg, 92%) as a slightly yellow solid. ¹**H NMR** (400 MHz, MeCN-$d_3$): $\delta = 8.78$ (ddt, $J = 6.2$, 1.5, 0.7 Hz, 1H, H$_{Ar}$), 8.42 (td, $J = 8.0$, 1.5 Hz, 1H, H$_{Ar}$), 7.95 (ddd, $J = 7.8$, 6.1, 1.5 Hz, 1H, H$_{Ar}$), 7.34 (d, $J = 7.8$ Hz, 1H, H$_{Ar}$), 6.26 (d, $J = 5.6$ Hz, 2H, methylen), 4.38 (s, 3H, Py-CH₃), 1.47 (d, $J = 1.5$ Hz, 9H,C(CH₃)₃) ppm. ¹³**C{¹H NMR** (101 MHz, MeCN-$d_3$): $\delta = 200.3$ (d, $J = 56.8$ Hz, C=P), 154.3 (C$_{Ar}$), 148.1 (C$_{Ar}$), 147.4 (C$_{Ar}$), 128.3 (C$_{Ar}$), 128.1 (C$_{Ar}$), 52.3 (d, $J = 14.4$ Hz, methylen), 47.2 (Py-CH₃), 36.0 (d, $J = 15.6$ Hz, $C(CH_3)_3$), 31.6 (d, $J = 7.7$ Hz, C(CH₃)₃) ppm. ³¹**P{¹H} NMR** (162 MHz, MeCN-$d_3$): $\delta = 177.4$ ppm. **ESI-TOF** (m/z): 249.1293 g/mol (calculated: 249.1264 g/mol) [M]⁺.

## General procedure to synthesize the dications (3 a', 3 a'', 3 b', 3 b'')

**Method A**: Trimethyloxonium tetrafluoroborate or triethyloxonium tetrafluoroborate (1.1 eq.) was added to a solution of the corresponding 3H-1,2,3,4-triazaphospholenium salt (1.0 eq.) in DCM (10 mL per 200 mg triazaphospholenium salt) and the reaction mixture was stirred at $T = 55\,°C$ for two days. The solvent was then removed in vacuo, the residue was washed with diethyl ether (3 x 10 mL per 200 mg reactant) and dried in vacuo.

**Method B**: (only for **3 a'** and **3 b''**) Trimethyloxonium tetrafluoroborate or triethyloxonium tetrafluoroborate (2.2 eq.) was added to a solution of the corresponding 3H-1,2,3,4-triazaphosphol (1.0 eq.) in DCM (10 mL per 200 mg triazaphosphol) and the reaction mixture was stirred at $T = 55\,°C$ for four days. The solvent was then removed in vacuo, the residue was washed with diethyl ether (3×10 mL per 200 mg reactant) and dried in vacuo.

## 2-((5-(tert-butyl)-1-methyl-3H-1,2,3,4-triazaphosphol-1-ium-3-yl)methyl)-1-methylpyridin-1-ium tetrafluoroborate (3 a')

**Method A**: The dication **3 a'** was synthesized from **2 a** (104 mg, 0.31 mmol) and trimethyloxonium tetrafluoroborate (50.0 mg,

0.34 mmol) in DCM (5 mL). **3 a'** was obtained as colorless solid (110 mg, 81%) **Method B**: The dication **3 a'** was synthesized from **1** (145 mg, 0.62 mmol) and trimethyloxonium tetrafluoroborate (201 mg, 1.36 mmol) in DCM (10 mL). **3 a'** was obtained as colorless solid (175 mg, 65%). ¹**H NMR** (500 MHz, MeCN-$d_3$): $\delta = 8.80$ (d, $J = 6.1$ Hz, 1H, HAr), 8.55 (t, $J = 8.0$ Hz, 1H, HAr), 8.06 (t, $J = 6.9$ Hz, 1H, HAr), 7.91 (d, $J = 8.1$ Hz, 1H, HAr), 6.23 (d, $J = 5.4$ Hz, 2H, methylen), 4.49 (d, $J = 1.0$ Hz, 3H, N-CH₃), 4.36 (s, 3H, Py-CH₃), 1.61 (d, $J = 2.5$ Hz, 9H, C(CH₃)₃) ppm. ¹³**C{¹H} NMR** (101 MHz, MeCN-$d_3$): $\delta = 193.4$ (d, $J = 64.0$ Hz, C=P), 150.6 (CAr), 149.0 (CAr), 147.9 (CAr), 130.2 (CAr), 129.5 (CAr), 55.2 (d, $J = 12.2$ Hz, methylen), 47.4 (Py-CH₃), 44.5 (N-CH₃), 36.3 (d, $J = 11.2$ Hz, C(CH₃)₃), 29.8 (d, $J = 11.1$ Hz, C(CH₃)3) ppm. ³¹**P {¹H} NMR** (162 MHz, MeCN-$d_3$): $\delta = 212.3$ ppm. ¹⁹**F-NMR** (377 MHz MeCN-$d_3$): $\delta = -151.6$ ppm. ¹¹**B NMR** (129 MHz MeCN-$d_3$): $\delta = -1.3$ ppm. ESI-TOF (m/z): 249.1285 g/mol (cal.: 249.1264 g/mol) [M–CH₃]⁺.

## 2-((5-(tert-butyl)-1-ethyl-3H-1,2,3,4-triazaphosphol-1-ium-3-yl)methyl)-1-methylpyridin-1-ium tetrafluoroborate (3 a'')

**Method A**: **2 a** (108 mg, 0.32 mmol) and triethyloxonium tetrafluoroborate (67.1 mg, 0.35 mmol) were dissolved in DCM (5 mL). **3 a''** was obtained as colorless solid (124 mg, 85%). ¹**H NMR** (500 MHz, MeCN-$d_3$): $\delta = 8.81$ (d, $J = 6.0$ Hz, 1H, *H*Ar), 8.55 (t, $J = 7.9$ Hz, 1H, *H*Ar), 8.05 (t, $J = 7.0$ Hz, 1H, *H*Ar), 7.96 (d, $J = 8.2$ Hz, 1H, *H*Ar), 6.26 (d, $J = 5.2$ Hz, 2H, methylen), 4.83 (q, $J = 7.2$ Hz, 2H, N-C*H*₂CH₃), 4.38 (s, 3H, Py-C*H*₃), 1.63 (t, $J = 7.2$ Hz, 3H, N-CH2C*H*₃), 1.60 (d, $J = 1.9$ Hz, 9H, C(C*H*₃)₃) ppm. ¹³**C{¹H} NMR** (101 MHz, MeCN-$d_3$): $\delta = 193.3$ (d, $J = 63.4$ Hz, C=P), 150.0 (CAr), 149.1 (CAr), 147.9 (CAr), 130.5 (CAr), 129.6 (CAr), 55.3 (d, $J = 12.7$ Hz, Methylen), 53.6 (N-CH2CH3), 47.4 (Py-CH₃), 36.3 (d, $J = 11.4$ Hz, $C(CH_3)_3$), 30.23 (d, $J = 11.3$ Hz, C(CH₃)₃), 15.28 (N-CH₂CH₃) ppm. ³¹**P{¹H} NMR** (162 MHz, MeCN-$d_3$): $\delta = 210.5$ ppm. ¹⁹**F NMR** (377 MHz MeCN-$d_3$): $\delta = -151.3$ (s) ppm. ¹¹**B NMR** (129 MHz MeCN-$d_3$): $\delta = -1.3$ ppm. **ESI-TOF** (m/z): 139.0846 g/mol (calculated: 139.0825 g/mol) [M]²⁺.

## 2-((5-(tert-butyl)-1-methyl-3H-1,2,3,4-triazaphosphol-1-ium-3-yl)methyl)-1-ethylpyridin-1-ium tetrafluoroborate (3 b')

**Method A**: **3 b'** was synthesized by adding trimethyloxonium tetrafluoroborate (76.0 mg, 0.51 mmol) to a solution of **2 b** (150 mg, 0.43 mmol) in DCM (5 mL). **3 b'** was obtained as colourless solid (173 mg, 89%). ¹**H NMR** (500 MHz, MeCN-$d_3$): $\delta = 8.87$ (dd, $J = 6.2$, 1.5 Hz, 1H, H$_{Ar}$), 8.54 (td, $J = 8.0$, 1.5 Hz, 1H, H$_{Ar}$), 8.10 (ddd, $J = 7.8$, 6.1, 1.5 Hz, 1H, H$_{Ar}$), 7.93 (d, $J = 8.1$ Hz, 1H, H$_{Ar}$), 6.26 (d, $J = 5.3$ Hz, 2H, methylen), 4.70 (q, $J = 7.3$ Hz, 2H, Py-C*H*₂CH₃), 4.48 (d, $J = 1.0$ Hz, 3H, N-CH₃), 1.64 (t, $J = 7.3$ Hz, 3H, Py-CH₂C*H*₃), 1.60 (d, $J = 2.4$ Hz, 9H, C(C*H*₃)₃) ppm. ¹³**C{¹H} NMR** (101 MHz, MeCN-$d_3$): $\delta = 193.4$ (d, $J = 64.0$ Hz, C=P), 150.0 (CAr), 149.1 (CAr), 147.9 (CAr), 130.3 (CAr), 129.6 (CAr), 55.2 (d, $J = 12.1$ Hz, methylen), 47.4 (Py-CH₃), 44.5 (N-CH₃), 36.3 (d, $J = 11.0$ Hz, C(CH₃)₃), 29.81 (d, $J = 11.2$ Hz, C(CH₃)₃) ppm. ³¹**P {¹H} NMR** (162 MHz, MeCN-$d_3$): $\delta = 212.1$ ppm. ¹⁹**F NMR** (377 MHz MeCN-$d_3$): $\delta = -151.4$ (s) ppm. ¹¹**B NMR** (129 MHz MeCN-$d_3$): $\delta = -1.3$ ppm. ESI-TOF (m/z): 139.0847 g/mol (calculated: 139.0825 g/mol) [M]²⁺

## 2-((5-(tert-butyl)-1-ethyl-3H-1,2,3,4-triazaphosphol-1-ium-3-yl)methyl)-1-ethylpyridin-1-ium tetrafluoroborate (3 b'')

**Method B**: **1** (236 mg, 1.01 mmol) was disolved in DCM (10 mL) and triethyloxonium tetrafluoroborate (402 mg, 2.12 mmol) was added to the reaction mixture. **3 b''** was obtained as colourless solid (395 mg, 84%). ¹**H NMR** (500 MHz, MeCN-$d_3$): $\delta = 8.87$ (dd, $J = 6.2$, 1.5 Hz, 1H, HAr), 8.55 (td, $J = 8.0$, 1.5 Hz, 1H, HAr), 8.11 (ddd, $J = 7.9$, 6.2, 1.6 Hz, 1H, HAr), 7.98 (dd, $J = 8.1$, 1.5 Hz, 1H, HAr), 6.27 (d, $J =$

**Chemistry–A European Journal**

Research Article
**doi.org/10.1002/chem.202400592**

**Chemistry Europe**
European Chemical
Societies Publishing

5.2 Hz, 2H, methylen), 4.82 (qd, $J = 7.2$, 1.0 Hz, 2H, N-C$H_2$CH$_3$), 4.72 (q, $J = 7.3$ Hz, 2H, Py-C$H_2$CH$_3$), 1.65 (t, $J = 7.3$ Hz, 3H, Py-CH$_2$C$H_3$), 1.61 (d, $J = 2.4$ Hz, 9H, C(CH$_3$)$_3$), 1.61 (t, $J = 7.2$ Hz, 3H, N-CH$_2$C$H_3$) ppm. $^{13}$C {$^1$H} NMR (101 MHz, MeCN-$d_3$): $\delta = 193.0$ (d, $J = 63.6$ Hz, C=P), 149.1 (CAr), 147.7 (CAr), 147.4 (CAr), 131.1 (d, $J = 0.9$ Hz, (CAr)), 129.9 (CAr), 55.3 (Py-CH$_2$CH$_3$), 54.7 (d, $J = 12.2$ Hz, methylen), 53.4 (N-CH$_2$CH$_3$), 36.2 (d, $J = 11.3$ Hz, $C$(CH$_3$)$_3$), 30.0 (d, $J = 11.5$ Hz, C(CH$_3$)$_3$), 16.0 (Py-CH$_2$CH$_3$), 15.1 (N-CH$_2$CH$_3$) ppm. $^{31}$P{$^1$H}-NMR (162 MHz, MeCN-$d_3$): $\delta = 210.1$ ppm. $^{19}$F NMR (377 MHz MeCN-$d_3$): $\delta = -151.7$ (s) ppm. $^{11}$B NMR (129 MHz MeCN-$d_3$): $\delta = -1.3$ ppm. **ESI-TOF** (m/z): 263.1430 g/mol (calculated.: 263.1420 g/mol) [M–C$_2$H$_5$]$^+$.

### Cu(I) complexes of triazaphosphole salts 2a, 2c

The corresponding the Cu(I) salt (3.0 eq) was added to a solution of the alkylated triazaphosphole (1.0 eq) in THF (3 mL per 20.0 mg triazaphospholenium salt) and stirred at $T = 60\,°C$ for overnight. The solvent was reduced to half in vacuum and $n$-pentane (10 mL per 20.0 mg triazaphospholenium salt) was added to complete the precipitation of the product. The solid obtained was washed with n-pentane (3×10 mL per 20.0 mg reactant), dried in vacuo and recrystallized from acetonitrile.

#### [C$_{12}$H$_{18}$N$_4$P]$_n$ [Cu$_2$Br$_3$]$_n$ (4a$_{\mu2}$)

**2a** (20.0 mg, 0.06 mmol) and CuBr·SMe$_2$ (37.1 mg, 0.18 mmol) were dissolved in THF (3 mL). **4a$_{\mu2}$** was obtained quantitatively according to $^{31}$P NMR spectroscopy as yellow solid. $^1$H NMR (400 MHz, MeCN-$d_3$): $\delta = 8.70$ (d, $J = 6.1$ Hz, 1H, H-1), 8.41 (t, $J = 7.9$ Hz, 1H, H-3), 7.94 (t, $J = 6.9$ Hz, 1H, H-2), 7.34 (d, $J = 8.1$ Hz, 1H, H-4), 6.20 (d, $J = 5.6$ Hz, 2H, CH$_2$), 4.35 (s, 3H, N-CH$_3$), 1.48 (d, $J = 1.4$ Hz, 9H, C(CH$_3$)$_3$) ppm. $^{31}$P {$^1$H} NMR (162 MHz, MeCN-$d_3$): $\delta = 175.6$ ppm.

#### [C$_{12}$H$_{18}$N$_4$P]$_2$ [Cu$_2$I$_4$] (4c$_{\eta1}$)

**2c** (15.0 mg, 0.05 mmol) and CuI·SMe$_2$ (36.5 mg, 0.15 mmol) were dissolved in THF (3 mL). **4c$_{\eta1}$** was obtained quantitatively according to $^{31}$P NMR spectroscopy as orange solid. $^1$H NMR (400 MHz, MeCN-$d_3$): $\delta = 8.72$ (ddd, $J = 6.2$, 1.4, 0.7 Hz, 1H, $H$Ar), 8.41 (td, $J = 7.7$, 1.1 Hz, 1H, $H$Ar), 7.95 (ddd, $J = 7.8$, 6.1, 1.5 Hz, 1H, $H$Ar), 7.33 (d, $J = 8.5$ Hz, 1H, $H$Ar), 6.28 (d, $J = 5.7$ Hz, 2H, methylen), 4.38 (s, 3H, Py-CH$_3$), 1.49 (d, $J = 1.4$ Hz, 9H, C(CH$_3$)$_3$) ppm. $^{13}$C{$^1$H} NMR (101 MHz, MeCN-$d_3$): $\delta = 195.8$ (d, $J = 63.1$ Hz, C=P), 154.3 (CAr), 148.0 (CAr), 147.4 (CAr), 128.4 (CAr), 128.1 (CAr), 52.3 (d, $J = 13.6$ Hz, methylen), 47.3 (Py-CH$_3$), 36.0 (d, $J = 15.8$ Hz, $C$(CH$_3$)$_3$), 31.6 (d, $J = 7.7$ Hz, C(CH$_3$)$_3$) ppm. $^{31}$P{$^1$H} NMR (162 MHz, MeCN-$d_3$): $\delta = 170.8$ ppm. **ESI-TOF** (m/z): 249.1261 g/mol (calculated: 249.1264 g/mol) [M]$^+$ (only cation detected).

### Cu(I) complexes of triazaphosphole salt 2b

#### [C$_{13}$H$_{20}$N$_4$P]$_n$ [Cu$_2$Br$_3$]$_n$ (4b$_{\mu2}$) / [C$_{13}$H$_{20}$N$_4$P]$_2$ [Cu$_2$Br$_4$] (4b$_{\eta1}$)

**2b** (30.0 mg, 0.09 mmol) and CuBr·SMe$_2$ (55.0 mg, 0.27 mmol) were dissolved in THF (3 mL) and acetonitrile (0.5 mL) and stirred at $T = 60\,°C$ for 2 h. The reaction mixture was allowed to stand at room temperature for overnight. Yellow crystals of **4b$_{\mu2}$** and **4b$_{\eta1}$** were obtained directly from the reaction mixture. $^1$H NMR (400 MHz, MeCN-$d_3$): $\delta = 8.77$ (dd, $J = 6.2$, 1.2 Hz, 1H, $H$Ar), 8.42 (td, $J = 7.9$, 1.3 Hz, 1H, $H$Ar), 7.99 (ddd, $J = 7.5$, 6.2, 1.1 Hz, 1H, $H$Ar), 7.49 (d, $J = 8.1$ Hz, 1H, $H$Ar), 6.26 (d, $J = 3.9$ Hz, 2H, methylen), 4.73 (q, $J = 7.4$ Hz, 2H, CH$_2$CH$_3$), 1.57 (t, $J = 7.2$ Hz, 3H, CH$_2$CH$_3$), 1.47 (d, $J = 1.4$ Hz, 9H, C(CH$_3$)$_3$) ppm. $^{13}$C{$^1$H} NMR (101 MHz, MeCN-$d_3$): $\delta = 198.7$ (d, $J = 70.2$ Hz, C=P), 152.8 (CAr), 147.3 (CAr), 146.7 (CAr),

129.4 (CAr), 128.8 (CAr), 54.9 (CH$_2$CH$_3$), 51.7 (d, $J = 14.0$ Hz, methylen), 36.0 (d, $J = 15.4$ Hz, $C$(CH$_3$)$_3$), 31.6 (d, $J = 7.8$ Hz, C(CH$_3$)$_3$), 15.9 (CH$_2$CH$_3$) ppm. $^{31}$P{$^1$H} NMR (162 MHz, MeCN-$d_3$): $\delta = 174.0$ ppm.

### Cu(I) complexes of triazaphospholenium salts 3a", 3b"

The corresponding dication (1.0 eq) and a Cu(I) salt (3.0 eq) were dissolved in THF (3 mL per 20.0 mg dication) and stirred at $T = 60\,°C$ for overnight. The solvent was reduced to half in vacuum and $n$-pentane (10 mL per 20.0 mg triazaphospholenium salt) was added to complete the precipitation of the product. The solid obtained was washed with $n$-pentane (3×10 mL per 20.0 mg reactant), dried in vacuo and recrystallized from acetonitrile.

#### [C$_{14}$H$_{23}$N$_4$P][CuBr$_3$] (5$_{\eta1}$)

**3a'** (30.0 mg, 0.06 mmol) and CuBr·SMe$_2$ (40.9 mg, 0.20 mmol) were dissolved in a mixture of THF: acetonitrile 1:1 (4 mL). **5$_{\eta1}$** was obtained as orange solid.

#### [C$_{14}$H$_{23}$N$_4$P]$_n$[Cu$_4$I$_6$]$_n$ (6)

**3a'** (10.0 mg, 0.02 mmol) and CuI·SMe$_2$ (33.6 mg, 0.14 mmol) were dissolved in THF (3 mL). **6** was obtained quantitatively according to $^{31}$P-NMR as orange solid. $^1$H NMR (400 MHz, MeCN-$d_3$): $\delta = 8.79$ (dd, $J = 6.4$, 1.2 Hz, 1H, HAr), 8.55 (td, $J = 7.9$, 1.6 Hz, 1H, HAr), 8.06 (ddd, $J = 7.6$, 6.1, 1.1 Hz, 1H, HAr), 7.98 (d, $J = 8.3$ Hz, 1H, HAr), 6.27 (d, $J = 5.4$ Hz, 2H, methylen), 4.82 (qd, $J = 7.2$, 1.0 Hz, 2H, N-CH$_2$CH$_3$), 4.38 (s, 3H, Py-CH$_3$), 1.62 (d, $J = 2.6$ Hz, 9H, C(CH$_3$)$_3$), 1.62 (t, $J = 7.2$ Hz, 3H, N-CH$_2$CH$_3$) ppm. $^{31}$P{$^1$H} NMR (162 MHz, MeCN-$d_3$): $\delta = 206.5$ ppm. **ESI-TOF** (m/z): 263.1492 g/mol (calculated: 263.1420 g/mol) [M]$^+$ (only cation of the structure C$_{13}$H$_{20}$N$_4$P$^+$ could be detected).

#### [C$_{15}$H$_{25}$N$_4$P]$_n$[BF$_4$]$_n$[CuBr$_2$]$_n$ (7$_{\eta1}$)

**3b"** (30.0 mg, 0.06 mmol) and CuBr·SMe$_2$ (24.5 mg, 0.12 mmol) were dissolved in a Mixture of THF: acetonitrile 1:1 (4 mL). **7$_{\eta1}$** was obtained quantitatively according to $^{31}$P NMR spectroscopy as orange solid. $^1$H NMR (400 MHz, MeCN-$d_3$): $\delta = 8.86$ (dd, $J = 6.3$, 1.5 Hz, 1H, $H$Ar), 8.53 (td, $J = 7.9$, 1.5 Hz, 1H, $H$Ar), 8.19–8.02 (m, 2H, $H$Ar), 6.46 (d, $J = 5.2$ Hz, 2H, methylen), 4.78 (qd, $J = 7.3$, 1.3 Hz, 2H, N-CH$_2$CH$_3$), 4.47 (q, $J = 7.5$ Hz, 2H, Py-CH$_2$CH$_3$), 1.67 (d, $J = 7.3$ Hz, 3H, Py-CH$_2$CH$_3$), 1.64 (d, $J = 2.4$ Hz, 9H, C(CH$_3$)$_3$), 1.60 (t, $J = 7.2$ Hz, 3H, N-CH$_2$CH$_3$) ppm. $^{31}$P{$^1$H} NMR (162 MHz, MeCN-$d_3$): $\delta = 200.9$ ppm. $^{19}$F NMR (377 MHz MeCN-$d_3$): $\delta = -151.7-{-}151.8$ (m) ppm. $^{11}$B NMR (129 MHz MeCN-$d_3$): $\delta = -1.1-{-}1.3$ (m) ppm.

## Conflict of Interests

The authors declare no conflict of interest.

*Chem. Eur. J.* **2024**, e202400592 (9 of 10)

© 2024 The Authors. Chemistry - A European Journal published by Wiley-VCH GmbH

58

## Data Availability Statement

The data that support the findings of this study are available in the supplementary material of this article.

[1] a) J. A. W. Sklorz, C. Müller, *Eur. J. Inorg. Chem.* **2016**, 595–606; b) K. B. Dillon, F. Mathey, J. F. Nixon, *Phosphorus: The Carbon Copy: From Organophosphorus to Phospha-Organic Chemistry*, John Wiley & Sons, **1998**.

[2] a) Y. C. Yeung, L. Y. Ko, R. Carrié, *Chem. Commun.* **1984**, 1640–1641; b) W. Rösch, M. Regitz, *Angew. Chem. Int. Ed.* **1984**, *23*, 900–901.

[3] a) E. Yue, L. Dettling, J. A. W. Sklorz, S. Kaiser, M. Weber, C. Müller, *Chem. Commun.* **2022**, *58*, 310–313; b) L. Dettling, M. Papke, J. A. W. Sklorz, D. Buzsáki, Z. Kelemen, M. Weber, L. Nyulászi, C. Müller, *Chem. Commun.* **2022**, *58*, 7745–7748; c) L. Dettling, N. Limberg, R. Küppers, D. Frost, M. Weber, N. T. Coles, D. M. Andrada, C. Müller, *Chem. Commun.* **2023**, *59*, 10243–10246.

[4] S. L. Choong, C. Jones, A. Stasch, *Dalton Trans.* **2010**, *39*, 5774–5776.

[5] S. L. Choong, A. Nafady, A. Stasch, A. M. Bond, C. Jones, *Dalton Trans.* **2013**, *42*, 7775–7780.

[6] J. A. W. Sklorz, S. Hoof, M. G. Sommer, F. Weißer, M. Weber, J. Wiecko, B. Sarkar, C. Müller, *Organometallics* **2014**, *33*, 511–516.

[7] M. Papke, L. Dettling, J. A. W. Sklorz, D. Szieberth, L. Nyulászi, C. Müller, *Angew. Chem. Int. Ed.* **2017**, *56*, 16484–16489.

[8] a) M. Heckenroth, E. Kluser, A. Neels, M. Albrecht, *Dalton Trans.* **2008**, 6242–6249; b) G. Guisado-Barrios, J. Bouffard, B. Donnadieu, G. Bertrand, *Angew. Chem. Int. Ed.* **2010**, *49*, 4759–4762.

[9] J. J. Daly, *J. Chem. Soc.* **1964**, 3799–3810.

[10] T. A. Van Der Knaap, T. C. Klebach, F. Visser, F. Bickelhaupt, P. Ros, E. J. Baerends, C. H. Stam, M. Konijn, *Tetrahedron Lett.* **1984**, *40*, 765–776.

[11] Y. Charbonnel, J. Barrans, *Tetrahedron Lett.* **1976**, *32*, 2039–2043.

[12] a) Y. Jeong, J. S. Ryu, *J. Org. Chem.* **2010**, *75*, 4183–4191; b) S. Hohloch, C. Y. Su, B. Sarkar, *Eur. J. Inorg. Chem.* **2011**, 3067–3075; c) Z. K. Reeder, A. M. Adler, K. M. Miller, *Tetrahedron Lett.* **2016**, *57*, 206–209.

[13] a) P. J. Stang, M. Hanack, L. R. Subramanian, *Synthesis* **1982**, 85–126; b) E. S. Lewis, S. Vanderpool, *J. Am. Chem. Soc.* **1977**, *99*, 1946–1949; c) D. N. Kevill, G. M. L. Lin, *Tetrahedron Lett.* **1978**, *11*, 949–952.

[14] A. Bastero, D. Font, M. A. Pericàs, *J. Org. Chem.* **2007**, *72*, 2460.

[15] S. Burck, J. Daniels, T. Gans-Eichler, D. Gudat, K. Nättinen, M. Nieger, *Z. Anorg. Allg. Chem.* **2005**, *631*, 1403–1412.

[16] K. Wang, A. K. Chinnam, N. Petrutik, E. P. Komarala, Q. Zhang, Q. Yan, R. Dobrovetsky, M. Gozin, *J. Mater. Chem. A* **2018**, *6*, 22819–22829.

[17] a) T. E. Kokina, L. A. Glinskaya, D. A. Piryazev, A. M. Agafontsev, E. V. Vorontsova, A. S. Bogomyakov, A. V. Tkachev, S. V. Larionov, *Russ. Chem. Bull. Int. Ed.* **2018**, *67*, 1251–1260; b) G. Hu, E. M. Holt, *Acta Crystallogr.* **1994**, *C50*, 1578–1580; c) S. Anderson, S. Jagner, *Acta Chem. Scand.* **1985**, *A40*, 181–186; d) N. P. Rath, E. M. Holt, *Chem. Commun.* **1985**, *7*, 665–667.

[18] C. Pardin, I. Roy, W. D. Lubell, J. W. Keillor, *Chem. Biol. Drug Des.* **2008**, *72*, 189–196.

[19] G. Becker, H. Schmidt, G. Uhl, W. Uhl, M. Regitz, W. Rösch, U.-J. Vogelbacher, *Inorg. Synth.* **1990**, *27*, 249–253.

[20] Bruker (**2010**). APEX2, SAINT, SADABS and XSHELL. Bruker AXS Inc., Madison, Wisconsin, USA.

[21] a) Sheldrick, G. SADABS. University of Göttingen: Göttingen, Germany: **2014**; b) Coppens, P. The Evaluation of Absorption and Extinction in Single-Crystal Structure Analysis. Crystallographic Computing. Copenhagen, Muksgaard: **1979**.

[22] a) G. M. Sheldrick, *Acta Crystallogr. Sect. A* **2008**, *64*, 112–122; b) G. M. Sheldrick, *Acta Crystallogr. Sect. C* **2015**, *71*, 3–8.

[23] O. V. Dolomanov, L. J. Bourhis, R. J. Gildea, J. A. K. Howard, H. Puschmann, *J. Appl. Crystallogr.* **2009**, *42*, 339.

[24] C. F. Macrae, I. Sovago, S. J. Cottrell, P. T. A. Galek, P. McCabe, E. Pidcock, M. Platings, G. P. Shields, J. S. Stevens, M. Towler, P. A. Wood, *J. Appl. Crystallogr.* **2020**, *53*, 226–235.

# RESEARCH ARTICLE

Pyridyl-functionalized triazaphospholes provide the possibility for a post-synthesis modification, affording a variety of mono- and dicationic species. This is achieved by a chemoselective and stepwise alkylation exclusively of the nitrogen atoms and can be controlled by the choice and by the stoichiometry of the used electrophile. This targeted synthesis opens up a fascinating coordination chemistry.
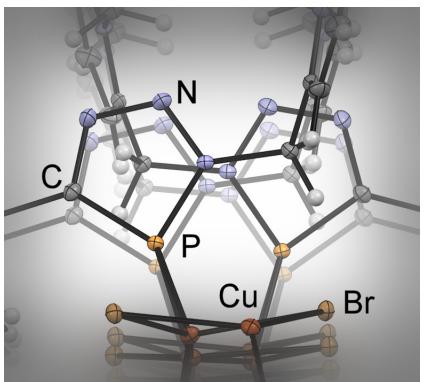
*M. Sc. L. Dettling, Dr. M. Papke, M. Sc. M. J. Ernst, M. Weber, Prof. Dr. C. Müller\**

1 – 11

**Chemoselective Post-Synthesis Modification of Pyridyl-Substituted, Aromatic Phosphorus Heterocycles: Cationic Ligands for Coordination Chemistry**

## 7. Conclusion

*Au(I)-mediated N₂-elimination from triazaphospholes: a one-pot synthesis of novel $N_2P_2$-heterocycles:* Triazaphospholes can easily be synthesized from the corresponding phosphaalkynes and organoazides. However, limited accessibility of phosphaalkynes lead to a primary focus in this thesis on changes in the reactivity of the triazaphosphole by introduction of different substituents through the corresponding organoazide. It could now be shown that the introduction of electron withdrawing tosyl- and mesitylsulfonyl- groups at the N(3) atom leads to an unprecedented $N_2$ release upon coordination to a gold(I) center and the subsequent formation of $N_2P_2$-heterocycles (Scheme 20). This is a surprising observation as $N_2$ release from triazaphospholes is uncommon. UV irradiation and temperatures up to $T$ = 400 °C for example did not lead to an observable $N_2$ release.[88] The stability of these heterocycles is attributed to the highly delocalized aromatic system, which is for example reflected in the very similar N(1)–N(2) and N(2)–N(3) bond lengths in classical triazphospholes.[59][61][62][63] Single crystals suitable for X-ray diffraction were obtained for the tosyl- and mesitylsulfonyl substituted triazaphospholes. The introduction of an electron-withdrawing aryl-sulfonyl-substituent at the N(3) position has a noticeable influence on the bond distances observed. Most significantly a lengthening of the N(2)–N(3) bond distance and a shortening of the N(1)–N(2) bond distance was detected, indicating that in these previously unknown aryl-sulfonyl-substituted triazaphospholes the double bonds are more localized between N(1)–N(2) and the P(1)–C(1) atoms. Interestingly, the introduction of electron withdrawing groups at the N(3) position had no noticeable effect on the ³¹P NMR shift of the corresponding triazaphospholes. (*Attention: for the sake of uniformity, the nomenclature has been kept unchanged throughout this thesis (see Scheme 20); the publication uses a different nomenclature.*)

Addition of chloro(dimethylsulfide)gold(I) (AuCl·S(CH₃)₂) to the aryl-sulfonyl-substituted triazaphospholes directly lead to a vigorous release of $N_2$. Crystallographic characterization of the product shows the formation of a cyclo-diphosphadiazane which coordinates two gold(I) chloride fragments *via* the lone pair of the pyramidal coordinated $\lambda^3,\sigma^3$-phosphorus atom (scheme 20, **20 A**).[136][137][138][139] Selectively, the *trans* isomer was formed as expected for sterically more demanding ligands (aryl-sulfonyl) at the phosphorus atoms.[140] However, the addition of the gold(I) precursor to the triazaphosphole is necessary for the formation of the $P_2N_2$ heterocycle as just heating of the aryl-sulfonyl substituted triazaphosphole alone does not lead to the same reactivity.
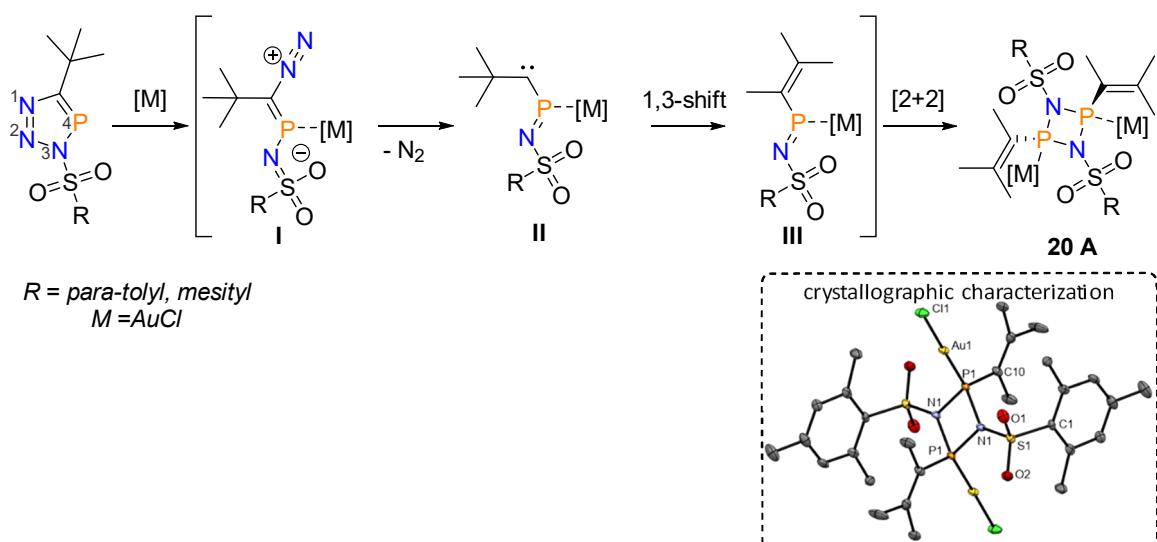
Scheme 20: unprecedented formation of $N_2P_2$-heterocycles upon coordination of a tosyl- and mesitylsulfonyl-substituted triazaphosphole to a gold(I) center, crystallographic characterization of the product **20 A** (R = mesityl).

A mechanism for this novel highly selective ''one-pot'' formation of a $P_2N_2$ heterocycle was proposed: After $N_2$ release the formation of a carbene intermediate (Scheme 20, **II**) is assumed, which leads to the conversion of the $^tBu$-substituent into an *iso*-pentenyl-substituent after an 1,3 shift (Scheme 20, **III**). A similar carbene intermediate was also reported in literature of similar 1-sulfonyl-1,2,3-triazoles in a rhodium(II)-catalyzed denitrogenation.[141] The 1,3 shift of the $^tBu$-substituent should give an iminophosphine intermediate (Scheme 20, **III**) which would undergo a intermolecular [2+2] cycloaddition giving the observed $P_2N_2$ heterocycle (scheme 20, **20 A**). A trapping experiment was performed with dimethylbutadiene and a crossover experiment was performed by mixing both aryl-sulfonyl substituted triazaphospholes. The results found were in agreement with the formation of an iminophosphine intermediate (Scheme 20, **III**). Iminophosphines have been known to undergo cyclisation reactions forming dimers or trimers.[140]

While $P_2N_2$ heterocycles are a versatile and widely used compounds, no example of this specific substitution pattern was known, probably due to the difficulties in the synthesis. The above described approach gives access to previously inaccessible novely substituted $P_2N_2$ heterocycles.

*A new access to diazaphospholes via cycloaddition–cycloreversion reactions on triazaphospholes:* Cycloaddition reactions are known to play an important role in the synthesis of phosphorus heterocycles. For example, phosphinines can be synthesized in a [4 + 2] cycloaddition from pyrones and phosphaalkynes or from azaphosphinines and alkynes.[17][142][143][144][145][146][147] However, there is only one example of a 1,2,3,4-triazaphosphol participating in a cyclisation reaction: in a 1,3 dipolar cycloaddition, the P=C double bond of the

3-phenyl-5-*tert*-butyl substituted triazaphosphole reacts as a dienophile with an α-diazo-β-diketone and forms a new heterocycle system (chapter 1.3.3, scheme 13).[89] For the first time it could now be shown that the 1,2,3,4-triazaphosphole can react as a diene in a [4 + 2] cycloaddition reaction. Addition of the electron-poor, sterically not very demanding hexafluoro-2-butyne leads to the formation of the corresponding CF$_3$-substituted 2*H*-1,2,3-diazaphosphole derivative in a concerted cycloaddition-cycloreversion process (Scheme 21). According to $^{31}$P NMR spectroscopic tracing of the reaction progress, the elimination of pivaloyl nitrile leads to the quantitative formation of the diazaphosphole (Scheme 21, **21 B**). However, the cycloaddition intermediate (Scheme 21, **21 A**) was not detectable during the reaction despite a relatively long reaction time of eight weeks. This indicates that the cycloaddition is the rate-determining step. Similar observations were also made for the 1,2,4,3-triazaphospholes.[148] Interestingly no reaction was observed between the 1,2,3,4-triazaphospholes and dimethylacetylenedicarboxylate (DMAD). This observation is contrary to the reactivity of triazoles, which are known to undergo cycloaddition reactions with DMAD but not with hexafluoro-2-butyne.[149] Crystallographic characterization of the products shows that the bis-CF$_3$-substituted diazaphosphole heterocycle is planar and the bond distances are very similar to those of the starting material.[59] The replacement of the pivaloyl nitrile by a hexafluoro-2-butyne group does not lead to a significant structural change within the heterocycle.
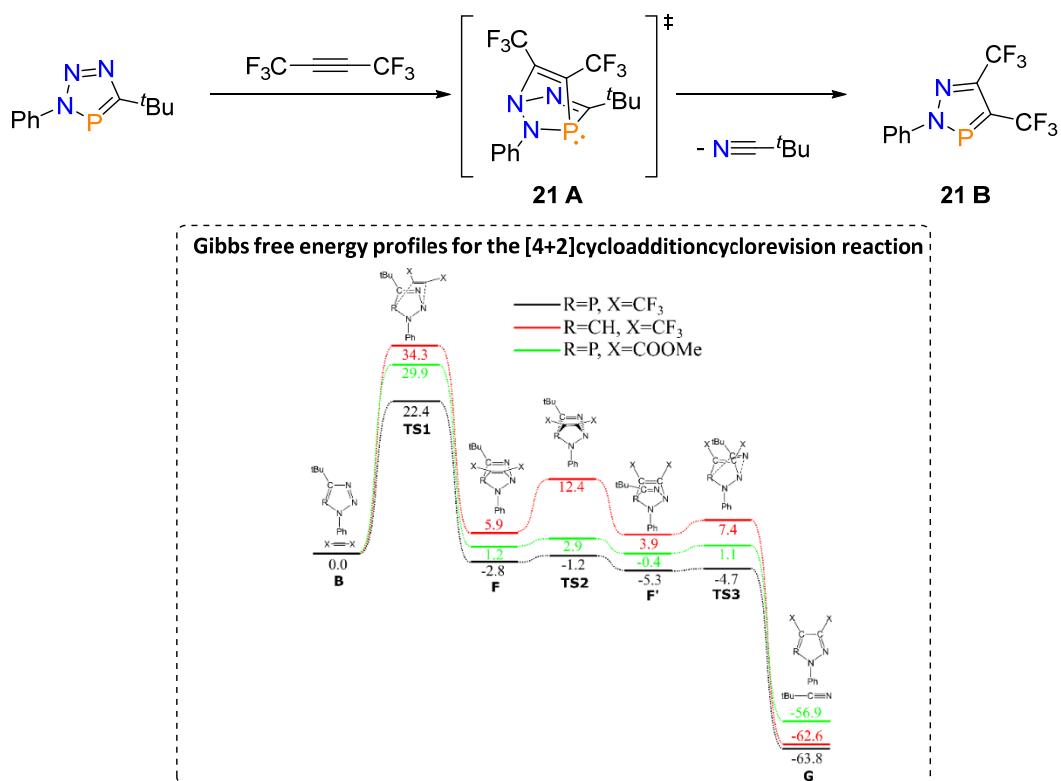


Scheme 21: Formation of a CF$_3$-substituted 2H-1,2,3-diazaphosphole **21 B** in a concerted cycloaddition-cycloreversion process (top). Gibbs free Energy profile of the cycloaddition-cycloreversion process (bottom).

DFT calculations performed to investigate the reaction mechanism show a concerted cycloaddition-cycloreversion process (Scheme 21, bottom). As anticipated, the cycloaddition step is the rate-determining step, while the pivaloylnitrile-eliminating cycloreversion step is strongly exergonic. Comparison of the cycloaddition reaction of triazaphospholes with hexafluoro-2-butyne (Scheme 21, black) to the cycloaddition reaction with DMAD (Scheme 21, green) shows that the energy barrier in the rate-determining cycloaddition step is higher in the latter, which explains why only the [4 + 2]-cycloaddition cycloreversion product with hexafluoro-2-butyne is observed. The calculation of frontier orbitals indicates that the $CF_3$-groups have a stabilizing effect on the diazaphosphole. The $CF_3$-substituted diazaphosphole should also be a stronger $\pi$-acceptor than the triazaphosphole, when coordinated to a metal center.

Diazaphospholes are ambidentate ligands analogous to triazaphospholes (Scheme 22, **I** and **II**).[150] They can coordinate to a metal center either *via* the phosphorus lone pair or a nitrogen donor. Few examples of the coordination chemistry of diazaphospholes are known in the literature.[151][152] However, in a recent publication it could be shown that in Si-bridged, chelating diazaphospholes, harder Lewis acids favor coordination to the nitrogen donor of the ambidentate ligands, while M(0)-carbonyls preferentially coordinate *via* the phosphorus lone pair.[153] To get further insight into the possible coordination modes of these heterocycles the Gibbs energies of the optimized structures of potential [**L**W(CO)$_5$] complexes (L = diazaphosphole, triazaphosphole; N- or P-bonded) were calculated and compared. A preference for the coordination *via* the phosphorus atom of 10.6 kcal/mol was calculated for the diazaphosphole. In case of the triazaphosphole the result was much less clear with a calculated preference for coordination *via* the phosphorus atom over a coordination *via* a nitrogen donor (N(1), N(2) is much less favored) of only 0.6 kcal/mol.
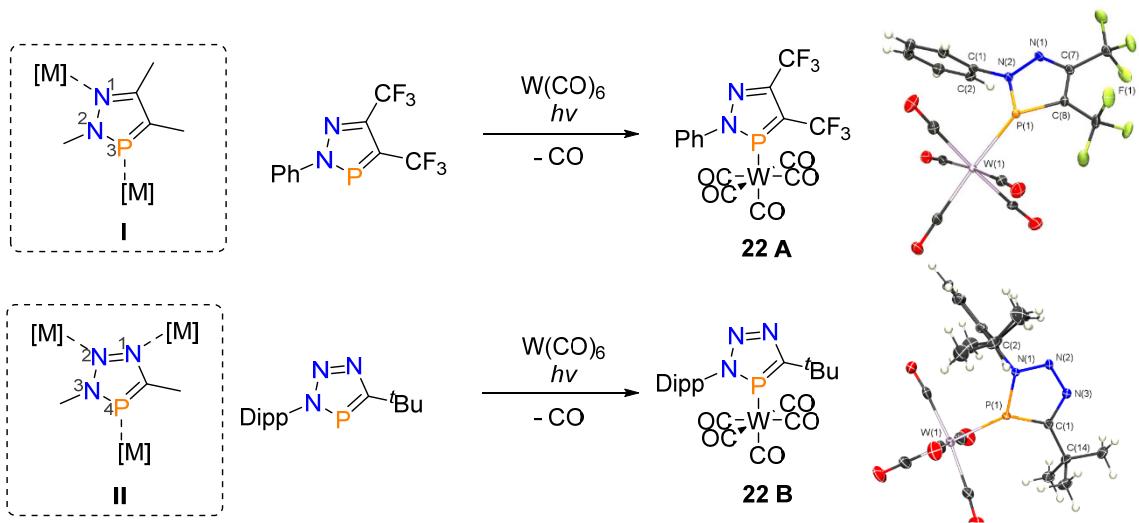
*Scheme 22: potential coordination modes of diazaphospholes and triazaphospholes (left), formation of tungsten(0) pentacarbonyl complexes of the diazaphosphole and triazaphosphole (center) and crystallographic characterization of the corresponding tungsten(0) pentacarbonyl complexes (right).*

The addition of an equimolar amount of tungsten hexacarbonyl ($W(CO)_6$) to the bis-$CF_3$-substituted diazaphosphole and subsequent UV-irradiation yielded the corresponding coordination complex (Scheme 22, **22 A**). Similarly, the tungsten complexes of the phenyl-substituted and Dipp-substituted triazaphospholes were synthesized (Scheme 22, **22 B**). Crystallographic characterization of the diazaphosphole and triazaphosphole coordination compounds clearly confirms that the heterocycles coordinate to the $W(CO)_5$ fragment *via* the phosphorus atom (Scheme 22, left). A comparison of the CO stretching frequencies in the recorded IR spectra also shows that the wavelengths in the tungsten complex of a bis-$CF_3$-substituted diazaphosphole ligand (Scheme 22, **22 A**) are shifted to higher wavenumbers, indicating lower net donor properties of the bis-$CF_3$-substituted diazaphosphole ligand compared to the triazaphosphole ligands (Scheme 22, **22 B**).

Bis-$CF_3$-substituted diazaphospholes are an interesting class of compounds as they are the phosphorus analogues of bis-$CF_3$-substituted pyrazoles. Fluorinated pyrazoles have been used in many pharmacologically relevant and bioactive compounds.[154][155][156][157] In addition, the observed tungsten(0) pentacarbonyl complex of the triazaphosphole is of particular interest as it is the first example of a tungsten complex of a triazaphosphole and one of the few examples of coordination *via* the phosphorus atom of a triazaphosphole.

*Phosphorus derivatives of mesoionic carbenes: synthesis and characterization of triazaphosphole-5-ylidene → BF₃ adducts:* The first tiazaphospholenium salt (Scheme 23, **I**), the 3-benzyl-5-*tert*-butyl-1-methyl-triazaphospholenium tetrafluoroborate, was introduced by the group of MÜLLER in 2017.[60] These salts can be synthesized by treatment of the corresponding triazaphospholes with Meerwein's reagent. Following the principle of the valence

isoelectronicity, these compounds represent the formal phosphorus analogues of the well-known mesoionic 1,2,3-triazolylidenes (Scheme 23, **II**).[124] The effect different substituents have on the heterocycle is of particular interest, especially the exchange of the $^t$Bu-group in 5-position by a TMS group was in the focus of this investigation. TMS-groups attached to an aromatic system are known to provide interesting electronic effects to the aromatic ring. In case of phosphinines, TMS-substitution increases the reactivity for example in the formation of phosphinine selenides.[158] The TMS-group in 5-TMS-triazaphospholes was observed to undergo a [1,5] shift to the neighboring N(2) atom in early works as well.[88] Now for the first time it could be shown that the [BF$_4$]$^-$ salts of the TMS-substituted triazaphospholenium cations undergo fluorotrimethylsilane (TMS–F) elimination yielding BF$_3$ adducts of a triazaphosphol-5-ylidenes (Scheme 23).

The quaternization of the TMS-substituted triazaphospholes with [Me$_3$O][BF$_4$] has to be carried out at room temperature, as higher temperatures lead to the formation of two initially undefined new products. Deliberately heating a solution of the TMS-substituted triazaphospholenium tetrafluoroborate in DME to $T$ = 60 °C led to the complete consumption of the triazaphospholenium salt and the formation of the previously observed products. Separation of the products and subsequent analysis revealed that they were the protodesilylated product (Scheme 23, **23 A**) and the BF$_3$ adduct (Scheme 23, **23 B**). Interestingly, protonated side-products had previously been observed in literature in the thermal degradation of free 1,2,3-triazol-5-ylidenes (Scheme 23, **III**).[124][159] The BF$_3$ adduct is probably formed by elimination of a fluorotrimethylsilane (TMS–F) which initially forms the carbene intermediate, that subsequently reacts with the remaining BF$_3$. A similar reactivity, albeit under harsh conditions, had been observed in the formation of NHC-based BF$_3$ and PF$_5$ Lewis pairs.[160] While the postulated carbene intermediate cannot be observed, fluorotrimethylsilane (TMS-F) can be detected spectroscopically.
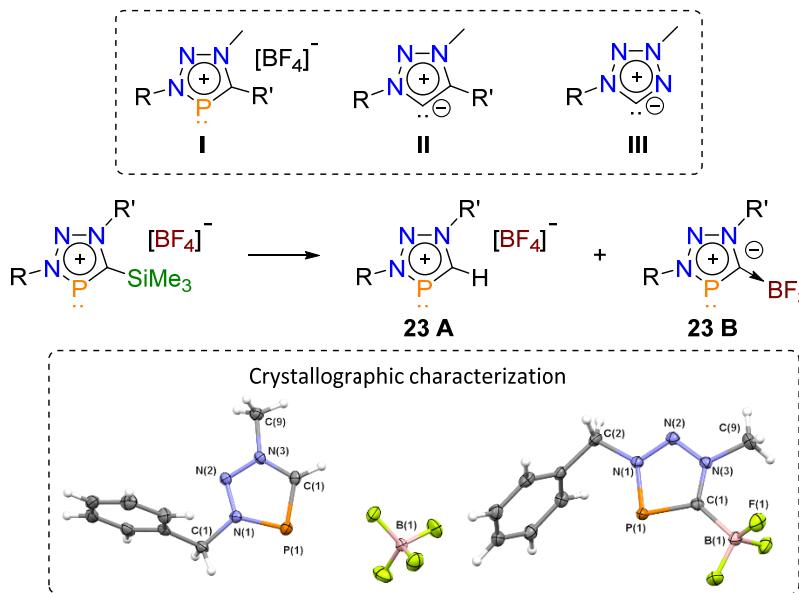
Scheme 23: Selected phosphorus and nitrogen-based heterocycles (top) formation of the protodesilylated triazaphospholenium salt **23 A** and the BF$_3$ adduct **23 B** (middle) and the molecular structure of **23 A** and **23 B** in the crystal (bottom).

Single crystals suitable for X-ray diffraction, were obtained for both compounds (Scheme 23, **23 A** and **23 B**). Comparison of bond lengths an angles show a decrease of the N(3)–C(1)–P(1) bond angle as well as a elongation of the N(3)–C(1) and C(1)–P(1) distances from the protodesilylated product to the BF$_3$ adduct. Such changes in geometry have commonly been observed in related NHC–boranes. The smaller bond angles around the carbene carbon reflect an increase in s-character for the lone pair orbital typically observed for singlet carbenes.[161] The bond distance of the C(1)–B(1) bond length is very similar to the C–B-bond distance in the Lewis pairs of classical Arduengo carbenes.[162] These properties indicate the presence of an abnormal carbene → BF$_3$-adduct, which would make this compound the BF$_3$ adduct of an unprecedented triazaphosphol-5-ylidene. Therefore this compound could be considered the phosphorus congener of the known tetrazol-5-ylidene with an abnormal substitution pattern (Scheme 23, **III**).[163]

The isolated yields of the compounds were moderate, since the protodesilylated product and the BF$_3$ adduct are apparently formed by competing reactions. However, it was assumed that an exchange of the counterion from [BF$_4$]$^-$ to [PF$_6$]$^-$ would lead to a more stable triazaphospholenium salt, which would then allow for a targeted synthesis of each product (Scheme 24). Quaternization of the corresponding triazaphosphole with triethyloxonium hexafluorophosphate ([Et$_3$O][PF$_6$]) gave the corresponding [PF$_6$]$^-$ triazaphospholenium salts (Scheme 24, **24 A**). The targeted synthesis of a BR$_3$ adduct was achieved by adding BEt$_3$ and potassium fluoride (KF) to the triazaphospholenium salt (Scheme 24, **24 A**) which, indeed, yielded only the corresponding BEt$_3$-adduct (Scheme 24, **24 C**). Also in this reaction the

formation of fluorotrimethylsilane (TMS–F) is detected spectroscopically. Formation of only the protodesilylated product was also possible (Scheme 24, **24 B**). Formation of both compounds was confirmed by means of X-ray structural analysis.
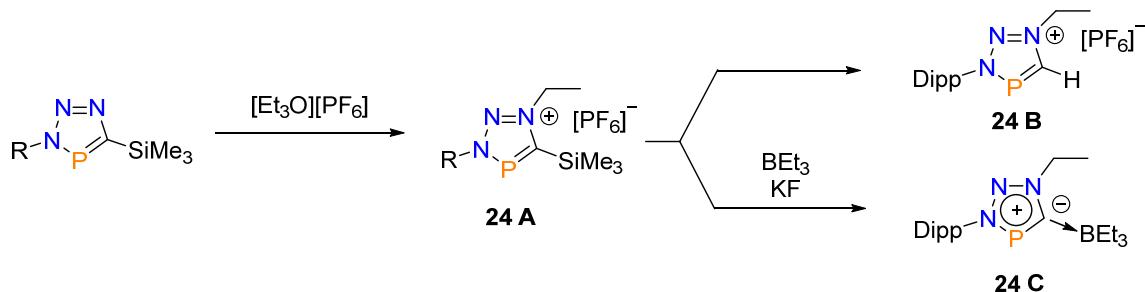


*Scheme 24: Synthesis of the protodesylated product **24 B** and BEt$_3$ adduct **24 C**.*

Investigation of the C$_{carb}$ → B bond by means of DFT calculations indicate a strong donation of electrons as the BF$_3$ bears a negative partial charge (NBO) as well as a single bond character (WBI). The bond dissociation energy is slightly weaker than in other carbene-borane adducts.[164] However, the dissection into preparation energy and interaction energy suggests that the geometrical deformation of BF$_3$ or BEt$_3$ brings a significant energy penalty (EDA-NOCV). The interaction energy, however, is comparable to other known carbene-borane adducts.[164] Further investigation reveals an ionic nature of the bond with approximately 53% electrostatic interaction and 45% orbital interaction. Analysis of the covalent part shows that the $\sigma$-donation counts for 81% of the orbital interaction while the $\pi$-back donation is only 5%.

Thes BR$_3$-adducts display a new and interesting compound class as they are considered the phosphorus analogs of tetrazol-5-ylidene carbenes (Scheme 23, **III**) with abnormal substitution pattern. The protodesilylated product is also of interest as protodesilylation is rather uncommonly observed in the classical triazaphospholes and this marks the first example of a protodesilylated triazaphospholenium salt.

*Chemoselective Post-Synthesis Modification of Pyridyl-Substituted, Aromatic Phosphorus Heterocycles: Cationic Ligands for Coordination Chemistry:* The first coordination compound of a triazaphospholenium salt was synthesized by the group of MÜLLER. It was a dimeric neutral coordination compound with two triazaphospholenium cations bridged by a di-anionic [Cu$_2$Br$_4$]$^{2-}$ unit (chapter 1.4.2, Scheme 18).[60] Looking at the coordination chemistry of classical triazaphospholes, functionalization at the 3-position of a triazaphosphole with a 2-pyridylmethyl group provided application as chelating ligands. However, only a *N,N*-chelating mode was observed upon coordination to rhenium centers.[93] The reactivity of pyridylmethyl-functionalized triazaphospholes in quaternization reactions with Meerwein reagents and their

coordination chemistry has now been investigated for the first time. Both chemoselective and stepwise quaternization of the triazaphosphole derivative is observed due to different nucleophilicities at the different nitrogen atoms. This provides access to new mono- and di-cationic triazaphospholenium ligands that exhibit a versatile coordination chemistry when treated with Cu(I) halides.

The addition of one equivalent of the Meerwein salt ([Me$_3$O][BF$_4$] or [Et$_3$O][BF$_4$]) to the triazaphosphole provided access to the corresponding pyridinium-methyl-triazaphospholes (Scheme 25, **25 A**). NMR spectroscopic and crystallographic characterization confirms that alkylation occurs only at the pyridine nitrogen atom of the triazaphosphole and no alkylation of the nitrogen atoms of the phosphorus heterocycle is observed. This can be explained by the nucleophilicity of the pyridine nitrogen atom being higher than the nucleophilicity of the nitrogen atoms of the triazaphosphole heterocycle.[60][59][165][92][93] Earlier works have already shown that the quaternization of the triazaphosphole heterocycle with MeI is not possible.[60] However, the addition of four equivalents of MeI in this case lead to quaternization of the pyridine nitrogen atom of the triazaphosphole (Scheme 25, **25 A**). Nevertheless, quaternization of the triazaphosphole heterocycle was again not possible with MeI.
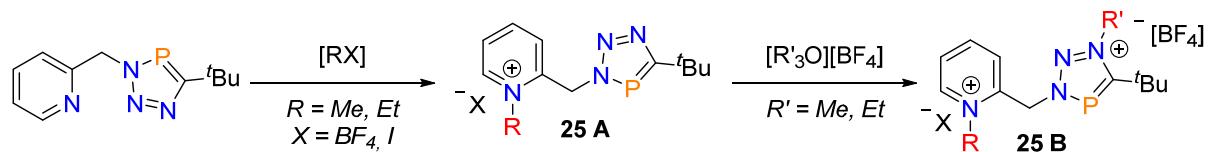


*Scheme 25: Formation of the mono- (**25 A**) and di-cationic- (**25 B**) triazaphospholes.*

The di-cationic triazaphospholenium salt (Scheme 25, **25 B**) was obtained *via* alkylation of pyridinium-methyl-triazaphospholes (Scheme 25, **25 A**) with an additional equivalent of the Meerwein salt ([Me$_3$O][BF$_4$] or [Et$_3$O][BF$_4$]). The direct formation of the triazaphospholenium salt (Scheme 25, **25 B**) from the pyridylmethyl-functionalized triazaphospholes was also possible by directly adding two equivalents of Meerwein salt. Quaternization of the phosphorus heterocycle takes place exclusively at the nitrogen atom with the highest nucleophilicity (N(1) atom).[60][59][165][92][93] The second alkylation was confirmed by NMR spectroscopic investigation and crystallographic characterization. These observations illustrate that the alkylation of the nitrogen atoms in triazaphosphole is chemoselective and stepwise and can be controlled by the choice and the stoichiometry of the alkylation reagent (Scheme 25).

After alkylation of the pyridine nitrogen atom, coordination as a chelating ligand is no longer possible. Nevertheless, both the mono-cationic pyridinium-methyl-triazaphospholes (Scheme

25, **25 A**) and the di-cationic triazaphospholenium salts (Scheme 25, **25 B**) were reacted with copper(I) halides.

The mono-cationic ligands coordinate in two different modes. The $\mu_2$-P coordination mode is observed upon the formation of a coordination polymer (Scheme 26, **26$\mu_2$**). In this case, the phosphorus atom bridges two different Cu(I) centres of an [Cu$_2$Br$_3$]$^-$ unit in the polymer. The other coordination mode is the $\eta^1$-P coordination mode. This is observed in the formation of a neutral Cu(I) dimer of the type [L$_2$Cu$_2$Br$_4$] (Scheme 26, **26$\eta^1$**) The phosphorus atom of each ligand coordinates to only one copper center of the [Cu$_2$Br$_4$]$^{2-}$ core. These complexes are the first examples in literature of Cu(I) complexes of a triazaphosphole ligand.
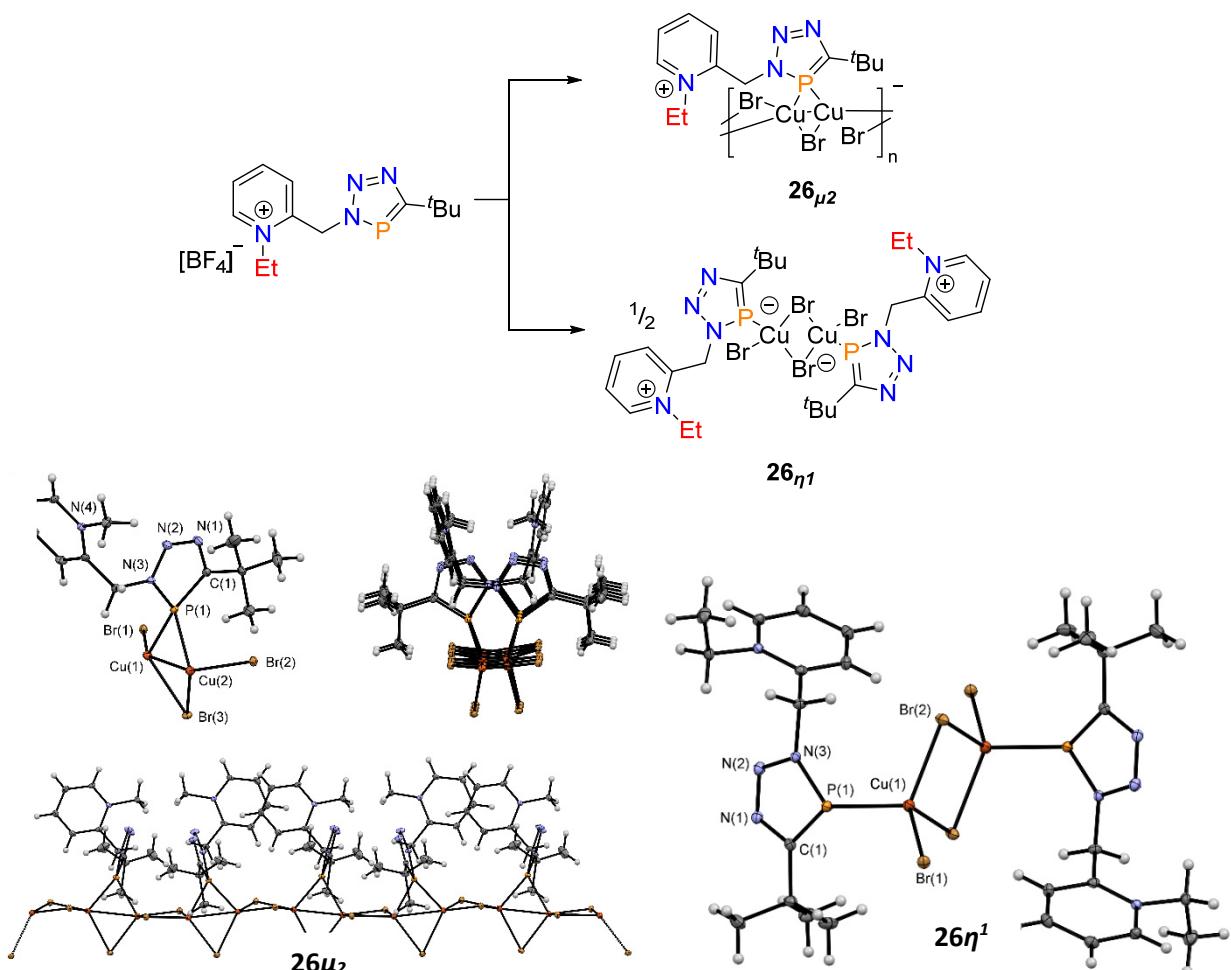


*Scheme 26: Synthesis of Cu(I) complexes of triazaphospholenium ligands and their different coordination modes (top) and the molecular structure of* **26$\mu_2$** *(left) and* **26$\eta^1$** *(right) in the crystal (bottom).*

Addition of CuBr·SMe$_2$ to the di-cationic triazaphospholenium ligands yields a neutral mononuclear Cu(I) complex with an $\eta^1$-P coordination mode (Scheme 27, **27 A**). The phosphorus atom coordinates to a [CuBr$_3$]$^{2-}$ core. It is noteworthy that the phosphorus atom adopts a pyramidal geometry, while the Cu(I) center is located below the plane of the heterocycle (similar to the previously observed Cu(I) complex of the benzyl-substituted triazaphospholenium salt

(chapter 1.4.2, Scheme 18). The formation of an ion pair was observed with a $CuI·SMe_2$ precursor (Scheme 27, **27 B**). Direct coordination of the phosphorus atom to the $[Cu_4I_6]^{2-}$ core is not observed. The di-cationic ligands are located between polymeric ribbons of the anions. This observation shows that the choice of Cu(I) halide also appears to have a major influence on the coordination modes of the ligands.
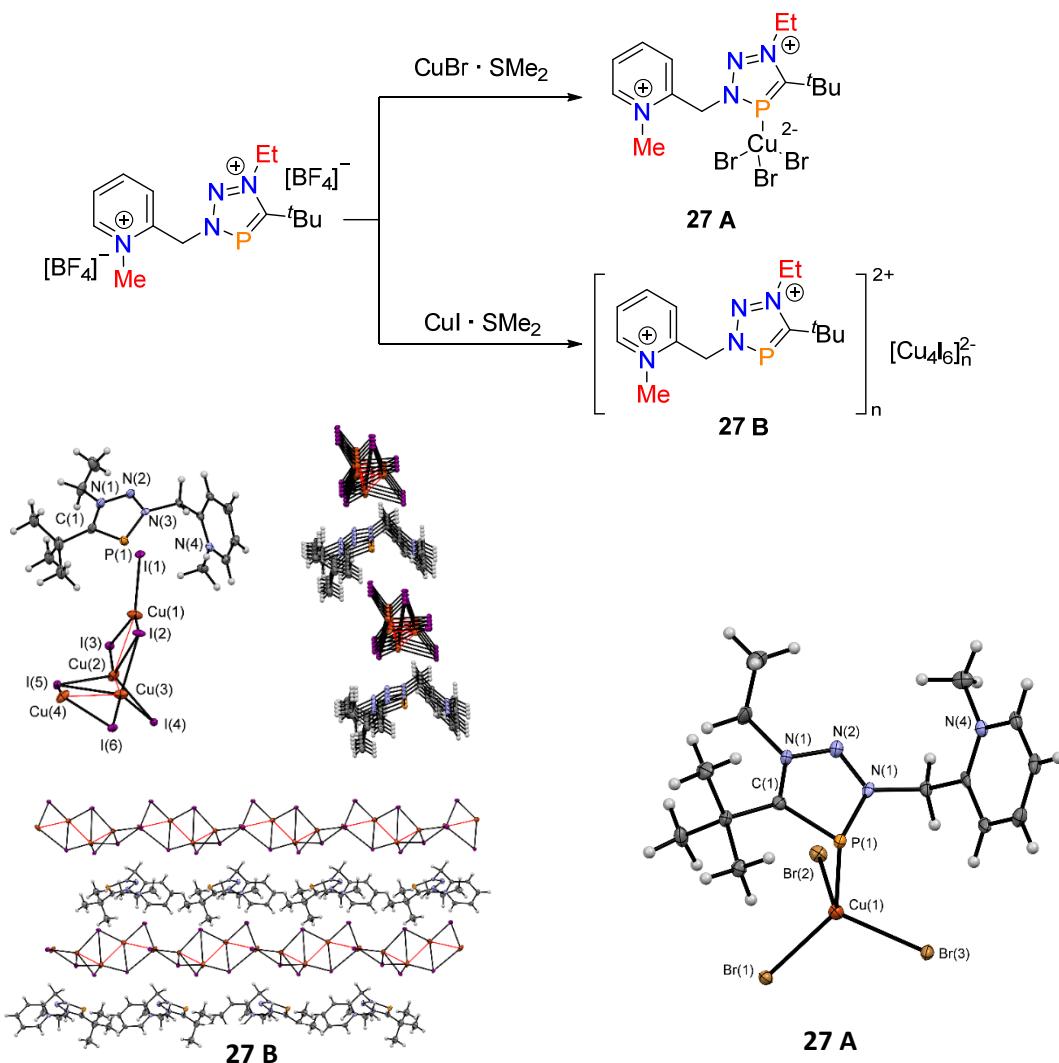


Scheme 27: synthesis of Cu(I) complexes of triazaphospholeenium ligands and their different coordination modes (top) and the molecular structure of **27 B** (left) and **27 A** (right) in the crystal (bottom).

For the first time it could be shown that pyridyl-functionalized triazaphospholes can be modified by chemoselective and stepwise alkylation. This allows access to a large number of mono- and di-cationic species. The investigation of the coordination chemistry of these charged triazaphospholes and the triazaphospholenium salts with Cu(I) halides revealed a versatile coordination chemistry, which manifests itself in different coordination modes depending on the charge of the ligand as well as the type of Cu(I) halide. Only coordination *via* the phosphorus atom is observed. These compounds thus represent one of the few examples in which

coordination of the triazaphosphole- as well as the triazaphospholenium- heterocycle occurs *via* the π-acidic phosphorus atom.

## 8. Outlook

In the course of this work, triazaphospholes and triazaphospholenium salts were investigated in detail regarding their reactivity and coordination chemistry. The presented results illustrate the central role of different substituents on the reactivity of both the triazaphosphole and the triazaphospholenium salts. In addition, the number of known coordination compounds with a phosphorus coordination to the metal center for both compound classes could be significantly increased. The first example of a tungsten complex with a coordinated triazaphosphole demonstrates that especially electron-rich metal centers ($W(CO)_5$, Cu(I)) favor coordination *via* the phosphorus atom.

The described [4+2] cycloaddition cyclorevision reaction of triazaphospholes with a suitable alkyne is a promising way of gaining access to diazaphospholes with a novel substitution pattern. During the investigation of these reactions, it was found that electron-poor alkynes, with small substituents, are particularly suitable. Diiodoacetylenes, fulfil this requirement and have the advantage that the iodo substituents may be subsequently replaced, thus potentially enabling access to a versatile substituted diazaphosphole.[166] The investigation of [4+2] cycloaddition reactions with diiodoacetylenes would therefore be of interest.

The first example of a tungsten complex of a triazaphosphole with a rare coordination *via* the phosphorus atom of a triazaphosphole could also be reported. Motivated by these results, it might be interesting to aim for the synthesis of further coordination compounds with electron-rich metal centers such as M(0) (M = Cr, Mo, Ni) for a deeper insight into triazaphospholes as ligands.[153] This would open up the possibility of potential catalytic reactions with such ligands.

Unprecedented $BF_3$ adducts of triazaphosphol-5-ylidenes which can be regarded as phosphorus analogues of the tetrazole-5-ylidene carbenes (chapter 7, Scheme 23, **III**) with an abnormal substitution pattern were described in detail. Transition metal complexes with a coordination *via* the potential "carbene" carbon atom are of great interest as they would help to further understand the ligand properties of these unusual ligands. However substituting the Lewis acid ($BR_3$) with a metal center has not been possible so far. Another possibility to gain access to these coordination compounds should be the quaternization of a metallo-triazaphosphole with, Meerwein's reagent or other suitable alkylation reagents. Such reactions are known for the tetrazol-5-ylidenes.[167][168] A first step in this direction is the recently published addition of a Lewis acid $B(C_6F_5)_3$ to the N(1) atom of gold(I) triazaphosphole (chapter 1.4.1, Scheme 17). The products can be regarded as gold(I) complexes of anionic abnormal carbenes.[82] However, the

actual synthesis of a phosphorus analogue of a neutral abnormal carbene coordination compound is still pending.

It would also be interesting to investigate the possible coordination of a metal center *via* the phosphorus atom to the metallo-triazaphospholes. While the formation of multimetal transition metal complexes featuring bridging cyaphide anions ($[C \equiv P]^-$) are known,[169] a similar coordination chemistry of a metallo-triazaphosphol has not yet been observed. It would also be interesting to investigate the coordination chemistry of the $BR_3$ adducts for a possible coordination of a metal center *via* the phosphorus atom of the heterocycle; based on the observations to date, copper(I) or tungsten(0) might be the most promising.

## 9.      References

[1]      D. E. C. Corbridge, in *Studies in Inorganic Chemistry 20, Phosphorus - An Outline of its Chemistry, Biochemistry and Uses,* Elsevier Science B.V., **1995**, pp. 27–28.

[2]      P. Jutzi, *Chem. Unserer Zeit* **1981**, *15*, 149–154.

[3]      D. Klaus, B. W. Rawe, M. R. Scott, D. P. Gates, *Angew. Chem. Int. Ed.* **2017**, *56*, 9507–9511.

[4]      N. T. Coles, A. Sofie, J. Leitl, R. Wolf, H. Grützmacher, C. Müller, *Coord. Chem. Rev.* **2021**, *433*, 213729.

[5]      M. Caporali, L. Gonsalvi, A. Rossin, M. Peruzzini, *Chem. Rev.* **2010**, *110*, 4178–4235.

[6]      T. E. Gier, *J. Am. Chem. Soc.* **1961**, *83*, 1769–1770.

[7]      G. Märkl, *Angew. Chem. Int. Ed.* **1966**, *5*, 846–847.

[8]      A. J. Ashe III, *J. Am. Chem. Soc.* **1971**, 3293–3295.

[9]      G. Becker, *ZAAC* **1976**, *423*, 242–254.

[10]     G. Becker, G. Gresser, *J. Mol. Struct.* **1981**, *75*, 283–289.

[11]     G. Becker, G. Gresser, W. Uhl, *Z. Naturforsch. B* **1981**, *36*, 16–19.

[12]     W. Rösch, M. Regitz, *Angew. Chem. Int. Ed.* **1984**, *23*, 900–901.

[13]     Y. C. Yeung, L. Y. Ko, R. Carrié, *Chem. Commun.* **1984**, 1640–1641.

[14]     D. W. N. Wilson, S. J. Urwin, E. S. Yang, J. M. Goicoechea, *J. Am. Chem. Soc.* **2021**, *143*, 10367–10373.

[15]     T. Görlich, D. S. Frost, N. Boback, N. T. Coles, B. Dittrich, P. Müller, W. D. Jones, C. Müller, *J. Am. Chem. Soc.* **2021**, *143*, 19365–19373.

[16]     W. Rösch, U. Vogelbacher, T. Allspach, M. Regitz, *J. Organomet. Chem.* **1986**, *306*, 39–53.

[17]     W. Rösch, M. Regitz, *Z. Naturforsch.* **1986**, 931–933.

[18]  M. H. Habicht, F. Wossidlo, M. Weber, C. Müller, *Chem. Eur. J.* **2016**, 12877–12883.

[19]  G. Becker, W. Schwarz, N. Seidler, M. Westerhausen, *ZAAC* **1992**, *612*, 72–82.

[20]  F. F. Puschmann, D. Stein, D. Heift, C. Hendriksen, Z. A. Gal, H. F. Grützmacher, H. Grützmacher, *Angew. Chem. Int. Ed.* **2011**, *50*, 8420–8423.

[21]  J. M. Goicoechea, H. Grützmacher, *Angew. Chem. Int. Ed.* **2018**, *57*, 16968–16994.

[22]  J. G. Cordaro, D. Stein, H. Rüegger, H. Grützmacher, *Angew. Chem. Int. Ed.* **2006**, *45*, 6159–6162.

[23]  M. Y. Antipin, A. N. Chernega, K. A. Lysenko, Y. T. Struchkov, J. F. Nixon, *Chem. Commun.* **1995**, *548*, 505–506.

[24]  R. Appel, A. Westerhaus, *Tetrahedron Lett.* **1981**, *22*, 2159–2160.

[25]  A. M. Arif, A. R. Barron, A. H. Cowley, S. W. Hall, *Chem. Commun.* **1988**, *171*, 171–172.

[26]  C. Jones, M. Waugh, *J. Organomet. Chem.* **2007**, *692*, 5086–5090.

[27]  M. Brym, C. Jones, *Dalton Trans.* **2003**, *3*, 3665–3667.

[28]  M. Finze, E. Bernhardt, H. Willner, C. W. Lehmann, *Angew. Chem. Int. Ed.* **2004**, *43*, 4160–4163.

[29]  J. C. T. R. B.-S. Laurent, M. A. King, H. W. Kroto, J. F. Nixon, R. J. Suffolk, *Dalton Trans.* **1983**, 755–759.

[30]  K. Jayasuriya, *J. Mol. Struct. THEOCHEM* **1992**, *256*, 17–27.

[31]  O. Mo, M. Yáñez, J.-C. Guillemin, E. H. Riague, J.-F. Gal, C. D. Maria, Pierre-Charles Poliart, *Chem. Eur. J.* **2002**, *8*, 4919–4924.

[32]  M. F. Lucas, M. C. Michelini, N. Russo, E. Sicilia, *J. Chem. Theory Comput.* **2008**, *4*, 397–403.

[33]  D. González-Pinardo, J. M. Goicoechea, I. Fernández, *Chem. Eur. J.* **2023**, *30*, e202303977.

[34]  M. J. Hopkinson, H. W. Kroto, J. F. Nixon, N. P. C. Simmons, *Chem. Phys. Lett.* **1976**, *42*, 460–461.

[35]  H. Eshtiagh-Hosseini, H. W. Kroto, J. F. Nixon, S. Brownstein, J. R. Morton, K. F. Preston, *Chem. Commun.* **1979**, *10*, 653–654.

[36]  R. Appel, F. Knoll, I. Ruppert, *Angew. Chem. Int. Ed.* **1981**, *20*, 731–744.

[37]  E. P. O. Fuchs, M. Hermesdorf, W. Schnurr, W. Rösch, H. Heydt, M. Regitz, P. Binger, *J. Organomet. Chem.* **1988**, *338*, 329–340.

[38]  J. Guillemin, T. Janati, J. Denis, *J. Org. Chem.* **2001**, *66*, 7864–7868.

[39]  S. M. Mansell, M. Green, R. J. Kilby, M. Murray, C. A. Russell, *Comptes Rendus Chim.* **2010**, *13*, 1073–1081.

[40]  R. Appel, G. Maier, H. P. Reisenauer, A. Westerhaus, *Angew. Chem. Int. Ed.* **1981**, *20*, 197–197.

[41]  T. Allspach, M. Regitz, G. Becker, W. Becker, *Synthesis (Stuttg).* **1986**, 31–36.

[42]  W. Rösch, U. Hess, M. Regitz, *Chem. Ber.* **1987**, 1645–1652.

[43]    M. Regitz, W. Rösch, T. Allspach, U. Annen, K. Blatter, J. Fink, M. Hermesdorf, H. Heydt, U. Vogelbacher, O. Wagner, *Phosphorus Sulfur Silicon Relat. Elem.* **1987**, *30*, 479–482.

[44]    A. Mack, E. Pierron, T. Allspach, U. Bergsträßer, M. Regitz, *Synthesis (Stuttg).* **1998**, 1305–1313.

[45]    G. Fritz, W. Hölderich, *ZAAC* **1976**, *422*, 104–114.

[46]    F. Uhlig, R. Hummeltenberg, *J. Organomet. Chem.* **1993**, *452*, 6–7.

[47]    D. Heift, Z. Benko, H. Grützmacher, *Dalton Trans.***2014**, *43*, 831–840.

[48]    R. Suter, Z. Benkő, M. Bispinghoff, H. Grützmacher, *Angew. Chem. Int. Ed.* **2017**, 11226 – 11231.

[49]    W. J. Transue, J. Yang, M. Nava, I. V. Sergeyev, T. J. Barnum, M. C. McCarthy, C. C. Cummins, *J. Am. Chem. Soc.* **2018**, *140*, 17985–17991.

[50]    E. Yue, L. Dettling, J. A. W. Sklorz, S. Kaiser, M. Weber, C. Müller, *Chem. Commun.* **2022**, *58*, 310–313.

[51]    L. Dettling, M. Papke, J. A. W. Sklorz, D. Buzsáki, Z. Kelemen, M. Weber, L. Nyulászi, C. Müller, *Chem. Commun.* **2022**, *58*, 7745–7748.

[52]    L. Dettling, N. Limberg, R. Küppers, D. Frost, M. Weber, N. T. Coles, D. M. Andrada, C. Müller, *Chem. Commun.* **2023**, *59*, 10243–10246.

[53]    L. Dettling, M. Papke, M. Ernst, M. Weber, C. Müller, *Chem. Eur. J.* **2024**, e202400592.

[54]    R. Huisgen, *Proc. Chem. Soc.* **1961**, 357–396.

[55]    G. Pfeifer, M. Papke, D. Frost, J. A. W. Sklorz, M. Habicht, C. Müller, *Angew. Chem. Int. Ed.* **2016**, *55*, 11760–11764.

[56]    L. Nyulászi, T. Veszprémi, J. Réffy, B. Burkhardt, M. Regitz, *J. Am. Chem. Soc.* **1992**, *114*, 9080–9084.

[57]    L. Nyulászi, G. Csonka, J. Réffy, T. Veszprémi, J. Heinicke, *J. Organomet. Chem.* **1989**, *373*, 49–55.

[58]    B. Niaz, F. Iftikhar, M. K. Kindermann, P. G. Jones, J. Heinicke, *Eur. J. Inorg. Chem.* **2013**, 4220–4227.

[59]    J. A. W. Sklorz, S. Hoof, N. Rades, N. Derycke, L. Könczöl, D. Szieberth, M. Weber, J. Wiecko, L. Nyulászi, M. Hissler, C. Müller, *Chem. Eur. J.* **2015**, *21*, 11096–11109.

[60]    M. Papke, L. Dettling, J. A. W. Sklorz, D. Szieberth, L. Nyulászi, C. Müller, *Angew. Chem. Int. Ed.* **2017**, *56*, 16484 –16489.

[61]    J. A. W. Sklorz, M. Schnucklake, M. Kirste, M. Weber, J. Wiecko, C. Müller, *Phosphorus Sulfur Silicon Relat. Elem.* **2016**, *191*, 558–562.

[62]    S. L. Choong, A. Nafady, A. Stasch, A. M. Bond, C. Jones, *Dalton Trans.***2013**, *42*, 7775–7780.

[63]    S. L. Choong, C. Jones, A. Stasch, *Dalton Trans.***2010**, *39*, 5774–5776.

[64]    C. Elschenbroich, *Organometallchemie*, Teubner Verlag, Wiesbaden, **2008**.

[65]    J. J. Daly, *J. Chem. Soc.* **1964**, 3799–3810.

[66] T. A. Van Der Knaap, T. C. Klebach, F. Visser, F. Bickelhaupt, P. Ros, E. J. Baerends, C. H. Stam, M. Konijn, *Tetrahedron Lett.* **1984**, *40*, 765–776.

[67] J. A. W. Sklorz, PhD Thesis, **2016**.

[68] P. Le Floch, *Coord. Chem. Rev.* **2006**, *250*, 627–681.

[69] D. S. Frost, PhD Thesis, **2022**.

[70] J. A. W. Sklorz, S. Hoof, M. G. Sommer, F. Weißer, M. Weber, J. Wiecko, B. Sarkar, C. Müller, *Organometallics* **2014**, *33*, 511–516.

[71] R. Huisgen, *Angew. Chem. Int. Ed.* **1963**, *2*, 565–632.

[72] V. V. Rostovtsev, L. G. Green, V. V. Fokin, K. B. Sharpless, *Angew. Chem. Int. Ed.* **2002**, *41*, 2596–2599.

[73] F. Himo, T. Lovell, R. Hilgraf, V. V. Rostovtsev, L. Noodleman, K. B. Sharpless, V. V. Fokin, *J. Am. Chem. Soc.* **2005**, *127*, 210–216.

[74] L. Zhang, X. Chen, P. Xue, H. H. Y. Sun, I. D. Williams, K. B. Sharpless, V. V. Fokin, G. Jia, *J. Am. Chem. Soc.* **2005**, *127*, 15998–15999.

[75] B. C. Boren, S. Narayan, L. K. Rasmussen, L. Zhang, H. Zhao, Z. Lin, G. Jia, V. V Fokin, *J. Am. Chem. Soc.* **2008**, *130*, 8923–8930.

[76] H. C. Kolb, M. G. Finn, K. B. Sharpless, *Angew. Chem. Int. Ed.* **2001**, *40*, 2004–2021.

[77] Nobel Prize Outreach, *Nobelprize.Org* **2022**, 1.

[78] E. M. Sletten, C. R. Bertozzi, *Acc. Chem. Res.* **2011**, *44*, 666–676.

[79] D. González-Pinardo, J. M. Goicoechea, I. Fernández, *Chem. Eur. J.* **2024**, *30*, e202303977.

[80] J. A. W. Sklorz, C. Müller, *Eur. J. Inorg. Chem.* **2016**, 595–606.

[81] S. P. Chia, Y. Li, C. W. So, *Organometallics* **2013**, *32*, 5231–5234.

[82] E. S. Yang, A. Mapp, A. Taylor, P. D. Beer, J. M. Goicoechea, *Chem. Eur. J.* **2023**, *29*, e202301648.

[83] A. Mapp, J. T. Wilmore, P. D. Beer, J. M. Goicoechea, *Angew. Chem. Int. Ed.* **2023**, *62*, e202309211.

[84] W. J. Transue, A. Velian, M. Nava, M. A. Martin-Drumel, C. C. Womack, J. Jiang, G. L. Hou, X. Bin Wang, M. C. McCarthy, R. W. Field, C. C. Cummins, *J. Am. Chem. Soc.* **2016**, *138*, 6731–6734.

[85] G. Märkl, I. Troetsch-Schaller, W. Hölzl, *Tetrahedron Lett.* **1988**, *29*, 785–788.

[86] H.-P. Schrodel, A. Schmidpeter, *Chem. Ber.* **1997**, *130*, 89–93.

[87] G. Bouhadir, R. W. Reed, R. Réau, G. Bertrand, *Heteroat. Chem.* **1995**, *6*, 371–375.

[88] W. Rösch, T. Facklam, M. Regitz, *Tetrahedron* **1987**, *43*, 3247–3256.

[89] J. Kerth, U. Werz, G. Maas, *Tetrahedron* **2000**, *56*, 35–42.

[90] C. Müller, L. E. E. Broeckx, I. De Krom, J. J. M. Weemers, *Eur. J. Inorg. Chem.* **2013**, 187–202.

[91] T. L. Mindt, H. Struthers, L. Brans, T. Anguelov, C. Schweinsberg, V. Maes, D. Tourwé, R.

Schibli, *J. Am. Chem. Soc.* **2006**, *128*, 15096–15097.

[92]    A. Bastero, D. Font, M. A. Pericàs, *J. Org. Chem.* **2007**, *72*, 2460–2468.

[93]    J. A. W. Sklorz, S. Hoof, M. G. Sommer, F. Weißer, M. Weber, J. Wiecko, B. Sarkar, C. Müller, *Organometallics* **2014**, *33*, 511–516.

[94]    M. Papke, PhD Thesis, **2019**.

[95]    S. Burck, J. Daniels, T. Gans-Eichler, D. Gudat, K. Nättinen, M. Nieger, *ZAAC* **2004**, *631*, 1403–1412.

[96]    A. J. Arduengo, R. L. Harlow, M. Kline, *J. Am. Chem. Soc.* **1991**, *113*, 361–363.

[97]    S. Fleming, M. K. Lupton, K. Jekot, *Inorg. Chem.* **1972**, *11*, 2534–2540.

[98]    B. E. Maryanoff, R. O. Hutchins, *J. Org. Chem.* **1972**, *37*, 3475–3480.

[99]    D. Enders, O. Niemeier, A. Henseler, *Chem. Rev.* **2007**, *107*, 5606–5655.

[100]   N. Marion, S. Díez-González, S. P. Nolan, *Angew. Chem. Int. Ed.* **2007**, *46*, 2988 – 3000.

[101]   S. Díez-González, N. Marion, S. P. Nolan, *Chem. Rev.* **2009**, *109*, 3612–3676.

[102]   H. V. Huynh, *Chem. Rev.* **2018**, *118*, 9457–9492.

[103]   P. Bellotti, M. Koy, M. N. Hopkinson, F. Glorius, *Nat. Rev. Chem.* **2021**, *5*, 711–725.

[104]   T. M. Trnka, R. H. Grubbs, *Acc. Chem. Res.* **2001**, *34*, 18–29.

[105]   G. C. Vougioukalakis, R. H. Grubbs, *Chem. Rev.* **2010**, *110*, 1746–1787.

[106]   G. C. Fortman, S. P. Nolan, *Chem. Soc. Rev.* **2011**, *40*, 5151–5169.

[107]   B. Stadelmann, J. Bender, D. Förster, W. Frey, M. Nieger, D. Gudat, *Dalton Trans.***2015**, *44*, 6023–6031.

[108]   H. M. Tuononen, R. Roesler, J. L. Dutton, P. J. Ragogna, *Inorg. Chem.* **2007**, *46,* 10693–10706.

[109]   L. D. Hutchins, R. T. Paine, C. F. Campana, *J. Am. Chem. Soc.* **1980**, *102*, 4521–4523.

[110]   D. Gudat, A. Haghverdi, M. Nieger, *J. Organomet. Chem.* **2001**, *617*, 383–394.

[111]   D. Gudat, *Coord. Chem. Rev.* **1997**, *163*, 71–106.

[112]   L. K. Oliemuller, C. E. Moore, C. M. Thomas, *Inorg. Chem.* **2022**, *61*, 19440–19451.

[113]   C. A. Caputo, M. C. Jennings, H. M. Tuononen, N. D. Jones, *Organometallics* **2009**, *28*, 990–1000.

[114]   L. Rosenberg, *Coord. Chem. Rev.* **2012**, *256*, 606–626.

[115]   M. L. H. Green, *J. Organomet. Chem.* **1995**, *500*, 127–148.

[116]   L. D. Hutchins, E. N. Duesler, R. T. Paine, *Organometallics* **1982**, *1*, 1254–1256.

[117]   B. Pan, Z. Xu, M. W. Bezpalko, B. M. Foxman, C. M. Thomas, *Inorg. Chem.* **2012**, *51*, 4170–4179.

[118]   D. A. Evers-McGregor, M. W. Bezpalko, B. M. Foxman, C. M. Thomas, *Dalton Trans.* **2016**, *45*, 1918–1929.

[119]  C. W. Tornøe, C. Christensen, M. Meldal, *J. Org. Chem.* **2002**, *67*, 3057–3064.

[120]  Y. Jeong, J. S. Ryu, *J. Org. Chem.* **2010**, *75*, 4183–4191.

[121]  S. Hohloch, C. Y. Su, B. Sarkar, *Eur. J. Inorg. Chem.* **2011**, 3067–3075.

[122]  Z. K. Reeder, A. M. Adler, K. M. Miller, *Tetrahedron Lett.* **2016**, *57*, 206–209.

[123]  M. Heckenroth, E. Kluser, A. Neels, M. Albrecht, *Dalton Trans.* **2008**, *130*, 6242–6249.

[124]  G. Guisado-Barrios, J. Bouffard, B. Donnadieu, G. Bertrand, *Angew. Chem. Int. Ed.* **2010**, *49*, 4759–4762.

[125]  K. F. Donnelly, A. Petronilho, M. Albrecht, *Chem. Commun.* **2013**, *49*, 1145–1159.

[126]  C. Hering, A. Schulz, A. Villinger, *Inorg. Chem.* **2013**, *52*, 5214–5225.

[127]  S. Burck, D. Gudat, *Inorg. Chem.* **2008**, *47*, 315–321.

[128]  P. J. Stang, M. Hanack, L. R. Subramanian, *Synthesis (Stuttg).* **1982**, 85–126.

[129]  E. S. Lewis, S. Vanderpool, *J. Am. Chem. Soc.* **1977**, *99*, 1946–1949.

[130]  D. N. Kevill, G. M. L. Lin, *Tetrahedron Lett.* **1978**, 949–952.

[131]  S. S. Batsanov, *Inorg. Mater.* **2001**, *37*, 871–885.

[132]  E. C. Alyea, G. Ferguson, J. Malito, B. L. Ruhl, *Inorg. Chem.* **1985**, *24*, 3720–3722.

[133]  G. A. Bowmaker, J. D. Cotton, P. C. Healy, J. D. Kildea, B. Silong, B. W. Skelton, A. H. White, *Inorg. Chem.* **1989**, *28*, 1462–1466.

[134]  J. I. Van Der Vlugt, E. A. Pidko, D. Vogt, M. Lutz, A. L. Spek, *Inorg. Chem.* **2009**, *48*, 7513–7515.

[135]  J. Chen, X. Cao, J. Wang, L. He, Z. Liu, H. Wen, Z.-N. Chen, *Inorg. Chem.* **2013**, *52*, 9727–9740.

[136]  M. S. Balakrishna, V. S. Reddy, S. S. Krishnamurthy, J. F. Nixon, J. C. T. R. B. S. Laurent, *Coord. Chem. Rev.* **1994**, *129*, 1–90.

[137]  G. G. Briand, T. Chivers, M. Krahn, *Coord. Chem. Rev.* **2002**, *233*, 237–254.

[138]  M. M. Siddiqui, J. T. Mague, M. S. Balakrishna, *Inorg. Chem.* **2015**, *54*, 6063–6065.

[139]  A. J. Plajer, J. Zhu, P. Pröhm, F. J. Rizzuto, U. F. Keyser, D. S. Wright, *J. Am. Chem. Soc.* **2020**, *142*, 1029–1037.

[140]  M. Lehmann, A. Schulz, A. Villinger, *Struct. Chem.* **2011**, *22*, 35–43.

[141]  N. Selander, B. T. Worrell, V. V. Fokin, *Angew. Chem. Int. Ed.* **2012**, *51*, 13054–13057.

[142]  G. Märkl, G. Y. Jin, E. Silbereisen, *Angew. Chem. Int. Ed.* **1982**, *5*, 370–371.

[143]  M. H. Habicht, F. Wossidlo, M. Weber, C. Müller, *Chem. Eur. J.* **2016**, *22*, 12877 –12883.

[144]  M. H. Habicht, F. Wossidlo, T. Bens, E. A.Pidko, C. Müller, *Chem. Eur. J.* **2018**, *24*, 944–952.

[145]  N. Avarvari, P. Le Floch, F. Mathey, *J. Am. Chem. Soc.* **1996**, *118*, 11978–11979.

[146]  G. Frison, A. Sevin, N. Avarvari, F. Mathey, P. Le Floch, *J. Org. Chem.* **1999**, *64*, 5524–5529.

[147] R. O. Kopp, S. L. Kleynemeyer, L. J. Groth, M. J. Ernst, S. M. Rupf, M. Weber, L. J. Kershaw Cook, N. T. Coles, S. E. Neale, C. Müller, *Chem. Sci.* **2024**, *15*, 5405–5788.

[148] A. Schmidpeter, H. Klehr, *Z. Naturforsch. B* **1983**, *38b*, 1484–1487.

[149] Á. Díaz-Ortiz, A. de Cózar, P. Prieto, A. de la Hoz, A. Moreno, *Tetrahedron Lett.* **2006**, *47*, 8761–8764.

[150] J. A. W. Sklorz, C. Müller, *Eur. J. Inorg. Chem.* **2016**, 595–606.

[151] J. G. Kraaijkamp, G. van Koten, K. Vrieze, D. M. Grove, E. A. Klop, A. L. Spek, A. Schmidpeter, *J. Organomet. Chem.* **1983**, *256*, 375–389.

[152] J. G. Kraaijkamp, D. M. Grove, G. van Koten, A. Schmidpeter, *Inorg. Chem.* **1988**, *27*, 2612–2617.

[153] P. Kozáček, L. Dostál, A. Růžička, I. Císařová, Z. Černošek, M. Erben, *New J. Chem.* **2019**, *43*, 13388–13397.

[154] D. Gladow, S. Doniz-Kettenmann, H.-U. Reissig, *Helv. Chim. Acta* **2014**, *97*, 808–821.

[155] E. Y. Slobodyanyuk, O. S. Artamonov, O. V. Shishkin, P. K. Mykhailiuk, *Eur J. Org. Chem.* **2014**, 2487–2495.

[156] P. K. Mykhailiuk, *Beilstein J. Org. Chem.* **2015**, *11*, 16–24.

[157] Y. L. Yagupolskii, N. V. Pavlenko, I. I. Gerus, S. Peng, M. Nappa, *ChemistrySelect* **2019**, *4*, 4604–4610.

[158] F. Wossidlo, D. S. Frost, J. Lin, N. T. Coles, K. Klimov, M. Weber, T. Böttcher, C. Müller, *Chem. Eur. J.* **2021**, *27*, 12788–12795.

[159] J. Bouffard, B. K. Keitz, R. Tonner, G. Guisado-Barrios, G. Frenking, R. H. Grubbs, G. Bertrand, *Organometallics* **2011**, *30*, 2617–2627.

[160] C. Tian, W. Nie, M. V. Borzov, P. Su, *Organometallics* **2012**, *31*, 1751–1760.

[161] L. B. De Oliveira Freitas, P. Eisenberger, C. M. Crudden, *Organometallics* **2013**, *32*, 6635–6638.

[162] A. J. Arduengo, F. Davidson, R. Krafczyk, W. J. Marshall, R. Schmutzler, *Monatshefte für Chemie* **2000**, *131*, 251–265.

[163] L. A. Schaper, X. Wei, P. J. Altmann, K. Öfele, A. Pöthig, M. Drees, J. Mink, E. Herdtweck, B. Bechlars, W. A. Herrmann, F. E. Kühn, *Inorg. Chem.* **2013**, *52*, 7031–7044.

[164] S. Dutta, S. De, S. Bose, E. Mahal, D. Koley, *Eur. J. Inorg. Chem.* **2020**, 638–655.

[165] A. Maisonial, P. Serafin, M. Traïkia, E. Debiton, V. Théry, D. J. Aitken, P. Lemoine, B. Viossat, A. Gautier, *Eur. J. Inorg. Chem.* **2008**, 298–305.

[166] A. Haupt, L. M. Keller, M. Kutter, D. Lentz, *Chem. Eur. J.* **2018**, *24*, 10756–10765.

[167] W. F. Gabrielli, S. D. Nogai, J. M. McKenzie, S. Cronje, H. G. Raubenheimer, *New J. Chem.* **2009**, *33*, 2208–2218.

[168] M. A. Kinzhalov, A. S. Legkodukh, T. B. Anisimova, A. S. Novikov, V. V. Suslonov, K. V. Luzyanin, V. Y. Kukushkin, *Organometallics* **2017**, *36*, 3974–3980.

[169] E. S. Yang, J. M. Goicoechea, *Angew. Chem. Int. Ed.* **2022**, *134*, 1–5.

## 10.    Curriculum Vitae

**Education:**

**2020– 2024**          **Doctoral candidate in Inorganic Chemistry (Freie Universität Berlin):**

Thesis "Aromatic phosphorus heterocycles: from triazaphospholes to phosphorus derivatives of mesoionic carbenes"

**2014 – 2020**          **Freie Universität Berlin**:

**Bachelor of Chemistry**: Bachelor thesis titled: "Synthesis and reactivity of low-coordinated phosphorus compounds"

**Master of Chemistry**: Master thesis with the title: "Reactivity studies on 3*H*-1,2,3,4-triazaphospholes"

**International experience:**

**University of British Columbia (Vancouver, BC) Spring 2023, research stay**

research stay with the research group of Prof. Derik Gates: Working on the Polymerization of Phosphaalkynes.

**Scripps Research Institute (San Diego, CA) Summer 2019, Internship**

Internship with the research group of Prof. Keary Engle: Development of chiral "directing groups" and their potential application in hydroformylation and hydroboration reactions

**National University of Singapore Summer 2017, Internship**

Internship with the research group of Prof. Han Vinh Huynh: Synthesis of bridged NHCs and their use as chelating ligands in nickel(II) complexes

**WWF Paraguay (Asunción) Spring 2014, Internship**

Working in a forest conservation project in the Atlantic Rainforest with an indigenous community

**Work Experience:**

**2016 – 2018**          **Atotech Berlin Trainee**

**2013 – 2015**          **Tutor for Mathematics and Chemistry**

**Voluntary Work:**

**2019 – 2020**          **Project CyberMentor Volunteer**

Meeting weekly with a female high school student to support them in carrying out joint scientific projects with the aim of giving them an insight into and inspire them for the STEM field

**11.      Appendix**

Au(I)-mediated N2-elimination from triazaphospholes: a one-pot synthesis of novel N2P2-heterocycles

# Supporting Information

## Au(I)-Mediated $N_2$-Elimination from Triazaphospholes: A One-Pot Synthesis of Novel $N_2P_2$-Heterocycles

Erlin Yue, Lea Dettling, Julian A. W. Sklorz, Selina Kaiser, Manuela Weber, and
Christian Müller

**Table of Content**

# 1. Experimental Procedures

## 1.1 General information

### General Remarks

All reactions were performed under an argon atmosphere in oven-dried glassware using modified Schlenk techniques or in an MBraun glovebox. All common solvents and chemicals were commercially available. Tosyl azide **1a** and mesitylsulfonyl azide **1b** were prepared according to literature methods.[1] *Tert*-butylphosphaalkyne was prepared according to the previous literature.[2] Commercially available chemicals were used without further purification. Dry Toluene, EtOH, *n*-hexane, *n*-pentane and $CH_2Cl_2$ were prepared by using an MBraun Solvent Purification System. $Et_2O$ was dried over Na/benzophenone and THF was dried over K/benzophenone under argon. The deuterated dry solvents benzene-$d_6$ and DCM-$d_2$ were dried over $CaH_2$ and THF-$d_8$ over sodium-potassium alloy. $^1H$, $^{13}C\{^1H\}$, and $^{31}P\{^1H\}$ NMR spectra were recorded by using a JEOL ECS400 spectrometer (400 MHz), or a JEOL ECZ600 spectrometer (600Hz). All chemical shifts are reported relative to the residual resonance in the deuterated solvents. ESI-MS spectra were recorded on an Agilent 6210 ESI-TOF (4 kV) from Agilent Technologies. EI measurements were conducted with a modified device of a MAT 711 from Varian MAT. CHN-Analysis was performed on an ELEMENTAR VARIO EL.

**Caution**: Azides are potentially hazardous compounds and adequate safety measures should be taken when weighing, heating and working up.

## 1.2 Synthesis and characterization

**Synthesis of 5-(*tert*-butyl)-3-tosyl-3*H*-1,2,3,4-triazaphosphole (2a)**
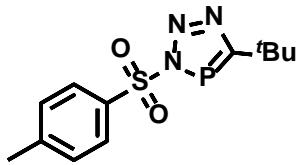
The tosyl azide **1a** (739.6 mg, 3.75 mmol) was dissolved in 20 mL of dry toluene and the solution was frozen at $T$ = -78 °C and degassed. The freshly prepared *tert*-butyl phosphaalkyne (412.9 mg, 4.13 mmol, 1.5 eq.) in 30 mL dry toluene was added by means of trap-to-trap condensation. The reaction mixture was allowed to warm to room temperature and stirred for 24 h. Excess alkyne and the solvent were removed under vacuum. The crude product was recrystallized from a hot saturated solution of dry pentane. **2a** was obtained as a white solid (948.4 mg, 85%). $^1$H NMR (400 MHz, CD$_2$Cl$_2$): $\delta$ (ppm) = 8.06 (d, $J$ = 8.5 Hz, 2H, *m*-tosyl-H), 7.44 (d, $J$ = 8.5 Hz, 2H, *o*-tosyl-H), 2.47 (s, 3H, CH$_{3\text{-tosyl}}$), 1.47 (d, $J$ = 3.2 Hz, 9H, CH$_3$). $^{13}$C{$^1$H} NMR (100 MHz, CD$_2$Cl$_2$): $\delta$ (ppm) = 200.0 (d, $J$ = 61.8 Hz, Ar-C), 147.0 (s, Ar-C), 133.9 (s, Ar-C), 130.2 (s, Ar-C), 128.5 (s, Ar-C), 33.5 (d, $J$ = 14.5 Hz, $C$Me$_3$), 30.8 (d, $J$ = 8.5 Hz, C$Me_3$), 21.5 (s, *p*-Ar-Me). $^{31}$P{$^1$H} NMR (162 MHz, CD$_2$Cl$_2$): $\delta$ (ppm) = 177.2 (s). EI-MS(m/z): 297.078 m/z (Calc.: 297.0701). Elemental analysis: N: 11.51; C: 48.61; H: 5.513; (Calc.: N: 14.13; C: 48.48; H: 5.42).

**Synthesis of 5-(*tert*-butyl)-3-(2-mesitylenesulfonyl)-3*H*-1,2,3,4-triazaphosphole (2b)**
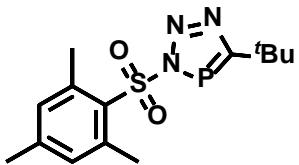
The 2-mesitylenesulfonyl azide **1b** (1500 mg, 6.66 mmol) was dissolved in 20 mL toluene and the solution was frozen at $T$ = -78 °C and degassed. The freshly prepared *tert*-butyl phosphaalkyne (998.8 mg, 9.99 mmol, 1.5 eq.) in 30 mL dry toluene was added by means of trap-to-trap condensation. The reaction mixture was allowed to warm to room temperature and stirred for 24 h. Excess alkyne and the solvent was removed under vacuum. The crude product was recrystallized from a hot saturated solution of dry pentane. **2b** was obtained as a white solid (998.0 mg, 46%). $^1$H NMR (400 MHz, CD$_2$Cl$_2$): $\delta$ (ppm) = 7.04 (s, 2H, Ar-H), 2.71 (s, 6H, Ar$_{Me}$-H), 2.31 (s, 3H, Ar$_{Me}$-H), 1.43 (s, 9H, CMe$_3$-H). $^{13}$C{$^1$H} NMR (100 MHz, CD$_2$Cl$_2$): $\delta$ (ppm) = 199.5 (d, $J$ = 61.0 Hz, TAP-C), 146.3 (s, Ar-C), 142.1 (s, Ar-C), 133.0 (s, Ar-C), 131.5 (s, Ar-C), 36.0 (d, $J$ = 15.0 Hz, $C$Me$_3$), 31.4 (d, $J$ = 8.0 Hz, C$Me_3$), 23.6 (s, *o*-Ar-Me), 21.4 (s, *p*-Ar-Me). $^{31}$P{$^1$H} NMR (162 MHz, CD$_2$Cl$_2$): $\delta$ (ppm) = 175.2 (s). Elemental analysis: N: 12.93; C: 51.72; H: 6.614 (Calc.: N: 12.91; C: 51.68; H: 6.20).

**Reaction of 2a with AuCl(SMe₂):**

In a *J*-Young NMR tube, tosyl-substituted triazaphosphole **2a** (50.0 mg, 0.17 mmol) and AuCl(SMe₂) (48.5 mg, 0.17 mmol) was dissolved in 0.5 mL of $CD_2Cl_2$ under an argon atmosphere. A gas evolution was immediately observed, while the reaction solution turned yellow. The reaction is not selective and several resonances were found by means of NMR spectroscopy (see Figure S9). $^{31}P\{^1H\}$ NMR (162 MHz, $CD_2Cl_2$): $\delta$ (ppm) = 11.5 (s), 16.7 (s), 115.4 (s), 120.5 (s), 130.2 (s), 138.4 (s). Crystals of diauro 2,4-bis(3-methylbut-2-en-2-yl)-1,3-ditosyl-1,3,2,4-diazadiphosphetidine dichloride **(3a)**, suitable for single crystal X-ray diffraction analysis, were obtained from the reaction mixtures at low temperature.

**Synthesis of diauro 2,4-bis(3-methylbut-2-en-2-yl)-1,3-bis(2-mesitylenesulfonyl)-1,3,2,4-diazadiphosphetidine dichloride (3b).**
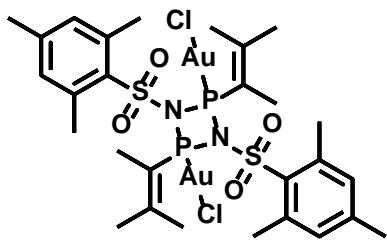


Mesitylsulfonyl-substituted triazaphosphole **2b** (50.0 mg, 0.15 mmol) and AuCl(SMe₂) (45.3 mg, 0.15 mmol) was dissolved in 2.0 mL of $CH_2Cl_2$ under an argon atmosphere. A gas evolution was immediately observed (Figure S1). The reaction solution was first heated to $T = 60°C$ for 2h and then left to cool to room temperature over the next 12 h. The Solvent was evaporated and a yellow solid was obtained. When adding 1.0 mL of toluene the product precipitated as a white solid. The desired complex was obtained as a white solid (28.6 mg, 36%). Crystals suitable for single crystal X-ray diffraction analysis were obtained from the reaction mixtures at low temperature.

$^1H$ NMR (401 MHz, $CD_2Cl_2$): $\delta$ = 7.03 (s, 2H), 2.74 (d, *J* = 1.2 Hz, 3H), 2.72 (s, 6H), 2.32 (s, 3H), 1.95 (d, *J* = 11.5 Hz, 3H), 1.88 (s, 3H). $^{13}C\{^1H\}$ NMR (151 MHz, $CD_2Cl_2$): $\delta$ = 169.57 – 169.15 (m)145.98, 140.47, 132.96, 131.08, 125.55 – 125.03 (m), 26.83 – 26.56 (m), 25.35 – 24.95 (m), 24.56, 20.93, 16.28. $^{31}P\{^1H\}$ NMR (162 MHz, $CD_2Cl_2$): $\delta$ = 133.9 (s). Elemental analysis: N: 2.658; C: 31.88; H: 4.73 (Calc.: N: 2.64; C: 31.75; H: 3.81).
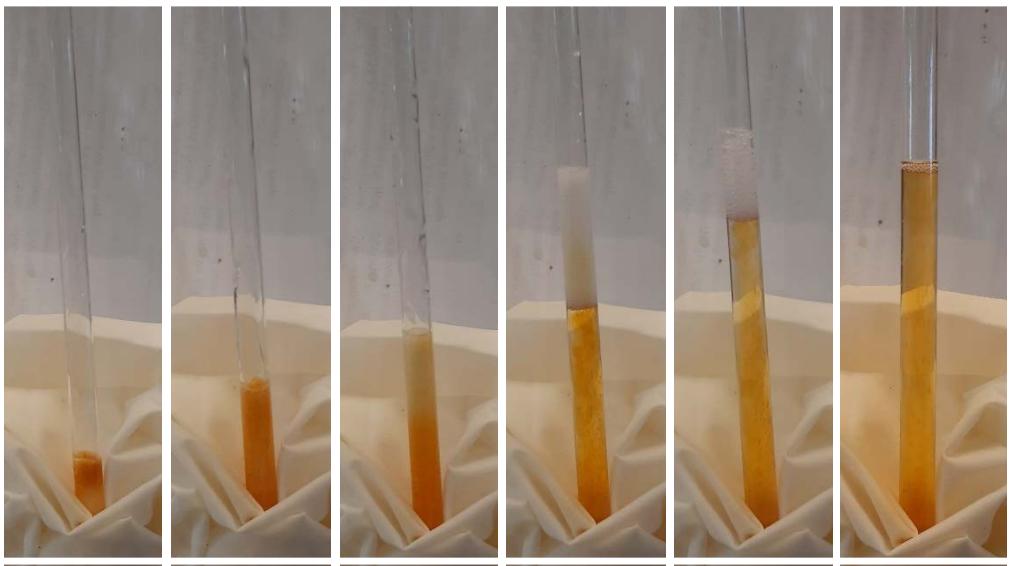
**Figure S1.** Nitrogen generation upon addition of DCM to a mixture of **2b** and AuCl(SMe$_2$). Left picture: start, right picture: after one minute.

## 1.3 Low-temperature $^{31}$P{$^1$H} NMR spectroscopy

Under exclusion of light gold(I)chloride dimethylsulfide (18.1 mg, 0.06 mmol) was dissolved in DCM-$d_2$ in a *J*-Young-NMR-tube and cooled to $T$ = -78 °C. A prestirred solution of 5-(*tert*-butyl)-3-(mesitylsulfonyl)-3*H*-1,2,3,4-triazaphosphole **2b** (20.0 mg, 0.06 mmol) in DCM-$d_2$ (0.3 mL) was likewise cooled to $T$ = -78 °C and then carefully added. The low temperature $^{31}$P{$^1$H} NMR-measurement was started at $T$ = -70 °C, the temperature of the reaction solution was increased by $T$ = 10 °C every 30 minutes until reaching room temperature (Figure S2).
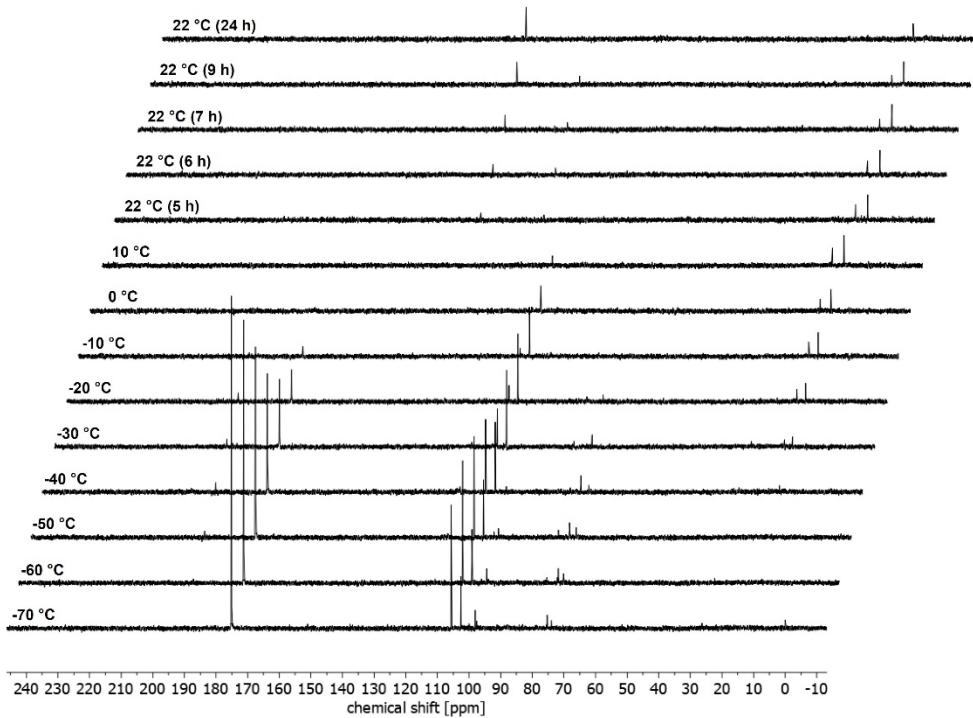
**Figure S2.** Temperature-dependent $^{31}P\{^{1}H\}$ NMR spectra for the reaction of **2b** with an equimolar amount of AuCl·SMe$_2$.

At $T$ = -70 °C, free ligand and a new species with a sharp resonance at $\delta$(ppm) = 105.4 is present in solution in a ratio of 3:2. The strong upfield shift of the signal is consistent with the formation of the Au(I)-complex [(**2b**)AuCl], in which coordination of the heterocycle to the AuCl-fragment proceeds *via* the phosphorus donor. The presence of larger amounts of free ligand might be attributed to the low solubility of AuCl·S(CH$_3$)$_2$ in CH$_2$Cl$_2$ at $T$ = -70 °C. Indeed, with increasing temperature up to $T$ = -10°C, both the signal of the free ligand and the proposed [(**2b**)AuCl] complex decrease in intensity, which indicates that fluxional coordination processes start to take place, while the AuCl-fragment can coordinate to the donor atoms P$^4$, N$^1$ and N$^2$ of the ambidentate triazaphosphole. Between $T$ = 0 °C and r.t., the formation of the products with the resonances at $\delta$(ppm) = 133.81 (**3b**) and $\delta$(ppm) = 2.18 can be observed. It should be noted that during the temperature dependent NMR spectroscopic investigations, also several minor, unidentified phosphorus compounds were detected. However, the exclusive formation of the above-mentioned two phosphorus species in the ratio of approximately 4:1 is completed within 24 h.

## 1.4 Trapping Experiment

In a *J*-Young NMR tube, *N*-tosyl-triazaphosphole **2a** (20 mg, 0.067 mg) and AuCl(SMe$_2$) (20 mg, 0.067 mmol) were cooled to *T* = -196 °C. Subsequently, a solution of dimethylbutadiene (22 mg, 0.26 mmol, 4 eq.) as a trapping reagent in CD$_2$Cl$_2$ was condensed into the reaction vessel. The solution was first placed into a dry ice bath (*T* = -78 °C) and then slowly warmed to room temperature over 6-8 hours. The reaction solution was analysed by means of NMR spectroscopy (*T* = 25 °C) $^1$H NMR (400 MHz, CD$_2$Cl$_2$): $\delta$ (ppm) = 7.91–7.85 (m, 3 H), 7.45 (d, *J* = 8.0 Hz, 1 H), 7.40 (dd, *J* = 8.5, 0.5 Hz, 2H), 7.37–7.33 (m, 2H), 7.10 (dd, *J* = 8.6, 0.7 Hz, 1H), 2.67 (s, 3H), 2.52–2.25 (m), 1.57 (s, 9H), 1.49–1.44 (m), 1.32 (s, 1H), 1.13 (s, 1H), 1.24 (s, 1H). $^{13}$C{$^1$H} NMR (100 MHz, CD$_2$Cl$_2$): $\delta$ = 143.41, 132.24, 131.34, 130.95, 129.74, 129.29, 128.75, 128.65, 128.39, 128.34, 128.23, 127.57, 126.25, 126.12, 124.70, 112.77, 30.94, 28.12, 27.64, 21.62, 20.26, 0.70. $^{31}$P{$^1$H} NMR (162 MHz, CD$_2$Cl$_2$): $\delta$ = 133.2 (s), 104.8 (s, main species), 13.6 (s). ESI-TOF-MS (m/z): [(**6a**)AuCl] m/z calc. for C$_{18}$H$_{26}$AuClNO$_2$PS [M + Na]$^+$: 606.0668; found 606.0655; [(**6a**)AuCl] m/z calc. for C$_{18}$H$_{26}$AuClNO$_2$PS [M + K]$^+$: 622.0407; found 622.0392.

## 1.5 Crossover Experiment

Tosyl-substituted triazaphosphole **2a** (30.0 mg, 0.10 mmol), mesitylsulfonyl-substituted triazaphosphole **2b** (32.8 mg, 0.10 mmol) and AuCl(SMe$_2$) (29.7 mg, 0.10 mmol) were dissolved in 2.0 mL of CH$_2$Cl$_2$ under an argon atmosphere. A gas evolution was immediately observed. The reaction solution was first heated to *T* = 60°C for 2 h and then left to cool to room temperature over the next 12 h. The reaction solution was analysed by means of NMR spectroscopy. $^{31}$P{$^1$H} NMR (162 MHz, NONE): $\delta$ = 133.9 (s), 133.0 (s), 132.3 (s). The above-mentioned three phosphorus species are in the ratio of approximately 4:4:1 (see Figure S13).

## 2. Crystallographic Details

Crystals of **2b** suitable for X-ray diffraction were obtained by laying diethyl ether on a dichloromethane solution of **2b** at low temperature. Crystals of **3a** and **3b** suitable for X-ray diffraction were obtained from their reaction mixtures at low temperature. X-ray studies were carried out on a D8 Venture, Bruker Photon CMOS diffractometer[3] with a rotating anode (MoKα radiation; $\lambda$ = 0.71073 Å) up to a resolution of (sin$\Theta$/$\lambda$)$_{max}$ = 0.60 Å at 104(2) K (**2b**), 100(2) K (**3a**) and 102(2) K (**3b**). The structures were solved with SHELXT-2014/5[4a] by using direct methods and refined with SHELXL-2017/1[4b] on $F^2$ for all reflections. Non-

hydrogen atoms were refined by using anisotropic displacement parameters. The positions of the hydrogen atoms were calculated for idealized positions. Geometry calculations and checks for higher symmetry were performed with the PLATON program.[5] Crystal data for the structures reported in this paper have been deposited in the Cambridge Crystallographic Database Center: CCDC number: 1983603 (**2b**), CCDC number: 1983601 (**3a**) and CCDC number: 1983602 (**3b**). Details of the X-ray structure determinations and refinements are provided in Table S1.

**Table S1.** Crystal data and structure refinement for **2b**, **3a** and **3b** (CCDC: 1983603, 1983601, 1983602).

| Identification code | 2b | 3a | 3b |
|---|---|---|---|
| Empirical formula | $C_{14}H_{20}N_3O_2PS$ | $C_{24}H_{32}Au_2Cl_2N_2O_4P_2S_2$ | $C_{28}H_{40}Au_2Cl_2N_2O_4P_2S_2$ |
| Formula weight | 325.36 | 1003.42 | 1059.52 |
| Temperature/K | 104(2) | 100(2) | 102(2) |
| Crystal system | monoclinic | monoclinic | monoclinic |
| Space group | $P2_1/c$ | $P2_1/n$ | $P2_1/c$ |
| a/Å | 10.6589(3) | 8.8016(5) | 9.6463(2) |
| b/Å | 17.7200(4) | 9.8055(4) | 17.8725(4) |
| c/Å | 8.8396(2) | 17.4622(9) | 10.9159(2) |
| α/° | 90 | 90 | 90 |
| β/° | 102.6651(9) | 96.710(2) | 114.0878(7) |
| γ/° | 90 | 90 | 90 |
| Volume/Å$^3$ | 1628.96(7) | 1496.74(13) | 1718.06(6) |
| Z | 4 | 2 | 2 |
| $\rho_{calc}$g/cm$^3$ | 1.327 | 2.227 | 2.048 |
| $\mu$/mm$^{-1}$ | 0.304 | 10.250 | 8.935 |
| $F(000)$ | 688 | 952 | 1016 |
| Crystal size/mm$^3$ | 0.660×0.110×0.050 | 0.115×0.035×0.020 | 0.170×0.100×0.040 |
| Radiation | MoKα(λ = 0.71073) | MoKα(λ = 0.71073) | MoKα(λ = 0.71073) |
| 2Θ range for | 4.54 to 52.83 | 4.70 to 52.89 | 4.62 to 51.44 |

data collection/°

| | | | |
|---|---|---|---|
| Index ranges | $-13 \le h \le 13$, <br> $-22 \le k \le 21$, <br> $-11 \le l \le 11$ | $-11 \le h \le 11$, <br> $-12 \le k \le 10$, <br> $-21 \le l \le 21$ | $-11 \le h \le 11$, <br> $-21 \le k \le 21$, <br> $-13 \le l \le 13$ |
| Reflections collected | 17318 | 18922 | 24932 |
| Independent reflections | 3335 [$R_{int}$ = 0.0524, $R_{sigma}$ = 0.0408] | 3072 [$R_{int}$ = 0.0245, $R_{sigma}$ = 0.0423] | 3267 [$R_{int}$ = 0.0452, $R_{sigma}$ = 0.0236] |
| Data/restraints/parameters | 3335/0/196 | 3072/0/176 | 3267/0/196 |
| Goodness-of-fit on $F^2$ | 1.033 | 1.186 | 1.133 |
| Completeness to $\theta$ | 99.9% | 99.7% | 99.8% |
| Final R indexes [I>=2σ (I)] | R1 = 0.0370 <br> wR2 = 0.0817 | R1 = 0.0335 <br> wR2 = 0.0582 | R1 = 0.0233 <br> wR2 = 0.0465 |
| Final R indexes [all data] | R1 = 0.0575 <br> wR2 = 0.0896 | R1 = 0.0434 <br> wR2 = 0.0582 | R1 = 0.0296 <br> wR2 = 0.0465 |
| Largest diff. peak/hole/e Å$^{-3}$ | 0.292/-0.408 | 1.832/-1.617 | 1.369/-0.778 |
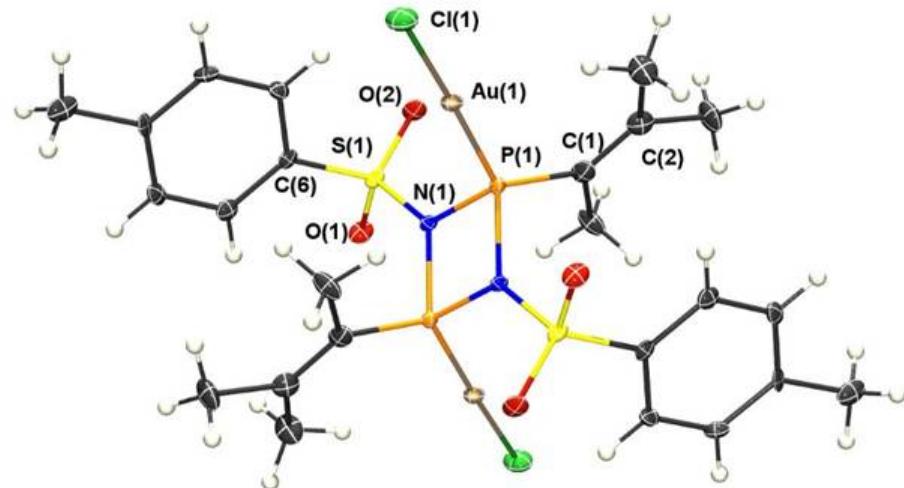


**Figure S3.** Molecular structure of **3a** in the crystal. Displacement ellipsoids are shown at the 50% probability level. Selected bond lengths (Å) and angels (°): P(1)-N(1): 1.720(5), N(1)-P(1)_i: 1.732 (5), N(1)-S(1): 1.658(5), P(1)-Au(1): 2.203(1), P(1)-C(1): 1.796(7), C(1)-C(2): 1.337(9), N(1)-P(1)-N(1)_i: 79.9(2), P(1)-N(1)-P(1)_i: 100.1(2).

## 3. NMR Spectroscopic Data
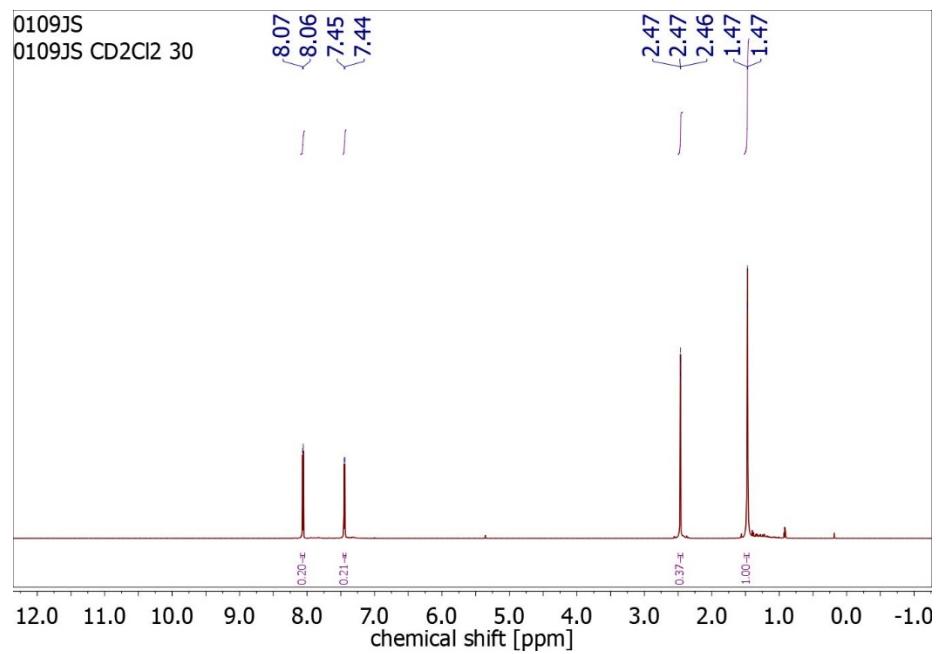


**Figure S4**. $^1$H NMR spectrum of **2a** in CD$_2$Cl$_2$
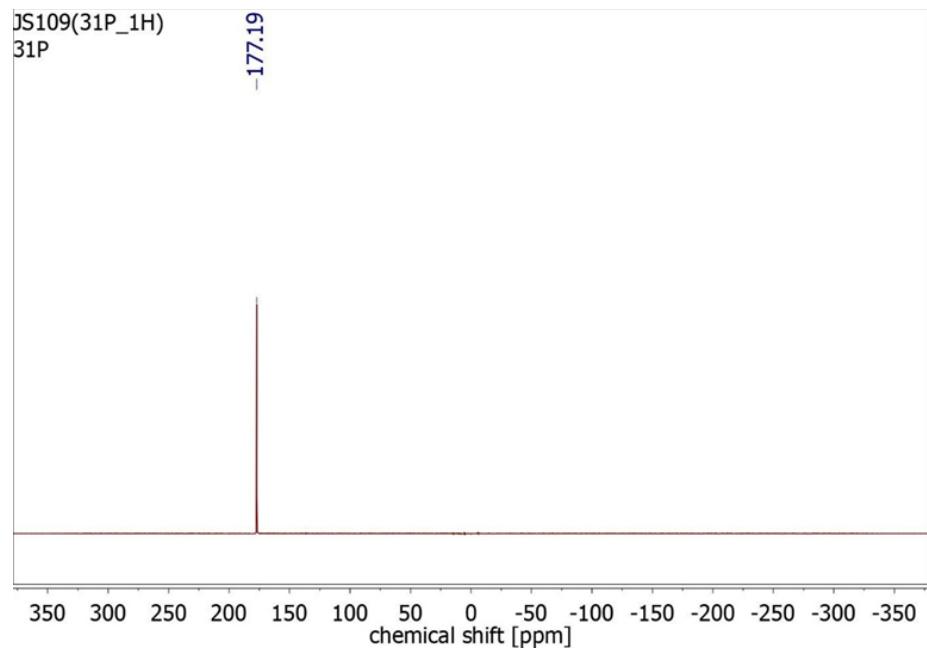


**Figure S5.** $^{31}$P{$^1$H} NMR spectrum of **2a** in CD$_2$Cl$_2$.
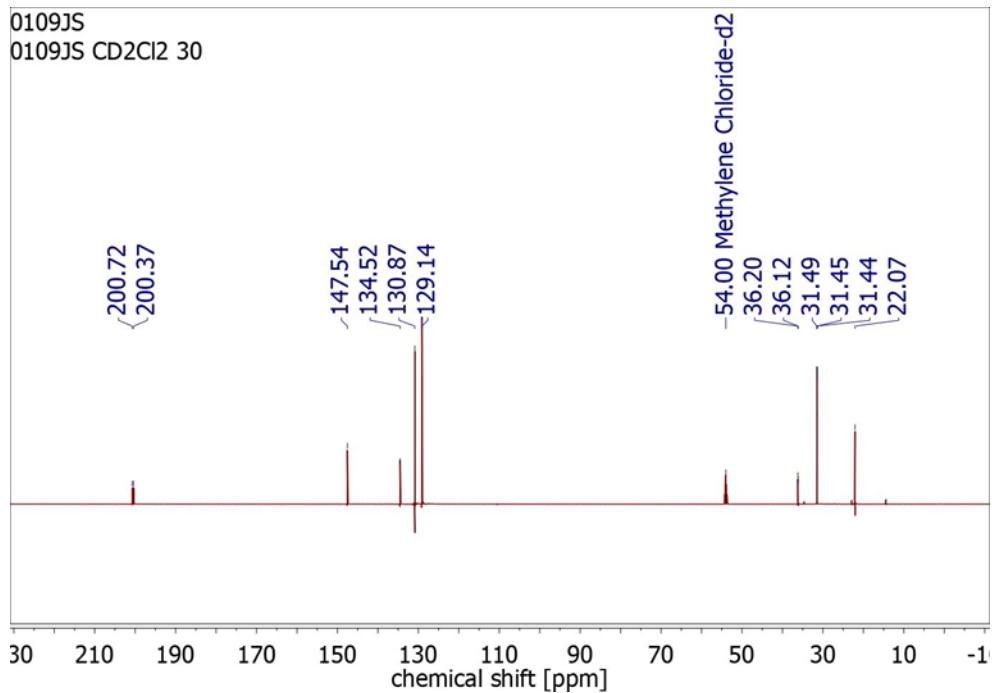
**Figure S6**. $^{13}C\{^1H\}$ NMR spectrum of **2a** in $CD_2Cl_2$.
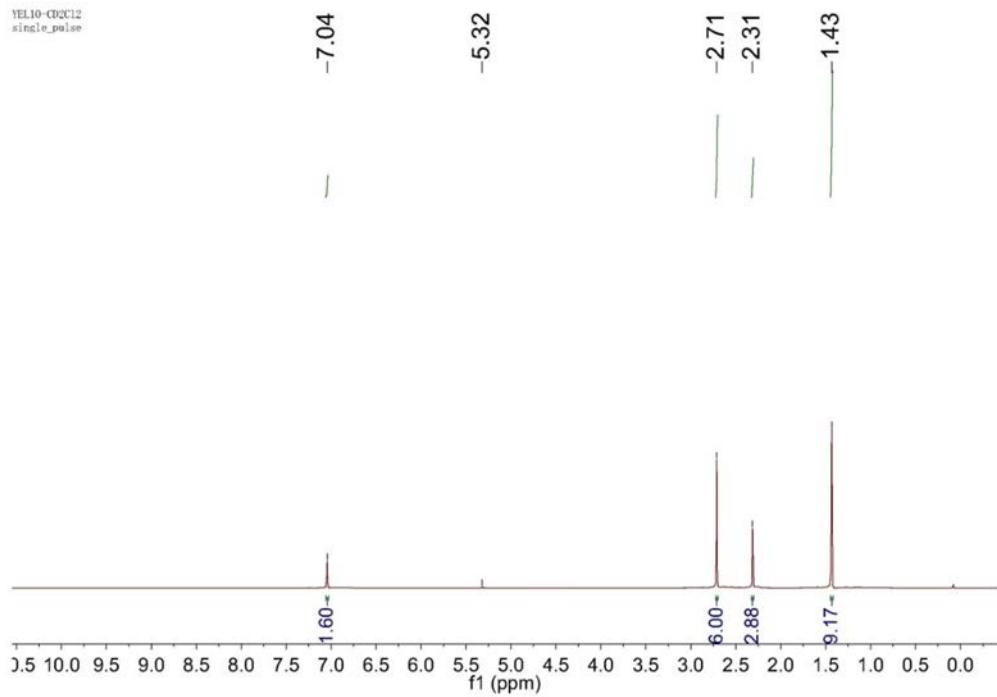


**Figure S7**. $^1H$ NMR spectrum of **2b** in $CD_2Cl_2$.

S12

94
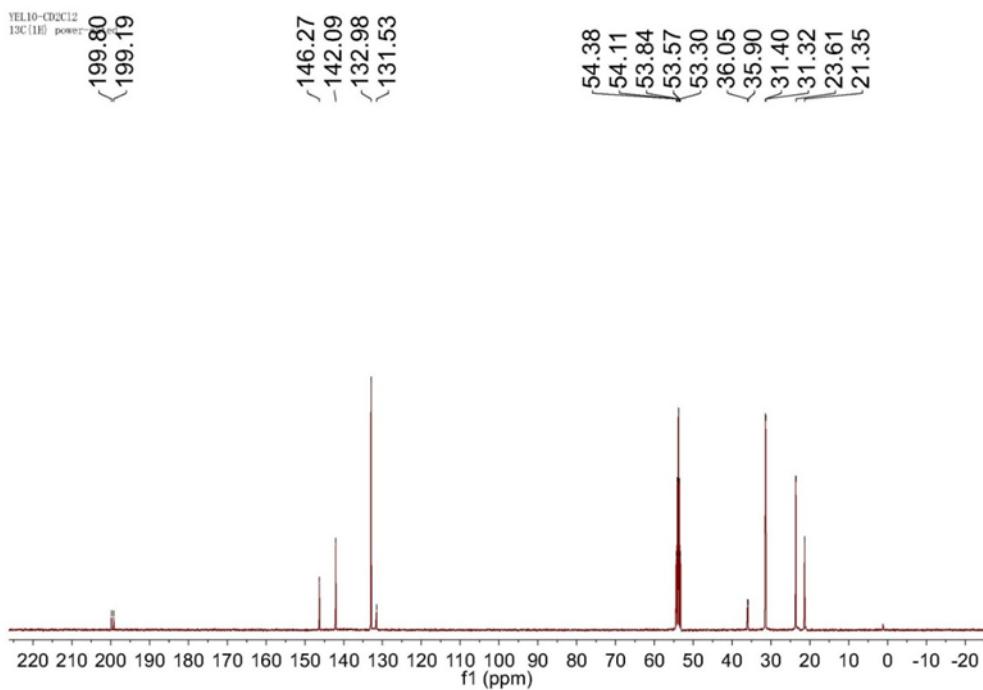
**Figure S8**. $^{13}C\{^1H\}$ NMR spectrum of **2b** in $CD_2Cl_2$.
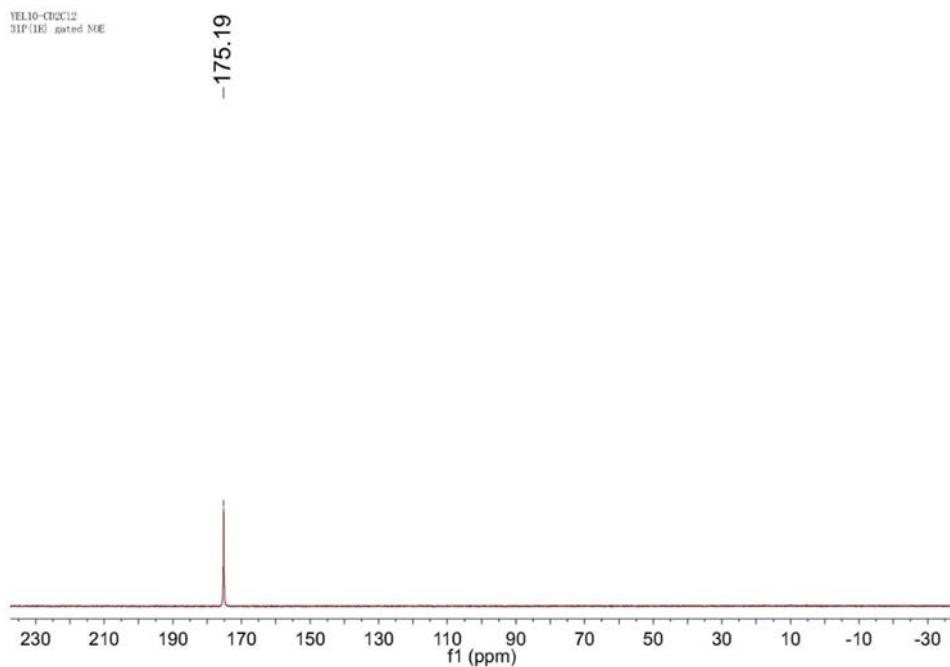


**Figure S9**. $^{31}P\{^1H\}$ NMR spectrum of **2b** in $CD_2Cl_2$.

S13

95
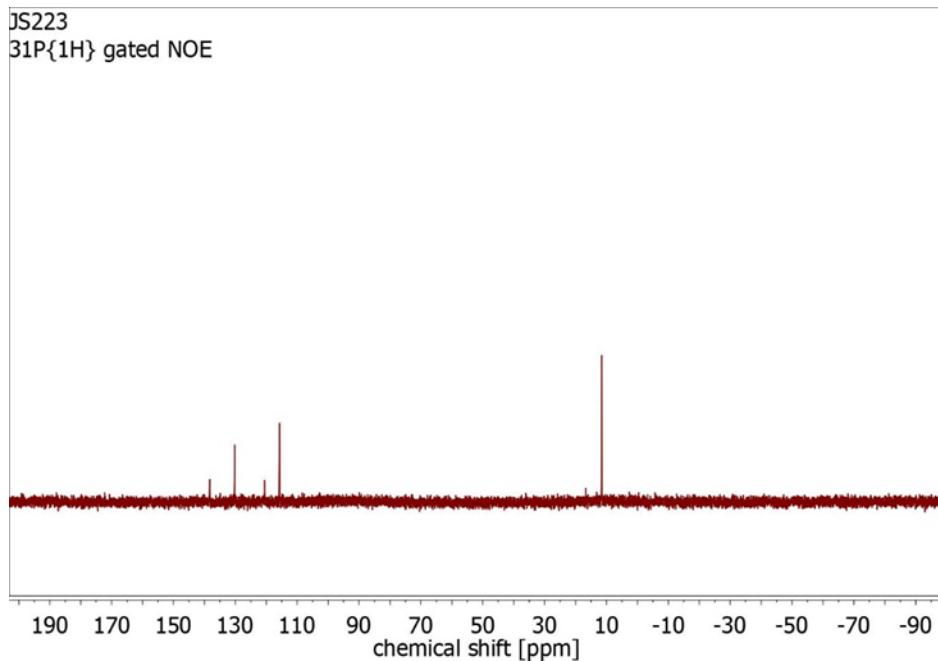
**Figure S10**. $^{31}P\{^1H\}$ NMR spectrum for the unselective reaction of **2a** with AuCl·SMe$_2$ in CD$_2$Cl$_2$.
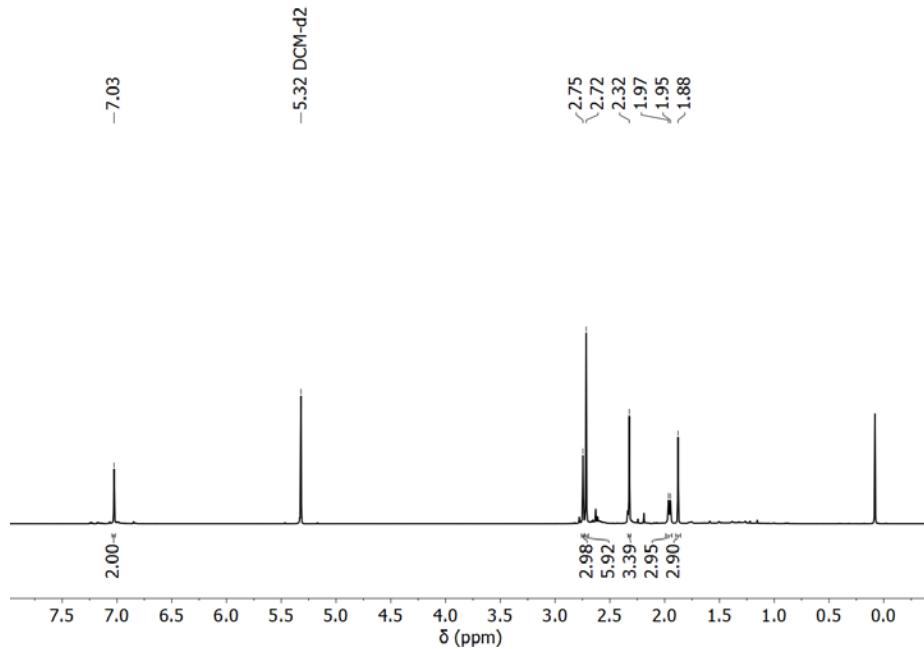


**Figure S10**. $^1H$ NMR spectrum of **3b** in CD$_2$Cl$_2$.
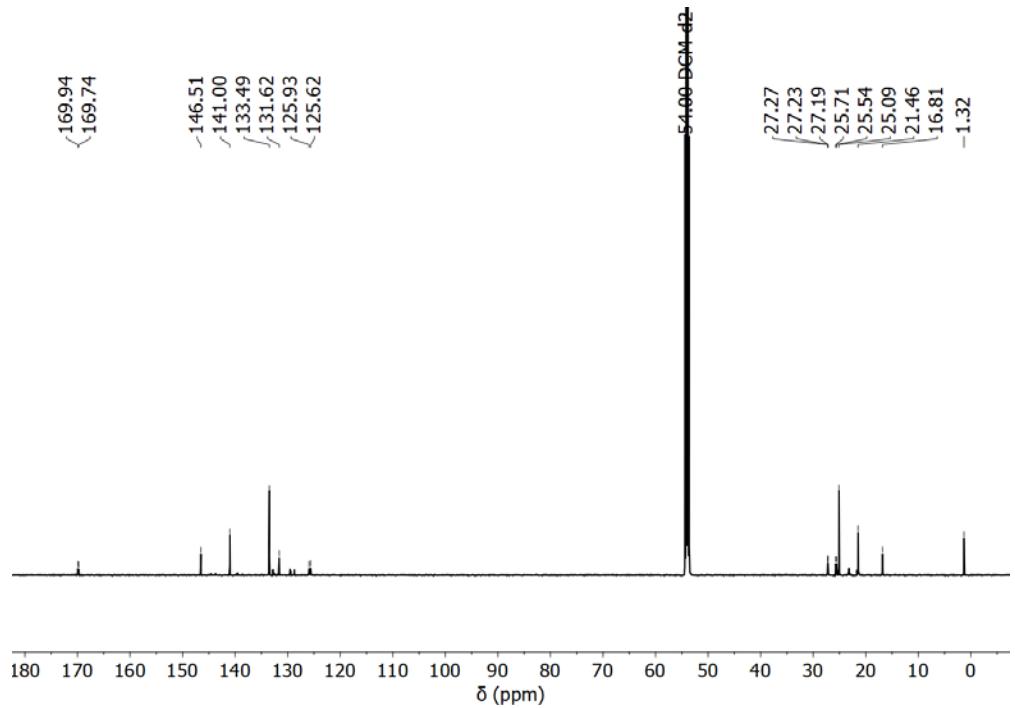
**Figure S11**. $^{13}C\{^1H\}$ NMR spectrum of **3b** in $CD_2Cl_2$.
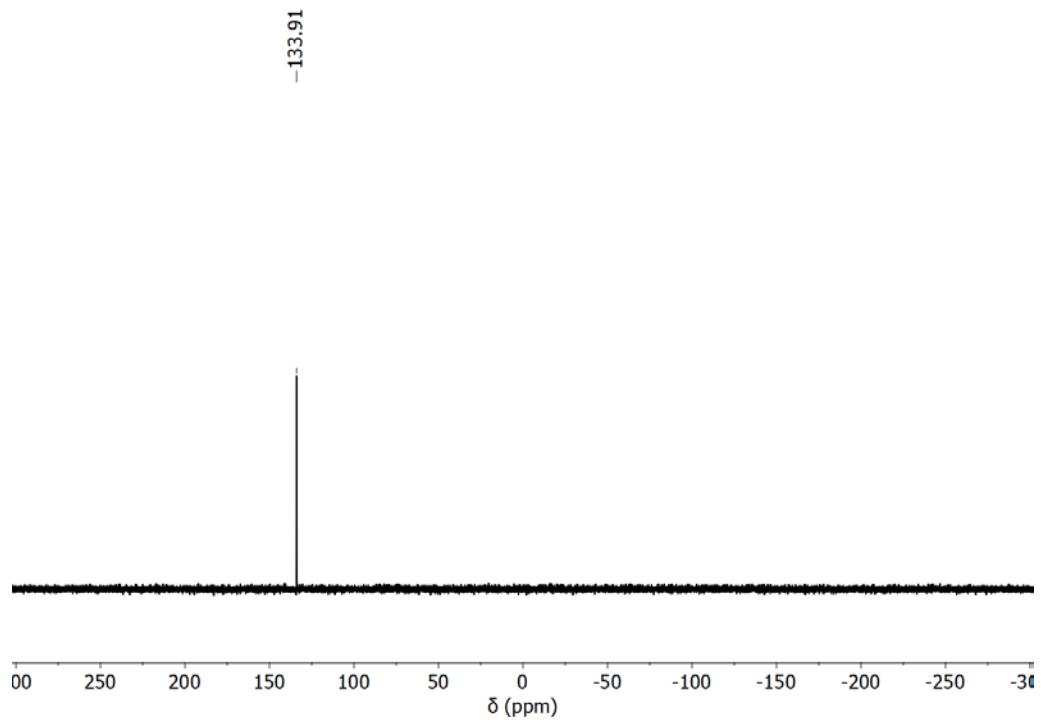


**Figure S12**. $^{31}P\{^1H\}$ NMR spectrum of **3b** in $CD_2Cl_2$.
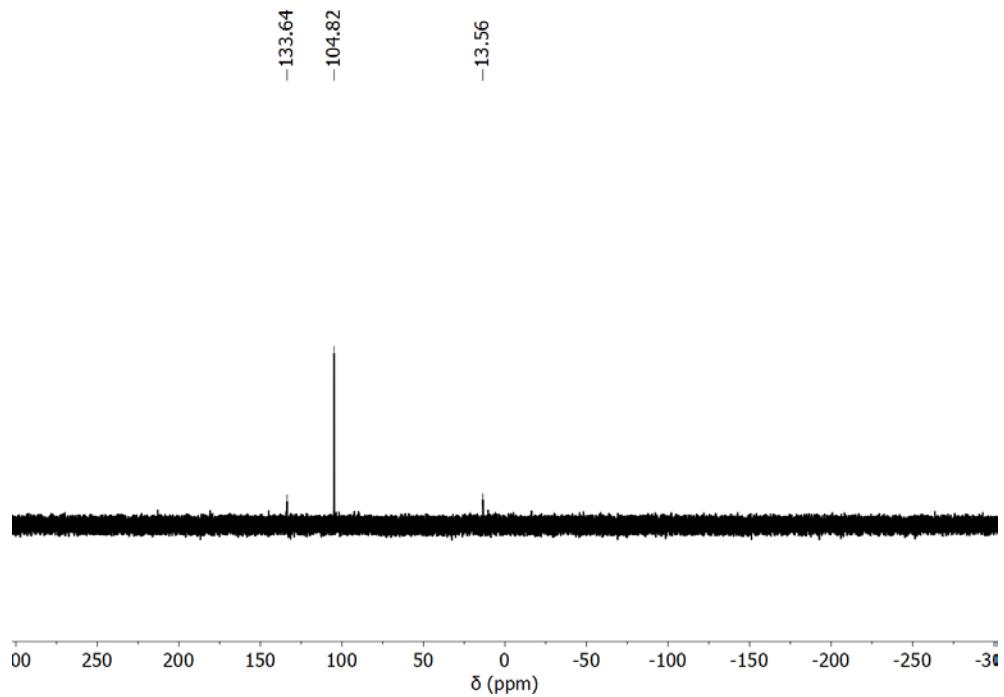
**Figure S13.** $^{31}P\{^1H\}$ NMR spectrum of trapping experiment.
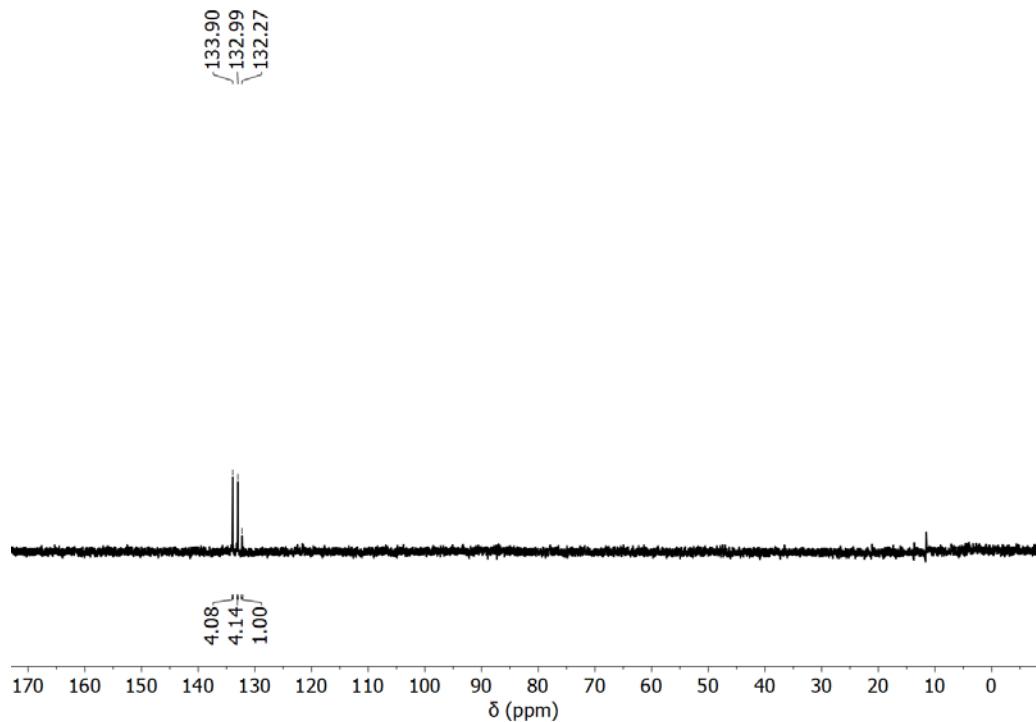


**Figure S13.** $^{31}P\{^1H\}$ NMR spectrum of crossover experiment.

# 4. References

[1]  a) T. J. Curphey, *Org. Prep. Proced. Int.* 1981, **13**, 112; b) R. A. Abramovitch, T.Chellathurai, D. W. Holcomb, T. I. McMaster, D. P. Vanderpool, *J. Org. Chem.* 1977, **42**, 2920.

[2]  a) G. Becker, G. Gresser, W. Uhl, *Z. Naturforsch., B* 1981, **36**, 16; b) W. Rösch, U. Vogelbacher, T. Allspach, M. Regitz. *J. Organomet. Chem.* 1986, **306**, 39; c) R. W. Miller, J. T. Spencer, *Organometallics* 1996, **15**, 4293.

[3]  Bruker (**2010**). APEX2, SAINT, SADABS and XSHELL. Bruker AXS Inc., Madison, Wisconsin, USA.

[4]  a) G. M. Sheldrick, *Acta Cryst*. 2015, **C71**, 3; b) G. M. Sheldrick, *Acta Cryst*. 2015, **A71**, 3.

[5]  A. L. Spek, *Acta Cryst*. 2009, **D65**, 148.

A new access to diazaphospholes via cycloaddition–cycloreversion reactions on triazaphospholes:

# Supporting Information

# A New Access to Diazaphospholes *via* Cycloaddition-Cycloreversion Reactions on Triazaphospholes

Lea Dettling, Martin Papke, Julian A. W. Sklorz, Dániel Buzsáki, Zsolt Kelemen, Manuela Weber, László Nyulászi, and Christian Müller

## Table of Contents

# 1.    DFT Calculations

All calculations have been carried out with the Gaussian 09 program package [1]. First the structure of **3** was optimized at different levels of the theory and the structural parameters obtained were compared to the X-ray data (more information can be seen in Table S2). Unless otherwise stated, subsequent calculations were carried out at the ωB97X-D/6-311+G** level of theory [2] (for the W atom, def2TZVP basis set was applied), with the correction of the PCM implicit solvent model (in toluene) [3]. Harmonic vibrational frequency calculations were applied on the fully optimized systems to establish their nature, as characterized by only positive eigenvalues of the Hessian for minima and by a single negative eigenvalue for transition states. The reaction path was checked by IRC calculations starting from the transition structures. Gibbs free energies were obtained at atmospheric pressure utilizing the calculated harmonic frequencies. In accordance with the experimental conditions for the studied cycloaddition reactions 403 K, while for the complex formations (**6** and **7**) 298.15 K was considered. Aromatic properties were investigated by calculating NICS values, which can be accessed by performing NMR calculations on ghost atoms 1 Å above and below the geometric center of the ring in question [4]. Furthermore, Bird indices (aromaticity descriptor based on the standard deviation from the average bond indices) were also calculated [5]. For the visualization of the Kohn-Sham orbitals, the program IQmol [6] was used.

**Table S1.** NICS(1) and NICS (-1) values in ppm and Bird indexes for **1**, **3**, **6** and **7**.

| Compound no. | NICS(1), NICS(-1) (ppm) | Bird indices (-) |
|:---:|:---:|:---:|
| **1** | -12.3,-12.3 | 66 |
| **3** | -10.7,-10.7 | 67 |
| **6** | -9.6, -8.9 | 67 |
| **7** | -11.2,-11.1 | 64 |

Both measures indicate significant aromaticity. For comparison, the B3LYP/6-311+G** NICS(1) and BI values for pyrrole are -10.1 ppm and 73, respectively.

**Table S2.** Comparison of results of optimized geometries obtained by DFT calculations with X-ray data for **3**. As the best match can be seen in case of ωB97X-D/6-311+G** (highlighted in green), unless otherwise stated this level of theory was applied for all calculations.
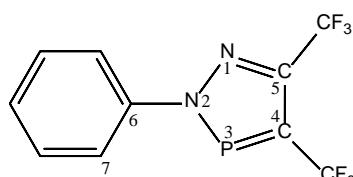


| Funct. Basis set | X-ray | B3LYP 6-311+G** | B3LYP cc-pVTZ | B3LYP def2-TZVP | M06-2X 6-311+G** | M06-2X cc-pVTZ | M06-2X def2-TZVP | ωB97X-D 6-311+G** | ωB97X-D cc-pVTZ | ωB97X-D def2-TZVP |
|---|---|---|---|---|---|---|---|---|---|---|
| N1-N2 | 1.349 | 1.335 | 1.333 | 1.333 | 1.329 | 1.328 | 1.328 | 1.329 | 1.327 | 1.327 |
| N2-P3 | 1.693 | 1.724 | 1.718 | 1.71 | 1.707 | 1.701 | 1.695 | 1.700 | 1.695 | 1.688 |
| P3-C4 | 1.712 | 1.728 | 1.723 | 1.718 | 1.713 | 1.710 | 1.706 | 1.714 | 1.710 | 1.705 |
| C4-C5 | 1.406 | 1.413 | 1.408 | 1.41 | 1.408 | 1.404 | 1.406 | 1.410 | 1.406 | 1.408 |
| C5-N1 | 1.323 | 1.321 | 1.318 | 1.318 | 1.314 | 1.312 | 1.311 | 1.315 | 1.312 | 1.311 |
| N2-C6 | 1.436 | 1.435 | 1.431 | 1.431 | 1.433 | 1.431 | 1.43 | 1.432 | 1.429 | 1.429 |
| dihedr1-2-6-7 | 145.9 | 149.5 | 153.9 | 152.1 | 151.4 | 157.3 | 154.5 | 146.1 | 150.2 | 149.2 |

**Table S3**. The comparison of the experimental of computational CO stretching nodes.

| | | $\tilde{v}_{(CO)}$ [cm$^{-1}$] | | | | |
|---|---|---|---|---|---|---|
| **6** | Experimental | 2089 | 2017 | 2002 | 1934 | - |
| | Computational[a] | 2085 | 2014 | 1989 | 1985 | 1977 |
| **7** | Experimental | 2077 | 2023 | 1980 | 1885 | - |
| | Computational[a] | 2077 | 2000 | 1973 | 1970 | 1967 |

[a]Calculated at the B3LYP/def2TZVP level of theory modified by a scaling factor of 0.968, as suggested by M.K.Assefa, J.L.Devera, A.D.Brathwaite, J.D.Mosley, M.A.Duncan, *Chem. Phys. Lett.* **2015**, *640*, 175-179.
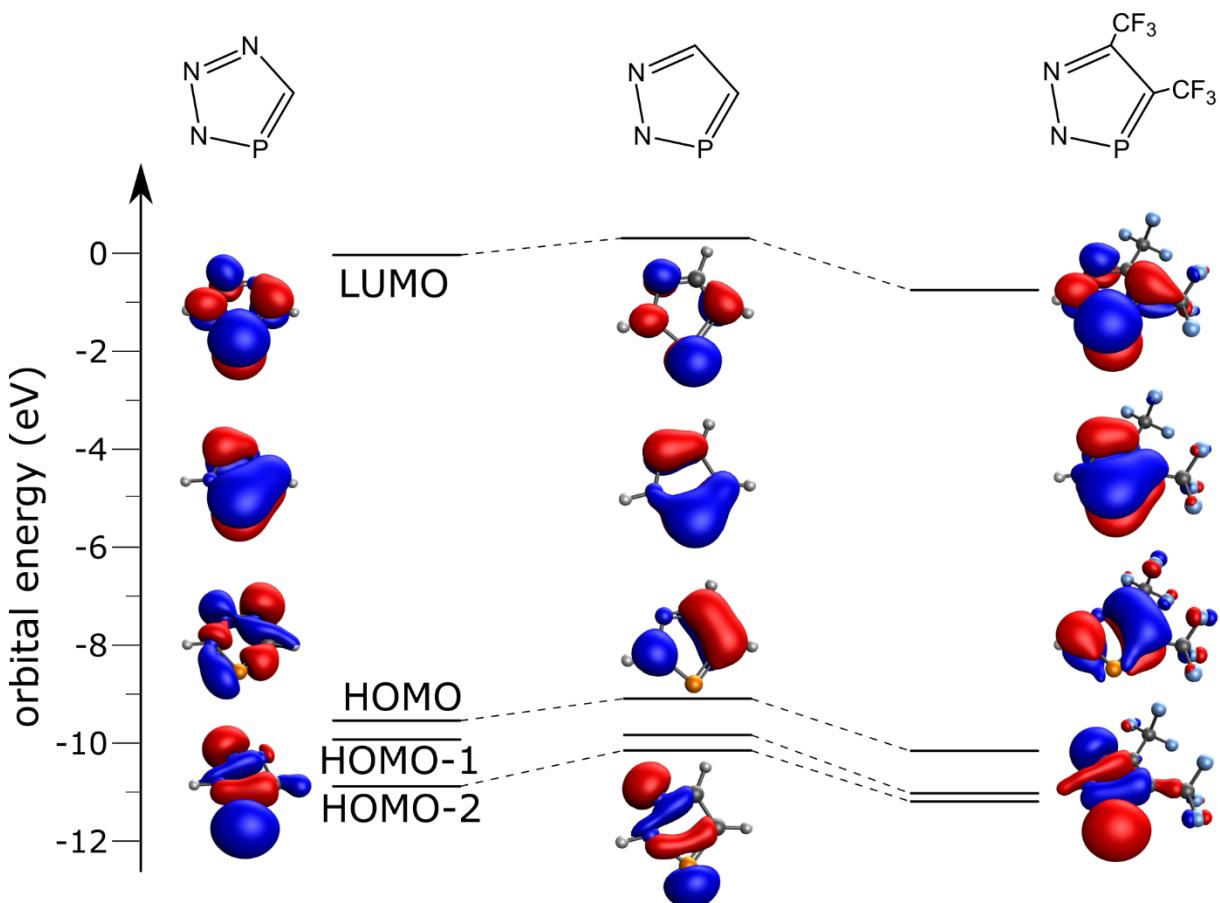


**Figure S1.** Kohn-Sham orbitals of the 3*H*-1,2,3,4-triazaphosphole, the 2*H*-1,2,3-diazaphosphole and CF$_3$-substituted diazaphosphole at the ωB97X-D/6-311+G** level of theory.

**XYZ coordinates of the investigated systems**

**XYZ coordinates of the intermediates of the a) reaction on Scheme 1**

**B** intermediate (van der Waals complex of 1 + DMAD)
E(ωB97X-D/6-311+G**) = -1466.21184374
G(403K)=      -1465.950793
C 2.97732800 -1.85264800 -1.30033300
C 2.37272300 -0.72039300 -0.76814300
C 3.06839500 0.13669100 0.07713400
C 4.39325000 -0.14663000 0.38109300
C 5.00998300 -1.27885500 -0.14148700
C 4.29943700 -2.13172400 -0.97810100
N 1.00876400 -0.43520600 -1.08429700
P -0.30096200 -1.52807800 -1.03870500
C -1.28534300 -0.17931000 -1.45016600
C -2.78677400 -0.12544900 -1.63201600
C -3.09796400 0.37504600 -3.05194500
N 0.69512800 0.82286700 -1.38512700
N -0.56883000 0.96231600 -1.58924400
C -3.37073700 0.84762400 -0.59327700
C -3.39962800 -1.51520400 -1.42895400
O 1.10512500 2.92201800 0.90860100
C 1.44923800 4.12048700 0.19788700
C -0.18677600 2.73864900 1.14661600
O -1.06076600 3.53713700 0.94080800
C -0.42768700 1.41410600 1.69525200
C -0.70077400 0.31517100 2.09029500
C -0.98982900 -1.02452200 2.56913700
O -2.15616300 -1.45210100 2.09627800
C -2.52365500 -2.79417900 2.44609400
O -0.25833900 -1.64908400 3.29037000
H -3.19394300 -1.89225700 -0.42241400
H -4.48483700 -1.46356500 -1.55129900
H -3.01672500 -2.23578000 -2.15911100
H -2.66260000 1.36236300 -3.21827000
H -4.18053700 0.44438600 -3.19412300
H -2.69559100 -0.31001100 -3.80404700
H -2.91642600 1.83603000 -0.68509700
H -3.19319600 0.48152400 0.42097300
H -4.45043900 0.94429000 -0.74274400
H 2.56796200 1.00555200 0.48701000
H 4.94329400 0.51634500 1.03877600
H 6.04360100 -1.49513600 0.10234400
H 4.77596300 -3.01231700 -1.39255900
H 2.42343300 -2.49968900 -1.97064500
H 2.52740200 4.07732100 0.06879600
H 0.94787500 4.12763900 -0.77018500
H 1.16256500 4.99989800 0.77503100
H -3.48730200 -2.96033200 1.97129000
H -1.78068700 -3.49657200 2.06617600
H -2.60677700 -2.89529500 3.52839000

**TS1**
E(ωB97X-D/6-311+G**) = -1466.16424154
G(403K)= -1465.899906
C -2.91659400 -0.94995300 -1.81533100
C -2.05527200 0.03718200 -1.34629200
C -2.55304700 1.24251400 -0.86282500
C -3.92490100 1.46453100 -0.86843300
C -4.79269700 0.48507100 -1.33447200
C -4.28498100 -0.72330700 -1.80178700
N -0.65381400 -0.22058300 -1.36198600
P 0.57840800 0.93001300 -1.28713500
C 1.70216200 -0.46588400 -1.23203600
C 3.20281300 -0.39757400 -1.38468700

C 3.53839500 -0.16782800 -2.86903800
N -0.26629300 -1.38116500 -0.76600900
N 1.07012800 -1.55707000 -0.91969700
C 3.72037400 0.78603200 -0.54841600
C 3.85032500 -1.69733200 -0.89865000
C -0.10946300 -0.51732600 1.14466100
C -0.71176200 -1.53223100 1.99443100
O 0.13759300 -2.52556000 2.23646600
C -0.37279300 -3.60790600 3.02410200
C 0.37757500 0.61926600 0.94540000
C 0.80494800 1.80191400 1.69961600
O 0.02996400 2.85208700 1.42256700
C 0.34921600 4.06950200 2.10941300
O 1.74182200 1.82632900 2.45522500
O -1.84304100 -1.47120000 2.40623100
H 3.61839800 -1.88164100 0.15257800
H 3.49797700 -2.55470700 -1.47530900
H 4.93585900 -1.62548800 -1.00976300
H 3.16629100 -0.99107200 -3.48440300
H 4.62283800 -0.10546000 -2.99736700
H 3.09906100 0.76315500 -3.23901000
H 3.47983900 0.66110300 0.51049400
H 4.80659900 0.85969800 -0.64690800
H 3.29882100 1.73847400 -0.88986600
H -1.88240100 1.99509100 -0.46332100
H -4.31371900 2.40261000 -0.48997100
H -5.86231200 0.65952100 -1.32908700
H -4.95722300 -1.49221800 -2.16437600
H -2.50721400 -1.88274200 -2.18220600
H -0.37405100 4.79970200 1.75541100
H 0.25675900 3.93154300 3.18707500
H 1.36432700 4.38618100 1.86689400
H 0.44634300 -4.31791300 3.10364500
H -0.66975300 -3.25283200 4.01173700
H -1.22920100 -4.06474200 2.52677000

**F** intermediate
E(ωB97X-D/6-311+G**) = -1466.20985218
G(403K)= -1465.938975
C -4.12827200 -1.40480600 0.49209500
C -2.79236300 -1.12083500 0.75556800
C -1.79676900 -1.69479700 -0.03479200
C -2.15287800 -2.54840000 -1.08303000
C -3.48922200 -2.81302900 -1.33955000
C -4.48747300 -2.24389000 -0.55382400
N -0.42671800 -1.46388400 0.21803500
N -0.13836500 -0.49378600 1.23694400
N 1.29147800 -0.71684300 1.54413600
C 1.90886900 -1.02090300 0.47914300
C 3.38553900 -1.29387100 0.39061400
C 3.59014800 -2.73483900 -0.10722300
P 0.72630700 -1.06054500 -1.01373800
C 0.27915500 0.74170100 -0.70987700
C -0.16212200 0.80416500 0.54388600
C -0.53993500 2.03134200 1.29370300
O -1.22405500 1.74836100 2.39457200
C -1.62983700 2.87064500 3.18761100
C 0.51177300 1.83191400 -1.68134000
O -0.60458600 2.46148200 -2.01732000
C -0.45624400 3.56728400 -2.91776300
O 1.60535000 2.06583000 -2.13397500
O -0.25227800 3.14319100 0.92783900
C 3.97133300 -0.30054500 -0.62813700
C 4.05301800 -1.10929700 1.75567800
H 5.12633600 -1.29561700 1.66173800
H 3.90827400 -0.09426100 2.13140500

H 3.64321100 -1.80341000 2.49244600
H 4.66026900 -2.93565200 -0.20584900
H 3.16841100 -3.45689700 0.59673900
H 3.12835600 -2.89428800 -1.08567200
H 5.04614000 -0.47311900 -0.72821500
H 3.52280100 -0.42114600 -1.61920000
H 3.81395400 0.73325600 -0.31169700
H -3.75106400 -3.47664700 -2.15608900
H -5.53107600 -2.45517000 -0.75485500
H -4.89387500 -0.95623800 1.11554600
H -2.51961400 -0.46955900 1.57538000
H -1.38184100 -3.01077400 -1.68973800
H -1.45992300 3.95693900 -3.06604600
H 0.18764800 4.32646700 -2.47291400
H -0.02984400 3.23123800 -3.86368900
H -2.15613300 2.44741600 4.03909800
H -0.75668400 3.43443300 3.51777800
H -2.28849800 3.52084500 2.61061200

**TS2**
E(ωB97X-D/6-311+G**) =  -1466.20721192
G(403K)= -1465.93483
C 3.30270800 0.29070400 -1.45205000
C 2.61077200 -0.10470800 -0.30322200
C 3.26710000 -0.85779300 0.67287500
C 4.60106500 -1.20038300 0.49396300
C 5.29618900 -0.80930900 -0.64457400
C 4.63468700 -0.06252500 -1.61377700
N 1.27424000 0.26143600 -0.13899400
N 0.54631400 -0.15573200 0.99760100
N -0.10264000 1.10055800 1.51942300
C -0.41445300 1.83737900 0.53971600
P 0.10971800 1.02950200 -1.12638800
C -0.99990600 -0.43211900 -0.73310100
C -0.57531000 -0.90938000 0.43666000
C -1.22483400 -1.98147400 1.23336000
C -1.09003700 3.17771800 0.64372800
C -2.33445600 3.14486400 -0.25892100
C -1.49233700 3.46971600 2.09188900
C -0.10762000 4.25034600 0.14171500
C -2.18178900 -0.83144700 -1.53043000
O -2.02580800 -2.01468100 -2.10536400
O -3.14159300 -0.11353700 -1.66426300
O -0.53518000 -2.28205100 2.32450600
O -2.26529400 -2.49945500 0.90993000
H -1.97523400 4.44934100 2.14507700
H -2.19192300 2.71805600 2.46395500
H -0.62114800 3.47563000 2.75008900
H 0.19257200 4.07052900 -0.89457500
H -0.58822300 5.23136300 0.18570600
H 0.79146200 4.27945300 0.76251600
H -2.07043100 2.97925000 -1.30827500
H -3.02672400 2.35535600 0.04275000
H -2.85424500 4.10456700 -0.19682100
H 2.72628300 -1.16221100 1.55885200
H 5.09996800 -1.78395500 1.26001900
H 6.33637200 -1.08233600 -0.77608900
H 5.15816100 0.25184100 -2.50993500
H 2.80074300 0.87413400 -2.21622200
C -1.10588100 -3.28778100 3.17018800
H -0.42111600 -3.38265500 4.00880700
H -2.09320600 -2.97675600 3.51348800
H -1.18738200 -4.23250000 2.63133700
C -3.14737700 -2.50509400 -2.85229200
H -2.83127000 -3.46549800 -3.25092100
H -4.00702000 -2.62823200 -2.19292700
H -3.39695000 -1.81622800 -3.66004900

**F' intermediate**

E(ωB97X-D/6-311+G**) =  -1466.21252337
G(403K)= -1465.942267
C 4.40239500 -1.72245200 0.38161000
C 3.03181900 -1.49884400 0.45902400
C 2.35312100 -0.99989400 -0.65066400
C 3.05270500 -0.72646000 -1.82841100
C 4.42178600 -0.93945000 -1.88612700
C 5.10572700 -1.44052700 -0.78220900
N 0.95357900 -0.77741400 -0.63541300
P 0.26831400 0.76210900 -1.07513100
C 0.52238800 1.19179300 0.79620200
C 0.70232200 2.59694500 1.30571700
C 0.81712300 2.61377900 2.83212300
N 0.30130100 -1.07322900 0.59437600
N 0.52457900 0.15502300 1.51119700
C -1.09623700 -0.96933900 0.23152900
C -2.05370100 -1.80919100 1.01849800
O -2.41220300 -2.88925500 0.34627400
C -1.35575200 -0.01225500 -0.66222300
C -2.70106400 0.38125500 -1.11211800
O -3.71868800 -0.19504600 -0.81648300
O -2.65239700 1.47749700 -1.87306800
C 1.97800200 3.17783900 0.67234000
C -0.52517900 3.40706800 0.85512000
O -2.40282000 -1.52009200 2.13113000
H 0.93884900 3.64392500 3.17847600
H -0.07605700 2.19267000 3.29827100
H 1.67821800 2.03149400 3.16659800
H 2.12276000 4.20364500 1.02202300
H 2.85617300 2.59120300 0.95442600
H 1.91459800 3.19994000 -0.41916700
H -0.42560800 4.44130100 1.19491600
H -0.62340900 3.42442200 -0.23536400
H -1.44513200 2.99486100 1.27854100
H 4.95476800 -0.72276900 -2.80509000
H 6.17446500 -1.61254100 -0.83258800
H 4.92194800 -2.11516700 1.24855700
H 2.48837500 -1.71210800 1.36963000
H 2.52045900 -0.35929300 -2.69911000
C -3.91039000 1.97874100 -2.33982800
H -3.67234900 2.86545400 -2.92179500
H -4.40632300 1.23345400 -2.96259000
H -4.55220100 2.23390300 -1.49584300
C -3.35030600 -3.75619000 1.00132000
H -3.52113800 -4.57406800 0.30657500
H -2.93124200 -4.12658500 1.93729100
H -4.27775700 -3.21778200 1.19783700

**TS3**
E(ωB97X-D/6-311+G**) =  -1466.21011763
G(403K)= -1465.940143
P 0.27736400 0.70356800 -1.09925100
C 0.49790100 1.12364000 0.86942100
N 0.50436600 0.11638700 1.58123800
N 0.28704800 -1.25132200 0.45005400
C -1.07264400 -1.06226900 0.13379100
C -1.32418800 -0.05789100 -0.72767800
C -2.66535900 0.41948900 -1.09436400
O -3.69718500 -0.13595900 -0.80731100
N 0.97999000 -0.81108900 -0.66201200
C 2.38687600 -1.00135800 -0.64201900
C 3.11453000 -0.67786000 -1.78776000
C 4.49207400 -0.84098300 -1.79867200
C 5.15083600 -1.34178600 -0.67984200
C 4.41711500 -1.67515400 0.45172000
C 3.03784400 -1.50217300 0.48221700
C 0.65849300 2.56614000 1.30000600
C 1.94634700 3.11597500 0.66710800
C -0.56186100 3.34493600 0.78617500

C 0.74069500 2.65855400 2.82671100
C -2.06152400 -1.85710400 0.93327700
O -2.38058000 -1.56486100 2.05374200
O -2.49121400 -2.90722700 0.25283900
C -3.47706200 -3.71978100 0.90629000
O -2.59694700 1.56961900 -1.77271400
C -3.84739000 2.15836200 -2.14668200
H 0.84894000 3.70484000 3.12614100
H -0.16065800 2.25464000 3.29251600
H 1.59813300 2.09869000 3.20602200
H 2.08222800 4.15744900 0.97116000
H 2.81825000 2.54494800 0.99617000
H 1.90705100 3.08668000 -0.42509400
H -0.47344800 4.39444800 1.07937800
H -0.63935600 3.31022200 -0.30521300
H -1.48821700 2.94807000 1.21007200
H 5.05087600 -0.58723600 -2.69227200
H 6.22615800 -1.47560400 -0.69381100
H 4.91932900 -2.06829800 1.32847700
H 2.46669200 -1.75094300 1.36608700
H 2.59999100 -0.31335100 -2.67003100
H -3.59185400 3.07409600 -2.67388800
H -4.40303000 1.48367300 -2.79881400
H -4.44207100 2.37953500 -1.25957600
H -3.70901100 -4.51470100 0.20254700
H -3.07388900 -4.13083000 1.83228100
H -4.36509900 -3.12468300 1.12099600

**G** intermediate (van der Waals complex of **2** + <sup>*t*</sup>BuCN)
E(ωB97X-D/6-311+G**) = -1466.30259288
G(403K)= -1466.038074
C -2.65173400 -1.89305800 0.38348800
C -3.99104000 -2.18760200 0.15797500
C -4.54229200 -2.02292300 -1.10700200
C -3.74614300 -1.57139400 -2.15548300
C -2.40347200 -1.29087200 -1.94665200
C -1.86575100 -1.45228100 -0.67451600
N -0.49247000 -1.13312400 -0.44640100
P 0.56601100 -1.99126200 0.56204400
C 1.77939400 -0.84376500 0.17078500
C 1.25096300 0.11714200 -0.71498900
N -0.00849500 -0.04242700 -1.05615400
C 3.13038200 -0.77967600 0.75416000
O 3.44901500 -1.92586500 1.36770600
O 3.85653900 0.18287000 0.71227900
C 1.98177000 1.28209100 -1.31132900
O 3.00476600 0.87098800 -2.05019500
O 1.66065300 2.43122600 -1.15769900
N -1.05410400 0.35020600 2.42661100
C -1.53942500 1.22265100 1.85248600
C -2.17628100 2.35315300 1.15466200
C -2.81753400 1.84474200 -0.14708700
C -3.24917600 2.93920600 2.08896800
C -1.09438500 3.40069400 0.84291000
H -4.60720300 -2.52737000 0.98215400
H -5.59012300 -2.24217200 -1.27603800
H -4.17064200 -1.44175400 -3.14421900
H -1.77295300 -0.93795700 -2.75270600
H -4.01968800 2.19924600 2.31752600
H -2.80975200 3.28635600 3.02676600
H -3.72325200 3.79030000 1.59336600
H -0.31475600 2.98732000 0.19985700
H -0.63193700 3.77213700 1.76047300
H -1.56039400 4.24410600 0.32609100
H -2.05724200 1.46420300 -0.83062600
H -3.54266700 1.05013700 0.04719200
H -3.33544900 2.67797800 -0.62965200
H -2.23049400 -1.96715600 1.37878000
C 3.84317700 1.89809700 -2.59181300

H 4.62345300 1.37715400 -3.14078400
H 3.27102400 2.54475900 -3.25809300
H 4.27368000 2.48995500 -1.78329300
C 4.71689200 -1.95854800 2.02994200
H 4.78866100 -2.94903900 2.47243800
H 5.52367800 -1.80123200 1.31300300
H 4.76152800 -1.19030200 2.80295600

**XYZ coordinates of the intermediates of the b) reaction on Scheme 1**

**B** intermediate (van der Waals complex of 1 + hexafluoro-2-butyne)
E(ωB97X-D/6-311+G**) = -1684.56991593
G(403K)= -1684.382812
C 0.94537200 -1.62787900 -0.77217400
C 1.60927100 -1.07560900 -1.86312100
C 2.94102300 -1.39736200 -2.08186500
C 3.61151400 -2.25204400 -1.21357300
C 2.93982700 -2.79552500 -0.12585000
C 1.60231100 -2.49266900 0.09569600
N -0.42270400 -1.29092800 -0.53464900
N -1.19858400 -1.06756700 -1.59782300
N -2.39873400 -0.76128600 -1.25581900
C -2.60785500 -0.73376400 0.08410300
C -3.98494300 -0.37874200 0.60384500
C -4.33369100 1.04944600 0.15189200
P -1.19210600 -1.11350200 0.98103100
C -5.00597500 -1.37093200 0.02314400
C -4.01428600 -0.45002800 2.13461900
F 0.35940700 2.11936600 -2.27404200
C 0.10603900 2.53110000 -1.02897300
F 0.21787700 3.86302800 -1.00622100
C 1.03551900 1.91730000 -0.07317600
C 1.79701000 1.42410000 0.70112600
C 2.74338900 0.84540400 1.66208500
F 2.17448900 -0.13739900 2.36494300
F 3.16440100 1.77586000 2.52555800
F 3.81273700 0.34702100 1.04041500
F -1.15648800 2.21799400 -0.73695600
H 4.65484900 -2.49065900 -1.38308300
H 3.45830100 -0.96785300 -2.93179600
H 1.08119400 -0.40437000 -2.52678800
H 3.45358200 -3.46488800 0.55396300
H 1.07382400 -2.93232100 0.93341200
H -5.00918100 -1.33002300 -1.06779500
H -6.00943700 -1.12595700 0.38374700
H -4.77235900 -2.39513200 0.32766400
H -5.01035400 -0.18741800 2.50079000
H -3.30208700 0.25096100 2.58209700
H -3.78365300 -1.45779100 2.49449000
H -4.29602500 1.13374300 -0.93607600
H -3.63342900 1.77438100 0.57517100
H -5.34245300 1.30867500 0.48682100

**TS1**
E(ωB97X-D/6-311+G**) = -1684.53262105
G(403K)= -1684.339296
C -2.46407400 -0.85335700 -1.46744300
C -1.95714500 -1.39185700 -0.28982500
C -2.80607200 -1.95638500 0.65707900
C -4.17211000 -1.97855200 0.41780800
C -4.68915900 -1.45365400 -0.76246300
C -3.83278200 -0.89499500 -1.70269000
N -0.55613800 -1.36802200 -0.02376400
N -0.20143400 -0.95375900 1.21634700
N 1.13513200 -1.06145700 1.38290400
C 1.78960300 -1.19490000 0.26528500
C 3.29278300 -1.34558600 0.21669700

S5

C 3.86234100 -0.39334500 -0.84600000
P 0.68295200 -1.12196600 -1.13655300
C 3.90771200 -1.02551300 1.58267600
C 3.61491000 -2.80157900 -0.16899700
C -0.16230100 1.07670700 0.71109900
C -0.77458700 1.71505700 1.88742200
F -0.80899400 3.05171900 1.74909300
C 0.30649400 1.13241100 -0.43807100
C 0.58559800 2.06401200 -1.54523100
F 1.81181200 1.87794400 -2.06290600
F -2.03586800 1.30247900 2.06005300
F -0.09621100 1.45012500 3.00788400
F -0.29565400 1.88817400 -2.54735000
F 0.50895400 3.34607700 -1.17066300
H 4.99378800 -1.13680800 1.52288700
H 3.67958500 -0.00192100 1.88823000
H 3.53205400 -1.69868000 2.35527800
H 4.69889700 -2.94113800 -0.20751200
H 3.20461400 -3.49971000 0.56523000
H 3.20535600 -3.05489100 -1.15103900
H 4.94438400 -0.52974100 -0.91860400
H 3.44133800 -0.58785200 -1.83804400
H 3.66549800 0.64992100 -0.59005200
H -4.22798700 -0.47479400 -2.61996600
H -5.75681600 -1.47844100 -0.94646700
H -4.83557900 -2.41408300 1.15571500
H -2.39139400 -2.36595300 1.56917000
H -1.80455200 -0.39319000 -2.19402800

**F** intermediate
E(ωB97X-D/6-311+G**) = -1684.57593715
G(403K)= -1684.377916
C 3.03886900 -0.68724500 -0.97783200
C 2.15941400 -1.27201300 -0.06811600
C 2.66406600 -1.94016800 1.05036800
C 4.03384300 -2.01448400 1.25391600
C 4.91704900 -1.43252800 0.35030500
C 4.40944300 -0.77466800 -0.76211100
N 0.76128200 -1.24621800 -0.27957600
P -0.42072000 -1.09813600 0.97328900
C -0.33779000 0.77062500 0.71211300
C -0.73296000 1.78677400 1.73804000
F -1.71922400 2.58753900 1.30785100
N 0.28372500 -0.32328600 -1.26666100
C 0.08233100 0.93755900 -0.53508800
C 0.29193200 2.17611900 -1.36022800
F 0.16737400 3.29108900 -0.63880500
N -1.09055900 -0.79564000 -1.56528000
C -1.62087900 -1.23318500 -0.50069700
C -3.01685700 -1.78214400 -0.39804100
C -3.74587100 -0.98295000 0.69614500
C -3.75004600 -1.64403000 -1.73463500
C -2.92637000 -3.26323200 0.00824900
F -1.19019800 1.17338700 2.84556000
F 0.29143000 2.56119700 2.11145800
F 1.50994400 2.18472300 -1.91283200
F -0.60441100 2.22486100 -2.35411100
H -4.75960600 -2.05219300 -1.63783600
H -3.82597700 -0.59723000 -2.03635700
H -3.23112200 -2.18663000 -2.52725500
H -3.93421000 -3.67517000 0.10585300
H -2.38944500 -3.84373100 -0.74602800
H -2.41899700 -3.38959300 0.96889500
H -4.76662500 -1.35882800 0.80179300
H -3.25763700 -1.08668700 1.67093300
H -3.79891000 0.07991900 0.44497700
H 4.41133500 -2.53369300 2.12755000
H 5.98648000 -1.49376100 0.51286300
H 5.08383600 -0.31760800 -1.47753400

H 2.65138000 -0.17988700 -1.85015200
H 1.98787500 -2.40862600 1.75716600

**TS2**
E(ωB97X-D/6-311+G**) = -1684.57396709
G(403K)= -1684.374221
C -3.25234500 0.82385500 1.28904300
C -2.60570000 0.29683300 0.16857100
C -3.34985600 -0.32738100 -0.83301400
C -4.73007300 -0.41653600 -0.70464900
C -5.38186200 0.10391300 0.40695100
C -4.63172800 0.72360800 1.40052600
N -1.21425700 0.40364400 0.06137900
N -0.53135500 -0.12825900 -1.05109500
N 0.35825300 0.99158800 -1.53471300
C 0.76203000 1.65049000 -0.53390200
P 0.02974600 0.94329100 1.09792000
C 0.88861900 -0.69143500 0.71968700
C 0.40661400 -1.08048800 -0.45516900
C 0.69551600 -2.28103400 -1.31046600
F -0.43234500 -2.95304000 -1.57039800
C 1.70289500 2.82267800 -0.59166100
C 2.93299800 2.45205300 0.25565900
C 2.12094300 3.11007000 -2.03607800
C 1.00102200 4.05031500 0.01261500
C 1.91401400 -1.33143100 1.60333100
F 1.50566000 -2.51012300 2.08748600
F 2.17395000 -0.53760200 2.65897900
F 3.08161500 -1.52880500 0.97456600
F 1.22445100 -1.90506000 -2.48081200
F 1.54603300 -3.12639500 -0.72633000
H 2.82294100 3.94799400 -2.05163400
H 2.60648600 2.24162600 -2.48580300
H 1.25680400 3.36940800 -2.65121500
H 0.72103300 3.88420300 1.05656600
H 1.67975600 4.90656500 -0.01908500
H 0.10059300 4.30600100 -0.55174100
H 2.66739500 2.25910100 1.30051400
H 3.43623800 1.56791100 -0.14435800
H 3.64443800 3.28159900 0.24786100
H -2.84457500 -0.73483900 -1.69823100
H -5.29866300 -0.90421000 -1.48873800
H -6.45831300 0.02553100 0.50057500
H -5.12095100 1.13629100 2.27570500
H -2.68064100 1.31078400 2.07168800

**F'** intermediate
E(ωB97X-D/6-311+G**) = -1684.58003252
G(403K)= -1684.381027
C 4.42983400 -1.11301500 -1.63388000
C 3.05369500 -0.94045300 -1.64629600
C 2.33514400 -1.00564300 -0.45141500
C 2.99637200 -1.25681800 0.74765200
C 4.37461800 -1.44329300 0.74250600
C 5.09843300 -1.36692400 -0.44003200
N 0.92683500 -0.83214400 -0.50645600
P 0.21811300 0.58386600 -1.22119100
C -1.40847100 -0.16049100 -0.70722800
C -2.71771200 0.12839700 -1.37681900
F -3.57721700 0.75081500 -0.55679400
N 0.25085200 -0.92027700 0.74036900
C -1.13736600 -0.94089800 0.33635300
C -2.01998800 -1.79791200 1.20132700
F -3.31434500 -1.63751800 0.91933300
N 0.41256300 0.44963700 1.42989800
C 0.39961900 1.34785700 0.54742100
C 0.53413700 2.82466500 0.80214900
C 1.82823200 3.30787100 0.12477800
F -1.72280600 -3.09229400 1.03694100

F -1.84011800 -1.49794800 2.49164100
C -0.68445400 3.51641300 0.16818700
C 0.58629700 3.11237900 2.30491000
F -3.31588200 -0.97740600 -1.83366900
F -2.53070500 0.94248700 -2.43116900
H 0.68502800 4.18901300 2.46719600
H -0.32179700 2.76687600 2.80341300
H 1.43818900 2.61265300 2.77045000
H 1.81178000 3.13268800 -0.95463800
H 1.94367700 4.38252500 0.28850200
H 2.70140600 2.80101000 0.54345600
H -0.73486000 3.34726500 -0.91258200
H -1.61681700 3.16493600 0.61809800
H -0.61448200 4.59536100 0.32741000
H 2.43545400 -1.31202700 1.67100200
H 4.88238900 -1.64365000 1.67920900
H 6.17261100 -1.50967300 -0.43489300
H 4.97948400 -1.06102300 -2.56681500
H 2.53380600 -0.77048700 -2.58285300

**TS3**
E(ωB97X-D/6-311+G**) = -1684.57718424
G(403K)= -1684.378819
C 2.97975500 -1.29640800 0.72511200
C 2.33848500 -1.01786900 -0.47778000
C 3.07282200 -0.88664900 -1.65579600
C 4.45352000 -1.01907400 -1.62228300
C 5.10465700 -1.29785400 -0.42474500
C 4.36242200 -1.44122100 0.74074700
N 0.92607500 -0.86273100 -0.54480800
N 0.22471900 -1.13095300 0.60993300
C -1.13342600 -1.02862400 0.25086600
C -1.39426300 -0.16847400 -0.74709900
C -2.70783100 0.25427400 -1.32757500
F -3.49179700 0.86766800 -0.42771900
N 0.40378600 0.39490500 1.51860400
C 0.39514300 1.28278100 0.66375500
C 0.56415900 2.77452300 0.85629600
C 1.89593700 3.18369900 0.20653800
P 0.21203700 0.55071900 -1.22069800
C -2.05730300 -1.84769400 1.11414800
F -1.84932200 -3.15592200 0.91674500
F -1.84107400 -1.59182200 2.40750800
F -3.34336000 -1.60035100 0.85577300
C -0.60685100 3.48380900 0.16189100
C 0.57974800 3.11398700 2.34996800
F -2.51010600 1.13509500 -2.32709700
F -3.39950100 -0.77126300 -1.83736800
H 0.70657900 4.19221500 2.47963600
H -0.35438200 2.81430100 2.82979800
H 1.40168200 2.60510200 2.85759100
H 2.04393300 4.25892800 0.33729700
H 2.73568900 2.66168900 0.67187700
H 1.90852600 2.97166400 -0.86609900
H -0.50640100 4.56392700 0.29484000
H -0.62407700 3.28723900 -0.91513800
H -1.56538900 3.17649900 0.58793900
H 5.01946200 -0.91748500 -2.54111600
H 6.18229800 -1.41002400 -0.40301100
H 4.85970100 -1.66131600 1.67850900
H 2.40017800 -1.39862400 1.63251800
H 2.56420100 -0.69933700 -2.59512600

**G** intermediate (van der Waals complex of **3** + *t*BuCN)
E(ωB97X-D/6-311+G**) = -1684.67113362
G(403K)= --1684.478090
C 2.51461600 -1.85688800 -0.75737100
C 3.85615900 -2.18777800 -0.60823200
C 4.42953200 -2.23545200 0.65654600

C 3.65576300 -1.96204800 1.78084700
C 2.31117700 -1.64818600 1.64632700
C 1.75349300 -1.59524000 0.37464600
N 0.37634000 -1.23693400 0.22727900
P -0.71768900 -1.97338200 -0.83647100
C -1.90307000 -0.86279100 -0.29194700
C -1.33746400 -0.00628800 0.67346000
N -0.07099400 -0.21709900 0.95528900
C -3.31658300 -0.86892800 -0.77274900
F -3.44256400 -1.64616000 -1.86564100
F -3.75692600 0.35316500 -1.10365400
F -4.16806500 -1.35729000 0.14617000
C -2.00383900 1.15648400 1.36453200
F -3.22896100 0.83360700 1.80139500
F -1.29681900 1.57661000 2.41634000
F -2.14149000 2.20401100 0.53454000
N 0.83322200 0.76231500 -2.21167400
C 1.41577100 1.49547600 -1.54158300
C 2.17272800 2.45076000 -0.71366000
C 2.89256600 1.68614300 0.40910500
C 3.19193200 3.15956100 -1.62230300
C 1.18322000 3.46419400 -0.11515600
H 4.45565600 -2.38922900 -1.48811300
H 5.47920400 -2.48071100 0.76834900
H 4.09974300 -2.00003800 2.76860200
H 1.69661700 -1.43245500 2.51137400
H 3.89927300 2.44534400 -2.04979100
H 2.69448400 3.68844000 -2.43815200
H 3.75167600 3.88619600 -1.02794500
H 0.45770500 2.96661000 0.52984400
H 0.64427100 4.00217300 -0.89787400
H 1.73941100 4.18831000 0.48555900
H 2.17346300 1.21219500 1.07853800
H 3.55583900 0.91529400 0.00868200
H 3.49205400 2.39438900 0.98705000
H 2.07338300 -1.76337100 -1.74245400

**XYZ coordinates of the intermediates of the c) reaction on Scheme 1**

**B** intermediate (van der Waals complex of 4 + hexafluoro-2-butyne)
E(ωB97X-D/6-311+G**) = -1381.92254491
G(403K)= -1381.714429
C 2.73347900 0.21234200 -1.03649100
H 2.17068000 1.08323500 -1.34575000
C 4.11067200 0.26664200 -0.87155100
H 4.63178200 1.19892600 -1.05501200
C 4.81635400 -0.86014400 -0.46327100
H 5.89033000 -0.80886000 -0.32813800
C 4.14093800 -2.05256600 -0.23065500
H 4.68574500 -2.93707200 0.07785100
C 2.76495100 -2.12433100 -0.40655000
H 2.24012400 -3.05957900 -0.25140800
C 2.07149300 -0.98663300 -0.80014700
N 0.65886200 -1.03845300 -0.94720500
N -1.23750900 -0.49192900 -1.73621100
C -0.69589300 2.95706200 -0.70832600
N 0.03437100 -0.28837600 -1.86326800
F -0.78705900 4.19644500 -0.20447700
F -1.84414600 2.67919600 -1.31746000
F 0.27847200 2.96170500 -1.61982100
C -0.16490500 1.28722100 1.29501900
C -0.24335400 -1.73852300 -0.21506500
H 0.04642500 -2.39018900 0.59046400
C 0.14489100 0.46760400 2.46971100
F -0.86621800 -0.35698100 2.76586500
F 0.36784300 1.23867000 3.53802000
F 1.23562500 -0.27826600 2.26953700

C -1.46348000 -1.37880700 -0.72847500
C -2.85763300 -1.78317300 -0.32329800
C -0.40909600 2.00117800 0.37063200
C -3.57943900 -2.38724000 -1.53803200
C -2.79586500 -2.81537600 0.80734700
C -3.61353800 -0.53268700 0.15587900
H -4.60356800 -2.66217900 -1.26806300
H -3.61932800 -1.66925900 -2.35991000
H -3.06446200 -3.28479200 -1.89213100
H -4.63896100 -0.79509600 0.43332600
H -3.12482400 -0.09174400 1.02925100
H -3.65064800 0.22188600 -0.63274700
H -3.80836000 -3.10890900 1.09715000
H -2.26313600 -3.71824000 0.49338600
H -2.29996900 -2.40915800 1.69319400

**TS1**
E(ωB97X-D/6-311+G**) = -1381.86788451
G(403K)= -1381.655577
N 0.14914400 -0.57803000 -1.55479100
C 0.17457200 1.09896400 -0.53342800
C -0.29532500 0.80315100 0.58642800
C -0.65772700 -1.24999500 0.34296300
N -1.21583000 -0.63440700 -1.71463700
C -1.73479400 -1.05785200 -0.59849500
N 0.43058300 -1.35565500 -0.46578100
C 1.78538800 -1.46539900 -0.06096700
C 2.75600700 -1.64254100 -1.04200000
C 4.08730900 -1.74290500 -0.66799700
C 4.44891100 -1.68056000 0.67446900
C 3.47111400 -1.50677100 1.64499200
C 2.13425300 -1.38991700 1.28274000
C -3.20556400 -1.24570100 -0.34824800
C -3.60555100 -0.43642200 0.89617400
C -0.56484200 1.37977000 1.91209100
F -0.77324700 0.43083000 2.85155400
C 0.78716200 2.11962800 -1.39853600
F 0.78287100 3.32731500 -0.80823500
C -4.01328600 -0.77230700 -1.55929600
C -3.46606200 -2.74219100 -0.09818600
F -1.65810200 2.15868000 1.90240600
F 0.45892400 2.12725500 2.34981800
F 2.06264400 1.81753500 -1.67713700
F 0.13470900 2.24348300 -2.55995100
H 4.84592900 -1.87534700 -1.43034300
H 3.74434900 -1.44690600 2.69184400
H 5.49055700 -1.76504000 0.96087200
H 2.46161600 -1.69156100 -2.08243500
H 1.38261500 -1.23007100 2.04596900
H -0.71227300 -1.75227400 1.29731100
H -4.53208800 -2.90496000 0.08207800
H -3.16997400 -3.34089300 -0.96354800
H -2.91898600 -3.10678900 0.77598200
H -4.66904000 -0.58485800 1.10016300
H -3.05032000 -0.75204200 1.78397300
H -3.43437300 0.63132600 0.74354300
H -5.07809700 -0.93007600 -1.36826700
H -3.84892200 0.28996600 -1.75210100
H -3.73784900 -1.32342600 -2.46088000

**F** intermediate
E(ωB97X-D/6-311+G**) = -1381.91312973
G(403K)= -1381.695442
H 4.83996300 -1.38519100 -1.63954000
C 4.08542100 -1.48562700 -0.86767200
C 4.46225700 -1.76114900 0.44428800
H 5.50893200 -1.87767500 0.69914600
C 3.48460900 -1.88282100 1.42100900
H 3.76125100 -2.09155800 2.44813200

C 2.14004600 -1.72514800 1.09923200
H 1.39458500 -1.81911600 1.87961500
C 1.76940200 -1.45820500 -0.21643700
C 2.74882400 -1.33911900 -1.20361600
H 2.45379900 -1.12451500 -2.22274300
N 0.40490700 -1.35778100 -0.58890500
N 0.12488400 -0.26588100 -1.51853800
N -1.33603900 -0.48582700 -1.73685200
C -1.76535500 -0.92744600 -0.62441400
C -0.59942300 -0.96263700 0.38759400
C 0.17588500 0.89504100 -0.60922100
C -0.23821400 0.52429500 0.59446900
C -3.18045000 -1.31325100 -0.31482300
C 0.62385600 2.19701500 -1.18801000
F 1.89750700 2.12831400 -1.59153000
C -0.40525300 1.28550400 1.86955800
F -0.75296300 0.44971400 2.86624700
F 0.72027200 1.90034800 2.24282500
F -1.36969300 2.21393100 1.78552600
F -0.12179100 2.51716100 -2.25267700
F 0.52708700 3.19431600 -0.30382800
H -0.71594100 -1.58629100 1.26597000
C -4.08789200 -1.01355400 -1.51003300
C -3.21431000 -2.81677800 0.01276300
C -3.62850800 -0.49799700 0.91107000
H -4.66648700 -0.74308000 1.14913200
H -3.02533300 -0.72240500 1.79531100
H -3.57165800 0.57611700 0.71559600
H -5.11398400 -1.30427700 -1.27000000
H -4.07804200 0.05100300 -1.75361500
H -3.76881800 -1.56535400 -2.39640600
H -4.23934400 -3.10994800 0.25394300
H -2.87844200 -3.41030900 -0.84083500
H -2.58589600 -3.06376400 0.87277700

**TS2**
E(ωB97X-D/6-311+G**) = -1381.90276101
G(403K) =-1381.684548
C 4.46514300 -0.51466600 1.41066600
C 3.09908100 -0.64408700 1.19848200
C 2.51027200 -0.04159900 0.08153300
C 3.30212300 0.69102000 -0.80944800
C 4.66442000 0.80709600 -0.57706500
C 5.25969400 0.20880400 0.52934200
N 1.15471800 -0.17173300 -0.14036400
C 0.05786500 -0.78160800 0.54643600
C -0.86655400 0.44920000 0.66439200
F -3.11983300 0.55691800 1.34805000
N 0.43935900 0.40785100 -1.20605500
C -0.59408900 1.12665700 -0.44513700
C -1.15768500 2.36538400 -1.06138100
F -2.16936500 2.86173900 -0.34378000
N -0.31859400 -0.81508500 -1.73699700
C -0.51700600 -1.52570100 -0.70490400
C -1.21027700 -2.85441000 -0.65909200
C -0.21293000 -3.90111000 -0.13065200
F -0.22113100 3.31651200 -1.16318300
F -1.61167900 2.11023800 -2.29380800
C -2.39993500 -2.72867100 0.30851700
C -1.69999100 -3.25205300 -2.05337200
F -1.72373100 1.90647000 2.29825600
F -1.66829900 -0.20467400 2.75283200
H -2.20400200 -4.22061500 -1.99943100
H -2.40355700 -2.51632700 -2.44826100
H -0.86715300 -3.33326100 -2.75486300
H 0.12915600 -3.66633200 0.88102900
H -0.70008100 -4.87887900 -0.09684700
H 0.66056700 -3.97578300 -0.78300300

H -2.07962100 -2.46653100 1.32095600
H -3.11249100 -1.97495700 -0.03602200
H -2.92165700 -3.68712200 0.36664200
H 2.84094200 1.15777100 -1.67005200
H 5.26782900 1.37721200 -1.27486100
H 6.32455300 0.30657400 0.70206700
H 4.90857800 -0.98718900 2.28016400
H 2.49782200 -1.21174700 1.89907300
H 0.26243600 -1.35440700 1.44250300

**F' intermediate**
E(ωB97X-D/6-311+G**) = -1381.91630651
G(403K)= -1381.698815
C 2.81231900 -1.66914900 0.46328600
C 2.15236200 -1.02188200 -0.57656400
H 2.24720300 -2.05672300 1.30036100
C 4.19511400 -1.80676100 0.41515900
H 4.70342600 -2.31245200 1.22836800
C 4.92406900 -1.29532800 -0.65083800
H 6.00207900 -1.40223900 -0.67850800
C 4.25640900 -0.65120100 -1.68775100
H 4.81058200 -0.25627300 -2.53162700
C 2.87570800 -0.52088400 -1.65890000
H 2.35929900 -0.04457100 -2.48501300
N 0.73788300 -0.88372100 -0.60342100
N 0.06645300 -1.21432100 0.62760700
N 0.39633400 -0.00552100 1.53177100
C -1.29808400 -0.95317500 0.19574600
C -2.38035500 -1.78448400 0.80567600
F -2.30700400 -1.73946000 2.14106100
F -3.59436300 -1.35806000 0.44560000
F -2.26830100 -3.06551700 0.43663000
H 0.49651300 1.06435400 -1.55993900
F -3.19297500 -0.06210400 -2.04347200
C -2.41147600 0.77820000 -1.35994600
F -1.91247400 1.66560700 -2.23910100
C 0.17187700 0.46151700 -0.71953900
C 0.48939400 0.96466400 0.72539700
C -1.30008600 0.07165600 -0.65075900
C 0.86230000 2.37591500 1.06721500
F -3.19284800 1.46436800 -0.51271100
C 0.98864000 2.54764200 2.58253800
C 2.21302800 2.67177600 0.38802600
C -0.22542100 3.30974900 0.51186200
H 1.27089400 3.57913300 2.80965500
H 0.04283500 2.32911400 3.08305200
H 1.74990400 1.88034400 2.99152800
H 0.03759900 4.34743800 0.73170000
H -0.32974500 3.21862400 -0.57299900
H -1.19567300 3.10275300 0.97098100
H 2.51848400 3.69514200 0.62100200
H 2.98751700 1.98757100 0.74369200
H 2.15129800 2.57969500 -0.69965400

**TS3**
E(ωB97X-D/6-311+G**) = -1381.91070937
G(403K)= -1381.693164
C 4.18652900 -1.78234300 0.46605800
C 2.80122800 -1.66562100 0.47924100
C 2.16334200 -1.03471600 -0.58275800
C 2.89988900 -0.53158200 -1.65315100
C 4.28265600 -0.64065700 -1.64646300
C 4.93188500 -1.26673200 -0.58687800
N 0.75003000 -0.89222500 -0.62248800
C 0.15881700 0.40486200 -0.74756700
C 0.46948600 0.93207400 0.81207100
C 0.86250600 2.37592100 1.03574600
C 0.99259200 2.65003000 2.53694900
N 0.03458200 -1.40328400 0.43634100

N 0.38744300 0.01191900 1.62688100
C -1.28220400 -1.03976500 0.10476000
C -2.39078900 -1.81809100 0.74637100
F -3.57237700 -1.21075600 0.59485500
C -1.28244200 0.04699400 -0.68606800
C -2.40061100 0.83937400 -1.27727000
F -3.28459200 0.06291400 -1.91206500
F -3.07403000 1.54869100 -0.35747600
F -1.92451200 1.72137000 -2.17596900
C 2.21912200 2.59898000 0.34392700
C -0.20689300 3.29016400 0.42365000
F -2.49278600 -3.04222500 0.20967400
F -2.16930900 -1.96766000 2.05469900
H 1.28212600 3.69243100 2.69560800
H 0.04475100 2.47255800 3.04959800
H 1.74958800 2.00554600 2.98818800
H 2.55224200 3.62343400 0.52961400
H 2.97530900 1.91182000 0.73164400
H 2.15654800 2.46015000 -0.73851300
H 0.07498800 4.33372300 0.58532000
H -0.31274000 3.14140300 -0.65406600
H -1.18058500 3.12710600 0.89180300
H 4.85287400 -0.24623500 -2.47957500
H 6.01175000 -1.35789000 -0.58700300
H 4.68352100 -2.27362600 1.29470500
H 2.21706700 -2.05070400 1.30392600
H 2.39375800 -0.07102400 -2.49424000
H 0.52219500 1.05205100 -1.53731600

**G** intermediate (van der Waals complex of **5** + *t*BuCN)
E(ωB97X-D/6-311+G**) = -1382.02236899
G(403K)= -1381.815373
C 2.48645700 -0.13645100 -1.62514400
C 0.03896700 0.48438800 -1.31207000
C -4.78838000 1.92945400 -0.31595600
N 0.07630200 1.42513200 0.71308700
F 2.08095800 2.14882300 2.32290700
C 2.40236200 1.24302600 1.39934700
F 2.68647000 0.09613300 2.04354000
F 3.53311700 1.64678800 0.80180300
C -2.08017300 1.36606300 -0.33381400
C -2.94576100 0.56990500 -1.07331800
C -4.30339400 0.86421300 -1.06503700
H -2.57828100 -0.28543300 -1.62679500
H -4.98201400 0.24531500 -1.63987900
C -3.90873100 2.70919400 0.42730600
H -1.85302800 3.03757300 0.99066800
C -2.54769000 2.43591500 0.41959500
F 3.30608400 0.81097800 -2.11332200
H -0.40181000 0.14037800 -2.23248600
F 2.05742000 -0.85980800 -2.67063100
H -5.84944500 2.14949300 -0.30824100
F 3.23938300 -0.94351800 -0.85894000
C 1.29982800 1.04960300 0.40109200
C 1.33938000 0.43560900 -0.87080700
N -0.68058100 1.07867100 -0.33566800
N -1.43200600 -2.48977000 -1.65935600
C -1.26234600 -2.66486400 -0.53393300
C -1.04436500 -2.87303500 0.90746100
H -4.27989800 3.54166400 1.01335500
C -1.95170500 -1.90313200 1.68385600
C -1.39589200 -4.33076600 1.24825700
C 0.43341600 -2.58357000 1.21681200
H -1.79944500 -2.06118800 2.75432000
H -1.71133100 -0.86240100 1.45642400
H -3.00545500 -2.07510100 1.45416200
H -1.22729900 -4.49447400 2.31551100
H -2.44351400 -4.54575700 1.02685700
H -0.76956400 -5.02786800 0.68777000

H 0.61606000 -2.74412500 2.28193800
H 1.09598300 -3.23685500 0.64571500
H 0.68030400 -1.54731300 0.98415900


**XYZ coordinates of other investigated systems**


**6**
E(ωB97X-D/6-311+G**) = -2067.85434537
G(298K)= -2067.729907
C 1.04597800 5.06123200 -0.03183100
C 0.14242800 4.78304200 0.98885100
C -0.62009500 3.62461600 0.95184000
C -0.47545600 2.75926000 -0.12418000
C 0.40143000 3.03783300 -1.16228000
C 1.17343400 4.19084600 -1.10717400
N -1.22376800 1.53874000 -0.14748300
P -0.56106800 -0.00893800 -0.18485600
W 1.80039500 -0.66135500 0.03890800
C 1.53626800 -2.35873300 -1.13136300
O 1.43943800 -3.28653600 -1.78155400
N -2.55556300 1.60546500 -0.07042300
C -3.05566200 0.39259000 -0.05220400
C -2.12832400 -0.67365400 -0.11637800
C -2.42623700 -2.13788200 -0.06866800
F -2.73345300 -2.54945600 1.16955500
C -4.56361400 0.28106500 -0.01956500
F -5.04960600 -0.02033000 -1.23214200
F -4.95752100 -0.68241300 0.82386200
F -5.12806700 1.42056500 0.37132400
F -1.35246200 -2.85338500 -0.45820400
F -3.43998600 -2.48009000 -0.86994400
C 2.40414900 0.35786300 -1.65426400
O 2.76440300 0.90635700 -2.58727700
C 2.17242300 1.03113400 1.17808100
O 2.41874300 1.95031200 1.80363700
H 1.86602200 4.41092800 -1.91072300
H 1.64673100 5.96218700 0.00936700
H 0.03933100 5.46550800 1.82404000
H -1.32002300 3.38454000 1.74283900
H 0.46701100 2.36688200 -2.00985300
C 1.25829800 -1.73523800 1.73606300
O 0.98053300 -2.33038000 2.66481300
C 3.73037900 -1.22362300 0.35239400
O 4.81194500 -1.53741400 0.53630300


**6** (in case of coordination to the nitrogen atom)
E(ωB97X-D/6-311+G**) = -2067.83736022
G(298K) = -2067.711662
C 0.25169000 2.56100100 -0.22266000
C 0.57198500 3.43631100 0.80460900
C 1.59517800 4.35494200 0.61169600
C 2.29072300 4.38174600 -0.58974200
C 1.95432900 3.50075900 -1.61314300
C 0.91922800 2.59530100 -1.44046200
N -0.85526000 1.66433800 -0.05357600
N -0.73423400 0.35346700 -0.32722700
C -1.94906700 -0.19488600 -0.30078400
C -2.11770000 -1.64449300 -0.71461900
F -1.76153100 -2.49317500 0.25352300
P -2.39468700 2.25071400 0.30620200
C -2.99587300 0.66392800 0.06831300
C -4.45386800 0.35343000 0.25619000
F -5.09579900 0.14585100 -0.89679900
F -5.05400600 1.40848400 0.84852600
F -4.65647900 -0.70507700 1.04455300
F -3.39036900 -1.89798500 -1.01930800
F -1.39362500 -1.91306800 -1.80403800
H 1.86378100 5.03255400 1.41269800


H 3.09831700 5.09018800 -0.73046000
H 2.49249700 3.52240000 -2.55297400
H 0.62893800 1.91773100 -2.23367200
H 0.05280800 3.37625700 1.75403700
W 1.47463100 -0.79806400 0.14377100
C 2.34473600 -0.24623400 -1.64079600
O 2.86181200 0.03970200 -2.61927700
C 2.37029400 0.79490300 1.08673300
O 3.02200800 1.55336300 1.64365000
C 1.03633000 -2.63427500 -0.69977200
O 0.96163800 -3.69322500 -1.11743000
C 0.58832600 -1.34730700 1.93622500
O 0.13092100 -1.65151200 2.93555400
C 3.13732500 -1.70596100 0.67377500
O 4.11014300 -2.23432500 0.98906000


**7**
E(ωB97X-D/6-311+G**) = -1567.02813923
G(298K)= -1566.808566
C 2.24627300 3.04835700 0.96396200
C 3.63166000 3.11382400 1.00697100
C 4.39023400 2.57833400 -0.02823100
C 3.76303900 1.99229800 -1.12120100
C 2.37683500 1.93675400 -1.18083100
C 1.63195100 2.45379600 -0.13002900
N 0.20690300 2.35135900 -0.15634700
P -0.71553100 0.93536600 -0.20353300
W 0.20437200 -1.39869400 0.03859900
C 0.94153600 -3.25539000 0.33245500
O 1.35967000 -4.30652700 0.50325700
N -0.51356300 3.47575300 -0.07210800
N -1.77289100 3.22920600 -0.05168300
C -2.11201300 1.91637500 -0.11096300
C -3.58035300 1.54826800 -0.07402300
C -4.30962500 2.31302100 -1.19073700
C -3.77939600 0.04458000 -0.27427100
C -4.14204900 1.96537300 1.29621400
C -0.89425200 -1.57605500 1.78681000
O -1.49822800 -1.68760500 2.74722700
C 1.29884000 -1.26360900 -1.70936700
O 1.90714900 -1.21993100 -2.67404300
C 1.82842500 -0.67747200 1.11403800
O 2.73953800 -0.34621200 1.71183000
C -1.33407600 -2.25268100 -1.04459300
O -2.15308200 -2.77116100 -1.64567900
H 5.47220600 2.62094700 0.01662000
H 4.11948500 3.57273600 1.85867000
H 1.63851800 3.44586400 1.76749000
H 4.35006800 1.58381700 -1.93518800
H 1.87594300 1.50661600 -2.03924800
H -4.17530800 3.38966700 -1.07475700
H -5.37933900 2.08717700 -1.15644700
H -3.92866300 2.02301900 -2.17404900
H -4.84544500 -0.19396100 -0.23920000
H -3.28764000 -0.53781300 0.51006000
H -3.39917900 -0.28369200 -1.24541800
H -4.00212500 3.03536000 1.46205100
H -3.64284800 1.42322800 2.10462900
H -5.21195600 1.74256300 1.34448100


**7** (in case of coordination to the nitrogen atom closer to the Ph substituent)
E(ωB97X-D/6-311+G**) = -1567.02904162
G(298K)= -1566.811500
C 1.71099900 3.62781200 1.23628500
C 0.66262900 2.71964300 1.21980100
C -0.01938000 2.49937100 0.03074900
C 0.30841200 3.18357700 -1.13064700
C 1.35131400 4.09978300 -1.10046500

C 2.05397300 4.31723100 0.07815200
N -1.10603800 1.56328700 0.01076500
N -0.85821000 0.24883600 0.05418000
N -1.94717900 -0.44623100 0.06468900
C -3.07189200 0.29148400 0.02645400
C -4.40578100 -0.42421100 0.04399000
C -4.51920200 -1.21254200 1.35981000
P -2.75191700 1.98378500 -0.02035600
C -5.55192000 0.58798400 -0.05466900
C -4.46411900 -1.39213500 -1.14909500
H 2.87457000 5.02465200 0.09394700
H 1.62450800 4.63069600 -2.00425100
H -0.23575600 2.98386100 -2.04626000
H 2.25730200 3.79718800 2.15627500
H 0.37548100 2.18041700 2.11405200
H -3.71020400 -1.94050900 1.44782900
H -5.47230200 -1.74815300 1.39070100
H -4.47550500 -0.54202300 2.22284000
H -6.51212200 0.06685400 -0.02818000
H -5.50907200 1.15339400 -0.99120000
H -5.53909400 1.29594000 0.78064700
H -3.65815800 -2.12630700 -1.09403900
H -4.37371600 -0.85367200 -2.09670000
H -5.41945400 -1.92462400 -1.14778500
W 1.16034700 -0.94249400 -0.01982300
C 2.36022100 0.53059000 -0.80594800
O 3.11529800 1.27461000 -1.23755600
C 1.73244600 -0.36505500 1.87031300
O 2.09059100 -0.05925600 2.91377000
C 0.63143800 -1.53337000 -1.93656200
O 0.37002700 -1.87389600 -2.99409200
C 0.09978300 -2.54144800 0.77769400
O -0.42771300 -3.45388700 1.21303500
C 2.76333000 -2.11165800 -0.10609900
O 3.69093200 -2.79176200 -0.15660800

**7** (in case of coordination to the nitrogen atom closer to the $^t$Bu substituent)
E(ωB97X-D/6-311+G**) = -1567.02378855
G(298K)= -1566.804627
C 6.05346700 -0.61106400 0.63831200

C 4.90353800 0.16732900 0.65811600
C 3.76798700 -0.28581200 -0.00075500
C 3.75900300 -1.50608900 -0.66587800
C 4.91038300 -2.28025000 -0.66543000
C 6.05871800 -1.83440200 -0.02031700
N 2.58444700 0.52211400 0.00082100
N 1.43281500 -0.10879900 0.04235200
N 0.42364200 0.71082100 0.00223500
C 0.78863700 2.02395800 -0.06601100
C -0.20704900 3.16664400 -0.10980600
C -1.05445900 3.15461300 1.17341400
P 2.49750300 2.22174800 -0.10046900
C 0.54315500 4.50661700 -0.17256200
C -1.07307700 3.04950700 -1.37497900
H 6.95608100 -2.44182400 -0.02792200
H 4.90903800 -3.23496900 -1.17763700
H 2.86027000 -1.84078800 -1.16726800
H 6.94223300 -0.26269400 1.15073800
H 4.88706600 1.10958500 1.19372600
H -1.55220800 2.19876900 1.32453500
H -1.81987200 3.93305800 1.12037200
H -0.42576200 3.34888000 2.04686800
H -0.18136000 5.32392900 -0.20304800
H 1.16323500 4.58496200 -1.07136500
H 1.17558100 4.66204200 0.70727800
H -1.58295900 2.09013600 -1.43395700
H -0.45602600 3.15865900 -2.27116900
H -1.83001400 3.83789500 -1.38001400
W -1.57748400 -0.66292400 0.03835800
C -1.55974700 -0.67661600 -2.02649300
O -1.56044200 -0.69119500 -3.16916000
C -0.32711800 -2.32161900 0.05545200
O 0.26473000 -3.29757000 0.05646200
C -3.08511700 0.72500500 0.01871600
O -4.01302800 1.39790900 0.00793600
C -1.53497100 -0.59140700 2.10586000
O -1.52364300 -0.55613800 3.24721000
C -3.06725400 -1.96149300 0.06965200
O -3.93223700 -2.72250100 0.08702900

## 2.    Experimental Procedures

### 2.1    General Information

All reactions involving air- and moisture-sensitive compounds were carried out using standard Schlenk techniques or in an MBraun glovebox under an argon atmosphere. All common chemicals and solvents were commercially available. 2,5-diisopropylphenyl azide [7], *tert*-butylphosphaalkyne [8] and 5-(*tert*-butyl)-3-phenyl-3*H*-1,2,3,4-triazaphosphole (**1**)[9] were prepared by methods described in the literature. Hexafluoro-2-butyne was purchased at 99% purity from ABCR. Commercially available chemicals were used without further purification. Toluene and *n*-pentane were prepared using an MBraun Solvent Purification System MB-SPS 800. THF was dried over K/benzophenone under argon. The deuterated dry solvents DCM-$d_2$ were dried over $CaH_2$ and THF-$d_8$ and benzene-$d_6$ over a sodium-potassium alloy. $^1$H, $^{13}$C{$^1$H}, $^{19}$F and $^{31}$P{$^1$H} NMR spectra were recorded by using a JEOL ECS400 spectrometer (400 MHz), or a JEOL ECZ600 spectrometer (600 Hz). All chemical shifts are reported relative to the residual resonance in the deuterated solvents. IR spectra were recorded on a 5 SXC Nicolet FT-IR spectrometer with a DTGS detector (**6**) and on a Bruker Alpha FTIR spectrometer equipped with a diamond ATR in the solid state (pure powder) under an argon atmosphere (**7**, **9**). Characteristic absorption bands are given in wavenumbers (in cm$^{-1}$). ESI-MS spectra were recorded on an Agilent 6210 ESI-TOF (4 kV) from Agilent Technologies. EI measurements were conducted with a modified device of a MAT 711 from Varian MAT. CHN-Analysis was performed on an ELEMENTAR VARIO EL.

**Caution**: Azides are potentially hazardous compounds and adequate safety measures should be taken when weighing, heating and working up.

### 2.2    Synthesis and Characterization

**2-phenyl-4,5-bis(trifluoromethyl)-2*H*-1,2,3-diazaphosphole (3)**
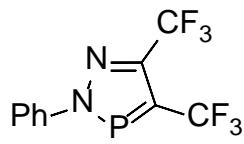


**1** (500 mg, 2.28 mmol, 1 eq.) was placed in a pressure tube, and dissolved in dry toluene (10 mL). The solution was frozen at $T$ = -160°C and hexafluoro-2-butyne was condensed in excess (11 mmol, 5 eq.). The reaction mixture was warmed overnight and heated at $T$ = 60 °C for eight weeks. The excess hexafluoro-2-butyne was removed with the solvent in vacuo, and the compound was crystallized from DCM. **3** was obtained as a light brown crystalline material (590 mg, 87%).

$^1$H-NMR (400 MHz, THF-$d_8$): $\delta$ = 7.93 – 7.85 (m, 2H, H$_{Ar}$), 7.60 – 7.51 (m, 2H, H$_{Ar}$), 7.51 – 7.44 (m, 1H, H$_{Ar}$) ppm. $^{13}$C{$^1$H}-NMR (176 MHz, THF-$d_8$): $\delta$ = 146.4 - 145.6 (m, P$C$CF$_3$), 144.5 - 143.6 (m, N$C$CF$_3$), 143.5 (d, $J$ = 11.5 Hz, C$_{Ar}$), 130.9 (C$_{Ar}$), 130.2 (d, $J$ = 1.7 Hz, C$_{Ar}$), 124.6 (q, $J$ = 269.2 Hz, $C$F$_3$), 124.5 (q, $J$ = 269.4 Hz, $C$F$_3$), 122.1 (d, $J$ = 9.6 Hz, C$_{Ar}$) ppm. $^{31}$P{$^1$H}-NMR (162 MHz, THF-$d_8$): $\delta$ = 233.9 (q, $^3J_{P-F}$ = 22.9 Hz) ppm. $^{19}$F-NMR (377 MHz, THF-$d_8$): $\delta$ = -53.3 (dq, $J$ = 25.7, 7.2 Hz, PCCF$_3$), -61.8 (qd, $J$ = 7.3, 1.2 Hz, NCCF$_3$) ppm. EI (m/z): 298.0097 g/mol (calc.: 298.0095 g/mol) [M]$^+$. ESI-TOF (m/z): 299.1622 g/mol (calc.: 299.0167 g/mol) [M+H]$^+$.

### 2-Benzyl-4,5-bis(trifluoromethyl)-2*H*-1,2,3-diazaphosphole-*P*-pentacarbonyl-tungsten(0) (6)
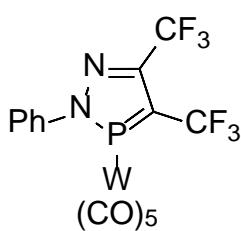
In a J-Young NMR tube, **3** (15.0 mg, 0.05 mmol) was placed together with W(CO)$_6$ (17.7 mg, 0.05 mmol) and dissolved in dry deuterated THF (0.5 mL). The reaction mixture was irradiated with a UV lamp (100 W, 365 nm) for 68 h at room temperature. The reaction solution was filtered over Celite and the solvent was removed in vacuo. According to NMR spectroscopy, **6** was quantitatively obtained as a dark brown solid. Single Crystals of were obtained by evaporation of the solvent of a saturated *n*-pentane solution of **6**.

$^1$H-NMR (400 MHz, THF-$d_8$): $\delta$ = 7.70 - 7.65 (m, 2H, $H_{Ar}$), 7.61 - 7.54 (m, 3H, $H_{Ar}$) ppm. $^{13}$C{$^1$H}-NMR (101 MHz, THF-$d_8$): δ = 196.0 (d, *J* = 43.3 Hz, CO$_{trans}$), 192.8 (d, *J* = 9.0 Hz, CO$_{cis}$), 140.9 (m, *C*CF$_3$), 131.4 (C$_{Ar}$), 130.9 (C$_{Ar}$), 130.6 (C$_{Ar}$), 128.3 (d, *J* = 4.0 Hz, C$_{Ar}$), 124.6 (q, *J* = 268.6 Hz, C*C*F$_3$), 120.9 (q, *J* = 222.2 Hz. C*C*F$_3$) ppm. $^{31}$P{$^1$H}-NMR (162 MHz, THF-$d_8$): $\delta$ = 217.3 (q, $^1J_{P\text{-}W}$ = 326.5 Hz, $^3J_{P\text{-}F}$ = 16.1 Hz) ppm. $^{19}$F-NMR (377 MHz, THF-$d_8$): $\delta$ = -51.3 (dq, *J* = 16.2, 8.1 Hz), -62.9 (qd, *J* = 8.1, 0.3 Hz) ppm. IR (solid): $\tilde{\nu}$ = 2089, 2017, 2002, 1934 cm$^{-1}$. EI (m/z): 621.9389 g/mol (calc.: 621.9350 g/mol) [M]$^+$.

### 5-(*tert*-butyl)-3-phenyl-3*H*-1,2,3,4-triazaphosphole-*P*-pentacarbonyl-tungsten(0) (7)
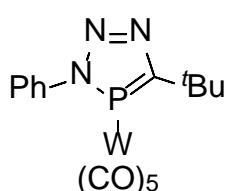
**1** (30.0 mg, 0.14 mmol) and tungsten hexacarbonyl (40.9 mg, 0.14 mmol) were placed in a *J*-Young NMR tube and dissolved in THF-d$_8$ (0.7 mL). The reaction mixture was irradiated with a UV lamp (100 W, 365 nm) for 5 days at room temperature, with overpressure released from the J-Young NMR tube twice a day. After removing the solvent under high vacuum, **7** was obtained as a brown solid.

$^{31}$P{$^1$H}-NMR (162 MHz, THF-$d_8$): $\delta$ = 136.1 ($^1J_{P\text{-}W}$ = 260 Hz) ppm, $^1$H-NMR (400 MHz, DCM-$d_2$): $\delta$ = 7.58 (dd, *J* = 5.1, 1.8 Hz, 2H, $H_{Ar}$), 7.51 (td, *J* = 7.3, 2.0 Hz, 3H, $H_{Ar}$), 1.61 (d, *J* = 0.9 Hz, 9H, C(C*H*$_3$)$_3$) ppm. $^{13}$C{$^1$H}-NMR (101 MHz, THF-$d_8$): δ = 197.53(CO$_{trans}$), 196.08 (d, *J* = 8.8 Hz, CO$_{cis}$), 162.56 (C=P), 124.47 (d, *J* = 6.6 Hz, C$_{Ar}$), 121.9 (C$_{Ar}$), 121.36 (d, *J* = 14.9 Hz, C$_{Ar}$), 120.84 (d, *J* = 2.5 Hz, C$_{Ar}$), 36.35 (d, *J* = 13.7 Hz, *C*(CH$_3$)$_3$), 32.84 (d, *J* = 11.1 Hz, C(C*H*$_3$)$_3$) ppm. EI (m/z): 543.0168 g/mol (calc.: 543.0180 g/mol) [M]$^+$. IR (solid): $\tilde{\nu}$ = 2077, 2023, 1980, 1885 cm$^{-1}$.

### 5-(*tert*-butyl)-3-(2,6-diisopropylphenyl)-3*H*-1,2,3,4-triazaphosphole (8)

2,6-Diisopropylphenyl azide (0.46 g, 2.27 mmol) was added to a 100 mL Normag flask with a stir bar, the azide was frozen at *T* = -160°C, and the flask was evacuated. Subsequently, an excess of *tert*-butylphosphaalkyne in 50 mL dry toluene was condensed into the reaction flask. The reaction solution was warmed to r.t. and stirred for 24 h. The reaction was stopped and the solvent and excess alkyne were removed in vacuo. The resulting solid was recrystallized from a hot saturated n-pentane solution. Triazaphosphole **8** was obtained as an off white solid (0.69 g, 64%).
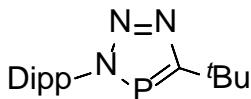
$^1$H-NMR (400 MHz, DCM-$d_2$): $\delta$ = 7.49 (t, *J* = 7.8 Hz, 1H, $H_{Ar}$), 7.32 (d, *J* = 7.8 Hz, 2H, $H_{Ar}$), 2.18 (hept, *J* = 6.8 Hz, 2H, $H_{i\text{-Propyl}}$), 1.55 (d, *J* = 1.3 Hz, 9H, C(CH$_3$)$_3$), 1.13 (dd, *J* = 6.8, 4.7 Hz, 12H, $H_{i\text{-Propyl}}$) ppm. $^{13}$C{$^1$H}-NMR (101 MHz, DCM-$d_2$): $\delta$ = 199.9 (d, *J* = 57.9 Hz, C=P), 149.6 (C$_2$), 136.0 (d, *J* = 7.8 Hz, C$_4$), 130.6 (C$_1$), 124.3 (C$_1$), 35.9 (d, *J* = 14.9 Hz, *C*(CH$_3$)$_3$), 32.03 (d, *J* = 7.5 Hz, C(C*H*$_3$)$_3$), 28.86 ($H_{i\text{-Propyl}}$), 24.66 (d, *J* = 20.7 Hz, $H_{i\text{-Propyl}}$) ppm. $^{31}$P{$^1$H}-NMR (162 MHz, DCM-$d_2$): $\delta$ = 179.5 ppm.

### 5-(*tert*-butyl)-3-(2,6-diisopropylphenyl)-3*H*-1,2,3,4-triazaphosphole *P*-pentacarbonyl-tungsten(0) (9)

N=N

Dipp—N   ⁀  ᵗBu
        P
        ‖
        W
      (CO)₅
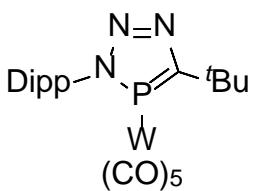
**8** (50.0 mg, 0.16 mmol) and tungsten hexacarbonyl (58.0 mg, 0.16 mmol) were placed in a *J*-Young NMR tube and dissolved in THF-$d_8$ (0.7 mL). The reaction mixture was irradiated with a UV lamp (100 W, 365 nm) for 5 days at room temperature, with overpressure released from the J-Young NMR tube twice a day. The crude product was sublimed at $T = 60°C$ for 2 hours. **9** stayed behind during sublimation and was obtained as a green solid. Single Crystals of were obtained by evaporation of the solvent of a saturated THF solution of **9**.

$^1$H-NMR (400 MHz, DCM-$d_2$): $δ = 7.54$ (t, *J* = 7.8 Hz, 1H, $H_{Ar}$), 7.35 (d, *J* = 7.8 Hz, 2H, $H_{Ar}$), 2.24 (hept, *J* = 6.8 Hz, 2H, $H_{i\text{-Propyl}}$), 1.65 (s, 9H, $C(CH_3)_3$), 1.24 (d, *J* = 6.8 Hz, 6H, $H_{i\text{-Propyl}}$), 1.06 (d, *J* = 6.8 Hz, 6H, $H_{i\text{-Propyl}}$) ppm. $^{31}$P{$^1$H}-NMR (162 MHz, DCM-$d_2$): $δ = 160.6$ ($^1J_{P\text{-}W} = 285.6$ Hz) ppm. IR (solid): $\tilde{v}$ =2081, 2000, 1954, 1934 cm$^{-1}$. EI (m/z): 627.1133 g/mol (calc.: 627.1119 g/mol) [M]$^+$. C-H-N-Analysis: N: 6.85; C: 42.92; H: 5.85, (Calc.: N: 6.70; C: 42.13; H: 4.18).

## 2. Crystallographic Details

X-ray studies were carried out on a D8 Venture, Bruker Photon CMOS diffractometer[10] (MoKα radiation; $λ$ = 0.71073 Å) up to a resolution of (sinΘ/$λ$) $_{max}$ = 0.58 Å (**6**) 0.60 Å (**3**, **9**) at 100(2) K. The structures of **3** and **6** were solved with SHELXS-2014[10] using direct methods and refined with SHELXL-2014[11] on $F^2$ for all reflections. The structure of **9** was solved with SHELXT-2014/5[12a] by using direct methods and refined with SHELXL-2017/1[12b] on $F^2$ for all reflections. Non-hydrogen atoms were refined by using anisotropic displacement parameters. The positions of the hydrogen atoms were calculated for idealized positions. Geometry calculations and checks for higher symmetry were performed with the PLATON program.[13] Crystal data for the structures reported in this paper have been deposited in the Cambridge Crystallographic Database Center: CCDC number: 2163856 (**3**), CCDC number: 2163857 (**6**) and CCDC number: 2163858 (**9**). Details of the X-ray structure determinations and refinements are provided in Table S4.

**Table S4.** Crystal data and structure refinement for **3**, **6** and **9** (CCDC: 2163856 (**3**), 2163857 (**6**) 2163858 (**9**)).

| Identification code | 3 | 6 | 9 |
|---|---|---|---|
| Empirical formula | $C_{10}H_5F_6N_2P$ | $C_{15}H_5F_6N_2O_5PW$ | $C_{22}H_{26}N_3O_5PW$ |
| Formula weight | 298.13 | 622.03 | 627.28 |
| Temperature/K | 100(2) | 100(2) | 100(2) |
| Crystal system | Orthorhombic | Monoclinic | triclinic |
| Space group | P b c a | $P2_1/c$ | P-1 |
| a/Å | 7.5247(5) | 6.6629(3) | 11.1075(2) |
| b/Å | 12.9354(9) | 18.3901(8), | 14.6470(2) |
| c/Å | 22.6658(15) | 15.6561(7) | 16.9008(3) |
| α/° | 90 | 90 | 112.5214(6) |
| β/° | 90 | 100.123(2) | 102.9855(5) |
| γ/° | 90 | 90 | 91.3575(5) |
| Volume/Å$^3$ | 2206.2(3) | 1888.50(15) | 2456.50(7) |
| Z | 8 | 4 | 4 |
| $\rho_{calc}$g/cm$^3$ | 1.795 | 2.188 | 1.696 |
| $\mu$/mm$^{-1}$ | 0.318 | 6.290 | 4.804 |
| $F$(000) | 1184 | 1168.0 | 1232.0 |
| Crystal size/mm$^3$ | 0.2 x 0.15 x 0.06 | 0.24x0.11x0.02 | 0.40 × 0.34 × 0.09 |
| Radiation | MoKα ($\lambda$ = 0.71073) | MoKα ($\lambda$ = 0.71073) | MoKα($\lambda$ = 0.71073) |
| 2$\theta$ range for data collection/° | 6.5 to 54.336 | 5.158 to 61.114 | 3.792 to 56.564 |
| Index ranges | -9 ≤ h ≤ 9, | -9 ≤ h ≤ 9, | -13 ≤ h ≤ 14, |
| | -16 ≤ k ≤ 16, | -25 ≤ k ≤ 25, | -19 ≤ k ≤ 19, |
| | -29 ≤ l ≤ 28 | -22 ≤ l ≤ 21 | -22 ≤ l ≤ 22 |
| Reflections collected | 18484 | 30420 | 68480 |
| Independent reflections | 2444 [$R_{int}$ = 0.0329, $R_{sigma}$ = 0.0229] | 5650 [$R_{int}$ = 0.0282, $R_{sigma}$ = 0.0210] | 12174 [$R_{int}$ = 0.0425, $R_{sigma}$ = 0.0292] |
| Data/restraints/parameters | 2444/0/172 | 5650/0/271 | 12174/0/591 |
| Goodness-of-fit on $F^2$ | 1.171 | 1.178 | 1.040 |
| Completeness to $\theta$ | 99.4% | 97.3% | 99.8% |
| Final R indexes [I>=2σ (I)] | $R_1$ = 0.0440, | $R_1$ = 0.0192 | $R_1$ = 0.0192, |
| | $wR_2$ = 0.1017 | $wR_2$ = 0.0413 | $wR_2$ = 0.0440 |
| Final R indexes [all data] | $R_1$ = 0.0514, | $R_1$ = 0.0223 | $R_1$ = 0.0220, |
| | $wR_2$ = 0.1047 | $wR_2$ = 0.0422 | $wR_2$ = 0.0452 |
| Largest diff. peak/hole/e Å$^{-3}$ | 0.52/-0.37 | 0.57/-1.70 | 1.15/-1.22 |

## 3. NMR Spectroscopic Data
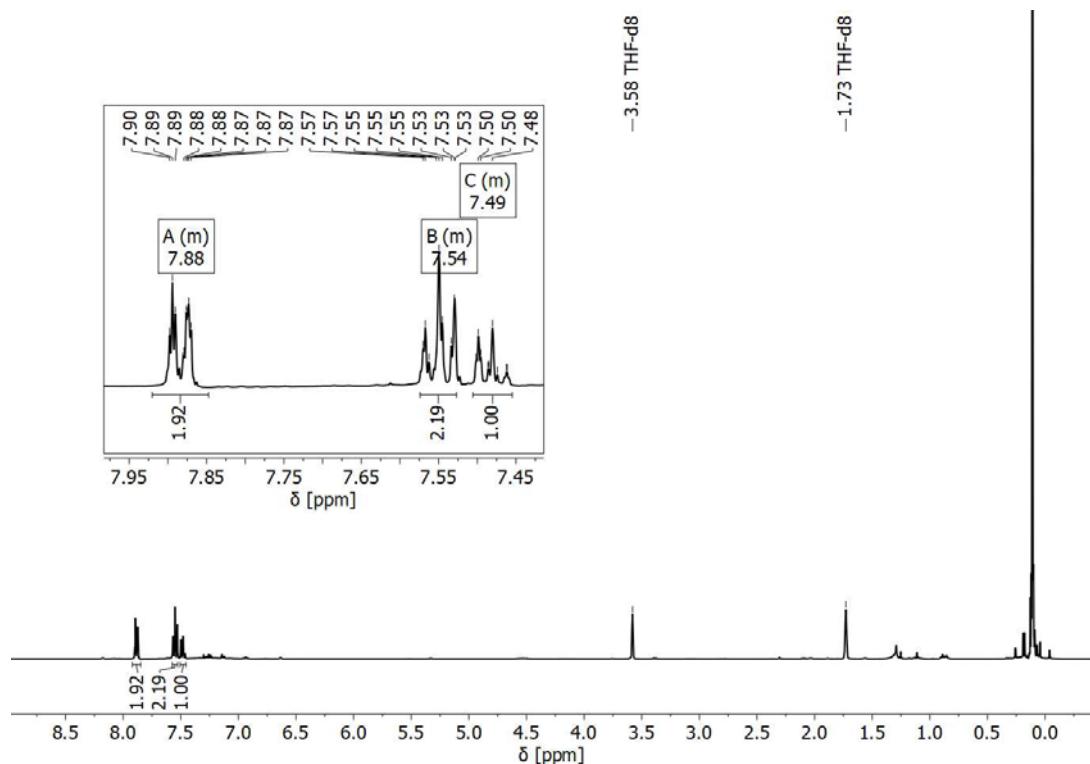


**Figure S2**. $^1$H NMR spectrum of **3** in THF-$d_8$.
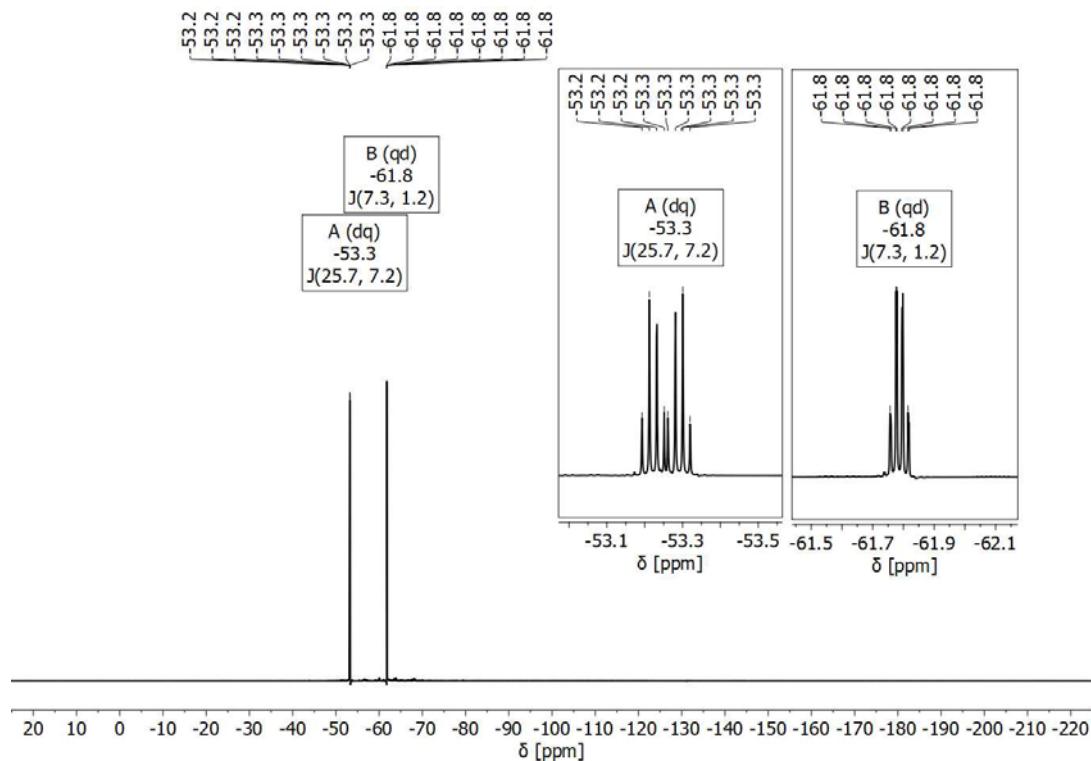


**Figure S3**. $^{19}$F NMR spectrum of **3** in THF-$d_8$.
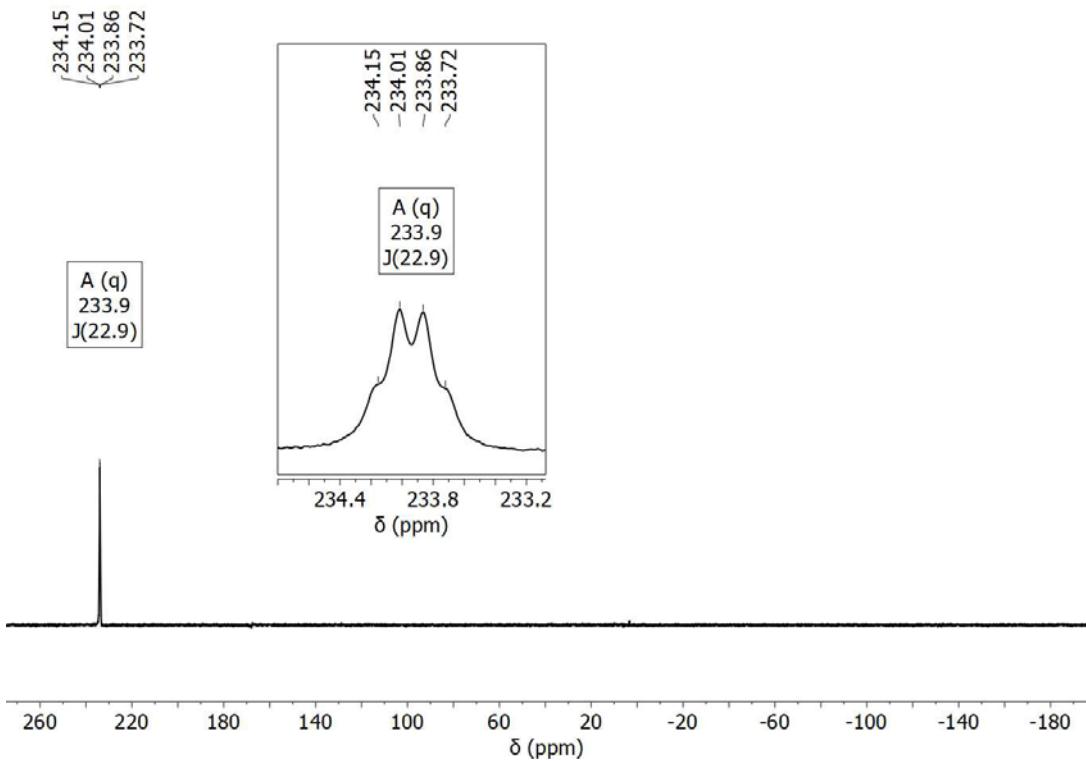
**Figure S4**. $^{31}P\{^1H\}$ NMR spectrum of **3** in THF-$d_8$.
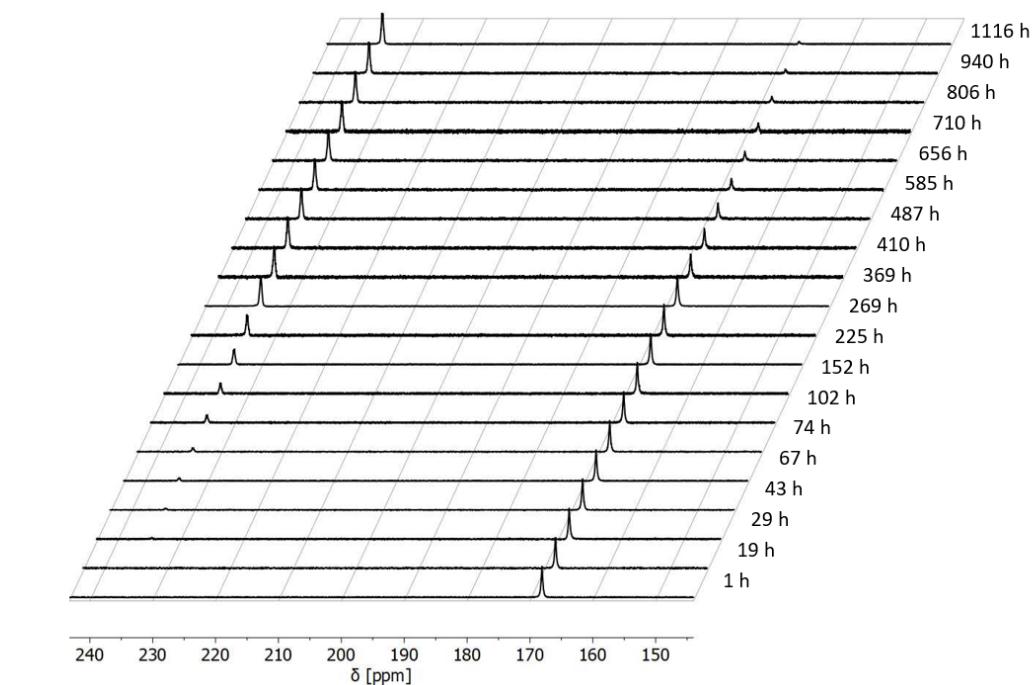


**Figure S5**. Advance of the [4+2]-cycloaddition reaction of **1** ($\delta$ = 169.3 ppm) with Hexafluoro-2-butyne according to $^{31}P\{^1H\}$ NMR spectroscopy over $t$ = 1116 h.

S17

118

7.69
7.68
7.68
7.67
7.66
7.59
7.59
7.58
7.57

−3.58 THF-d8

−1.73 THF-d8

1.93
2.03
0.91

8.0 7.5 7.0 6.5 6.0 5.5 5.0 4.5 4.0 3.5 3.0 2.5 2.0 1.5 1.0 0.5 0.0
δ [ppm]

**Figure S6**. $^1$H NMR spectrum of **6** in THF-$d_8$.

196.3
195.8
192.9
192.8

141.0
140.9
131.4
130.9
130.6
130.6
128.3
128.3
125.9
123.3
122.0
119.8

−67.6 THF-d8

−25.5 THF-d8

196.3
195.8
192.9
192.8

196 194 192 190
δ [ppm]

141.0
140.9
131.4
130.9
130.6
130.6
128.3
128.3
125.9
123.3
122.0
119.8

140 135 130 125 120
δ [ppm]

200 190 180 170 160 150 140 130 120 110 100 90 80 70 60 50 40 30 20 10 0
δ [ppm]
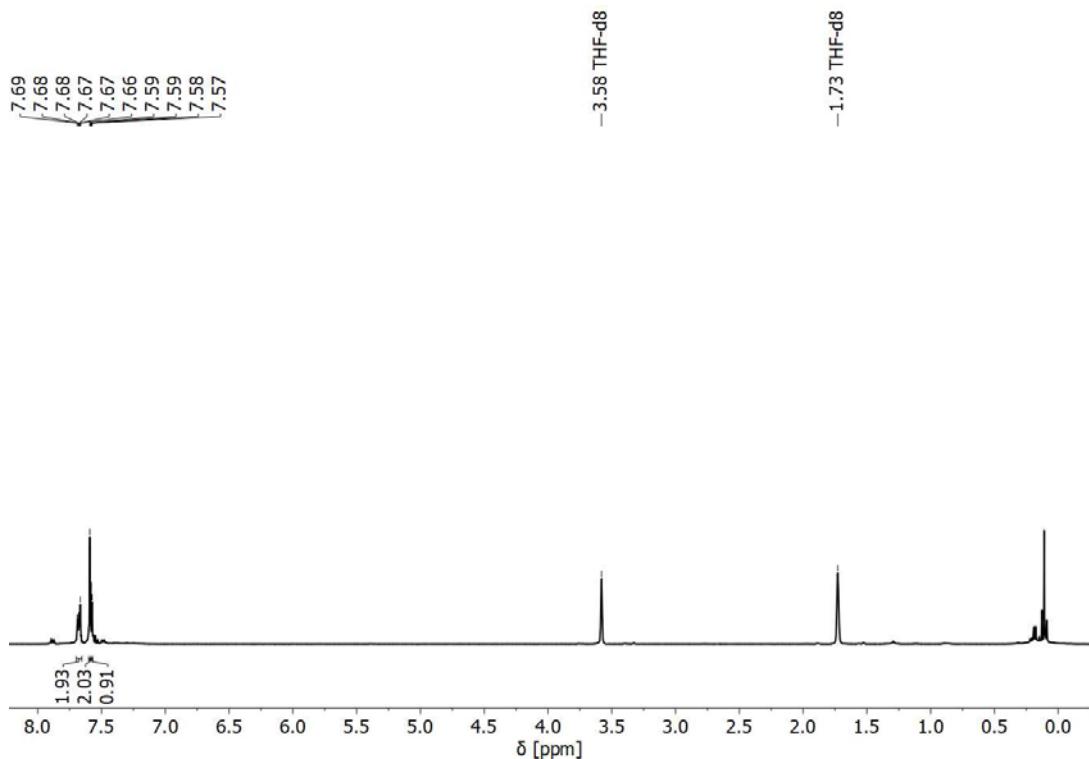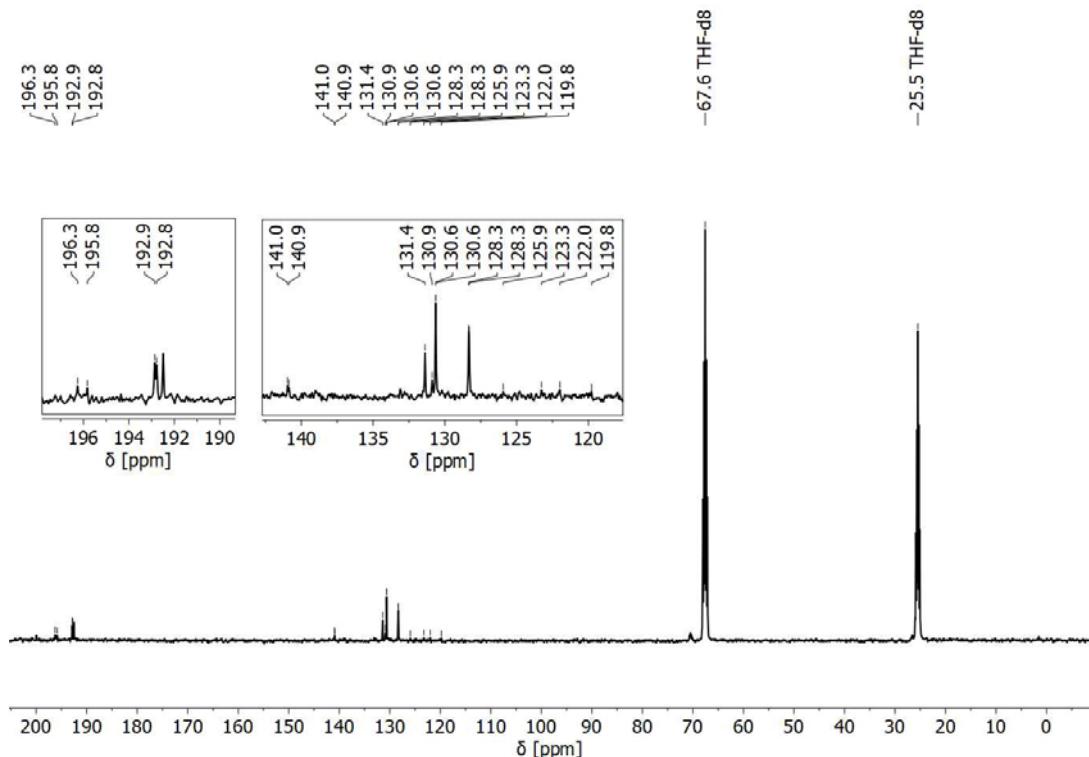
**Figure S7**. $^{13}$C{$^1$H} NMR spectrum of **6** in THF-$d_8$.
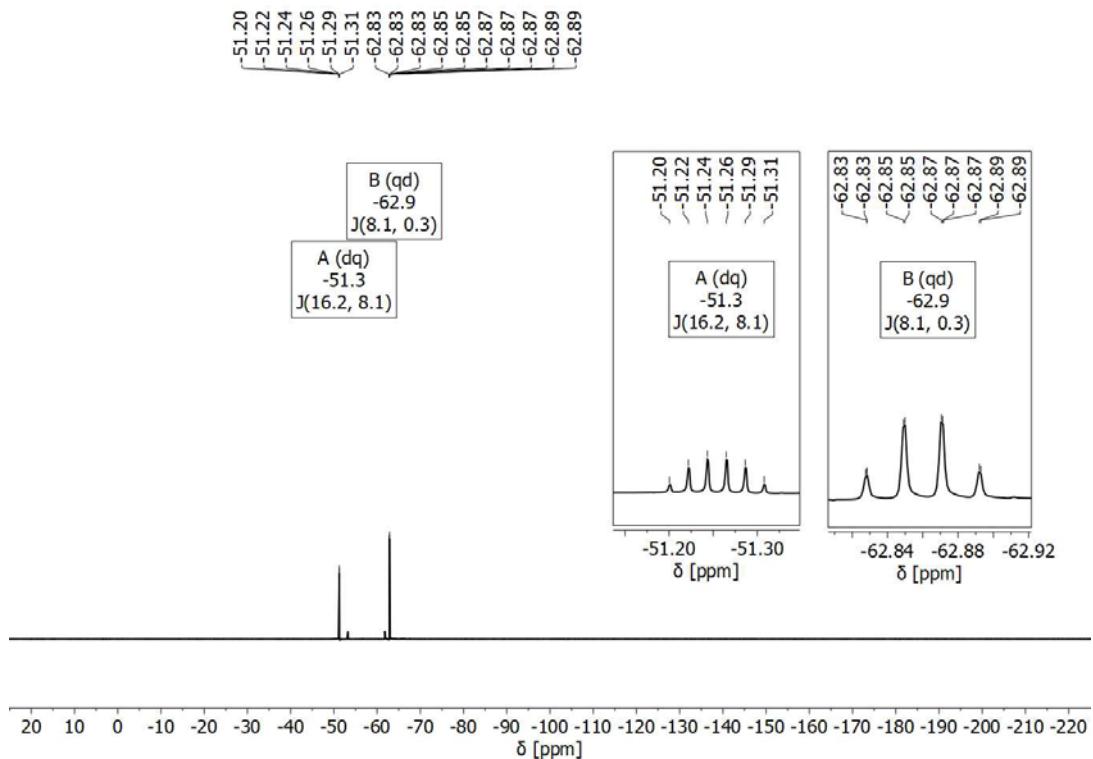
**Figure S8**. $^{19}$F NMR spectrum of **6** in THF-$d_8$.



**Figure S9**. $^{31}$P{$^1$H} NMR spectrum of **6** in THF-$d_8$.

**Figure S10**. $^{31}P\{^1H\}$ NMR spectrum of **7** in THF-$d_8$.



**Figure S11**. $^1H$ NMR spectrum of **7** in DCM-$d_2$.
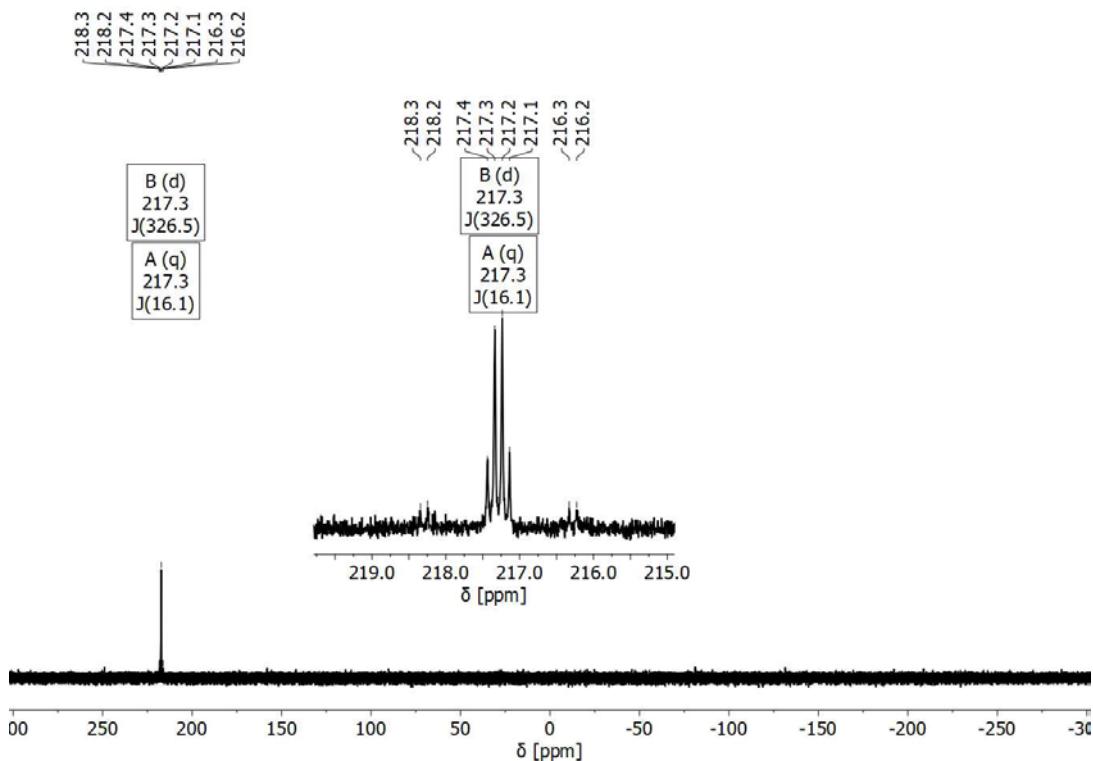
**Figure S12**. $^{13}C\{^1H\}$ NMR spectrum of **7** in THF-$d_8$.
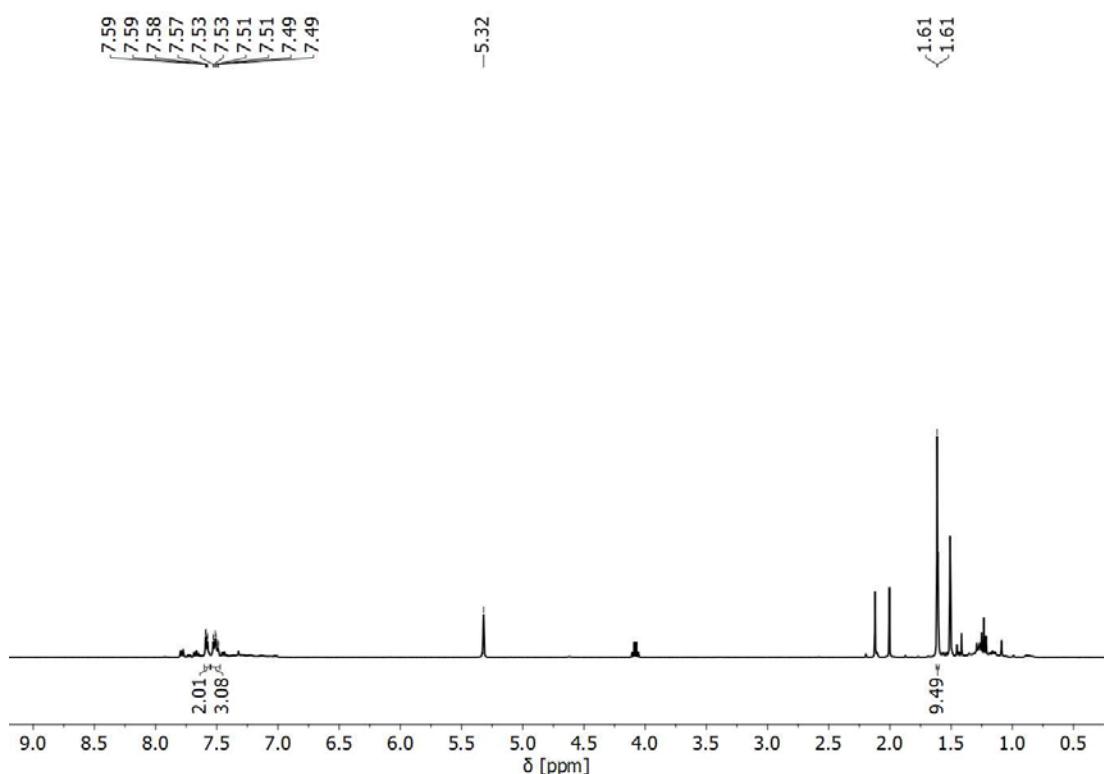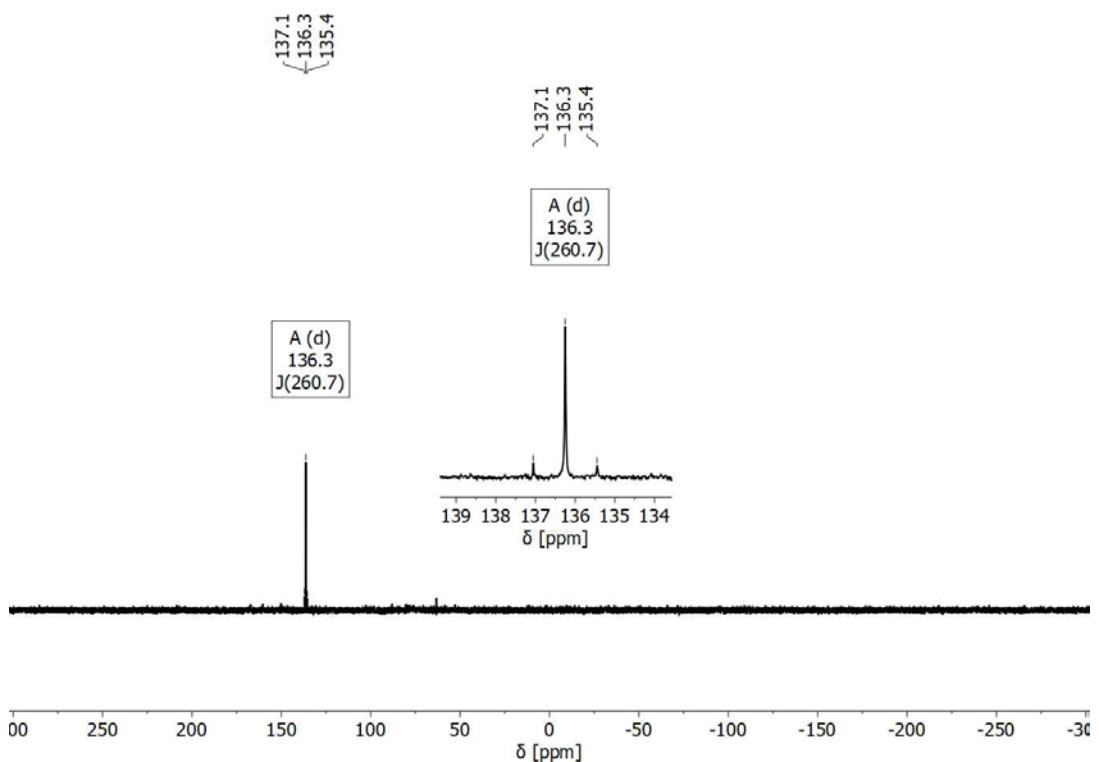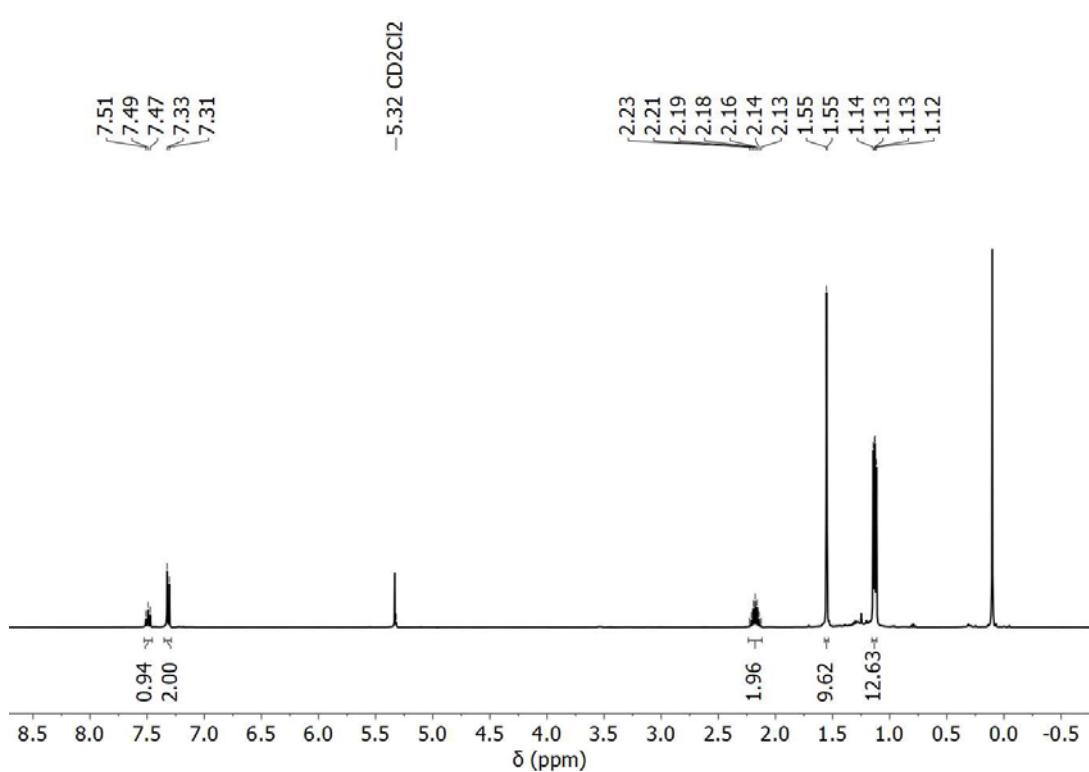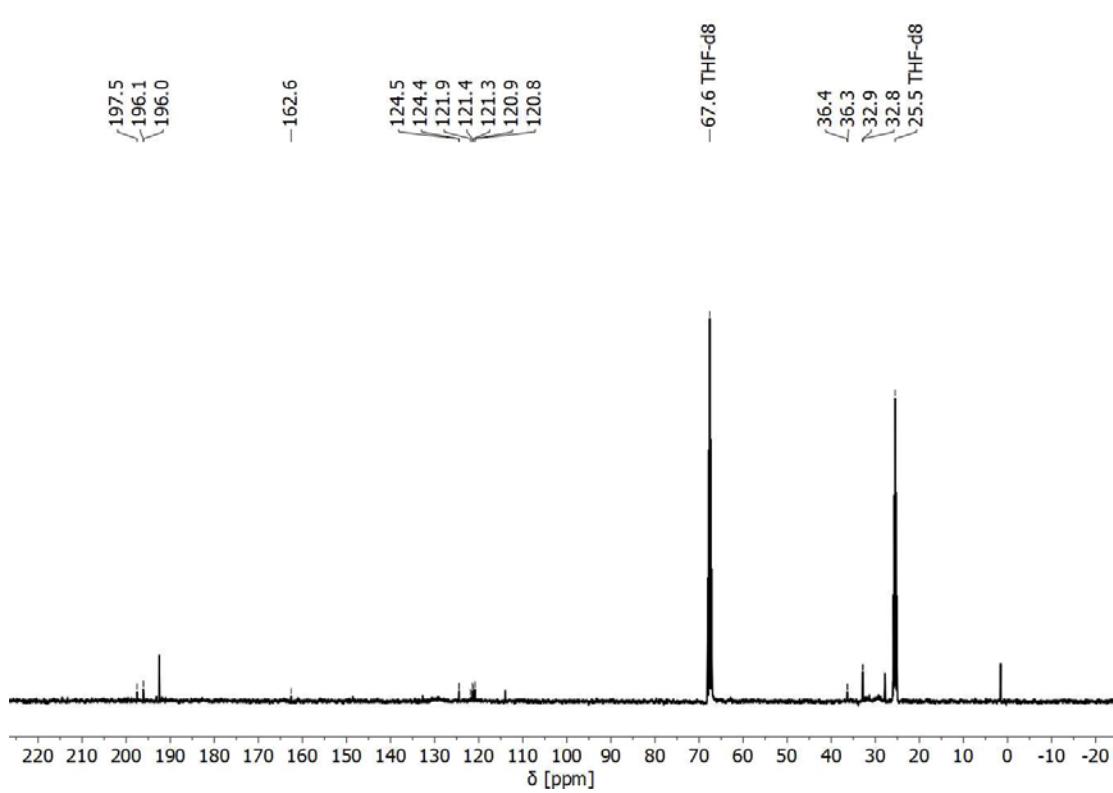


**Figure S13**. $^1H$ NMR spectrum of **8** in DCM-$d_2$.

199.9
199.3

146.6
136.1
136.0
130.6
124.3

36.0
35.8
32.1
32.0
28.9
24.8
24.6



220 210 200 190 180 170 160 150 140 130 120 110 100 90 80 70 60 50 40 30 20 10 0 -10 -20
δ (ppm)
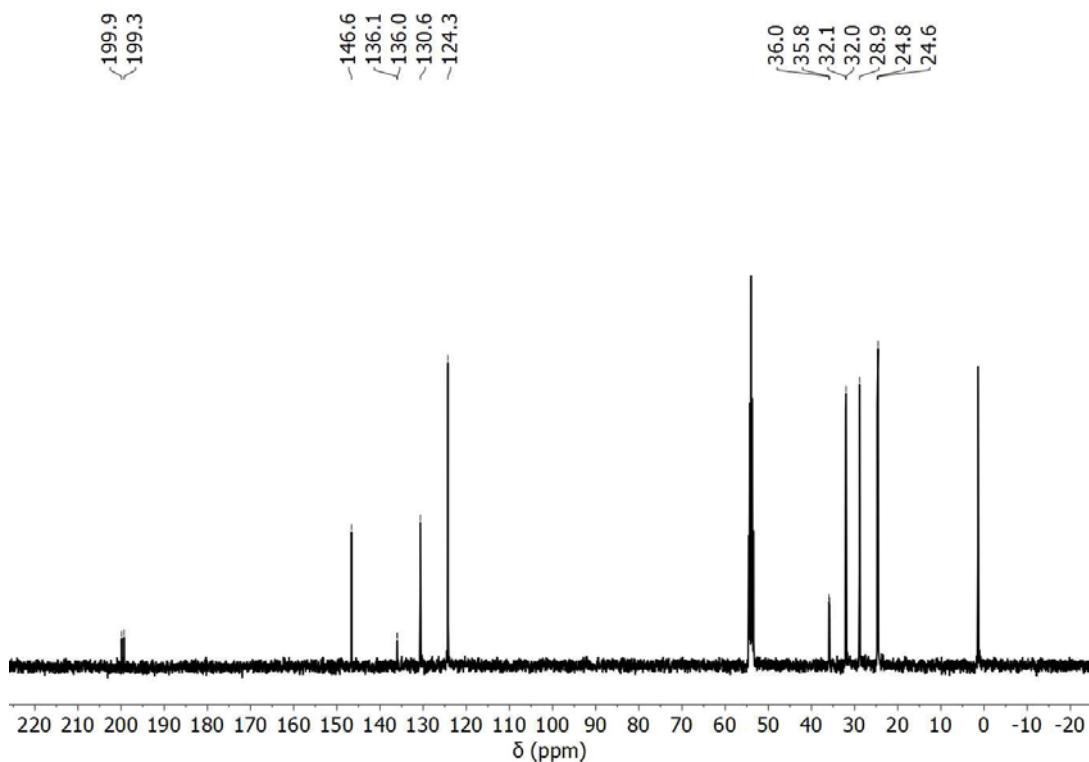
**Figure S14**. $^{13}$C{$^{1}$H} NMR spectrum of **8** in DCM-$d_2$.

−179.5



250    200    150    100    50    0    -50    -100    -150    -200    -250
δ (ppm)
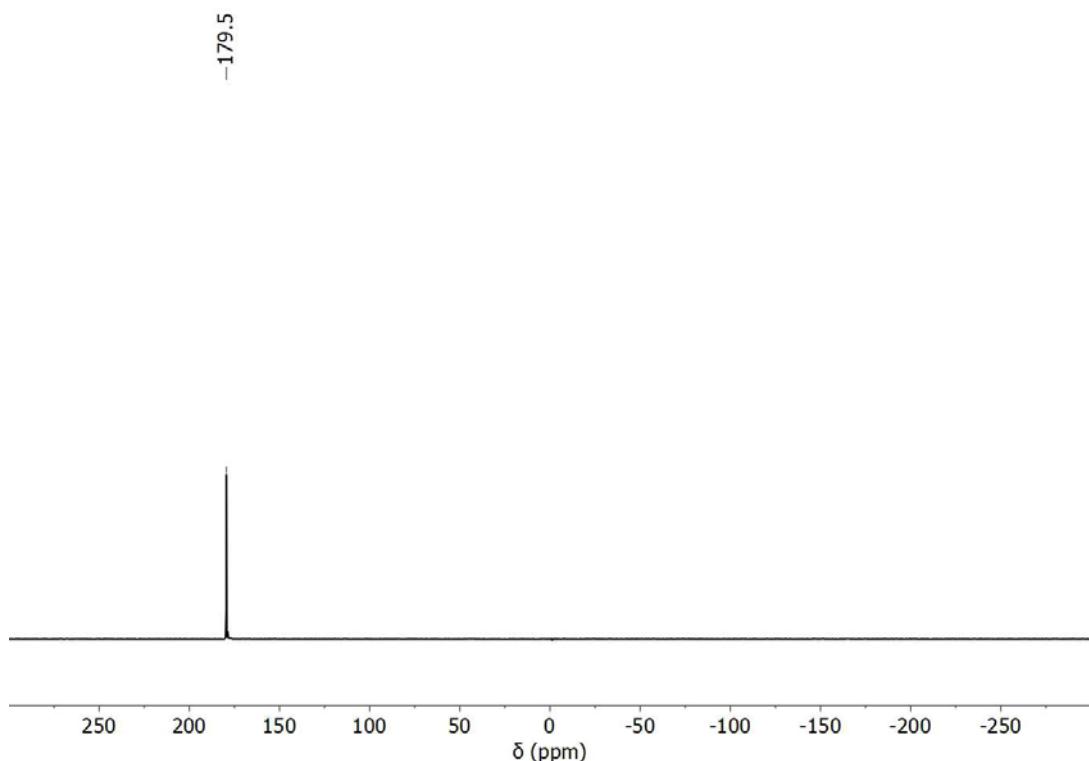
**Figure S15**. $^{31}$P{$^{1}$H} NMR spectrum of **8** in DCM-$d_2$
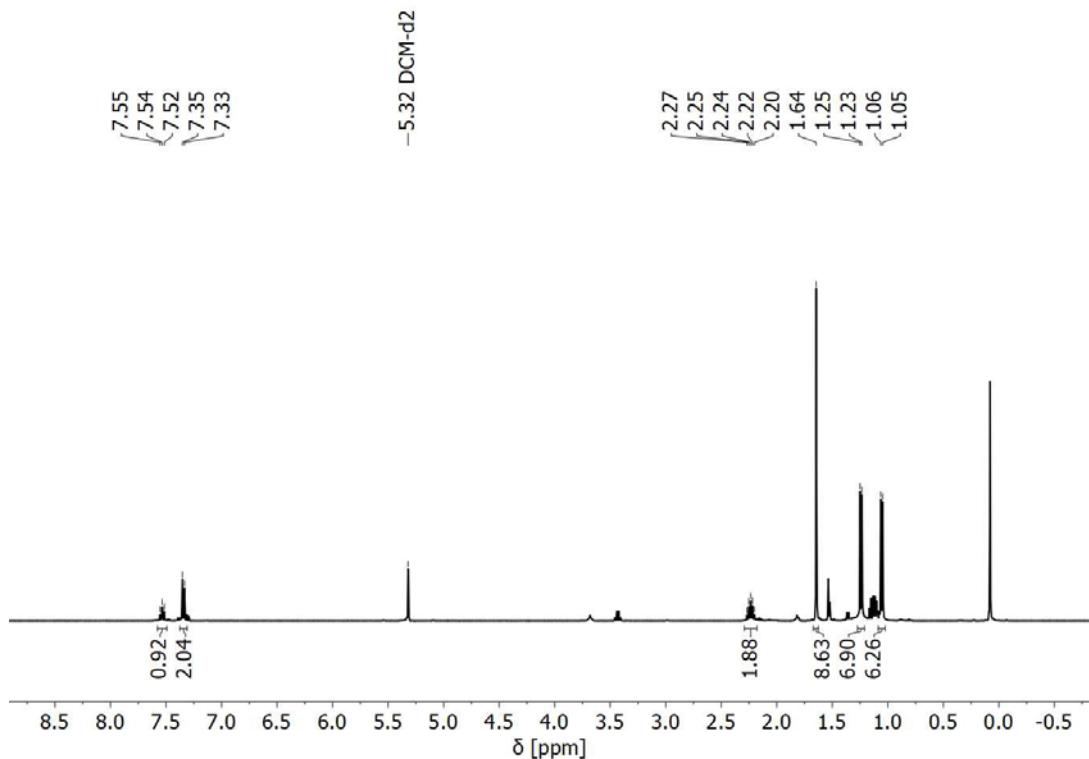
**Figure S16**. $^1H$ NMR spectrum of **9** in DCM-$d_2$.
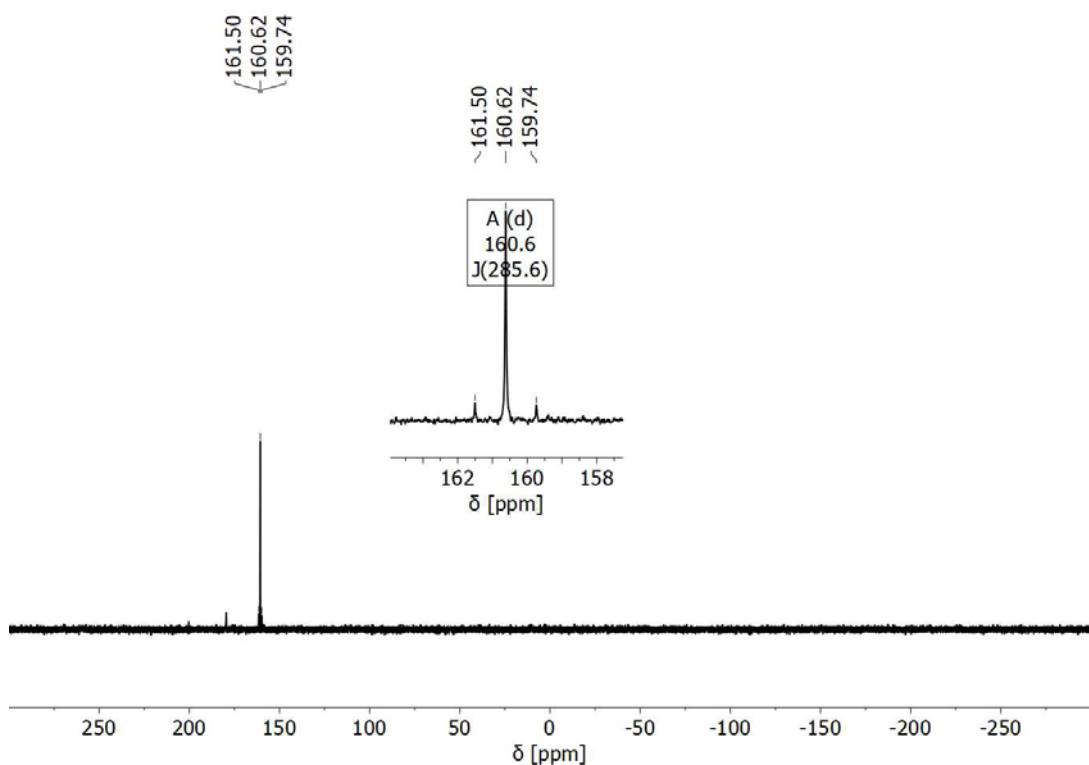


**Figure S17**. $^{31}P\{^1H\}$ NMR spectrum of **9** in DCM-$d_2$

## 5.    References

[1]     M. J. Frisch, G.; Trucks, W.; Schlegel, H. B.; Scuseria, G. E.; Robb, M. A.; Cheeseman, J. R.; Scalmani, G.; Barone, V.; Mennucci, B.; Petersson, G. A.; et al. Gaussian 09, Revision E.01. *Gaussian, Inc.: Wallingford, CT*. 2009.

[2]     J.-D. Chai, M. Head-Gordon. *Phys. Chem. Chem. Phys.* **2008**, *10* (44), 6615–6620.

[3]     S. Miertuš, E. Scrocco, J. Tomasi, *Chem. Phys.* **1981**, *55* (1), 117–129.

[4]     a) P. v. R. Schleyer, C. Maerker, A. Dransfeld, H. Jiao, N. J. R. V. E. Hommes, *J. Am. Chem. Soc.* **1996**, *118* (26), 6317–6318. b) Z. Chen, C. S. Wannere, C. Corminboeuf, R. Puchta, P. v. R. Schleyer, *Chem. Rev.* **2005**, *105* (10), 3842–3888.

[5]     a) C. W. Bird, *Tetrahedron* **1985**, *41* (7), 1409–1414. b) C. W. Bird, *Tetrahedron* **1986**, *42* (1), 89–92.

[6]     A. T. B. Gilbert, IQmol molecular viewer. Available at: http://iqmol.org (Accessed October, 2012).

[7]     G. Guisado-Barrios, J. Bouffard, B. Donnadieu, G.Bertrand, *Angew. Chem. Int. Ed.* **2010**, *49*, 4759-4762.

[8]     G. Becker, H. Schmidt, G. Uhl, W. Uhl, M. Regitz, W. Rösch, U.-J. Vogelbacher, *Inorg. Synth.* **1990**, *27*, 249–253.

[9]     Y. Y. C. Yeung Lam Ko, R. Carrié, A. Muench, G. Becker, *J. Chem. Soc. Chem. Commun.***1984**, 1634-1635.

[10]    Bruker (**2010**). APEX2, SAINT, SADABS and XSHELL. Bruker AXS Inc., Madison, Wisconsin, USA.

[11]    G. M. Sheldrick, *Acta Cryst.* **2008**, *A64*, 112.

[12]    a) G. M. Sheldrick, *Acta Cryst.* **2015**, *C71*, 3; b) G. M. Sheldrick, *Acta Cryst.* **2015**, *A71*, 3.

[13]    Spek, A. L. *Acta Cryst.* **2009**, *D65* (2), 148.

Phosphorus derivatives of mesoionic carbenes: synthesis and characterization of triazaphosphole-5-ylidene → BF$_3$ adducts:

# Supporting Information

# Phosphorus Derivatives of Mesoionic Carbenes: Synthesis and Characterization of Triazaphosphole-5-ylidene→BF₃ Adducts

Lea Dettling,[a] Niklas Limberg,[a] Raphaela Küppers,[a] Daniel Frost,[a] Manuela Weber,[a] Nathan T. Coles,[b] Diego M. Andrada,[c] Christian Müller*[a]

**Table of Contents**

## 1. Experimental Procedures
### 1.1 General Information

All reactions involving air- and moisture-sensitive compounds were carried out using an *MBRAUN* glovebox under an argon atmosphere or standard Schlenk techniques. All common chemicals and solvents were commercially available. Benzylazide[1], 2-azido-1,3-diisopropylbenzene[2] and trimethylsilyl-phosphaalkine[3] were prepared by methods described in the literature. Commercially available chemicals were used without further purification. Toluene, DCM and *n*-pentane were prepared using an *MBRAUN* Solvent Purification System *MB-SPS 800*. THF and DME were dried over K/benzophenone under argon. The deuterated dry solvents DCM-$d_2$ and acetonitrile-$d_3$ were dried over CaH$_2$ and THF-$d_8$ over a sodium-potassium alloy and chloroform-*d* over molecular sieve 4Å. $^1$H, $^{13}$C{$^1$H}, $^{19}$F, $^{19}$F{$^{31}$P}, $^{11}$B{$^{19}$F}, $^{11}$B and $^{31}$P{$^1$H} NMR spectra were recorded by using a *JEOL ECS400* spectrometer (400 MHz), or a *JEOL ECZ600* spectrometer (600 MHz). All chemical shifts are reported relative to the residual resonance in the deuterated solvents.

**Caution**: Azides are potentially hazardous compounds and adequate safety measures should be taken when weighing, heating and working up.

### 1.2 Synthesis and Characterization

**3-benzyl-5-(trimethylsilyl)-3*H*-1,2,3,4-triazaphosphole (1a)**
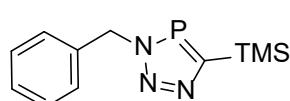
Benzylazide (200 mg, 1.50 mmol, 1.00 eq) was added to an excess of trimethylsilyl-phosphaalkine in toluene. After stirring the reaction mixture overnight at room temperature, the excess of trimethylsilyl-phosphaalkine in toluene was condensed out of the reaction mixture in a separate Schlenk flask (after determination of the concentration the trimethylsilyl-phosphaalkine could be reused for the next synthesis). The crude product was recrystallized from a *n*-pentane solution yielding the 3-benzyl-5-(trimethylsilyl)-3*H*-1,2,3,4-triazaphosphole (**1a**) as colorless solid (325 mg, 87%).

**$^1$H NMR (401 MHz, chloroform-*d*):** $\delta$ = 7.36 (s, 5H), 5.79 (d, $^3J_{P-H}$ = 6.1 Hz, 2H), 0.38 (s, 9H, Si(CH$_3$)$_3$) ppm.

**$^{31}$P{$^1$H} NMR (162 MHz, chloroform-*d*):** $\delta$ = 214.0 ppm.

**$^{13}$C NMR (101 MHz, chloroform-*d*):** $\delta$ = 185.27 (d, *J* = 75.0 Hz), 137.11, 129.08, 128.64, 128.59, 55.84 (d, *J* = 12.0 Hz), -0.26 (d, *J* = 3.5 Hz) ppm.

**ESI-TOF** (m/z): 250.0930 g/mol (calc.: 250,0923 g/mol) [M+H]$^+$.

The spectroscopic data obtained is in agreement with the literature.[4]

**3-(2,6-diisopropylphenyl)-5-(trimethylsilyl)-3*H*-1,2,3,4-triazaphosphole (1b)**
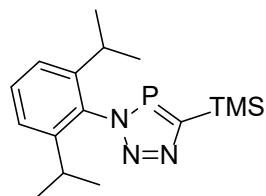
2-Azido-1,3-diisopropylbenzene (1.07 g, 5.26 mmol, 1.00 eq.) was added to an excess of trimethylsilyl-phosphaalkine in toluene. After stirring the reaction mixture overnight at room temperature, the excess of trimethylsilyl-phosphaalkine in toluene was condensed out of the reaction mixture in a separate Schlenk flask. The crude product was washed with *n*-pentane (3 x 2

1

mL) and the 5-rimethylsilyl-3*H*-1,2,3,4-triazaphosphole was isolated as a yellowish solid (1.39 g, 83%)

**¹H NMR (401 MHz, chloroform-*d*):** $\delta$ = 7.50 (t, *J* = 7.8 Hz, 1H, Dipp-*para*-HAr), 7.33 (d, *J* = 7.8 Hz, 2H, Dipp-*meta*-HAr), 2.10 (hept, *J* = 7.1 Hz, 2H, Dipp-*ortho*- ipr-CH), 1.12 (d, *J* = 6.7 Hz, 12H, Dipp-*ortho*- ipr-CH₃), 0.49 (s, 9H, C-TMS) ppm.

**³¹P{¹H} NMR (162 MHz, chloroform-*d*):** $\delta$ = 223.0 ppm.

**¹³C NMR (101 MHz, chloroform-*d*):** $\delta$ = 185.86 (d, *J* = 75.0 Hz), 145.96, 130.11, 123.82, 28.40, 24.41 (d, *J* = 22.8 Hz), -0.02 (d, *J* = 3.2 Hz) ppm.

**C-H-N-Analysis**: Found: C, 58.6; H, 8.8; N, 12.0. Calc. for $C_{16}H_{26}N_3PSi$: C, 60.2; H, 8.2; N, 13.1%.

### 3-benzyl-1-methyl-5-(trimethylsilyl)-3*H*-1,2,3,4-triazaphosphol-1-ium tetrafluoroborate (2a)
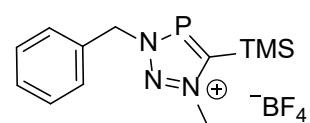
**2a** was prepared starting from **1a** (200 mg, 0.80 mmol) and trimethyloxonium tetrafluoroborate (143 mg, 0.96 mmol) in DCM (10 mL). The reaction mixture was stirred at room temperature for 2 hours, after which the solvent was removed in vacuo and the remaining solid was washed with dry diethyl ether (3 x 5 mL). **2a** was obtained as a colorless solid (222 mg, 79%).

**¹H-NMR (400 MHz, DCM-*d₂*):** $\delta$ = 7.54 – 7.50 (m, 5H), 5.82 (d, *J* = 5.6 Hz, 2H), 4.52 (s, 3H, CH₃), 0.53 (s, 9H, Si(CH₃)₃) ppm.

**¹³C{¹H}-NMR (101 MHz, DCM-*d₂*):** $\delta$ = 130.9, 130.7, 130.3, 60.3, 44.7, -0.9 ppm

**³¹P{¹H}-NMR (162 MHz, DCM-*d₂*):** $\delta$ = 239.3 ppm.

**¹⁹F-NMR (377 MHz, DCM-*d₂*):** $\delta$ = − 153.2 ppm.

**¹¹B-NMR (129 MHz, DCM-*d₂*):** $\delta$ = − 1.5 ppm.

**ESI-TOF** (m/z): 264.1159 g/mol (calc.: 264.1086 g/mol) [M-BF₄]⁺.

**C-H-N-Analysis**: Found: C, 40.1; H, 6.0; N, 11.2. Calc. for $C_{12}H_{19}N_3PSiBF_4$: C, 41.0; H, 5.5; N, 12.0%.

### 3-(2,6-diisopropylphenyl)-1-methyl-5-(trimethylsilyl)-3H-1,2,3,4-triazaphosphol-1-ium tetrafluoroborate (2b)
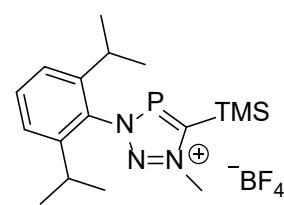
3-(2,6-diisopropylphenyl)-5-(trimethylsilyl)-3*H*-1,2,3,4-triazaphosphole (**1b**) (500 mg, 1.57 mmol) was dissolved in 10 ml DCM and trimethyloxonium tetrafluoroborate (255 mg, 1.72 mmol,) was added. The reaction mixture was stirred at room temperature overnight. Subsequently, the solvent was removed in vacuo and redissolved in acetonitrile. The solution was washed three times with 5 ml of dry diethyl ether. The solid was dried in vacuo to give product **2b** as an off white solid (636 mg, 97%).

**¹H-NMR (401 MHz DCM-*d₂*):** $\delta$ = 7.63 (t, *J* = 7.8 Hz, 1H, Dipp-*para*-H_Ar), 7.41 (d, *J* = 7.9 Hz, 2H, Dipp-*meta*-H_Ar), 4.70 (s, 3H, N-CH₃), 2.21 (hept, *J* = 6.6 Hz, 2H, Dipp-*orthoipr*-CH), 1.22 (d, *J* = 6.8 Hz, 6H, Dipp-*ortho*- ipr-CH₃), 1.18 (d, *J* = 6.8 Hz, 6H, Dipp-*ortho*- ipr-CH₃), 0.71 (s, 9H, C-TMS) ppm.

2

**13C{1H}-NMR (101 MHz, DCM-$d_2$):** δ = 133.04, 125.34, 45.39, 29.21, 24.59, -0.63 ppm.

**31P{1H}-NMR (162 MHz, DCM-$d_2$):** δ = 249.1 ppm.

**11B-NMR (129 MHz, DCM-$d_2$):** δ = − 1.3 ppm.

**19F-NMR (377 MHz, DCM-$d_2$):** δ = − 152.3 ppm.

**ESI-TOF** (m/z): 262.1476 g/mol (calc.: 262.1468 g/mol) [M-SiMe$_3$BF$_4$]$^+$, 334.1871 g/mol (calc.: 334.1868 g/mol) [M-BF$_4$]$^+$.

**C-H-N-Analysis**: Found: C, 48.3; H, 7.3; N, 10.0. Calc. for C$_{17}$H$_{29}$N$_3$PSiBF$_4$: C, 49.7; H, 7.2; N, 9.7%.


### 3-benzyl-1-methyl-3H-1,2,3,4-triazaphosphol-1-ium tetrafluoroborate (3a)
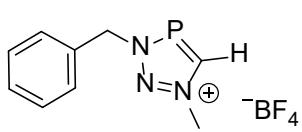


The corresponding triazaphospholenium salt **2a** (200 mg, 0.57 mmol) was dissolved in DME (10 mL) and stirred at $T$ = 60°C for 4 days. Subsequently, the solvent was removed in vacuo. After washing with *n*-pentane (3 x 5 mL) **3a** was obtained as a colorless oil (84 mg, 53%).

**1H-NMR (401 MHz, acetonitrile-$d_3$):** δ = 9.33 (d, $J$ = 37.5 Hz, 1H), 7.56 − 7.41 (m, 5H), 5.81 (d, $^3J_{P\text{-}H}$ = 6.0 Hz, 2H), 4.42 (s, 3H) ppm.

**13C{1H}-NMR (101 MHz, acetonitrile-$d_3$):** δ = 165.0 (d, $J$ = 62.3 Hz, C=P), 131.0 (C$_{Ar}$), 130.8 (C$_{Ar}$), 130.5 (C$_{Ar}$), 72.66 (CH$_2$), 44.5 (CH$_3$) ppm.

**31P{1H}-NMR (162 MHz, acetonitrile-$d_3$):** δ = 206.7 ppm.

**11B-NMR (129 MHz, acetonitrile-$d_3$):** δ = − 0.3 ppm.

**19F-NMR (377 MHz, acetonitrile-$d_3$):** δ = − 150.7 ppm.


### (3-benzyl-1-methyl-3H-1,2,3,4-triazaphosphol-1-ium-5-yl)trifluoroborate (4a)
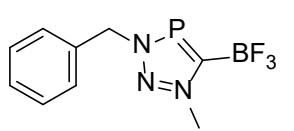


The corresponding triazaphospholenium salt **2a** (134.0 mg, 0.38 mmol) was dissolved in DME (5 mL) and stirred at $T$ = 60 °C for 6 hours. Subsequently, the solvent was removed under high vacuum, and the crude product was purified by column chromatography in hexane : ethyl acetate (1 : 9). **4a** was obtained as a colorless oil (45 mg, 42%).

**1H-NMR (401 MHz, DCM-$d_2$):** δ = 7.69 − 7.31 (m, 5H), 5.68 (d, $J$ = 5.6 Hz, 2H), 4.47 (d, $J$ = 0.9 Hz, 3H) ppm.

**13C{1H}-NMR (101 MHz, DCM-$d_2$):** δ = 133.9 (d, $J$ =49.7 Hz), 130.5 (C$_{Ar}$), 130.1 (C$_{Ar}$), 129.7 (C$_{Ar}$), 59.8 (d, $J$ = 10.0 Hz, CH$_2$), 42.8 (CH$_3$) ppm.

**31P{1H}-NMR (162 MHz, DCM-$d_2$):** δ = 229.3 ppm.

**11B-NMR (129 MHz, DCM-$d_2$):** δ = 0.65 (qd, $J$ = 37.9, 15.9 Hz) ppm.

**19F-NMR (377 MHz, DCM-$d_2$):** δ = − 140.5 (qd, $J$ = 37.7, 14.6 Hz) ppm.

3

## (3-(2,6-diisopropylphenyl)-1-methyl-3*H*-1,2,3,4-triazaphosphol-1-ium-5-yl)trifluoroborate (4b)
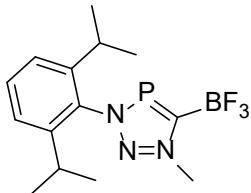
The corresponding triazaphospholenium salt **2b** (136 mg, 0.31 mmol) was dissolved in DME (2 mL), and stirred at *T* = 60 °C for 2 hours. Subsequently, the solvent was removed under high vacuum, and the crude product was purified by column chromatography in hexane : ethyl acetate (1 : 9). **4b** was obtained as a yellowish oil.

**$^{1}$H-NMR (401 MHz, THF-$d_8$):** $\delta$ = 7.66 (t, *J* = 3.0 Hz, 1H),7.49 (d, *J* = 7.8 Hz, 2H), 3.32 (s, 3H, N-CH$_3$), 2.46 (hept, *J* = 6.8 Hz, 2H), 1.25 (d, *J* = 6.8 Hz, 12H) ppm.

**$^{13}$C-NMR (101 MHz, THF-$d_8$):** $\delta$ = 146.2 (C$_{Ar}$), 145.7 (C$_{Ar}$), 132.4 (C$_{Ar}$), 124.9 (C$_{Ar}$), 72.5 (C=P), 44.1 (N-CH3), 28.9 (isopropyl), 24.1 (isopropyl) ppm.

**$^{31}$P{$^{1}$H}-NMR (162 MHz, THF-$d_8$):** $\delta$ = 240.1 ppm.

**$^{11}$B-NMR (129 MHz, THF-$d_8$):** $\delta$ = 0.6 (qd, *J* = 37.8, 15.3 Hz) ppm.

**$^{19}$F-NMR-Spektrum (377 MHz, DCM-$d_2$)**: $\delta$ = − 140.4 (qd, *J* = 72.0, 14.3 Hz) ppm.

**C-H-N-Analysis**: Found: C, 49.4; H, 6.4; N, 10.2. Calc. for C$_{14}$H$_{20}$N$_3$PBF$_3$: C, 51.1; H, 6.1; N, 12.8%.


## 3-benzyl-1-ethyl-5-(trimethylsilyl)-3*H*-1,2,3,4-triazaphosphol-1-ium hexafluorophosphate (5a)
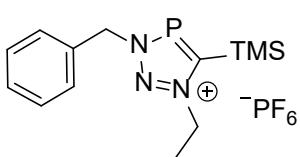
Triazaphosphol **1a** (300 mg, 1.20 mmol) and triethyloxonium hexafluorophosphate (298 mg, 1.20 mmol) were dissolved in DCM (10 mL) and stirred for two hours at room temperature. Removal of the solvent in vacuum gave the crude product which was purified by washing with *n*-pentane (3 x 3 mL) followed by drying the solid in vacuo. **5a** was obtained as a yellowish solid (407 mg, 80%).

**$^{1}$H-NMR (401 MHz, chloroform-*d*):** $\delta$ = 7.71 – 7.37 (m, 5H, H$_{Ar}$), 5.83 (d, *J* = 5.5 Hz,2H), 4.80 (q, *J* = 7.3 Hz, 2H, N-CH$_2$), 1.83 (t, *J* = 7.3 Hz, 3H, N-CH$_2$-CH$_3$), 0.57 (s, 9H, C-TMS) ppm.

**$^{31}$P{$^{1}$H}-NMR (162 MHz, chloroform-*d*):** $\delta$ = 238.3 (s, P=C), − 144.9 (hept, *J* = 712.9 Hz, PF$_6$) ppm.

**$^{19}$F-NMR (377 MHz, chloroform-*d*):** = -73.3 (d*, J* = 713.0 Hz) ppm.

**$^{13}$C NMR (101 MHz, chloroform-*d*):** $\delta$ = 181.3 (d, *J* = 61.6 Hz), 132.6, 130.9, 130.4, 60.4, 54.2, -0.4 (d, *J* = 6.4 Hz) ppm.

**ESI-TOF** (m/z): 278.1285 g/mol (calc.: 278.1242 g/mol) [M-PF$_6$]$^+$.


## 3-(2,6-diisopropylphenyl)-1-ethyl-5-(trimethylsilyl)-3*H*-1,2,3,4-triazaphosphol-1-ium hexafluorophosphate (5b)
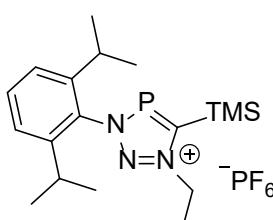
Triazaphosphol **1b** (1.73 g, 5.42 mmol) was dissolved in 10 ml DCM and triethyloxonium hexafluorophosphate (1.23 g, 4.92 mmol) was added. The reaction mixture was stirred overnight. Subsequently, the solvent was removed in vacuo and dissolved in acetonitrile. The solution was washed three times with 5 ml of *n*-pentane. The solvent of the acetonitrile fraction

4

was removed in vacuo and product **5b** was obtained as a colorless solid (2.26 g, 93%).

**¹H-NMR (400 MHz, DCM-$d_2$):** $\delta$ = 7.66 (t, $J$ = 7.8 Hz, 1H), 7.43 (d, $J$ = 7.9 Hz, 2H), 4.95 (q, $J$ = 7.3 Hz, 2H), 2.19 (p, $J$ = 6.9 Hz, 2H), 1.78 (t, $J$ = 7.2 Hz, 3H), 1.24 (d, $J$ = 6.8 Hz, 6H), 1.17 (d, $J$ = 6.7 Hz, 6H), 0.70 (s, 9H)ppm.

**³¹P{¹H}-NMR (162 MHz, DCM-$d_2$):** $\delta$ = 248.7 (s, P=C), 144.0 (hept, $J$ = 711.6 Hz, PF₆) ppm.

**¹⁹F-NMR (377 MHz, DCM-$d_2$):** = -72.8 (d, $J$ = 719.1 Hz) ppm.

**¹³C NMR (101 MHz, DCM-$d_2$):** $\delta$ = 145.7, 133.1, 125.4, 55.2, 29.4, 24.8, 24.3, 15.9, -0.4 ppm.

**C-H-N-Analysis:** Found: C, 44.5; H, 6.8; N, 8.9. Calc. for $C_{18}H_{31}N_3P_2SiF_6$: C, 43.8; H, 6.3; N, 8.5%.

### 3-(2,6-diisopropylphenyl)-1-ethyl-3$H$-1,2,3,4-triazaphosphol-1-ium hexafluorophosphate (6b)
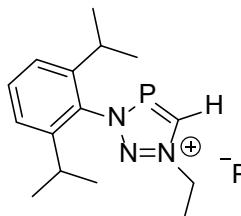


The triazaphospholenium Salt **5b** (200 mg, 0.41 mmol) and potassium fluoride (118 mg, 2.03 mmol) were dissolved in DCM (5 mL) and stirred at $T$ = -78°C for overnight. After adding $n$-pentane (3 mL) the precipitate was filtered of and the remaining solution dried in vacuo. The product **6b** was obtained as yellow solid (75 mg, 44%).

**¹H-NMR (401 MHz, DCM-$d_2$):** $\delta$ = 9.91 (d, $J$ = 35.9 Hz, 1H), 7.65 (t, $J$ = 7.9 Hz, 1H), 7.42 (d, $J$ = 7.9 Hz, 2H), 5.00 (q, $J$ = 7.5 Hz, 2H), 2.17 (hept, $J$ = 6.8 Hz, 2H), 1.78 (t, $J$ = 7.3 Hz, 3H), 1.23 (dd, $J$ = 29.6, 6.8 Hz, 12H) ppm.

**³¹P{¹H}-NMR (162 MHz, DCM-$d_2$):** $\delta$ = 214.4 (s, P=C), − 144.4 (hept, $J$ =711.6 Hz, PF₆) ppm.

**¹⁹F-NMR (377 MHz, DCM-$d_2$):** $\delta$ = − 72.1 (d, $J$ = 711.6 Hz) ppm.

**¹³C{¹H}-NMR (101 MHz, DCM-$d_2$):** $\delta$ = 165.3 (C=P), 145.7 (C$_{Ar}$), 145.7 (C$_{Ar}$), 133.2 (C$_{Ar}$), 125.3(C$_{Ar}$), 54.8 (N-CH₂), 29.4 (N-CH₂-CH₃), 24.7 (isopropyl), 24.2 (isopropyl), 15.3 (isopropyl) ppm.

### (3-(2,6-diisopropylphenyl)-1-ethyl-3$H$-1,2,3,4-triazaphosphol-1-ium-5-yl)triethylborate (7b)
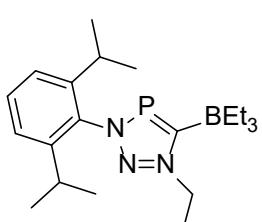


The triazaphospholenium salt **5b** (300 mg, 0.61 mmol) was added together with the potassium fluoride (70.6 mg, 1,22 mmol) and then dissolved in dry THF (5 mL). The reaction mixture was cooled to $T$ = − 78°C and carefully 0.9 mL of a 1 M solution of BEt₃ in THF (71.5 mg, 0.73 mmol) was added. The reaction mixture was allowed to warm to room temperature overnight. The solvent was removed in vacuo, dry DCM (3 mL) was added, and the solution was filtered. The product **7b** was obtained from the solution after removal of the solvent in vacuum as pale yellow oil (111 mg, 49%).

**¹H-NMR (401 MHz, DCM-$d_2$):** $\delta$ = 7.54 (t, $J$ = 7.9 Hz, 1H), 7.34 (d, $J$ = 7.9 Hz, 2H), 4.89 (q, $J$ = 7.3 Hz, 2H, N-CH₂), 2.20 (hept, $J$ = 6.8 Hz, 2H), 1.59 − 1.57 (m, 3H, N-CH₂-CH₃), 1.20 (d, $J$ = 6.8 Hz, 6H), 1.12 (d, $J$ = 6.9 Hz, 6H), 0.69 (t, J = 7.5 Hz, 9H, B-CH₂-CH₃), 0.44 (q, $J$ = 7.6 Hz, 6H, B-CH₂) ppm.

**³¹P{¹H}-NMR (162 MHz, DCM-$d_2$):** $\delta$ = 242.9 (s) ppm.

**¹¹B-NMR (129 MHz, DCM-$d_2$):** $\delta$ = − 13.5 (s) ppm.

5

**¹³C{¹H}-NMR (101 MHz, DCM-*d₂*):** $\delta$ = 177.7, 145.6, 131.6, 124.7, 71.1, 50.9, 27.2, 24.7, 24.3 (d, *J* = 39.8 Hz), 16.3, 11.0 ppm.

## 2. Additional Figures
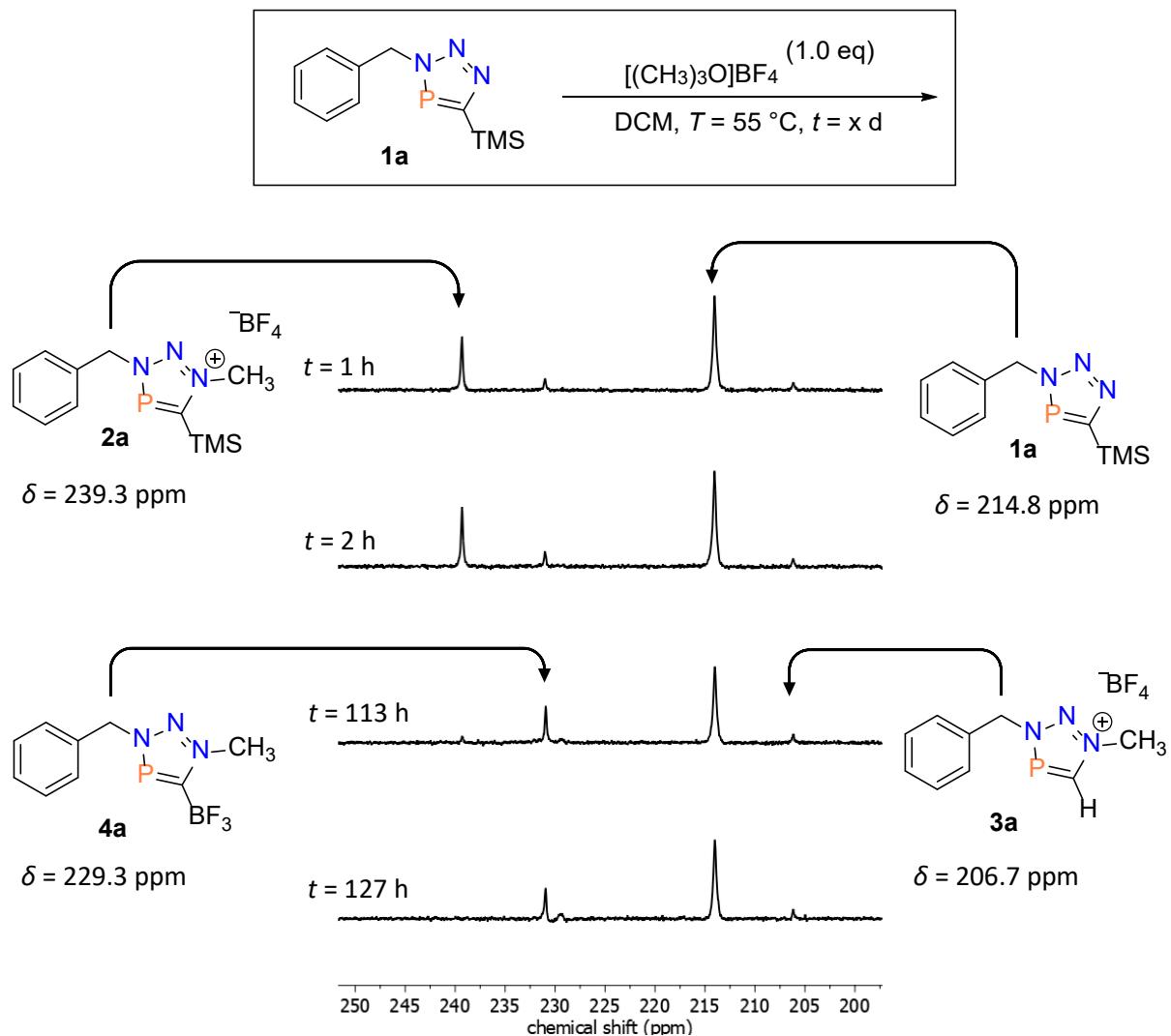


**Figure S1**: Monitoring the reaction progress by $^{31}P\{^{1}H\}$-NMR spectroscopy (without solvent) of the attempted preparation of quaternized 3*H*-1,2,3,4-triazaphosphole **1a**.
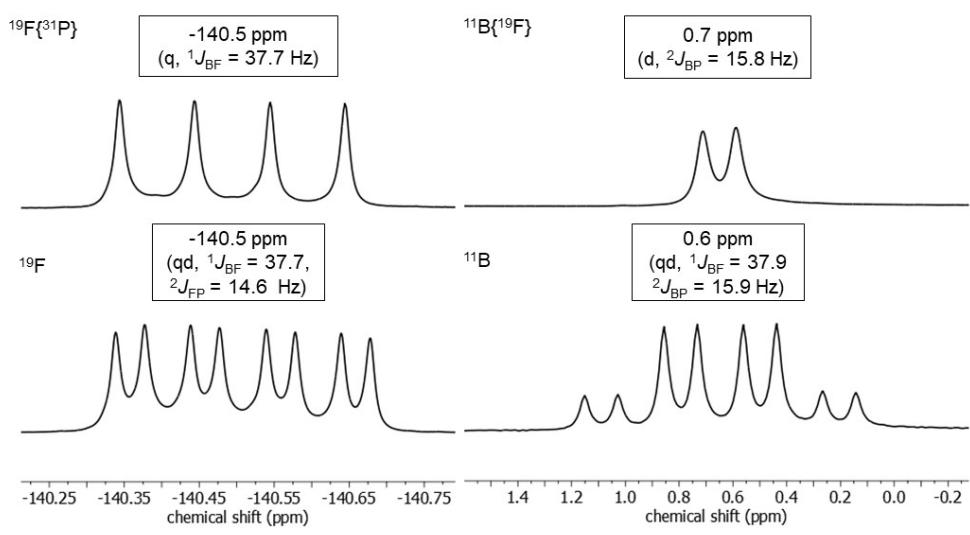
**Figure S2**: $^{11}B$ and $^{19}F$ NMR spectra of $BF_3$-3$H$ 1,2,3,4 triazaphospholenium salt adduct **4a** in MeCN-$d_3$.

### 3. Crystallographic Details

X-ray studies were carried out on a D8 Venture, Bruker Photon CMOS diffractometer[5] (MoKα radiation; λ = 0.71073 Å and CuKα radiation; λ = 1.54178 Å) up to a resolution of (sinΘ/λ) max = 0.58 Å (6) 0.60 Å (3, 9) at 100(2) K. The structures of were solved with SHELXT-2018[6] by using direct methods and refined with SHELXL-2018/3 [7] on F2 for all reflections. Non-hydrogen atoms were refined by using anisotropic displacement parameters. The positions of the hydrogen atoms were calculated for idealized positions. Geometry calculations and checks for higher symmetry were performed with the PLATON program.[8] The program Olex2 [9] was also used to aid in the refinement of the structures of compounds. All non-hydrogen atoms were refined anisotropically. All hydrogen atoms were included into the model at geometrically calculated positions and refined using a riding model. The isotropic displacement parameter of all hydrogen atoms were fixed to 1.2 times the U-value of the atoms they are linked to (1.5 times for methyl groups). Crystallographic data for the structures reported in this paper have been deposited in the Cambridge Crystallographic Database Center: CCDC number: 2279457(**3a**) 2279453(**4a**), 2279454(**4b**), 2279455 (**6b**) 2279456 (**7b**). Details of the X-ray structure determinations and refinements are provided in Table S1-S5.
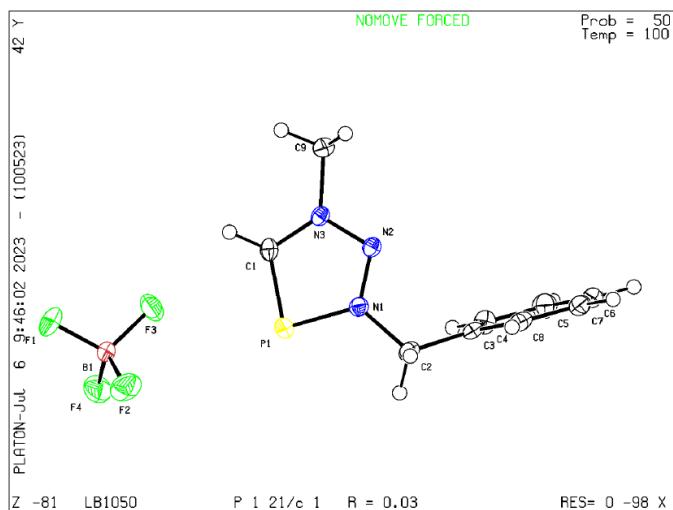
Table S1 Crystal data and structure refinement for **3a**.

| | |
|---|---|
| Identification code | LB1050 |
| Empirical formula | $C_9H_{11}BF_4N_3P$ |
| Formula weight | 278.999 |
| Temperature/K | 100.00 |
| Crystal system | monoclinic |
| Space group | $P2_1/c$ |
| a/Å | 10.71411(7) |
| b/Å | 8.96879(6) |
| c/Å | 13.55016(9) |
| α/° | 90 |
| β/° | 111.9100(2) |
| γ/° | 90 |
| Volume/Å$^3$ | 1208.023(14) |
| Z | 4 |
| $\rho_{calc}$g/cm$^3$ | 1.534 |
| μ/mm$^{-1}$ | 2.400 |
| F(000) | 571.6 |
| Crystal size/mm$^3$ | $0.7 \times 0.16 \times 0.05$ |
| Radiation | Cu Kα (λ = 1.54178) |
| 2Θ range for data collection/° | 8.9 to 136.56 |
| Index ranges | $-12 \leq h \leq 12, -10 \leq k \leq 10, -16 \leq l \leq 16$ |
| Reflections collected | 18430 |
| Independent reflections | 2174 [$R_{int}$ = 0.0343, $R_{sigma}$ = 0.0205] |
| Data/restraints/parameters | 2174/0/164 |
| Goodness-of-fit on F$^2$ | 1.062 |
| Final R indexes [I>=2σ (I)] | $R_1$ = 0.0301, w$R_2$ = 0.0771 |
| Final R indexes [all data] | $R_1$ = 0.0311, w$R_2$ = 0.0779 |
| Largest diff. peak/hole / e Å$^{-3}$ | 0.29/-0.31 |

10
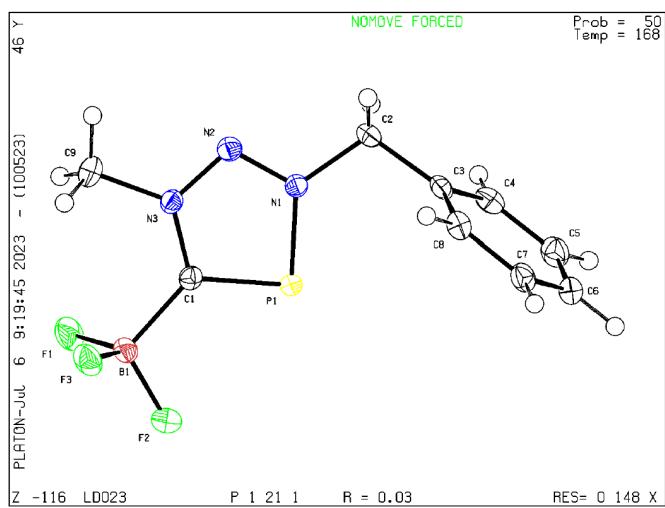
Table S2 Crystal data and structure refinement for **4a**

| | |
|---|---|
| Identification code | LD023 |
| Empirical formula | $C_9H_{10}BF_3N_3P$ |
| Formula weight | 258.993 |
| Temperature/K | 168.00 |
| Crystal system | monoclinic |
| Space group | $P2_1$ |
| a/Å | 5.80174(8) |
| b/Å | 8.60271(12) |
| c/Å | 11.79661(16) |
| α/° | 90 |
| β/° | 99.5596(5) |
| γ/° | 90 |
| Volume/Å$^3$ | 580.601(14) |
| Z | 2 |
| $\rho_{calc}$g/cm$^3$ | 1.481 |
| μ/mm$^{-1}$ | 0.255 |
| F(000) | 264.4 |
| Crystal size/mm$^3$ | 0.49 × 0.17 × 0.15 |
| Radiation | Mo Kα (λ = 0.71073) |
| 2Θ range for data collection/° | 5.88 to 52.76 |
| Index ranges | -7 ≤ h ≤ 7, -10 ≤ k ≤ 10, -14 ≤ l ≤ 14 |
| Reflections collected | 14658 |
| Independent reflections | 2376 [$R_{int}$ = 0.0304, $R_{sigma}$ = 0.0253] |
| Data/restraints/parameters | 2376/1/155 |
| Goodness-of-fit on F$^2$ | 1.159 |
| Final R indexes [I>=2σ (I)] | $R_1$ = 0.0261, $wR_2$ = 0.0590 |
| Final R indexes [all data] | $R_1$ = 0.0264, $wR_2$ = 0.0594 |
| Largest diff. peak/hole / e Å$^{-3}$ | 0.51/-0.32 |
| Flack parameter | -0.00(2) |
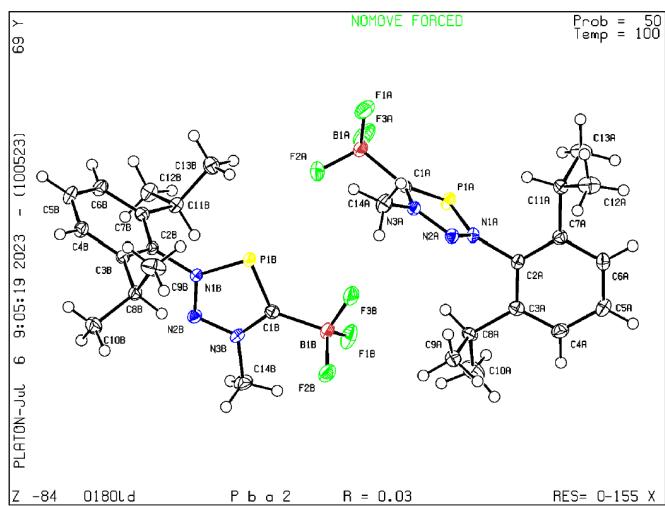
Table S3 Crystal data and structure refinement for **4b**.

| | |
|---|---|
| Identification code | 0180LD |
| Empirical formula | $C_{14}H_{20}BF_3N_3P$ |
| Formula weight | 329.11 |
| Temperature/K | 100.0 |
| Crystal system | orthorhombic |
| Space group | Pba2 |
| a/Å | 11.2355(2) |
| b/Å | 30.5407(5) |
| c/Å | 9.5592(2) |
| $\alpha$/° | 90 |
| $\beta$/° | 90 |
| $\gamma$/° | 90 |
| Volume/Å$^3$ | 3280.14(10) |
| Z | 8 |
| $\rho_{calc}g/cm^3$ | 1.333 |
| $\mu$/mm$^{-1}$ | 0.196 |
| F(000) | 1376.0 |
| Crystal size/mm$^3$ | 0.31 × 0.25 × 0.11 |
| Radiation | MoK$\alpha$ ($\lambda$ = 0.71073) |
| 2$\Theta$ range for data collection/° | 3.862 to 51.426 |
| Index ranges | -13 ≤ h ≤ 13, -37 ≤ k ≤ 37, -11 ≤ l ≤ 11 |
| Reflections collected | 41596 |
| Independent reflections | 6034 [$R_{int}$ = 0.0321, $R_{sigma}$ = 0.0211] |
| Data/restraints/parameters | 6034/1/408 |
| Goodness-of-fit on F$^2$ | 1.047 |
| Final R indexes [I>=2σ (I)] | $R_1$ = 0.0270, $wR_2$ = 0.0676 |
| Final R indexes [all data] | $R_1$ = 0.0286, $wR_2$ = 0.0688 |
| Largest diff. peak/hole / e Å$^{-3}$ | 0.27/-0.18 |
| Flack parameter | 0.03(2) |

12
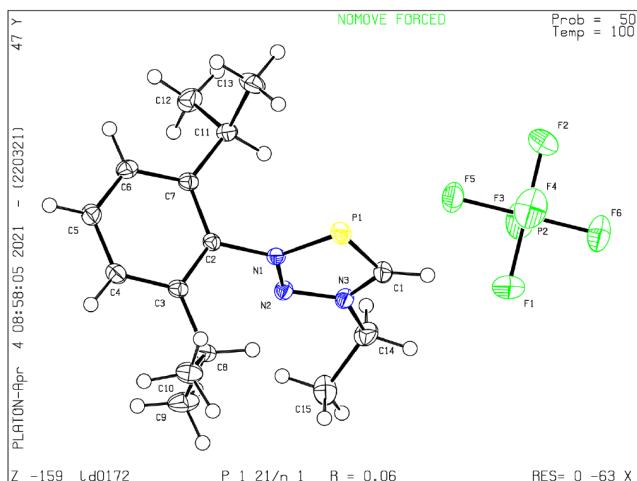
Table S4 Crystal data and structure refinement for **6b**.

| Identification code | LD0172 |
|---|---|
| Empirical formula | $C_{15}H_{23}F_6N_3P_2$ |
| Formula weight | 421.30 |
| Temperature/K | 99.95 |
| Crystal system | monoclinic |
| Space group | $P2_1/n$ |
| a/Å | 10.3822(4) |
| b/Å | 8.4426(2) |
| c/Å | 21.5901(7) |
| α/° | 90 |
| β/° | 95.4340(10) |
| γ/° | 90 |
| Volume/Å$^3$ | 1883.93(10) |
| Z | 4 |
| $\rho_{calc}$g/cm$^3$ | 1.485 |
| μ/mm$^{-1}$ | 0.292 |
| F(000) | 872.0 |
| Crystal size/mm$^3$ | 0.219 × 0.167 × 0.046 |
| Radiation | MoKα (λ = 0.71073) |
| 2Θ range for data collection/° | 4.208 to 61.054 |
| Index ranges | -14 ≤ h ≤ 14, -11 ≤ k ≤ 12, -30 ≤ l ≤ 29 |
| Reflections collected | 44368 |
| Independent reflections | 5744 [$R_{int}$ = 0.0467, $R_{sigma}$ = 0.0279] |
| Data/restraints/parameters | 5744/0/240 |
| Goodness-of-fit on F$^2$ | 1.048 |
| Final R indexes [I>=2σ (I)] | $R_1$ = 0.0597, w$R_2$ = 0.1619 |
| Final R indexes [all data] | $R_1$ = 0.0712, w$R_2$ = 0.1711 |
| Largest diff. peak/hole / e Å$^{-3}$ | 1.17/-0.67 |
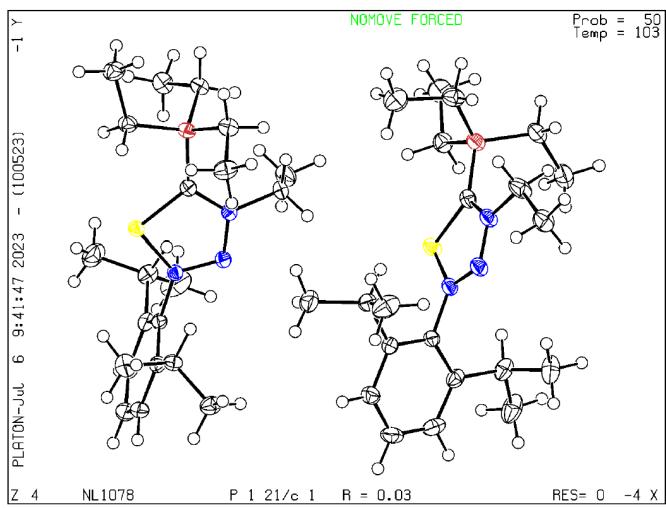
Table S5 Crystal data and structure refinement for **7b**.

| Identification code | NL1078 |
|---|---|
| Empirical formula | $C_{21}H_{37}BN_3P$ |
| Formula weight | 373.346 |
| Temperature/K | 102.60 |
| Crystal system | monoclinic |
| Space group | $P2_1/c$ |
| a/Å | 14.06027(9) |
| b/Å | 23.24206(15) |
| c/Å | 14.36186(9) |
| α/° | 90 |
| β/° | 102.7284(2) |
| γ/° | 90 |
| Volume/Å$^3$ | 4577.97(5) |
| Z | 8 |
| $\rho_{calc}$g/cm$^3$ | 1.083 |
| μ/mm$^{-1}$ | 1.110 |
| F(000) | 1638.6 |
| Crystal size/mm$^3$ | 0.3 × 0.23 × 0.12 |
| Radiation | Cu Kα (λ = 1.54178) |
| 2Θ range for data collection/° | 6.44 to 149.32 |
| Index ranges | -17 ≤ h ≤ 17, -29 ≤ k ≤ 27, -17 ≤ l ≤ 17 |
| Reflections collected | 78829 |
| Independent reflections | 9356 [$R_{int}$ = 0.0378, $R_{sigma}$ = 0.0201] |
| Data/restraints/parameters | 9356/0/485 |
| Goodness-of-fit on F$^2$ | 1.033 |
| Final R indexes [I>=2σ (I)] | $R_1$ = 0.0327, w$R_2$ = 0.0874 |
| Final R indexes [all data] | $R_1$ = 0.0348, w$R_2$ = 0.0896 |
| Largest diff. peak/hole / e Å$^{-3}$ | 0.35/-0.24 |

## 4. NMR Spectroscopic Data
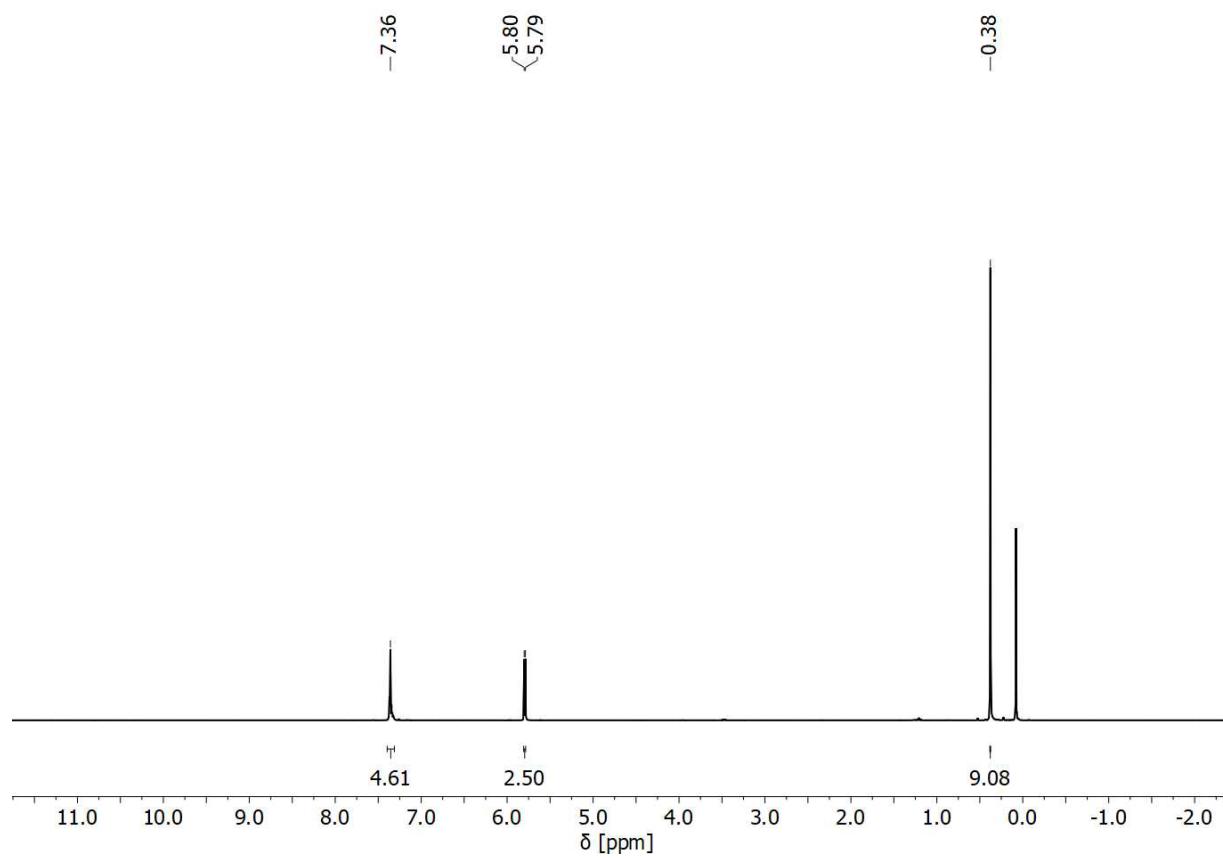


**Figure S3:** ^{1}H NMR spectrum of **1a**.
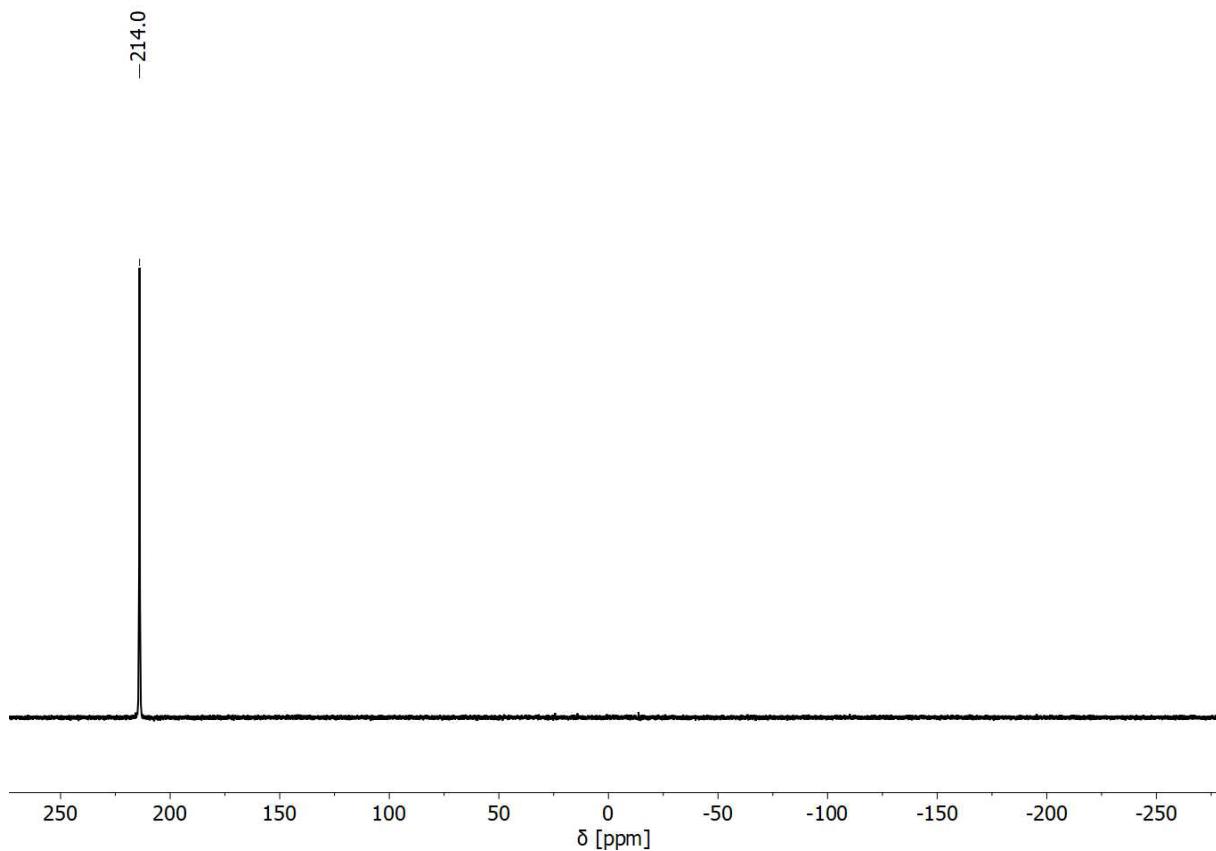
**Figure S4**: $^{31}P\{^1H\}$ NMR spectrum of **1a.**



| A (d) | B (d) | C (d) |
|---|---|---|
| 185.3 | 55.8 | -0.3 |
| J(75.0) | J(12.0) | J(3.5) |
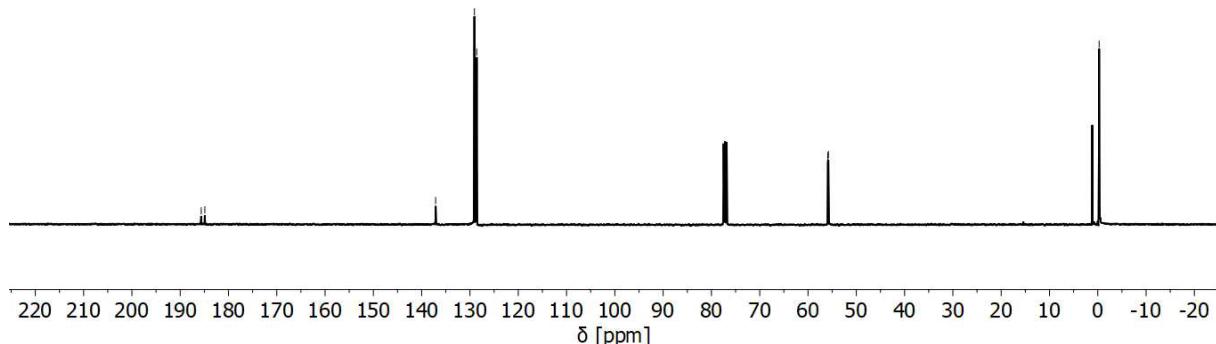
**Figure S5**: $^{13}C$ NMR spectrum of **1a.**

**Figure S6:** $^{1}H$ NMR spectrum of **1b**.
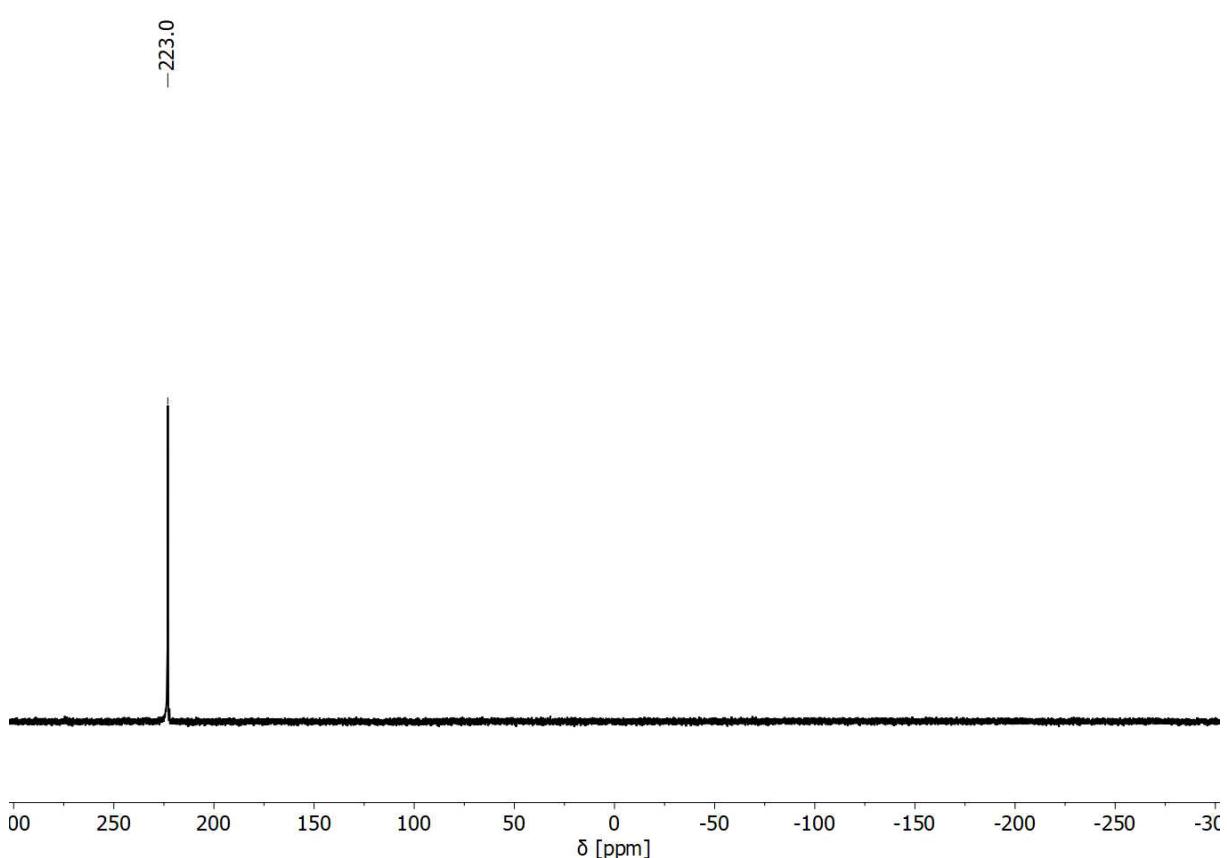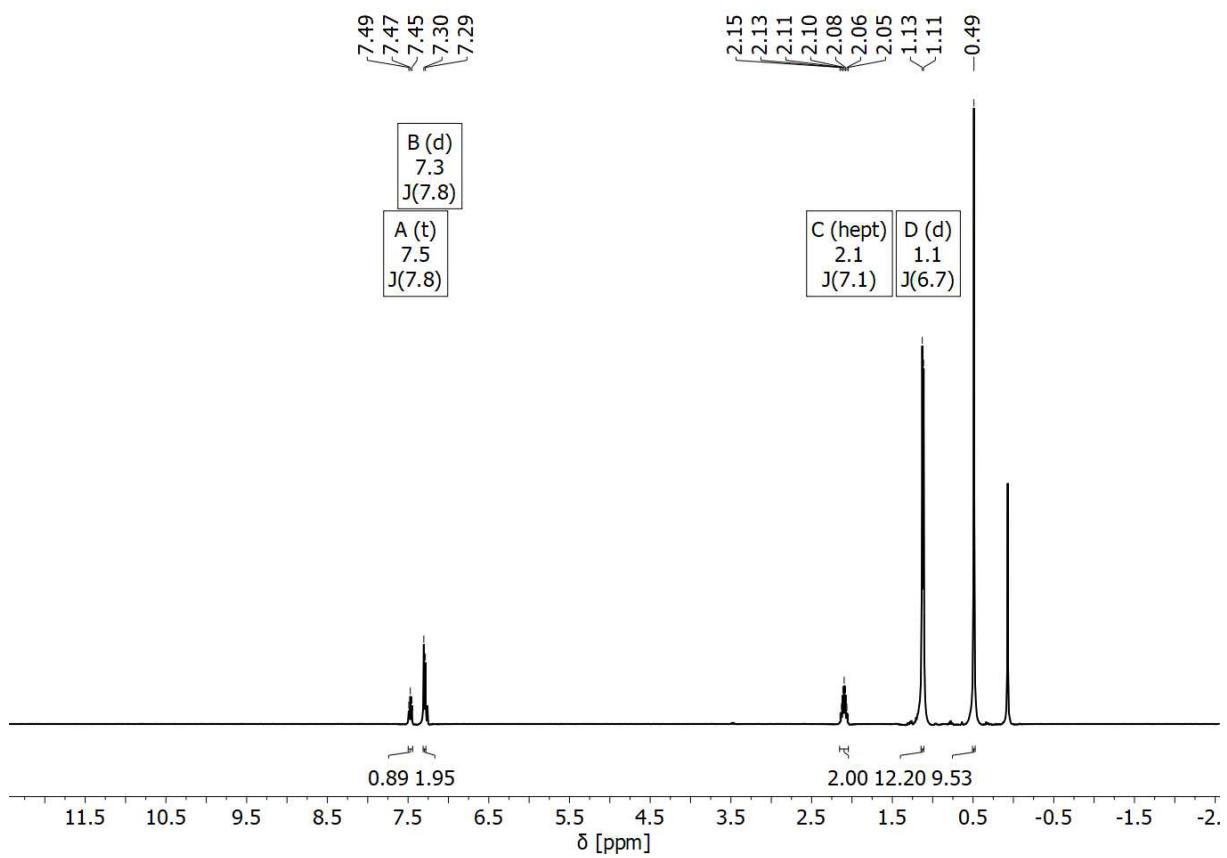


**Figure S7**: $^{31}P\{^{1}H\}$ NMR spectrum of **1b.**
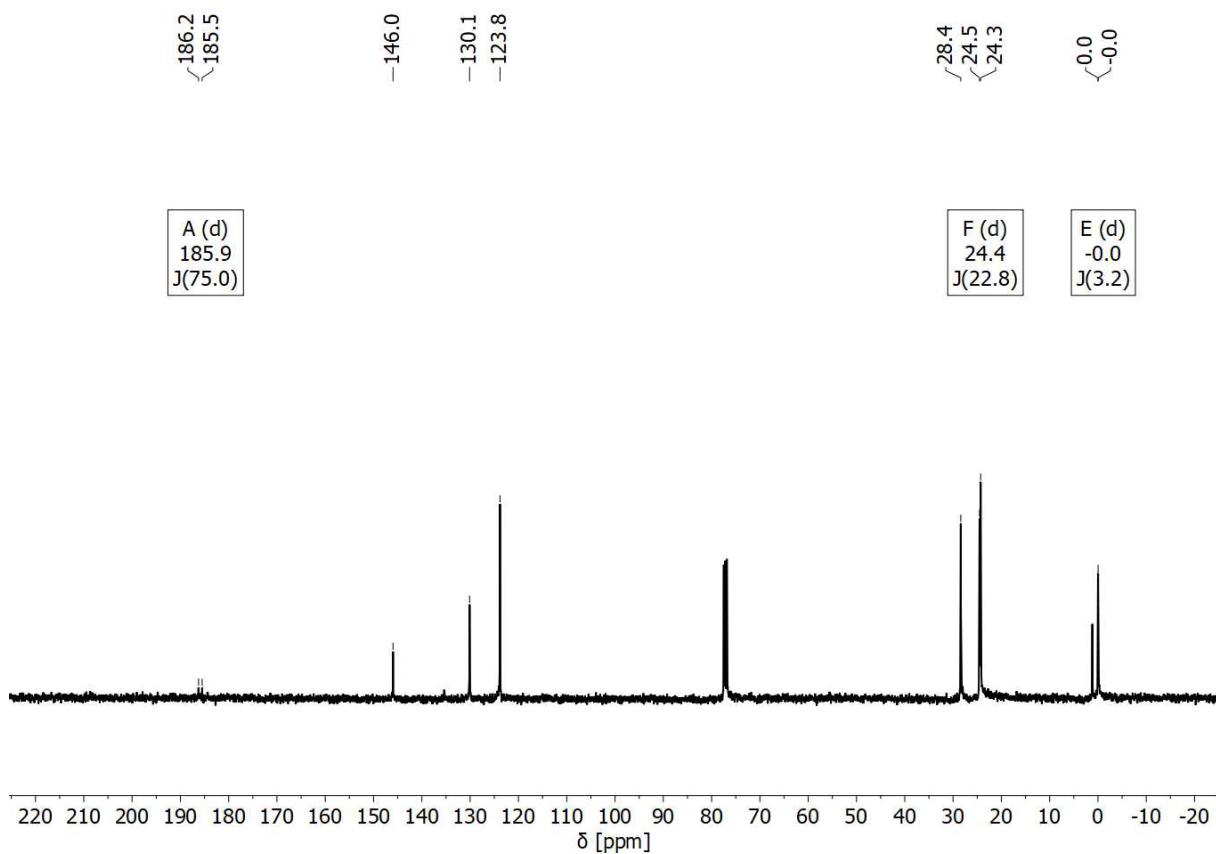
**Figure S8**: $^{13}C$ NMR spectrum of **1b.**
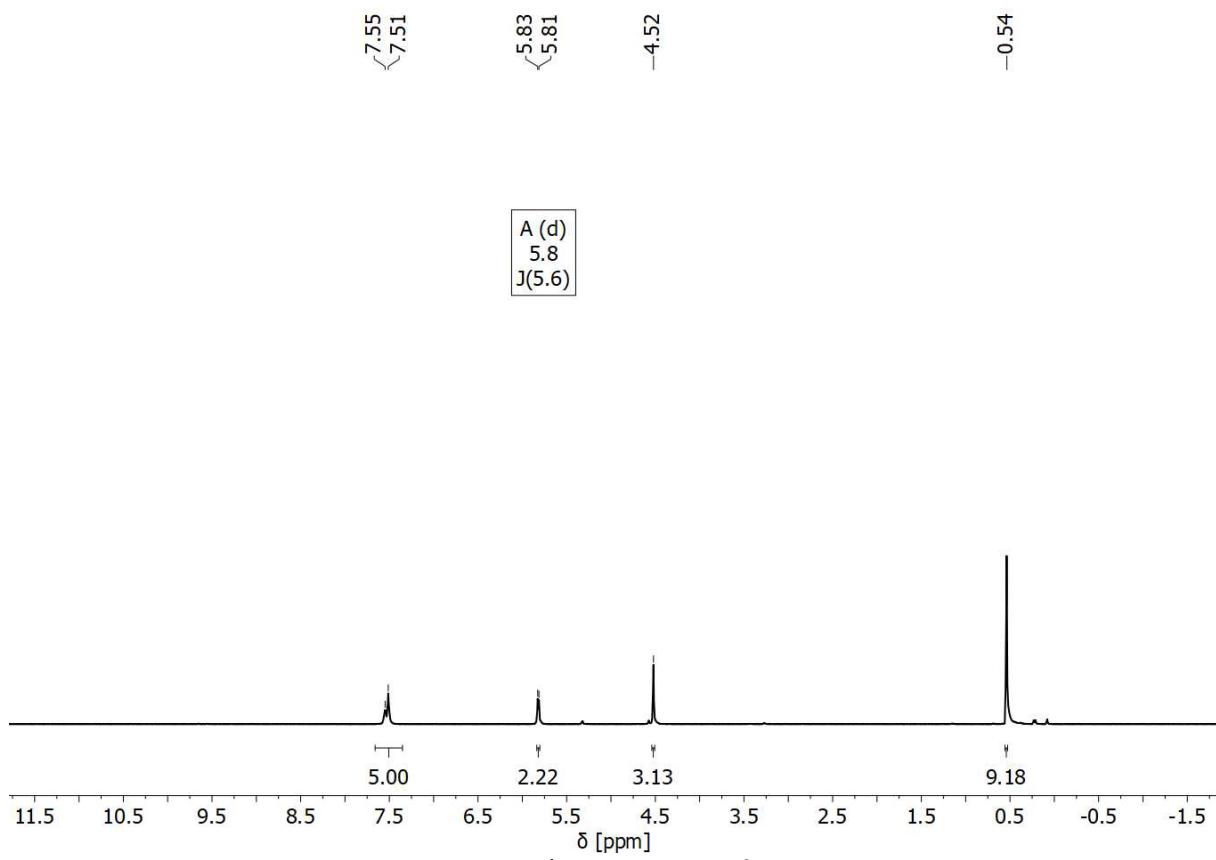


**Figure S9:** $^{1}H$ NMR spectrum of **2a**.
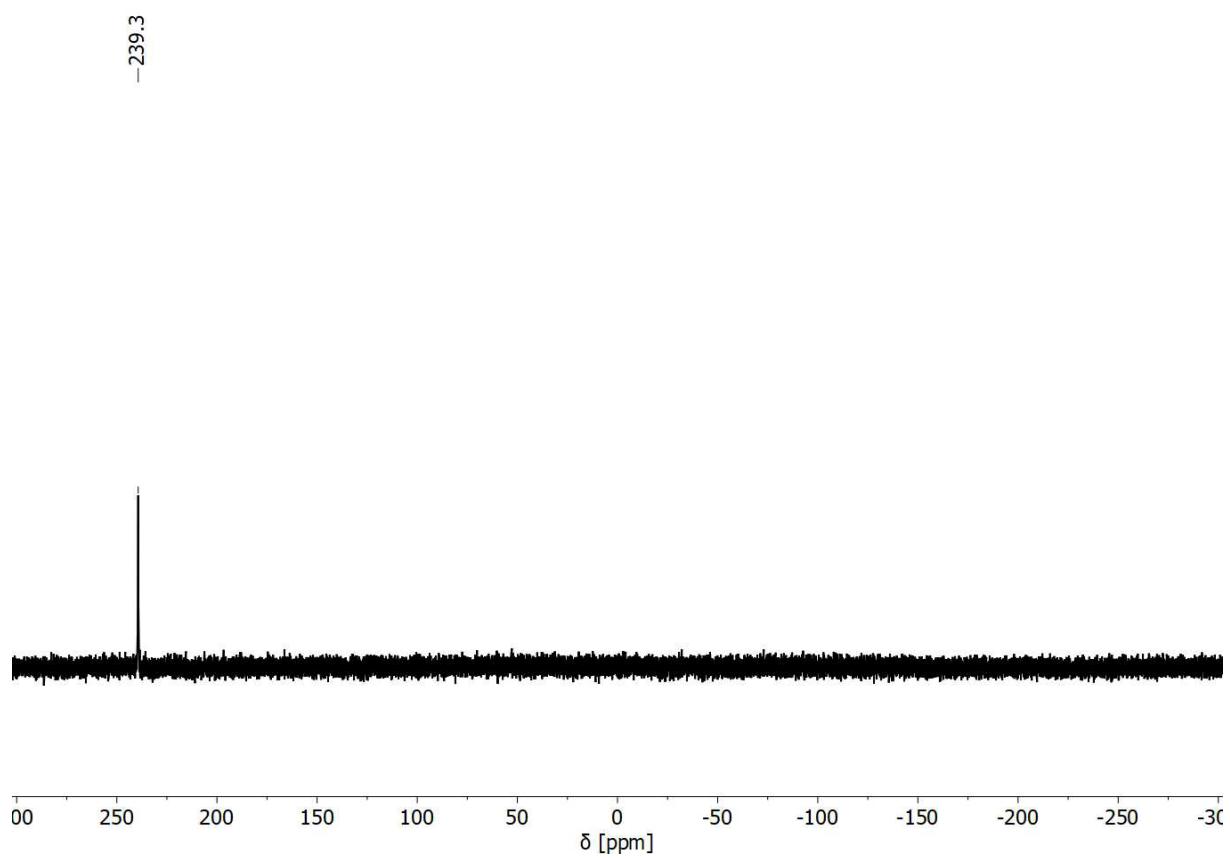
**Figure S10**: $^{31}P\{^1H\}$ NMR spectrum of **2a.**
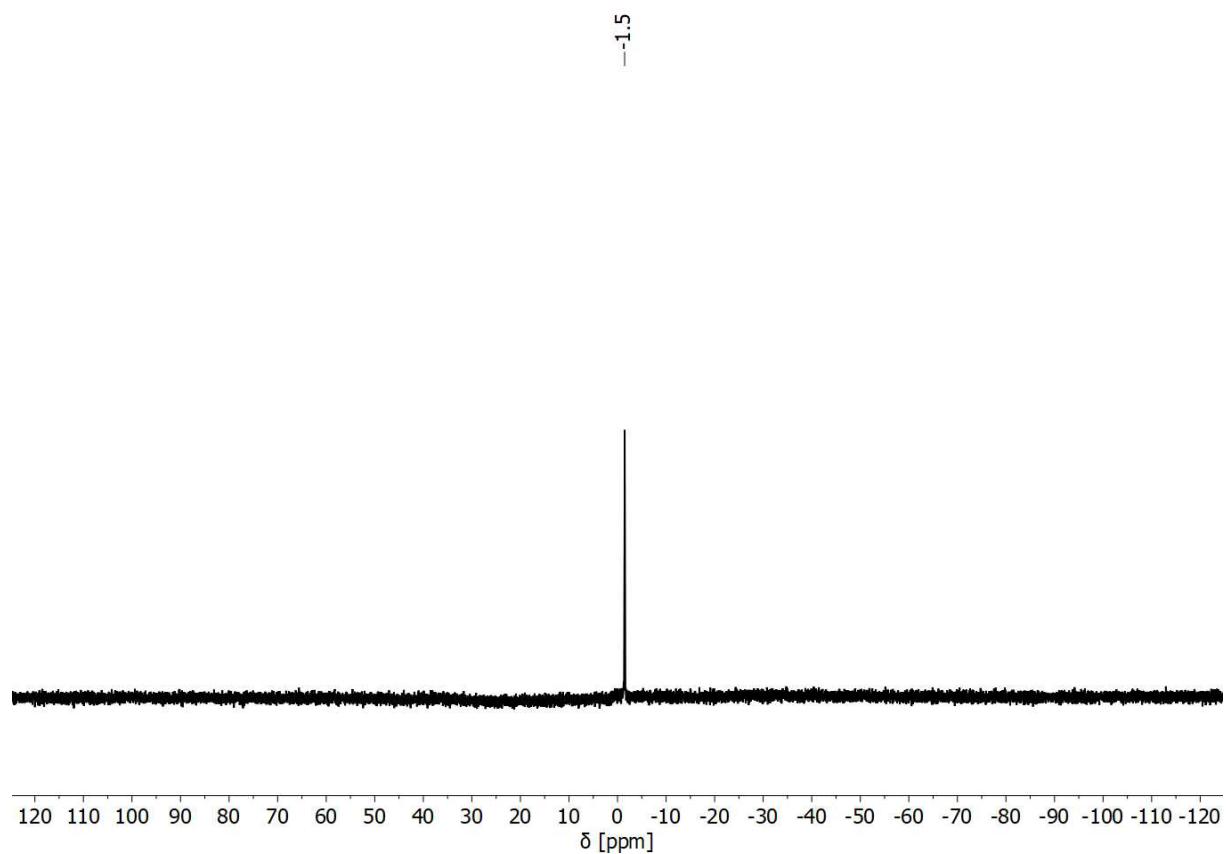


**Figure S11**: $^{11}B$ NMR spectrum of **2a.**
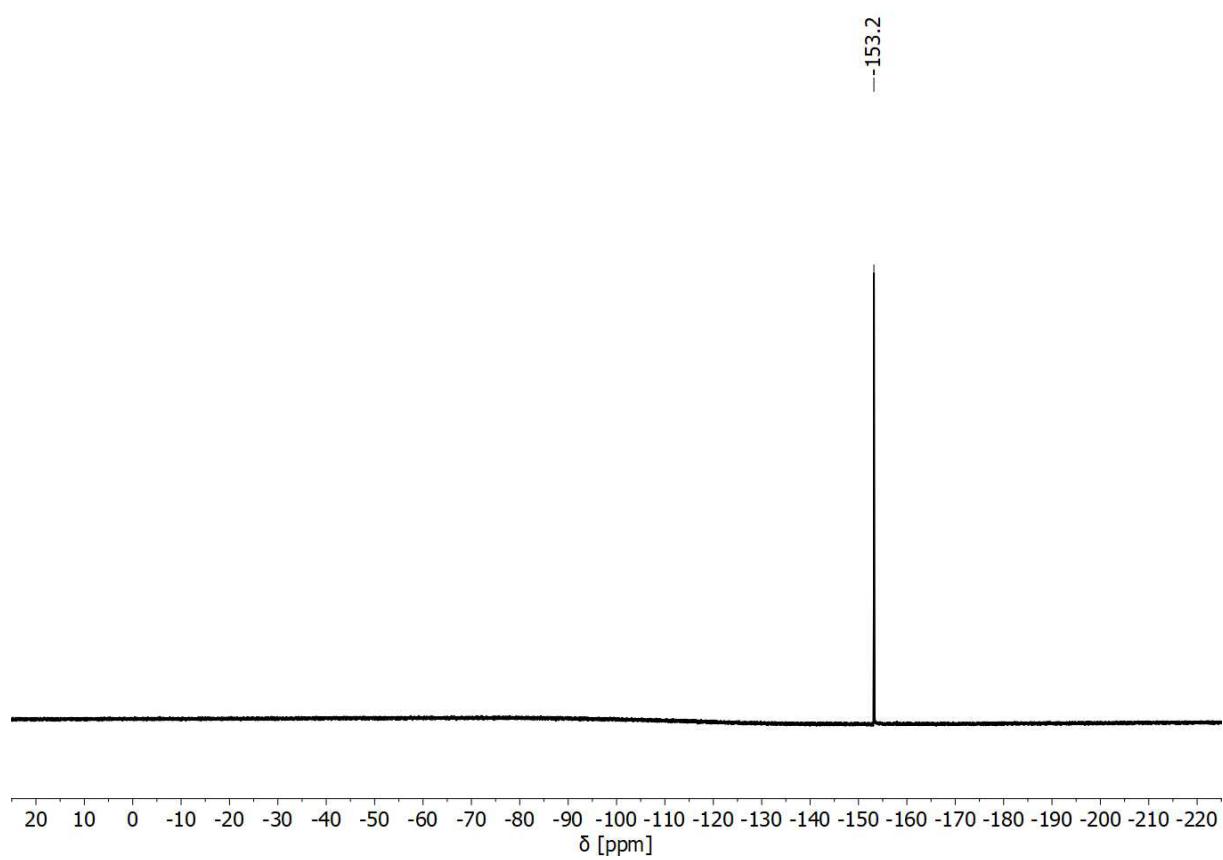
**Figure S12**: $^{19}$F NMR spectrum of **2a.**
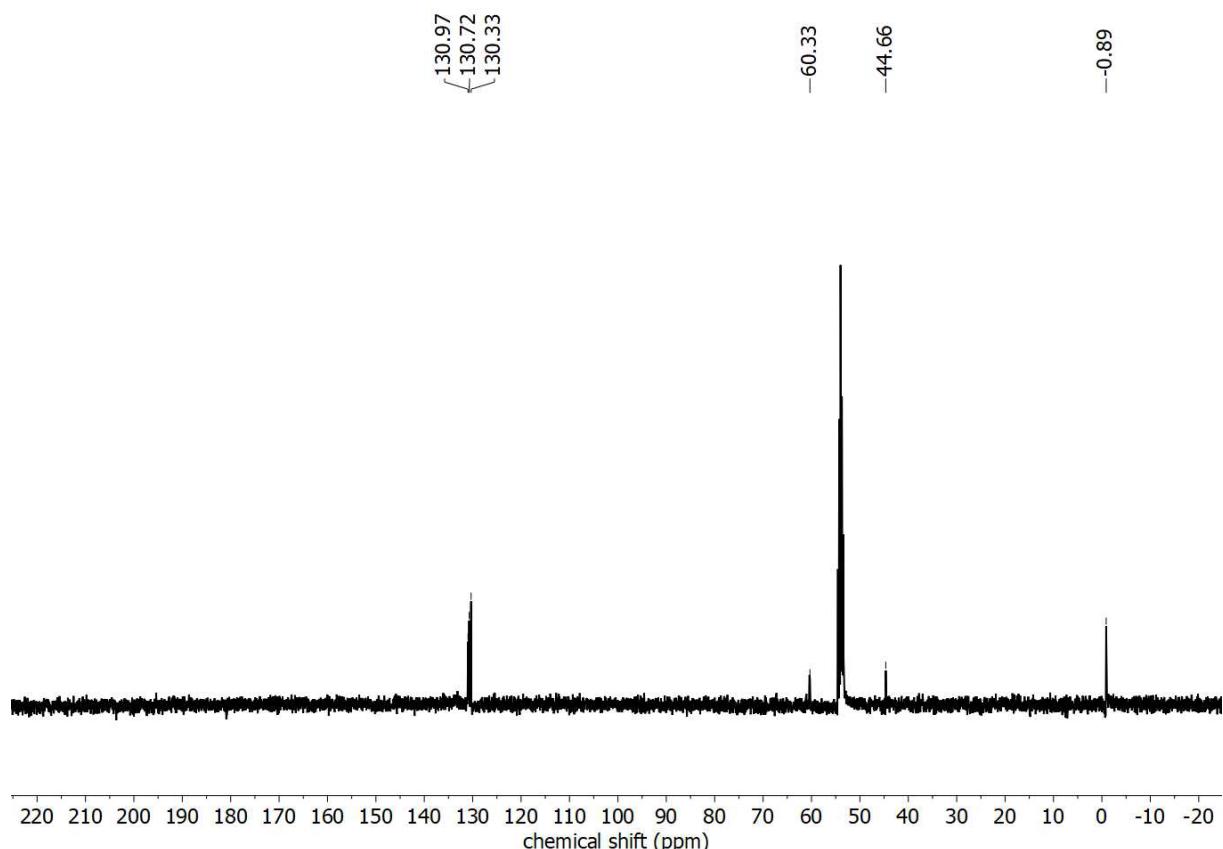


**Figure S13**: $^{13}$C NMR spectrum of **2a.**
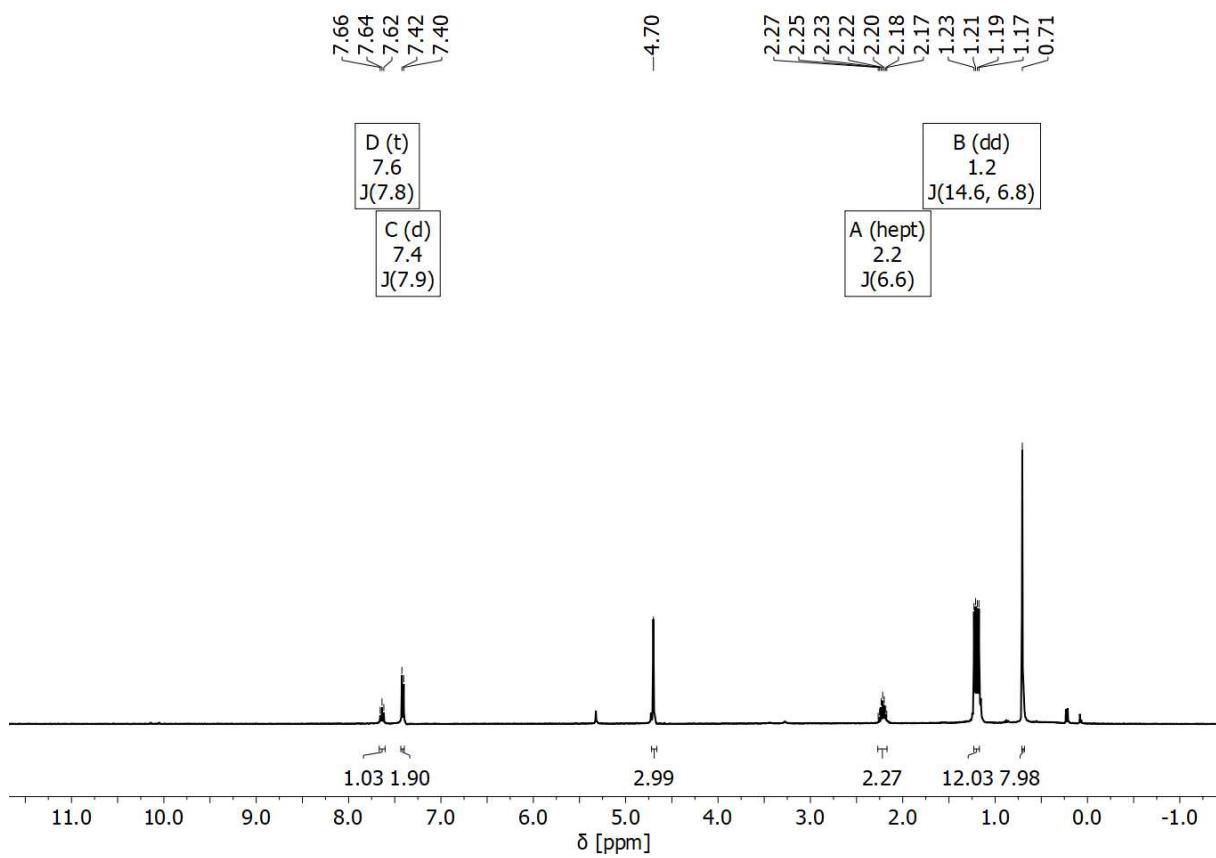
**Figure S14:** 1H NMR spectrum of **2b.**
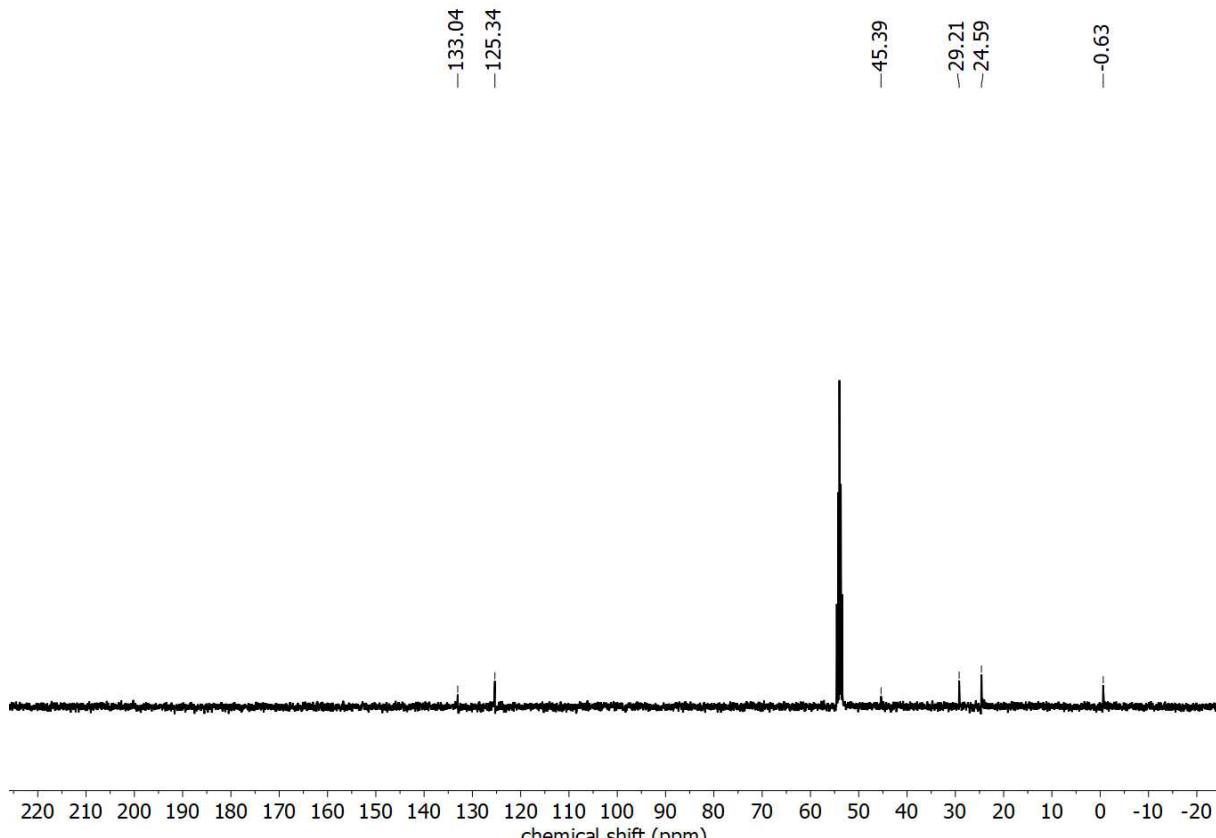


**Figure S15**: <sup>13</sup>C NMR spectrum of **2b.**
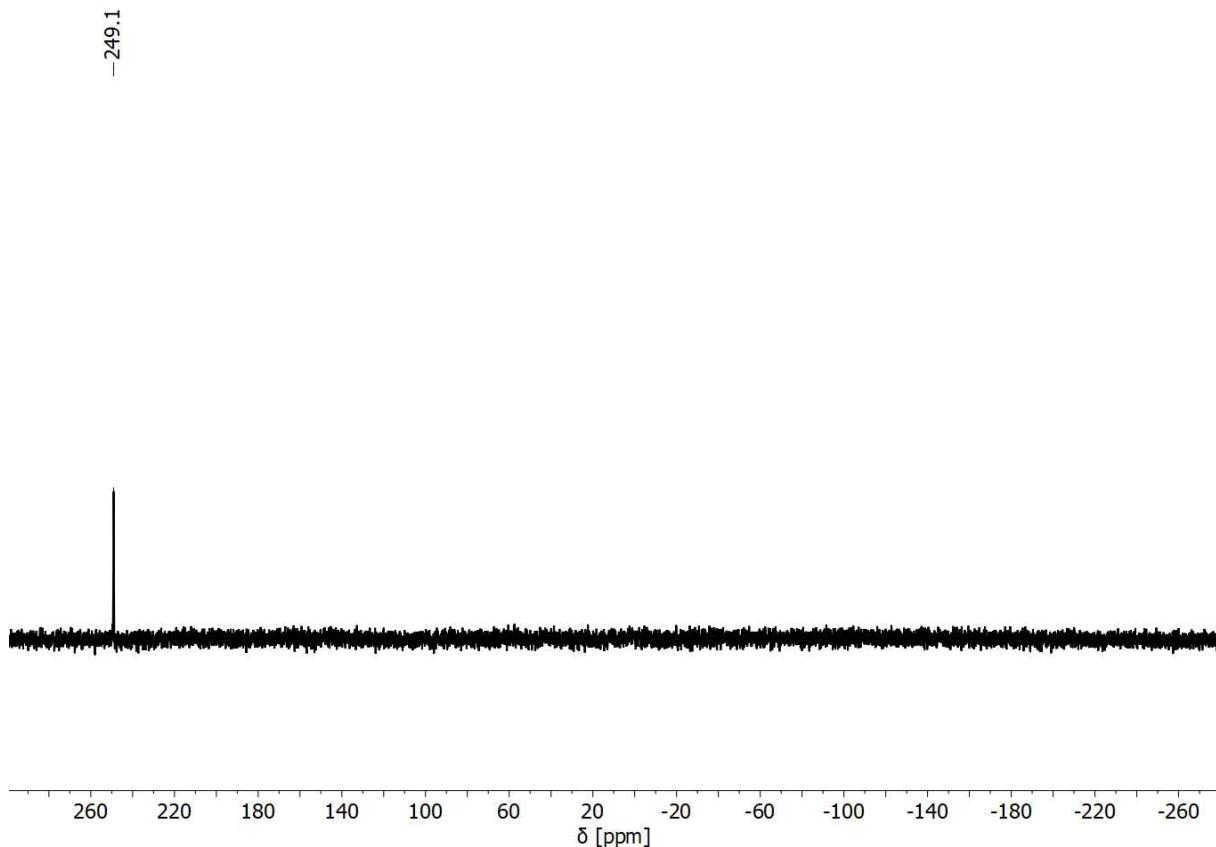
**Figure S16**: $^{31}$P{$^1$H} NMR spectrum of **2b.**
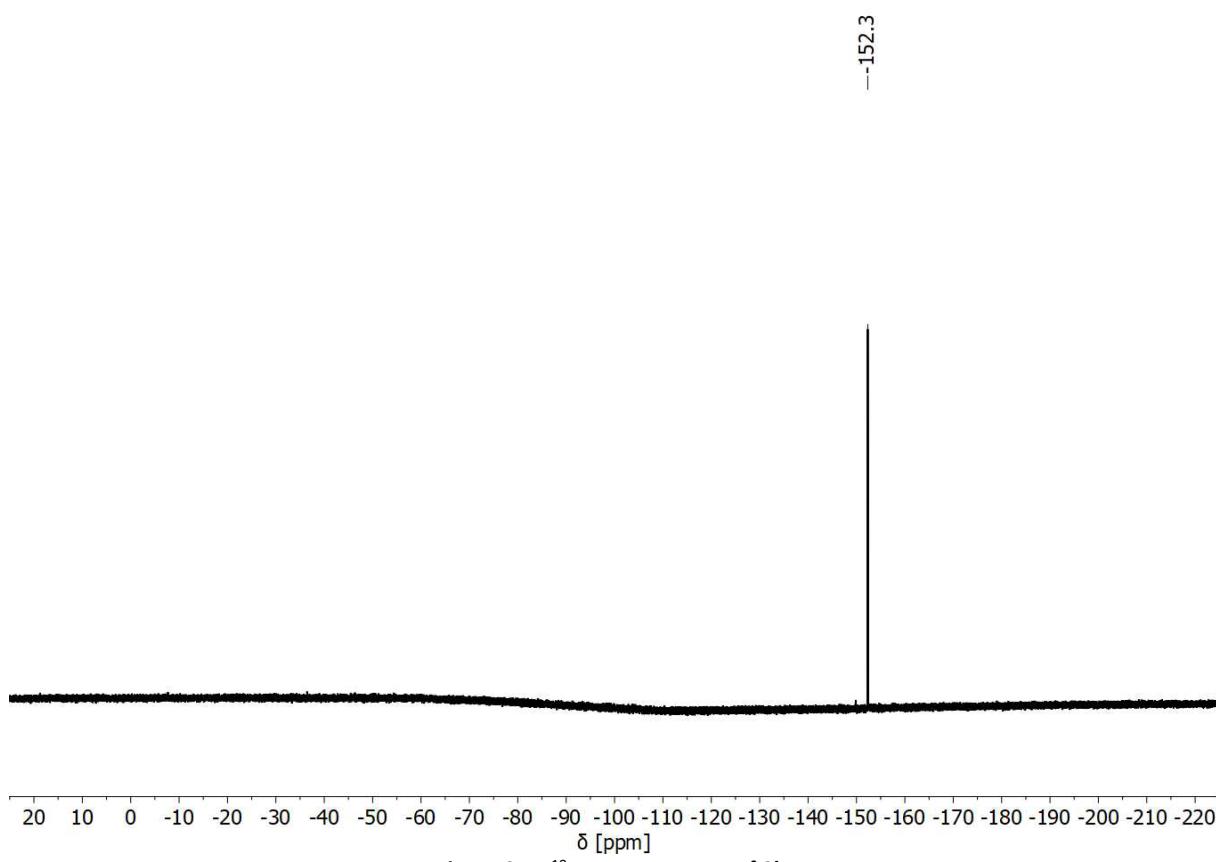


**Figure S17**: $^{19}$F NMR spectrum of **2b.**

−1.3

120 110 100 90 80 70 60 50 40 30 20 10 0 -10 -20 -30 -40 -50 -60 -70 -80 -90 -100 -110 -120
δ [ppm]

**Figure S18**: $^{11}$B NMR spectrum of **2b.**



9.38
9.29

7.51
7.50
7.49
7.48

5.82
5.80

−4.42

−1.94 CD3CN

| A (d) |
| 9.3 |
| J(37.5) |

| B (m) |
| 7.5 |

| C (d) |
| 5.8 |
| J(6.0) |

0.66

5.00

2.19

3.91

11.0 10.0 9.0 8.0 7.0 6.0 5.0 4.0 3.0 2.0 1.0 0.0 -1.0 -2.0
chemical shift (ppm)

**Figure S19:** 1H NMR spectrum of **3a.**
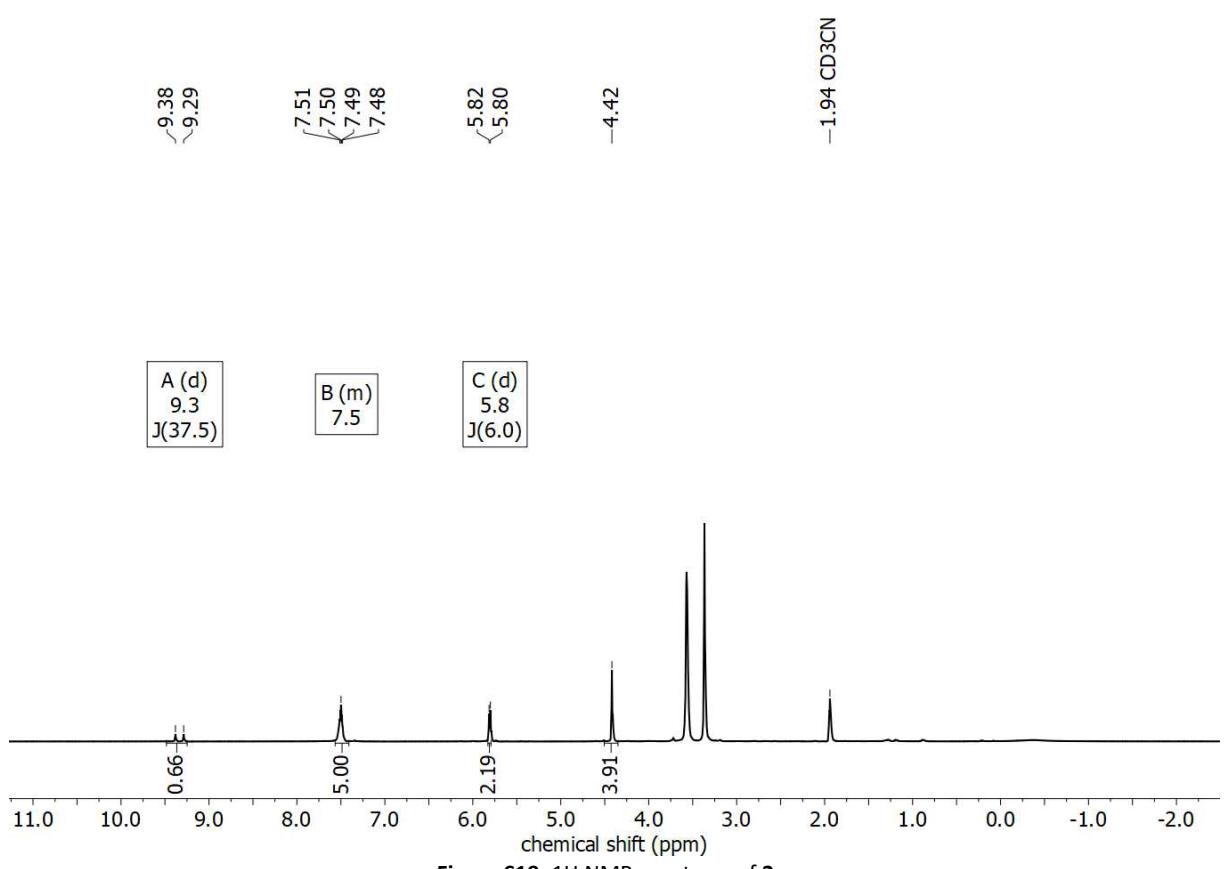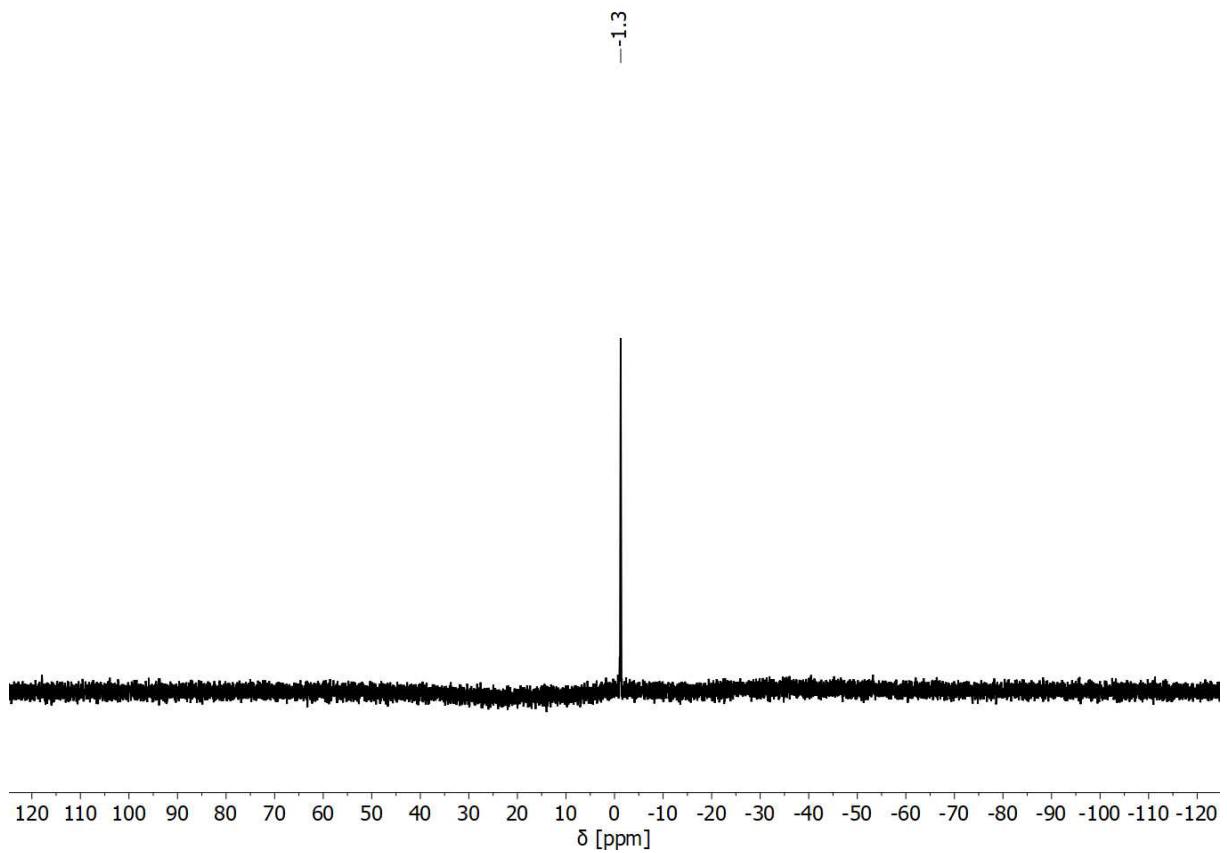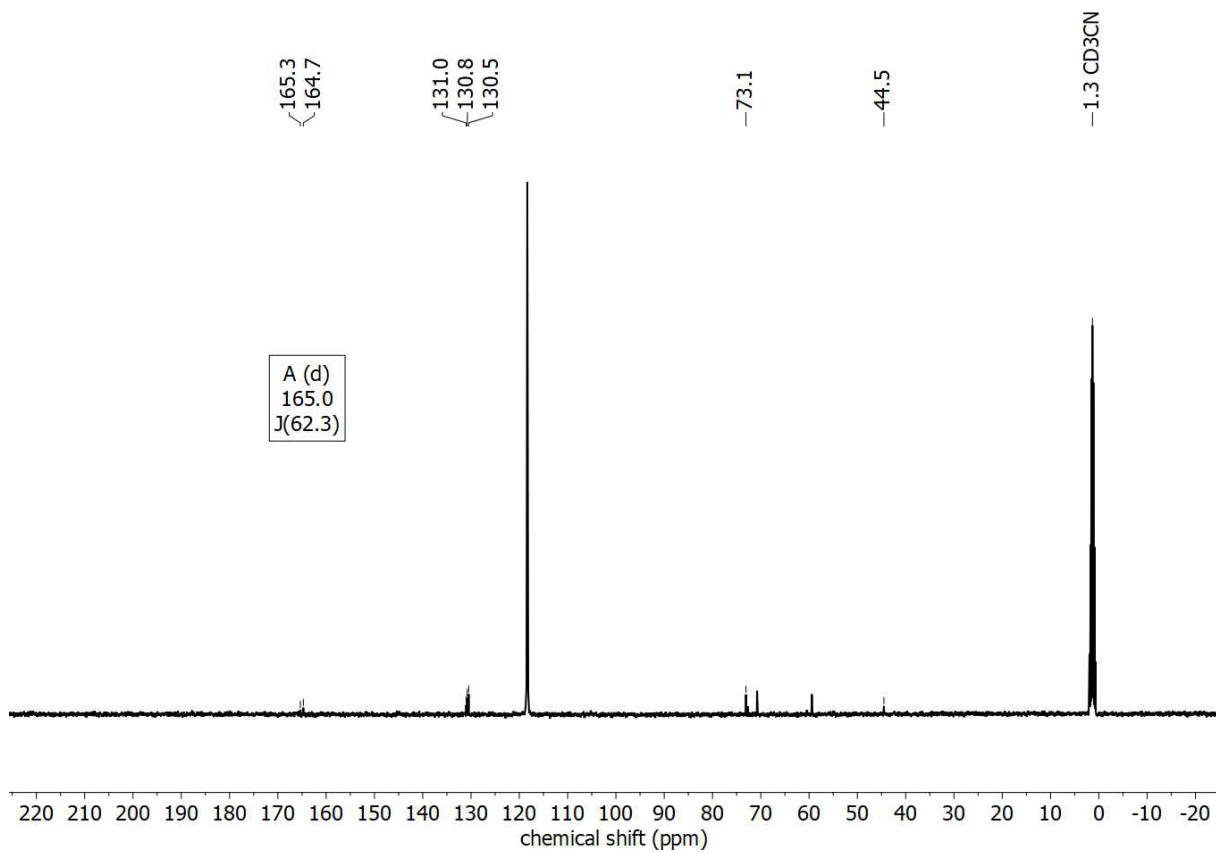
**Figure S20**: $^{13}C$ NMR spectrum of **3a.**
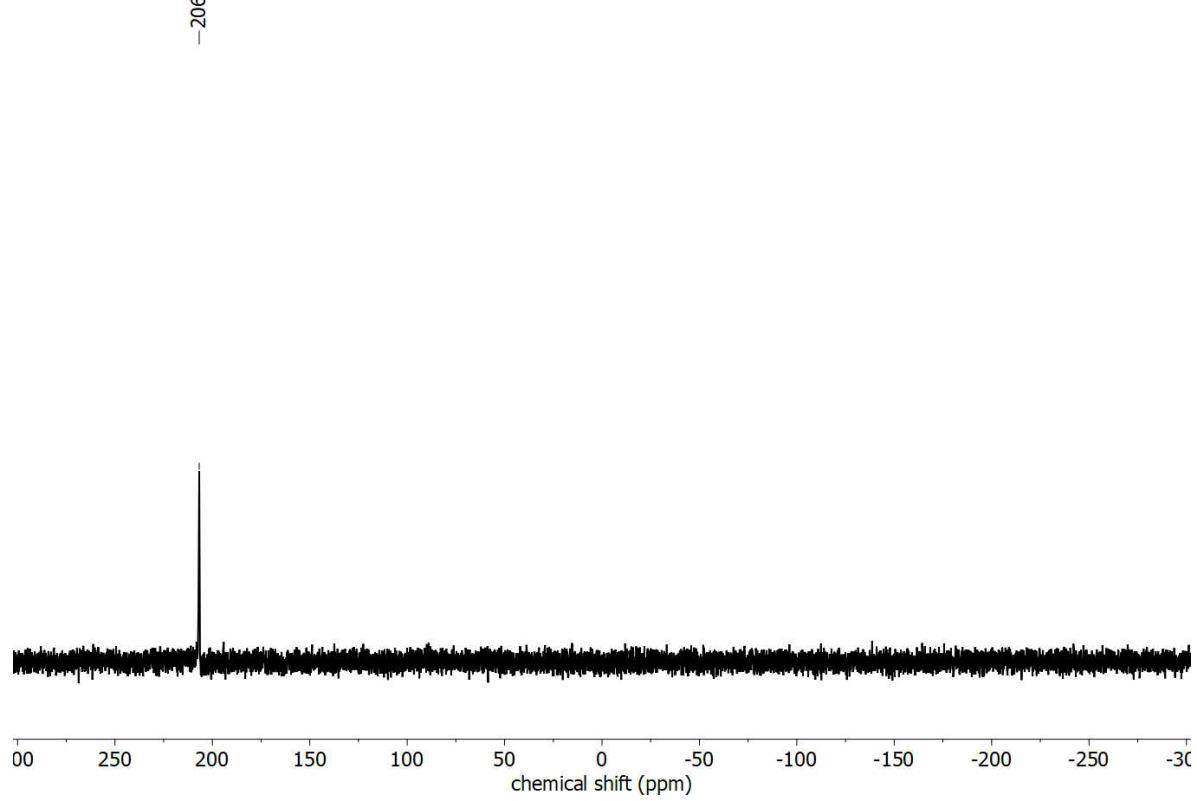


**Figure S21**: $^{31}P\{^{1}H\}$ NMR spectrum of **3a.**

24

—0.3

120 110 100 90 80 70 60 50 40 30 20 10 0 -10 -20 -30 -40 -50 -60 -70 -80 -90 -100 -110 -120
chemical shift (ppm)
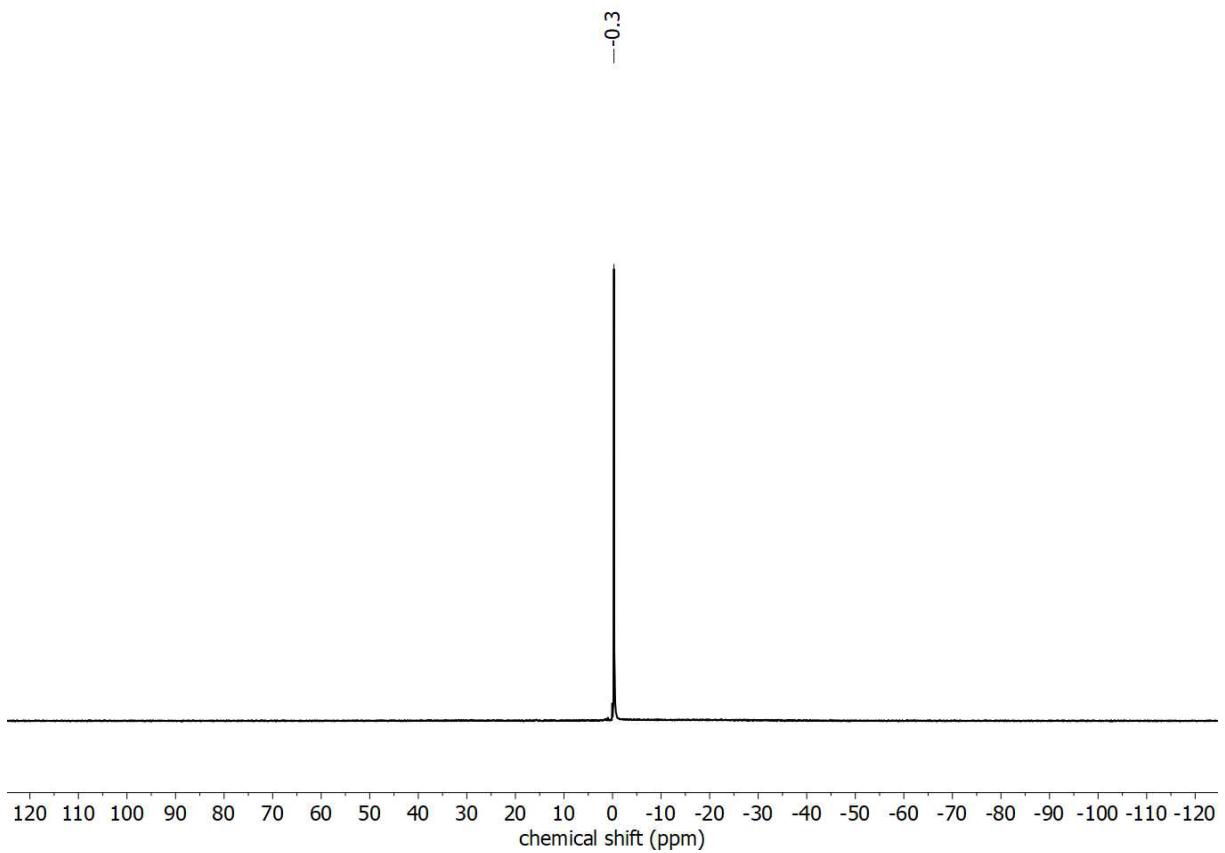
**Figure S22**: ^{11}B NMR spectrum of **3a.**

—-150.8

20 10 0 -10 -20 -30 -40 -50 -60 -70 -80 -90 -100 -110 -120 -130 -140 -150 -160 -170 -180 -190 -200 -210 -220
chemical shift (ppm)
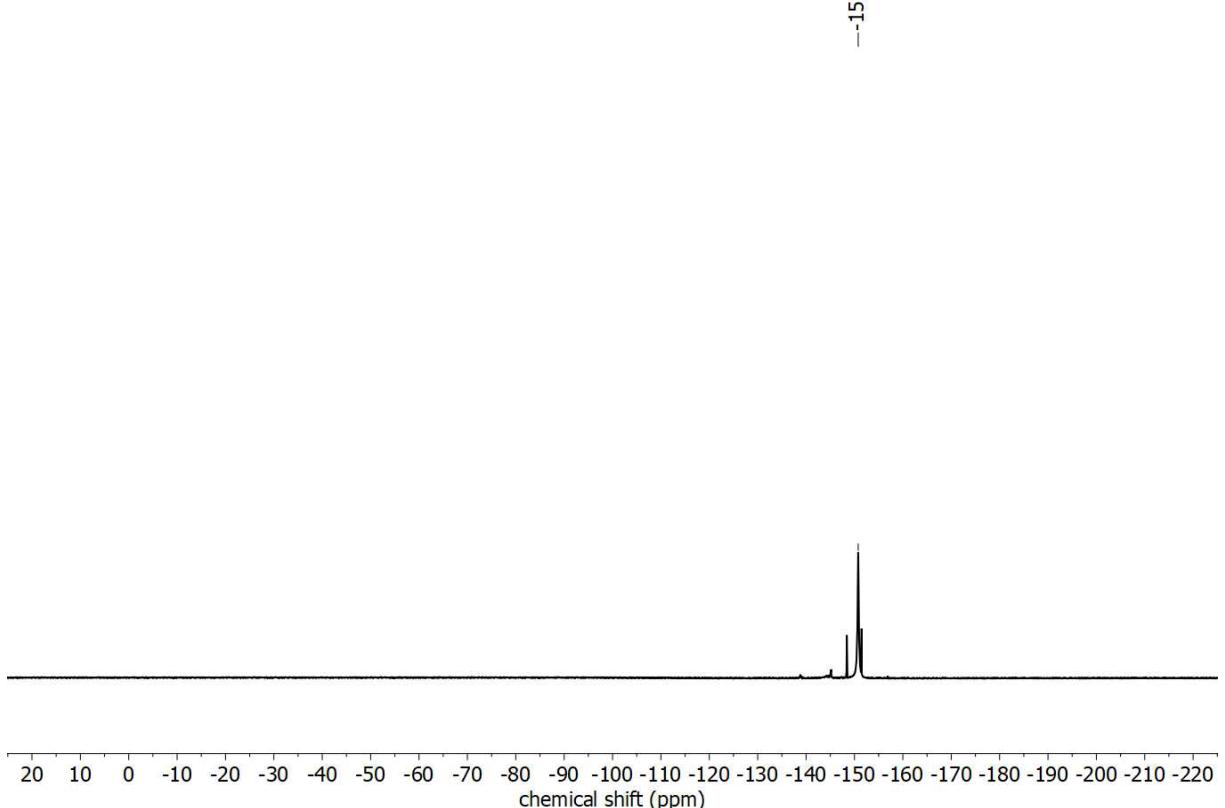
**Figure S23**: ^{19}F NMR spectrum of **3a.**

−229.3

260 255 250 245 240 235 230 225 220 215 210 205 200 195 190 185 180 175 170 165 160 155 150 145 140 135 13
chemical shift (ppm)

**Figure S24**: $^{31}P\{^1H\}$ NMR spectrum of **4a.**

7.47
7.46
7.46
7.45
7.44

5.69
5.67
5.32 CD2Cl2

4.47
4.47

| A (m) | B (d) | C (d) |
| 7.5 | 5.7 | 4.5 |
|  | J(5.6) | J(0.9) |

4.80
2.13
3.00

11.0 10.5 10.0 9.5 9.0 8.5 8.0 7.5 7.0 6.5 6.0 5.5 5.0 4.5 4.0 3.5 3.0 2.5 2.0 1.5 1.0 0.5
chemical shift (ppm)
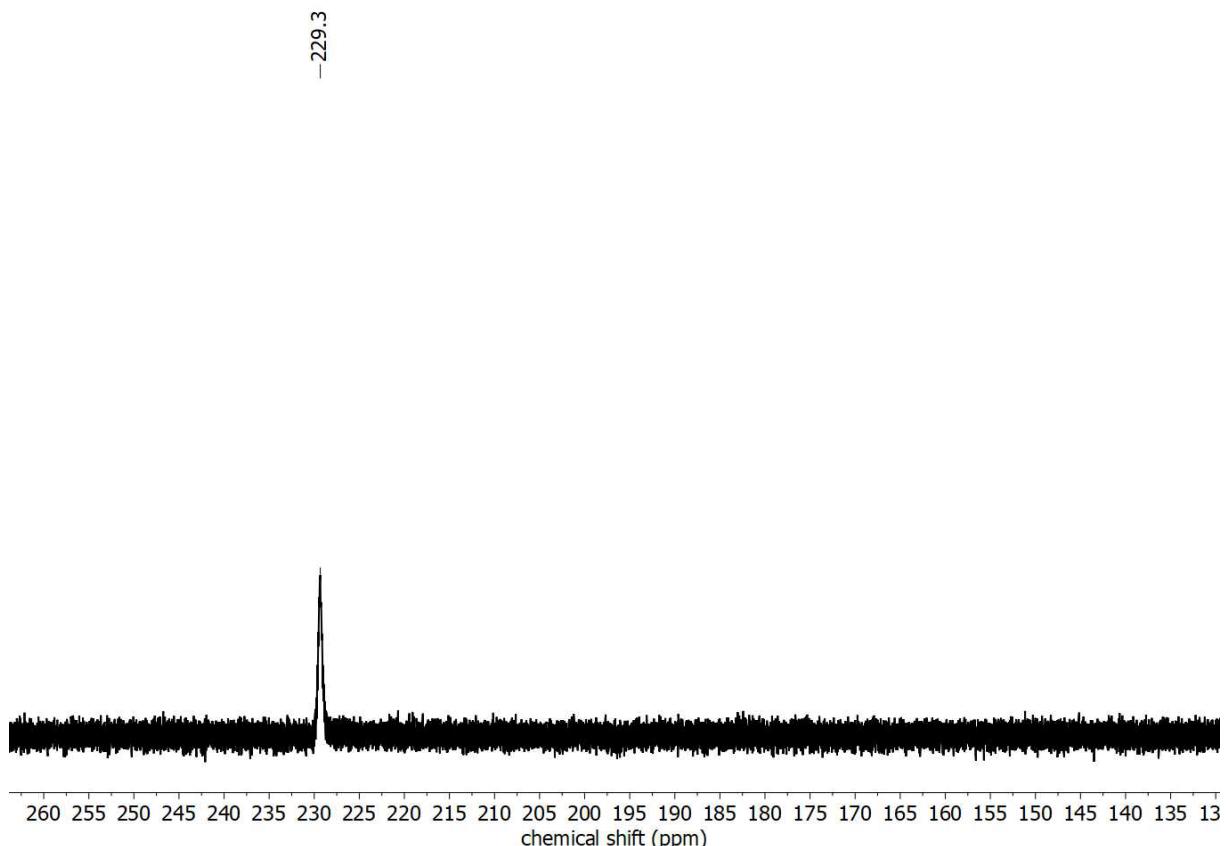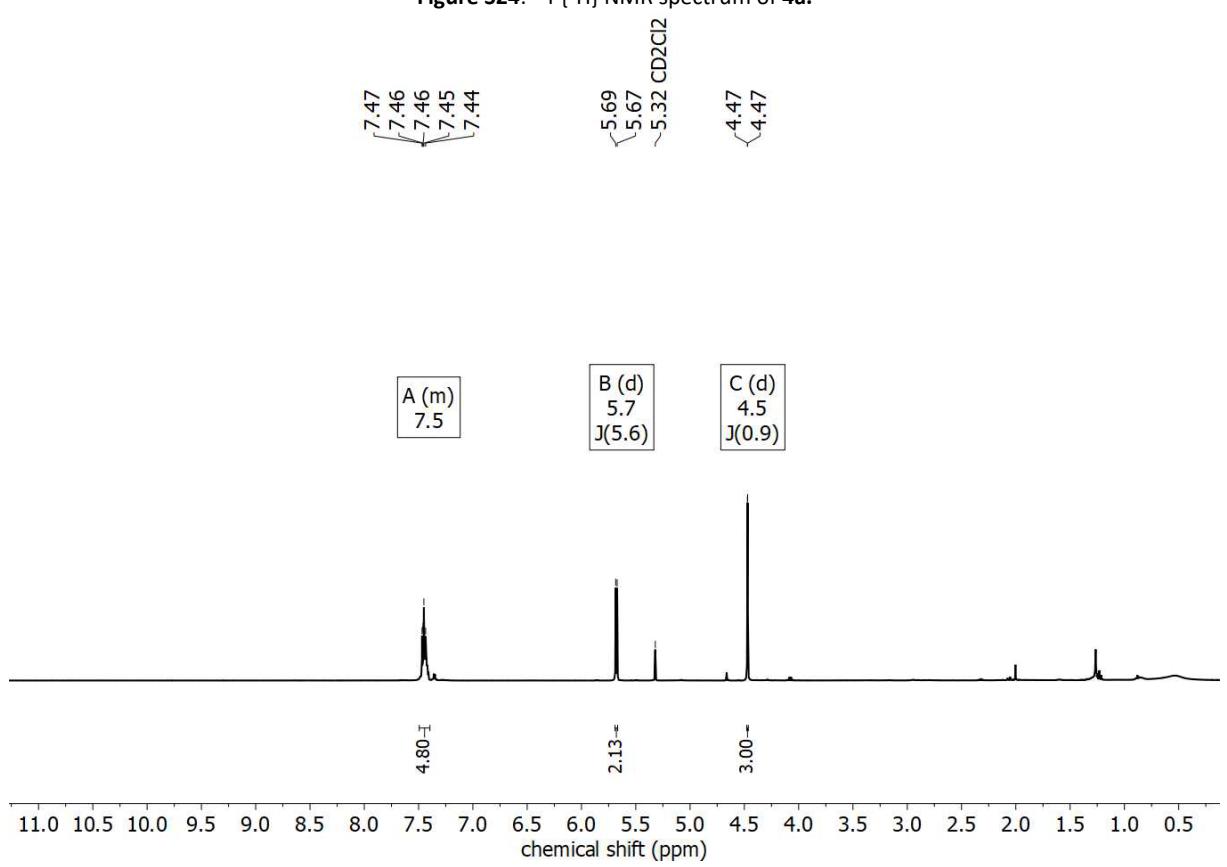
**Figure S25:** 1H NMR spectrum of **4a.**

**Figure S26**: ¹³C NMR spectrum of **4a.**



**Figure S27**: ¹⁹F NMR spectrum of **5a.**

27

154

**Figure S28**: $^{31}P\{^{1}H\}$ NMR spectrum of **5a.**

Peak labels: 238.3

131.7, 136.1, 140.5, 144.9, 149.3, 153.7, 158.1

A (hept)
-144.9
J(712.9)
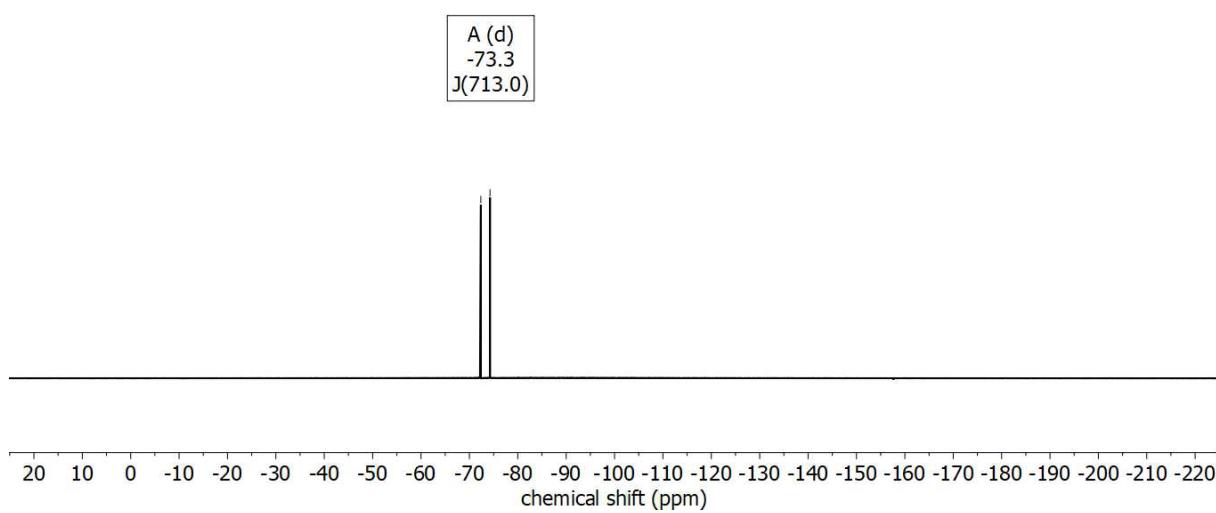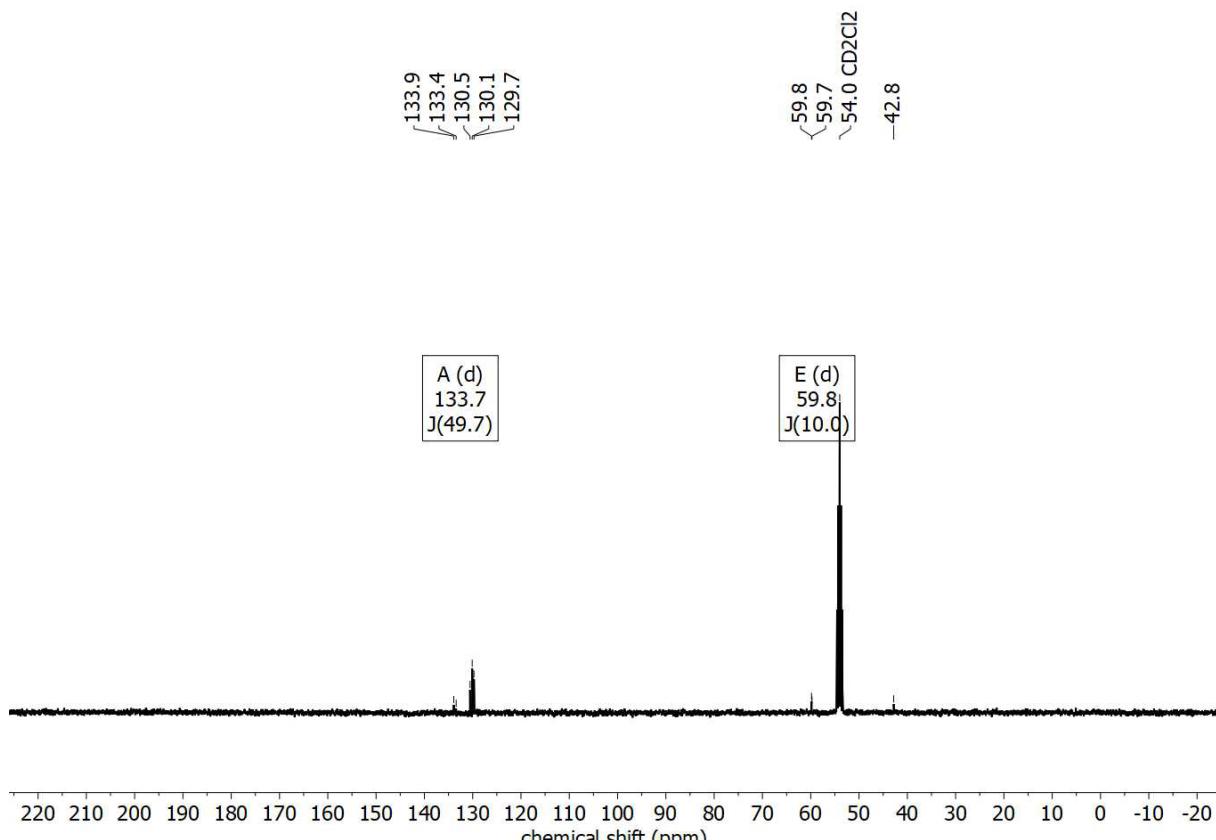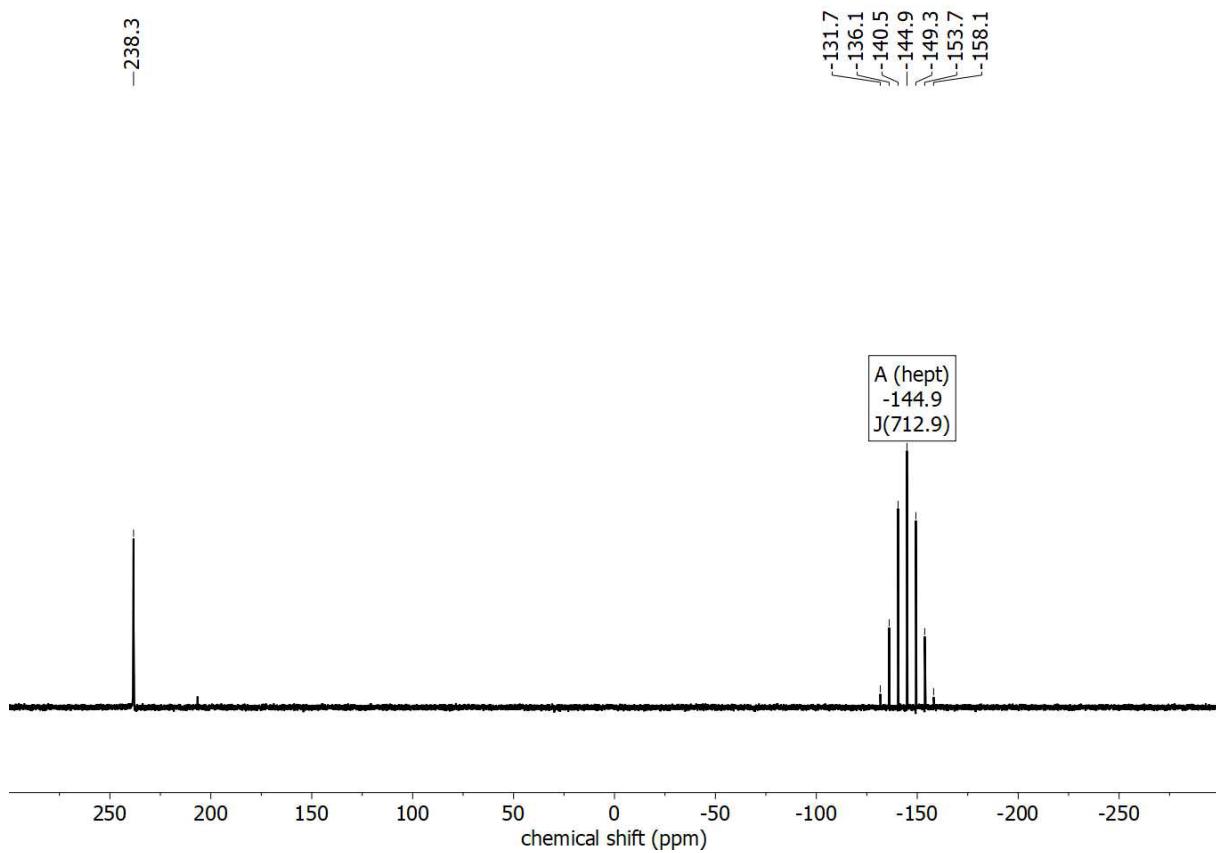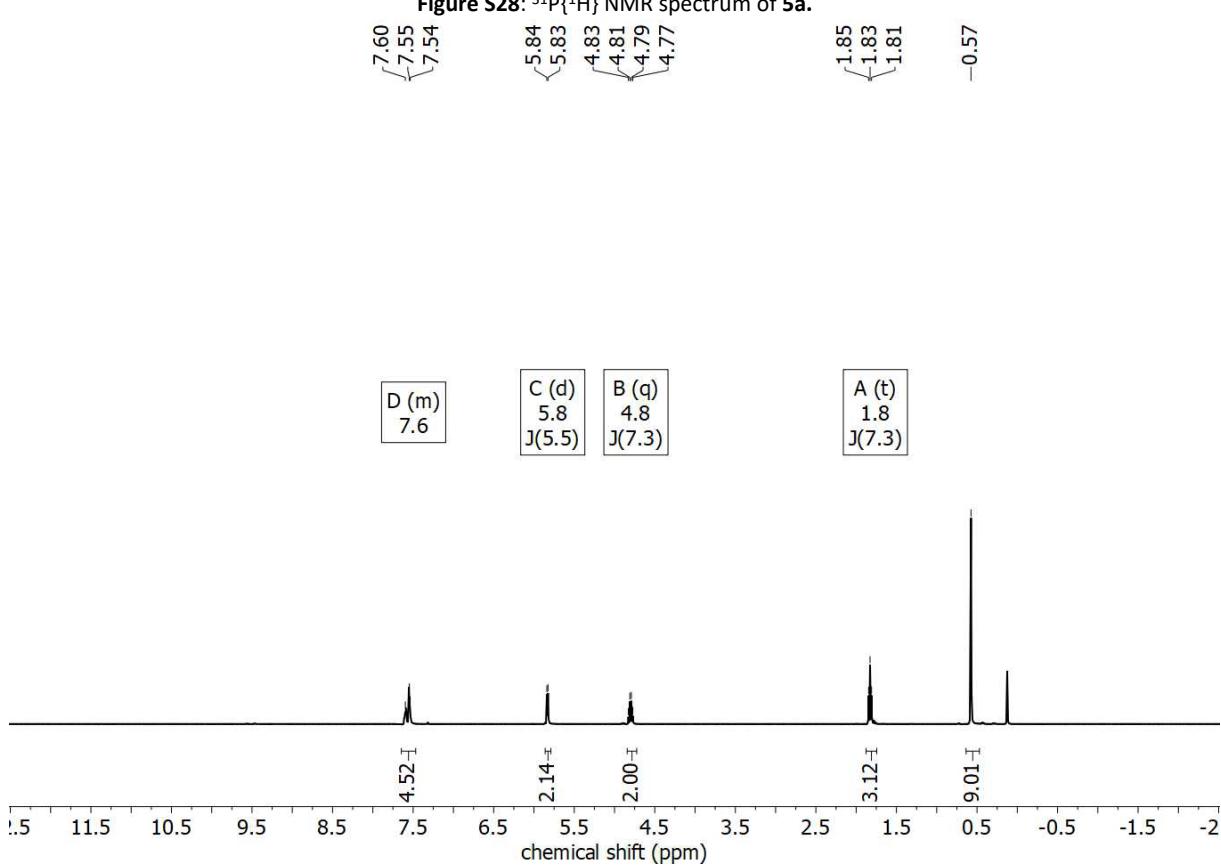


**Figure S29:** 1H NMR spectrum of **5a.**

Peak labels: 7.60, 7.55, 7.54, 5.84, 5.83, 4.83, 4.81, 4.79, 4.77, 1.85, 1.83, 1.81, −0.57

D (m)
7.6

C (d)
5.8
J(5.5)

B (q)
4.8
J(7.3)

A (t)
1.8
J(7.3)

Integrations: 4.52, 2.14, 2.00, 3.12, 9.01

181.60
180.99

132.59
130.89
130.38

60.37
54.22

-0.38
-0.44

B (d)
181.3
J(61.6)

A (d)
-0.4
J(6.4)

220 210 200 190 180 170 160 150 140 130 120 110 100 90 80 70 60 50 40 30 20 10 0 -10 -20
chemical shift (ppm)

**Figure S30**: $^{13}$C NMR spectrum of **5a.**



145.7

133.1
125.4

55.2

29.4
24.8
24.3
15.9

-0.4

220 210 200 190 180 170 160 150 140 130 120 110 100 90 80 70 60 50 40 30 20 10 0 -10 -20
chemical shift (ppm)

**Figure S31**: $^{13}$C NMR spectrum of **5b.**

-71.9
-73.8

A (d)
-72.8
J(719.1)

20 10 0 -10 -20 -30 -40 -50 -60 -70 -80 -90 -100 -110 -120 -130 -140 -150 -160 -170 -180 -190 -200 -210 -220
chemical shift (ppm)

**Figure S32**: $^{19}$F NMR spectrum of **5b.**

-248.7

-130.8
-135.2
-139.6
-144.0
-148.4
-152.8
-157.2

B (s)
248.7

A (hept)
-144.0
J(711.6)

250 200 150 100 50 0 -50 -100 -150 -200 -250
δ(ppm)
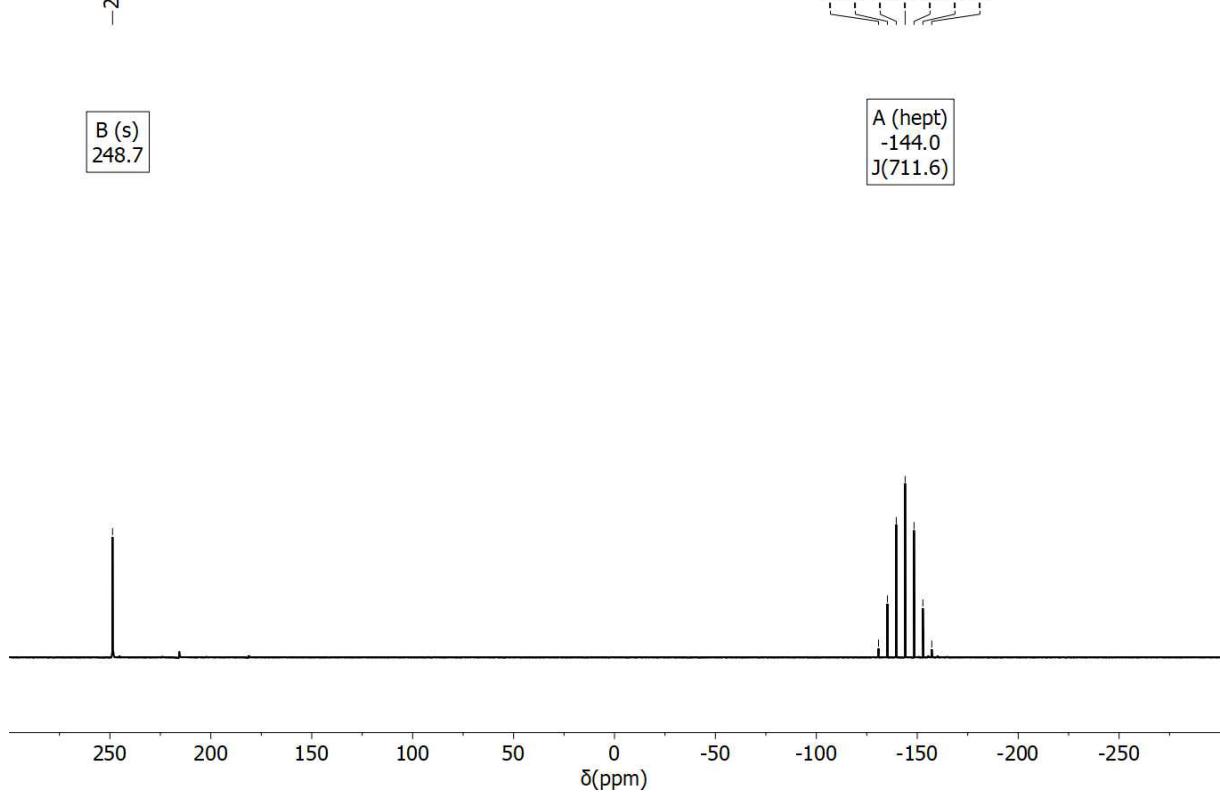
**Figure S33**: $^{31}$P{$^{1}$H} NMR spectrum of **5b.**
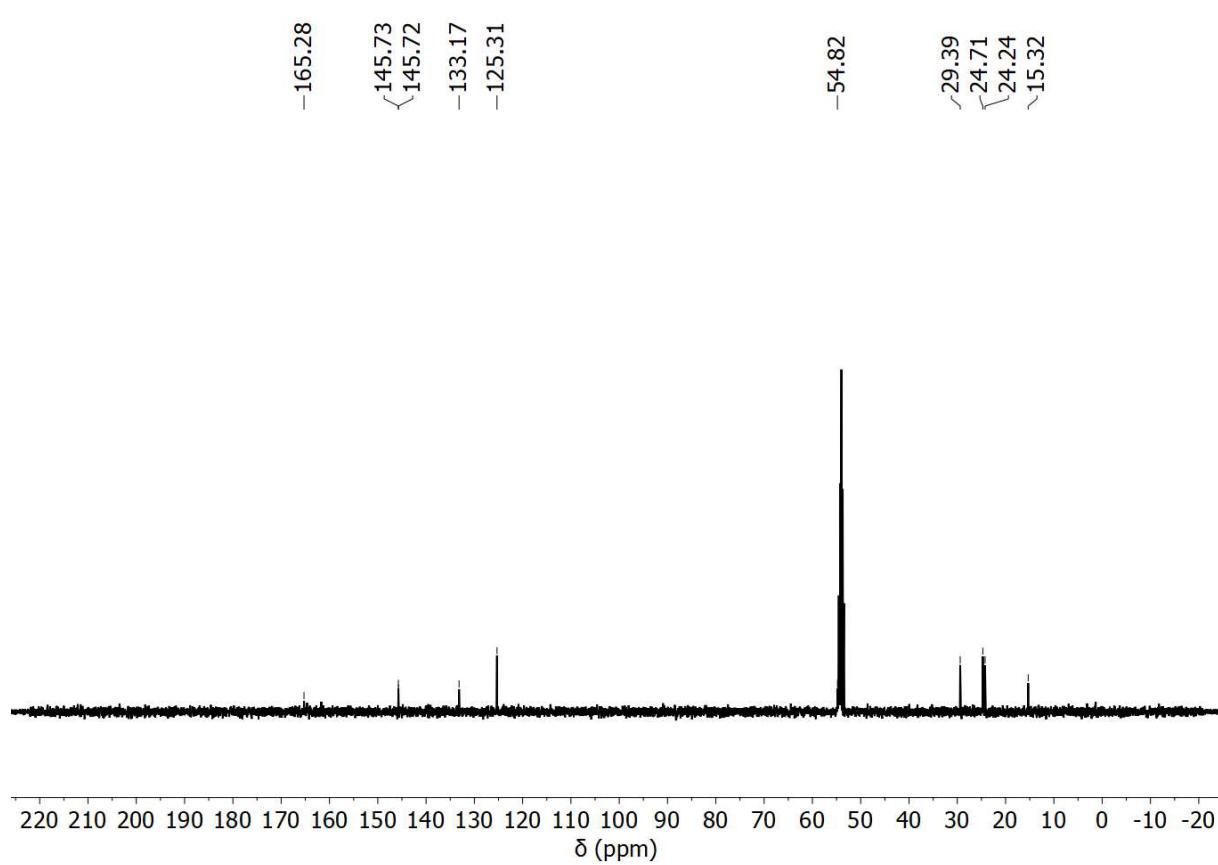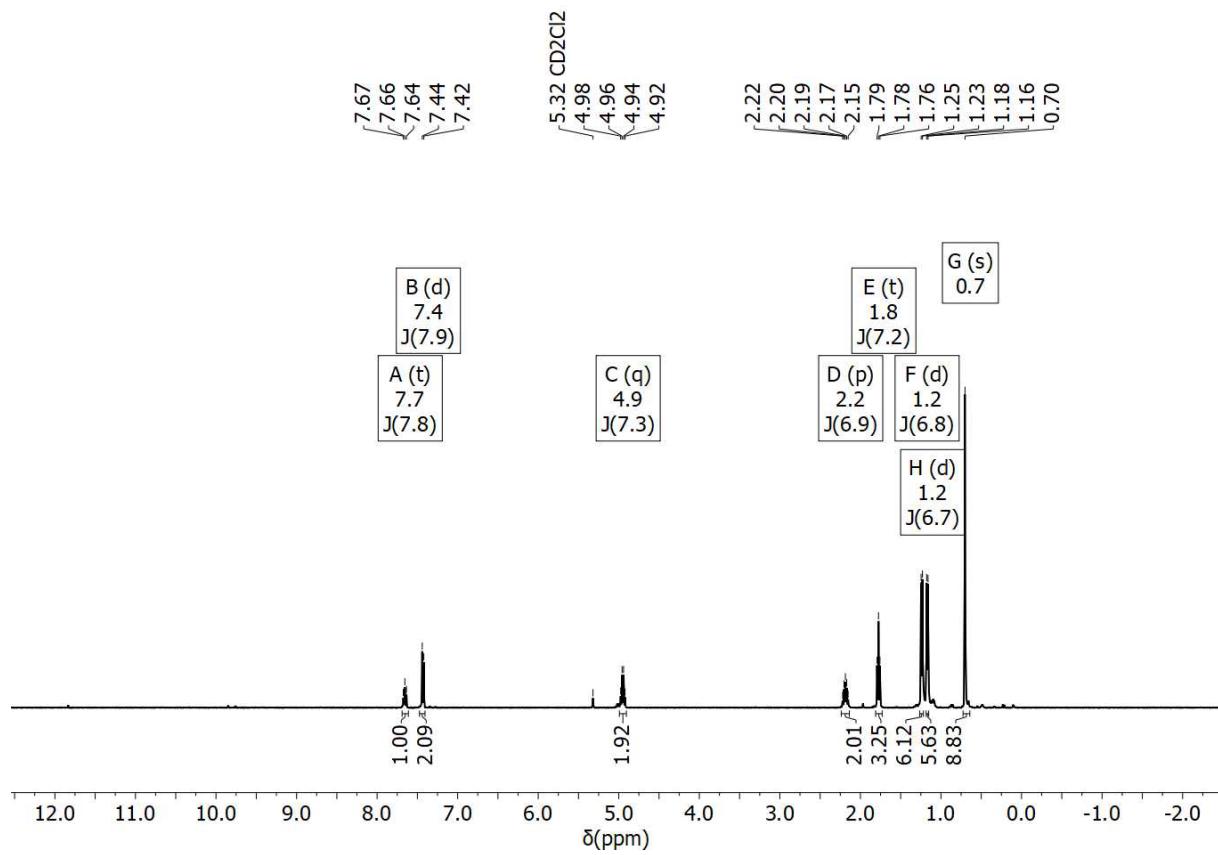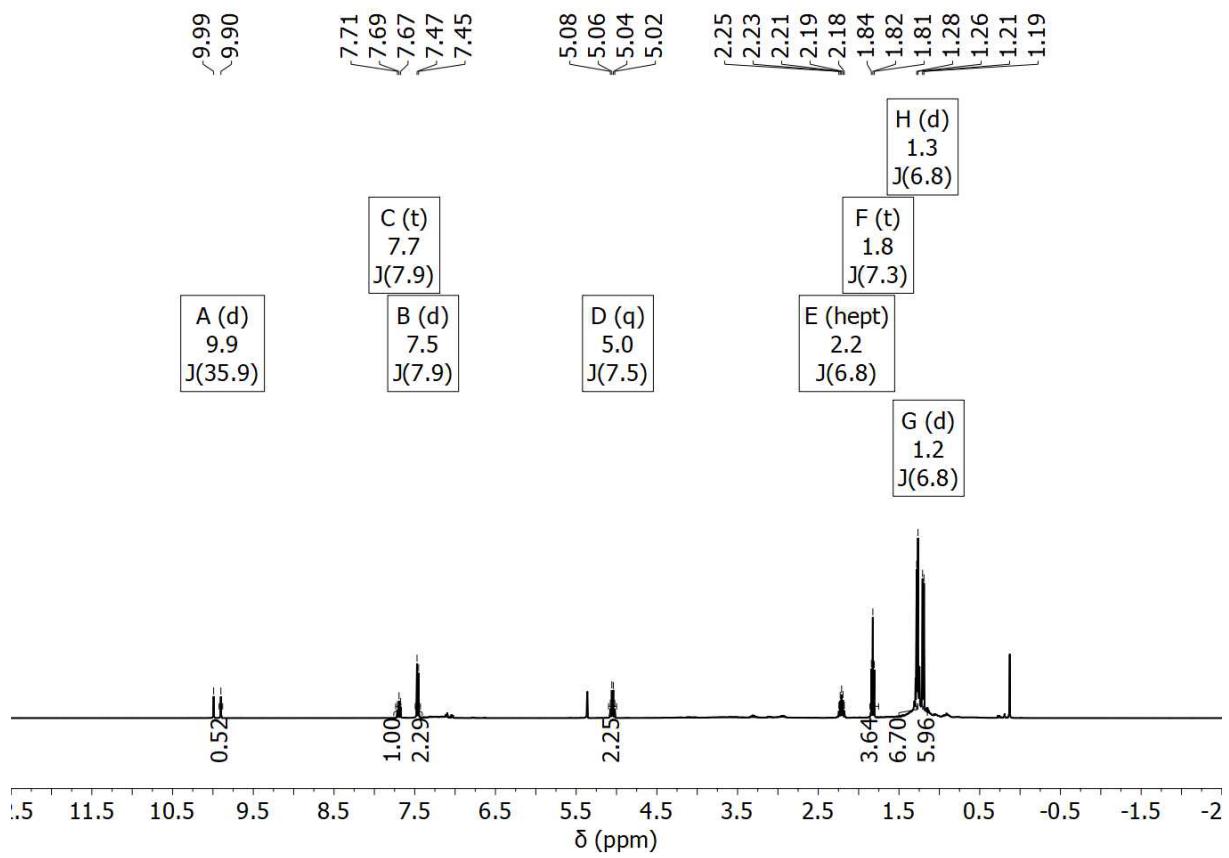
7.67
7.66
7.64
7.44
7.42

5.32 CD2Cl2
4.98
4.96
4.94
4.92

2.22
2.20
2.19
2.17
2.15
1.79
1.78
1.76
1.25
1.23
1.18
1.16
0.70

B (d)
7.4
J(7.9)

A (t)
7.7
J(7.8)

C (q)
4.9
J(7.3)

E (t)
1.8
J(7.2)

G (s)
0.7

D (p)
2.2
J(6.9)

F (d)
1.2
J(6.8)

H (d)
1.2
J(6.7)

1.00
2.09

1.92

2.01
3.25
6.12
5.63
8.83

**Figure S34:** 1H NMR spectrum of **5b.**

165.28
145.73
145.72
133.17
125.31

54.82

29.39
24.71
24.24
15.32

**Figure S35:** $^{13}$C NMR spectrum of **6b.**

**Figure S36:** 1H NMR spectrum of **6b.**



**Figure S37:** 19F NMR spectrum of **6b.**

32

159
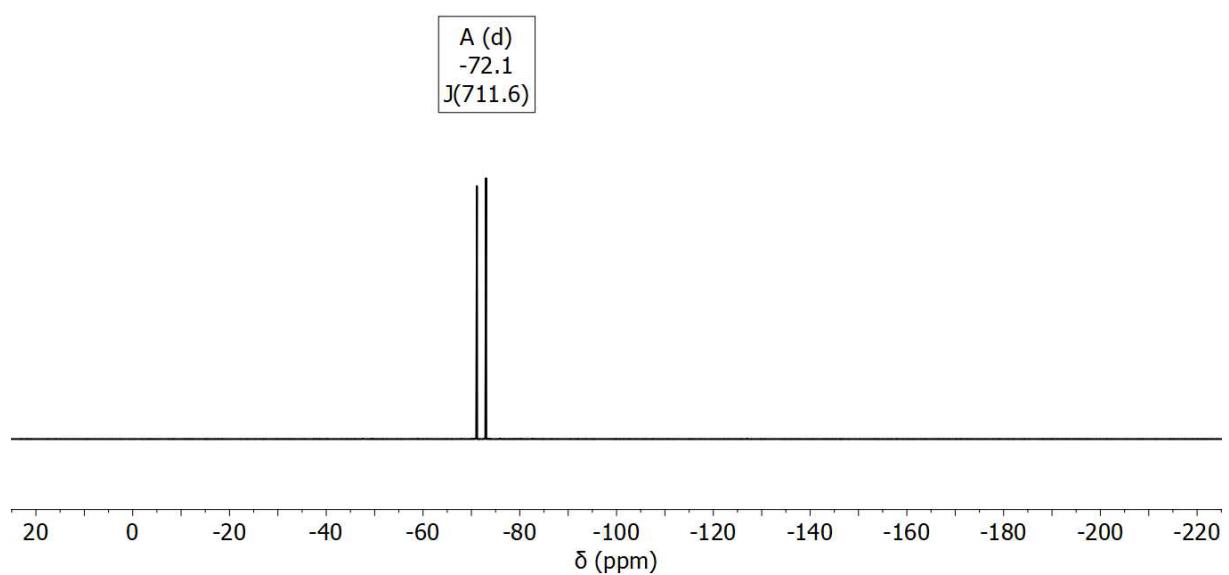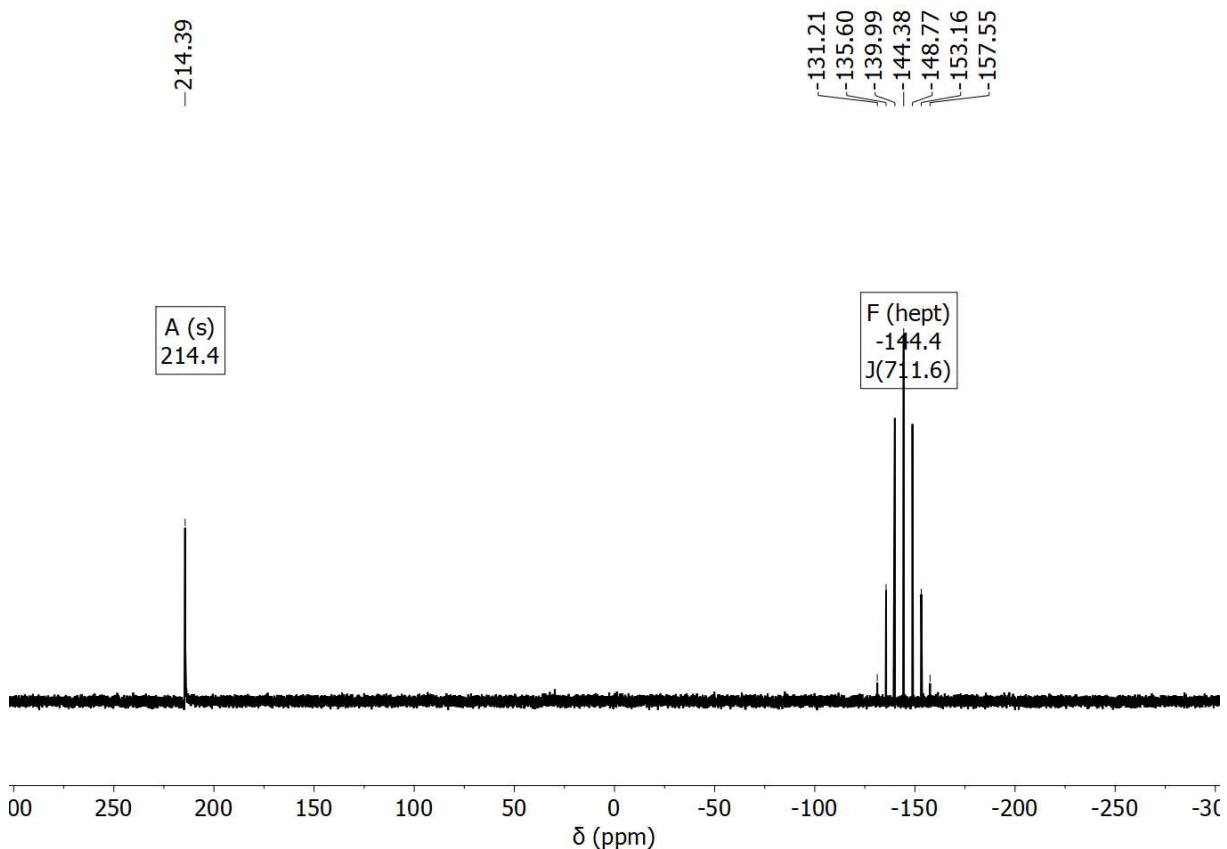
**Figure S38**: $^{31}P\{^1H\}$ NMR spectrum of **6b**
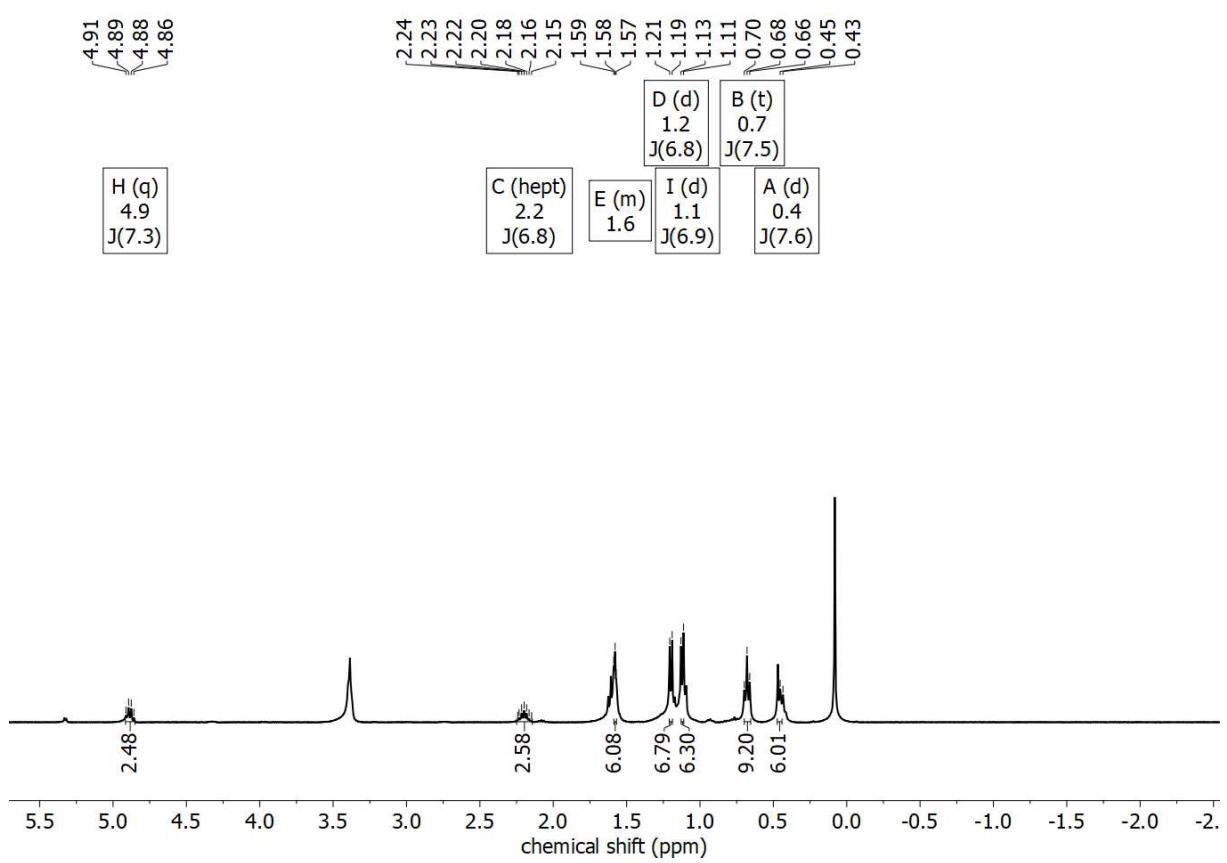


**Figure S39:** $^1H$ NMR spectrum of **7b.**
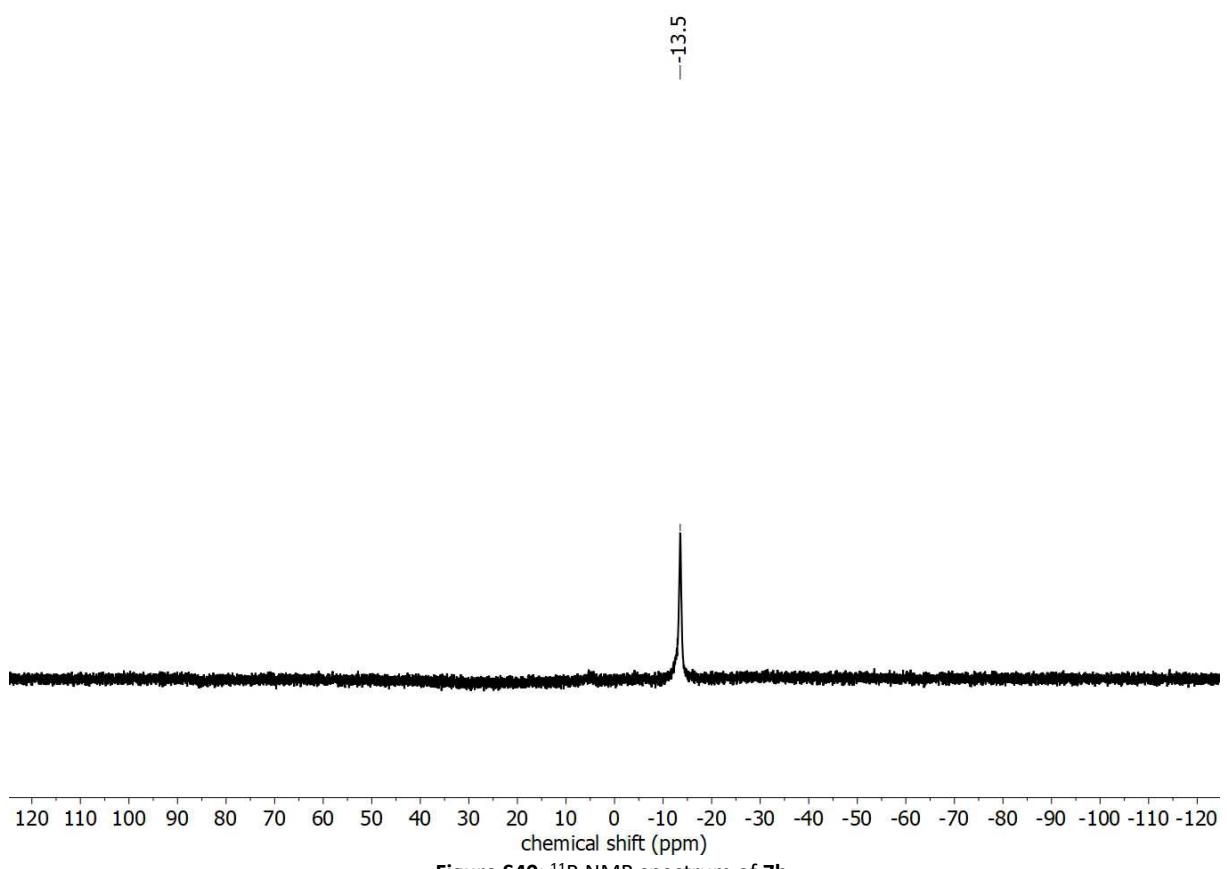
**Figure S40**: <sup>11</sup>B NMR spectrum of **7b.**

−13.5



−242.9
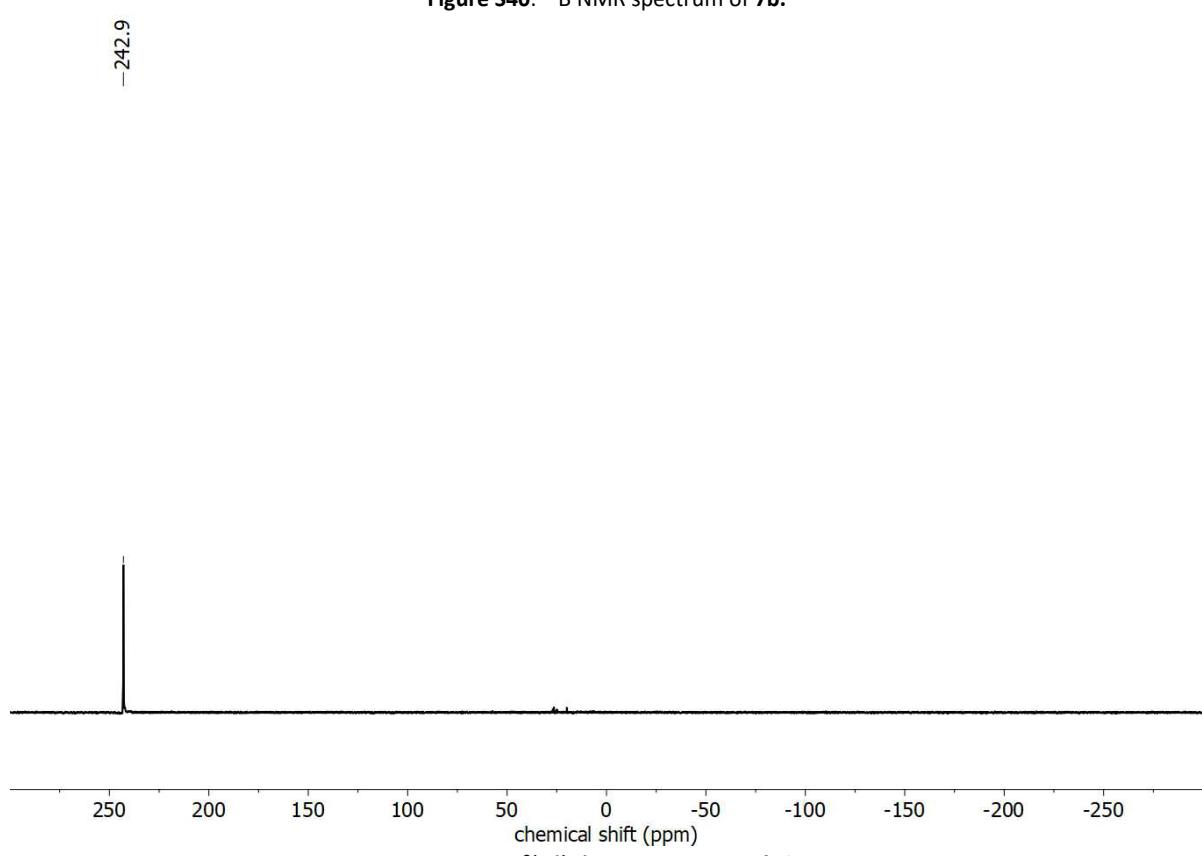
**Figure S41**: <sup>31</sup>P{<sup>1</sup>H} NMR spectrum of **7b.**
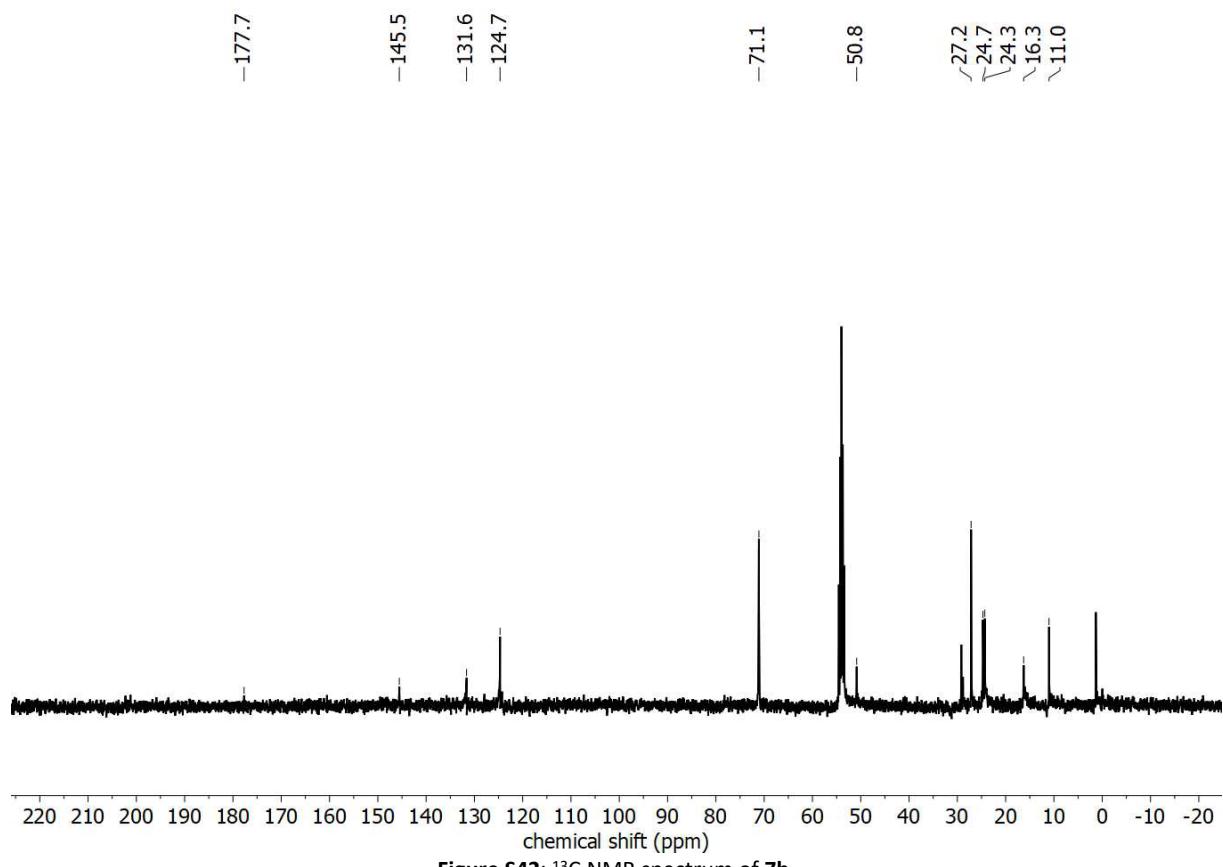
**Figure S42**: $^{13}$C NMR spectrum of **7b.**

177.7

145.5

131.6
124.7

71.1

50.8

27.2
24.7
24.3
16.3
11.0

220 210 200 190 180 170 160 150 140 130 120 110 100 90 80 70 60 50 40 30 20 10 0 -10 -20
chemical shift (ppm)

## 5. DFT Calculations



**4a**                    **4b**                    **7b**
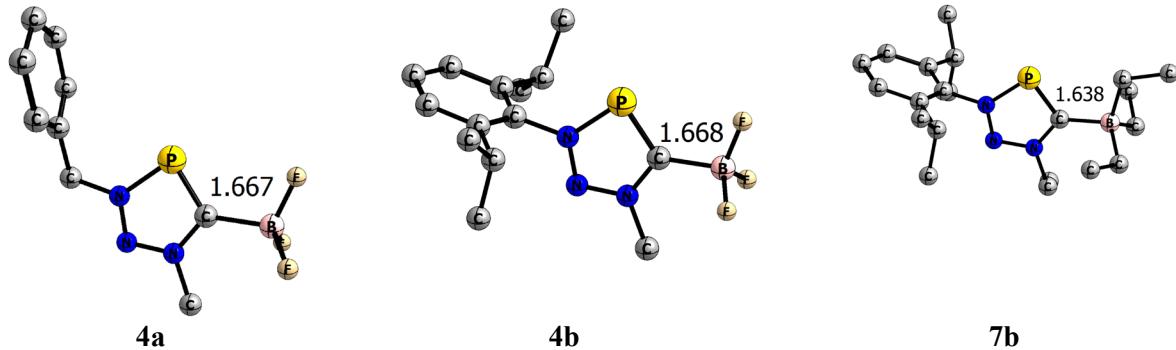
**Figure S43.** Optimized structures at the B3LYP-D3(BJ)/def2-TZVP level of theory. Hydrogen atoms are omitted for clarity.

**Table S6**. NBO results calculated at B3LYP-D3(BJ)/def2-TZVPP level of theory: partial charges, Q (in e), Wiberg bond order, WBI (in a.u.).

|                | 4a    | 4b    | 7b    |
|----------------|-------|-------|-------|
| Q(C$_{carb}$)  | -0.41 | -0.41 | -0.23 |
| Q(P)           | +0.81 | 0.81  | +0.78 |
| Q(PHC)         | +0.47 | +0.46 | +0.51 |
| Q(BR$_3$)      | -0.47 | -0.46 | -0.51 |
| WBI(C−B)       | 0.71  | 0.71  | 0.87  |



**4a**                    **4b**                    **7b**
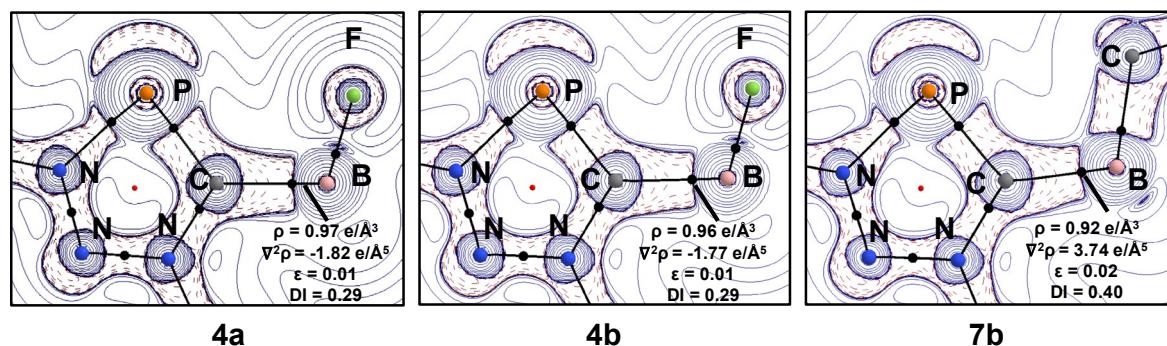
**Figure S44**. Laplacian distribution of the electron density of compounds **4a/b** and **7b** (B3LYP-D3(BJ)/def2-TZVP//B3LYP-D3(BJ)/def2-SVP). Contour line diagrams of the Laplacian distribution $\nabla^2\rho(r)$ in the PHC ring plane. Dashed red lines indicate areas of charge concentration ($\nabla^2\rho(r)<0$) while solid blue lines show areas of charge depletion ($\nabla^2\rho(r)>0$). The thick solid lines connecting the atomic nuclei are the bond paths and the small dots are the critical points. Bond Critical Points (in black), Ring Critical Points (in red).

**Table S7. EDA-NOCV results (in kcal/mol) on the $C_{carb}$-B bond of 4a/b and 7b at the BP86-D3(BJ)/TZ2P level of theory.[a]**

|  | 4a | 4b | 7b |
|---|---|---|---|
| $\Delta E_{int}$ | -72.1 | -70.7 | -68.4 |
| $\Delta E_{Pauli}$ | 179.5 | 177.6 | 192.1 |
| $\Delta E_{disp}$[b] | -4.6 (1.8 %) | -4.8 (1.9 %) | -14.7 (5.6 %) |
| $\Delta E_{elstat}$[b] | -133.7 (53.1 %) | -130.7 (52.7 %) | -126.2 (48.4 %) |
| $\Delta E_{orb}$[b] | -113.3 (45.0 %) | -112.8 (45.4 %) | -119.7 (45.9 %) |
| $\Delta E_{orb\text{-}\sigma}$[c] | -92.7 (81.8 %) | -92.3 (81.8 %) | -93.3 (77.9 %) |
| $\Delta E_{orb\text{-}\pi}$[c] | -6.1 (5.4 %) | -6.1 (5.4 %) | -7.8 (6.5 %) |
| $\Delta E_{orb\text{-}rest}$[c] | -14.5 (12.9 %) | -14.5 (12.8 %) | -18.6 (15.6 %) |
| $\Delta E_{prep\ BR3}$ | 31.2 | 30.9 | 26.4 |
| $\Delta E_{prep\ PHC}$ | 2.5 | 2.3 | 2.0 |
| $\Delta E_{prep\ total}$ | 33.7 | 33.2 | 28.4 |
| $D_e$ | 38.4 | 37.5 | 40.0 |

[a] Geometries optimized at the B3LYP-D3(BJ)/def2-SVP level of theory. [b] The value in parenthesis gives the percentage contribution to the total attractive interactions $\Delta E_{elstat} + \Delta E_{orb} + \Delta E_{disp}$. [c] The values in parenthesis gives the percentage contribution to the total orbital interaction.

ΔE$_{orb-σ}$= -92.7; |ν|= 0.72          ΔE$_{orb-π}$= -6.11; |ν|= 0.21

**4a**

ΔE$_{orb-σ}$= -92.3 kcal/mol; |ν|= 0.73          ΔE$_{orb-π}$= -6.1 kcal/mol; |ν|= 0.21

**4b**

ΔE$_{orb-σ}$ = -93.3 kcal/mol; |ν|= 0.74          ΔE$_{orb-π}$ = -7.8 kcal/mol; |ν|= 0.36

**7b**
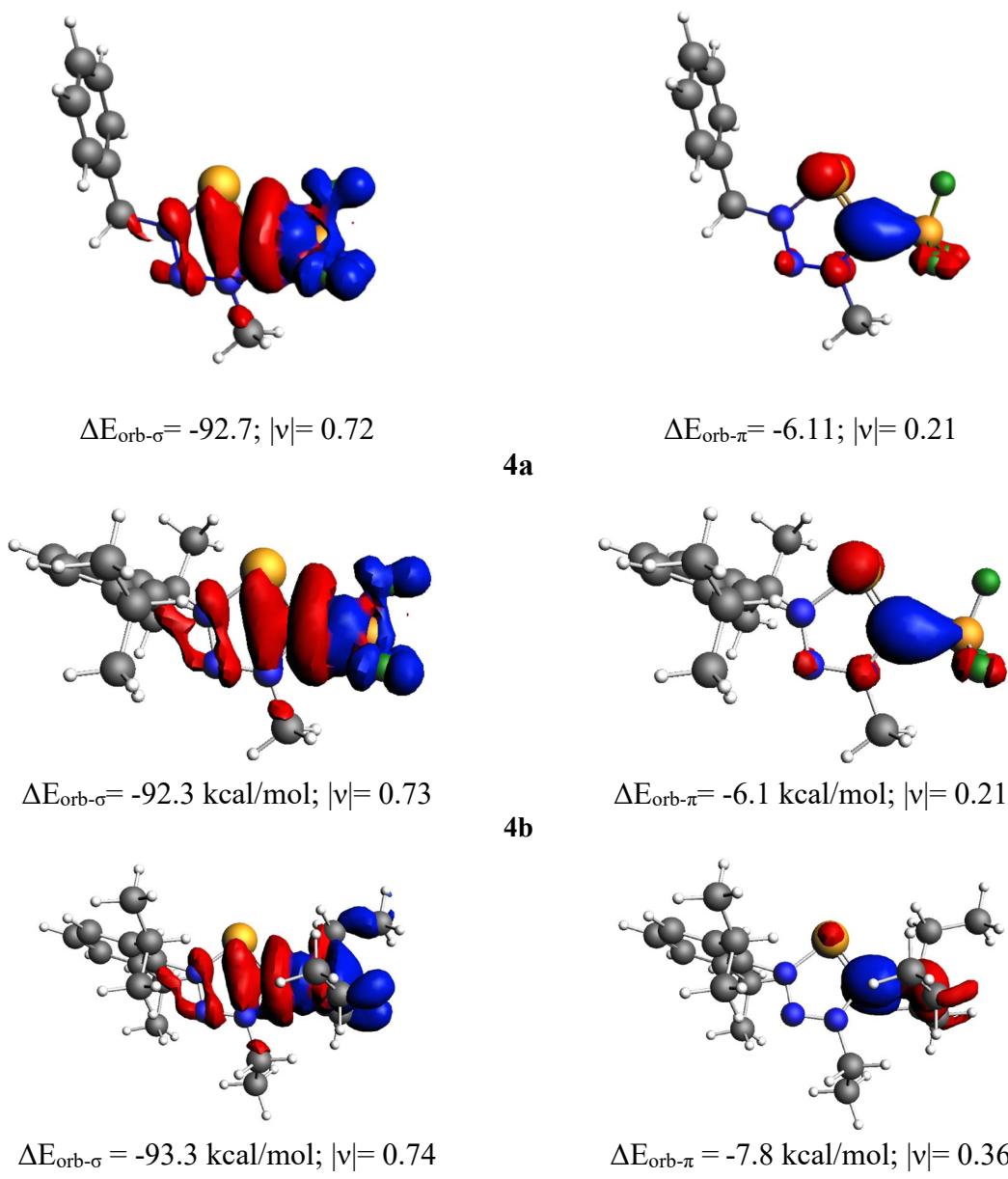
**Figure S45.** Plot of deformation densities Δρ of the pairwise orbital interactions (isovalue 0.001 au), associated energies ΔE in kcal/mol and eigenvalues ν in a.u.. The red color shows the charge outflow, whereas blue shows charge density accumulation.

38
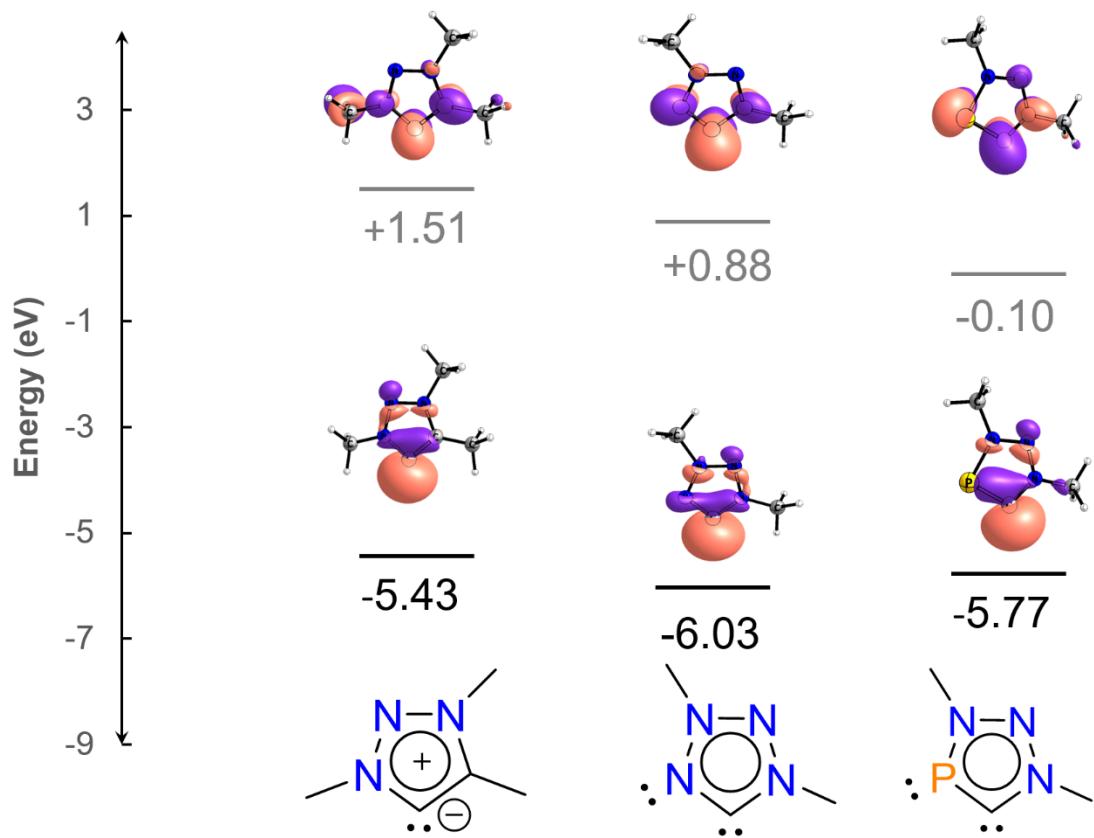
**Figure S46**. Molecular orbital energies (in eV) for the lone pairs (σ) and the unoccupied π* orbitals of 1,2,3-triazolylidene, tetrazol-5-ylidene and triazaphosphole-5-ylidene models systems at the B3LYP-D3(BJ)/def2-TZVPP// B3LYP-D3(BJ)/def2-SVP level of theory.

## 5.1 Computational Details

Geometry optimizations were performed using the Gaussian 16 optimizer[10] together with TurboMole V7.0.[11] energies and gradients. All geometry optimizations were computed using the functional B3LYP[12,13] functional with Grimme dispersion corrections D3[14] and the Becke-Jonson damping function[15] in combination with the def2-SVP basis set.[16] The stationary points were located with the Berny algorithm[17] using redundant internal coordinates. Analytical Hessians were computed to determine the nature of stationary points (one and zero imaginary frequencies for transition states and minima, respectively)[18] and to calculate unscaled zero-point energies (ZPEs) as well as thermal corrections and entropy effects using the standard statistical-mechanics relationships for an ideal gas

The atomic partial charges were estimated with the natural bond orbital (NBO)[19,20] method using NBO 7.0.[21] The topological quantum theory of atoms in molecules (QTAIM),[22] and Laplacian of the electron density analyses were carried out with AIMAII.[23] All these analysis were performed at the B3LYP-D3(BJ)/def2-TZVPP level of theory.

The nature of the chemical bonds were investigated by means of the Energy Decomposition Analysis (EDA) method, which was developed by Morokuma[24] and by Ziegler and Rauk.[25,26] The bonding analysis focuses on the instantaneous interaction energy $\Delta E_{int}$ of a bond A–B between two fragments A and B in the particular electronic reference state and in the frozen geometry AB. This energy is divided into four main components (Eq S1).

$$\Delta E_{int} = \Delta E_{elst} + \Delta E_{Pauli} + \Delta E_{orb} + \Delta E_{disp} \tag{S1}$$

The term $\Delta E_{elst}$ corresponds to the quasiclassical electrostatic interaction between the unperturbed charge distributions of the prepared atoms (or fragments) and it is usually attractive. The Pauli repulsion $\Delta E_{Pauli}$ is the energy change associated with the transformation from the superposition of the unperturbed wave functions (Slater determinant of the Kohn-Sham orbitals) of the isolated fragments to the wave function $\Psi_0 = N\hat{A}[\Psi^A\Psi^B]$, which properly obeys the Pauli principle through explicit antisymmetrization ($\hat{A}$ operator) and renormalization (N = constant) of the product wave function. It comprises the destabilizing interactions between electrons of the same spin on either fragment. The orbital interaction $\Delta E_{orb}$ accounts for charge transfer and polarization effects.[27] In the case that the Grimme dispersion corrections[14,15] are computed the term $\Delta E_{disp}$ is added to equation S1. Further details on the EDA method can be found in the literature.[28,29] In the case of the dimers, relaxation of the fragments to their equilibrium geometries at the electronic ground state is termed $\Delta E_{prep}$, because it may be considered as preparation energy for chemical bonding. The addition of $\Delta E_{prep}$ to the intrinsic interaction energy $\Delta E_{int}$ gives the total energy $\Delta E$, which is, by definition, the opposite sign of the bond dissociation energy $D_e$:

$$\Delta E(-D_e) = \Delta E_{int} + \Delta E_{prep} \tag{S2}$$

The EDA–NOCV method combines the EDA with the natural orbitals for chemical valence (NOCV) to decompose the orbital interaction term $\Delta E_{orb}$ into pairwise contributions. The NOCVs $\Psi_i$ are defined as the eigenvector of the valence operator, $\hat{V}$, given by Equation (S3).

$$\hat{V}\Psi_i = v_i\Psi_i \tag{S3}$$

In the EDA–NOCV scheme the orbital interaction term, $\Delta E_{orb}$, is given by Equation (S4),

$$\Delta E_{orb} = \sum_k \Delta E_k = \sum_{k=1}^{N/2} v_k\left[-F_{-k,k}^{TS} + F_{k,k}^{TS}\right] \tag{S4}$$

in which $F_{-k,-k}^{TS}$ and $F_{k,k}^{TS}$ are diagonal transition state Kohn–Sham matrix elements corresponding to NOCVs with the eigenvalues $-v_k$ and $v_k$, respectively. The $\Delta E_k^{orb}$ term for a particular type of bond is assigned by visual inspection of the shape of the deformation density $\Delta\rho_k$. The latter term is a measure of the size of the charge deformation and it provides a visual notion of the charge flow that is associated with the pairwise orbital interaction. The EDA–NOCV scheme thus provides both qualitative and quantitative information about the strength of orbital interactions in chemical bonds. The EDA-NOCV calculations were carried out with ADF2019.101. The basis sets for all elements have triple-$\zeta$ quality augmented by two sets of polarizations functions and one set of diffuse function. Core electrons were treated by the frozen-core approximation. This level of theory is denoted BP86-D3(BJ)/TZ2P.[30] Scalar relativistic effects have been incorporated by applying the zeroth-order regular approximation (ZORA).[31]

**xyz coordinations (in Å) and Energies (in Hartree)**


**4a**
**Energy(B3LYP-D3(BJ)/def2-SVP) = -1178.45912782**
P   -0.134390000000   -0.597706000000   -0.335633000000
F   -3.999540000000   -0.638180000000   -0.974486000000
F   -2.700853000000   -2.377127000000   -0.169975000000
F   -3.675381000000   -0.869798000000    1.291273000000
N    0.274992000000    1.104867000000   -0.221616000000
N   -0.705072000000    1.932281000000   -0.005514000000
N   -1.822008000000    1.241000000000    0.074921000000
C   -1.763697000000   -0.106995000000   -0.071349000000
C    1.616458000000    1.704333000000   -0.390630000000
H    1.669578000000    2.554364000000    0.303543000000
H    1.682231000000    2.096836000000   -1.416476000000
C    2.703664000000    0.696465000000   -0.128818000000
C    3.351393000000    0.056226000000   -1.192971000000
H    3.086340000000    0.314265000000   -2.221681000000
C    4.328144000000   -0.911713000000   -0.946334000000
H    4.827036000000   -1.406166000000   -1.782650000000
C    4.661727000000   -1.247246000000    0.367764000000
H    5.423653000000   -2.005550000000    0.561812000000
C    4.020137000000   -0.611283000000    1.435826000000
H    4.280622000000   -0.870648000000    2.464315000000
C    3.046653000000    0.356372000000    1.188363000000
H    2.542757000000    0.849862000000    2.023829000000
C   -3.070052000000    1.968849000000    0.330932000000
H   -3.500945000000    1.589890000000    1.265681000000
H   -3.767570000000    1.742359000000   -0.484519000000
H   -2.838425000000    3.037285000000    0.389141000000
B   -3.121883000000   -1.069609000000    0.023794000000


**4b**
**Energy(B3LYP-D3(BJ)/def2-SVP) = -1374.92121233**
P   -0.965251000000    0.168110000000   -1.298646000000
F   -4.408914000000    1.123071000000    0.290598000000
F   -4.409253000000   -1.158865000000   -0.003934000000
F   -4.050405000000    0.235230000000   -1.816767000000
N    0.122973000000   -0.009627000000    0.064635000000
N   -0.428456000000   -0.162029000000    1.237380000000
N   -1.734580000000   -0.142147000000    1.085987000000
C   -2.247378000000    0.020539000000   -0.162029000000
C    1.566495000000   -0.004477000000   -0.006998000000
C    2.230598000000   -1.238715000000   -0.149887000000
C    3.626752000000   -1.201493000000   -0.250180000000
H    4.182287000000   -2.133763000000   -0.358684000000
C    4.317116000000    0.010239000000   -0.214160000000
H    5.406328000000    0.015829000000   -0.298347000000
C    3.627932000000    1.212793000000   -0.070622000000
H    4.182249000000    2.152451000000   -0.043122000000
C    2.230980000000    1.234226000000    0.040435000000

| C | 1.472570000000 | -2.557859000000 | -0.134846000000 |
|---|---|---|---|
| H | 0.442438000000 | -2.354843000000 | -0.466521000000 |
| C | 1.394221000000 | -3.106750000000 | 1.301044000000 |
| H | 0.805440000000 | -4.037348000000 | 1.328102000000 |
| H | 0.925684000000 | -2.379645000000 | 1.980206000000 |
| H | 2.402730000000 | -3.328595000000 | 1.685896000000 |
| C | 2.053897000000 | -3.599375000000 | -1.097763000000 |
| H | 3.046569000000 | -3.949981000000 | -0.774024000000 |
| H | 2.150074000000 | -3.197560000000 | -2.117974000000 |
| H | 1.396587000000 | -4.481364000000 | -1.138183000000 |
| C | 1.481852000000 | 2.551966000000 | 0.173302000000 |
| H | 0.447373000000 | 2.325670000000 | 0.469722000000 |
| C | 2.072702000000 | 3.448642000000 | 1.269764000000 |
| H | 2.122272000000 | 2.920756000000 | 2.234316000000 |
| H | 1.449348000000 | 4.346674000000 | 1.401039000000 |
| H | 3.088964000000 | 3.789634000000 | 1.016930000000 |
| C | 1.424157000000 | 3.278830000000 | -1.180254000000 |
| H | 0.948860000000 | 2.653212000000 | -1.951240000000 |
| H | 2.436328000000 | 3.534942000000 | -1.532481000000 |
| H | 0.845767000000 | 4.212108000000 | -1.095040000000 |
| C | -2.570961000000 | -0.298523000000 | 2.281840000000 |
| H | -3.201053000000 | -1.185406000000 | 2.142856000000 |
| H | -3.224955000000 | 0.578769000000 | 2.355069000000 |
| H | -1.912074000000 | -0.394308000000 | 3.150845000000 |
| B | -3.890091000000 | 0.058512000000 | -0.450526000000 |

**7b**
**Energy(B3LYP-D3(BJ)/def2-SVP) = -1352.27572773**

| P | -0.454750000000 | -0.191518000000 | -1.258740000000 |
|---|---|---|---|
| N | 0.750923000000 | -0.015716000000 | -0.002866000000 |
| N | 0.308706000000 | 0.131643000000 | 1.212108000000 |
| N | -1.009533000000 | 0.108491000000 | 1.187207000000 |
| C | -1.653695000000 | -0.056972000000 | -0.008884000000 |
| C | 2.181023000000 | -0.032863000000 | -0.200565000000 |
| C | 2.842481000000 | -1.275455000000 | -0.171374000000 |
| C | 4.226985000000 | -1.264014000000 | -0.384918000000 |
| H | 4.780987000000 | -2.203320000000 | -0.368802000000 |
| C | 4.906783000000 | -0.068679000000 | -0.617144000000 |
| H | 5.986592000000 | -0.083162000000 | -0.782900000000 |
| C | 4.219953000000 | 1.144644000000 | -0.640569000000 |
| H | 4.768052000000 | 2.069971000000 | -0.822375000000 |
| C | 2.835199000000 | 1.191496000000 | -0.433561000000 |
| C | 2.096693000000 | -2.563372000000 | 0.146709000000 |
| H | 1.049775000000 | -2.428333000000 | -0.165733000000 |
| C | 2.093025000000 | -2.810082000000 | 1.666171000000 |
| H | 1.658887000000 | -1.956424000000 | 2.206876000000 |
| H | 3.120185000000 | -2.958791000000 | 2.037056000000 |
| H | 1.506483000000 | -3.710039000000 | 1.910262000000 |
| C | 2.635559000000 | -3.780487000000 | -0.612472000000 |
| H | 2.678695000000 | -3.594044000000 | -1.696449000000 |
| H | 1.981361000000 | -4.648996000000 | -0.441035000000 |
| H | 3.644960000000 | -4.063586000000 | -0.274101000000 |
| C | 2.081225000000 | 2.512603000000 | -0.394216000000 |
| H | 1.030486000000 | 2.303508000000 | -0.647762000000 |
| C | 2.104153000000 | 3.090197000000 | 1.032402000000 |
| H | 1.508853000000 | 4.015640000000 | 1.085989000000 |

| | | | |
|---|---|---|---|
| H | 3.136042000000 | 3.328407000000 | 1.337413000000 |
| H | 1.695448000000 | 2.371475000000 | 1.757452000000 |
| C | 2.593239000000 | 3.533337000000 | -1.416295000000 |
| H | 2.614830000000 | 3.110915000000 | -2.432492000000 |
| H | 3.607372000000 | 3.887377000000 | -1.172203000000 |
| H | 1.936051000000 | 4.416422000000 | -1.427121000000 |
| C | -1.659422000000 | 0.320232000000 | 2.494057000000 |
| H | -1.119322000000 | -0.305629000000 | 3.217639000000 |
| H | -2.679052000000 | -0.059852000000 | 2.391322000000 |
| C | -1.638220000000 | 1.786850000000 | 2.900477000000 |
| H | -2.165529000000 | 2.404392000000 | 2.160185000000 |
| H | -0.606217000000 | 2.155034000000 | 3.001424000000 |
| H | -2.144512000000 | 1.906248000000 | 3.870131000000 |
| C | -4.058317000000 | 1.152202000000 | 0.226871000000 |
| H | -5.130991000000 | 0.994137000000 | 0.011815000000 |
| H | -4.019171000000 | 1.260671000000 | 1.326952000000 |
| C | -3.610324000000 | 2.465109000000 | -0.422477000000 |
| H | -3.725260000000 | 2.430086000000 | -1.518190000000 |
| H | -2.540581000000 | 2.671228000000 | -0.233007000000 |
| H | -4.176003000000 | 3.343812000000 | -0.065257000000 |
| C | -3.412975000000 | -0.419563000000 | -1.907243000000 |
| H | -2.887369000000 | 0.390740000000 | -2.455098000000 |
| H | -2.895022000000 | -1.350902000000 | -2.216218000000 |
| C | -4.850530000000 | -0.479505000000 | -2.432119000000 |
| H | -5.389861000000 | 0.461787000000 | -2.236099000000 |
| H | -5.424833000000 | -1.282371000000 | -1.940922000000 |
| H | -4.901500000000 | -0.662889000000 | -3.519553000000 |
| C | -3.811531000000 | -1.534923000000 | 0.544447000000 |
| H | -3.967240000000 | -1.319846000000 | 1.619748000000 |
| H | -4.829335000000 | -1.735600000000 | 0.163645000000 |
| C | -2.972020000000 | -2.809670000000 | 0.412116000000 |
| H | -2.794020000000 | -3.065751000000 | -0.646090000000 |
| H | -3.442272000000 | -3.690464000000 | 0.883253000000 |
| H | -1.975437000000 | -2.695045000000 | 0.877326000000 |
| B | -3.263332000000 | -0.202296000000 | -0.275921000000 |

## 6. Literature

[1]     C. Pardin, I. Roy, W. D. Lubell, J. W. Keillor, *Chem. Biol. Drug Des.* **2008**, *72*, 189–196.

[2]     G. Guisado-Barrios, J. Bouffard, B. Donnadieu, G. Bertrand, *Angew. Chem. Int. Ed*. **2010**, *49*, 4759–4762.

[3]     C. E. Averre, M. P. Coles, I. R. Crossley, I. J. Day, *Dalton Trans*. **2012**, *41*, 278–284; S. M. Mansell, M. Green, R. J. Kilby, M. Murray, C. A. Russell, *C. R. Chim*. **2010**, *13*, 1073–1081.

[4]     J. A. W. Sklorz, S. Hoof, N. Rades, N. De Rycke, L. Könczöl, D. Szieberth, M. Weber, J. Wiecko, L. Nyulászi, M. Hissler, C. Müller, *Chem. Eur.J.* **2015**, *21*, 11096–11109.

[5]     Bruker (2010). APEX2, SAINT, SADABS and XSHELL. Bruker AXS Inc., Madison, Wisconsin, USA.

[6]     G. M. Sheldrick, *Acta Cryst*. **2015**, C71, 3;

[7]     G. M. Sheldrick, *Acta Cryst*. **2015,** A71, 3.

[8]     Spek, A. L. *Acta Cryst.* **2009**, D65 (2), 148.

[9]     O. V. Dolomanov, L. J. Bourhis, R. J Gildea, J. A. K. Howard, H. Puschmann, *J. Appl. Cryst.* **2009**, *42*, 339

[10]    M. J. Frisch; G. W. Trucks; H. B. Schlegel; G. E. Scuseria; M. A. Robb; J. R. Cheeseman; G. Scalmani; V. Barone; B. Mennucci; G. A. Petersson; H. Nakatsuji; M. Caricato; X. Li; H. P. Hratchian; A. F. Izmaylov; J. Bloino; G. Zheng; J. L. Sonnenberg; M. Hada; M. Ehara; K. Toyota; R. Fukuda; J. Hasegawa; M. Ishida; T. Nakajima; Y. Honda; O. Kitao; H. Nakai; T. Vreven; J. A. Montgomery, J.; J. E. Peralta; F. Ogliaro; M. Bearpark; J. J. Heyd; E. Brothers; K. N. Kudin; V. N. Staroverov; R. Kobayashi; J. Normand; K. Raghavachari; A. Rendell; J. C. Burant; S. S. Iyengar; J. Tomasi; M. Cossi; N. Rega; J. M. Millam; M. Klene; J. E. Knox; J. B. Cross; V. Bakken; C. Adamo; J. Jaramillo; R. Gomperts; R. E. Stratmann; O. Yazyev; A. J. Austin; R. Cammi; C. Pomelli; J. W. Ochterski; R. L. Martin; K. Morokuma; V. G. Zakrzewski; G. A. Voth; P. Salvador; J. J. Dannenberg; S. Dapprich; A. D. Daniels; O. Farkas; J. B. Foresman; J. V. Ortiz; J. Cioslowski; D. J. Fox Gaussian 09, Revision C.01. Gaussian, Inc.: Wallingford CT, 2009.

[11]    TURBOMOLE V7.0 2015 a development of University of Karlsruhe and Forschungszentrum Karlsruhe GmbH, 1989-2007; TURBOMOLE GmbH, since 2007; available from http://www.turbomole.com: Karlsruhe.

[12]    Becke, A. D., Density-functional thermochemistry. III. The role of exact exchange. *J. Chem. Phys.* **1993**, 98 (7), 5648-5652.

[13]    Lee, C.; Yang, W.; Parr, R. G., Development of the Colle-Salvetti correlation-energy formula into a functional of the electron density. *Phys. Rev. B* **1988**, *37* (2), 785-789.

[14]    Grimme, S.; Antony, J.; Ehrlich, S.; Krieg, H., A consistent and accurate ab initio parametrization of density functional dispersion correction (DFT-D) for the 94 elements H-Pu. *J. Chem. Phys*. **2010**, 132 (15).

[15]    Grimme, S.; Ehrlich, S.; Goerigk, L., Effect of the Damping Function in Dispersion Corrected Density Functional Theory. *J. Comp. Chem.* **2011,** *32* (7), 1456-1465.

[16]    Weigend, F.; Ahlrichs, R., Balanced basis sets of split valence, triple zeta valence and quadruple zeta valence quality for H to Rn: Design and assessment of accuracy. *Phys. Chem. Chem. Phys.* **2005**, *7* (18), 3297-3305.

[17]    Peng, C. Y.; Ayala, P. Y.; Schlegel, H. B.; Frisch, M. J., Using redundant internal coordinates to optimize equilibrium geometries and transition states. *J. Comp. Chem*. **1996,** *17* (1), 49-56.

[18]    McIver, J. W.; Komornic.A, Structure of Transition-state in organic reactions - General theory and an applications to cyclobutene-butadiene isomerization using a semiempirical molecular-orbital method. *J. Am. Chem. Soc*. **1972,** *94* (8), 2625-2633.

[19]    Reed, A. E.; Weinstock, R. B.; Weinhold, F., Natural-population analysis. *J. Chem. Phys.* **1985**, *83* (2), 735-746.

[20]    Reed, A. E.; Curtiss, L. A.; Weinhold, F., Intermolecular interactions from a natural bond orbital, donor-acceptor viewpoint. *Chem. Rev.* **1988**, *88* (6), 899-926.

45

[21] Glendening, E. D.; Landis, C. R.; Weinhold, F., NBO 7.0: New Vistas in Localized and Delocalized Chemical Bonding Theory. *J. Comp. Chem.* **2019**, *40* (25), 2234-2241.

[22] Bader, R. F. W., Atoms in Molecules: A Quantum Theory, Clarendon, Oxford, 1990.

[23] Keith, T. A.; Gristmill, T. K. AIMAll, 19.02.13; Overland Park KS, USA (aim.tkgristmill.com), 2019.

[24] Morokuma, K., Moluecular orbital studies of hydrogen bonds 3. C=O H-O hydrogen bond in H2CO and H2O and H2CO 2H2O. J. Chem. Phys. 1971, 55 (3), 1236-1244.

[25] Ziegler, T.; Rauk, A., Theoretical-study of the ethylene-metal bond in complexes between Cu+, Ag+, Au+, Pt0, or Pt2+ and ethylene, based on the Hartree-Fock Slater Transition-State method. *Inorg. Chem.* **1979,** 18 (6), 1558-1565.

[26] Ziegler, T.; Rauk, A., CO, CS, N2, PF3, and CNCH3 as s-donors and p-acceptors - Theoretical-study by the Hartree-Fock-Slater Transition-State method. *Inorg. Chem.* **1979,** *18* (7), 1755-1759.

[27] Bickelhaupt, F. M.; Nibbering, N. M. M.; Van Wezenbeek, E. M.; Baerends, E. J., *J. Phys. Chem.* **1992**, 96 (12), 4864-4873.

[28] Bickelhaupt, F. M.; Baerends, E. J., Kohn-Sham density functional theory: Predicting and understanding chemistry. In Reviews in Computational Chemistry, Lipkowitz, K. B.; Boyd, D. B., Eds. 2000; Vol. 15, pp 1-86.

[29] te Velde, G.; Bickelhaupt, F. M.; Baerends, E. J.; Fonseca Guerra, C.; van Gisbergen, S. J. A.; Snijders, J. G.; Ziegler, T., Chemistry with ADF. *J. Comp. Chem.* **2001,** 22 (9), 931-967.

[30] Krijn, J.; Baerends, E. J., Fit Functions in the HFS-Method 1984.

[31] Van Lenthe, E.; Baerends, E. J.; Snijders, J. G., Relativistic regular two-component Hamiltonians. *J. Chem. Phys*. **1993,** *99* (6), 4597-4610.[]

Chemoselective Post-Synthesis Modification of Pyridyl-Substituted, Aromatic Phosphorus Heterocycles: Cationic Ligands for Coordination Chemistry:

# Chemistry–A European Journal

## Chemoselective Post-Synthesis Modification of Pyridyl-Substituted, Aromatic Phosphorus Heterocycles: Cationic Ligands for Coordination Chemistry

Lea Dettling, Martin Papke, Moritz J. Ernst, Manuela Weber, and Christian Müller*

# Supporting Information

# Chemoselective Post-Synthesis Modification of Pyridyl-Substituted, Aromatic Phosphorus Heterocycles: Cationic Ligands for Coordination Chemistry

Lea Dettling,[a]† Martin Papke,[a]† Moritz J. Ernst,[a] Manuela Weber,[a] Christian Müller*[a]

**Table of Content**

# 1. NMR Spectroscopic Data

**General Remarks:**

$^1$H, $^{13}$C{$^1$H}, $^{19}$F, $^{11}$B and $^{31}$P{$^1$H} NMR spectra were recorded by using a JEOL ECS400 spectrometer (400 MHz), or a JEOL ECZ600 spectrometer (600 MHz). All chemical shifts are reported relative to the residual resonance in the deuterated solvents.
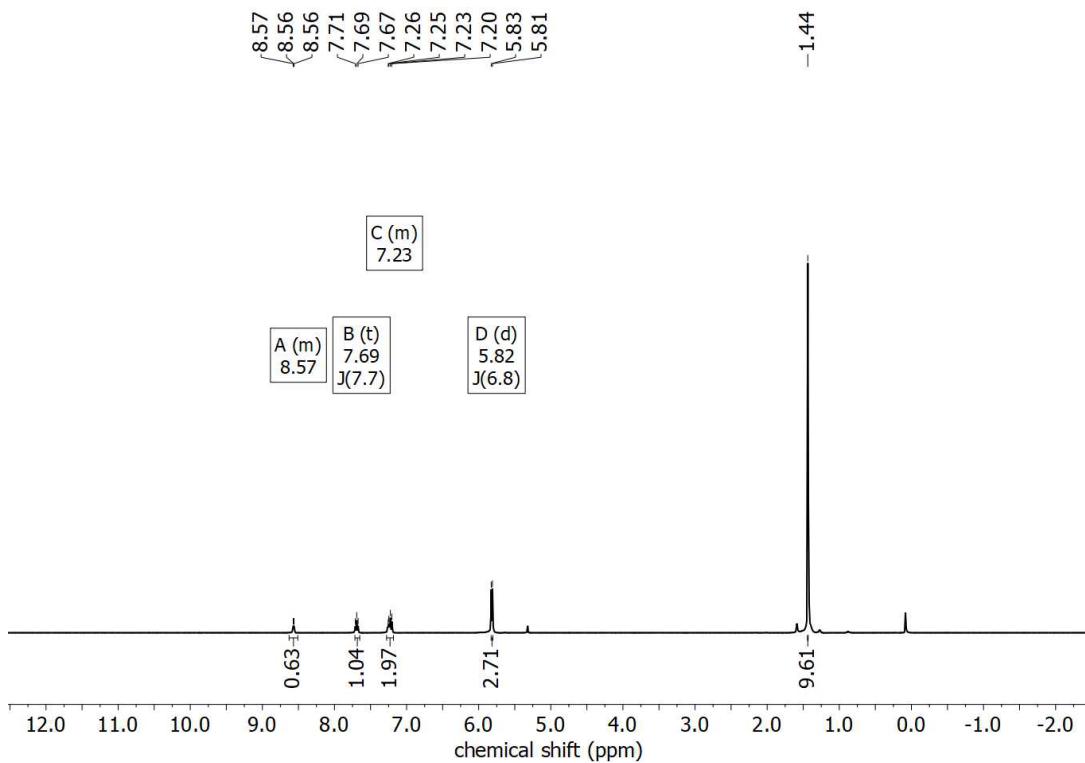


**Figure S1:** $^1$H-NMR of **1** in DCM-$d_2$.
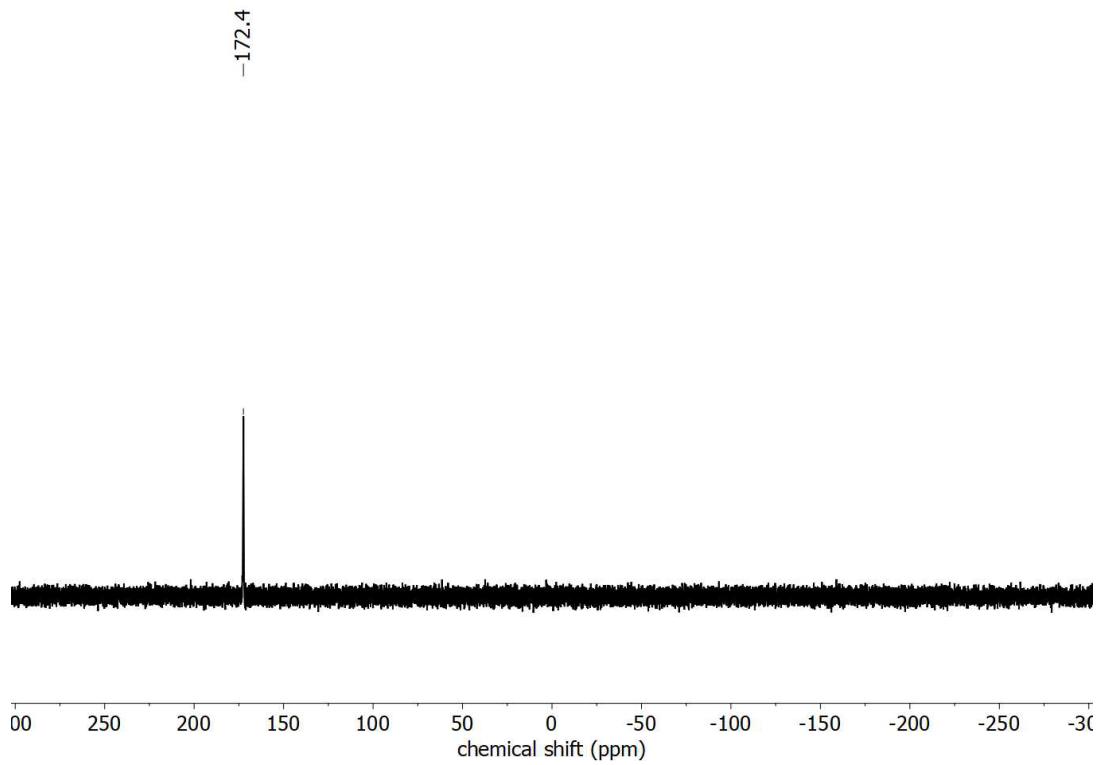
**Figure S2:** $^{31}P\{^{1}H\}$-NMR of **1** in DCM-$d_2$.
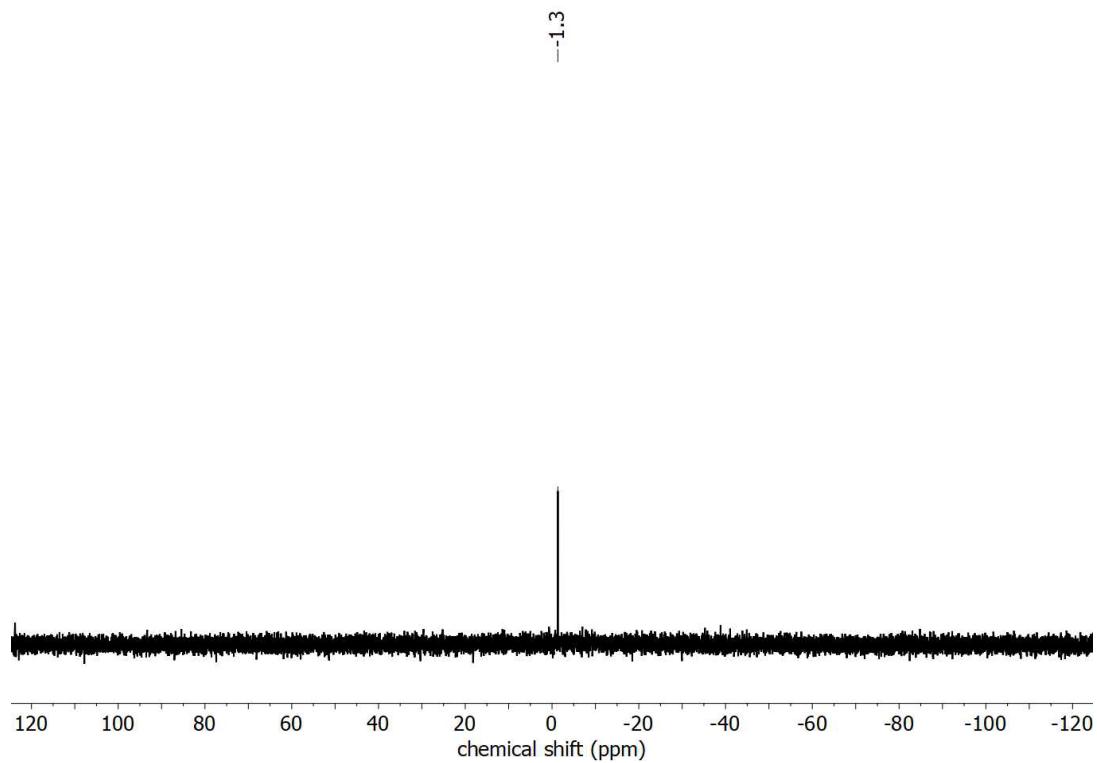


**Figure S3:** $^{11}B$-NMR of **2a** in DCM-$d_2$.

−151.3

20   0   -20   -40   -60   -80   -100   -120   -140   -160   -180   -200   -220
chemical shift (ppm)
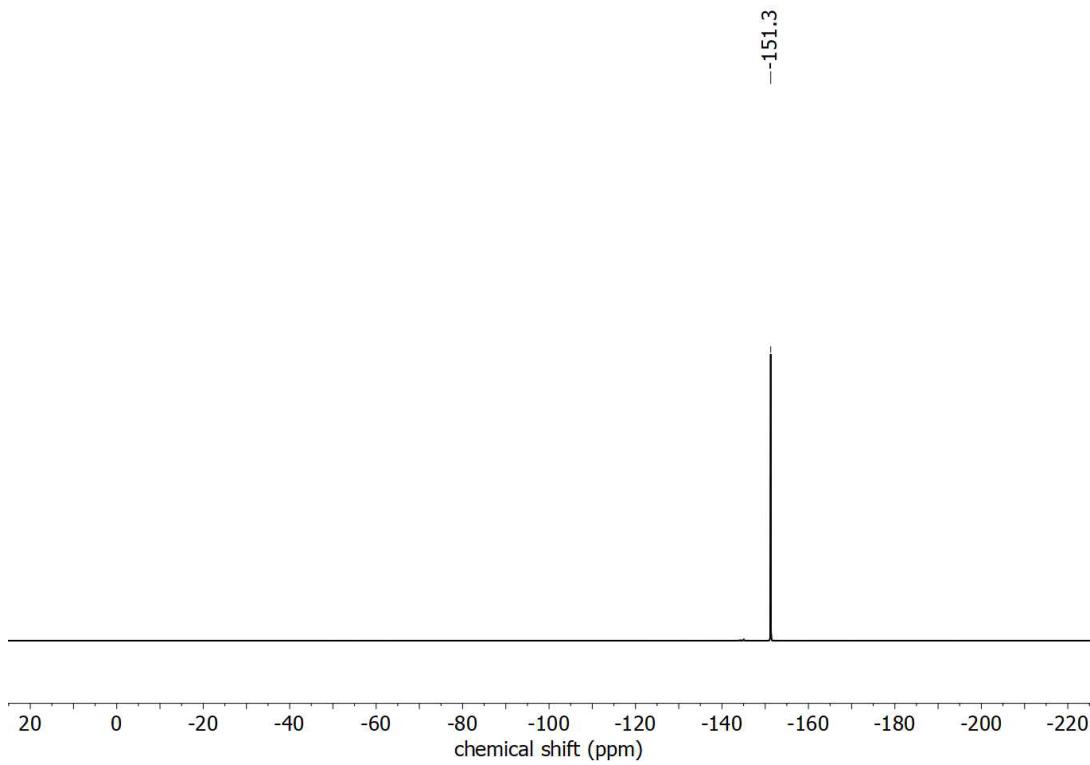
**Figure S4:** $^{19}$F-NMR of **2a** in DCM-$d_2$.

200.4
199.8

153.5
147.8
146.7

128.0
128.0

51.5
51.4
46.7
35.9
35.8
31.7

| C (d) |
| 35.8 |
| J(15.3) |

| A (d) |
| 200.1 |
| J(57.6) |

| B (d) |
| 51.5 |
| J(14.7) |

220 210 200 190 180 170 160 150 140 130 120 110 100 90  80  70  60  50  40  30  20  10  0  -10 -20
chemical shift (ppm)
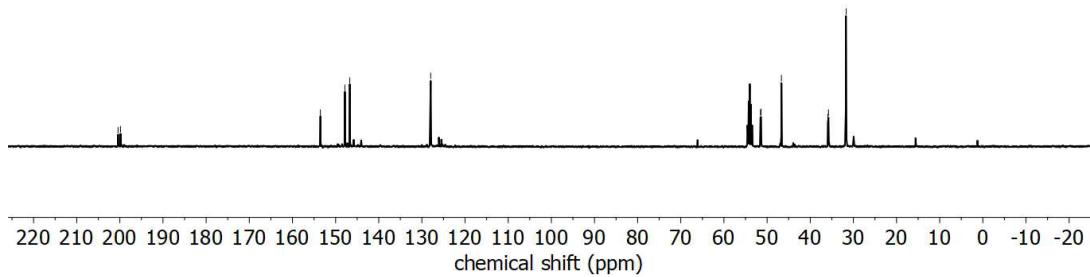
**Figure S5:** $^{13}$C{$^1$H}-NMR of **2a** in DCM-$d_2$.

S3

180

8.80
8.79
8.39
8.37
8.35
7.94
7.92
7.90
7.35
7.33
6.21
6.19
4.45
1.43

| D (d) |
| 8.37 |
| J(8.2) |

| E (d) | C (t) | B (d) | A (d) |
| 8.79 | 7.92 | 7.34 | 6.20 |
| J(6.1) | J(7.0) | J(8.0) | J(5.3) |

1.00
0.96
1.08
0.97
2.10
3.02
9.42

9.5  9.0  8.5  8.0  7.5  7.0  6.5  6.0  5.5  5.0  4.5  4.0  3.5  3.0  2.5  2.0  1.5  1.0  0.5
chemical shift (ppm)
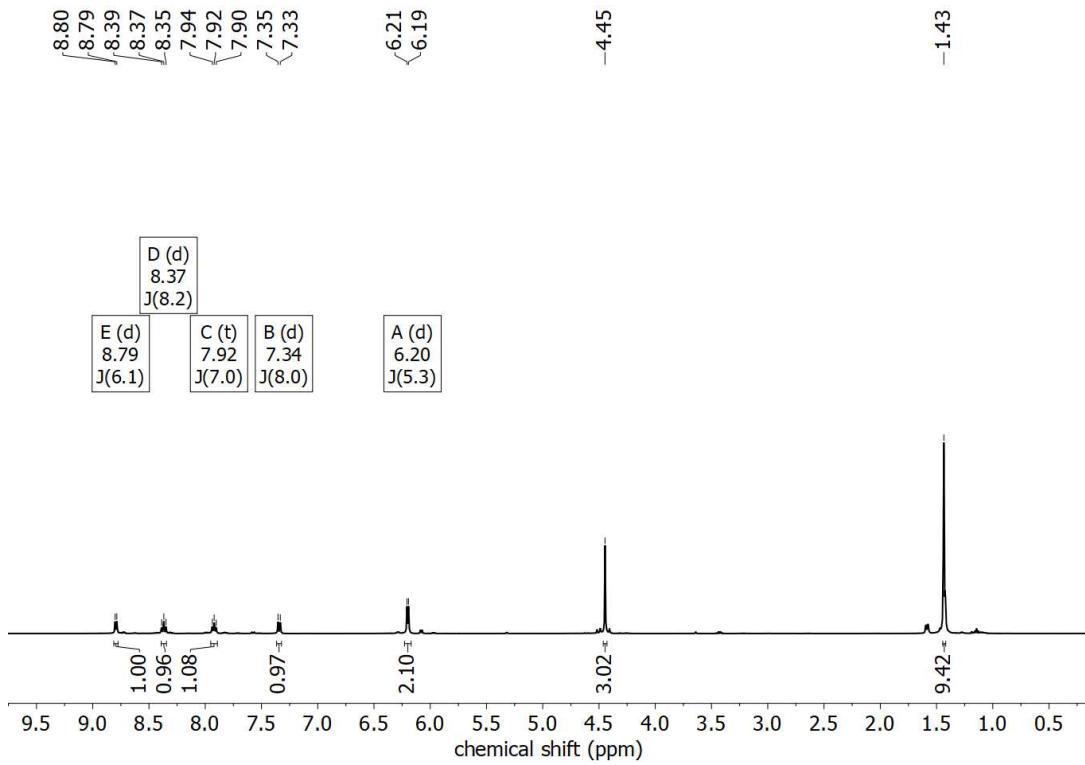
**Figure S6:** $^1$H-NMR of **2a** in DCM-$d_2$.

−178.4

00  250  200  150  100  50  0  −50  −100  −150  −200  −250  −30
chemical shift (ppm)
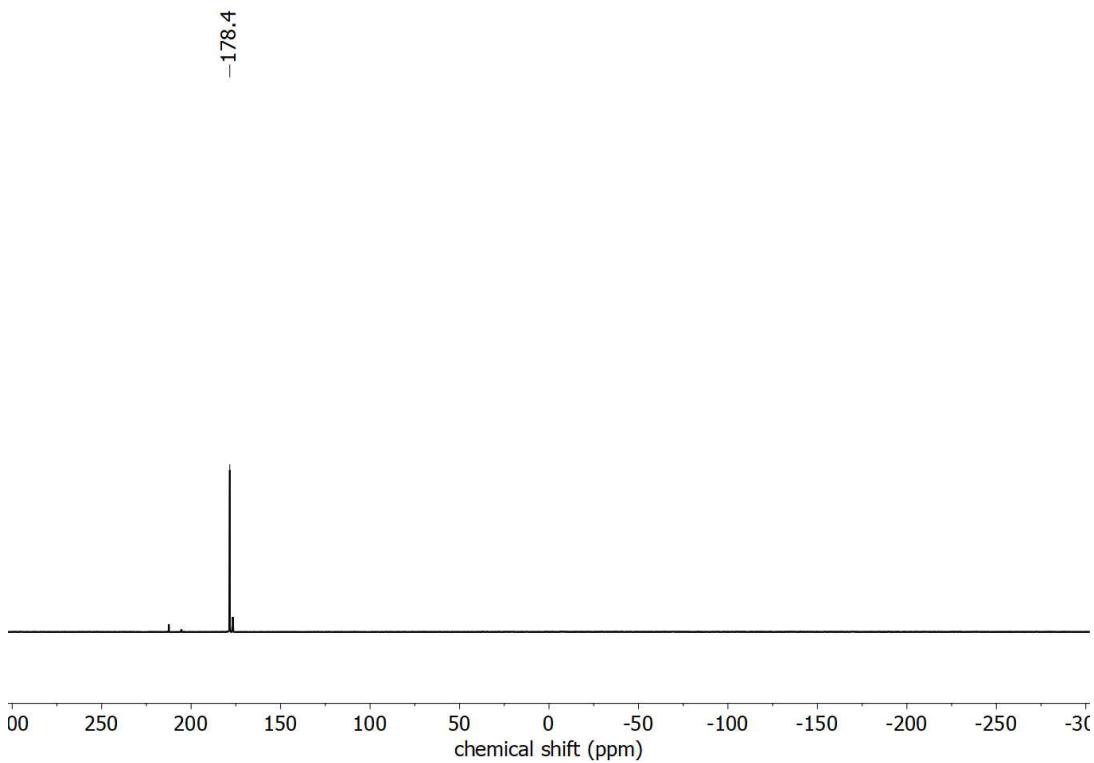
**Figure S7:** $^{31}$P{$^1$H}-NMR of **2a** in DCM-$d_2$.
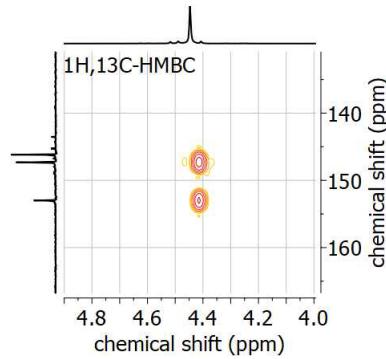
**Figure S8:** $^1H$-$^{13}C$-HMBC-NMR of **2a** in DCM-$d_2$.
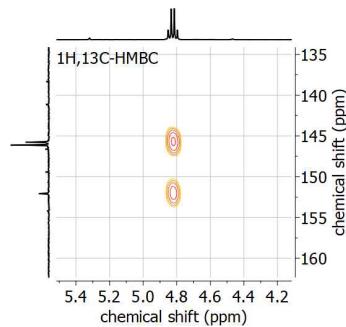


**Figure S9:** $^1H$-$^{13}C$-HMBC-NMR of **2b** in DCM-$d_2$.



A (d)
200.4
J(58.0)

G (s)
152.7

H (s)
146.7

I (s)
146.4

F (s)
129.4

E (s)
128.7

K (s)
54.8

B (d)
51.3
J(14.9)

C (d)
36.0
J(15.4)

D (t)
31.8
J(6.9)

J (s)
16.1
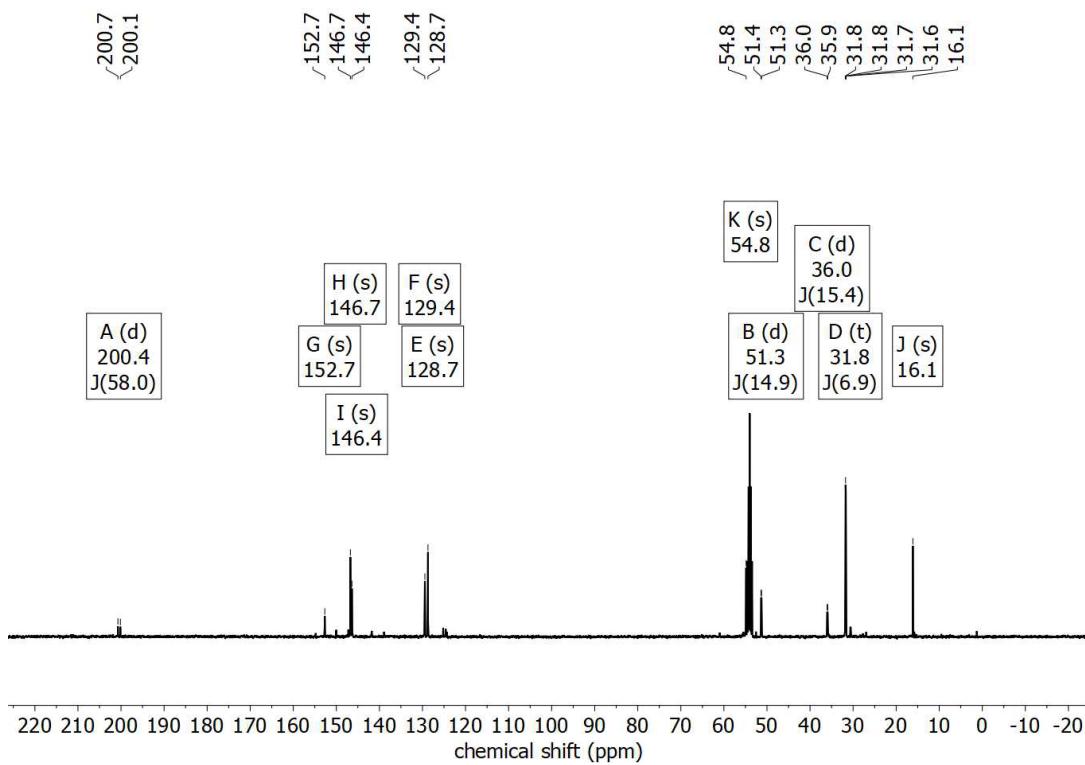
**Figure S10:** $^{13}C\{^1H\}$-NMR of **2b** in DCM-$d_2$.

8.87
8.87
8.86
8.85
8.43
8.43
8.41
8.41
8.39
8.39
8.04
8.03
8.02
8.02
8.01
8.00
8.00
7.54
7.52
6.24
6.23

4.85
4.83
4.81
4.80

1.62
1.60
1.58
1.45
1.45

B (td)
8.41
J(7.9, 1.4)

A (dd)
8.86
J(6.2, 1.2)

D (d)
7.53
J(8.0)

E (d)
6.23
J(5.2)

F (q)
4.82
J(7.3)

H (d)
1.45
J(1.4)

G (t)
1.60
J(7.3)

C (ddd)
8.02
J(7.7, 6.3, 1.5)

11.5   10.5   9.5   8.5   7.5   6.5   5.5   4.5   3.5   2.5   1.5   0.5
chemical shift (ppm)
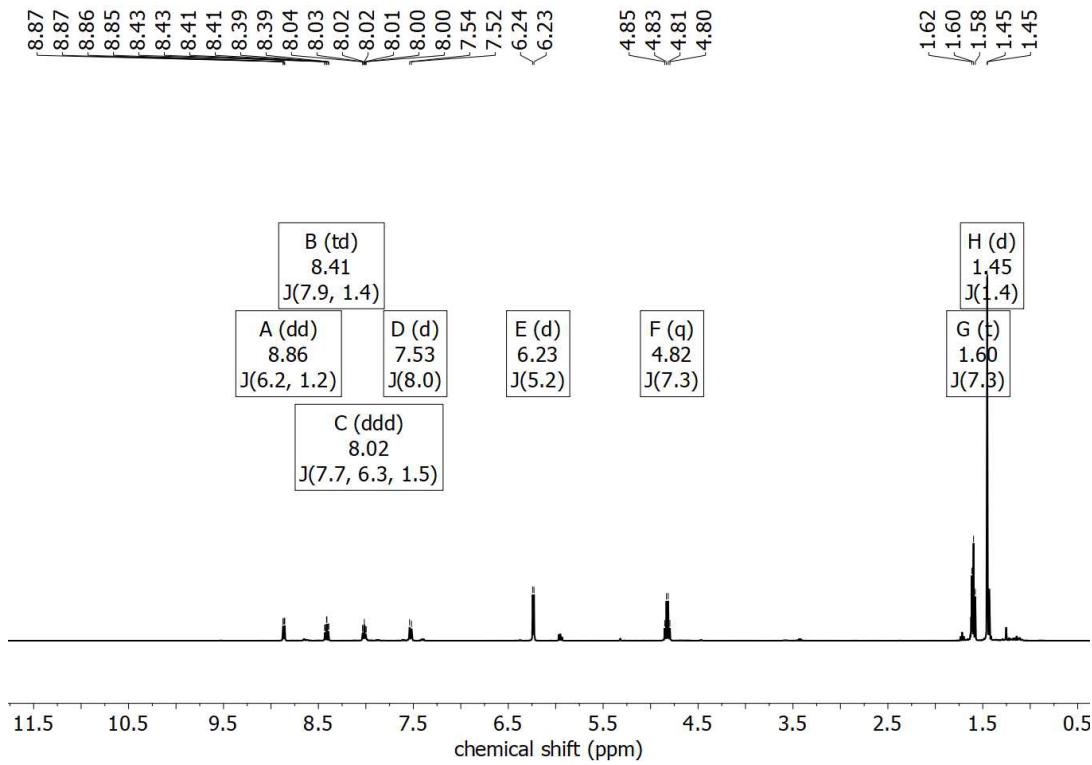
**Figure S11:** $^1$H-NMR of **2b** in DCM-$d_2$.

−1.3

120   100   80   60   40   20   0   -20   -40   -60   -80   -100   -120
chemical shift (ppm)
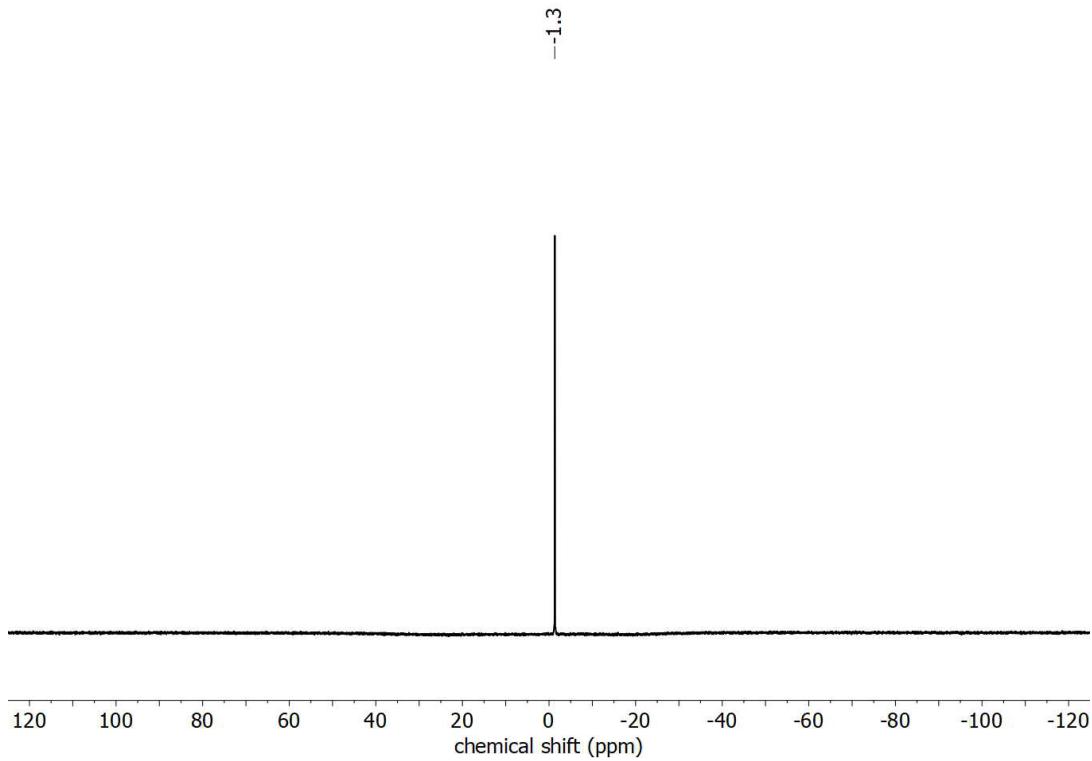
**Figure S12:** $^{11}$B-NMR of **2b** in DCM-$d_2$.

S6
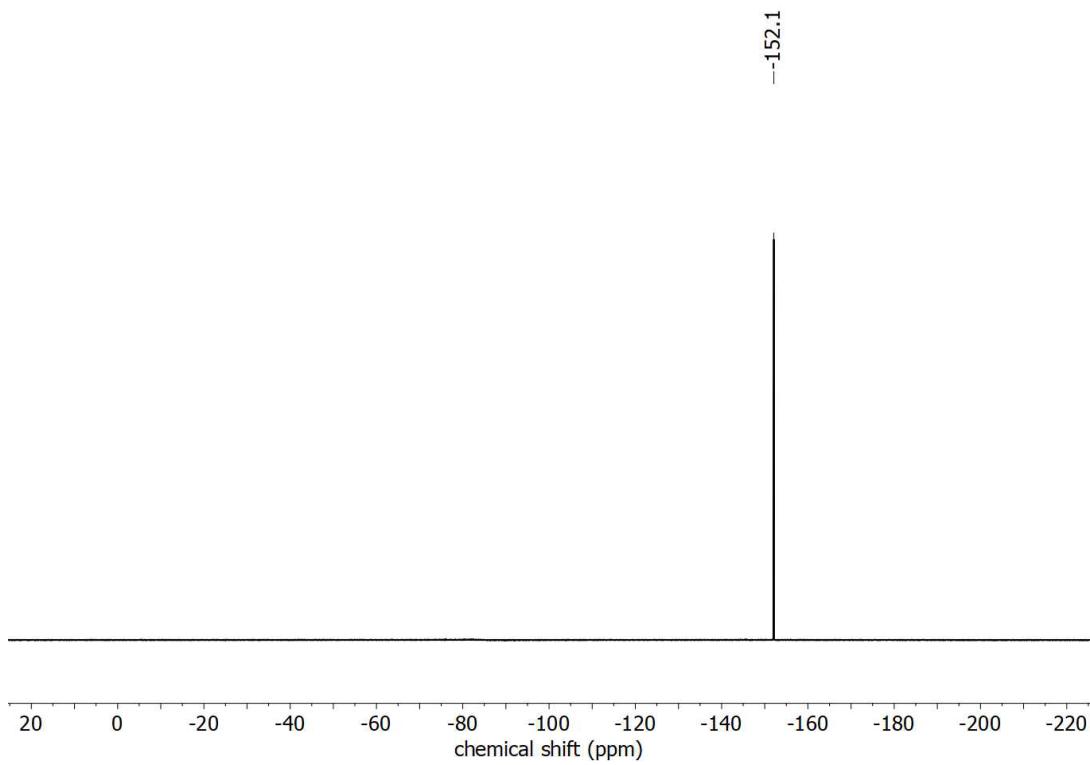
**Figure S13:** $^{19}$F-NMR of **2b** in DCM-$d_2$.
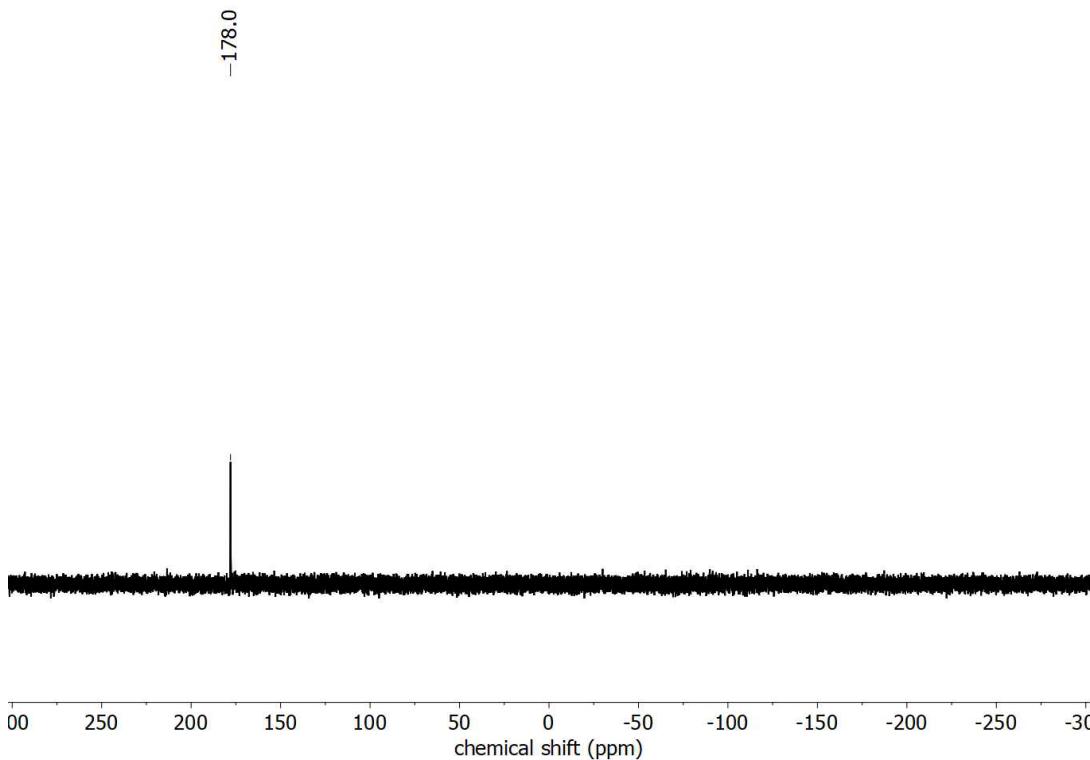


**Figure S14:** $^{31}$P{$^1$H}-NMR of **2b** in DCM-$d_2$.

S7

184
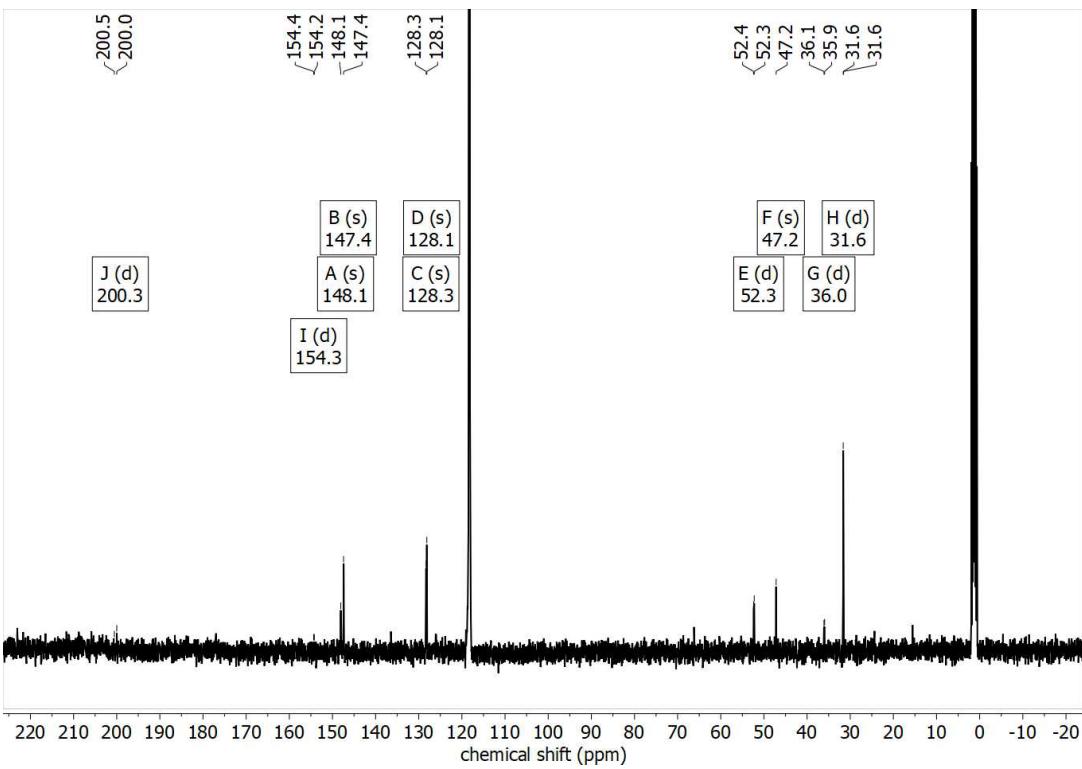
**Figure S15:** $^{13}C\{^1H\}$-NMR of **2c** in MeCN-$d_3$.
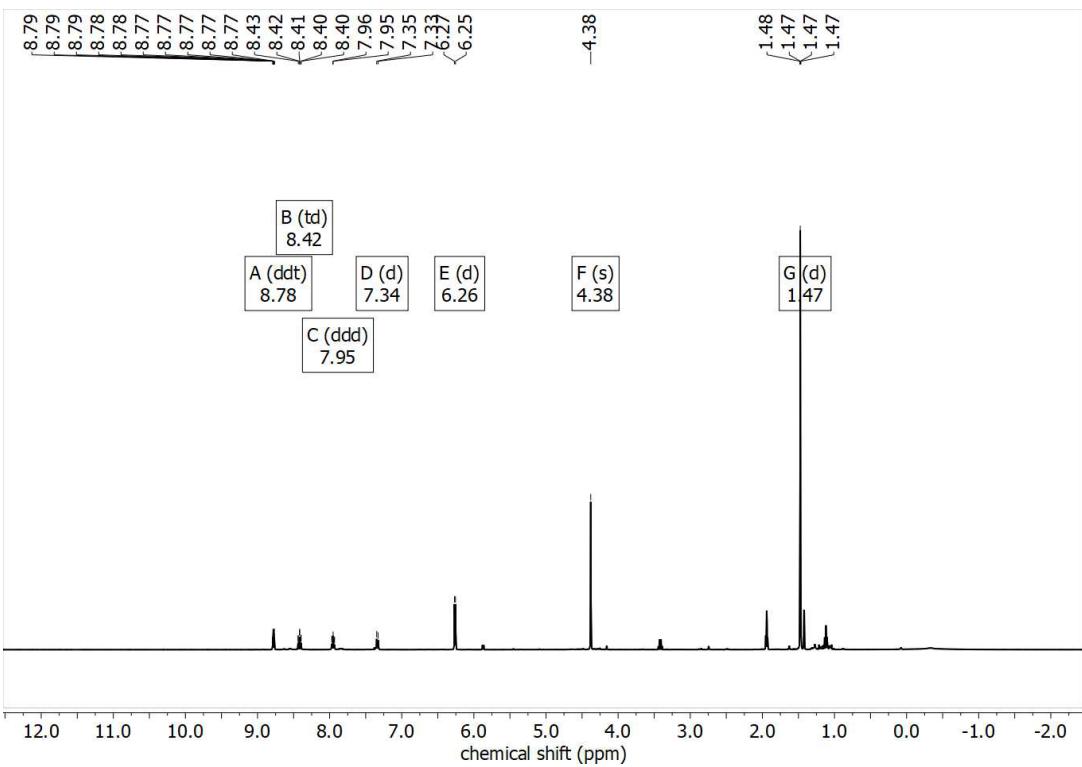


**Figure S16:** $^1H$-NMR of **2c** in MeCN-$d_3$.
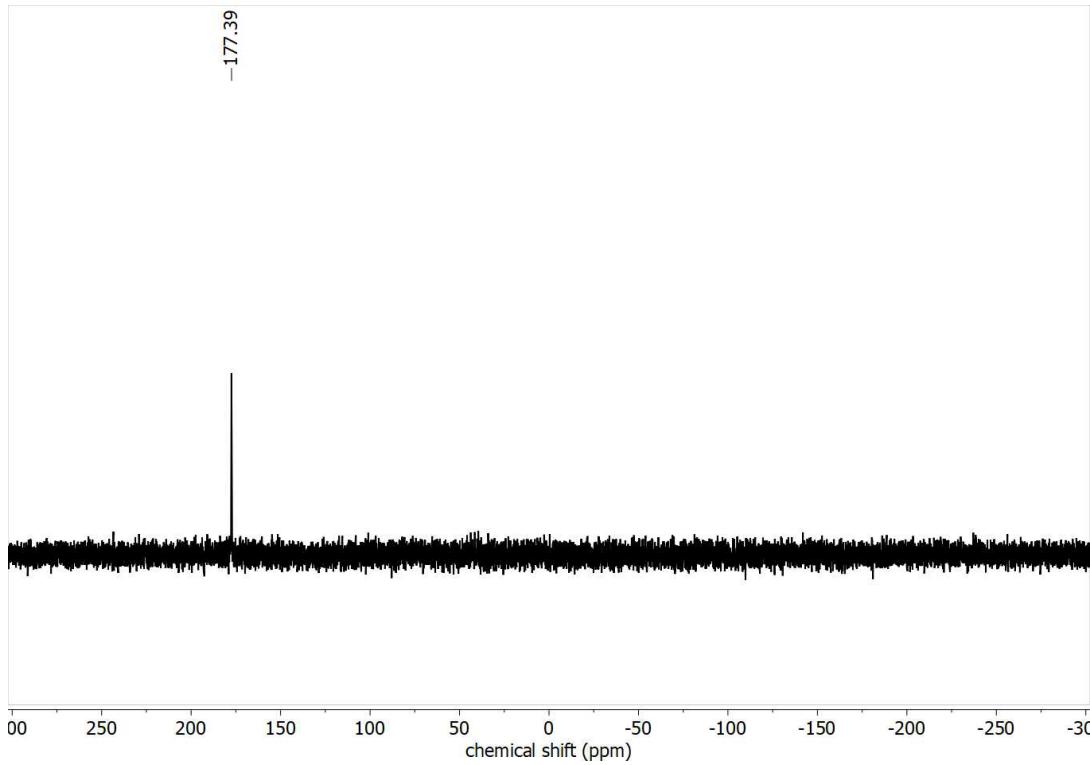
**Figure S17:** $^{31}$P{$^1$H}-NMR of **2c** in MeCN-$d_3$.
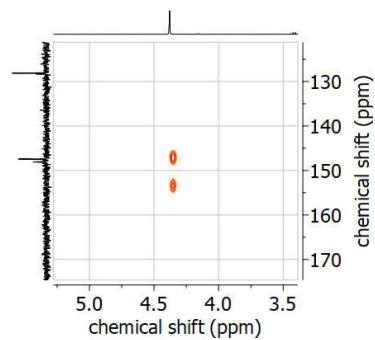


**Figure S18:** $^1$H-$^{13}$C-HMBC-NMR of **2c** in MeCN-$d_3$.

S9
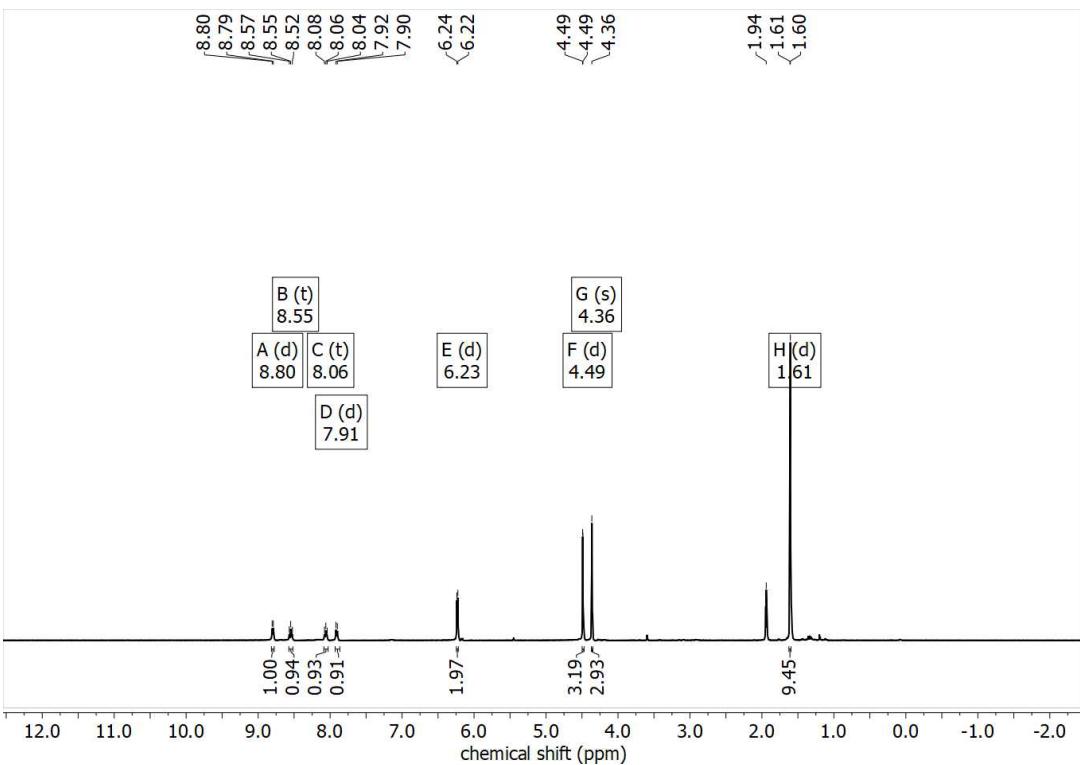
**Figure S19:** $^1$H-NMR of **3a'** in MeCN-$d_3$.
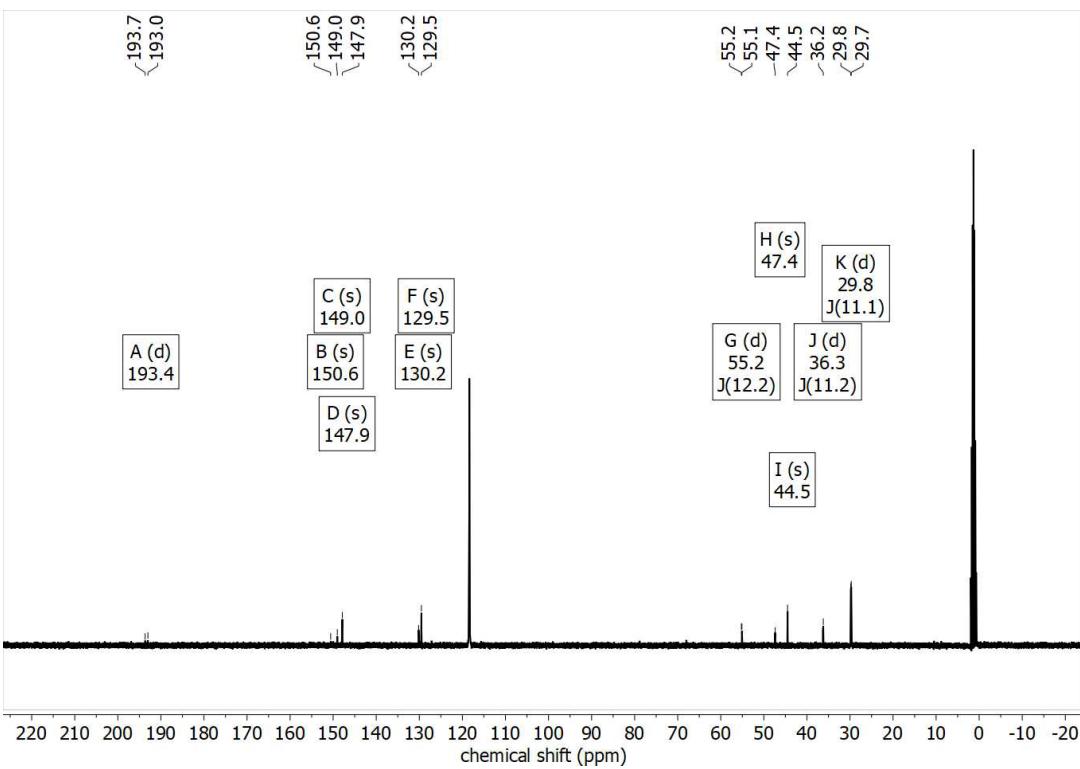


**Figure S20:** $^{13}$C{$^1$H}-NMR of **3a'** in MeCN-$d_3$.
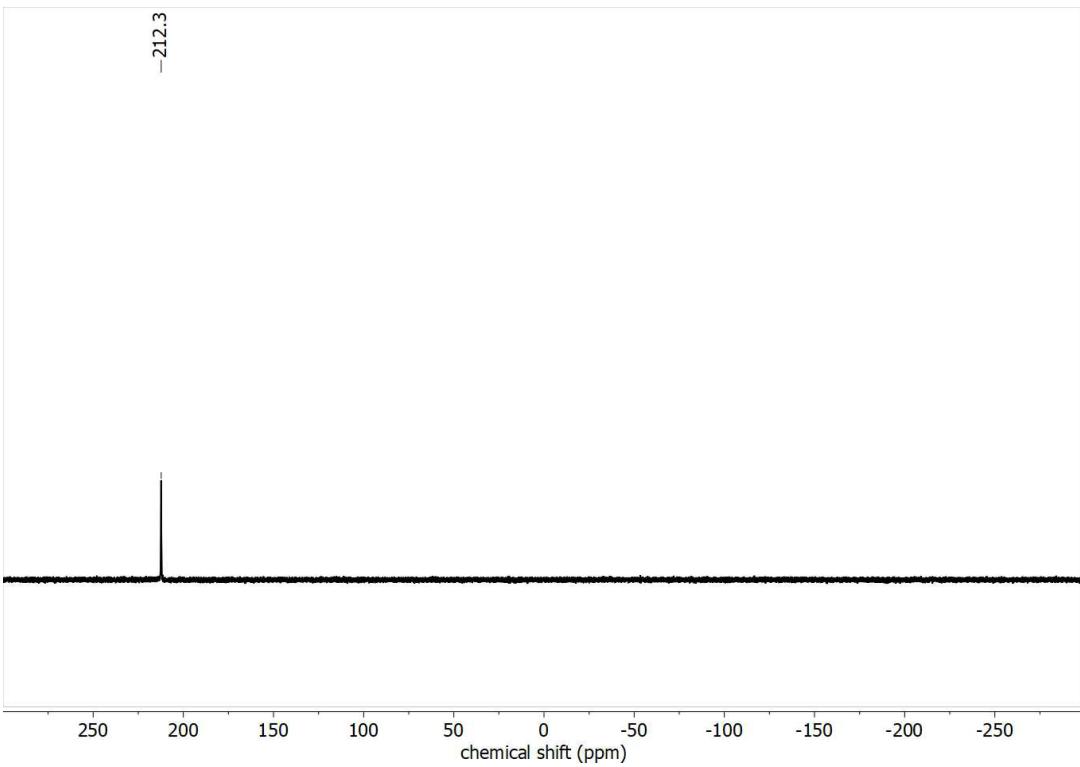
**Figure S21:** $^{31}P\{^1H\}$-NMR of **3a'** in MeCN-$d_3$.
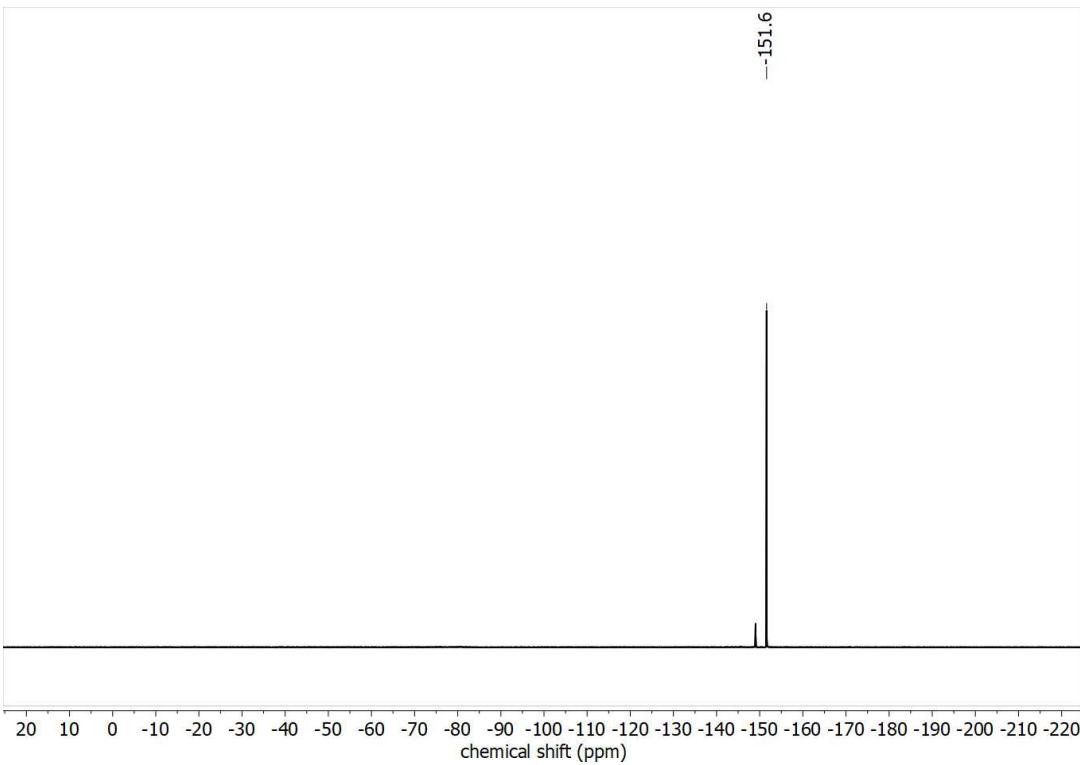


**Figure S22:** $^{19}F$-NMR of **3a'** in MeCN-$d_3$.
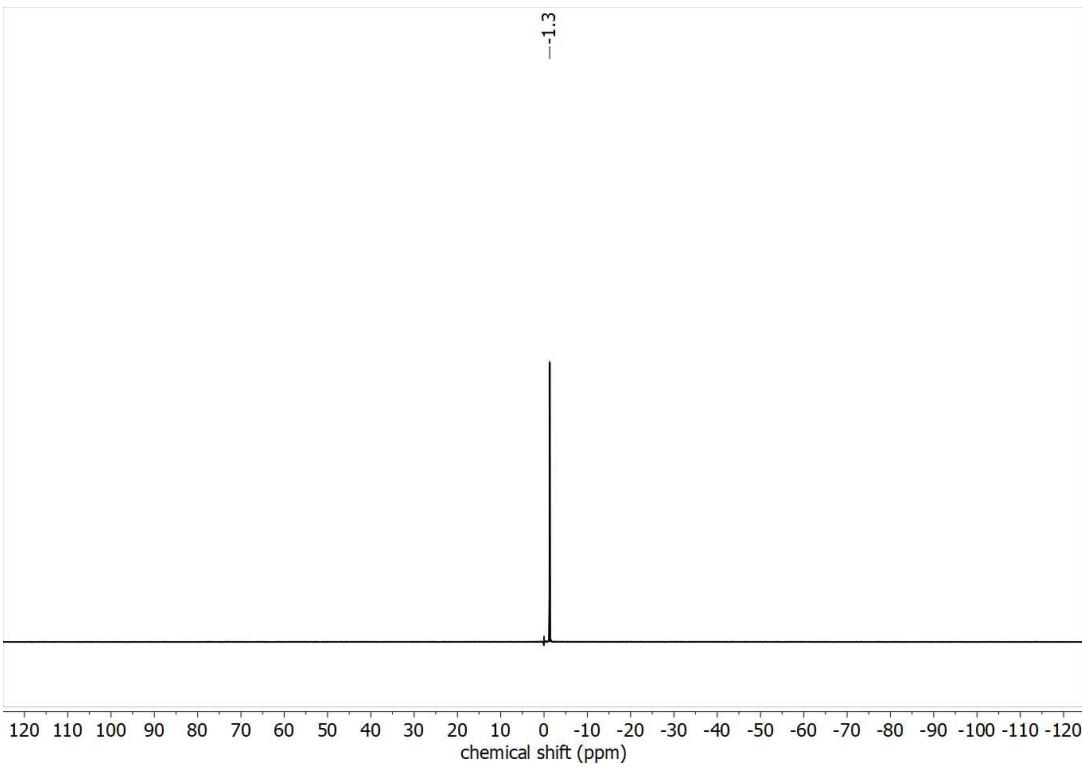
**Figure S23:** $^{11}$B-NMR of **3a'** in MeCN-$d_3$.
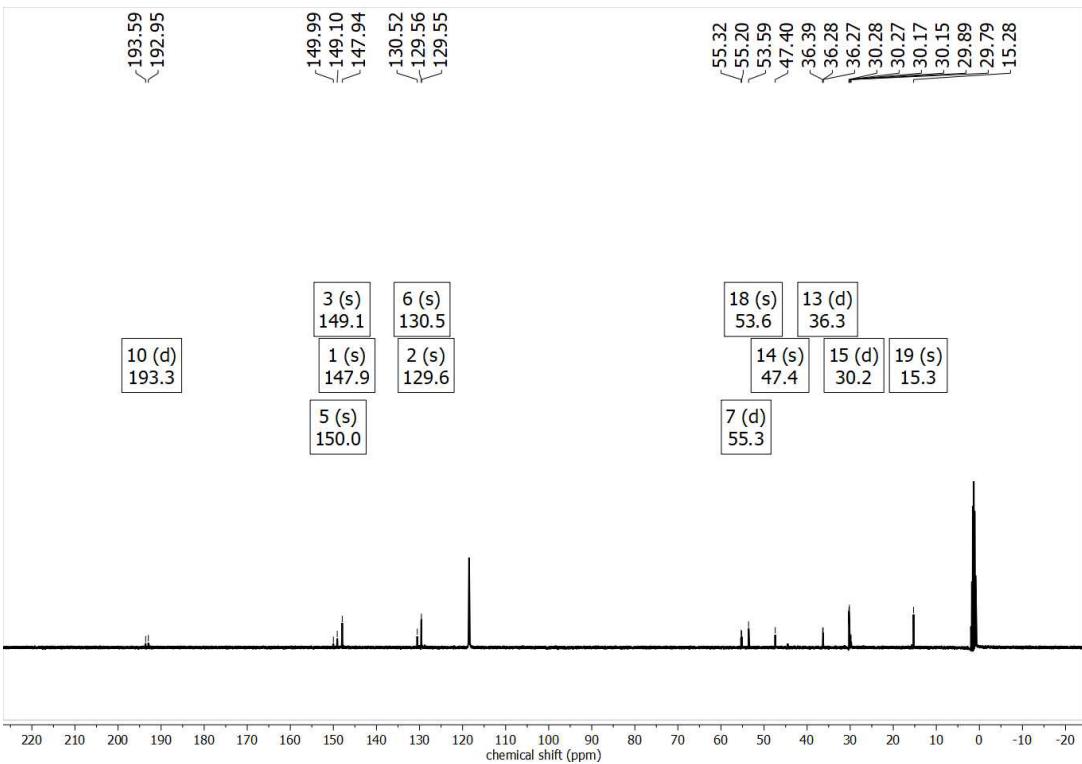


**Figure S24:** $^{13}$C{$^1$H}-NMR of **3a''** in MeCN-$d_3$.
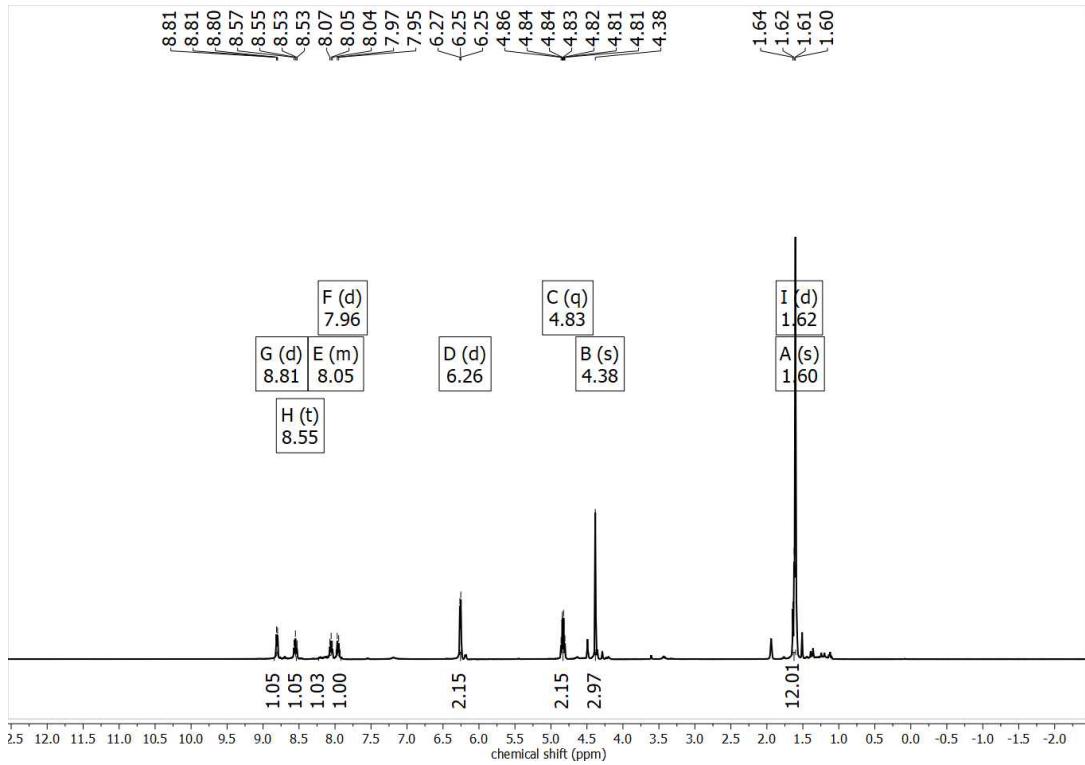
**Figure S25:** $^1$H-NMR of **3a''** in MeCN-$d_3$.



**Figure S26:** $^{31}$P{$^1$H}-NMR of **3a''** in MeCN-$d_3$
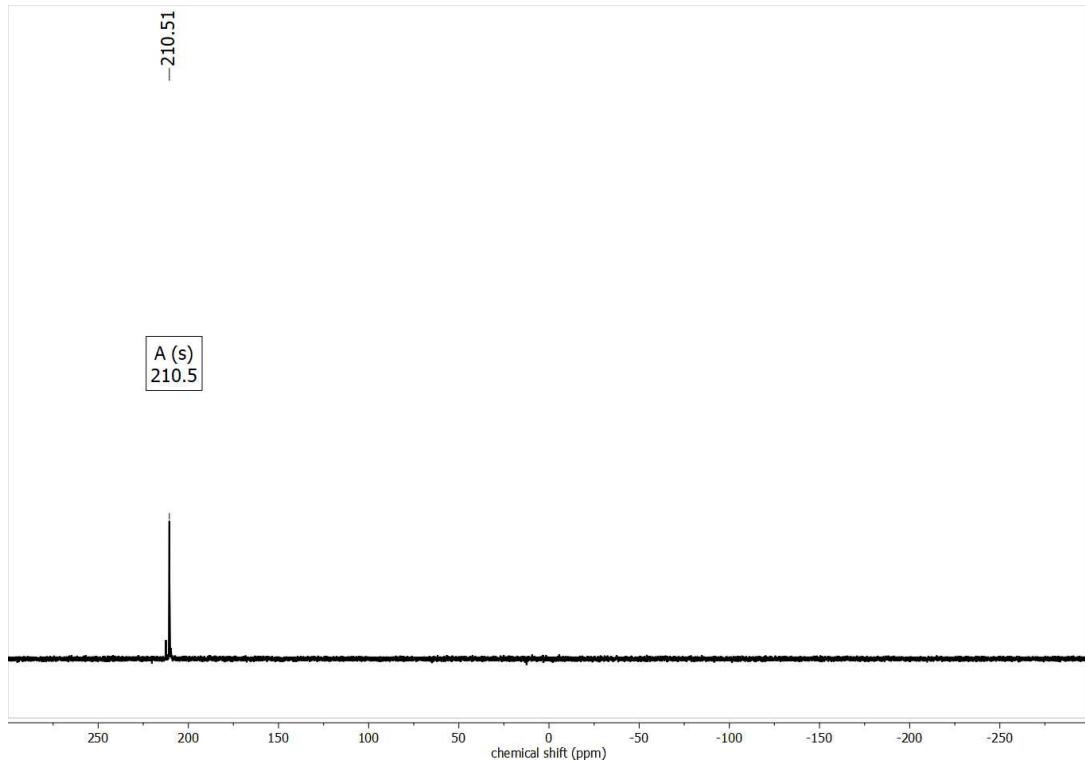
**Figure S27:** $^{19}$F-NMR of **3a''** in MeCN-*d$_3$*.
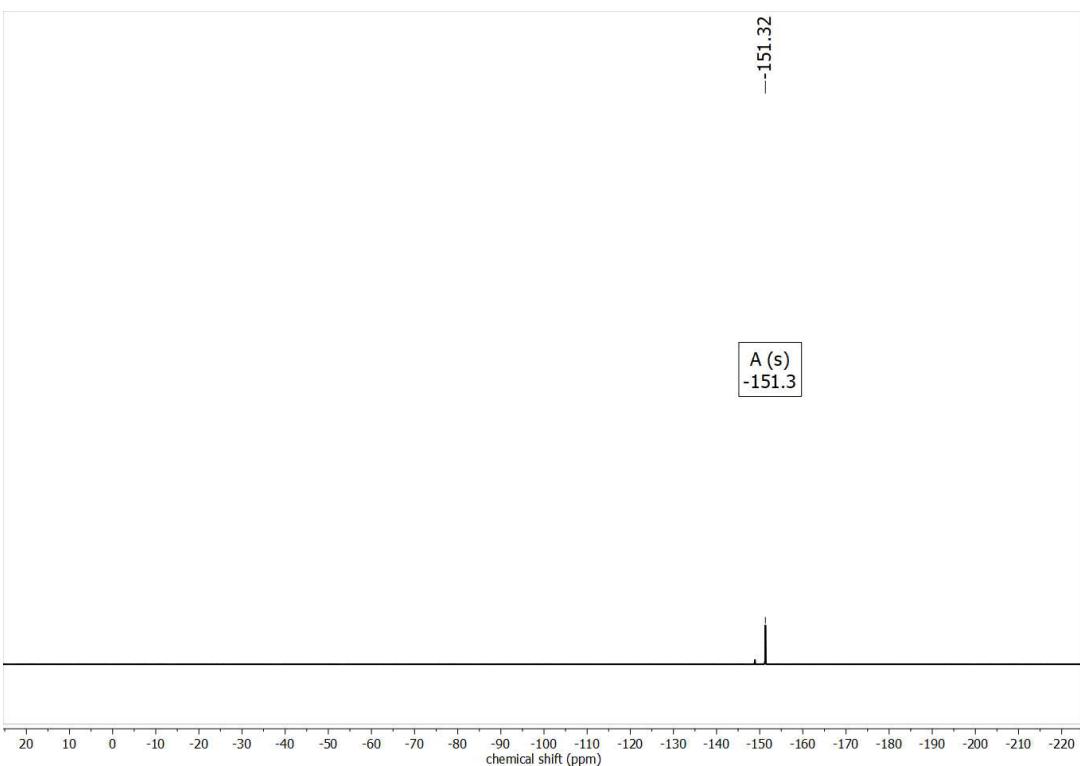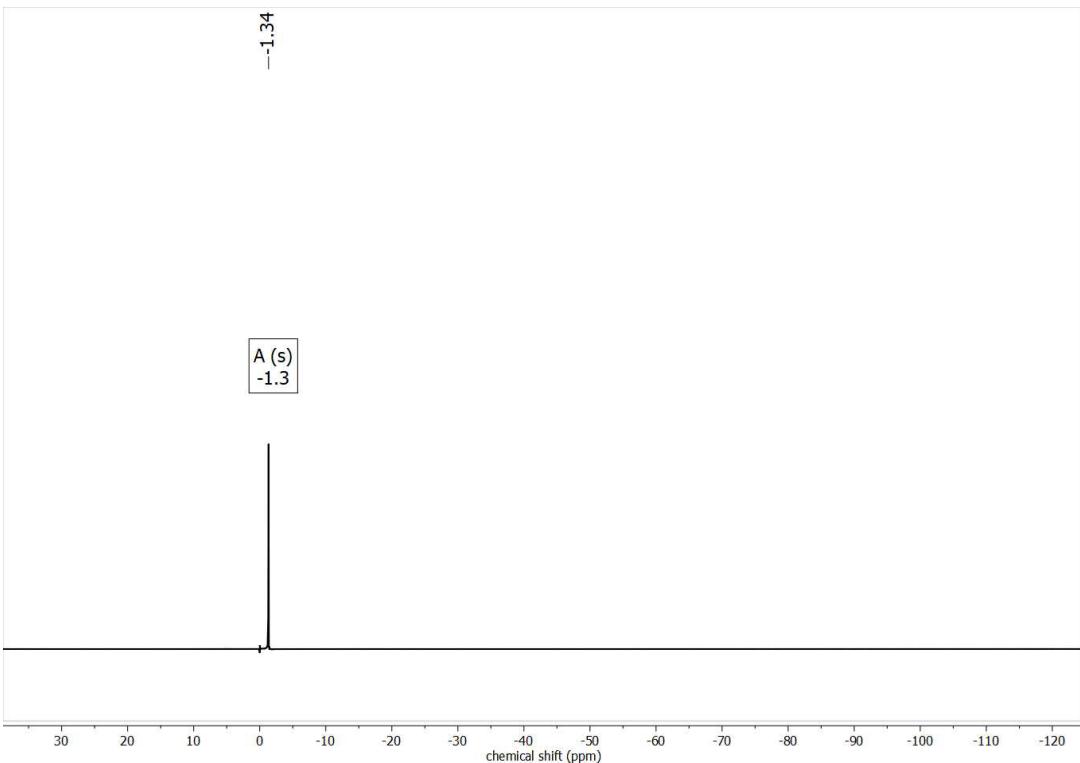


**Figure S28:** $^{11}$B-NMR of **3a''** in MeCN-*d$_3$*.

8.88
8.88
8.86
8.56
8.55
8.54
8.52
8.12
8.12
8.11
8.10
8.08
7.94
7.94
7.92
6.27
6.27
6.26
4.73
4.72
4.71
4.71
4.70
4.68
4.48
1.66
1.64
1.64
1.62
1.61
1.61
1.60

G (t)
8.54

D (q)
4.70

B (t)
1.64

F (d)   H (m)
8.87    8.10

E (s)
6.26

C (s)
4.48

A (d)
1.60

I (d)
7.93

1.00
1.04
1.02
0.83

2.19

2.21
2.94

2.92
9.11

12.0  11.0  10.0  9.0  8.0  7.0  6.0  5.0  4.0  3.0  2.0  1.0  0.0  -1.0  -2.0
chemical shift (ppm)
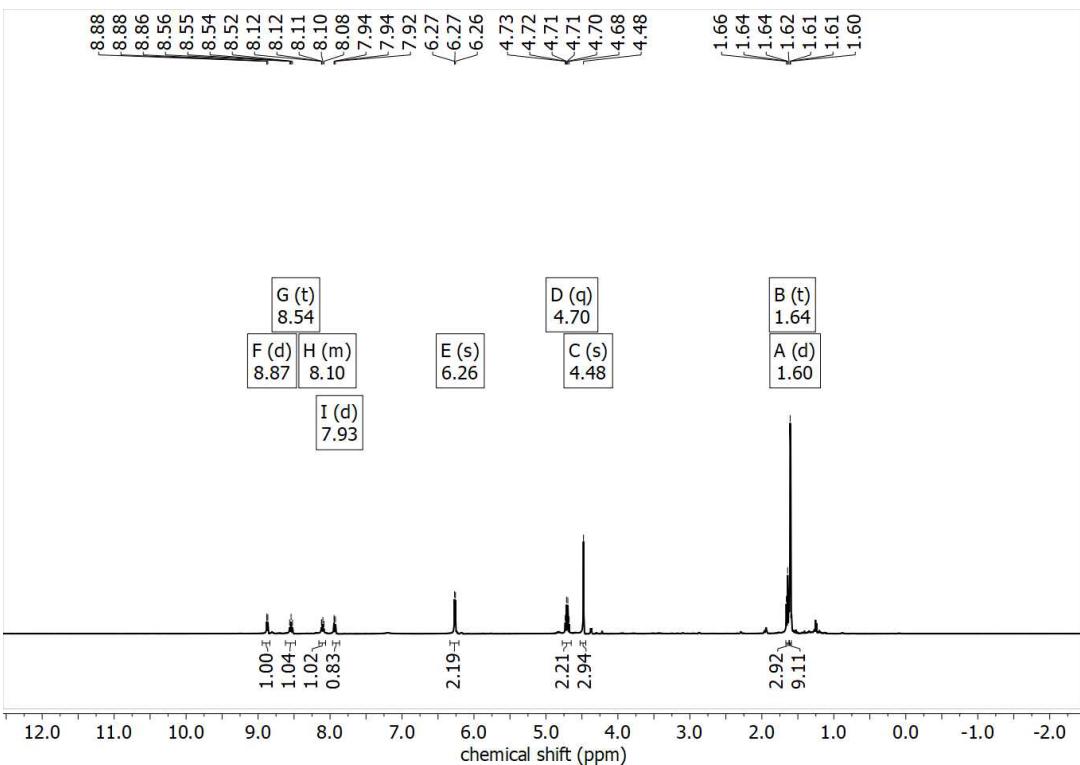
**Figure S29:** $^1$H-NMR of **3b'** in MeCN-$d_3$.

193.6
193.0
149.3
147.8
147.5
131.0
130.0
55.5
54.9
54.8
44.5
36.3
36.2
29.9
29.8
16.0

A (s)     6 (s)
147.8    131.0

7 (d)     13 (d)
54.8      36.3

10 (d)
193.3

3 (s)     2 (s)
147.5    130.0

18 (s)   15 (d)   19 (s)
44.5     29.8     16.0

5 (s)
149.3

14 (s)
55.5

220 210 200 190 180 170 160 150 140 130 120 110 100 90 80 70 60 50 40 30 20 10 0 -10 -20
chemical shift (ppm)
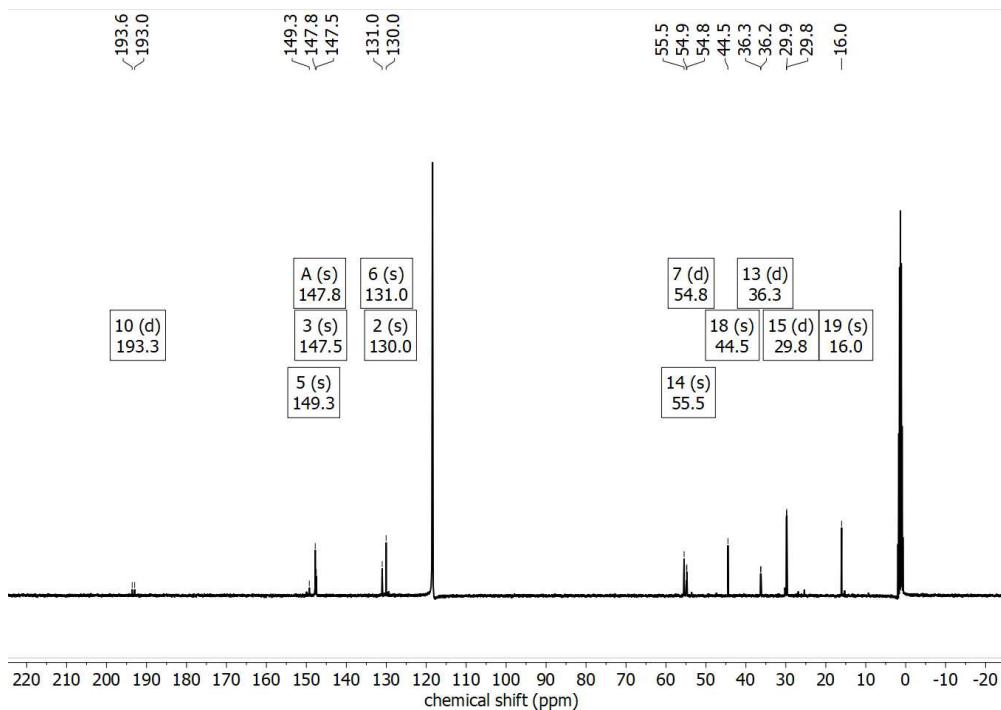
**Figure S30:** $^{13}$C{$^1$H}-NMR of **3b'** in MeCN-$d_3$.
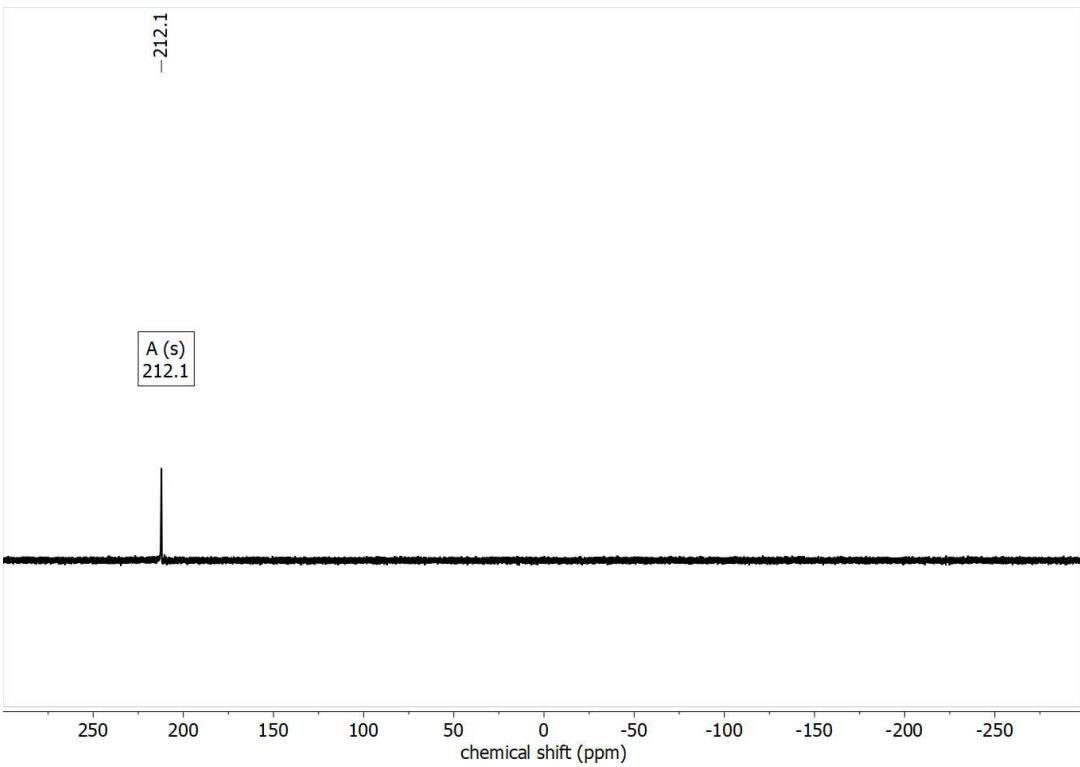
**Figure S31:** $^{31}$P{$^{1}$H}-NMR of **3b'** in MeCN-$d_3$.
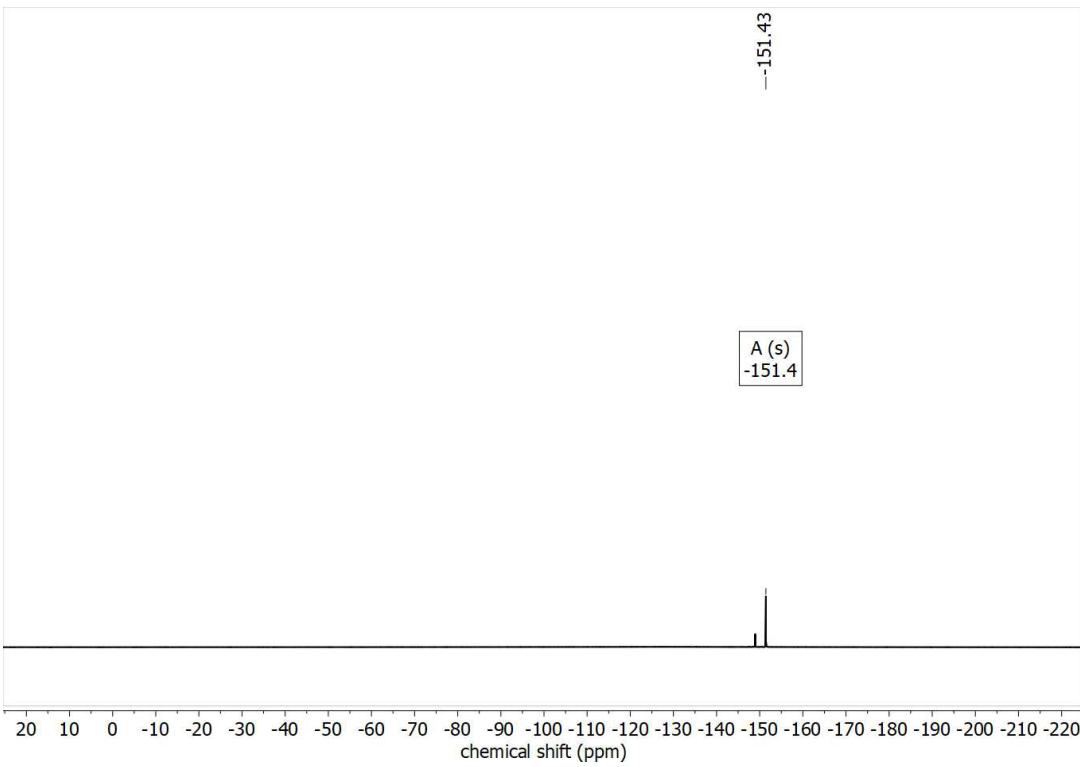


**Figure S32:** $^{19}$F-NMR of **3b'** in MeCN-$d_3$.

193
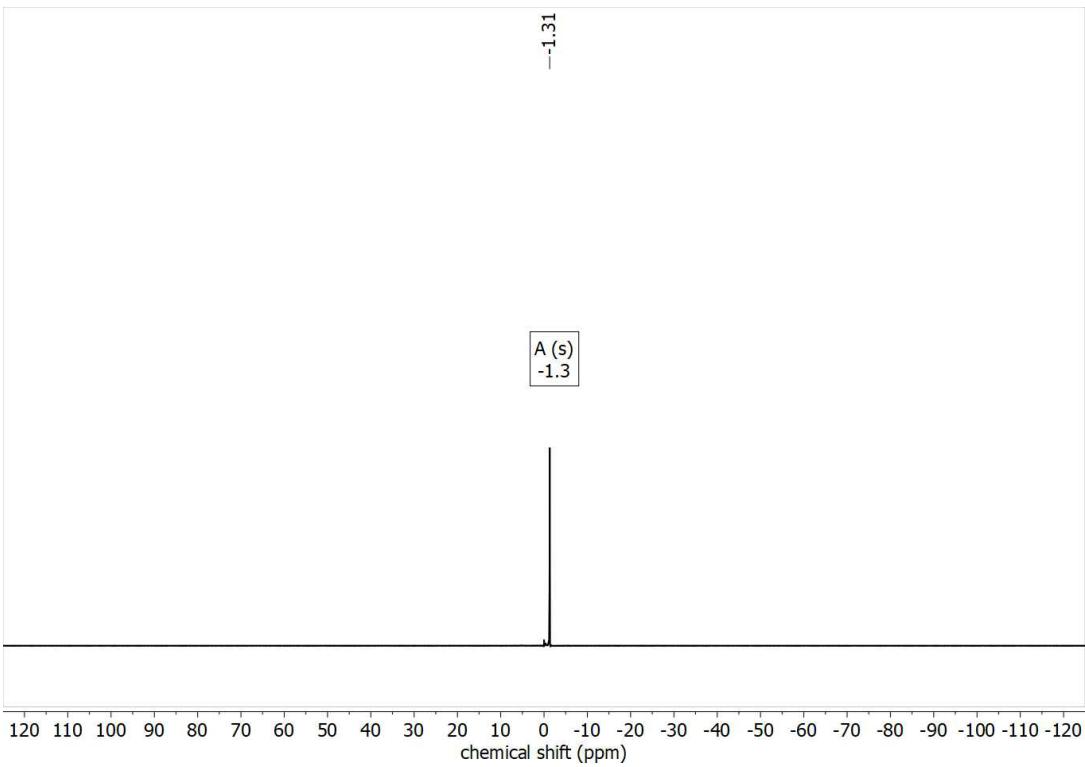
**Figure S33:** ¹¹B-NMR of **3b'** in MeCN-*d₃*.
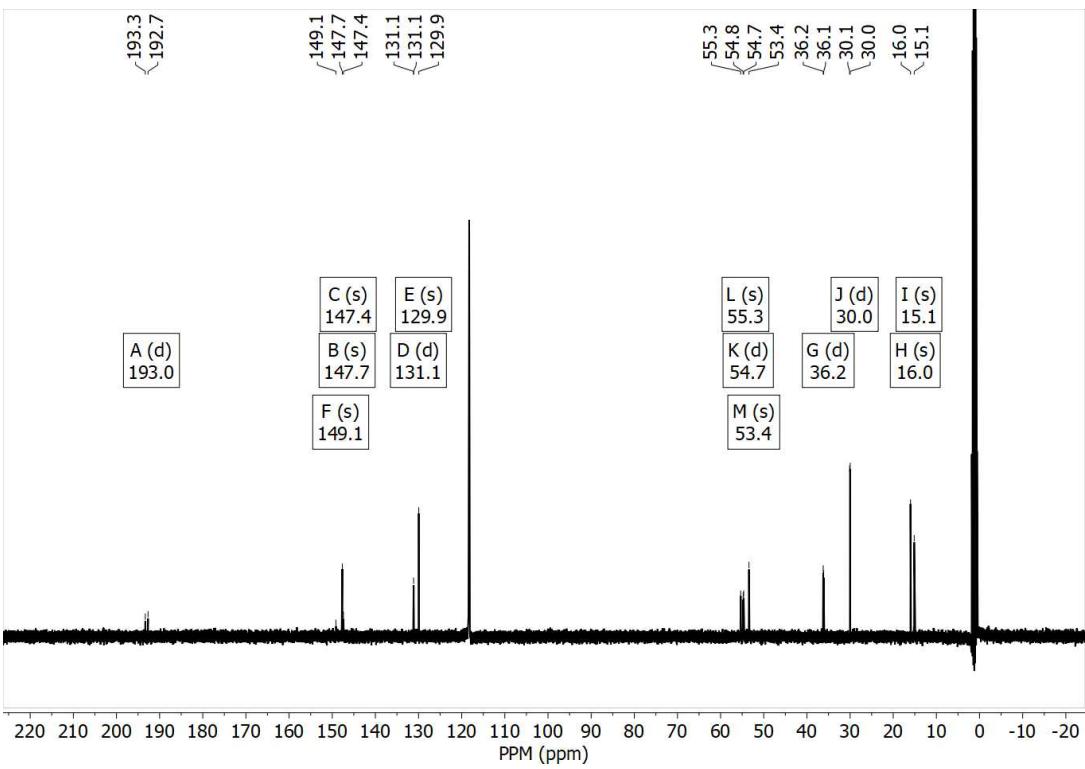


**Figure S34:** ¹³C{¹H}-NMR of **3b''** in MeCN-*d₃*.
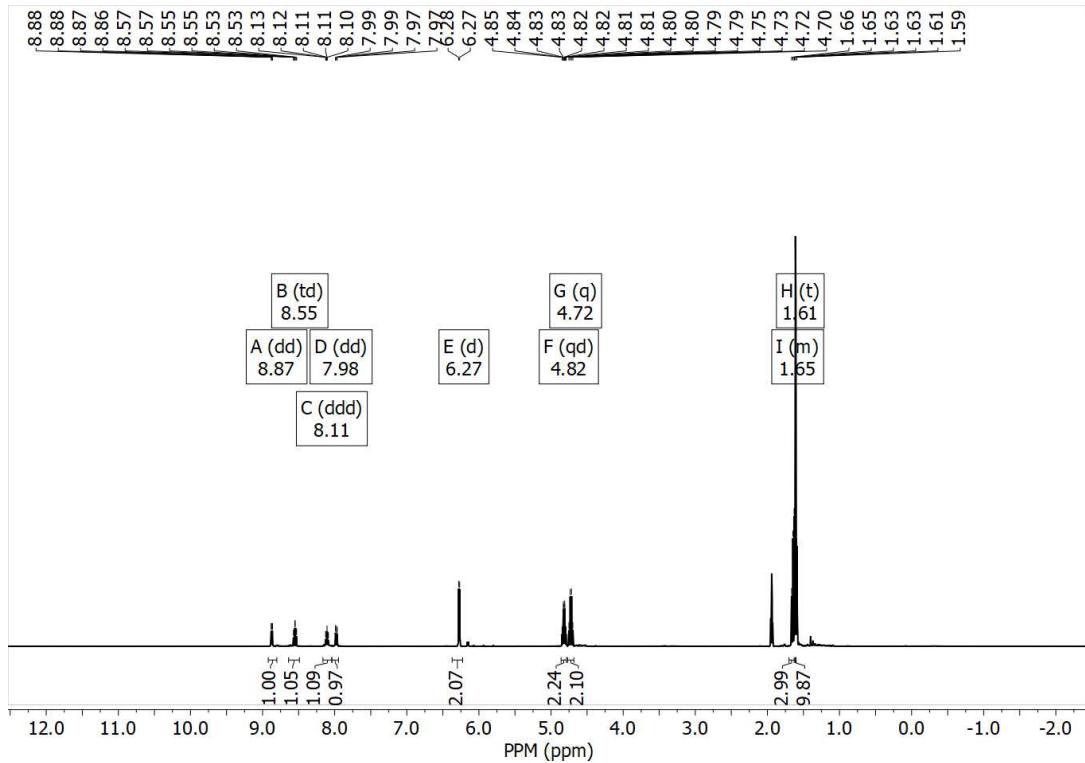
**Figure S35:** $^1$H-NMR of **3b''** in MeCN-$d_3$.
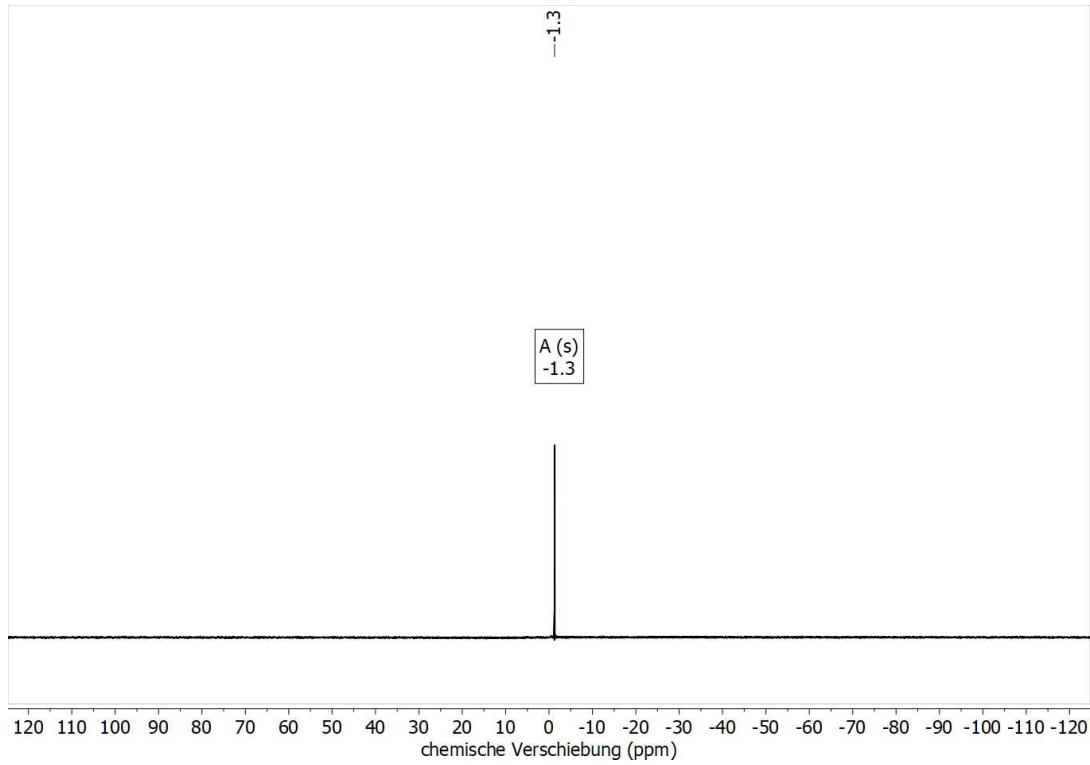


**Figure S36:** $^{11}$B-NMR of **3b''** in MeCN-$d_3$.
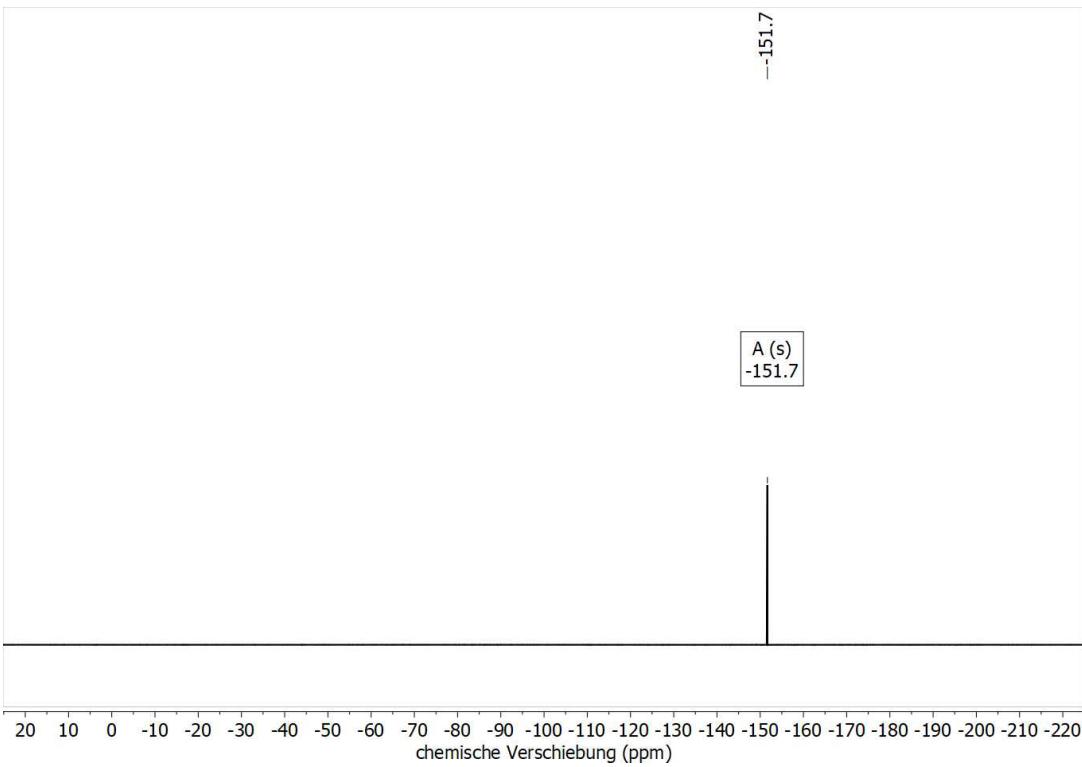
**Figure S37:** $^{19}$F-NMR of **3b''** in MeCN-$d_3$.
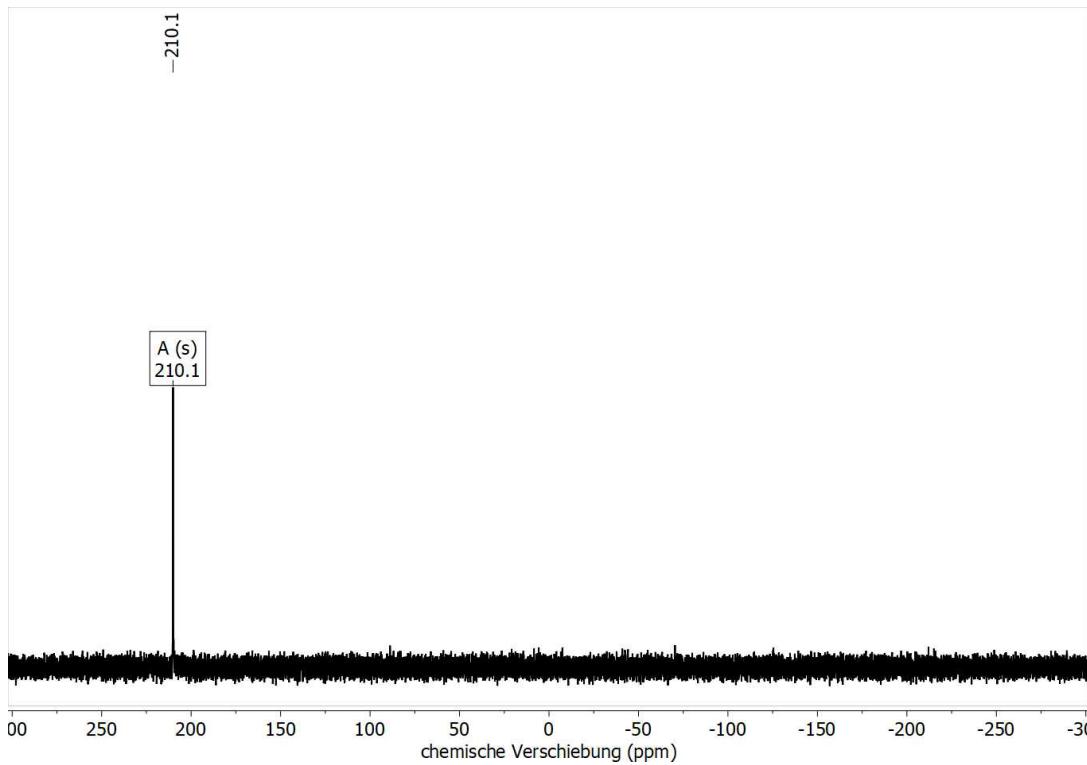


**Figure S38:** $^{31}$P{$^1$H}-NMR of **3b''** in MeCN-$d_3$.
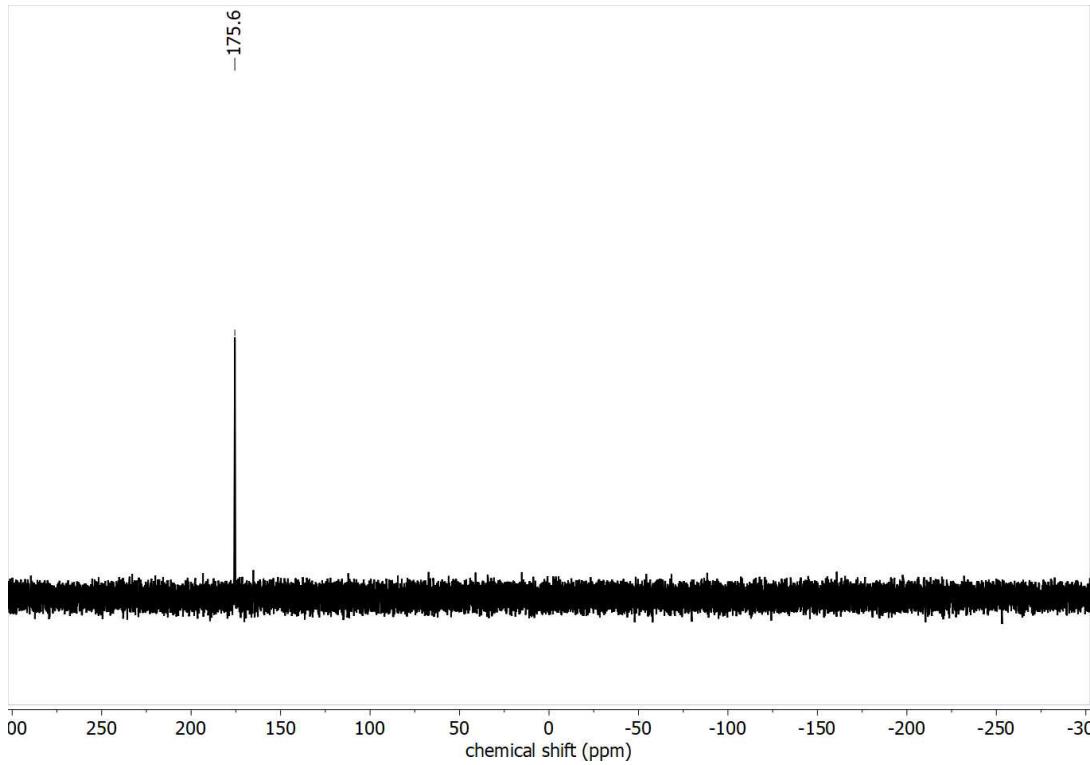
**Figure S39:** $^{31}P\{^{1}H\}$-NMR of **4a$_{\mu2}$** in MeCN-$d_3$.
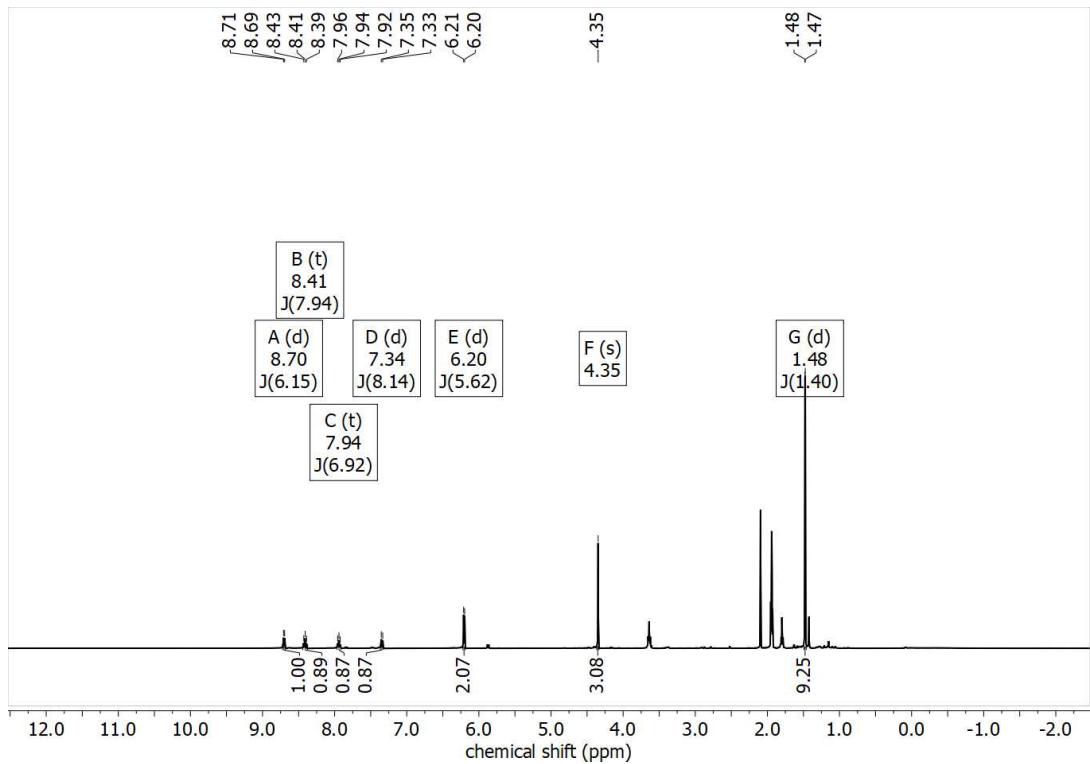


**Figure S40:** $^{1}H$-NMR of **4a$_{\mu2}$** in MeCN-$d_3$.
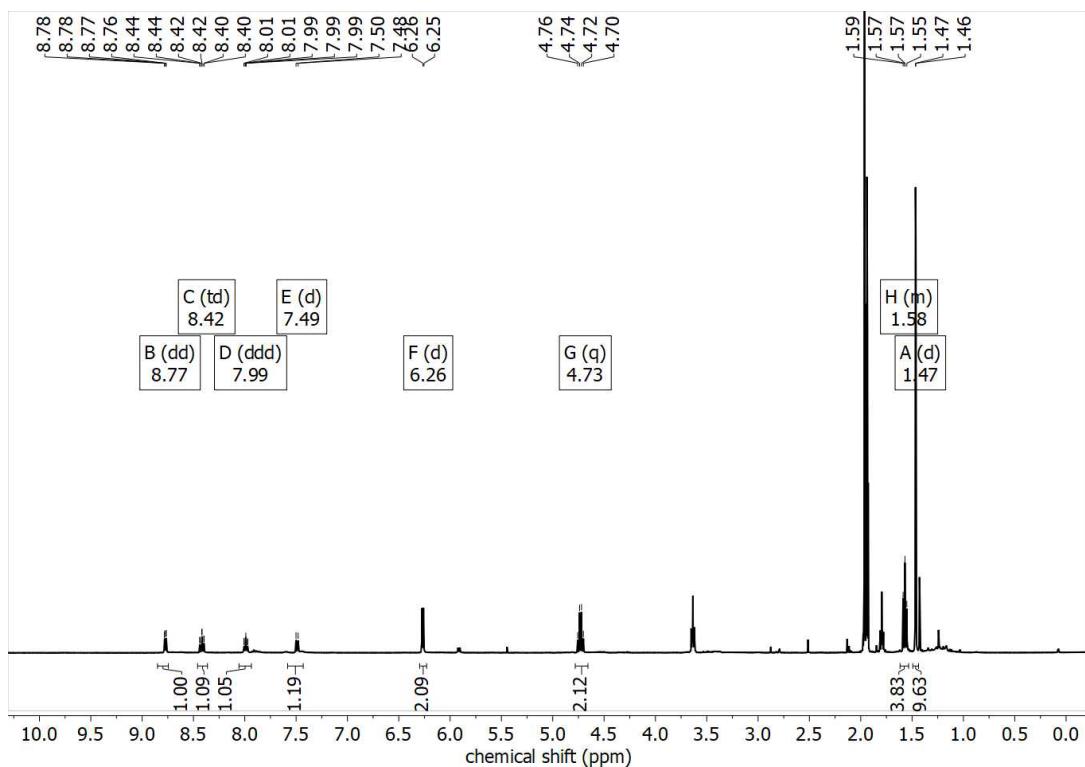
**Figure S41:** $^1$H-NMR of **4b$_{η1}$ / 4b$_{μ2}$** in MeCN-$d_3$.



**Figure S42:** $^{13}$C{$^1$H}-NMR of **4b$_{η1}$ / 4b$_{μ2}$** in MeCN-$d_3$.

**Figure S43:** $^{31}P\{^1H\}$-NMR of **4b**$_{\eta1}$ / **4b**$_{\mu2}$ in MeCN-$d_3$.
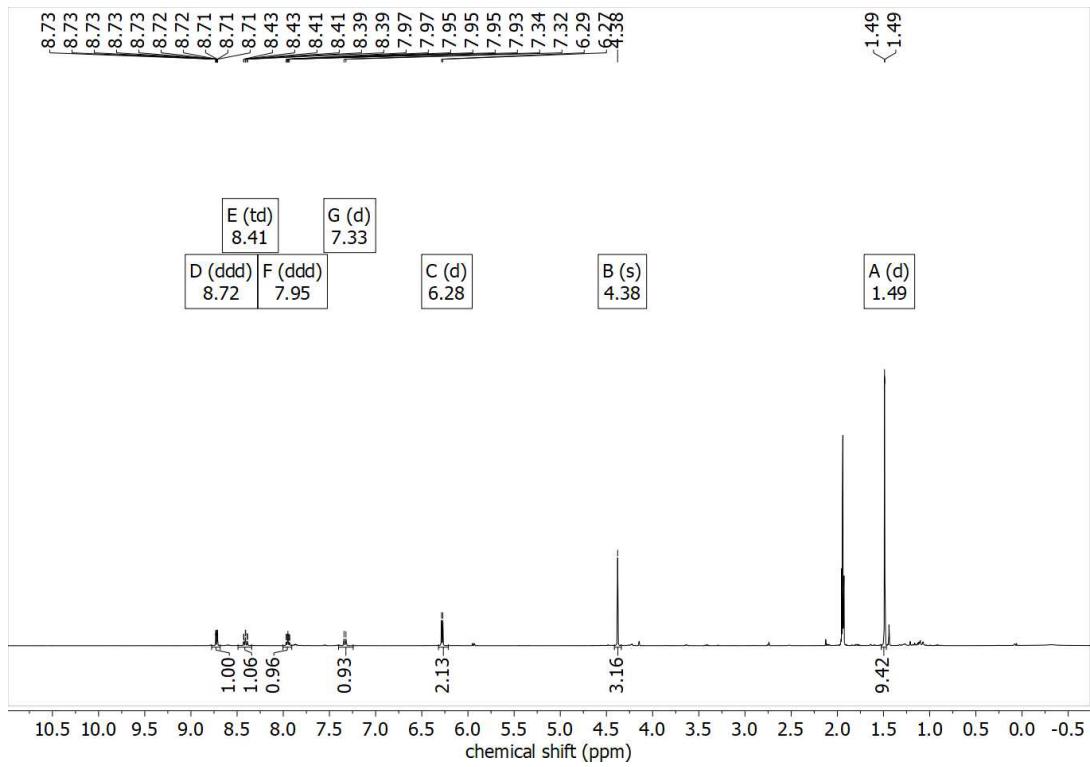


**Figure S44:** $^1H$-NMR of **4c**$_{\eta1}$ in MeCN-$d_3$.

**Figure S45:** $^{31}P\{^1H\}$-NMR of **4c$_{η1}$** in MeCN-$d_3$.
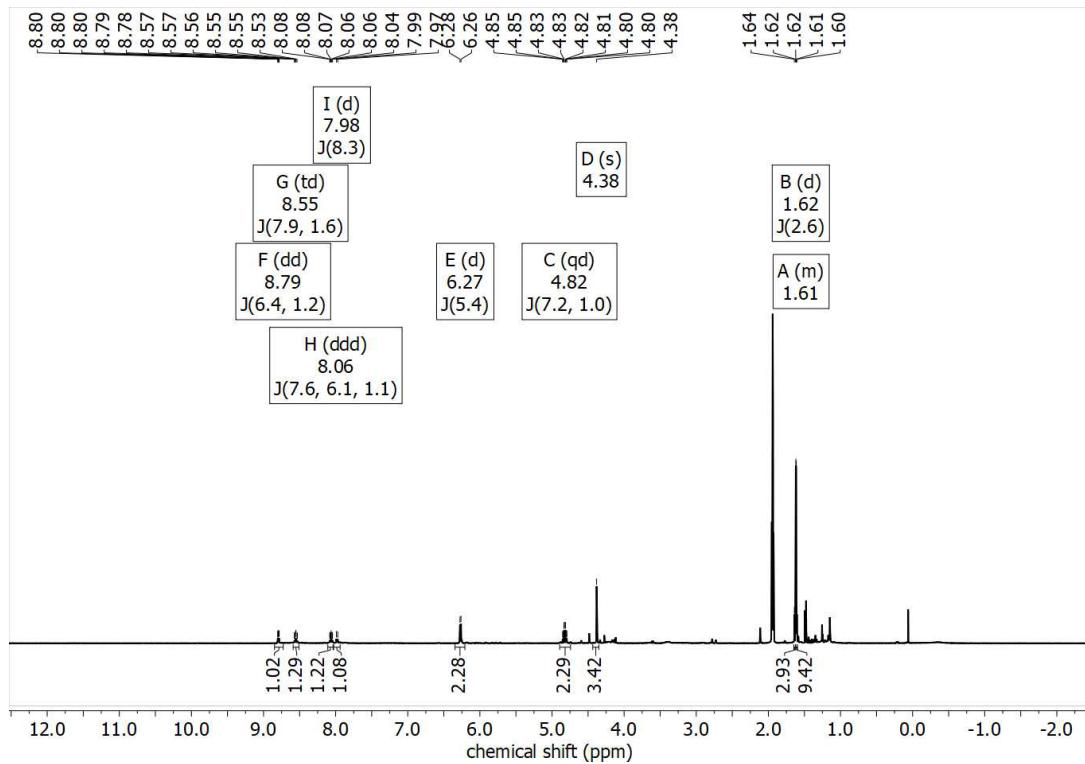


**Figure S46:** $^1H$-NMR of **6** in MeCN-$d_3$.
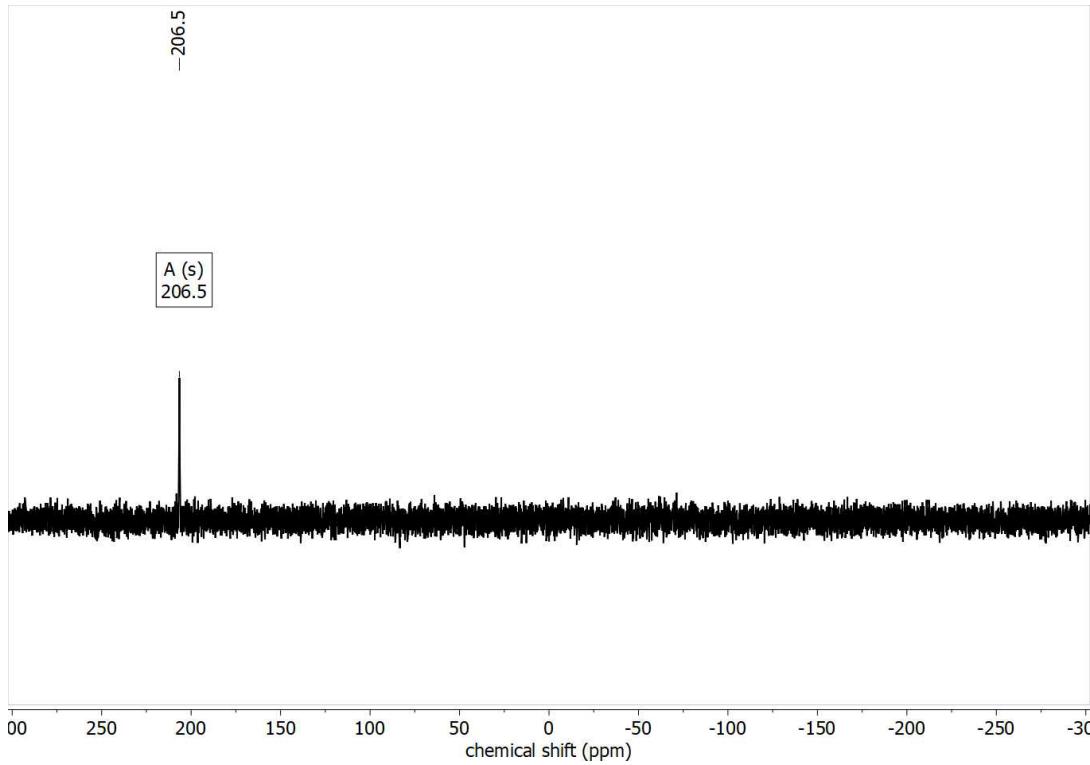
**Figure S47:** $^{31}P\{^1H\}$-NMR of **6** in MeCN-$d_3$.
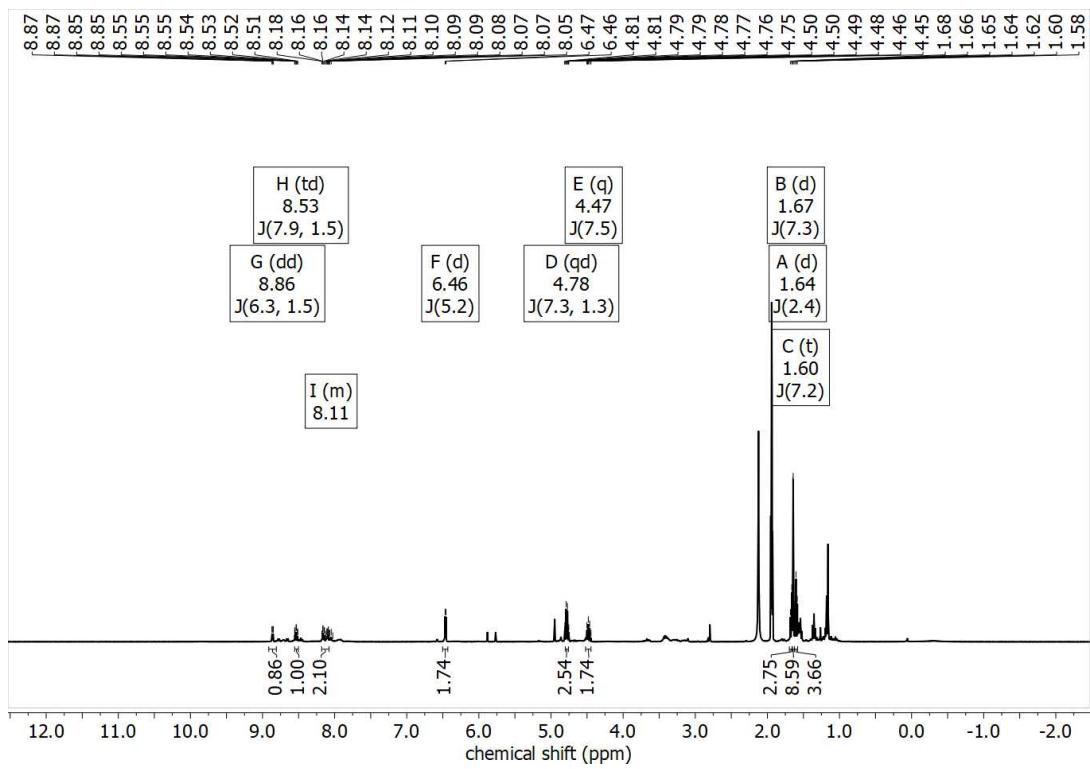


**Figure S48:** $^1$H-NMR of **7$_{η1}$** in MeCN-$d_3$.

**Figure S49:** $^{31}P\{^1H\}$-NMR of **7$_{\eta1}$** in MeCN-$d_3$.
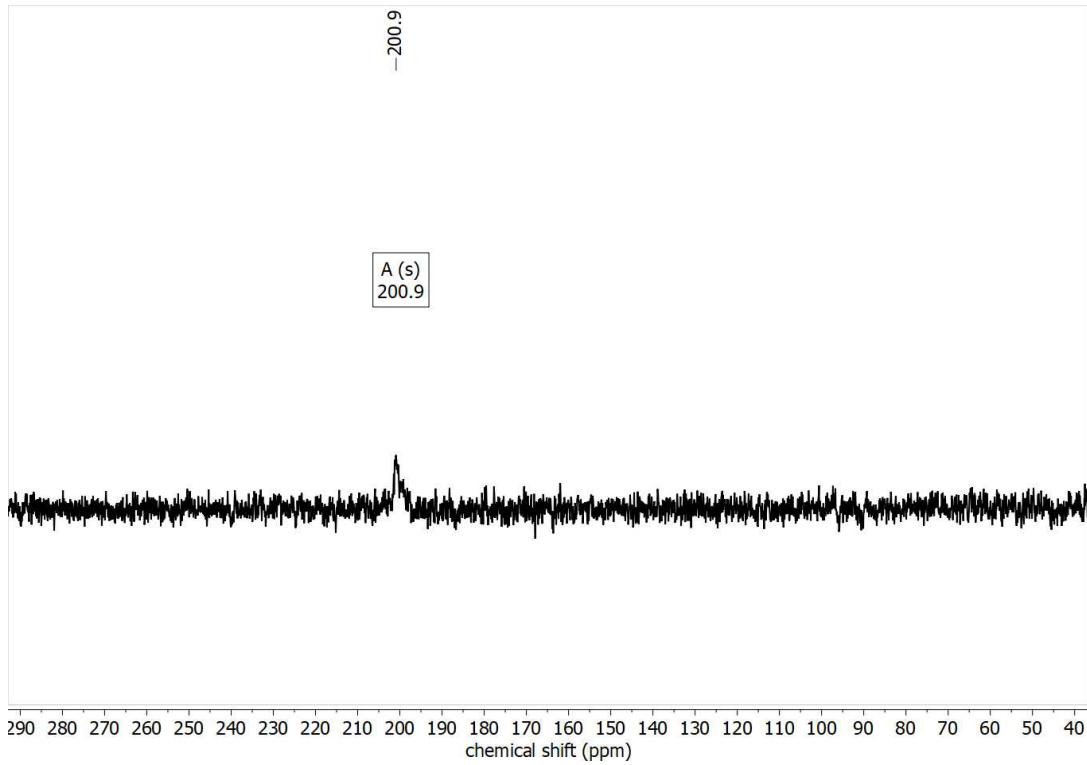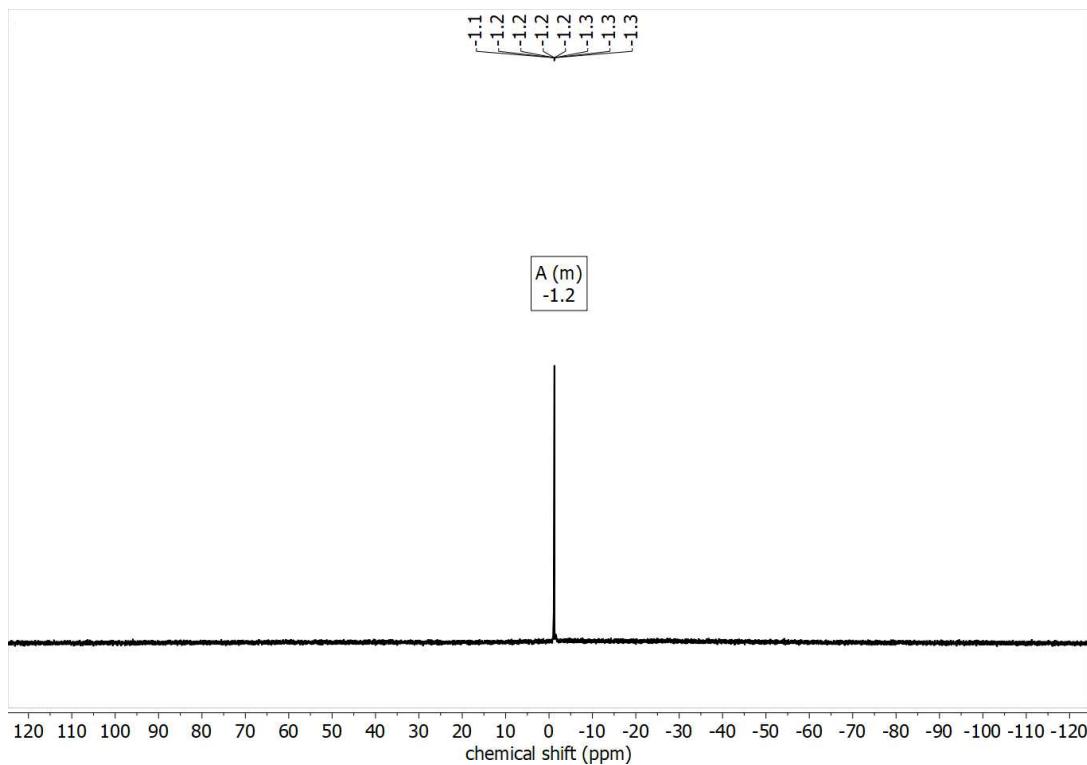


**Figure S50:** $^{11}B$-NMR of **7$_{\eta1}$** in MeCN-$d_3$.
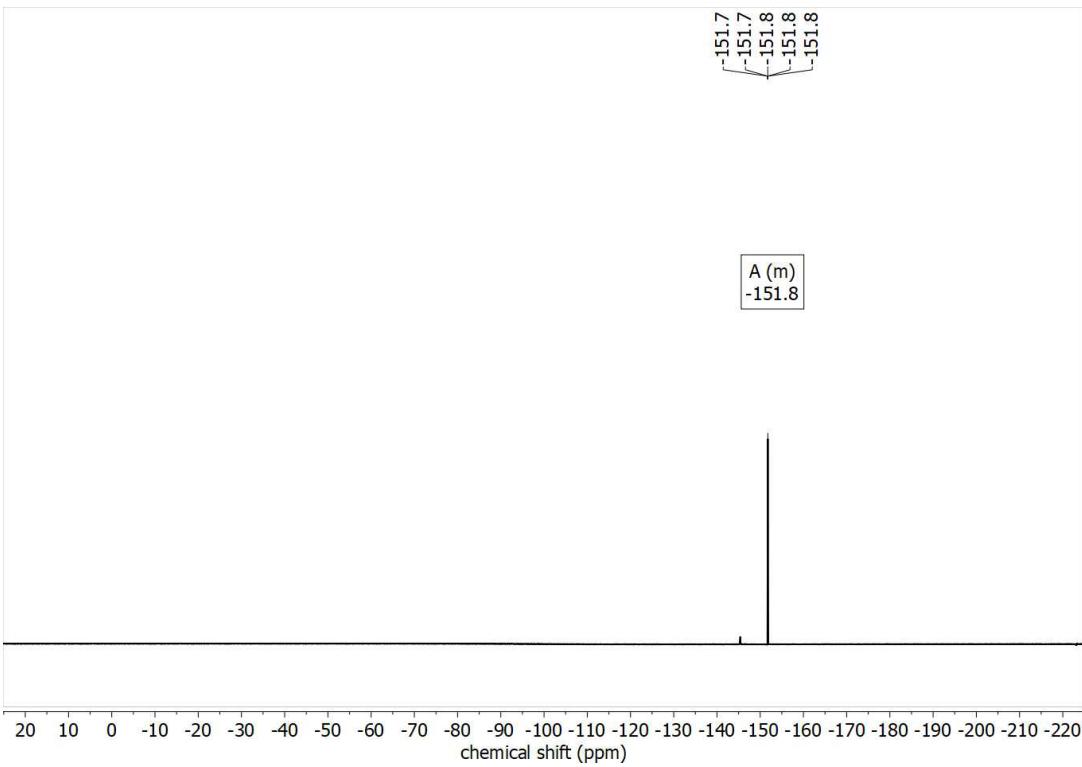
**Figure S51:** $^{19}$F-NMR of $\mathbf{7_{\eta1}}$ in MeCN-$d_3$.

## 2. Crystallographic Details

Crystals of **2b** suitable for X-ray diffraction were obtained diffusion of *n*-hexane into a saturated THF solution of **2b**. Crystals of **3b''** were obtained by Vapor diffusion of DCM into a concentrated solution of **3b''** in MeCN. Crystals of **4a**$_{\mu 2}$ were obtained by cooling a saturated solution of **4a**$_{\mu 2}$ in acetonitrile to $T = -21$ °C. **4b**$_{\eta 1}$ and **4b**$_{\mu 2}$ were obtained directly from the reaction mixture. Crystals of **4c**$_{\eta 1}$ were obtained by cooling a saturated solution of **4c**$_{\eta 1}$ in THF/acetonitrile (10:1) to $T = -21$ °C. Crystals of **5**$_{\eta 1}$ were obtained from a mixture of THF/acetonitrile (5:1). Crystals of **6** cooling a saturated solution of **6** in acetonitrile to $T = -21$ °C. Crystals of **7**$_{\eta 1}$ were obtained by cooling a saturated solution of **7**$_{\eta 1}$ in acetonitrile to $T = -21$ °C.

The intensities for the X-ray determinations were collected on a D8 Venture, Bruker Photon CMOS diffractometer with Mo/K$\alpha$ or Cu/K$\alpha$ radiation.[1] Semi-empirical or numerical absorption corrections were carried out by the SADABS or X-RED32 programs[2] Structure 535 solution and refinement were performed with the SHELX programs[3] included in OLEX2.[4] Hydrogen atoms were calculated for the idealized positions and treated with the 'riding model' option of SHELXL. Since some of the compounds crystallized together with disordered solvent molecules (partially close to special positions), the refinements of such structures were undertaken with the removal of the disordered solvent molecules using the solvent mask option of OLEX2. The representation of molecular structures was done using the program Mercury 3.0 (2022).[5] Deposition Numbers https://www.ccdc.cam.ac.uk/services/structures?id=doi:10.1002/chem.202400592 2331037 (for **2b**), 2331035 (for **3b''**), 2331040 (for **4a**$_{\mu 2}$), 2331042 (for **4b**$_{\mu 2}$), 2331036 (for **4b**$_{\eta 1}$), 2331038 (for **4c**$_{\eta 1}$), 2331034 (for **5**$_{\eta 1}$), 2331041 (for **6**), 2331039 (for **7**$_{\eta 1}$) contain the supplementary crystallographic data for this paper. These data are provided free of charge by the joint Cambridge Crystallographic Data Centre and Fachinformationszentrum Karlsruhe http://www.ccdc.cam.ac.uk/structures. Details of the X-ray structure determinations and refinements are provided in Table S1-S9.

**Table S1:** Crystal data and structure refinement for $C_{13}H_{20}BF_4N_4P$ (**2b**).

| | |
|---|---|
| Identification code | $C_{13}H_{20}BF_4N_4P$ |
| Empirical formula | $C_{13}H_{20}BF_4N_4P$ |
| Formula weight | 350.11 |
| Temperature/K | 100.02 |
| Crystal system | monoclinic |
| Space group | $P2_1/c$ |
| a/Å | 14.1130(5) |
| b/Å | 10.0903(3) |
| c/Å | 11.7750(4) |
| α/° | 90 |
| β/° | 105.4080(10) |
| γ/° | 90 |
| Volume/Å$^3$ | 1616.54(9) |
| Z | 4 |
| $\rho_{calc}$g/cm$^3$ | 1.439 |
| μ/mm$^{-1}$ | 1.927 |
| F(000) | 728.0 |
| Crystal size/mm$^3$ | 0.22 × 0.06 × 0.03 |
| Radiation | CuKα (λ = 1.54178) |
| 2Θ range for data collection/° | 6.496 to 159.298 |
| Index ranges | -17 ≤ h ≤ 17, -12 ≤ k ≤ 12, -14 ≤ l ≤ 14 |
| Reflections collected | 35817 |
| Independent reflections | 3495 [$R_{int}$ = 0.0496, $R_{sigma}$ = 0.0235] |
| Data/restraints/parameters | 3495/0/212 |
| Goodness-of-fit on F$^2$ | 1.066 |
| Final R indexes [I>=2σ (I)] | $R_1$ = 0.0313, w$R_2$ = 0.0750 |
| Final R indexes [all data] | $R_1$ = 0.0352, w$R_2$ = 0.0775 |
| Largest diff. peak/hole / e Å$^{-3}$ | 0.29/-0.30 |
| CCDC access code | 2331037 |
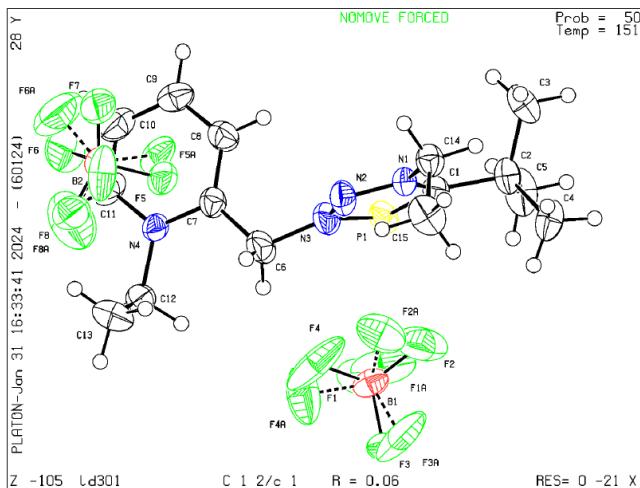
**Table S2:** Crystal data and structure refinement for $C_{15}H_{25}B_2F_8N_4P$ (**3b''**).

| | |
|---|---|
| Identification code | $C_{15}H_{25}B_2F_8N_4P$ |
| Empirical formula | $C_{15}H_{25}B_2F_8N_4P$ |
| Formula weight | 465.98 |
| Temperature/K | 150.50 |
| Crystal system | monoclinic |
| Space group | C2/c |
| a/Å | 24.3146(8) |
| b/Å | 12.9358(5) |
| c/Å | 13.5851(6) |
| α/° | 90 |
| β/° | 96.2730(10) |
| γ/° | 90 |
| Volume/Å$^3$ | 4247.3(3) |
| Z | 8 |
| $\rho_{calc}$g/cm$^3$ | 1.457 |
| μ/mm$^{-1}$ | 0.208 |
| F(000) | 1920.0 |
| Crystal size/mm$^3$ | 0.44 × 0.28 × 0.16 |
| Radiation | MoKα (λ = 0.71073) |
| 2Θ range for data collection/° | 4.554 to 51.36 |
| Index ranges | -29 ≤ h ≤ 28, -15 ≤ k ≤ 14, -16 ≤ l ≤ 16 |
| Reflections collected | 28439 |
| Independent reflections | 4017 [$R_{int}$ = 0.0390, $R_{sigma}$ = 0.0224] |
| Data/restraints/parameters | 4017/86/350 |
| Goodness-of-fit on F$^2$ | 1.065 |
| Final R indexes [I>=2σ (I)] | $R_1$ = 0.0600, $wR_2$ = 0.1605 |
| Final R indexes [all data] | $R_1$ = 0.0671, $wR_2$ = 0.1680 |
| Largest diff. peak/hole / e Å$^{-3}$ | 0.74/-0.26 |
| CCDC access code | 2331035 |
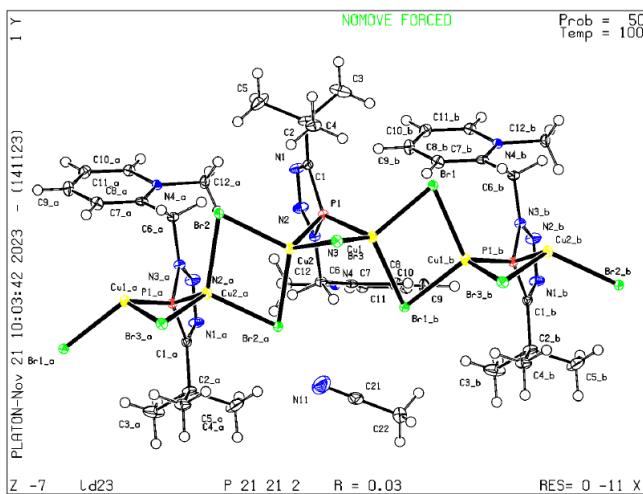
**Table S3:** Crystal data and structure refinement for $[C_{12}H_{18}N_4P]_n$ $[Cu_2Br_3]_n$ (**4a$_{\mu2}$**).

| | |
|---|---|
| Identification code | $[C_{12}H_{18}N_4P]_n$ $[Cu_2Br_3]_n$ |
| Empirical formula | $C_{14}H_{21}Br_3Cu_2N_5P$ |
| Formula weight | 657.14 |
| Temperature/K | 100.02 |
| Crystal system | orthorhombic |
| Space group | $P2_12_12$ |
| a/Å | 10.5062(11) |
| b/Å | 20.338(2) |
| c/Å | 9.7981(8) |
| α/° | 90 |
| β/° | 90 |
| γ/° | 90 |
| Volume/Å$^3$ | 2093.7(4) |
| Z | 4 |
| $\rho_{calc}$g/cm$^3$ | 2.085 |
| μ/mm$^{-1}$ | 7.841 |
| F(000) | 1272.0 |
| Crystal size/mm$^3$ | 0.36 × 0.04 × 0.01 |
| Radiation | MoKα (λ = 0.71073) |
| 2Θ range for data collection/° | 4.614 to 61.258 |
| Index ranges | -15 ≤ h ≤ 15, -29 ≤ k ≤ 29, -14 ≤ l ≤ 14 |
| Reflections collected | 76946 |
| Independent reflections | 6441 [$R_{int}$ = 0.0728, $R_{sigma}$ = 0.0371] |
| Data/restraints/parameters | 6441/0/232 |
| Goodness-of-fit on F$^2$ | 1.029 |
| Final R indexes [I>=2σ (I)] | $R_1$ = 0.0256, w$R_2$ = 0.0443 |
| Final R indexes [all data] | $R_1$ = 0.0332, w$R_2$ = 0.0458 |
| Largest diff. peak/hole / e Å$^{-3}$ | 0.54/-0.63 |
| Flack parameter | 0.035(8) |
| CCDC access code | 2331040 |
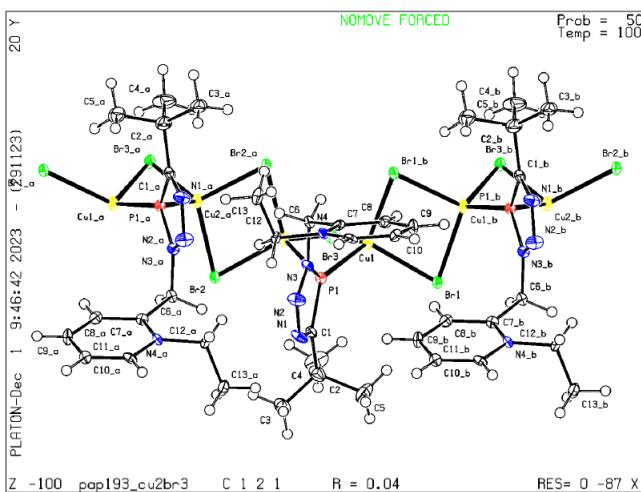
**Table S4:** Crystal data and structure refinement for $[C_{13}H_{20}N_4P]_n$ $[Cu_2Br_3]_n$ (**4b$_{\mu 2}$**).

| | |
|---|---|
| Identification code | $[C_{13}H_{20}N_4P]_n$ $[Cu_2Br_3]_n$ |
| Empirical formula | $C_{13}H_{20}Br_3Cu_2N_4P$ |
| Formula weight | 630.11 |
| Temperature/K | 100.00 |
| Crystal system | monoclinic |
| Space group | C2 |
| a/Å | 23.1483(19) |
| b/Å | 9.8144(7) |
| c/Å | 10.6338(8) |
| α/° | 90 |
| β/° | 99.906(7) |
| γ/° | 90 |
| Volume/Å$^3$ | 2379.8(3) |
| Z | 4 |
| $\rho_{calc}$g/cm$^3$ | 1.759 |
| μ/mm$^{-1}$ | 6.893 |
| F(000) | 1216.0 |
| Crystal size/mm$^3$ | 0.2 × 0.17 × 0.01 |
| Radiation | MoKα (λ = 0.71073) |
| 2Θ range for data collection/° | 4.518 to 61.188 |
| Index ranges | -32 ≤ h ≤ 32, -14 ≤ k ≤ 14, -15 ≤ l ≤ 15 |
| Reflections collected | 39503 |
| Independent reflections | 7247 [$R_{int}$ = 0.0899, $R_{sigma}$ = 0.0750] |
| Data/restraints/parameters | 7247/1/213 |
| Goodness-of-fit on F$^2$ | 0.979 |
| Final R indexes [I>=2σ (I)] | $R_1$ = 0.0396, $wR_2$ = 0.0739 |
| Final R indexes [all data] | $R_1$ = 0.0533, $wR_2$ = 0.0773 |
| Largest diff. peak/hole / e Å$^{-3}$ | 1.12/-0.79 |
| Flack parameter | 0.029(13) |
| CCDC access code | 2331042 |
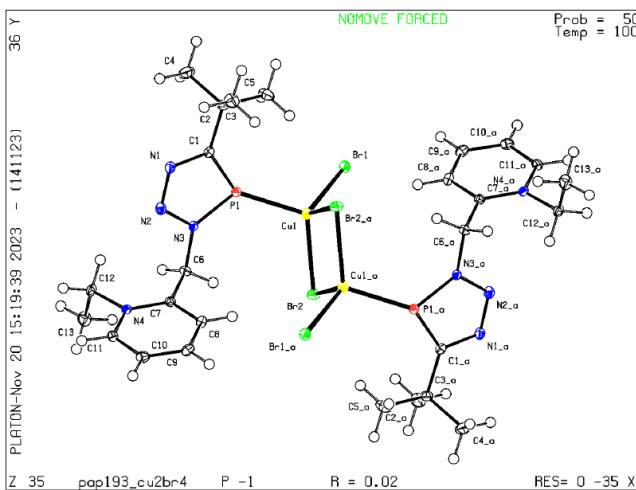
**Table S5:** Crystal data and structure refinement for $[C_{13}H_{20}N_4P]_2[Cu_2Br_4]_n$ (**4b$_{\eta1}$**).

| | |
|---|---|
| Identification code | $[C_{13}H_{20}N_4P]_2[Cu_2Br_4]_n$ |
| Empirical formula | $C_{26}H_{40}Br_4Cu_2N_8P_2$ |
| Formula weight | 973.32 |
| Temperature/K | 100.00 |
| Crystal system | triclinic |
| Space group | P-1 |
| a/Å | 9.1540(13) |
| b/Å | 10.0348(11) |
| c/Å | 10.5489(15) |
| α/° | 93.756(6) |
| β/° | 98.769(5) |
| γ/° | 112.775(4) |
| Volume/Å$^3$ | 874.7(2) |
| Z | 1 |
| $\rho_{calc}$g/cm$^3$ | 1.848 |
| μ/mm$^{-1}$ | 5.906 |
| F(000) | 480.0 |
| Crystal size/mm$^3$ | 0.23 × 0.15 × 0.03 |
| Radiation | MoKα (λ = 0.71073) |
| 2Θ range for data collection/° | 4.918 to 61.184 |
| Index ranges | -13 ≤ h ≤ 13, -14 ≤ k ≤ 14, -15 ≤ l ≤ 15 |
| Reflections collected | 34087 |
| Independent reflections | 5366 [R$_{int}$ = 0.0358, R$_{sigma}$ = 0.0245] |
| Data/restraints/parameters | 5366/0/194 |
| Goodness-of-fit on F$^2$ | 1.048 |
| Final R indexes [I>=2σ (I)] | R$_1$ = 0.0225, wR$_2$ = 0.0541 |
| Final R indexes [all data] | R$_1$ = 0.0254, wR$_2$ = 0.0554 |
| Largest diff. peak/hole / e Å$^{-3}$ | 0.68/-0.92 |
| CCDC access code | 2331036 |
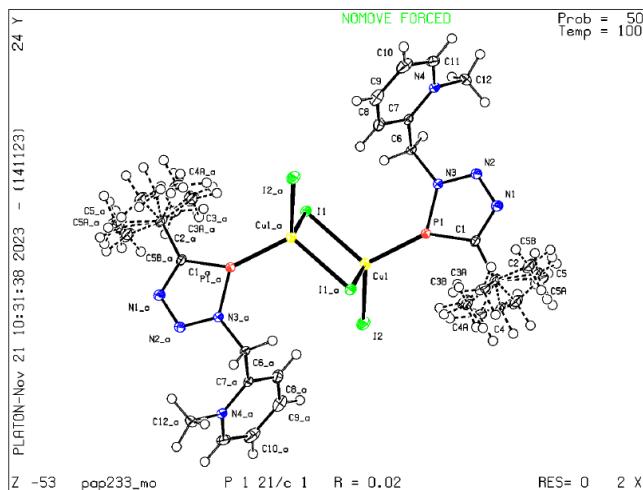
**Table S6:** Crystal data and structure refinement for [C$_{12}$H$_{18}$N$_4$P]$_2$ [Cu$_2$I$_4$]$_2$ (**4c$_{\eta 1}$**).

| | |
|---|---|
| Identification code | [C$_{12}$H$_{18}$N$_4$P]$_2$ [Cu$_2$I$_4$]$_2$ |
| Empirical formula | C$_{24}$H$_{36}$Cu$_2$I$_4$N$_8$P$_2$ |
| Formula weight | 1133.23 |
| Temperature/K | 100.05 |
| Crystal system | monoclinic |
| Space group | P2$_1$/c |
| a/Å | 10.7747(6) |
| b/Å | 10.8023(6) |
| c/Å | 15.1569(7) |
| α/° | 90 |
| β/° | 103.912(2) |
| γ/° | 90 |
| Volume/Å$^3$ | 1712.39(16) |
| Z | 2 |
| ρ$_{calc}$g/cm$^3$ | 2.198 |
| μ/mm$^{-1}$ | 4.970 |
| F(000) | 1072.0 |
| Crystal size/mm$^3$ | 0.15 × 0.08 × 0.02 |
| Radiation | MoKα (λ = 0.71073) |
| 2Θ range for data collection/° | 4.678 to 61.102 |
| Index ranges | -15 ≤ h ≤ 15, -15 ≤ k ≤ 15, -21 ≤ l ≤ 21 |
| Reflections collected | 71354 |
| Independent reflections | 5245 [R$_{int}$ = 0.0389, R$_{sigma}$ = 0.0156] |
| Data/restraints/parameters | 5245/10/212 |
| Goodness-of-fit on F$^2$ | 1.118 |
| Final R indexes [I>=2σ (I)] | R$_1$ = 0.0228, wR$_2$ = 0.0513 |
| Final R indexes [all data] | R$_1$ = 0.0285, wR$_2$ = 0.0540 |
| Largest diff. peak/hole / e Å$^{-3}$ | 1.59/-1.46 |
| CCDC access code | 2331038 |

S33
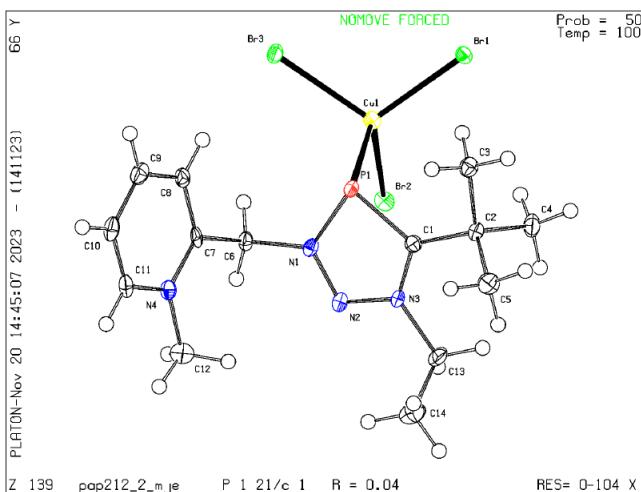
**Table S7:** Crystal data and structure refinement for [C$_{14}$H$_{23}$N$_4$P][CuBr$_3$] (**5$_{η1}$**).

| | |
|---|---|
| Identification code | [C$_{14}$H$_{23}$N$_4$P][CuBr$_3$] |
| Empirical formula | C$_{14}$H$_{23}$Br$_3$CuN$_4$P |
| Formula weight | 581.60 |
| Temperature/K | 99.98 |
| Crystal system | monoclinic |
| Space group | P2$_1$/c |
| a/Å | 6.9051(3) |
| b/Å | 14.2784(5) |
| c/Å | 20.3158(7) |
| α/° | 90 |
| β/° | 96.578(2) |
| γ/° | 90 |
| Volume/Å$^3$ | 1989.82(13) |
| Z | 4 |
| ρ$_{calc}$g/cm$^3$ | 1.941 |
| μ/mm$^{-1}$ | 9.391 |
| F(000) | 1136.0 |
| Crystal size/mm$^3$ | 0.18 × 0.04 × 0.01 |
| Radiation | CuKα (λ = 1.54178) |
| 2Θ range for data collection/° | 7.584 to 137 |
| Index ranges | -8 ≤ h ≤ 7, -17 ≤ k ≤ 17, -24 ≤ l ≤ 24 |
| Reflections collected | 16925 |
| Independent reflections | 16925 [R$_{int}$ = ?, R$_{sigma}$ = 0.0598] |
| Data/restraints/parameters | 16925/0/214 |
| Goodness-of-fit on F$^2$ | 1.038 |
| Final R indexes [I>=2σ (I)] | R$_1$ = 0.0364, wR$_2$ = 0.0822 |
| Final R indexes [all data] | R$_1$ = 0.0453, wR$_2$ = 0.0857 |
| Largest diff. peak/hole / e Å$^{-3}$ | 1.96/-0.88 |
| CCDC access code | 2331034 |
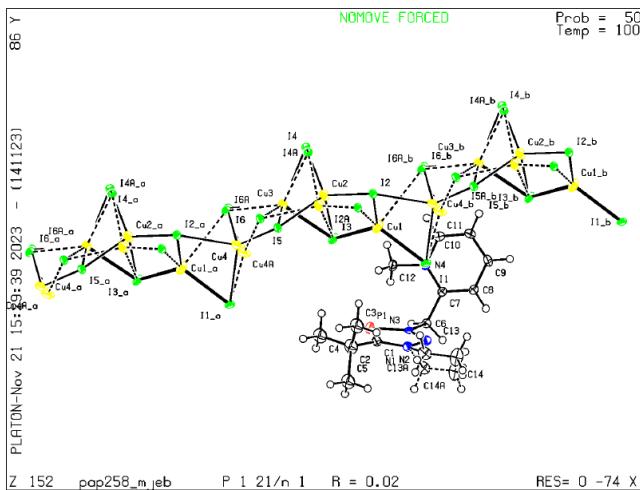
**Table S8:** Crystal data and structure refinement for [C₁₄H₂₃N₄P][Cu₄I₆] (**6**).

| | |
|---|---|
| Identification code | [C₁₄H₂₃N₄P][Cu₄I₆] |
| Empirical formula | C₁₄H₂₃Cu₄I₆N₄P |
| Formula weight | 1293.89 |
| Temperature/K | 100.10 |
| Crystal system | monoclinic |
| Space group | P2₁/n |
| a/Å | 18.6654(13) |
| b/Å | 8.5221(6) |
| c/Å | 19.9329(13) |
| α/° | 90 |
| β/° | 115.795(2) |
| γ/° | 90 |
| Volume/Å³ | 2854.8(3) |
| Z | 4 |
| ρ$_{calc}$g/cm³ | 3.010 |
| μ/mm$^{-1}$ | 9.495 |
| F(000) | 2336.0 |
| Crystal size/mm³ | 0.08 × 0.05 × 0.02 |
| Radiation | MoKα (λ = 0.71073) |
| 2Θ range for data collection/° | 4.54 to 50.828 |
| Index ranges | -22 ≤ h ≤ 22, -10 ≤ k ≤ 10, -24 ≤ l ≤ 24 |
| Reflections collected | 142872 |
| Independent reflections | 5259 [R$_{int}$ = 0.0642, R$_{sigma}$ = 0.0145] |
| Data/restraints/parameters | 5259/12/264 |
| Goodness-of-fit on F² | 1.094 |
| Final R indexes [I>=2σ (I)] | R₁ = 0.0241, wR₂ = 0.0512 |
| Final R indexes [all data] | R₁ = 0.0295, wR₂ = 0.0529 |
| Largest diff. peak/hole / e Å$^{-3}$ | 2.03/-1.39 |
| CCDC access code | 2331041 |
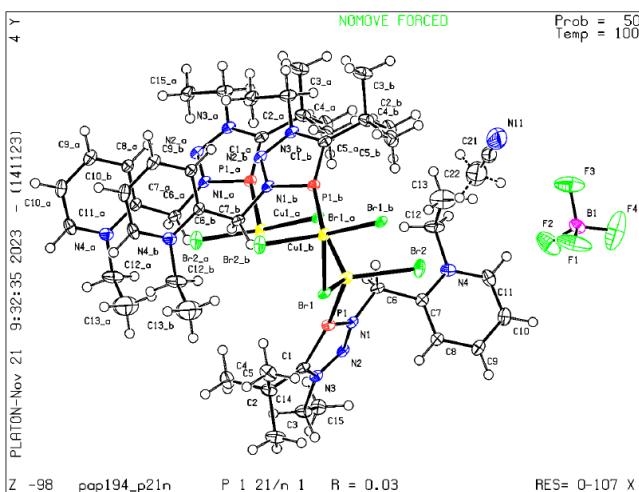
**Table S9:** Crystal data and structure refinement for [C$_{15}$H$_{25}$N$_4$P][BF$_4$][CuBr$_2$] (**7$_{\eta 1}$**).

| | |
|---|---|
| Identification code | [C$_{15}$H$_{25}$N$_4$P][BF$_4$][CuBr$_2$] |
| Empirical formula | C$_{15.67}$H$_{26}$BBr$_2$CuF$_4$N$_{4.33}$P |
| Formula weight | 616.21 |
| Temperature/K | 100.00 |
| Crystal system | monoclinic |
| Space group | P2$_1$/n |
| a/Å | 14.5353(9) |
| b/Å | 6.9730(4) |
| c/Å | 22.7438(14) |
| α/° | 90 |
| β/° | 90.042(3) |
| γ/° | 90 |
| Volume/Å$^3$ | 2305.2(2) |
| Z | 4 |
| ρ$_{calc}$g/cm$^3$ | 1.776 |
| μ/mm$^{-1}$ | 4.526 |
| F(000) | 1221.0 |
| Crystal size/mm$^3$ | 0.45 × 0.04 × 0.02 |
| Radiation | MoKα (λ = 0.71073) |
| 2Θ range for data collection/° | 5.606 to 52.852 |
| Index ranges | -18 ≤ h ≤ 18, -8 ≤ k ≤ 8, -28 ≤ l ≤ 28 |
| Reflections collected | 33558 |
| Independent reflections | 4729 [R$_{int}$ = 0.0411, R$_{sigma}$ = 0.0231] |
| Data/restraints/parameters | 4729/48/281 |
| Goodness-of-fit on F$^2$ | 1.033 |
| Final R indexes [I>=2σ (I)] | R$_1$ = 0.0312, wR$_2$ = 0.0718 |
| Final R indexes [all data] | R$_1$ = 0.0389, wR$_2$ = 0.0754 |
| Largest diff. peak/hole / e Å$^{-3}$ | 1.87/-1.13 |
| CCDC access code | 2331039 |

## 3. References

[1]  Bruker (**2010**). APEX2, SAINT, SADABS and XSHELL. Bruker AXS Inc., Madison, Wisconsin, USA.

[2]  Sheldrick, G. SADABS. University of Göttingen: Göttingen, Germany: **2014**; Coppens, P. The Evaluation of Absorption and Extinction in Single-Crystal Structure Analysis. Crystallographic Computing. Copenhagen, Muksgaard: **1979**.

[3]  Sheldrick, G. M. A short history of SHELX. *Acta Crystallogr. Sect. A: Found. Crystallogr*. **2008**, *64*, 112-122; Sheldrick, G. M. Crystal structure refinement with SHELXL. *Acta Crystallographica Section C: Structural Chemistry* **2015**, *71*, 3-8.

[4]  O. V. Dolomanov, L. J. Bourhis, R. J Gildea, J. A. K. Howard, H. Puschmann, *J. Appl. Cryst.* **2009**, *42*, 339.

[5]  Mercury 3.0. C. F. Macrae, I. Sovago, S. J. Cottrell, P. T. A. Galek, P. McCabe, E. Pidcock, M. Platings, G. P. Shields, J. S. Stevens, M. Towler, P. A. Wood, *J. Appl. Cryst.* **2020**, *53*, 226–235.